

Bahman Zohuri

# Nuclear Energy for Hydrogen Generation through Intermediate Heat Exchangers

A Renewable Source of Energy



Springer

# Nuclear Energy for Hydrogen Generation through Intermediate Heat Exchangers



Bahman Zohuri

# Nuclear Energy for Hydrogen Generation through Intermediate Heat Exchangers

A Renewable Source of Energy



Springer

Bahman Zohuri  
Galaxy Advanced Engineering, Inc.  
Albuquerque, NM, USA

ISBN 978-3-319-29837-5      ISBN 978-3-319-29838-2 (eBook)  
DOI 10.1007/978-3-319-29838-2

Library of Congress Control Number: 2016943831

© Springer International Publishing Switzerland 2016

This work is subject to copyright. All rights are reserved by the Publisher, whether the whole or part of the material is concerned, specifically the rights of translation, reprinting, reuse of illustrations, recitation, broadcasting, reproduction on microfilms or in any other physical way, and transmission or information storage and retrieval, electronic adaptation, computer software, or by similar or dissimilar methodology now known or hereafter developed.

The use of general descriptive names, registered names, trademarks, service marks, etc. in this publication does not imply, even in the absence of a specific statement, that such names are exempt from the relevant protective laws and regulations and therefore free for general use.

The publisher, the authors and the editors are safe to assume that the advice and information in this book are believed to be true and accurate at the date of publication. Neither the publisher nor the authors or the editors give a warranty, express or implied, with respect to the material contained herein or for any errors or omissions that may have been made.

Printed on acid-free paper

This Springer imprint is published by Springer Nature  
The registered company is Springer International Publishing AG Switzerland

*This book is dedicated to my daughter  
Dr. Natasha Zohuri (MD), who always  
encouraged me in my scholarly work.*



# Preface

Today's global energy market places many demands on power generation technology, particularly in terms of high thermal efficiency, low cost, rapid installation, reliability, environmental compliance, and operational flexibility.

The demand for clean, non-fossil-based electricity is growing; therefore, the world needs to develop new nuclear reactors with higher thermal efficiency in order to increase electricity generation and decrease the detrimental effects of energy production on the environment. The current fleet of nuclear power plants is classified as Generation III or less. However, these models are not as energy efficient as they should be because the operating temperatures are relatively low. Currently, groups of countries have initiated international collaboration to develop the next generation of nuclear reactors, called Generation IV. The ultimate goal of developing such reactors is to increase the thermal efficiency from what currently is in the range of 30–35 % to 45–50 %. This increase in thermal efficiency would result in a higher production of electricity compared to current pressurized water reactor (PWR) or boiling water reactor (BWR) technologies.

Recent technological developments in next generation nuclear reactors have created renewed interest in nuclear process heat for industrial applications. The Next Generation Nuclear Plants (NGNPs) will most likely produce electricity and process heat for hydrogen production. Process heat is not restricted to hydrogen production but is also envisioned for various other technologies such as the extraction of iron ore, coal gasification, and enhanced oil recovery. To utilize process heat, a thermal device is needed to transfer the thermal energy from a NGNP to a hydrogen plant in the most efficient way possible, which has launched a quest for the most cost-effective, high-performance, and efficient intermediate heat exchanger (IHX); this book was written around this quest. The option of transferring heat and thermal energy either via a single-phase forced convection loop, where a fluid is mechanically pumped between the heat exchanger at nuclear and hydrogen plants, is presented, and challenges associated with this problem are discussed.

As a second option, heat pipes and thermosyphons, which have the ability to transport very large quantities of heat over relatively long distances with small temperature losses, are also examined and presented in the book.

A number of technologies are being investigated for NGNPs that will produce heated fluids at significantly higher temperatures than current generation power plants. The higher temperatures offer the opportunity to significantly improve the thermodynamic efficiency of the energy conversion cycle. One of the concepts currently under study is the molten salt reactor. The coolant from a molten salt reactor may be available at temperatures as high as 800–1000 °C. At these temperatures, an open Brayton cycle, combined with a Rankine bottoming cycle, appears to have some strong advantages.

Combined-cycle thermal efficiency increases as gas turbine specific power increases. The gas turbine firing temperature is the primary determinant of specific power.

Gas turbine engines, used in both aircraft and industrial power generation, represent one of the most aggressive applications for structural materials. With ever growing demands for increasing performance and efficiencies, all classes of materials are being pushed to higher temperature capabilities. These materials must also satisfy stringent durability and reliability criteria. As materials are developed to meet these demanding requirements, the processing of these materials often becomes very complicated and expensive. As a result, the cost of materials and processes has become a much larger consideration in the design and application of high-performance materials. Both the aircraft engine and power generation industries are highly cost competitive, and market advantage today relies on reducing cost and increasing performance and efficiency.

In the distributed power generation market, and renewed attention to nuclear power plants, in particular next generation and small modular reactors (SMRs), one of the most economical solutions today is to generate power through small gas turbine systems in the form of the Brayton cycle in combination with these reactors. These gas turbines can be categorized arbitrarily as micro turbines with an output of 5–200 kW and mini turbines with an output of 200–500 kW. The thermal efficiency of such micro turbines is around 20 % or less if no recuperator is used in the system. Using a recuperator (a regenerator can also be considered but has a number of problems) operating at 87 % effectiveness, the efficiency of the gas turbine system increases to around 30 %, a substantial performance improvement. However, the cost of a recuperator is around 25–30 % of the total power plant, so the total cost of ownership and return on investments are not very well justified. This necessitates the use of all prime surface heat exchangers with no brazing. Thus there exists a quest for a novel design of a new generation of compact heat exchangers in support of such combined cycle, and understanding such an innovative approach among engineers and scientists in the field is rising rapidly.

In this book, after providing the necessary concise information on all aspects of this innovative approach, such as combined cycles, and associated turbines, such as micro turbines, we launch into a discussion of the various types of compact heat

exchanger surfaces and novel designs that can be considered for cost-effective heat exchangers and packaging in a system.

The simple Brayton cycle is modified to include a recuperator (which transfers heat from the turbine exhaust to preheated, compressed high-pressure air before going to the combustion chamber), so less fuel will be needed to obtain the desired turbine inlet temperature of compressed air, and the optimum pressure ratio (for either the compressor or turbine) can be reduced to typically 3–4. This improves the thermal efficiency of the cycle. Alternatively, a regenerator can also be used instead of a recuperator.

The development of high-temperature/high-strength materials, corrosion-resistant coatings, and improved cooling technology has led to increases in gas turbine firing temperatures. This increase in firing temperature is the primary development that has led to increases in combined-cycle gas turbine (CCGT) thermal efficiencies. The improvements in combined-cycle thermal efficiencies and the commercial development of combined-cycle power plants have proceeded in parallel with advances in gas turbine technologies.

The Generation IV International Forum program has narrowed the design options of nuclear reactors to six concepts. These concepts are the gas-cooled fast reactor, very-high-temperature reactor, sodium-cooled fast reactor, lead-cooled fast reactor, molten salt reactor, and supercritical water-cooled reactor. These nuclear-reactor concepts differ in their design in aspects such as the neutron spectrum, coolant, moderator, and operating temperature and pressure.

There are many different types of power reactors. What is common to all of them is that they produce thermal energy that can be used for its own sake or converted into mechanical energy and, ultimately, in the vast majority of cases, into electrical energy. Thermal-hydraulic issues related to both operating and advanced reactors are presented. Further thermal-hydraulics research and development continues in both experimental and computational areas for operating reactors, reactors under construction or ready for near-term deployment, and advanced Generation IV reactors. As computing power increases, fine-scale multiphysics computational models, coupled with systems analysis code, are expected to provide answers to many challenging problems in both operating and advanced reactor designs.

Compact heat exchangers, filters, turbines, and other components in integrated NGNP combined-cycle systems must withstand the demanding conditions of high temperatures and pressure differentials. Under the highly sulfiding conditions of high temperature, such as inlet hot steam or other related environmental effects, the performance of components degrades significantly with time unless expensive high alloy materials are used. The deposition of a suitable coating on a low-cost alloy may improve its resistance to such sulfidation attacks and decrease capital and operating costs. A review of the literature indicates that corrosion reaction reflects the competition between oxidation and sulfidation reactions. Fe- and Ni-based high-temperature alloys are susceptible to sulfidation attack unless they are fortified with high levels of Cr, Al, and Si. To impart corrosion resistance, these elements need not be in the bulk of the alloy but present only at the surface layers.

Those who practice the art of nuclear engineering must have a physical and intuitive understanding of the mechanisms and balances of the forces that control the transport of heat and mass in all physical systems. This understanding starts at the molecular level, with intermolecular forces and the motion of molecules, and continues to the macroscopic level, where gradients of velocity, temperature, and concentration drive the diffusion of momentum, heat, and mass, and the forces of pressure, inertia, and buoyancy balance to drive the convection of fluids.

This text covers the fundamentals of combined cycles, which are required to understand electrical power generation systems and driven efficiency of combined cycles. It then covers the application of these principles to nuclear reactor power systems. It represents a general approach to Brayton combined cycles and aims at explaining the fundamentals of combined cycles with compact heat exchangers in a loop and applying them to the challenges facing actual nuclear power systems. It is written at an undergraduate level but should also be useful to practicing engineers and scientists as well.

Chapter 1 presents information about energy resources and the role of nuclear energy from past to present and the future of energy with a roadmap to the next generation of nuclear power plants. Chapter 2 covers the basic thermodynamics of combustion by examining mass and mole fractions and discussing the enthalpy of formation and combustion and the temperature of adiabatic flames. Chapter 3 explains the need for hydrogen production plants and the need for hydrogen as a transport fuel cell and industrial needs for hydrogen for use in oil refineries and other applications. This chapter also explains the efficiency of these power plants, from the entire system to the subsystem level, by discussing the basic Brayton cycle and thermal characteristics of coupling a nuclear plant to a hydrogen production plant using an intermediate heat exchanger for thermal energy transport from the nuclear side to a hydrogen plant. Chapter 4 discusses energy conversion and how to use waste heat and recover it for use as a new source of renewable energy during on-peak and off-peak times of nuclear power plants on the grid in electricity production plants; the chapter also introduces the reader to basic concepts of heat exchangers, which includes their types and how they operate from a thermal-hydraulic point of view; the discussion will allow one to think about their design and application to the nuclear power industry and how compact heat exchangers play a role in increasing the thermal efficiency of the next generation of power plants, with respect to either gas or nuclear produced energy.

Chapter 5 explains and evaluates the next generation of nuclear power plants, along with intermediate heat exchanger operation conditions, from a component point of view and the entire system of such facilities from the nuclear side to the hydrogen side; furthermore, it discusses how the overall output efficiency of combined systems could be improved to make them very cost effective, from operation to production. Chapter 6 covers all classifications and types of heat exchangers in more detailed form, giving the reader a deeper understanding of the thermodynamics involved in their design based on their type and classification. Last but not least, Chapter 7 talks about compact heat exchangers and the roles they play in both gas power plants and nuclear power plants and how their design and

performance impact the thermal output efficiencies of these power plants in order to make them cost effective. This chapter also explains the thermal hydraulic analysis that is involved with the design of compact heat exchangers.

Chapter 4 also concentrates on the fundamentals of a new approach to energy conversion technology to cover power conversion systems and their components and how the waste heat from a power plant can be recovered and put to use in improving overall output efficiency, allowing the owners of such plants to enjoy increased revenue for day-to-day operations.

Finally, the book discusses hybrid energy as a new source of renewable energy, in particular in the utilization of hydrogen as a source of energy in application, where appropriate, to the given subject matter of each chapter's topic.

Detailed appendices provide metric and English system units and conversions, detailed steam and gas tables, heat transfer properties, and nuclear reactor system descriptions, as well as a holistic approach to understanding nuclear power plants and each generation of plants in general.

Albuquerque, NM, USA

Bahman Zohuri



# Acknowledgments

The author would like to acknowledge all those individuals who helped make this book possible with their help, encouragement, and support. I have decided not to name them all since some of them may not be around to see the end result of their encouragement, but we hope they can at least read this acknowledgment wherever they may be.

Last but not least, special thanks go to my parents, wife, children, and friends for providing constant encouragement, without which this book could not have been written. I especially appreciate their patience with my frequent absences from home and long hours in front of the computer during the preparation of this book.

My sincere appreciation goes to Professor Patrick McDaniel of the Department of Nuclear Engineering at the University of New Mexico in Albuquerque, New Mexico, who gave me the knowledge that I have now and continues to teach me what I need to know to go forward. He is a true gentleman.

I am also indebted to another teacher, mentor, and now close friend, Professor Dimiter N. Petsev of the University of New Mexico, Chemical Engineering Department, for whom I have the deepest respect.

I would also like to acknowledge the contributions of Dr. Ronald E. Mizia and Dr. Piyush Sabharwall of Idaho National Laboratory, which are evident throughout the book, and the time they spent on the phone to discuss and advise regarding their ideas, discussions which are ongoing. Appreciation also goes to Dr. C. H. Oh and Dr. C. B. Davis for thier collaboration.

I would also like to take this opportunity to thank Mrs. Tiffany Gasbarrini, Senior Editor at Springer, to whom I am indebted for all her encouragement, Without her tireless efforts and support, none of my publications would have seen the light of day.



# Contents

<b>1 Energy Resources and the Role of Nuclear Energy . . . . .</b>	<b>1</b>
1.1 The World's Energy Resources . . . . .	1
1.2 Today's Global Energy Market . . . . .	2
1.3 The End of Cheap Oil and the Future of Energy . . . . .	3
1.4 What to Do about Coal . . . . .	5
1.5 The Future of Energy . . . . .	7
1.6 Nuclear Reactors for Power Production . . . . .	8
1.7 Future Nuclear Power Plant System . . . . .	10
1.8 Next Generation of Nuclear Power Reactors for Power Production . . . . .	11
1.9 Goals for Generation IV Nuclear Energy Systems . . . . .	12
1.10 A Technology Roadmap for Generation IV Nuclear Energy Systems . . . . .	13
1.11 Description of Six Most Promising Nuclear Power Systems . .	15
1.12 Hybrid Energy Systems . . . . .	19
1.12.1 Hybrid Energy Systems as Sources of Renewable Energy . . . . .	23
1.13 Energy Storage Systems . . . . .	25
1.14 Variable Electricity with Base-Load Reactor Operations . .	29
References . . . . .	35
<b>2 Large-Scale Hydrogen Production . . . . .</b>	<b>37</b>
2.1 Hydrogen Production by Steam Reforming of Hydrocarbons .	38
2.1.1 Steam Reforming Technologies . . . . .	38
2.1.2 Heat of Combustion . . . . .	42
2.1.3 Reforming Reactions . . . . .	44
2.2 Introduction to Combustion . . . . .	45
2.3 Chemical Combustion . . . . .	46
2.4 Combustion Equations . . . . .	48
2.5 Mass and Mole Fractions . . . . .	51

2.6	Enthalpy of Formation . . . . .	53
2.7	Enthalpy of Combustion . . . . .	56
2.8	Adiabatic Flame Temperature . . . . .	57
	References . . . . .	60
<b>3</b>	<b>Hydrogen Production Plant . . . . .</b>	<b>61</b>
3.1	Introduction . . . . .	61
3.2	Electrical Energy Supply and Demand . . . . .	66
3.3	Hydrogen as a Source of Renewable Energy . . . . .	72
3.3.1	Why Hydrogen as a Source of Renewable Energy Now? . . . . .	73
3.3.2	Technical Development of Hydrogen Production . . . . .	75
3.3.3	Technical Development for Hydrogen Product Transport and Storage . . . . .	79
3.4	Development of a Hydrogen Combustion Turbine . . . . .	79
3.5	Feasibility Study on Hydrogen Energy Use . . . . .	81
3.6	Hydrogen Production Using Nuclear Energy . . . . .	83
3.7	Constraints on Hydrogen Production Using Nuclear Energy . . . . .	92
3.7.1	Safety: Hydrogen Generation . . . . .	92
3.7.2	Safety: Hydrogen Generation by Facility Location . . . . .	94
3.8	Efficient Generation of Hydrogen Fuels Utilizing Nuclear Power . . . . .	97
3.9	Thermal Characteristics for Coupling a Hydrogen Product Plant to HTR/VHTR . . . . .	102
3.10	Next Generation Nuclear Plant Intermediate Heat Exchanger Acquisition . . . . .	111
3.11	Applicability of Heat Exchanger to Process Heat Applications . . . . .	116
	References . . . . .	119
<b>4</b>	<b>A New Approach to Energy Conversion Technology . . . . .</b>	<b>123</b>
4.1	Power Conversion Study and Technology Options Assessment . . . . .	123
4.2	Waste Heat Recovery . . . . .	128
4.2.1	Advantages and Disadvantages of Waste Heat Recovery . . . . .	128
4.3	Power Conversion System Components . . . . .	129
4.3.1	Heat Exchangers . . . . .	129
4.3.2	Compact Heat Exchangers . . . . .	142
4.4	Development of Gas Turbine . . . . .	144
4.5	Turbomachinery . . . . .	147
4.6	Heat Transfer Analysis . . . . .	148
4.7	Combined-Cycle Power Plant . . . . .	149
4.8	Advanced Computational Materials Proposed for Generation IV Systems . . . . .	151

4.9	Material Classes Proposed for Generation IV Systems . . . . .	154
4.10	Generation IV Materials Challenges . . . . .	154
4.11	Generation IV Materials Fundamental Issues . . . . .	156
4.12	Capital Cost of Proposed Generation IV Reactors . . . . .	157
4.12.1	Economic and Technical Aspects of Combined-Cycle Performance . . . . .	159
4.12.2	Economic Evaluation Technique . . . . .	159
4.12.3	Output Enhancement . . . . .	161
	References . . . . .	164
<b>5</b>	<b>Evaluation of Next Generation Nuclear Plant Intermediate Heat Exchanger Operating Conditions . . . . .</b>	<b>165</b>
5.1	Introduction . . . . .	165
5.2	Hydrogen Production Plant Requirements . . . . .	172
5.2.1	Nuclear Reactor System . . . . .	173
5.2.2	Turbomachinery System . . . . .	173
5.2.3	Overall Efficiency of Plants . . . . .	179
5.2.4	Heat Exchanger System . . . . .	185
5.2.5	Heat Exchanger Design Configuration . . . . .	188
5.2.6	Intermediate Heat Exchanger Stress Analysis . . . . .	190
5.2.7	Heat Exchanger Materials and Comparisons . . . . .	191
5.2.8	Sizing of Components . . . . .	195
5.2.9	Heat Exchanger Cost Analysis . . . . .	197
5.3	Reactor and Power Conversion Unit . . . . .	198
5.4	Thermochemical Hydrogen Production . . . . .	199
5.5	High-Temperature Electrolysis . . . . .	201
5.6	System Thermal Transfer for Process Heat Application . . . . .	202
5.7	System Stress Analysis Model . . . . .	205
5.8	System Cost Analysis Model . . . . .	205
5.9	Verification and Validation Model . . . . .	205
5.10	System Integration . . . . .	207
	References . . . . .	208
<b>6</b>	<b>Heat Exchangers . . . . .</b>	<b>211</b>
6.1	Heat Exchanger Types . . . . .	211
6.2	Classification According to Transfer Processes . . . . .	214
6.2.1	Indirect-Contact Heat Exchangers . . . . .	214
6.2.2	Direct-Contact Heat Exchangers . . . . .	214
6.3	Classification of Heat Exchanger by Construction Type . . . . .	215
6.3.1	Tubular Heat Exchangers . . . . .	216
6.3.2	Plate Heat Exchangers . . . . .	217
6.3.3	Plate-Fin Heat Exchangers . . . . .	217
6.3.4	Tube-Fin Heat Exchangers . . . . .	218
6.3.5	Regenerative Heat Exchangers . . . . .	219
6.4	Condensers . . . . .	219

6.5	Boilers . . . . .	220
6.6	Classification According to Compactness . . . . .	220
6.7	Types of Applications . . . . .	221
6.8	Cooling Towers . . . . .	221
6.9	Regenerators and Recuperators . . . . .	222
6.10	Heat Exchanger Analysis: Use of LMTD . . . . .	227
6.11	Effectiveness-NTU Method for Heat-Exchanger Design . . . . .	234
6.12	Special Operating Conditions . . . . .	240
6.13	Compact Heat Exchangers and Their Classifications . . . . .	241
	References . . . . .	244
<b>7</b>	<b>Effective Design of Compact Heat Exchangers for Next Generation Nuclear Plants . . . . .</b>	<b>247</b>
7.1	Introduction . . . . .	247
7.2	Classification of Heat Exchangers . . . . .	250
7.3	Compact-Heat-Exchanger-Driven Efficiencies in Brayton Cycle . . . . .	253
7.4	Thermal Energy Transfer for Process Heat Application in Enhanced Mode . . . . .	263
7.5	Design Criteria for Process Heat Exchangers . . . . .	273
7.6	Thermal and Hydraulic Design . . . . .	277
7.6.1	Equations and Parameters . . . . .	278
7.7	Overall Heat Exchanger Design Process . . . . .	295
7.7.1	Input Information Needed . . . . .	295
7.8	Design Summary . . . . .	297
7.9	CHEs in Practice . . . . .	307
7.10	Heat-Exchanger Materials and Comparisons . . . . .	307
7.11	Guide to CHEs . . . . .	308
7.11.1	Generic Advantages of Compact Design . . . . .	310
	References . . . . .	311
	<b>Appendix A: Table and Graph Compilations . . . . .</b>	<b>313</b>
	<b>Appendix B: Gas Property Tables for Selected Gases . . . . .</b>	<b>331</b>
	<b>Appendix C: Thermodynamic Properties for Water . . . . .</b>	<b>367</b>
	<b>Appendix D: Thermodynamic Property Tables for Carbon Dioxide . . . . .</b>	<b>387</b>
	<b>Appendix E: Thermodynamic Property Tables for Sodium . . . . .</b>	<b>391</b>
	<b>Nuclear System Acronyms . . . . .</b>	<b>397</b>
	<b>Index . . . . .</b>	<b>401</b>

## About the Author

**Bahman Zohuri** currently works for Galaxy Advanced Engineering, Inc., a consulting firm that he started in 1991 when he left both the semiconductor and defense industries after many years working as a chief scientist. After graduating from the University of Illinois in the field of physics and applied mathematics and the University of New Mexico, where he studied nuclear engineering, he joined Westinghouse Electric Corporation, where he performed thermal hydraulic analysis and studied natural circulation in an inherent shutdown heat removal system (ISHRS) in the core of a liquid metal fast breeder reactor (LMFBR) as a secondary fully inherent shutdown system for secondary loop heat exchange. All these designs were used in nuclear safety and reliability engineering for a self-actuated shutdown system. He designed a mercury heat pipe and electromagnetic pumps for large pool concepts of a LMFBR for heat rejection purposes for this reactor around 1978, when he received a patent for it. He was subsequently transferred to the defense division of Westinghouse, where he oversaw dynamic analysis and methods of launching and controlling MX missiles from canisters. The results were applied to MX launch seal performance and muzzle blast phenomena analysis (i.e., missile vibration and hydrodynamic shock formation). Zohuri was also involved in analytical calculations and computations in the study of nonlinear ion waves in rarefying plasma. The results were applied to the propagation of so-called soliton waves and the resulting charge collector traces in the rarefaction characterization of the corona of laser-irradiated target pellets. As part of his graduate research work at Argonne National Laboratory, he performed computations and programming of multiechange integrals in surface physics and solid state physics. He earned various patents in areas such as diffusion processes and diffusion furnace design while working as a senior process engineer at various semiconductor companies, such as Intel Corp., Varian Medical Systems, and National Semiconductor Corporation. He later joined Lockheed Martin Missile and Aerospace Corporation as Senior Chief Scientist and oversaw research and development (R&D) and the study of the vulnerability, survivability, and both radiation and laser hardening of different components of the Strategic Defense Initiative, known as Star Wars.

This included payloads (i.e., IR sensor) for the Defense Support Program, the Boost Surveillance and Tracking System, and Space Surveillance and Tracking Satellite against laser and nuclear threats. While at Lockheed Martin, he also performed analyses of laser beam characteristics and nuclear radiation interactions with materials, transient radiation effects in electronics, electromagnetic pulses, system-generated electromagnetic pulses, single-event upset, blast, thermo-mechanical, hardness assurance, maintenance, and device technology.

He spent several years as a consultant at Galaxy Advanced Engineering serving Sandia National Laboratories, where he supported the development of operational hazard assessments for the Air Force Safety Center in collaboration with other researchers and third parties. Ultimately, the results were included in Air Force Instructions issued specifically for directed energy weapons operational safety. He completed the first version of a comprehensive library of detailed laser tools for airborne lasers, advanced tactical lasers, tactical high-energy lasers, and mobile/tactical high-energy lasers, for example.

He also oversaw SDI computer programs, in connection with Battle Management C<sup>3</sup> and artificial intelligence, and autonomous systems. He is the author of several publications and holds several patents, such as for a laser-activated radioactive decay and results of a through-bulkhead initiator. He has published the following works: *Heat Pipe Design and Technology: A Practical Approach* (CRC Press); *Dimensional Analysis and Self-Similarity Methods for Engineering and Scientists* (Springer); *High Energy Laser (HEL): Tomorrow's Weapon in Directed Energy Weapons Volume I* (Trafford Publishing Company); *Thermodynamics in Nuclear Power Plant Systems* (Springer ); and *Thermal-Hydraulic Analysis of Nuclear Reactors* (Springer).

# **Chapter 1**

## **Energy Resources and the Role of Nuclear Energy**

Energy is broadly defined as the ability to produce a change from existing conditions. Thus, the term *energy* implies that a capacity for action is present. The evaluation of energy is done by measuring certain effects that are classified by descriptive names, and these effects can be produced under controlled conditions. For example, mass that is located at a certain position may have a potential energy; if the same mass is in motion, then it may possess kinetic energy; or if its characteristics of composition such as temperature or pressure changes, then it is undergoing an energy process called internal energy. Internal energy can be measured by the release of an amount by the change in potential energy experienced by an external load.

### **1.1 The World's Energy Resources**

For the past half century fossil fuels, namely, coal, oil, and natural gas, have supplied the major portion of the world's energy requirements. It has long been realized, however, that in the not-too-distant future these sources of energy will be largely exhausted. At the present time the total energy consumption, for all countries, is about  $1 \times 10^{17}$  Btu per year. Since the world's population is steadily growing and the power use per capita is increasing, the rate of energy utilization by the year 2020 could well be five to ten times the current value. According to one estimate, the known coal, oil, gas, and oil shale that can be extracted at no more than twice the present cost would be equivalent to roughly  $4 \times 10^{19}$  Btu [10]. This means that in about 100 years the world's economically useful reserves of fossil fuels may approach exhaustion.

## 1.2 Today's Global Energy Market

Today's global energy market places many demands on power generation technology, including high thermal efficiency, low cost, rapid installation, reliability, environmental compliance, and operational flexibility. The conclusion to draw, even considering some margin of error, is that it is inevitable that new sources of power must be found during the next 50 years or so if Earth is to support a growing population with some increase in living standards. Some consideration has been given to a few such sources, for example, solar, wind, and nuclear energy. Although solar and wind energy is very attractive, developing large-scale processes along with large farms of such systems are still some years away; on the other hand nuclear energy has been made available through advances in fission of the heaviest elements or the fusion of very light nuclei. The technology of a fusion process is used commercially and involves the controlled release of energy using the magnetic confinement of a laser-driven pellet of deuterium and tritium the two isotopes of hydrogen is too far advanced. Nuclear fission, on the other hand, has already been established as a practical means for producing energy and getting to the point where it will be economically very competitive with energy produced from fossil fuels in the very near future.

The total amount of basic raw materials as a source of fuel for fission power plants, such as uranium and thorium, in Earth's crust, to a depth of 4.8 km, is very large, possibly something like  $10^{12}$  tons. However, much of this is present in minerals containing such a small proportion of the desired element that extraction would be very expensive and not very cost effective, in particular for high-grade ore reserves that are believed to be on the order of  $2 \times 10^6$  tons; therefore, we need to reduce the cost of recovery from moderately low-grade ores to at least \$100 or less per pound of metal with advanced technology.

The development of plant layout and modularization concepts requires an understanding of both primary and secondary systems.

General Electric's STeam And Gas (STAG)<sup>TM</sup> combined-cycle power generation equipment meets these demands and surpasses them, taking power plant performance to unprecedented levels.

The development of steam and gas turbine combined cycles has paralleled gas turbine development, resulting in reliable combined-cycle plants. Those incorporating GE's advanced gas turbine technology have achieved efficiency levels approaching 58 %, due primarily to the higher firing temperatures of advanced technology gas turbines. The MS9001H gas turbine will achieve 60 % efficiency in combined-cycle application when it goes into full operation.

In addition to advances in gas turbine technology, steam turbine performance has also evolved. GE's STAG combined-cycle power generation product line includes steam cycle options that satisfy a wide range of economic considerations, including fuel flexibility, fuel cost, duty cycle, and space limitations.

Heat exchangers, filters, turbines, and other components in integrated coal gasification combined-cycle systems must withstand the demanding conditions of

high temperatures and pressure differentials. Under the highly sulfiding conditions of high-temperature coal gas, the performance of components degrades significantly with time unless expensive high alloy materials are used. The deposition of a suitable coating on a low-cost alloy may improve resistance to such sulfidation attack and decrease capital and operating costs. A review of the literature indicates that corrosion reaction reflects the competition between oxidation and sulfidation reactions. Fe- and Ni-based high-temperature alloys are susceptible to sulfidation attack unless they are fortified with high levels of Cr, Al, and Si. To impart corrosion resistance, these elements need not be in the bulk of the alloy, but present only at the surface layers.

### **1.3 The End of Cheap Oil and the Future of Energy**

Global production of conventional oil will begin to decline sooner than most people think, probably within 10 years. Recall the two sudden price increases that took place in 1973 and 1979 and rudely awakened the industrial world and forced it to recognize its dependence on cheap crude oil. The first oil shock, in 1973, was in response to an Arab embargo during the Arab-Israeli war. The price tripled and then nearly doubled again when Iran's Shah was dethroned, sending the world's major economies into a tailspin. Just a few years earlier oil explorers had discovered enormous new reservoirs on the Northern Slope of Alaska and below the North Sea off the coast of Europe. The emotional and political reactions of most analysts have caused them to predict a shortage of crude oil in the world due to these types of crises. Not having enough underground reservoirs for the exploration of oil will put the future survival of the world economy on a critical path.

The five Middle Eastern nations that are members of the Organization of Petroleum Exporting Countries (OPEC) were able to hike the price of crude oil not because oil supplies were dwindling but because they controlled 36 % of the international market. Later, when, owing to oil pumped from Alaska and the North Sea, the demand for crude oil sagged, the price of oil dropped and OPEC's control of prices collapsed. The next oil crunch will not be so temporary. The exploration and discovery of oil fields, as well as oil production, around the world suggests that within the next decade, the supply of conventional oil will not support or keep up with demand. Whether this conclusion is in contradiction with what oil companies are reporting is an open question. Today's oil production rate of about 23.6 gigabarrels of oil (GBO) per year may suggest cheap crude oil for the next 43 years, or more, based on official charts showing that reserves are growing. But there are three critical errors in this projection:

- It relies on distorted estimates of reserves;
- It implies that production will remain constant;
- Most importantly, conventional wisdom erroneously assumes that the last bucket of oil can be pumped from the ground just as quickly as the barrels of oil gushing from wells today.

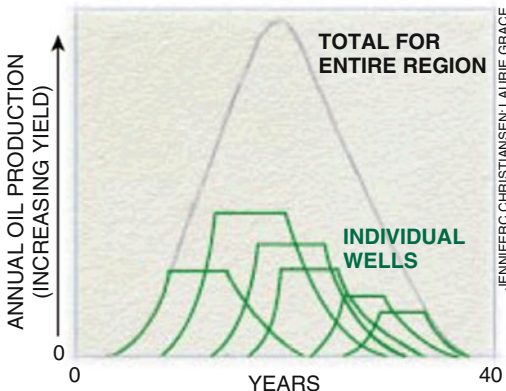


**Fig. 1.1** FLOW OF OIL starts to fall from any large region when about half the crude is gone. Adding the output of fields of various sizes and ages (green curves above) usually yields a *bell-shaped* production *curve* for the region as a whole. M. King Hubbert, a geologist with Shell Oil, exploited this fact in 1956 to predict correctly that oil from the lower 48 American states would peak around 1969

In fact, the rate at which any well – or any country – can produce oil always rises to a maximum and then, when about half the oil is gone, begins falling gradually back to zero.

*From an economic perspective, then, when the world runs completely out of oil is thus not directly relevant:*

What matters is when production begins to taper off. Beyond that point, prices will rise unless demand declines commensurately (Fig. 1.1).

Using several different techniques to estimate the current reserves of conventional oil and the amount still left to be discovered, many experts in the field concluded that the decline would begin before 2010.

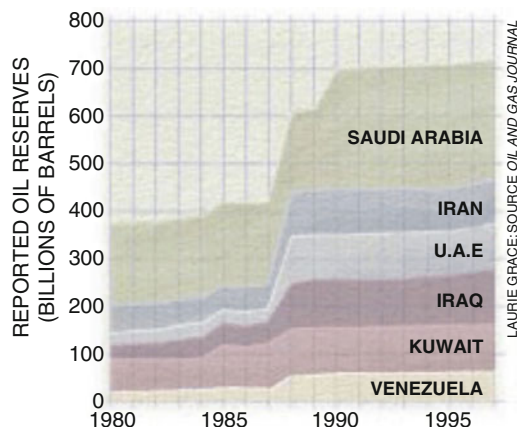
In practice, companies and countries are often deliberately vague about the likelihood of the reserves they report, preferring instead to publicize whichever figure, within a P10 to P90 range, best suits them. Exaggerated estimates can, for instance, raise the price of an oil company's stock (Fig. 1.2).

The members of OPEC have faced an even greater temptation to inflate their reports because the higher their reserves, the more oil they are allowed to export. National companies, which have exclusive oil rights in the main OPEC countries, need not (and do not) release detailed statistics on each field that could be used to verify the country's total reserves. There is thus good reason to suspect that when, during the late 1980s, 6 of the 11 OPEC nations increased their reserve figures by colossal amounts, ranging from 42 to 197 %, they did so only to boost their export quotas.

Meanwhile, global demand for oil is currently rising at more than 2 % a year. Since 1985, energy use is up by about 30 % in Latin America, 40 % in Africa, and 50 % in Asia. The Energy Information Administration forecasts that worldwide demand for oil will increase by 60 % (to about 40 GBO a year) by 2020.

The switch from growth to decline in oil production will thus almost certainly create economic and political tensions. Unless alternatives to crude oil quickly

**Fig. 1.2** A suspicious jump in reserves reported by six OPEC members added 300 billion barrels of oil to official reserve tallies yet followed no major discovery of new fields



Laurie Grace, SOURCE: OIL AND GAS JOURNAL

prove themselves, the market share of the OPEC states in the Middle East will rise rapidly. Within 2 years, these nations' share of the global oil business will pass 30 %, nearing the level reached during the oil-price shocks of the 1970s.

The world could thus see radical increases in oil prices. That alone might be sufficient to curb demand, flattening production for perhaps 10 years (demand fell more than 10 % after the 1979 shock and took 17 years to recover). Many Middle Eastern nations will themselves be past the midpoint soon. World production will then have to fall.

With sufficient preparation, however, the transition to the postoil economy need not be traumatic. If advanced methods of producing liquid fuels from natural gas can be made profitable and scaled up quickly, gas could become the next source of transportation fuel [see “Liquid Fuels from Natural Gas,” by Safaa A. Fouada, on page 92] [1]. Safer nuclear power, cheaper renewable energy, and oil conservation programs could all help postpone the inevitable decline of conventional oil.

Countries should begin planning and investing now. In November 2009 a panel of energy experts appointed by US President Bill Clinton strongly urged the administration to increase funding for energy research by \$1 billion over the next 5 years. That was a small step in the right direction, one that must be followed by giant leaps from the private sector.

The world is not running out of oil – at least not yet. What our society does face, and soon, is the end of the abundant and cheap oil on which all industrial nations depend.

## 1.4 What to Do about Coal

Cheap, plentiful coal is expected to fuel power plants for the foreseeable future, but can we keep it from devastating the environment?

Dealing with climate change means addressing the problems posed by emissions from coal-fired power plants. Unless we take prompt action to strictly limit the

amount of carbon dioxide ( $\text{CO}_2$ ) released into the atmosphere when consuming coal to make electricity, we have little chance of gaining control over global warming. The overview of the side effects from burning coal is as follows:

- Coal is widely burned for power plants to produce electricity, but it also produces large quantities of climate-changing carbon dioxide;
- Compared with conventional power plants, new gasification facilities can more effectively and affordably extract  $\text{CO}_2$  so it can be safely stored underground;
- The world must begin implementing carbon sequestration to stave off global warming.

Coal – the fuel that powered the Industrial Revolution – is a particularly worrisome source of energy, in part because burning it produces considerably more carbon dioxide per unit of electricity generated than burning either oil or natural gas does. In addition, coal is cheap and will remain abundant long after oil and natural gas have become very scarce. With coal plentiful and inexpensive, its use is expanding in the US and elsewhere and is expected to continue rising in areas with abundant coal resources [1] (Fig. 1.3).

Indeed, US power providers are expected to build the equivalent of nearly 280,500-MW, coal-fired electricity plants between 2003 and 2030. Meanwhile China is already constructing the equivalent of one large coal-fueled power station a week. Over their roughly 60-year life spans, the new generating facilities in



**Fig. 1.3** Iron hydroxide precipitate (*orange*) in a Missouri stream receiving acid drainage from surface coal mining (image: U.S. Geological Survey)

operation by 2030 could collectively introduce into the atmosphere about as much carbon dioxide as was released by all the coal burned since the dawn of the Industrial Revolution [1].

Coal use can lead to a range of harmful consequences, including decapitated mountains, air pollution from acidic and toxic emissions, and water fouled with coal wastes. Extraction also endangers and can kill miners. Together, such effects make coal production and conversion to useful energy one of the more destructive activities on the planet.

We need to find alternative answers to the aforementioned issues to deal with future demand. The only answer is to transition as quickly as possible to alternative fuels – including natural gas and nuclear power and solar, wind, and geothermal energy. “Running out of energy in the long run is not the problem, but the bind comes during the next 10 years and we need to get over our dependency on crude oil” [1].

## 1.5 The Future of Energy

The energy future will be very different than the present. For all the uncertainties highlighted in various reports by experts in the field, we can be certain that the energy world will look dramatically different in 2030 than it does today. The world energy system will be transformed, but not necessarily in the way we would like to see. We can be confident of some of the trends highlighted in reports on current global trends in energy supply and consumption, environmentally, economically, and socially. But that can – and must – be altered while there is still time to change the road we are on. The growing weight of China, India, the Middle East, and other non-OECD regions in energy markets and in CO<sub>2</sub> emissions is something we need to take into consideration to deal with global warming. The rapidly increasing dominance of national oil companies and the emergence of low-carbon-energy technologies seems one necessary solution to the problem at hand, but it is not sufficient. And while market imbalances could temporarily cause prices to fall back, it is becoming increasingly apparent that the era of cheap oil is over. But many of the key policy drivers (not to mention other, external, factors) remain in doubt. It is within the power of all governments, of producing and consuming countries alike, acting alone or in concert, to steer the world toward a cleaner, cleverer, and more competitive energy system. Time is running out, and the time to act is now. So what we need to ask is: *Can Nuclear Power Compete?*

A variety of companies that are in the energy production business say the answer may be yes. Manufacturers have submitted new designs to the Nuclear Regulatory Commission’s safety engineers, and that agency has already approved some as ready for construction – if they are built on a previously approved site. Utilities, reactor manufacturers, and architecture/engineering firms have formed partnerships to build plants, pending final approvals. Swarms of students are enrolling in



**Fig. 1.4** Typical nuclear plant in our backyard

college-level nuclear engineering programs, and rosy projections from industry and government predict a surge in construction (Fig. 1.4).

Like another moon shot, the launch of new reactors after a 35-year hiatus in orders is certainly possible, though not a sure bet. It would be easier this time, the experts say, because of technological progress over the intervening decades. But as with a project as large as a moon landing, there is another question: Would it be worthwhile?

To answer this question, we need to at least satisfy the four unresolved problems associated with nuclear power that were brought up by a report issued by the Massachusetts Institute of Technology; these points were mentioned at the beginning of this write up. To argue the first point, which is the cost of producing a nuclear power plant with its modern technologies from total ownership and return on investment, we need to understand the nature of the beast from the day it was born in the basement of the University of Chicago.

## 1.6 Nuclear Reactors for Power Production

In the USA, most reactor designs and development for the generation of electrical power stemmed from early naval nuclear research, when it was realized that a compact nuclear power plant would have great advantages in submarine propulsion.

Such a power plant would make possible long voyages across the oceans at high speeds without the necessity for resurfacing at frequent intervals. Argonne National Laboratory was assigned the task of designing such a reactor. Thus was born the first generation of pressurized water reactors (PWRs). It used highly enriched uranium as fuel and water under pressure as moderator as well as coolant. The first prototype of this reactor, named STR Mark 1, started operation at Arco, Idaho, in March 1953, and a production version of it was installed on the *USS Nautilus*, the first nuclear-powered submarine, in May 1953.

As a result of the experience gained in the successful operation of the submarine reactors, the first commercial version of a PWR was designed and installed at Shipping Port, Pennsylvania, and went into operation on December 2, 1957, with a water pressure of 13.8 MPa (2000 psi). The steam produced in the heat exchanger was at a temperature of around 254 °C (490 °F) and a pressure close to 4.14 MPa (600 psi). To make the reactor cost effective and reduce the cost of the power produced, only a small number of fuel elements were highly enriched in uranium-235 ( $U^{235}$ ) as an alloy with zirconium. The remainder was of normal uranium dioxide. The change in the core design required more real estate for the footprint of a commercialized PWR. This was not an issue for a land-based facility. The output power of this reactor was approximately 60 MWe and 230 MWt. Further enhancement in core design increased the power to 150 MWe and 505 MWt. PWRs, using slightly (2–6 %) enriched uranium dioxide as fuel, are now commonly used in the USA and other countries around the globe for commercial power generation. The most recent plants have electrical output in the neighborhood of 1000 MWe (3000 MWt).

Later on other reactor designs based on different fuel materials, moderators, and coolants, with various electrical and thermal powers output, were born. Examples are the following:

- Boiling water reactor (BWR), initiated in 1953;
- Water-cooled graphite moderated in 1954;
- High-temperature gas-cooled reactor (**HTGR**);
- Liquid metal fast breeder reactor (**LMFBR**).

Basically, all present commercial reactor power plants are systems for generating steam utilizing the heat of nuclear fission to boil water and produce steam for a turbine. They are often referred to as “Nuclear Steam Supply Systems” or **NSSS**. The steam is expanded in a turbine that drives a generator to produce electricity in the conventional manner. The exhaust steam from the turbine passes on to a condenser, where it is converted into liquid water, and this is returned as feed water to the steam generator of the **NSSS**.

The proportion of the heat supplied in a power plant that is actually converted into electrical energy is called the thermal efficiency of the system; thus, in a nuclear installation,

$$\text{Thermal Efficiency} = \frac{\text{Electrical Energy Generated}}{\text{Heat Produced in Reactor}}$$

The maximum possible value of the thermal efficiency is the *ideal thermodynamic efficiency*, which is given by following relationship

$$\text{Ideal Thermodynamic Efficiency} = \frac{T_1 - T_2}{T_1}$$

where

$T_1$  = absolute temperature of the steam entering the turbine (K) and

$T_2$  = temperature at which heat is rejected to the condenser (K)

The ideal thermodynamic efficiency can be increased by having  $T_2$  as high as possible and  $T_1$  as low as possible. In practice,  $T_1$  is more or less fixed by the ambient temperature; the thermal efficiency of a steam electric plant is then largely determined by the steam temperature, which should be as high as feasible [2].

Conditions in PWRs and BWRs are such that the steam temperature is lower than in modern fossil-fuel power plants, in which the heat is produced by burning coal, oil, or gas. The thermal efficiencies of these nuclear reactor plants are only about 33 %, compared with 40 % for the best fossil-fuel facilities. With the HTGRs and fast breeder reactors, however, the thermal efficiencies should equal those of the best fossil-fuel plants, i.e., about 40 %.

## 1.7 Future Nuclear Power Plant System

In response to the difficulties in achieving suitability, a sufficiently high degree of safety, and a competitive economic basis for nuclear power, the US Department of Energy initiated the Generation IV program in 1999. Generation IV refers to the broad division of nuclear designs into four categories as follows:

1. Early prototype reactor (Generation I).
2. The large central station nuclear power plants of today (Generation II),
3. The advanced light-water reactors and other systems with inherent safety features that have been designed in recent years (Generation III),
4. The next generation system to be designed and built two decades from now (Generation IV).

By 2000 international interest in the Generation IV project had resulted in a nine-country coalition that includes the following nations:

- (a) Argentina,
- (b) Brazil,
- (c) Canada,
- (d) France,
- (e) Japan,
- (f) South Africa,
- (g) South Korea,

- (h) United Kingdom.
- (i) USA.

Participants are mapping out and collaborating on the research and development of future nuclear energy systems.

Although the Generation IV program is exploring a wide variety of new systems, a few examples will serve to illustrate the broad approaches to reactor designs that are being developed to meet the coalition's objectives.

The next generation systems are based on three general classes of reactor:

1. Gas-cooled,
2. Water-cooled, and
3. Fast-spectrum.

All these categories and their designs are discussed briefly in the following sections.

## 1.8 Next Generation of Nuclear Power Reactors for Power Production

Experts are projecting that worldwide electricity consumption will increase substantially in the coming decades, especially in the developing world. The accompanying economic growth and social progress will have a direct impact on rising electricity prices. This has focused fresh attention on nuclear power plants. New, safer, and more economical nuclear reactors could not only satisfy many of our future energy needs but could combat global warming as well. Today's existing nuclear power plants on line in the USA provide a fifth of the nation's total electrical output.

Taking into account the expected increase in energy demand worldwide and the growing awareness about global warming, climate change issues, and sustainable development, nuclear energy will be needed to meet future global energy demand.

Nuclear power plant technology has evolved in distinct design generations, as mentioned in the previous section, and is briefly summarized here again as follows (Fig. 1.5):

- First generation: prototypes and first realizations (around 1950–1970),
- Second generation: current operating plants (around 1970–2030),
- Third generation: deployable improvements to current reactors (from around 2000),
- Fourth generation: advanced and new reactor systems (2030 and beyond).

The **Generation IV International Forum**, or **GIF**, was chartered in July 2001 to lead the collaborative efforts of the world's leading nuclear technology nations to develop next generation nuclear energy systems to meet the world's future energy needs.

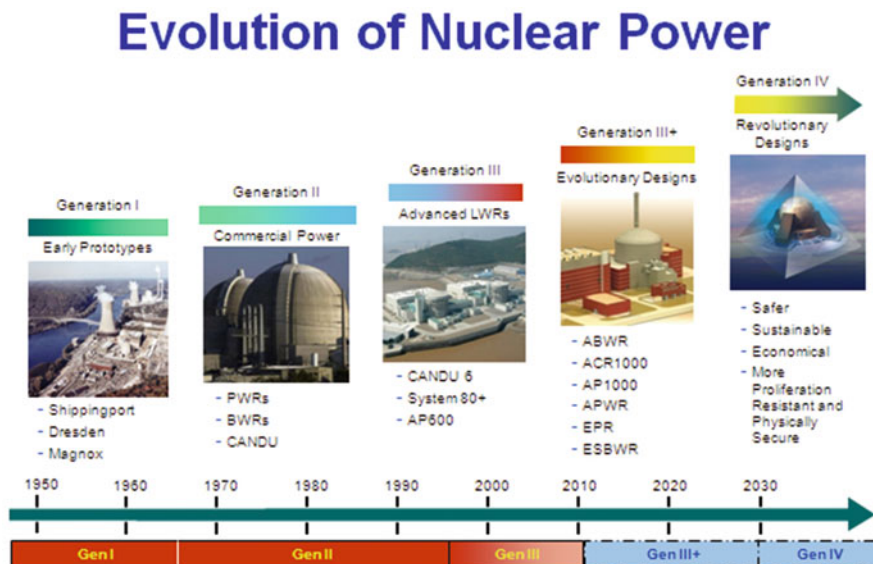


**Fig. 1.5** Evolution of nuclear power plants

Eight technology goals have been defined for Generation IV systems in four broad areas:

1. Sustainability,
2. Economics,
3. Safety and Reliability, and
4. Proliferation resistance and physical protection.

A large number of countries share these ambitious goals as they aim at responding to economic, environmental, and social requirements of the twenty-first century. They establish a framework and identify concrete targets for focusing GIF R&D efforts.

## 1.9 Goals for Generation IV Nuclear Energy Systems

The next generation (Generation IV) of nuclear energy systems is intended to meet the following goals (while being at least as effective as the third generation in terms of economic competitiveness, safety, and reliability) in order to provide a sustainable development of nuclear energy (Table 1.1).

In principle, the Generation IV systems should be marketable or deployable starting in 2030. The systems should also offer a true potential for new applications compatible with an expanded use of nuclear energy, in particular in the fields of hydrogen or synthetic hydrocarbon production, seawater desalination, and process heat production.

**Table 1.1** Goals for Generation IV nuclear energy systems

Sustainability 1	Generation IV nuclear energy systems will provide sustainable energy generation that meets clean air objectives and provides long-term availability of systems and effective fuel utilization for worldwide energy production.
Sustainability 2	Generation IV nuclear energy systems will minimize and manage their nuclear waste and noticeably reduce the long-term stewardship burden, thereby improving protection for public health and the environment.
Economics 1	Generation IV nuclear energy systems will have a clear life-cycle cost advantage over other energy sources.
Economics-2	Generation IV nuclear energy systems will have a level of financial risk comparable to other energy projects.
Safety and reliability 1	Generation IV nuclear energy systems operations will excel in safety and reliability.
Safety and reliability 2	Generation IV nuclear energy systems will have a very low likelihood and degree of reactor core damage.
Safety and reliability 3	Generation IV nuclear energy systems will eliminate the need for offsite emergency response.
Proliferation resistance and physical protection	Generation IV nuclear energy systems will dispel perceptions that they are very unattractive and the least desirable route for diversion or theft of weapons-grade materials and provide increased physical protection against acts of terrorism.

It has been recognized that these objectives, widely and officially shared by a large number of countries, should be the basis of an internationally shared R&D program, which will make it possible to keep open and consolidate technical options and avoid any early or premature selection.

In fact, because the next generation nuclear energy systems will address needed areas of improvement and offer great potential, many countries share a common interest in advanced R&D that will support their development. The international research community should explore such development benefits with the identification of promising research areas and collaborative efforts. The collaboration on R&D by many nations on the development of advanced next generation nuclear energy systems will in principle aid progress toward the realization of such systems by leveraging resources, providing synergistic opportunities, avoiding unnecessary duplication, and enhancing collaboration.

## 1.10 A Technology Roadmap for Generation IV Nuclear Energy Systems

The technology roadmap defines and plans the necessary research and development (R&D) to support the next generation of innovative nuclear energy systems known as Generation IV. The roadmap has been an international effort of ten countries,

including Argentina, Brazil, Canada, France, Japan, Republic of Korea, South Africa, Switzerland, the UK, and the USA, the International Atomic Energy Agency, and the OECD Nuclear Energy Agency.

Beginning in 2001, over 100 experts from these countries and international organizations began work on defining the goals for new systems, identifying many promising concepts and evaluating them, and defining the R&D needed for the most promising systems. By the end of 2002, the work resulted in a description of the six most promising systems and their associated R&D needs. They are as follows:

1. Gas-cooled fast reactor (**GFR**): features a fast-neutron-spectrum, helium-cooled reactor and closed fuel cycle;
2. Very-high-temperature reactor (**VHTR**): a graphite-moderated, helium-cooled reactor with a once-through uranium fuel cycle;
3. Supercritical water-cooled reactor (**SCWR**): a high-temperature, high-pressure, water-cooled reactor that operates above the thermodynamic critical point of water;
4. Sodium-cooled fast reactor (**SFR**): features a fast-spectrum, sodium-cooled reactor and closed fuel cycle for the efficient management of actinides and conversion of fertile uranium;
5. Lead-cooled fast reactor (**LFR**): features a fast-spectrum, lead/bismuth eutectic liquid-metal-cooled reactor and a closed fuel cycle for the efficient conversion of fertile uranium and management of actinides;
6. Molten salt reactor (**MSR**): produces fission power in a circulating molten salt fuel mixture with an epithermal-spectrum reactor and a full actinide recycling fuel cycle.

These systems offer significant advances in sustainability, safety and reliability, economics, proliferation resistance, and physical protection. These six systems feature increased safety, improved economics for electricity production and new products such as hydrogen for transportation applications, reduced nuclear wastes for disposal, and increased proliferation resistance.

In 2009, the Experts Group published an outlook on Generation IV R&D to provide a view of what GIF members hope to achieve collectively in the period 2010–2014. All Generation IV systems have features aiming at performance improvement, new applications of nuclear energy, and more sustainable approaches to the management of nuclear materials. High-temperature systems offer the possibility of efficient process heat applications and eventually hydrogen production. Enhanced sustainability is achieved primarily through the adoption of a closed fuel cycle with reprocessing and recycling of plutonium, uranium, and minor actinides using fast reactors; this approach provides significant reduction in waste generation and uranium resource requirements.

The following table summarizes the main characteristics of the six Generation IV systems (Table 1.2).

**Table 1.2** Summary of main characteristics of six Generation IV systems

System	Neutron spectrum	Coolant	Temperature (°C)	Fuel cycle	Size (MWe)
Very high temperature gas reactor	Thermal	Helium	900–1000	Open	250–300
Sodium-cooled fast reactor	Fast	Sodium	550	Closed	30–150, 300–1500, 1000–2000
Supercritical water-cooled reactor)	Thermal/fast	Water	510–625	Open/closed	300–700, 1000–2000
Gas-cooled fast reactor	Fast	Helium	850	Closed	1200
Lead-cooled fast reactor	Fast	Lead	480–800	Closed	20–180, 300–1200, 600–1000
Molten salt reactor	Epithermal	Fluoride salt	700–800	Closed	1000

## 1.11 Description of Six Most Promising Nuclear Power Systems

A brief summary of each Generation IV nuclear power systems follows.

**VHTR:** The very-high-temperature reactor is a next step in the evolutionary development of high-temperature reactors. The VHTR is a helium-gas-cooled, graphite-moderated, thermal-neutron spectrum reactor with a core outlet temperature exceeding 900 °C, and a goal of 1000 °C, sufficient to support production of hydrogen by thermochemical processes. The reference reactor thermal power is set at a level that allows passive decay heat removal, currently estimated to be about 600 MWth. The VHTR is primarily dedicated to the cogeneration of electricity and hydrogen, as well as to other process heat applications. It can produce hydrogen from water using thermochemical, electrochemical, or hybrid processes with reduced emissions of CO<sub>2</sub> gases. At first, a once-through low-enriched uranium (<20 % U<sup>235</sup>) fuel cycle will be adopted, but a closed fuel cycle will be assessed, as will potential symbiotic fuel cycles with other types of reactors (especially light-water reactors) for waste reduction (Fig. 1.6).

**SFR:** The sodium-cooled fast reactor system uses liquid sodium as the reactor coolant, allowing high power density with low coolant volume fraction. The reactor can be arranged in a pool layout or a compact loop layout. Reactor size options under consideration range from small (50–300 MWe) modular reactors to larger reactors (up to 1500 MWe). The two primary fuel recycle technology options are advanced aqueous and pyrometallurgical processing. A variety of fuel options are being considered for the SFR, with mixed oxide preferred for advanced aqueous recycling and mixed metal alloy preferred for pyrometallurgical processing. Owing to the significant past experience accumulated with sodium cooled reactors in several countries, the deployment availability of SFR systems is targeted for 2020 (Fig. 1.7).

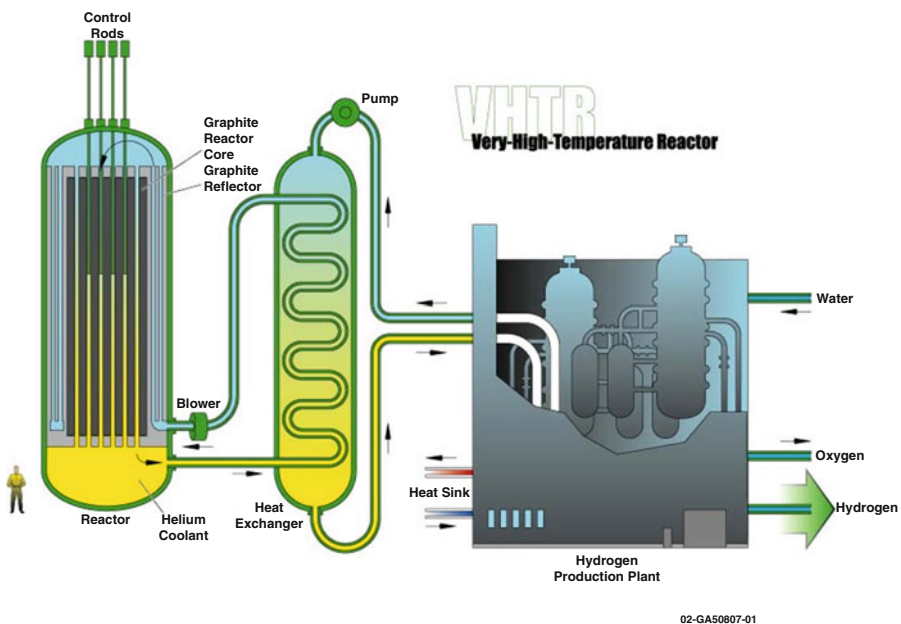


**Fig. 1.6** Very high temperature reactor

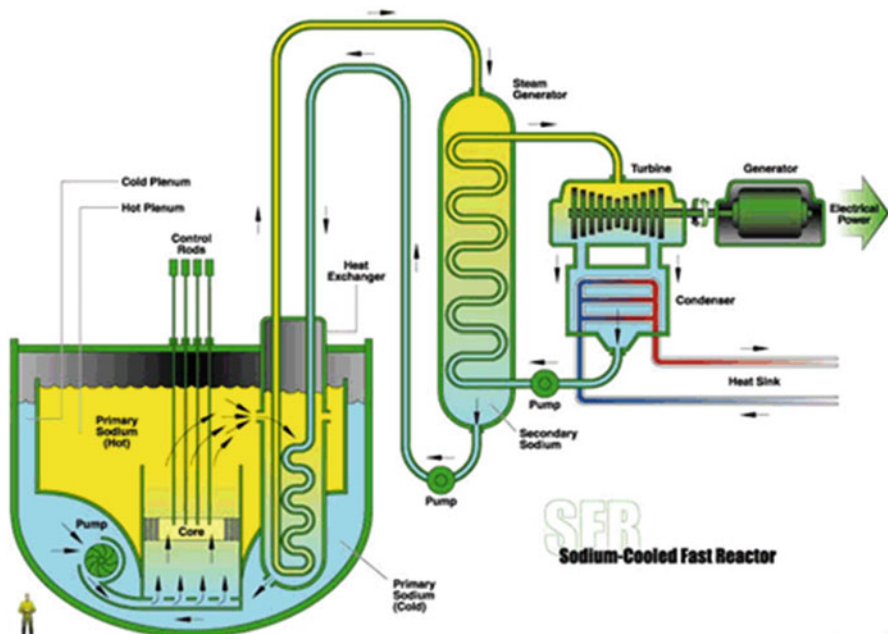


**Fig. 1.7** Sodium-cooled fast reactor

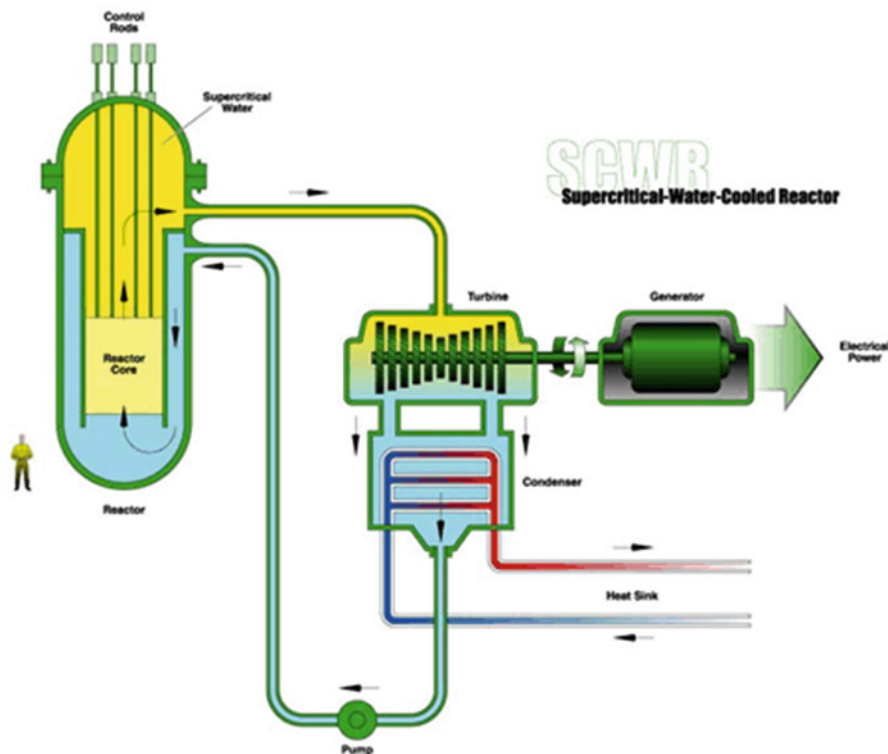


**Fig. 1.8** Supercritical water-cooled temperature reactor

**SCWR:** Supercritical water-cooled reactors are a class of high-temperature, high-pressure, water-cooled reactors operating with a direct energy conversion cycle and above the thermodynamic critical point of water ( $374^{\circ}\text{C}$ , 22.1 MPa). The higher thermodynamic efficiency and plant simplification opportunities afforded by a high-temperature, single-phase coolant translate into improved economics. A wide variety of options are currently being considered: both thermal-neutron and fast-neutron spectra are envisaged, and both pressure vessel and pressure tube configurations are being considered. The operation of a 30–150 MWe technology demonstration reactor is targeted for 2022 (Fig. 1.8).

**GFR:** The main characteristics of the gas-cooled fast reactor are fissile self-sufficient cores with a fast-neutron spectrum, robust refractory fuel, high operating temperature, high-efficiency electricity production, energy conversion with a gas turbine, and full actinide recycling possibly associated with an integrated on-site fuel reprocessing facility. A technology demonstration reactor needed to qualify key technologies could be put into operation by 2020 (Fig. 1.9).

**LFR:** The lead-cooled fast reactor system is characterized by a fast-neutron spectrum and a closed fuel cycle with full actinide recycling, possibly in central or

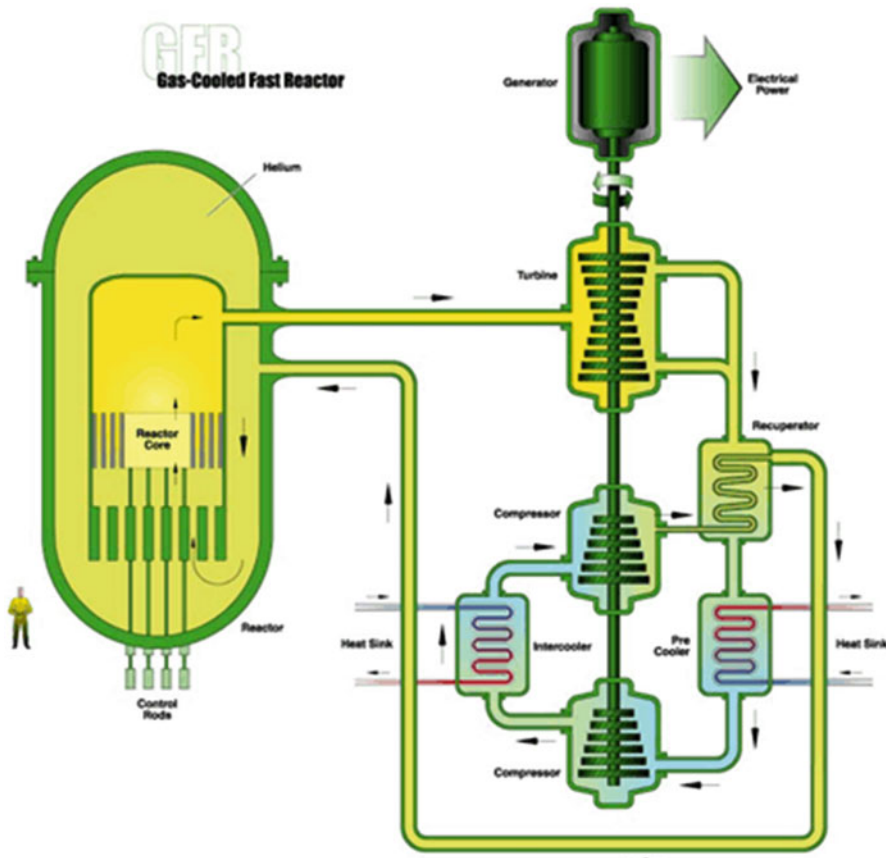


**Fig. 1.9** Gas Cooled fast reactor

regional fuel cycle facilities. The coolant could be either lead (preferred option) or lead/bismuth eutectic. The LFR can be operated as a breeder; a burner of actinides from spent fuel, using inert matrix fuel; or a burner/breeder using thorium matrices. Two reactor size options are being considered: a small transportable system of 50–150 MWe with a very long core life and a medium system of 300–600 MWe. In the long term a large system of 1200 MWe could be envisaged. The LFR system may be deployable by 2025 (Fig. 1.10).

**MSR:** The molten salt reactor system embodies the very special feature of a liquid fuel. MSR concepts, which can be used as efficient burners of TRU from spent LWR fuel, also have a breeding capability in any kind of neutron spectrum ranging from thermal (with a thorium-based fuel cycle) to fast (with a U–Pu fuel cycle). Whether configured for burning or breeding, MSRs hold considerable promise for the minimization of radiotoxic nuclear waste (Fig. 1.11).

**Fig. 1.10** Lead Lead-cooled fast reactor

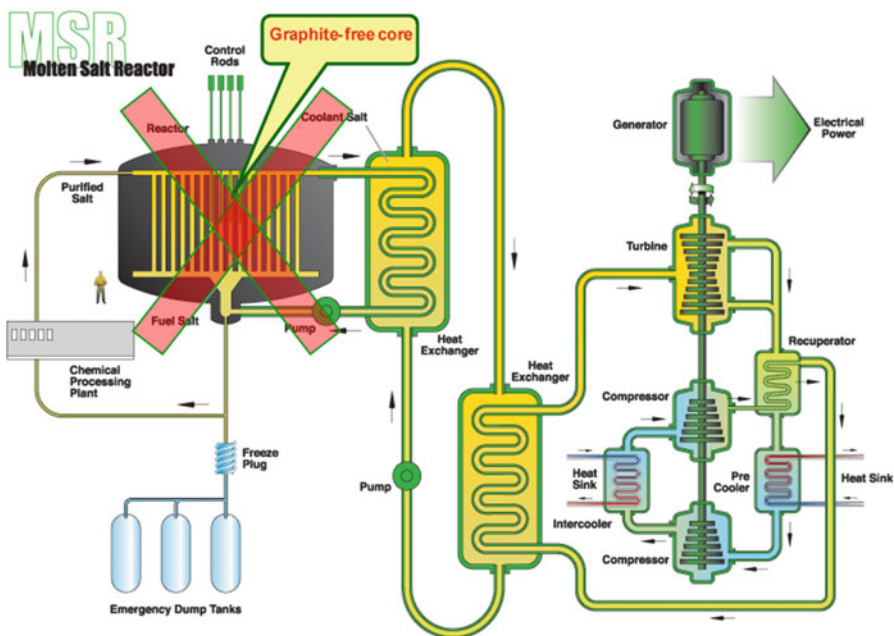
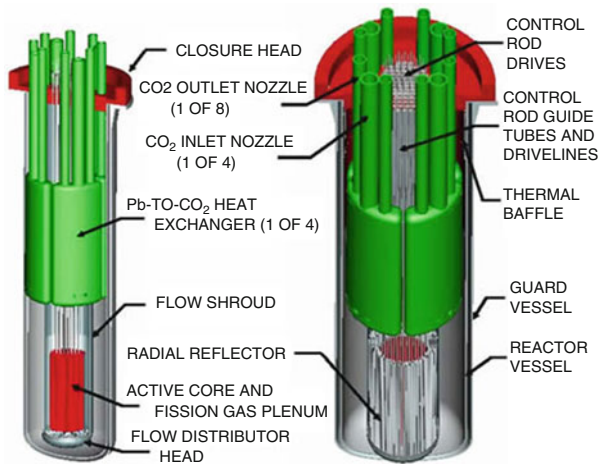


**Fig. 1.11** Molten salt reactor

## 1.12 Hybrid Energy Systems

The first questions that come to mind here are what is a hybrid system and what does the word hybrid stand for, and what do we really mean by looking at a hybrid energy system as a new source of renewable energy and the use of such a source

during on-peak demand for electricity? Heading toward the next century, demand for more electricity is on the rise and consequently the on-peak hours of such demand will pose challenges on electricity grids, so alternative sources of energy need to be found to meet such supply and demand constraints. Hence looking for a new source of renewable energy is becoming increasingly urgent.

The word *hybrid* can refer to phenomena that are a combination of two different elements:

1. Dramatic advances in hybrid technology, giving birth to hybrid cars, and
2. Incorporating information and communications technology (ICT) systems that automate smart houses and eco-homes.

Similarly, hybrid energy systems have been designed to generate electricity from different sources, such as solar panels and wind turbines, and now tap into such resources as hydrogen, which is stored in different forms and has emerged as a class of renewable energy source; thus, demand for its production in the most efficient and cost-effective way is a concern of every researcher and scientist at university, industry, and national laboratories who work in this field.

However, one of the biggest disadvantages of renewable energy is that the energy supply is not constant; sources like solar and wind power fluctuate in intensity because of weather and seasonal changes. Therefore, a reliable backup system is necessary for renewable energy generating stations that are not connected to a national power grid and that can produce energy during off-peak hours and store it for use during on-peak hours; this is the driving force behind the idea of producing hydrogen via nuclear power, which is indeed a solution to reducing carbon emissions. The costs of this type of energy production include those associated with nuclear waste storage and other related issues, such as the proliferation and security of fissionable weapons-grade waste coming out of reactor cores at the end of the burnup residue of fuel used in reactors or air or land contamination as a result of human-caused events (i.e., Three Mile Island or Chernobyl due to operator error) or natural disasters (i.e., Fukushima Daiichi in Japan).

Nevertheless, something could probably be done to avoid at least some of this pollution that may allay public fears of a nuclear disaster by increasing the safety design of these power plants going forward with Generation IV designs. In addition, we can tap into the waste of thermal energy generated by these reactors and put them to use in producing a new source of renewable energy, such as hydrogen production plants that are coupled to these VHTRs in particular.

As stated earlier, finding a reliable backup system for renewable energy is essential. Systems that consist of a variety of power control methods and storage equipment, including, for example, battery banks and diesel generators, do not have reliable endless life cycles that are sufficient to meet the demands that would be placed on electrical grids during on-peak hours or even on a small scale if power is to be stored for use at the residential level or in remote areas.

Power systems that are connected to the national grid do not have this problem because in most cases many different sources of power contribute to the national electricity supply.

The question about reducing the demand for energy in the future or meeting that demand is an open one and somehow solutions need to be found; thus, hybrid technology for the production of electrical energy seems very appealing, and research on these systems to make them cost effective and efficient has gathered huge momentum recently.

It is undoubtedly true that big centralized power stations are still needed to generate enough power for big industrial sites, but if we managed to dramatically reduce the amount of energy that the entire residential and small commercial building stock withdraws every year out of the national energy grid, we could very well need fewer nuclear power plants, which is arguably the viewpoint of opponents of nuclear energy, but it is something that remains to be seen and should not be a show stopper for solutions such as hybrid systems, and research to make them more productive and efficient must continue.

Hybrid energy systems often consist of a combination of fossil fuels and renewable energy sources and are used in conjunction with energy storage equipment (batteries) or hydrogen storage tanks. This is often done either to reduce the cost of generating electricity from fossil fuels or to provide backup for a renewable energy system, ensuring the continuity of the power supply when the renewable energy source fluctuates.

There are several types of hybrid energy systems such as wind–solar, solar–diesel, wind–hydro, and wind–diesel, which are among present production plants. The design of a system or the choice of energy source depends on several considerations. The factors affecting the choice of hybrid power technology can also tell us why people use hybrids and some of their advantages. The main factors are cost and resource availability. It is also worth mentioning some localized advantages, such as the standalone nature of operations and the fact that such systems are off the grid and function in a self-sustaining manner with respect to the need for electricity, for example, a solar system barn in a remote or isolated area, where farmers can take advantage of independence of the electricity feed from the grid. Solar energy can be produced on or off the grid.

On the grid means a house remains connected to the state electricity grid. Off the grid means there is no connection to an electricity grid, so the house, business, or whatever being powered relies solely on solar energy or a solar hybrid.

The ability to produce electricity off the grid is a major advantage of solar energy for people who live in isolated and rural areas. Power prices and the cost of installing power lines are often exorbitantly high in these places, and many have frequent power outages. Figure 1.12 illustrates a solar barn that can go off grid, which confers a huge advantage to solar power for people in isolated locations.

The cost of hybrid power technology greatly affects the choices people make, particularly in developing countries.

People's choices also depend on the aim of a given project. People who are planning to set up a hybrid energy project for their own use often focus on lowering the total investment and operational costs, while those planning to generate electricity for sale focus on long-term project revenue.

**Fig. 1.12** Solar barn



**Fig. 1.13** House with a solar system



As such, systems that incorporate hydrogen storage and fuel cells are not very common with small-scale projects. The viability of one hybrid energy system over another is usually pegged to the cost of generating each kilowatt [2, 3].

The availability of natural resources plays an enormous part when selecting the components of a hybrid energy system – the right power generation location and method must be chosen.<sup>1</sup>

Many city dwellers also choose to go off the grid with alternative energy as part of their self-reliant lifestyle (Fig. 1.13).

<sup>1</sup> <http://exploringgreentechnology.com/solar-energy/hybrid-energy-systems/>

Often, a hybrid system is chosen because the existing power resource is not enough to generate the amount of power needed – which is often the case when using micro-hydro plants.

In some developing countries, such as parts of Ethiopia, a wind–solar hybrid power system consisting of wind turbines and solar photovoltaic (PV) panels, was found to be most viable. This was because the wind resource alone was not sufficient to meet the electricity demand.

Solar PVs are used primarily for grid-connected electricity to operate residential appliances, commercial equipment, lighting, and air conditioning for all types of buildings. Through standalone systems and the use of batteries, they are also well suited for remote regions where there is no electricity source. Solar PV panels can be ground mounted, installed on building rooftops, or designed into building materials at the point of manufacture. Solar PV cells were once very expensive, so it was not feasible for project developers to use solar power alone [4].

The efficiency of solar PV panels increases in colder temperatures and makes them particularly well suited for Canada’s climate. A number of technologies are available that offer different solar conversion efficiencies and pricing.

Solar PV modules can be grouped together as an array of series and parallel connected modules to provide any level of power requirements, from mere watts (W) to kilowatt (kW) and megawatt (MW) sizes.

Hybrid systems are most suitable for small grids and isolated or standalone and self-reliant systems as hybrid power generation systems are by definition a solution for getting around problems where one energy source is not sufficient.

The popularity of hybrid energy systems has grown so much that it is now a niche industry in itself – with custom systems being engineered for specific functions.

For instance, Enercon, a German wind power company, has come up with unique factory-designed hybrid power technology, including the world’s first hybrid wind-diesel powered ship, the E-Ship 1 [5].

The German wind-turbine manufacturer Enercon launched and christened its new rotor ship E Ship 1 on the 2 August 2008. The vessel has now been in service for 5 years transporting wind turbines and other equipment to locations around the world (Fig. 1.14).

### ***1.12.1 Hybrid Energy Systems as Sources of Renewable Energy***

As was mentioned in the previous section, a hybrid energy system is a combination of energy sources of different characteristics and an energy storage medium. When it comes to standalone (Fig. 1.15) identifying applications depending on the hybrid energy system is a challenging process for a number of reasons, such as, for example, determining the best combination for reducing the initial capital



**Fig. 1.14** Enercon E-Ship 1

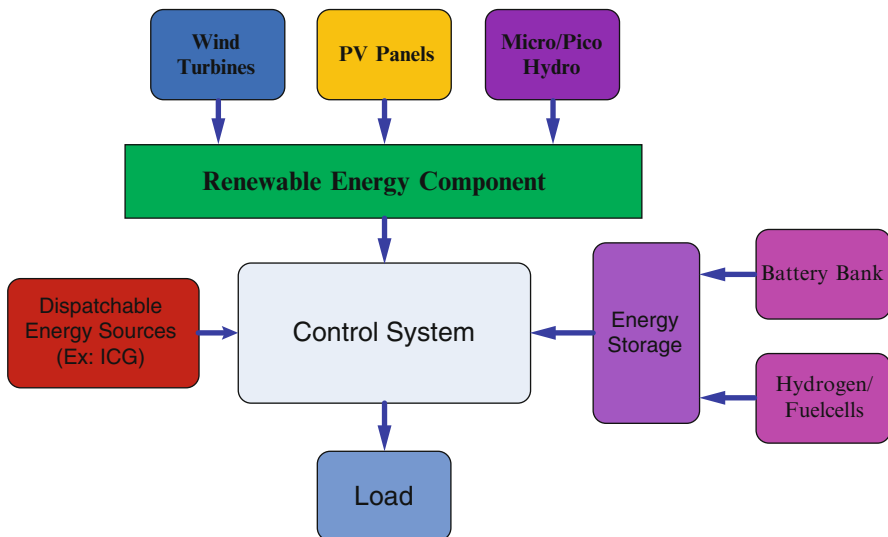


**Fig. 1.15** Schematic diagram of a standalone hybrid energy system

investment, maintaining power supply reliability, and reducing the maintenance of system components.<sup>2</sup>

A combination of energy sources having different characteristics reduces the impact of the time varying energy potential of renewable energy sources. Solar PV

<sup>2</sup> <http://hybrid-renewable.blogspot.com/2011/03/importance-of-hybrid-energy-systems.html>

(SPV) energy is available in the daytime but not at night, so you need to find some other alternative or store some SPV energy during the day. Wind energy share some similar qualities but generally with much chaotic variation. the time-varying nature of the renewable energy potential makes it essential to incorporate energy storage and dispatchable energy sources.

Energy systems play a major role in day-to-day life. Your refrigerator, air conditioner, or power generator that you use every day require electricity. Although we all use power and energy, very few of us are concerned with energy conservation. Even though we always try to take into account the financial aspects of conservation, there is something more to it, especially when we consider social responsibility. Fossil-fuel resources are being depleted at a rapid pace, and at the same time, we face many problems that have arisen as a result of emissions from fossil-fuel combustion. Therefore, we are living at a time when special consideration must be devoted to the conservation of energy.

Optimal designs of energy systems are vital in such circumstances. This is always a challenging process in which a number of techno-economical and environmental aspects need to be considered. Most of the time, modeling related to such energy systems is a difficult task. Meanwhile, a number of design parameters must be considered. This makes optimization work hard, and it is essential to move away from classical methods.

Current commercial, utility-scale hybrid energy systems include

- Geothermal + Solar Photo-Voltaic (PV),
- Biomass + Concentrated Solar Power (CSP),
- Solar PV + Fuel cells,
- Wind + Solar PV,
- Biodiesel + Wind,
- Gas + CSP,
- Coal + CSP.

More information on these commercial plants is freely available.<sup>3</sup>

## 1.13 Energy Storage Systems

The benefits of energy storage are significant and have long been recognized as necessary for the coordinated and reliable operation of utility grids. Energy storage is especially important for the integration of distributed renewable generation technologies. Storage protects against errors in forecasting, removes barriers to connecting renewable energy resources to a variety of grids, shifts demand at on-peak hours by storing off-peak energy, provides frequency regulation, and can

---

<sup>3</sup> [http://www.cleanenergyactionproject.com/CleanEnergyActionProject/Hybrid\\_Renewable\\_Energy\\_Systems\\_Case\\_Studies.html](http://www.cleanenergyactionproject.com/CleanEnergyActionProject/Hybrid_Renewable_Energy_Systems_Case_Studies.html)

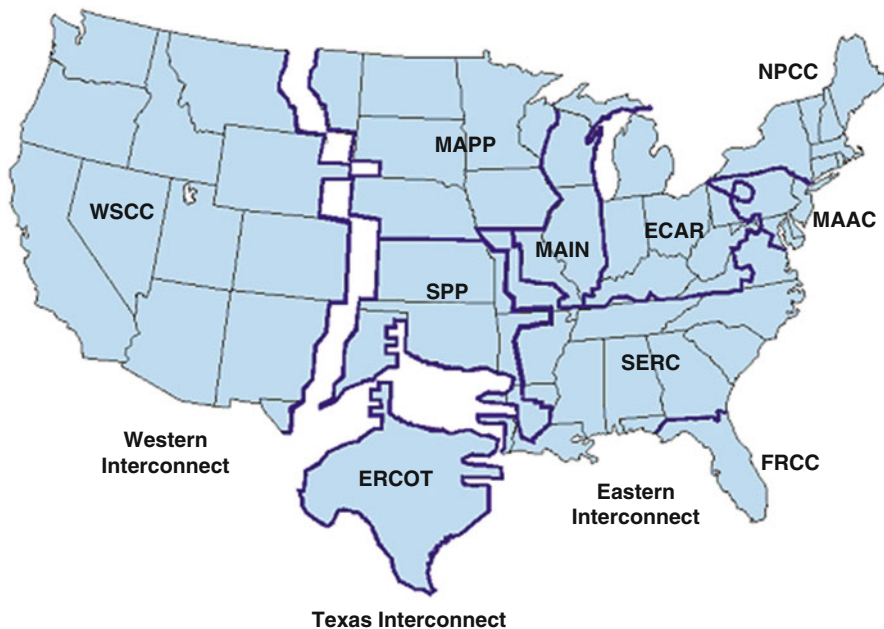


**Fig. 1.16** Electrical grid distribution in U.S. Department of Energy (graphics courtesy U.S. Department of Energy)

delay expensive grid upgrades or downtime owing to a sudden upsurge in demand or any trip-off of any sources attached to the nationwide grid system. See Chap. 17 of Zohuri and McDaniel [6].

It is important to know that there is no national power grid in the USA. In fact, the continental USA is divided into three main power grids (Fig. 1.16):

1. Eastern Interconnected System, or Eastern Interconnect;
2. Western Interconnected System, or Western Interconnect;
3. Texas Interconnected System, or Texas Interconnect.

Current commercial, utility-scale energy storage technologies include the following:

- Pumped hydropower storage,
- Compressed air energy systems (CAESs)
- Adiabatic compressed air energy storage for electricity (ADELE).
- Molten salt energy storage (MSES),
- Batteries, and
- Flywheels.

*Note that “adiabatic” here means the additional use of compression heat to increase efficiency.*



**Fig. 1.17** Herdecke pumped-storage power plant (courtesy RWE Power Company of Germany)

The technology of choice today is the pumped-storage power plant. In any excess power supply, water is electrically pumped into a reservoir on a hill, so that it can be discharged when power demand is high to drive a turbine in a valley downstream. Germany has pumped-storage power plants producing a total of about 7000 MW with an efficiency claimed to be *between 75 and 86 %*. The expansion potential is severely limited, especially in northern Germany, where the balancing need is greatest.

Figure 1.17 illustrates a CAES in Herdecke, Germany, and its conceptual design is similar in principle to pumped storage: during times of excess availability, electrically driven compressors compress air in a cavern to some 70 bar. For discharge of the stored energy, the air is conducted via an air turbine, which drives a generator.

Just as in pumped storage, its power can be released very quickly.

One advantage of a CAES over pumped storage, however, is that the visible impact on the landscape is low. What is more, facilities can be built near centers of wind-power production, especially in central and northern Germany. Today, there are two CAES plants in the world: one in Huntorf (Lower Saxony), in operation since 1978, and another in McIntosh (Alabama, USA), in operation since 1991. The efficiency of the 320-MW plant in Huntorf is about 42 %, that of McIntosh around 54 %. This means that they are more than 20 percentage points below the efficiency of pumped-storage plants (Fig. 1.18).<sup>4</sup>

<sup>4</sup> <http://www.rwe.com/web/cms/mediablob/en/391748/data/364260/1/rwe-power-ag/innovations/Brochure-ADELE.pdf>



**Fig. 1.18** Turbine hall of Vianden pumped-storage power plant (courtesy RWE Power Company of Germany)

It is worth asking in connection with this kind of storage the following question:  
*What lowers efficiency?*

We can seek the answer as follows:

1. First, the air that heats up during compression must be cooled down again to the ambient temperature before it can be stored in a cavern.
2. Second, cold air must be reheated for discharge of the storage facility since it cools strongly when expanding in a turbine for power generation. Today's plants use natural gas for this. Valuable efficiency percentages are lost.

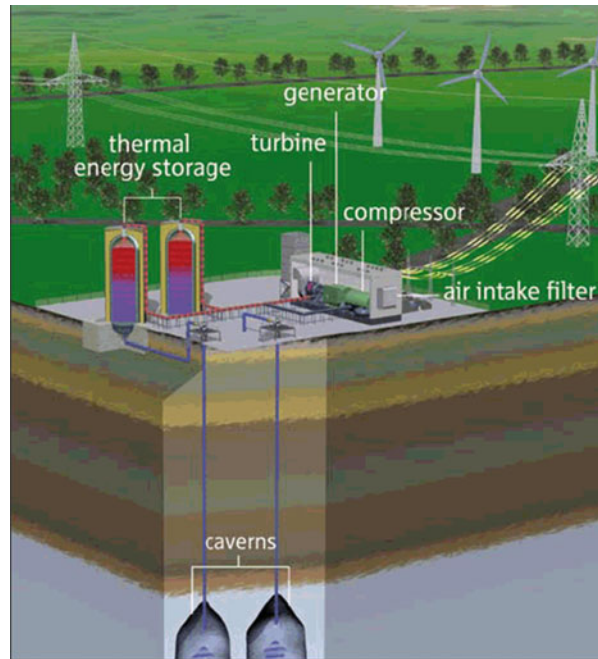
RWE Power, the largest Germany power producer company, and General Electric (GE) are leading players in the extraction of energy raw materials. The two companies have teamed up to work on the production of an adiabatic CAES facility and a project for electricity supply known as *ADELE*. The concept and principle of the process steps behind *ADELE* are as follows (Fig. 1.19 shows a conceptual layout of such a facility):

When air is compressed, heat is not released into the surroundings; most of it is captured in a heat-storage facility. During discharge, the heat-storage device re-releases its energy into the compressed air, so that no gas co-combustion to heat the compressed air is needed. The object is to make possible efficiencies of around 70 %. What is more, the input of fossil fuels is avoided.

Hence, this technology permits the CO<sub>2</sub>-neutral provision of peak-load electricity from renewable energy. That this technology is feasible has been shown by the EU project Advanced Adiabatic Compressed Air Energy Storage (AA-CAES) and by a study presented by GE and RWE in 2008.

The aim of a new joint project launched by the German Aerospace Center (DLR), Ed. Züblin AG, Erdgasspeicher Kalle GmbH, GE Global Research,

**Fig. 1.19** Illustration of ADELE facility (courtesy RWE Power Company of Germany)



Ooms-Ittner-Hof GmbH, and RWE Power AG – the project being officially kicked off in January 2010 – is to develop an adiabatic CAES power station to bidding maturity for a first demonstration plant. The federal ministry for economics has suggested that it might be willing to fund ADELE.

## 1.14 Variable Electricity with Base-Load Reactor Operations

Another way of storing energy to meet variable electricity needs with base-load reactor operation has been suggested by Charles Forsberg [7] of MIT based on recent technology and research by Forsberg et al. [8] on a nuclear air-Brayton combined cycle, which is the subject of ongoing collaboration.

The goal of the collaboration is not only to deal with a low-carbon world and use energy sources such as nuclear energy but to look at other sources of renewable energy such as wind, solar, and hydrogen produced by means of VHTRs of Next Generation Nuclear Plants (NGNP) coupled with hydrogen production plants (HPP) in coexisting circumstances.

The defining characteristics of these technologies are as follows:

1. High capital and low operating costs requiring full-capacity operation for economic energy production and
2. Output does not match human variable energy needs.

This challenge suggests a need to develop new nuclear technologies to meet the variable energy needs for a low-carbon world while promoting economic growth. Hence, to meet the aforementioned challenge, we have been developing a fluoride-salt-cooled high-temperature reactor (FHR) with a nuclear air-Brayton combined cycle (NACC) [7, 8] and firebrick resistance-heated energy storage (FIRES) system. The goals are as follows:

1. Improve nuclear power plant economics by 50–100 % relative to a base-load nuclear power plant,
2. Develop the enabling technology for a zero-carbon nuclear renewable electricity grid by providing dispatchable power, and
3. Eliminate major fuel failures and hence eliminate the potential for major offsite radionuclide releases in a beyond-design-basis accident.

Figure 1.20 shows the capabilities of a modular FHR when coupled to an electricity grid. FHR produces base-load electricity, with peak electricity produced by a topping cycle using auxiliary natural gas or stored heat – or, in the distant future, using hydrogen. The FIRES heat storage capability enables the FHR to replace energy storage technologies such as batteries and pumped storage – a storage requirement for a grid with significant nondispatchable solar or wind generating systems.

The FHR is a new class of reactor (Fig. 1.21) with characteristics different from light-water reactors (LWRs). The fuel is a graphite-matrix coated-particle fuel used

**Fig. 1.20** Capability of modular FHR with NACC and FIRES with base-load FHR operation [7, 8]

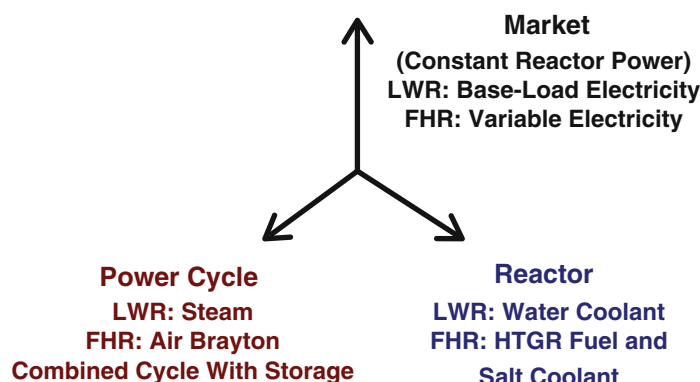
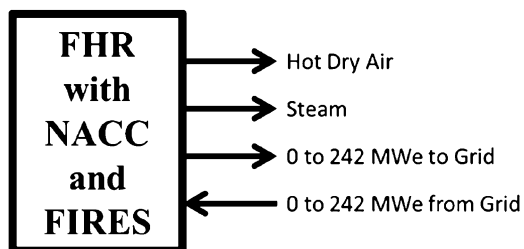


**Fig. 1.21** Comparison of LWR and FHR [7]

by high-temperature gas-cooled reactors (HTGRs), resulting in similar reactor core and fuel cycle designs – except the power density is greater because liquids are better coolants than gases. The coolant is a clean fluoride salt mixture. The coolant salts were originally developed for MSRs, where the fuel is dissolved in the coolant. Current coolant-boundary material limitations imply maximum coolant temperatures of about 700 °C. New materials are being developed that may allow exit coolant temperatures of 800 °C or higher. The power cycle is similar to that used in natural-gas-fired plants.

The fluoride salt coolants were originally developed for the US Aircraft Nuclear Propulsion program in the late 1950s. The goal was to develop a nuclear-powered jet bomber. These fluoride salts have low nuclear cross sections with melting points of 350–500 °C and boiling points in excess of 1200 °C – properties for efficient transfer of heat from a reactor to a jet engine. Since then there have been two developments. The first development was high-temperature graphite-matrix coated-particle fuels for HTGRs that are compatible with liquid salt coolants. The second is a half-century of improvements in utility gas turbines that now make it feasible to couple a nuclear reactor (the FHR) to a NACC.

The FHR is coupled to a NACC with FIRES (Fig. 1.22). In the power cycle external air is filtered, compressed, heated by hot salt from the FHR while going through a coiled tube air heater (CTAH), sent through a turbine producing electricity, reheated in a second CTAH to the same gas temperature, and sent through a second turbine producing added electricity. Warm low-pressure air flow from the gas turbine system exhaust drives a heat recovery steam generator (HRSG), which provides steam to either an industrial steam distribution system for process heat sales or a Rankine cycle for additional electricity production. The air from the HRSG is exhausted up the stack to the atmosphere. Additional electricity can be produced by injecting fuel (e.g., natural gas, hydrogen) or adding stored heat after

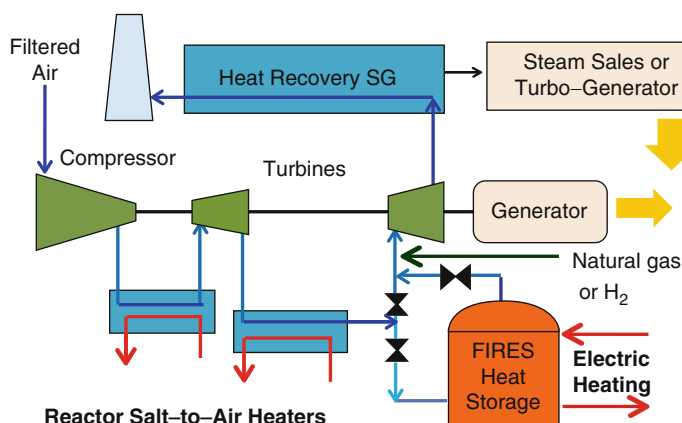


**Fig. 1.22** Nuclear air-Brayton combined cycle (NACC) with firebrick resistance-heated energy storage (FIRES) system [8]

nuclear heating by the second CTAH. This boosts temperatures in the compressed gas stream going to the second turbine and to the HRSG [8].

Since a NACC system functions quite well with a salt-cooled reactor, it is worth considering what it might do for a sodium-cooled reactor. With some modifications it could be competitive with other built systems. A computer model was built based on standard techniques for analyzing Brayton and Rankine systems. System performance was optimized by varying the turbine outlet temperatures for a fixed turbine inlet temperature. A second parameter that can usually be varied to obtain optimum performance is the peak pressure in the steam cycle. For most of the cases considered here this was held constant at 12.4 MPa (1800 psi) [8].

A fairly detailed design was attempted for the heat exchangers involved in the system because they tend to dominate the system size; more details are provided in Chaps. 5–7 of this book. The techniques and data were extracted from the text by Kays and London [9].

The stored heat option involves heating firebrick inside a prestressed concrete pressure vessel with electricity to high temperatures at times of low electricity prices, that is, below the price of natural gas. When peak power is needed, compressed air after nuclear heating and before entering the second turbine would be routed through the firebrick, heated to higher temperatures, and sent to the second turbine. The efficiency of converting electricity to heat is 100 %. The efficiency of converting auxiliary heat (natural gas or stored heat) to electricity in our current design is 66 %. This implies a round-trip efficiency of electricity to heat to electricity of approximately 66 %. Improvements in gas turbines in the next decade are expected to raise that efficiency to 70 %. FIRES would only be added to a NACC in electricity grids where there are significant amounts of electricity at prices less than the price of natural gas. As will be discussed later, these conditions are expected in any power grid with significant installed wind or solar capacity.

As stated earlier, much of the FIRES heat storage technology is being developed by GE and its partners for adiabatic a CAES system called ADELE (German abbreviation). The first prototype storage system is expected to be operational by 2018 with 90 MWe peak power and storing 360 MWh. When the price of electricity is low, the air is (1) adiabatically compressed to 70 bars with an exit temperature of 600 °C, (2) cooled to 40 °C by flowing the hot compressed air through firebrick in a prestressed concrete pressure vessel, and (3) stored as cool compressed air in underground salt caverns. At times of high electricity prices the compressed air from the underground cavern goes through the firebrick, is reheated, and sent through a turbine to produce electricity with the air exhausted to the atmosphere. The expected round-trip storage efficiency is 70 %. The ADELE project integrates firebrick heat storage into a gas turbine system. For a NACC system using FIRES there are differences: (1) the peak pressure would be about a third that of ADELE, (2) the firebrick is heated to higher temperatures, and (3) electricity is used to heat the firebrick to higher temperatures at times of low electricity prices. The technology for heat storage integration into a NACC system is partly under development.

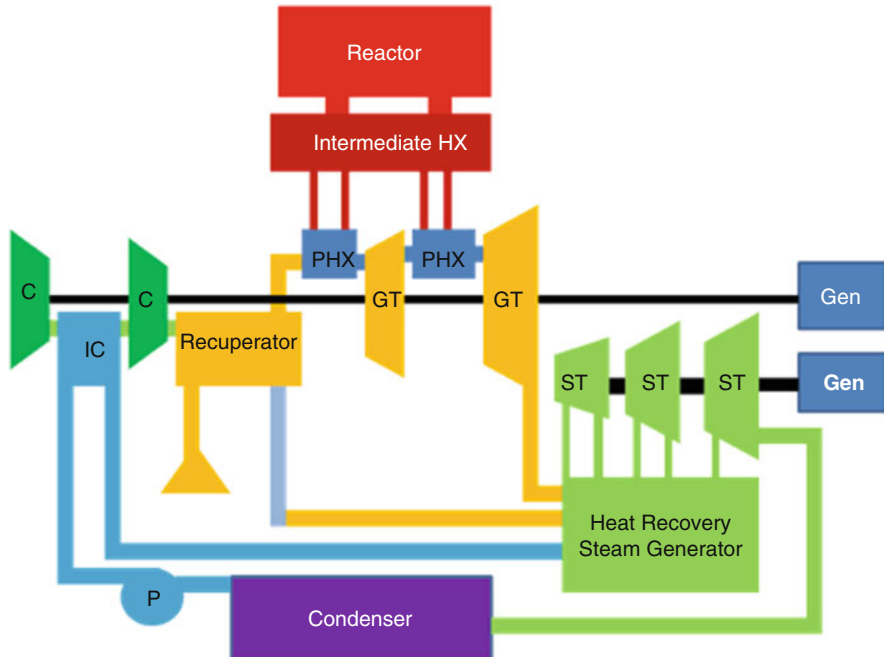


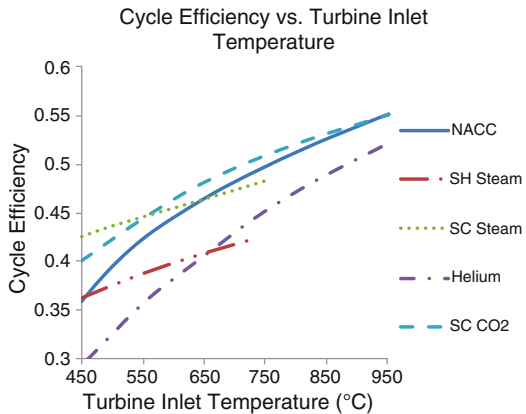
**Fig. 1.23** System layout with recuperator and intercooler [C = compressor, GT = gas turbine, ST = steam turbine, PHX = primary heat exchanger, IC = intercooler, P = pump] [10]

To show that utilization of a NACC system is very efficient and cost effective for such an innovative approach to storing energy in the form of a FIRES process, the following reasoning is presented here; for further information the reader is referred to the textbook by Zohuri [10].

Since the high-pressure water in the bottoming cycle must be heated and the heating of the air in the air compressor increases the work required, it is possible to split the compressor and add an intercooler that heats the high-pressure water in the bottoming cycle and cools the output from the first part of the compressor. If this is done, the efficiency goes to 40.3 % and the overall compressor pressure ratio goes to 2.0. A system diagram is provided in Fig. 1.23 [10].

The efficiency of NACC power systems continues to increase with increased turbine inlet temperatures. For the foreseeable future there does not appear to be a limitation to using off-the-shelf materials as it is not likely that a reactor-heated system will have a turbine inlet temperature exceeding 1300 K. A comparison of the cycle efficiencies for several cycles that have been proposed for the NGNP (Zohuri) [10] is presented in Fig. 1.24. The calculations for NACC systems are based on the system described in Fig. 1.24, with a peak steam pressure of 12.4 MPa.

**Fig. 1.24** Cycle efficiencies for various advanced cycles [8]



NACC systems can be applied to most of the proposed next generation systems. Their strongest competitor in terms of cycle efficiency is the supercritical CO<sub>2</sub> system. NACC systems will match or surpass the efficiency of these systems at or above 700 °C. But NACC systems have the competitive advantage of a large customer base for system hardware, significantly reduced circulating-water requirements for rejecting waste heat, and much greater efforts to improve the technology relative to other power cycles [8].

On 21 January 2010, the California Public Utilities Commission (CPUC) approved Pacific Gas and Electric's (PG&E's) request for matching funds of \$25 million for the Compressed Air Energy Storage (CAES) project. The CPUC found that the CAES demonstration project would provide PG&E a better understanding of a promising energy storage technology, which has the potential to lower costs for customers and reduce greenhouse gas emissions through greater integration of renewable energy sources. The California Energy Commission (CEC) has also shown support for the project with conditional approval of a \$1 million grant.

The commercial-scale project has a nominal output capacity of 300 megawatts (MW) – similar to a mid-sized power plant – for up to 10 h. It is estimated that a commercial plant could come on-line in the 2020–2021 time frame.

The time frame of this project is laid out here, and Fig. 1.25 shows a conceptual illustration of such a commercial facility.

PG&E is exploring this project in three primary phases:

- Phase 1: Reservoir feasibility, including site control, reservoir performance, economic viability, and environmental impacts;
- Phase 2: Commercial plant engineering, procurement and construction, and commissioning;
- Phase 3: Operations monitoring and technology transfer.

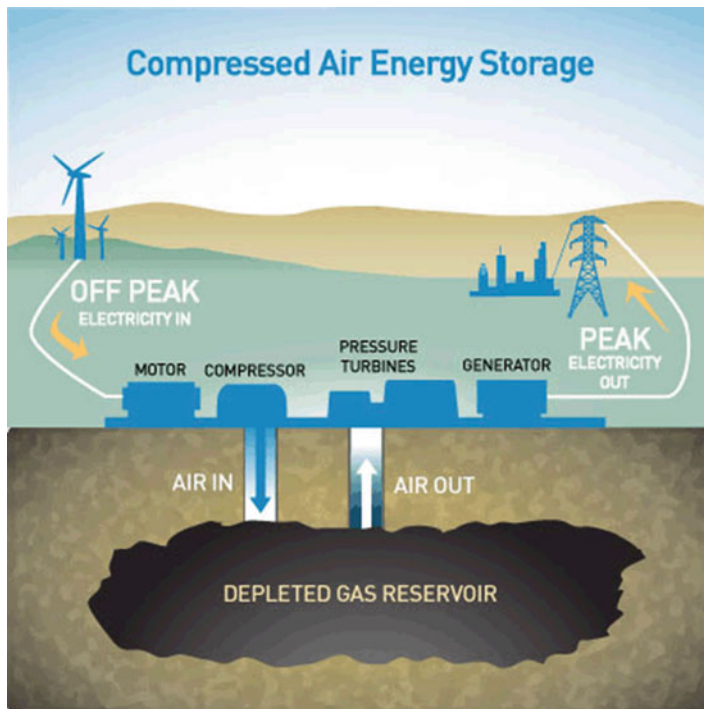


Fig. 1.25 Conceptual illustration of PG&E approach

## References

1. Scientific American. (2007). *Oil and the future of energy*. Guilford, CT: The Lyons Press.
2. U.S. Department of Energy – Fuel Cells Technologies Program: [https://www1.eere.energy.gov/hydrogenandfuelcells/pdfs/doe\\_h2\\_fuelcell\\_factsheet.pdf](https://www1.eere.energy.gov/hydrogenandfuelcells/pdfs/doe_h2_fuelcell_factsheet.pdf).
3. Khan, M., & Iqbal, M. (2005). Pre-feasibility study of stand-alone hybrid energy systems for applications in Newfoundland. *Renewable Energy*, 30, 835–854.
4. Bekele, G., & Palm, B. (2010). Feasibility for a standalone solar-wind-based hybrid energy system for application in Ethiopia. *Applied Energy*, 87, 487–495.
5. Got Powered – Enercon E-Ship 1: Wind-powered ship: <http://gotpowered.com/2011/enercon-e-ship-1-wind-powered-ship/>
6. Zohuri, B., & McDaniel, P. (2015). *Thermodynamics in nuclear power plant*. Heidelberg: Springer.
7. Forsberg, C. (2014). *Variable electricity with base-load reactor operations fluoride-salt-cooled high-temperature reactor (FHR) with nuclear air-Brayton combined cycle (NACC) and firebrick resistance-heated energy storage*. Cambridge, MA: MIT.
8. Forsberg, C., McDaniel, P., and Zohuri, B. (2015). Variable electricity and steam from salt, helium, and sodium cooled base-load reactors with gas turbines and heat storage. Proceedings of ICAPP 2015 May 03-06, 2015, Nice, France, Paper 15115.
9. Kays, W. M., & London, A. L. (1964). *Compact heat exchangers*. New York: McGraw Hill.
10. Zohuri, B. (2015). *Combined cycle driven efficiency for next generation nuclear power plants: An innovative design approach*. Heidelberg: Springer.

## Chapter 2

# Large-Scale Hydrogen Production

Industry's dependence on and demand for raw materials such as hydrogen are growing fast, and access to raw materials is high on the list of priorities of most industrial countries around the globe. But the question of where hydrogen comes from and how we can produce it for new applications besides the traditional ones is an important ones in industry. We have come to realize that hydrogen is an excellent source of renewable energy that can meet the fast growing energy demands of industrialized countries, during both on-peak and off-peak hours. The so-called sustainable routes of economic growth are still too expensive. The reformation of hydrocarbons using steam is the most feasible route today.

Hydrogen from biofuels, wind energy, solar energy, or, recently, nuclear energy is still expensive, which leaves fossil fuels as the most feasible feedstock for hydrogen generation in the near term while researchers try to come up with ways to use the aforementioned sources of energy in the long term for the production of hydrogen by coupling to power-generating plants. If CO<sub>2</sub> sequestration is adopted, then fossil fuels may play an important role in a rising so-called hydrogen economy. This will come about as a result of using reforming technologies. In this chapter we will discuss large-scale hydrogen production in stationary plants using a steam reforming approach from a big-picture point of view; for a more detailed understanding readers are encouraged to consult references [1–3] of this chapter.

To understand hydrogen production using a steam reforming process, one needs to understand combustion as well; thus, the bulk of this chapter is devoted to combustion.

## 2.1 Hydrogen Production by Steam Reforming of Hydrocarbons

The Green environmental and reform movement is pushing for low-sulfur gasoline and diesel fuels to be mandated for the purpose of dramatically reducing harmful emissions. Oil refiners are also trying to use more eco-friendly refining processes to produce cleaner products, for which they also require hydrogen. The growing fuel cell market is the source of additional demand for hydrogen, and fuel cell companies will also be dependent on hydrogen as a primary fuel source.

As was touched on in Chap. 1, another demand on the use of hydrogen in modern industry comes from fuel cells for transportation purposes, which are typically in units of 50 kW to 1 MW capacities. However, proposed applications for such fuel cells have not grown as fast as intended and predicted because of issues related to return on investment (ROI) and total cost of ownership (TCO). The high investment costs and challenging technology in advanced gas turbine machinery make it hard for fuel cells to compete with other sources of energy. The latest hydrogen fuel cells, with capacities of 30 to kW, are better positioned to attract more and more interest for use in cars. The question then becomes where and how to produce hydrogen so that it is more cost effective from a ROI point of view. The possible solutions to this problem are as follows:

1. Build large-scale hydrogen production plants (HPPs) that are driven by next generation nuclear plants, solar, or wind as the source of heat energy that these HPPs need for their production of hydrogen. In that case, very efficient and compact intermediate heat exchangers (IHXs) would be required that would impact the ROI and TCO;
2. Produce hydrogen in a medium-sized plant at gas stations; or
3. Produce hydrogen on smaller scales for mobile applications, i.e., cars.

Each of these solutions has pros and cons as well as technological challenges that would need to be addressed [1].

One of the common difficulties in terms of mobile applications is how to store sufficient amounts of hydrogen to have greater and more efficient mobility in, say, commercial vehicles. In this connection, it might be possible to build self-sustaining hydrogen generation plants with a small footprint that would make such applications feasible. This might enable the production of hydrogen from hydrocarbons or methanol [4].

### 2.1.1 Steam Reforming Technologies

In this section we will explore steam reforming technology, how it typically works, and the typical layout of a hydrogen plant based on this technology. To meet the industrial demand for hydrogen based on requirement variations, we must have some understanding of how to produce this element in a very cost-effective way.

For small-scale hydrogen production, below 0.1 million metric (MM) standard cubic feet per day (SCFD), the delivery of supply in cylinders or production by electrolysis may be a preferred method. Hydrogen production from methanol or ammonia cracking is suitable for small, constant, or intermittent requirements as used in the food, electronics, and pharmaceutical industries. On larger scales, hydrocarbons are used primarily as feedstock in the steam reforming process for the production of hydrogen and synthetic gas.

At least in North America the annual growth for hydrogen production is around 4 % above the present production rate of 6000 MM SCFD. Most of this growth is based on demand from refineries in the production of ultra-low-sulfur diesel and gasoline fuels. In spite of efforts to produce hydrogen by processes involving solar energy, wind energy, nuclear energy, and biofuels, fossil fuels remain the most feasible feedstock in the near term. For commercial-scale production of pure hydrogen, steam reforming remains the most economical and efficient technology for a wide range of hydrocarbon feedstock. To reduce the ROI and TCO of hydrogen production for near-term needs, some refineries have installed gasification units for power production and cogeneration of hydrogen as part of several existing methods of hydrogen production (Table 2.1). One of the important processes is the catalytic conversion method, also known as the method of *steam reforming* of hydrocarbons, followed by the gasification of, for example, coal or tar sands [5].

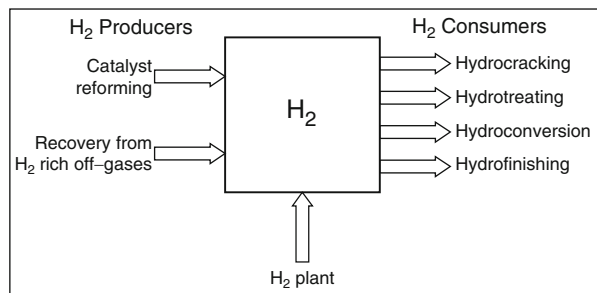
The steam reforming method for larger-scale production of hydrogen in the near term is the preferred solution, costwise, over more costly HPPs driven by solar, wind, or nuclear energy power plants until these plants become more efficient and their ROI and TCO are justified [6, 7].

Traditionally, a major part of hydrogen consumption in refineries was covered by hydrogen produced as a byproduct from other refinery processes ( $110 \times 10^9 \text{ Nm}^3/\text{year}$ ), mainly catalytic reforming (also known as platforming). A main reaction in catalytic reforming (not to be confused with catalytic steam reforming) is the conversion of paraffin into aromatics and hydrogen. Because aromatics are not wanted in reformulated fuels, less hydrogen becomes available from catalytic

**Table 2.1** Hydrogen production routes [5]

Natural gas • Refinery off-gases • LPG • Naphtha • Kerosene, gas oil	Steam reforming
Methanol, DME, NH <sub>3</sub>	Cracking
Coal • Biomass	Gasification
Water	Electrolysis

**Fig. 2.1** Schematic of refinery hydrogen balance [5]



reforming. Similarly, the gasoline and diesel fractions from catalytic crackers are highly unsaturated. The refined hydrogen balance is illustrated in Fig. 2.1 [5].

In conclusion, there is a fast growing need for increased hydrogen production capacity in refineries. This need is being met mainly by the installation of steam-reforming-based HPPs.

For small-scale production, simple equipment may be preferred over high energy efficiency. Electrolysis of water accounts for less than 5 % of production. For large-scale production, steam reforming of natural gas (or refinery off-gases) has emerged as the preferred solution. Gasification of heavy oil fractions may play an increasing role as these fractions are becoming more available because of falling demand.

The main application for hydrogen at present is as a carbon-free fuel; it is also coming to be seen as a new source of renewable energy that can meet the demand for electricity resulting from urbanization and growing industrial needs in newly industrialized countries (NICs).

As indicated at the beginning of this chapter, many technologies are being considered for the production of hydrogen that do not coproduce CO<sub>2</sub>. Hydrogen production using nonfossil energy for the electrolysis of water is one example. These schemes have not been introduced primarily owing to reluctance to adopt nuclear power and to the low efficiency of the electrolysis process. Hydrogen derived from biofuels, wind energy, and solar energy is still expensive, leaving fossil fuels as the most feasible feedstock for hydrogen production in the near term.

In areas with a high cost of hydrocarbon feedstocks, methanol may be considered as an alternative. One possible scheme involves the production of methanol in an area with very inexpensive natural gas, with the subsequent transport of the methanol to a hydrogen plant. A methanol-based hydrogen plant is a simple unit that is less costly than a natural-gas- or naphtha-based plant with a steam reformer. Figure 2.2 shows the conditions in which a methanol-based hydrogen plant would be more economical than a naphtha-based plant [6].

As stated previously and based on a cost analysis, despite efforts to produce hydrogen by processes involving solar energy, wind energy, nuclear energy, and biofuels, fossil fuels remain the most feasible feedstock in the near term, and for commercial-scale production of pure hydrogen, steam reforming remains the most economical and efficient technology for a wide range of hydrocarbon feedstocks.

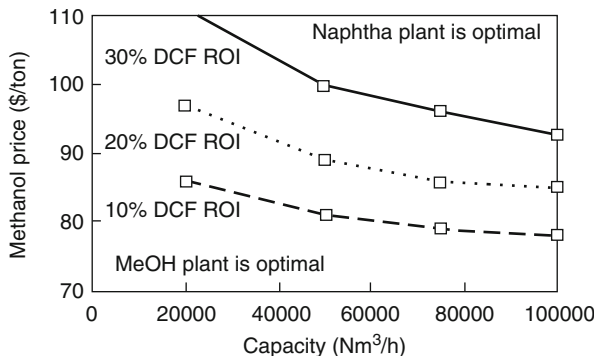


**Fig. 2.2** Hydrogen production from naphtha or methanol. Naphtha price: 140 USD/t. Steam credit: 8.3 USD/t. When competing against natural gas at 13 USD/Gcal, methanol prices must be about 10 USD/t less than indicated. *ROI* return on investment, *DFC* direct fixed capital. *ROI* means rate of return based on discounted cash flow

A typical layout of a hydrogen plant based on steam reforming includes the following steps, which are taken directly from the work of Niels R. Udengaard [3]:

- Natural gas feed is preheated in coils in the waste heat section of the reformer, and sulfur is removed over a zinc oxide catalyst. Process steam is added, and the mixture of natural gas and steam is further preheated before entering the tubular reformer. Here, conversion to equilibrium of hydrocarbons to hydrogen, carbon monoxide and carbon dioxide takes place over a nickel based reforming catalyst.
- The gas exits the reformer and is cooled by steam production before entering the shift converter, typically a medium temperature shift. Over the shift catalyst more hydrogen is produced by converting carbon monoxide and steam to carbon dioxide and hydrogen. The shifted gas is cooled further to ambient temperature before entering the PSA unit. High purity hydrogen product is obtained, and the off-gas from the PSA unit is used in the reformer as fuel supplemented with natural gas fuel.
- Combustion air for the tubular reformer burners can be preheated in coils in the reformer waste heat section. Part of the steam produced in the hydrogen plant is used as process steam, the excess steam is exported.
- In many situations when natural gas is not available, higher hydrocarbons become the preferred feedstock for the reforming process. Many refineries also can benefit from flexibility in feedstock, taking advantage of the surplus of various hydrocarbon streams in the refinery.

Fired tubular reforming is generally the most competitive technology for capacities of up to more than 100 MM SCFD hydrogen.

Based on the latest developments in steam reforming process technology, in advanced steam reforming, we can express the characteristics of this process as:

- High reformer outlet temperature,
- Low steam-to-carbon ratio,

- High combustion air preheats (optional),
- Adiabatic prereforming (optional),
- High heat flux reformer.

Low steam-to-carbon ratios, typically 2.5, in hydrogen plants reduce the mass flow through the plant and thus the size of the equipment. The lowest investment is therefore generally obtained for plants designed for low steam-to-carbon ratios. However, a low steam-to-carbon ratio also increases the methane leakage from the reformer. This can be compensated for by increasing the reformer outlet temperature to typically 922 °C (1690 °F) in hydrogen plants. Furthermore, operating at a low ratio requires the use of non-iron-containing catalyst, i.e., a copper-based medium-temperature shift catalyst, so as to eliminate the production of byproducts in the shift section.

The installation of an adiabatic prereformer upstream of a tubular reformer has been found to be very advantageous in naphtha-based plants and plants operating on fuel gases with higher concentrations of higher hydrocarbons. Since all higher hydrocarbons are converted over the prereformer catalyst, the inlet temperature of the gas inlet in the reformer can be increased to 1200 °F and the reformer can be designed for higher heat fluxes. This reduces the size of the tubular reformer, resulting in direct capital cost reductions.

High combustion air preheat temperatures result in reduced fuel consumption and reduced steam production. The combustion air temperature can be used to adjust the steam export to a desired level. Temperatures of up to 1020 °F have been industrially proven in radiant wall reformers.

As part of the cost analysis in terms of efficiency and production costs, with no steam export the theoretical energy consumption is 300 Btu/Scf H<sub>2</sub> at a lower heating value (LHV). The industrial value for natural-gas-based plants is about 320 Btu/Scf H<sub>2</sub>, corresponding to 94 % of the theoretical efficiency. At locations with high natural gas prices, the energy efficiency becomes critical. For a natural gas price of 4 USD/MM Btu, the feedstock and utility costs comprise about 65 % of total operating costs. For further information please refer to the presentation by Niels R. Udengaard [3].

### 2.1.2 Heat of Combustion

The energy that can be extracted from a fuel is often measured as the energy released as heat when the fuel undergoes complete combustion with oxygen. Table 2.2 shows this heat of combustion for several common fuels, including hydrogen.

The heat of combustion can be specified in terms of the higher heating value (HHV) or LHV. The HHV represents the entire produced heat while the LHV excludes any energy that is used to vaporize water during combustion. The difference between the two is higher for lower-carbon fuels (Table 2.2). The extent to

**Table 2.2** Heat of combustion of several fuels (MJ/kg)

	Higher heating value	Lower heating value	HHV/LHV ratio
Hydrogen	142	121	1.17
Methane	56	50	1.12
Gasoline	47	44	1.07
Coal (anthracite)	27	27	1.00
Wood	15	15	1.00

which energy is lost to water vaporization depends on the technology; the LHV is most appropriate where large amounts of water vapor are produced at a temperature below 150 °C or where condensation of the combustion products is impractical. Both the HHV and LHV are used in different sources in the literature, so it is necessary to use a consistent approach.

Some countries, such as the UK under their MARKAL energy efficiencies program, use the theoretical HHV, so HHV values are used throughout this report. However, the existing data in UK MARKAL have not always been consistently calculated using HHV data; for example, the vehicle technology data use the LHV (which inflates the costs of hydrogen storage in tanks because it effectively reduces the assumed usable energy in hydrogen). The high hydrogen HHV/LHV ratio as per Table 2.2 accentuates the discrepancies caused by using different approaches for different hydrogen technologies relative to other fuels [2].

### UK MARKAL

The UK MARKAL model was originally developed to provide insights for the Energy White Paper 2003. It was adopted and completely revised by the UCL Energy Systems team in 2005 and was under constant development until 2012. The development of the original model was funded by the UK government but the current academic version was developed and supported primarily by the UK Energy Research Centre.

UK MARKAL is a multiple-time-period linear optimization model. Its simplest formulation is to minimize discounted energy system costs, under a wide variety of physical and policy constraints. This minimization takes into account evolving costs and characteristics of resources, infrastructures, technologies, taxes, and conservation measures – to meet energy service demands – under a range of physical and policy constraints.

MARKAL is a very large model, with 1500 technology types, 250 energy carriers, plus constraints, taxes, emissions, and other model parameters. The model has well over half a million data elements.

For further information refer to the following link:

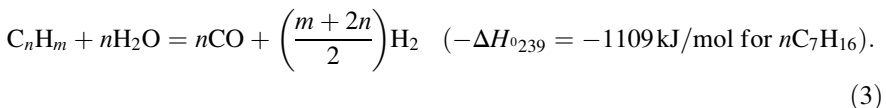
<https://www.ucl.ac.uk/energy-models/models/uk-markal>.

For solid fuels with higher carbon content (e.g., coal and biomass), the HHV and LHV can vary substantially depending on the exact fuel composition.

For example, the efficiency of coal gasification will be substantially influenced by the composition of the coal being used. Great care must be taken to match the fuel type to the process efficiency; if necessary, the process technology should be defined several times for different fuel compositions with different process efficiencies.

### 2.1.3 Reforming Reactions

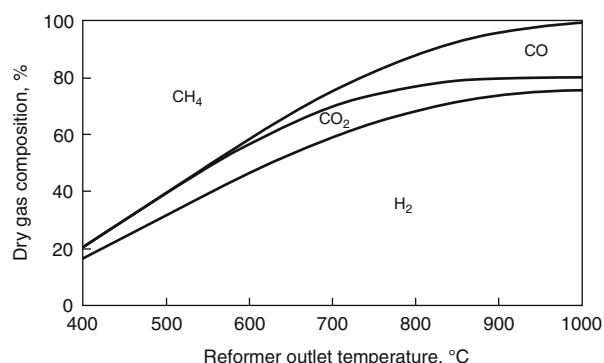
The principal process for converting hydrocarbons into hydrogen is steam reforming [1, 2], which involves the following reactions:



Reaction (1) is the steam reforming of methane. It is reversible and strongly endothermic, and according to the principle of le Chatelier, it must be carried out at a high temperature, high steam-to-methane ratio, and low pressure to achieve maximum conversion. The design of the steam reforming process is in part dictated by these constraints. The equilibrium composition out of the steam reformer is shown in Fig. 2.3 as a function of steam reformer outlet temperature under typical industrial conditions (26 bar with a feed steam-to-methane ratio of 2.5).

The reader may consult the work of Jens R. Rostrup-Nielsen and Thomas Rostrup-Nielsen [4].

**Fig. 2.3** Equilibrium composition out of a steam reformer at 26 bar with a feed steam-to-methane ratio of 2.5



## 2.2 Introduction to Combustion

Chemical combustion is the major source of energy used for transportation and the production of electricity. In this chapter, thermodynamic concepts important to the study of combustion are examined. Basic property relations for ideal gases and ideal-gas mixtures and the first law of thermodynamics are discussed in other chapters. A review of these concepts will be covered as they are integral to the study of combustion.

Combustion is a rapid exothermic reaction that releases substantial energy as heat and has the ability to propagate through a suitable medium. This propagation results from the strong coupling of the reaction with the molecular transport process. The chemistry and physics of combustion involves the destruction and rearrangement of certain molecules and a rapid energy release within a few millionths of a second. Currently, the study of combustion is a mature discipline and an integral element of diverse research and development programs from fundamental studies of the physics of flames and high-temperature molecular chemistry to applied engineering projects involved with developments such as advanced coal-burning equipment and improved combustion furnaces, boilers, and engines. These developments are important in optimizing fuel use and controlling the emission of pollutants.

The study of combustion starts with the *mass* and *energy balances* that limit the combustion process. Then the energy characteristics of various important fuel resources and their physical and chemical properties are considered. Finally, the practical stoichiometry and thermochemical requirements that apply during combustion processes, including chemical reactions, equilibrium compositions, and temperatures, are discussed.

Combustion is the conversion of a substance called a fuel into products of combustion by combination with an oxidizer. The combustion process is an exothermic chemical reaction, i.e., a reaction that releases energy as it occurs. Thus, combustion may be represented symbolically by the following formula:



Here the fuel and the oxidizer are reactants, i.e., the substances present before the reaction takes place. This relation indicates that the reactants produce combustion products and energy. Either the chemical energy released is transferred to the surroundings as it is produced or it remains in the combustion products in the form of elevated internal energy (temperature), or some combination thereof.

Fuels are evaluated, in part, based on the amount of energy or heat that they release per unit mass or per mole during the combustion of the fuel. Such a quantity is known as the fuel's heat of reaction or heating value.

Heats of reaction may be measured in a calorimeter, a device in which chemical energy release is determined by transferring the released heat to a surrounding fluid. The amount of heat transferred to the fluid in returning the products of combustion

to their initial temperature yields the heat of reaction. In combustion processes, the oxidizer is usually air but could be pure oxygen, an oxygen mixture, or a substance involving some other oxidizing element such as fluorine. Only oxygen-based oxidizers will be considered in what follows. Chemical fuels exist in gaseous, liquid, or solid form. Natural gas, gasoline, and coal are the most widely used examples of these three forms. Each is a complex mixture of reacting and inert compounds. The analysis process proceeds in three steps:

- Concepts and definitions related to element conservation;
- A definition of enthalpy that accounts for chemical bonds;
- First-law concepts defining, for example, the heat of reaction and heating values, and adiabatic flame temperature.

Actually, combustion is a result of dynamic, or time-dependent, events that occur on a molecular level among atoms, molecules, radicals, and solid boundaries. The rapid reactions produce gradients that transport processes convert into heat and species fluxes that speed up the reactions.

At the heart of fossil-fueled power plant operation is the combustion process. Through the combustion process, a modern power plant burns fuel to release the energy that generates steam – energy that ultimately is transformed into electricity. Yet, while the combustion process is one of a power plant's most fundamental processes, it is also one of the most complex.

Combustion, or the conversion of fuel to useable energy, must be carefully controlled and managed. Only the heat released that is successfully captured by steam is useful for generating power. Hence, the ability of the steam generator to successfully transfer energy from the fuel to steam is driven by the combustion process or, more precisely, the characteristics of the combustion process.

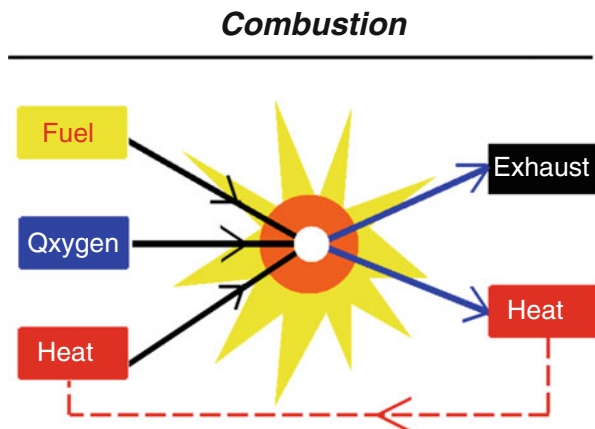
*A chemical reaction may be defined as the rearrangement of atoms due to the redistribution of electrons.* In a chemical reaction, the terms *reactants* and *products* are frequently used. Reactants comprise the initial constituents that start a reaction, while products are the final constituents formed by the chemical reaction. Although the basic principles, which will be discussed in this chapter, apply to any chemical reaction, the focus will be on combustion.

## 2.3 Chemical Combustion

Combustion is a chemical process in which a substance reacts rapidly with oxygen and gives off heat. The original substance is called the fuel, and the source of oxygen is called the oxidizer. The fuel can be a solid, liquid, or gas. For most forms of transportation propulsion, the fuel is usually a liquid. The oxidizer, likewise, could be a solid, liquid, or gas but is usually a gas (air). Rockets, on the other hand, usually carry their own oxidizer in addition to their fuel.

During combustion, new chemical substances are created from the fuel and the oxidizer. These substances will be called exhaust. Most of the exhaust comes from chemical combinations of the fuel and oxygen. When a hydrogen-carbon-based fuel

**Fig. 2.4** Simple chemical combustion illustration (courtesy NASA)



(like gasoline) burns, the exhaust includes water (hydrogen + oxygen) and carbon dioxide (carbon + oxygen). However, the exhaust can also include chemical combinations from the oxidizer alone. If the gasoline is burned in air, which contains 21 % oxygen and 78 % nitrogen, the exhaust can also include nitrous oxides (NO<sub>X</sub>, nitrogen + oxygen). The temperature of the exhaust is high because of the heat that is transferred to the exhaust during combustion. Because of the high temperatures, exhaust usually occurs as a gas, but there can be liquid or solid exhaust products as well. Soot, for example, is a form of solid exhaust that occurs in some combustion processes (Fig. 2.4).

During the combustion process, as the fuel and oxidizer are turned into exhaust products, heat is generated. Interestingly, some source of heat is also necessary to start combustion. Gasoline and air are both present in your automobile fuel tank; but combustion does not occur because there is no source of heat. Since heat is both required to start combustion and is itself a product of combustion, we can see why combustion takes place very rapidly. Once combustion gets started, we do not have to provide the heat source because the heat of combustion will keep things going. We do not have to keep lighting a campfire, it just keeps burning.

To summarize, for combustion to occur three things must be present:

1. A fuel to be burned,
2. A source of oxygen, and
3. A source of heat.

Because of combustion, exhaust products are created and heat is released. You can control or stop the combustion process by controlling the amount of the fuel available, the amount of oxygen available, or the source of heat.

Actually, combustion is a result of dynamic, or time-dependent, events that occur on a molecular level among atoms, molecules, radicals, and solid boundaries. Therefore, this chapter presents chemical kinetics that includes kinetic theory of gases, elementary reactions, and reaction rate theory. Furthermore, the rapid reactions produce gradients that transport processes convert into heat and species fluxes that speed up the reactions.

## 2.4 Combustion Equations

A simple chemical-reaction equation is the combustion of propane in a pure oxygen environment. The chemical reaction is represented by



Note that the number of moles on the left-hand side may not equal the number of moles on the right-hand side. However, the number of atoms of an element must remain the same, before, after, and during a chemical reaction; this demands that the mass of each element be conserved during combustion.

In writing the equation, some knowledge of the products of the reaction was assumed. *Complete combustion* was assumed. The products of *complete combustion* of a hydrocarbon fuel will be H<sub>2</sub>O and CO<sub>2</sub>. *Incomplete combustion* results in products that contain H<sub>2</sub>, CO, C, or OH.

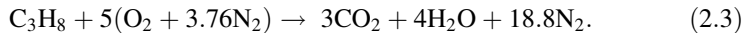
For a simple chemical reaction, such as Eq. (2.1), writing down a balanced chemical equation is straightforward. For reactions that are more complex the following systematic method proves useful [8]:

1. Set the number of moles of fuel equal to 1.
2. Balance CO<sub>2</sub> with the number of C from the fuel.
3. Balance H<sub>2</sub>O with H from the fuel.
4. Balance O<sub>2</sub> from CO<sub>2</sub> and H<sub>2</sub>O.

For the combustion of propane, it was assumed that the process occurred in a pure oxygen environment. Actually, such a combustion process normally occurs in air. Nominally air consists of 21 % O<sub>2</sub> and 79 % N<sub>2</sub> by volume, so that for each mole of O<sub>2</sub> in a reaction there are 3.76 mol of N<sub>2</sub>:

$$\frac{79}{21} = 3.76 \frac{\text{mol N}_2}{\text{mol O}_2}. \quad (2.2)$$

Thus, on the (simplistic) assumption that N<sub>2</sub> will not undergo any chemical reaction, Eq. (2.1) is replaced by



The minimum amount of air that supplies sufficient O<sub>2</sub> for the complete combustion of the fuel is called the *theoretical air* or *stoichiometric air*. When complete combustion is achieved with theoretical air, the products contain no O<sub>2</sub>, as in the reaction of Eq. (2.3). In practice, it is often found that if complete combustion is to occur, air must be supplied in an amount greater than theoretical air. This is due to the chemical kinetics and molecular activity of the reactants and products. The term *percent theoretical air* is used to compare the actual air provided to the combustion process compared to the *stoichiometric* air (Eq. 2.4a):

$$\% \text{ theoretical air} = 100\% + \% \text{ excess air.} \quad (2.4a)$$

Slightly insufficient air results in CO being formed; some hydrocarbons may result from larger deficiencies [8]. In summary, a mixture of air and fuel is called *stoichiometric* if it contains just enough oxygen for the complete combustion of the fuel. Moreover, the percent excess air is given by the following Eq. (2.4b):

$$\text{Percentage excess air} = \frac{\text{Actual (A/F) ratio} - \text{Stoichiometric (A/F) ratio}}{\text{Stoichiometric (A/F) ratio}}, \quad (2.4b)$$

where A denotes air while F denotes fuel.

The parameter that relates the amount of air used in a combustion process is the *air-fuel ratio* (A/F), which is the ratio of the mass of air to the mass of fuel. The reciprocal is the *fuel-air ratio* (F/A) (Eq. 2.5). Thus

$$AF = \frac{m_{\text{air}}}{m_{\text{fuel}}}, \quad FA = \frac{m_{\text{fuel}}}{m_{\text{air}}}. \quad (2.5)$$

Considering propane combustion with theoretical air as in (Eq. 2.3), the *air-fuel ratio* is (Eq. 2.6).

$$AF = \frac{m_{\text{air}}}{m_{\text{fuel}}} = \frac{(5)(4.76)(29)}{(1)(44)} = 15.69 \frac{\text{kg air}}{\text{kg fuel}}, \quad (2.6)$$

where the molecular weight of air is taken as 29 kg/kmol and that of propane as 44 kg/kmol. If for the combustion of propane  $AF > 15.69$ , a *lean or weak mixture* occurs; if  $AF < 15.69$ , a *rich mixture* results.

For solid and liquid fuels the ratios are expressed by mass, while for gaseous fuels the ratios are normally expressed by volume. For a boiler plant, the mixture is usually greater than 20 % lean; for gas turbines, it can be as much as 30 % lean. Petrol engines have to meet various conditions of load and speed and operate over a wide range of mixture strengths. The following definition is then used (Eq. 2.7):

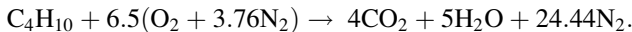
$$\text{Mixture strength} = \frac{\text{Stoichiometric (A/F) ratio}}{\text{Actual (A/F) ratio}} \quad (2.7)$$

In this situation, the working values range between 80 % (lean) and 120 % (rich). Where fuels contain some oxygen (e.g., ethyl alcohol  $C_2H_6O$ ) this oxygen is available for the combustion process, and so the fuel requires a smaller supply of air [1].

The combustion of hydrocarbon fuels involves  $H_2O$  in the products of combustion. The calculation of the dew point of the products is often of interest; it is the saturation temperature at the partial pressure of the water vapor. If the temperature drops below the dew point, the water vapor begins to condense. The condensate usually contains corrosive elements, and thus it is often important to ensure that the temperature of the products does not fall below the dew point.

*Example 2.1* Butane is burned with dry air at an air–fuel ratio of 20. Calculate (a) the percent excess air, (b) the volume percentage of CO<sub>2</sub> in the products, and (c) the dew-point temperature of the products.

**Solution** The reaction equation for theoretical air is



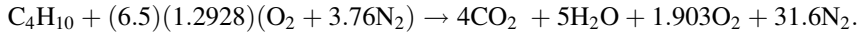
(a) The air–fuel ratio for theoretical air is

$$\text{AF} = \frac{m_{\text{air}}}{m_{\text{fuel}}} = \frac{(6.5)(4.76)(29)}{(1)(58)} = 15.47 \frac{\text{kg air}}{\text{kg fuel}}.$$

This represents 100 % theoretical air. The actual air–fuel ratio is 20. The excess air is then

$$\% \text{ excess air} = \left( \frac{\text{AF}_{\text{act}} - \text{AF}_{\text{th}}}{\text{AF}_{\text{th}}} \right) (100\%) = \frac{20 - 15.47}{15.47} (100\%) = 29.28\%.$$

(b) The reaction equation with 129.28 % theoretical air is



The volume percentage is obtained using the total moles in the products of combustion. For CO<sub>2</sub> we have

$$\% \text{ CO}_2 = \left( \frac{4}{42.5} \right) (100\%) = 9.41\%.$$

(c) To find the dew-point temperature of the products we need the partial pressure of the water vapor. It is found using a mole fraction of

$$p_{\text{H}_2\text{O}} = y_{\text{H}_2\text{O}} p_{\text{atm}} = \left( \frac{5}{42.5} \right) \times 101.325 \text{ kPa} = 11.76 \text{ kPa},$$

where we have assumed an atmospheric pressure of 101.325 kPa. Using Appendix C.2 we find the dew-point temperature to be  $T_{\text{d.p.}} = 49^\circ\text{C}$ .

When a chemical reaction occurs, there may be considerable change in the chemical composition of a system. The problem this creates is that for a control volume the mixture that exits is different from the mixture that enters.

## 2.5 Mass and Mole Fractions

The amount of a substance present in a sample may be indicated by its mass or by the number of moles of the substance. A *mole* is defined as the mass of a substance equal to its molecular mass or molecular weight. Molecular weights for substances of interest are given in the appendix. Compound molecular weights can be obtained by adding up the atomic weights of the constituents.

The composition of a mixture may be given as a list of the fractions of each of the substances present. Thus we define the mass fraction of a component  $i$ ,  $mf_i$ , as the ratio of the mass of the component,  $m_i$ , to the mass of the mixture (Eq. 2.8),  $m$ :

$$mf_i = \frac{m_i}{m}. \quad (2.8)$$

It is evident that the sum of the mass fractions of all the components must be 1. Thus (Eq. 2.9):

$$mf_1 = mf_2 + \cdots = 1 \quad (2.9)$$

The mole fraction of component  $i$ ,  $x_i$ , is the ratio of the number of moles of component  $i$ ,  $n_i$ , to the total number of moles in the mixture (Eq. 2.10),  $n$ :

$$x_i = \frac{n_i}{n}. \quad (2.10)$$

The total number of moles,  $n$ , is the sum of the number of moles of all the components of the mixture (Eq. 2.11):

$$n = n_1 + n_2 + n_3 + \cdots \quad (2.11)$$

It follows that the sum of all the mole fractions of the mixture (Eq. 2.12) must equal 1:

$$x_1 + x_2 + \cdots = 1. \quad (2.12)$$

The mass of component  $i$  in a mixture is the product of the number of moles of  $i$  and its molecular weight,  $M_i$ . The mass of the mixture is therefore the sum  $m = n_1M_1 + n_2M_2 + \cdots$  over all components of the mixture. Substituting  $x_i n$  for  $n_i$ , the total mass becomes (Eq. 2.13)

$$m = (x_1M_1 + x_2M_2 + \cdots)n. \quad (2.13)$$

But the average molecular weight of the mixture is the ratio of the total mass to the total number of moles. Thus, the average molecular weight is (Eq. 2.14)

$$M = m/n = x_1M_1 + x_2M_2 + \cdots \quad (2.14)$$

*Example 2.2* Express the mass fraction of component 1 of a mixture in terms of (a) the number of moles of the three components of the mixture,  $n_1$ ,  $n_2$ , and  $n_3$ , and (b) the mole fractions of the three components. (c) If the mole fractions of carbon dioxide and nitrogen in a three-component gas containing water vapor are 0.07 and 0.38, respectively, what are the mass fractions of the three components?

### Solution

- (a) Because the mass of  $i$  can be written as  $m_i = n_i M_i$ , the mass fraction of component  $i$  can be written as

$$mf_i = \frac{n_i M_i}{n_1 M_1 + n_2 M_2 + n_3 M_3 + \dots}.$$

For the first of the three components,  $i = 1$ , this becomes

$$mf_1 = \frac{n_1 M_1}{n_1 M_1 + n_2 M_2 + n_3 M_3}.$$

Similarly, for  $i = 2$  and  $i = 3$ :

$$mf_2 = \frac{n_2 M_2}{n_1 M_1 + n_2 M_2 + n_3 M_3},$$

$$mf_3 = \frac{n_3 M_3}{n_1 M_1 + n_2 M_2 + n_3 M_3}.$$

- (b) Substituting  $n_1 = x_1 n_1$ ,  $n_2 = x_2 n_2$ , and so forth in the earlier equations and simplifying, we obtain for the mass fractions

$$mf_1 = x_1 M_1 / (x_1 M_1 + x_2 M_2 + x_3 M_3),$$

$$mf_2 = x_2 M_2 / (x_1 M_1 + x_2 M_2 + x_3 M_3),$$

$$mf_3 = x_3 M_3 / (x_1 M_1 + x_2 M_2 + x_3 M_3).$$

- (c) Identifying the subscripts 1, 2, and 3 with carbon dioxide, nitrogen, and water vapor, respectively, we have  $x_1 = 0.07$ ,  $x_2 = 0.38$ , and  $x_3 = 1 - 0.07 - 0.038 = 0.55$ . Then

$$mf_1 = (0.07)(44) / [(0.07)(44) + (0.38)(28) + 0.55(18)]$$

$$= (0.07)(44) / (23.62) = 0.1304,$$

$$mf_2 = (0.38)(28) / (23.62) = 0.4505,$$

$$mf_3 = (0.55)(18) / (23.62) = 0.4191.$$

As a check we sum the mass fractions:  $0.1304 + 0.4505 + 0.4191 = 1.0000$ .

For a mixture of gases at a given temperature and pressure, the ideal gas law shows that  $pV_i = n_i \mathfrak{R}T$  holds for any component, and  $pV = n \mathfrak{R}T$  for the mixture as

a whole. Forming the ratio of the two equations, we observe that the mole fractions have the same values as the volume fraction (Eq. 2.15):

$$x_i = V_i/V = n_i/n. \quad (2.15)$$

Similarly, for a given volume of a mixture of gases at a given temperature,  $pV_i = n_i\mathfrak{R}T$  for each component and  $pV = n\mathfrak{R}T$  for the mixture. The ratio of the two equations shows that the *partial pressure* of any component  $i$  is the product of the mole fraction of  $i$  and the pressure of the mixture (Eq. 2.16):

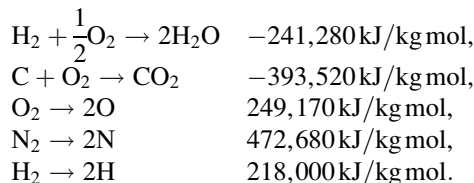
$$p_i = pn_i/n = px_i. \quad (2.16)$$

*Example 2.3* What is the partial pressure of water vapor in Example 2.2 if the mixture pressure is 2 atm?

**Solution** The mole fraction of water vapor in the mixture of Example 2.2 is 0.55. The partial pressure of the water vapor is therefore  $(0.55)(2) = 1.1$  atm.

## 2.6 Enthalpy of Formation

To deal with the heat produced in a chemical reaction, a reference point is required so that changes in enthalpy can be computed. The standard reference conditions are 25 °C (77 °F, 298 K, 537 °R) and 1 atm pressure. The enthalpy of a substance at the reference state is usually identified as  $h^0$ . In these conditions many of the elements in their normal form are defined to have a 0.0 enthalpy of formation or *heat of formation*,  $h_f^0$ . Typically this includes gases like oxygen, nitrogen, and hydrogen as well as the solid form of carbon. Other gases like carbon dioxide and water vapor have a negative heat of formation in standard conditions. This means that when they are formed by burning carbon with oxygen, or hydrogen with oxygen, a certain amount of energy will be given off. The reaction is exothermic. When oxygen, nitrogen, or hydrogen is decomposed to oxygen ions, nitrogen ions, or hydrogen ions, energy is required. The heat of formation for these reactions is positive because energy must be added to the molecule to break it down into ions. Therefore they are endothermic reactions:



The negative sign for the heats of formation means that when the reaction occurred, energy was given off by the reactants.

The first law for a chemical reaction can be written as Eq. (2.17):

$$Q = H_P - H_R. \quad (2.17)$$

$H_P$  is the enthalpy of the products of combustion that leave the combustion chamber and  $H_R$  is the enthalpy of the reactants that enter the combustion chamber. If the reactants are stable elements and the reaction occurs at constant temperature and pressure in the reference state (77 °F and 1 atm), then the  $H$  represent the heats of formation for the substances involved. If the temperature deviates from the reference state, each of the enthalpies must be corrected for the temperature changes.

The general equation for a flowing system is (Eq. 2.18)

$$Q - W_s = \sum_{\text{prod}} N_p [h_f^0 + (h(T) - h^0)]_p - \sum_{\text{react}} N_r [h_f^0 + (h(T) - h^0)]_r, \quad (2.18)$$

where  $N_p$  = moles of product,  $N_r$  = moles of reactants,  
 $h(T) - h^0$  = change in enthalpy from reference state.

The general equation for a rigid chamber is (Eq. 2.19)

$$\begin{aligned} Q - W_s &= U_p - U_r = \sum_{\text{prod}} N_p [h_f^0 + (h(T) - h^0) - Pv]_p \\ &\quad - \sum_{\text{react}} N_r [h_f^0 + (h(T) - h^0) - Pv]_r, \\ Q - W_s &= U_p - U_r = \sum_{\text{prod}} N_p [h_f^0 + (h(T) - h^0) - \mathfrak{R}T]_p \\ &\quad - \sum_{\text{react}} N_r [h_f^0 + (h(T) - h^0) - \mathfrak{R}T]_r. \end{aligned} \quad (2.19)$$

The changes in enthalpy from the reference state can be calculated using the following techniques:

For a solid or liquid:  $\Delta h = C\Delta T$ .

For gases:

1.  $\Delta h = C_p\Delta T$ ,
2. Use tabulated values for  $\Delta h$
3. Use generalized charts for a real gas,
4. Use tables for vapors like the steam tables.

*Example 2.4* Volumetric analysis of the products of combustion of an unknown hydrocarbon measured on a dry basis gives the following mole percentages:

$\text{CO}_2 = 10.4\%$ ,

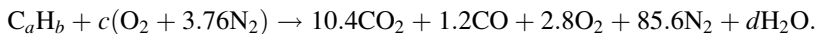
$\text{CO} = 1.2\%$ ,

$\text{O}_2 = 2.8\%$ ,

$\text{N}_2 = 85.6\%$ .

Determine the composition of the hydrocarbon and the percent theoretical air.

**Solution** The combustion equation is



Writing equations to balance each of the species gives

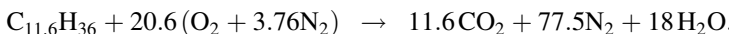
$$C : \quad a = 10.4 + 1.2, \quad a = 11.6,$$

$$N : \quad 3.76c = 85.6, \quad c = 22.8,$$

$$O : \quad 2c = 10.4(2) + 1.2 + 2.8(2) + d, \quad d = 2(22.8) - 20.8 - 1.2 - 5.6 = 18,$$

$$H : \quad b = 2d = 36.$$

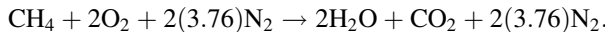
The actual equation for 100 % theoretical air must be



22.8 mol of air were used and only 20.6 were needed, so % theoretical air = 110.7 %.

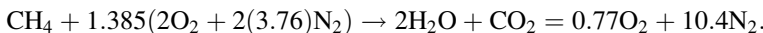
*Example 2.5* Methane is burned with dry air at an air–fuel ratio of 5. Calculate the percent excess air and the percent water vapor in the exhaust. Estimate the dew-point temperature of the products.

**Solution** The combustion equation is



The stoichiometric air–fuel mixture is  $AF_{st} = \frac{2(28.9669)}{16.043} = 3.611$ .

The percent excess air is  $100 \times (5 - 3.611)/3.611 = 38.47\%$ . So the balance equation is



There are  $2 + 1 + 0.77 + 10.4 = 14.17$  mol of products.

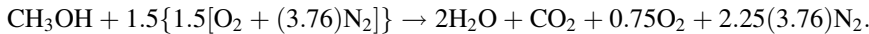
The mole percent of  $H_2O$  in the exhaust is  $2/14.17 = 14.1\%$ .

The partial pressure of  $H_2O$  in the exhaust is  $(2/14.17) \times 101,325 = 14.3$  kPa.

The saturation temperature (dew point) at 14.3 kPa is 326 K = 53 °C.

*Example 2.6* Gaseous methyl alcohol and air enter a combustion chamber at 25 °C and 1 atm and leave at 550 K and 1 atm. Assume 150 % theoretical air. Estimate the heat transfer to the chamber.

**Solution** The reaction equation is



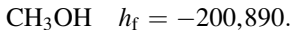
The first law gives

$$Q = \sum_{\text{prod}} N_p (h_f^0 + \Delta h)_p - \sum_{\text{react}} N_r (h_f^0 + \Delta h)_r.$$

Products:

$\text{H}_2\text{O}$	$h_f = -241,820$ ,	$\Delta h = h(550) - h(298) = 17,489.1 - 8853.3 = 8635.8$ ,
$\text{CO}_2$	$h_f = -393,520$ ,	$\Delta h = h(550) - h(298) = 18,878.8 - 8378.4 = 10,500.4$ ,
$\text{O}_2$	$h_f = 0$ ,	$\Delta h = h(550) - h(298) = 15,363.4 - 7766.2 = 7597.2$ ,
$\text{N}_2$	$h_f = 0$ ,	$\Delta h = h(550) - h(298) = 15,095.3 - 7754.3 = 7431.0$ .

Reactants:



The balance equation is

$$Q = (2 \times (-241,820 + 8635.8) + (-393,520 + 10,500.4) + 8.46 \times 7431.0 \\ + 0.75 \times 7597.2 - (-200,890)) \\ Q = -579,930 \text{ kJ/kmol methyl alcohol.}$$

The preceding calculation assumes the water in the exhaust is liquid, which at the temperature of the exhaust products is not very likely. So an additional enthalpy must be added to the  $\Delta h$  for  $\text{H}_2\text{O}$  to account for the vaporization of water:

$$\Delta h_{fg} = 2256.6 \text{ kJ/kg} = 40,619.0 \text{ kJ/kmol.}$$

Adding this to the negative  $Q$  gives  $Q = -539,311 \text{ kJ/kmol methyl alcohol}$ .

Note that the heat of formation for nitrogen and oxygen is zero on both sides of the equation. If the methyl alcohol had entered as a liquid, we would have had to add its heat of vaporization to the reactant side of the equation, further reducing the heat available per mole of the fuel.

## 2.7 Enthalpy of Combustion

With most hydrocarbons, normal combustion occurs with oxygen in the air. Therefore, the enthalpy change for the complete combustion of a substance with oxygen is called the **heat of combustion**. Several heats of combustion are tabulated in Table 2.3. If the products of combustion contain water in the vapor state, an allowance for the heat required to vaporize the water must be included in the

**Table 2.3** Selected enthalpies of combustion and enthalpies of vaporization

Substance	Formula	Higher heating value (kJ/kmol)	$h_{fg}$
Hydrogen	H <sub>2</sub> (g)	-285,840	
Carbon	C(s)	-393,520	
Carbon monoxide	CO(g)	-282,990	
Methane	CH <sub>4</sub> (g)	-890,360	
Acetylene	C <sub>2</sub> H <sub>2</sub> (g)	-1,299,600	
Ethylene	C <sub>2</sub> H <sub>4</sub> (g)	-1,410,970	
Ethane	C <sub>2</sub> H <sub>6</sub> (g)	-1,559,900	
Propylene	C <sub>3</sub> H <sub>6</sub> (g)	-2,058,500	
Propane	C <sub>3</sub> H <sub>8</sub> (g)	-2,220,000	15,060
<i>n</i> -Butane	C <sub>4</sub> H <sub>10</sub> (g)	-2,877,100	21,060
<i>n</i> -Pentane	C <sub>5</sub> H <sub>12</sub> (g)	-3,536,100	26,410
<i>n</i> -Hexane	C <sub>6</sub> H <sub>14</sub> (g)	-4,194,800	31,530
<i>n</i> -Heptane	C <sub>7</sub> H <sub>16</sub> (g)	-4,853,500	36,520
<i>n</i> -Octane	C <sub>8</sub> H <sub>18</sub> (g)	-5,512,200	41,460

change in enthalpy from the reference state. If the products of combustion include water in the liquid state, the heat of vaporization is not subtracted, and this gives the *higher heating value* for the *heat of combustion* for this fuel.

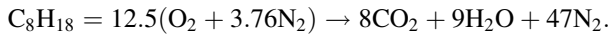
## 2.8 Adiabatic Flame Temperature

In many cases, the heat released in the combustion reaction will determine the final temperature of the products and the gases present in the combustion chamber. The temperature achieved, assuming no heat transfer to the surroundings, is called the adiabatic flame temperature. Since the change in enthalpy of the products will depend on this temperature, the adiabatic flame temperature must be found by iteration. Note also that when a fuel is burned in air, the heat required to bring the nitrogen in the air up to the adiabatic flame temperature must be included in the analysis. The adiabatic flame temperature can be lowered by adding excess air above that required for complete combustion. Typically, this will be required owing to peak temperature restrictions on the materials used for construction, for example, the strength of turbine blades downstream of the combustion process.

It is worth pointing out at this point that combustion in itself is an irreversible process and achieving complete combustion typically requires a pressure loss in the combustion chamber. Since the major part of the fluid flowing through an air combustion chamber does not participate in the chemical reactions (primarily the nitrogen), the combustion process can be thought of as simply heating the working fluid. A nuclear heated heat exchanger can often accomplish the same heating with a lower pressure loss. However, in the nuclear heated system the temperature drops are in the opposite direction, requiring the heat exchanger walls to operate at a higher temperature than the combustion chamber walls.

*Example 2.7* Calculate the enthalpy of combustion of gaseous octane and liquid octane assuming the reactants and products to be at a reference state of 25 °C and 1 atm. Assume liquid water in the products exiting the steady flow combustion chamber.

**Solution** The reaction is



Products:

$$\begin{array}{ll} \text{H}_2\text{O}, & h_f = -285,830, \\ \text{CO}_2, & h_f = -393,520, \\ \text{N}_2, & h_f = 0. \end{array}$$

Reactants:

$$\begin{array}{ll} \text{C}_8\text{H}_{18}(\text{l}), & h_f = -208,450, \quad h_{fg} = 41,460, \\ \text{C}_8\text{H}_{18}(\text{g}), & h_f = -208,450. \end{array}$$

Liquid octane:

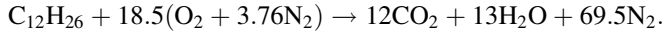
$$\begin{aligned} Q &= 8(-393,520) + 9(-285,830) - (-208,450 - 41,460) \\ &= 5.4707 \times 10^6 \text{ kJ/kmol}. \end{aligned}$$

Gaseous octane:

$$Q = 8(-393,520) + 9(-285,830) - (208,450) = 5.5122 \times 10^6 \text{ kJ/kmol}.$$

*Example 2.8* Kerosene is burned with theoretical air in a jet engine. Estimate the adiabatic flame temperature. Kerosene can be treated as *n*-Dodecane—C<sub>12</sub>H<sub>26</sub> and has a heat of formation of −291,010 kJ/kmol.

**Solution** The balance equation is

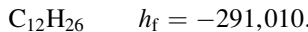


For the adiabatic flame temperature  $Q = 0$ , so:

Products:

$$\begin{array}{lll} \text{H}_2\text{O}, & h_f = -241,820, & \Delta h(\text{H}_2\text{O}) = ? \\ \text{CO}_2, & h_f = -393,520, & \Delta h(\text{CO}_2) = ? \\ \text{N}_2, & & \Delta h(\text{N}_2) = ? \end{array}$$

Reactants:



$$Q = 0 = 12(-393,520 + \Delta h(\text{CO}_2)) + 13(-241,820 + \Delta h(\text{H}_2\text{O})) \\ + 69.5\Delta h(\text{N}_2) - (-291,010).$$

At 25 °C we would have

$$Q = 12(-393,520) + 13(-241,820) + 291,010 = 7.5749 \times 10^6 \text{ kJ/kmol.}$$

Treating all of the products as nitrogen the dominant product, we would have 94.5 kg mol of product. Thus, the change in enthalpy per mole is 80,158 kJ/kmol. At 25 °C nitrogen has an enthalpy of 7754.3 kJ/kmol. So the gas tables are consulted looking for an enthalpy of 87,912 kJ/kmol. This corresponds to a temperature of 2660 K. Then, evaluating the  $\Delta h$  for  $\text{H}_2\text{O}$  and  $\text{CO}_2$  at 2660 K gives

$$\begin{aligned}\Delta h(\text{H}_2\text{O}) &= 116,547.5 - 8853.3 = 107,690.0, \\ \Delta h(\text{CO}_2) &= 140,041.3 - 8378.4 = 131,660.0, \\ \Delta h(\text{N}_2) &= 87,846.0 - 7754.3 = 80,092.0.\end{aligned}$$

At 2660 K the net heat balance is

$$Q = -7.5749 \times 10^6 + 13(107,690.0) + 12(131,660.0) + 69.5(80,092.0) \\ = 97,138 \text{ kJ/kmol.}$$

Since it is positive, the temperature does not quite reach 2660 K. Now noting that both  $\text{H}_2\text{O}$  and  $\text{CO}_2$  had larger enthalpy changes than nitrogen, the number of moles can be adjusted to represent them with the all-nitrogen model:

$$\begin{aligned}\Delta h(\text{H}_2\text{O})/\Delta h(\text{N}_2) &= 107,690.0/80,092 = 1.35, \\ \Delta h(\text{CO}_2)/\Delta h(\text{N}_2) &= 131,660/80,092 = 1.64.\end{aligned}$$

So the new number of moles will be  $N = 69.5 + 1.35(13) + 1.64(12) = 106.7$ .

Dividing the 25 °C enthalpy excess by 106.7 gives  $7.5749 \times 10^6 / 106.7 = 71,017 \text{ kJ/kmol}$ .

Add this to the nitrogen enthalpy at 25 °C to get 78,771 kJ/kmol. The gas table gives a temperature of about 2410 K:

$$\begin{aligned}\Delta h(\text{H}_2\text{O}) &= 103,045.9 - 8853.3 = 94,193, \\ \Delta h(\text{CO}_2) &= 124,671.2 - 8378.4 = 116,290.0, \\ \Delta h(\text{N}_2) &= 78,688.1 - 7754.3 = 70,934.0,\end{aligned}$$

$$Q = -7.5749 \times 10^6 + 13(94,193) + 12(116,290) + 69.5(70,934) \\ = -24,998 \text{ kJ/kmol.}$$

So now the temperature is bracketed. The new mole effectiveness ratios for H<sub>2</sub>O and CO<sub>2</sub> are 1.33 and 1.64. Therefore, 2410 K is very close, and in fact the best answer obtained by another iteration is  $T = 2416.3$  K, which is probably 2 or 3 too many digits for the round-offs that have been made in the solution process.

It is obvious that this would be a very stressing temperature, and so most jet engines run at a mixture ratio quite a bit lower than stoichiometric.

## References

1. [http://www.topsoe.com/sites/default/files/topsoe\\_large\\_scale\\_hydrogen\\_produc.pdf](http://www.topsoe.com/sites/default/files/topsoe_large_scale_hydrogen_produc.pdf)
2. Dodds, P. E., & McDowall, W. (2012). *A review of hydrogen production technologies for energy system models*. UKSHEC Working Paper No. 6, UCL Energy Institute, University College London Central House, London, UK.
3. Udengaard, N. R. (2004). Hydrogen production by steam reforming of hydrocarbons. Houston, TX: Haldor Topsoe Inc.
4. Rostrup-Nielsen, J. R., & Rostrup-Nielsen, T. (2001). Conversion of hydrocarbons and alcohols for fuel cells. *Physical Chemistry Chemical Physics*, 3, 283.
5. Pitt, R. (2001). World refining. p. 6.
6. Zohuri, B. (2015). *Combined cycle driven efficiency for next generation nuclear power plants: An innovative design approach*. New York: Springer Publishing Company.
7. Zohuri, B. (2014). *Innovative open air Brayton combined cycle systems for the next generation nuclear power plants*. Albuquerque, NM: University of New Mexico Publications.
8. Eastop, T. D., & McConkey, A. (1993). *Applied thermodynamics for engineering technologists* (5th ed.). Harlow, UK: Pearson Education Ltd.

# **Chapter 3**

## **Hydrogen Production Plant**

Research is going forward to produce hydrogen based on nuclear energy. Hydrogen production processes necessitate high temperatures that can be reached in fourth generation nuclear reactors. Technological studies are now under way that aim to define and qualify components that in the future will enable us to retrieve and transfer heat produced by these reactors. Hydrogen combustion turbine power could be one of the solutions to our future energy needs, particularly when it comes to on-peak demand for electricity, but until recently the problem with hydrogen power was its production for use as an energy source. Although hydrogen is the most common element in the known universe, actually capturing it for energy use is a process that itself usually requires some form of fuel or energy.

### **3.1 Introduction**

The aftermath of the Fukushima nuclear disaster has forced many countries such as Japan and Germany to take drastic measures in revising their nuclear energy policies, which had long heralded nuclear power plants as the countries' main source of energy. For example, while Germany decided to abandon all of its atomic power plants, the new energy policy announced by Japan aims to decrease the country's dependence on nuclear as much as possible while increasing and enhancing research and development (R&D) in search of an alternative renewable energy source. Also, in parallel efforts, the government is promoting a so-called Hydrogen Society and the use of hydrogen as a source of energy to pave the way to achieving the goal of such a society by making, for example, fuel cell vehicles (FCVs), where the Fuel Cell and Hydrogen Technology Group at the New Energy and Industrial Technology Development Organization (NEDO) oversees R&D.

Burning hydrogen in combustible form does not entail the emission of any carbon dioxide ( $\text{CO}_2$ ), so it is considered a source of clean energy that can greatly help reduce the effects of greenhouse gases. Although expectations are high, issues



**Fig. 3.1** A typical oil refinery plant

remain related to technical challenges, cost of ownership, and return on investment of R&D in hydrogen as a renewable energy source. Examples of the challenges associated with using hydrogen include setting up expensive hydrogen stations for FCVs, securing sufficient supplies of the gas, and coming up with ways to produce it without emitting carbon dioxide.

Another industrial application of hydrogen is in oil refining, where it is used to process crude oil into refined fuel, such as gasoline and diesel, and to remove contaminants, such as sulfur, from these fuels (Fig. 3.1).

Total hydrogen consumption in oil refineries is estimated at 12.4 billion standard cubic feet per day, which equates to an average hydrogen consumption of 100–200 standard cubic feet per barrel of oil processed. Hydrogen consumption in the oil refining industry grew at a compound annual growth rate of 4 % from 2000 to 2003, and growth in consumption is expected to increase to between 5 and 10 % through 2010 [Oil & Gas Journal, CryoGas International] (Fig. 3.2).<sup>1</sup>

The principal drivers of this growth in hydrogen refining demand are as follows:

- Low sulfur in diesel fuel regulations: hydrogen is used in refineries to remove sulfur from fuels such as diesel;
- Increased consumption of low-quality, heavy crude oil, which requires more hydrogen to refine;
- Increased oil consumption in developing economies such as China and India.

Approximately 75 % of hydrogen currently consumed worldwide by oil refineries is supplied by large hydrogen plants that generate hydrogen from natural gas or other hydrocarbon fuels, with the balance being recovered from hydrogen-containing

<sup>1</sup> <http://www.xebecinc.com/applications-industrial-hydrogen.php>

**Fig. 3.2** Hydrogen PSA unit – HYDROSWING (courtesy Mahler Advanced Gas Systems) (<http://www.mahler-agc.com/hydrogen/index.htm>)



streams generated in the refinery process. Pressure swing adsorption (PSA) (Fig. 3.3a, b) technology is used in both hydrogen generation plants and in hydrogen recovery.

### Pressure Swing Adsorption

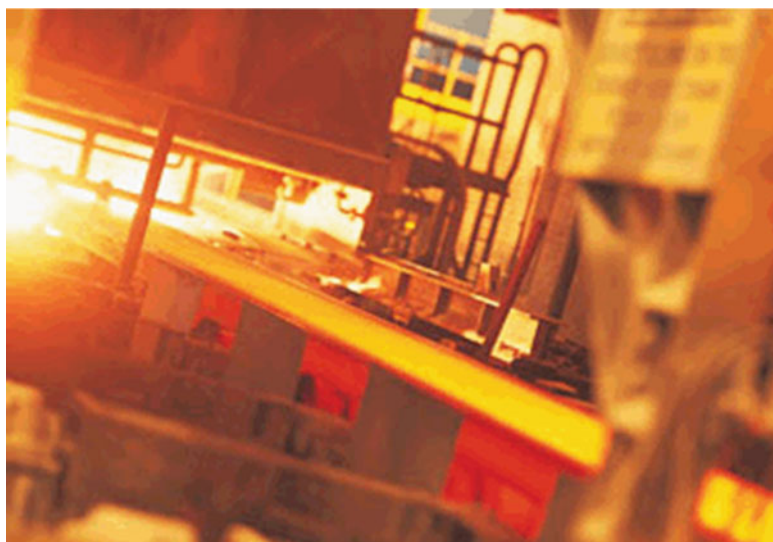
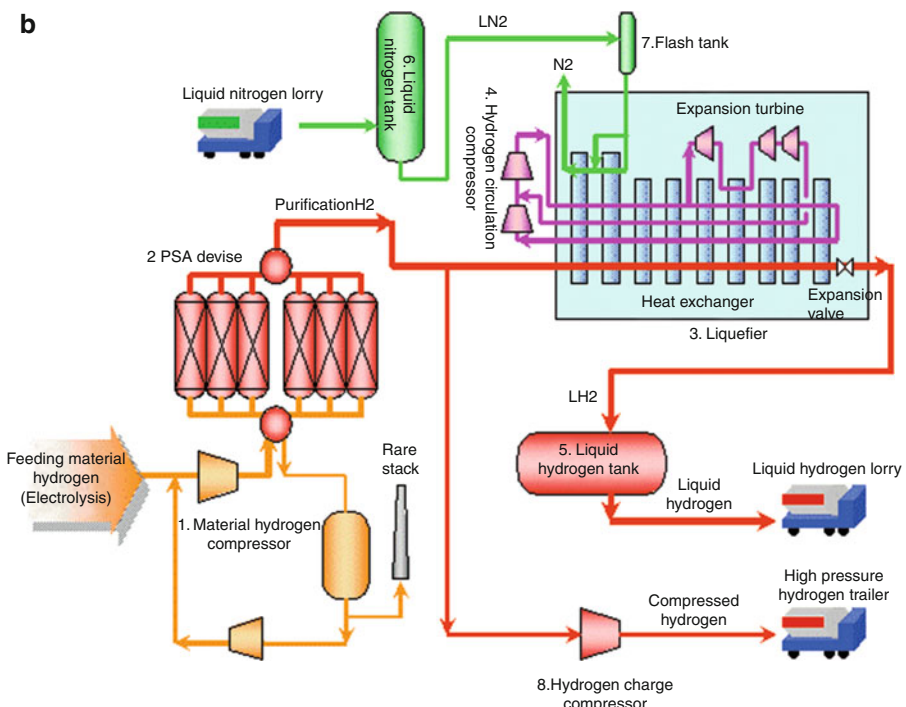
PSA technology is used to separate gas species from a mixture of gases under pressure according to the species' molecular characteristics and affinity for an adsorbent material. It operates at near-ambient temperatures and differs significantly from cryogenic distillation techniques of gas separation. Specific adsorptive materials (e.g., zeolites, activated carbon, molecular sieves) are used as a trap, preferentially adsorbing the target gas species at high pressure.<sup>2</sup> The process then switches to low pressure to desorb the adsorbed material.<sup>2</sup>

Hydrogen is used in a range of other industries, including chemical production, metal refining, food processing, and electronics manufacturing. Hydrogen is either delivered to customers in these industries as compressed or liquid hydrogen or generated on site from water using a process known as electrolysis or from natural gas using a process called reforming. In certain applications, there is a gradual shift toward on-site generation to replace delivered compressed or liquid hydrogen, largely based on the lower cost of new on-site hydrogen generation technologies compared to delivered hydrogen.

Other applications of hydrogen in industry worth mentioning are as follows:

1. In weather balloons in meteorology, where the balloons are fitted with equipment to record information necessary to study climate;
2. In fertilizers and paints;

<sup>2</sup> [http://en.wikipedia.org/wiki/Pressure\\_swung\\_adsorption](http://en.wikipedia.org/wiki/Pressure_swung_adsorption)

**a****b**

**Fig. 3.3** (a) Typical metal refining plant. (b) Flow of liquid hydrogen production facilities

3. In food-related industries, where it is used to make hydrogenated vegetable oils, using nickel as a catalyst;
4. In welding torches, which are used to melt steel;
5. In metal extraction in chemical industries; for example, hydrogen is needed to treat mined tungsten to make it pure.
6. In homes; hydrogen peroxide has nonmedical applications; other applications include pest control in gardens, stain removal on clothing, and as a bleaching agent for household cleaning.

As we can see, hydrogen plays an important role in numerous applications in multiple industries. Users in a wide range of industries can benefit from operating a cost-effective hydrogen plant and significantly reducing production costs (Fig. 3.3).

As we know from chemistry, hydrogen is the lightest and most common element in the universe. Its atomic number is 1. In its elemental state, hydrogen is rare. But it is one of the components of water and vital to life. Hydrogen alone does not exist as a natural resource but needs to be produced by separating it from other elements and molecules, such as water as waste in the oceans surrounding us. By far the most common method of producing hydrogen in industry today is by stripping it from natural gas using a process known as steam reforming.

When it comes to energy use, 95 % of the world's hydrogen is produced in this way. Steam reforming of natural gas requires temperatures as high as 850 °C and pressures of up to 365 pounds per square inch ( $2.517e+6$  Pa). If we are aiming for a sustainable future, producing hydrogen in this way from the world's finite resources of fossil fuels is not the answer, nor is it cost effective in long run.

Another way of producing hydrogen is through electric hydrolysis. Both methods are discussed in what follows.

Currently, fossil fuels, including naphtha, natural gas, and coal, are the main sources of hydrogen, which is generated using the steam reforming method, in which steam is added to methane to yield hydrogen. A huge amount of hydrogen is also produced as a byproduct of the production of caustic soda and from coke ovens.

In contrast, electric hydrolysis is a relatively simple process and involves methods used in typical high school chemistry labs, where two electrodes, one with a positive charge called the anode and the other negatively charged called the cathode, are placed in water. The results of the induced electric current flowing through the water splits a hydrogen ion from oxygen, with the positive hydrogen ion being attracted to the cathode and the negative oxygen ion to the anode. Once the ions touch the electrodes, the hydrogen gains an electron while oxygen loses one and they create fully fledged atoms of hydrogen and oxygen, which then rise and can then be collected separately at the top of the water container.

The Japanese National Economic Development Office (NEDO) published a white paper on hydrogen energy in July 2012 that states the importance of promoting hydrogen-related products, which in Japan are expected to develop into a market worth ¥1 trillion by 2030 and ¥8 trillion by 2050.<sup>3</sup>

---

<sup>3</sup><http://www.japantimes.co.jp/news/2014/10/12/national/japan-rises-challenge-becoming-hydrogen-society/>

### 3.2 Electrical Energy Supply and Demand

Consumer demand for electricity is a function of daily and seasonal changes. These variables are based on, for example, changes in demand at a manufacturing facility that has frequent starts and stops throughout the day and week, air conditioners that are turned off and on seasonally during early morning and late afternoon hours, and changes in demand for electricity by consumers at home or at work. Peak times occur when the most electricity is needed, which is known as the peak load, whereas a base load of electricity is needed year round.

Because electricity cannot be stored easily, utilities must anticipate demand, even on hot summer days, and supply enough electricity to meet demand. Consumption depends predominantly on the time of day and on the season. Utilities meet this demand with power plants in the state or region where the demand and peak load occur or by purchasing electricity from power plants in neighboring states or regions. Supply and demand must be balanced to maintain a reliable electricity grid without power interruptions to consumers and other end users.

Power supply companies must consider three main factors to meet supply and demand requirements:

1. **Demand**, or the need for electricity, is the total amount of electricity that consumers use at a particular time and is measured as electrical capacity in kilowatts; 1000 kilowatts (kW) equals 1 megawatt (MW). One kilowatt will power ten 100-W light bulbs. Most home air conditioners require 2 kW to operate. A power plant rated at 1 MW will supply enough energy for 500–1000 homes simultaneously. Electricity is also needed to supply industrial, commercial, and agricultural needs. Demand or energy use can be divided into base load, intermediate load, and peak load (Fig. 3.4). This helps to determine the type and quantity of power plants needed to produce electricity at the right

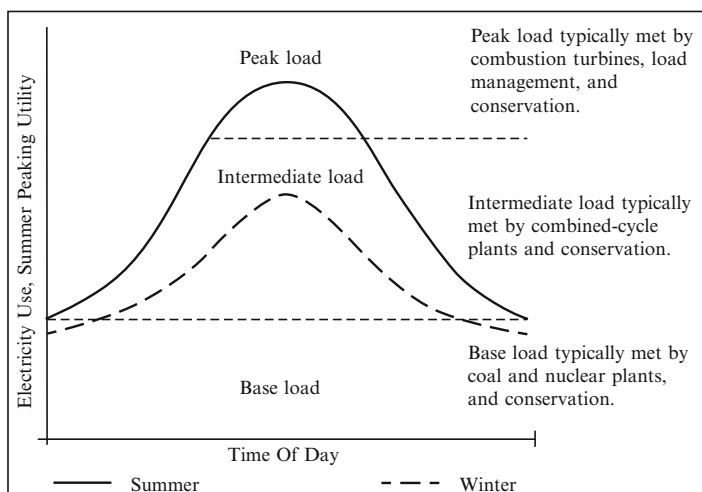


**Fig. 3.4** Typical electric load curve

times. Different types of plants using different fuels or combinations of fuels are needed to fulfill one or more of these three types of demand.

2. **Energy use**, as opposed to demand, is the total amount of measured electricity that consumers use over time. Energy use is typically measured in kilowatt-hours (kWh). A kWh is equal to the energy of 1 kW for 1 h, and 1000 kWh equals 1 megawatt-hour (MWh).
3. **The capacity factor** of a power plant is the actual output of the plant over a period of time compared to its potential output if it had operated at full nameplate capacity the entire time. It generally relates to how often a plant is run over the course of a year and is expressed as a ratio or percentage. For instance, new, more efficient coal-fired plants might have a capacity factor of 80 % because they would be producing electricity 80 % of the time, while older, less efficient coal-fired plants might have a capacity factor of 40 % because they would be in operation only 40 % of the time.

Base load plants provide a base level of electricity to the system and are typically large generating units. Base load plants operate almost continuously (approximately 70–80 % of the time), except when they are shut down for scheduled preventive maintenance, repairs, or unplanned outages. They take a long time to ramp back up to full capacity and have limited to no ability to vary their output of electricity.

In contrast, plants that satisfy peak demand (peaker plants) are highly responsive to changes in electricity demand. They can be turned off and on relatively quickly. However, they typically operate less than 10 % of the time. Peaker plants are most often natural gas combustion turbines and are relatively expensive to operate but cost less to build than base load or intermediate load plants.

As the preceding discussion makes clear, flexibility, control, and reliability are the key variables in electricity supply, and on this basis electricity sources can be ranked in the following categories.

1. **Class 1 electricity:** This class is derived from energy stores, can be switched on and off and ramped up and down with little reduction in efficiency; this category includes the following types of plants:
  - Combined-cycle gas turbines (CCGTs),
  - Coal-fired power,
  - Hydroelectric power,
  - Geothermal power.
2. **Class 2 electricity:** This class of energy is derived from energy stores, tends to be on all the time, providing a stable base load but contributing little to load variance; this category includes:
  - Nuclear power
3. **Class 3 electricity:** This class of energy refers to intermittent energy flows from renewable energy sources and these include the following types of power:
  - Solar power,
  - Tidal power,

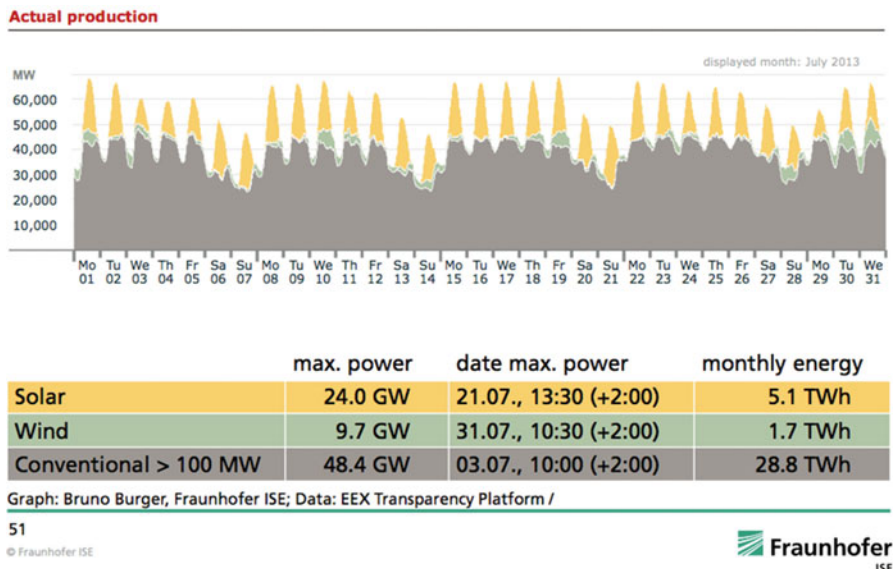


**Fig. 3.5** Electricity production in Germany: July 2013 (courtesy Professor Bruno Burger)

- Window power,
- Hydrogen power.

Of these, some power providers and owners of electricity generation plants strongly believe that solar is by far superior since it is predictably intermittent and on during the day, every day, when demand is highest (Fig. 3.5, German production electricity). Tidal power is also predictably intermittent but supply is not as well correlated with demand as solar. Wind is the worst of all and is best described as randomly intermittent. Class 3 electricity can be converted to Class 1 if large-capacity storage is available, but this remains an elusive goal.

The classification given earlier is based on the engineering requirements of balancing the grid. If you were to perform the same exercise from the perspective of CO<sub>2</sub> emissions, you would derive a different hierarchy. Solar may actually deserve to be elevated to Class 1. On the daily cycle, solar performs very well (Fig. 3.5), but on an annual cycle it does not at the high to middle latitudes of West Europe. Solar is on during the day when it is most needed, but largely off in winter, when it is also in high demand. This is one of the driving factors behind the push for hydrogen production plants (HPPs) as a means of renewable energy delivery for electricity. Bear in mind that as part of the power generation options, the need for a low-cost, continuous, reliable supply can be distinguished from peak demand, which occurs for a few hours daily and can command higher prices. Supply needs to match demand instantly and reliably over time.

This is another justification for satisfying world demand for more energy using nuclear power. In particular, consider the following factors:

- The world will need greatly increased energy supplies in the next 20 years, especially cleanly generated electricity.
- Electricity demand is increasing twice as fast as overall energy use and is likely to rise by more than two-thirds in the period 2011–2035. In 2012, 42 % of the primary energy used was converted into electricity.
- Nuclear power provides about 11 % of the world's electricity, and 21 % of the electricity in Organization for Economic Co-operation and Development (OECD) countries.
- Nuclear power is the most environmentally benign way of producing electricity on a large scale.
- Renewable energy sources such as solar and wind are costly per unit of output and are intermittent but can be helpful at the margins in terms of providing clean power.

Several characteristics of nuclear power make it particularly valuable apart from its actual generation cost per unit, megawatt-hour or kilowatt-hour. Fuel represents a low proportion of nuclear power costs, making power prices stable, its fuel is on site (not depending on continuous delivery), it is dispatchable on demand, it has fairly quick ramp-up, it contributes to clean air preservation and low-CO<sub>2</sub> objectives, and it gives good voltage support for grid stability. These attributes are mostly not monetized in commercial markets but have great value that is being increasingly recognized where dependence on intermittent sources has grown and governments are trying to address issues of long-term reliability and security of supply.

Knowing how one's electric use is billed and how demand and energy charges are calculated will help end users understand and manage their total energy costs. Figure 3.6 depicts a path to such understanding.

The following electricity use diagram shows the difference between energy (kWh) and demand (kW):

To have a better understanding of the energy charges on one's bill, the bill will indicate how much energy was used during on-peak hours (between 9 a.m. and 9 p.m. Monday–Friday) and off-peak hours (between 9 p.m. and 9 a.m. Monday–Friday) and on weekends and designated holidays (New Year's Day, Memorial Day, Independence Day, Labor Day, Thanksgiving Day, Christmas Day). Customers billed based on an amount of consumption that is less than 10,000 kWh/month or more, for example, will notice that the kilowatt-hour energy charge is more during on-peak hours than during off-peak hours.

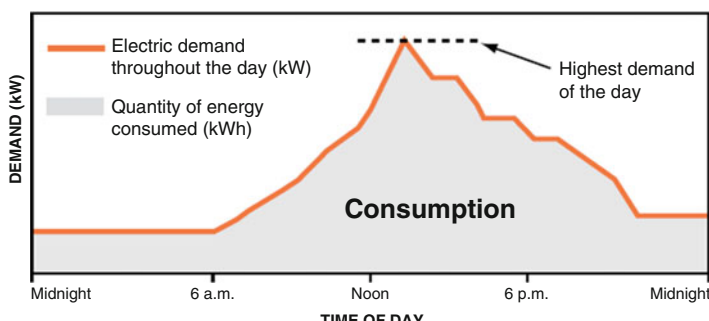


**Fig. 3.6** Sample of electricity use profile

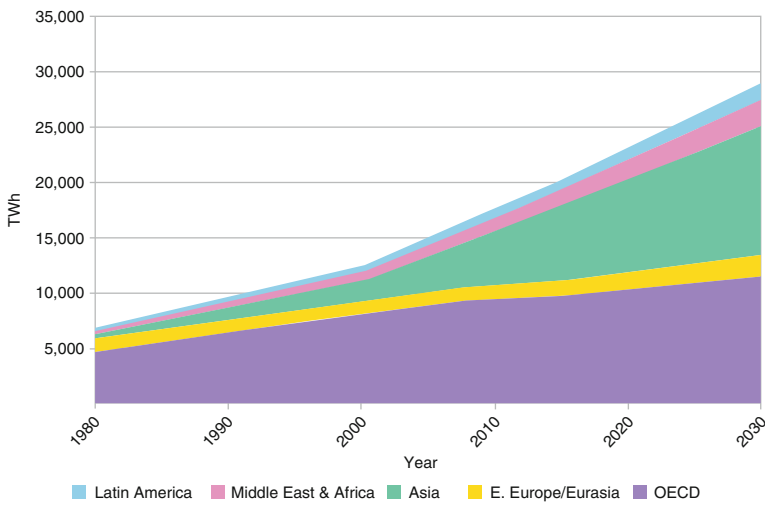


**Fig. 3.7** Worldwide electricity consumption by region

With the United Nations (UN) predicting world population growth from 6.7 billion in 2011 to 8.7 billion by 2035, demand for energy must increase substantially over that period. Both population growth and increasing standards of living for many people in developing countries will cause strong growth in energy demand, as outlined earlier. Over 70 % of the increased energy demand will come from developing countries, led by China and India; China overtook the USA as the top CO<sub>2</sub> emitter in 2007. Superimposed on this, the UN Population Division projects an ongoing trend of urbanization, from 52 % in 2011 to 62 % in 2035 and reaching 70 % worldwide by 2050, enabling world population to stabilize at about nine billion with better food supplies, clean water, sanitation, health, education, and communication facilities<sup>4</sup> (Fig. 3.7).

The World Energy Outlook 2013 from the OECD's International Energy Agency (IEA) sets out the present situation and also presents current policies, new policies, and carbon reduction (450) scenarios. From 2000 to 2010 total world primary energy demand grew by 26 %, and by 2020 it is projected to grow less (by 20 % under current policy scenarios, less under other scenarios). Growth to 2035 is projected to be 45 % under current policies and 33 % under a more restrained scenario. Electricity growth will approximately double this in each case. Electricity demand almost doubled from 1990 to 2011 and is projected to grow 81 % from 2011 to 2035 (from 19,004 to 34,454 TWh) in the current policy scenario and 69 % (to 32,150 TWh) in the central New Policies scenario. Increased demand is most dramatic in Asia, projected to average 4.0 % or 3.6 % per year to 2035. Currently some two billion people have no access to electricity, and it is a

<sup>4</sup> <http://www.nxuranium.com/primary-energy-and-electricity-outlook>

high priority to address this lack. Electricity Information 2013 from the IEA gives the latest available data on world electricity generation and its fuels.

As was demonstrated earlier, the renewable energy sources for electricity constitute a diverse group, from wind, solar, tidal, and wave energy to hydro, geothermal, and biomass-based power generation; currently Germany and Japan lead in R&D because they are looking closely at hydrogen production as another power generation option. Apart from hydropower in the few places where it is plentiful, none of these is suitable, intrinsically or economically, for large-scale power generation where a continuous, reliable supply is needed.

Growing use will, however, be satisfied by renewable energy sources in the coming years, although their role will be limited by their intermittent nature. In addition, their economic attractiveness remains an issue. Renewables will have most appeal where the demand is for a small-scale, intermittent supply of electricity. In the OECD about 2 % of electricity comes from renewables other than hydro and this is expected to increase to 4 % by 2015.<sup>5</sup> Figure 3.8 shows that much of the electricity demand is in fact for continuous, twenty-four-hour supply (base load), while some is for a lesser amount of predictable supply for about three-quarters of the day, and less still for variable peak demand up to half the time.

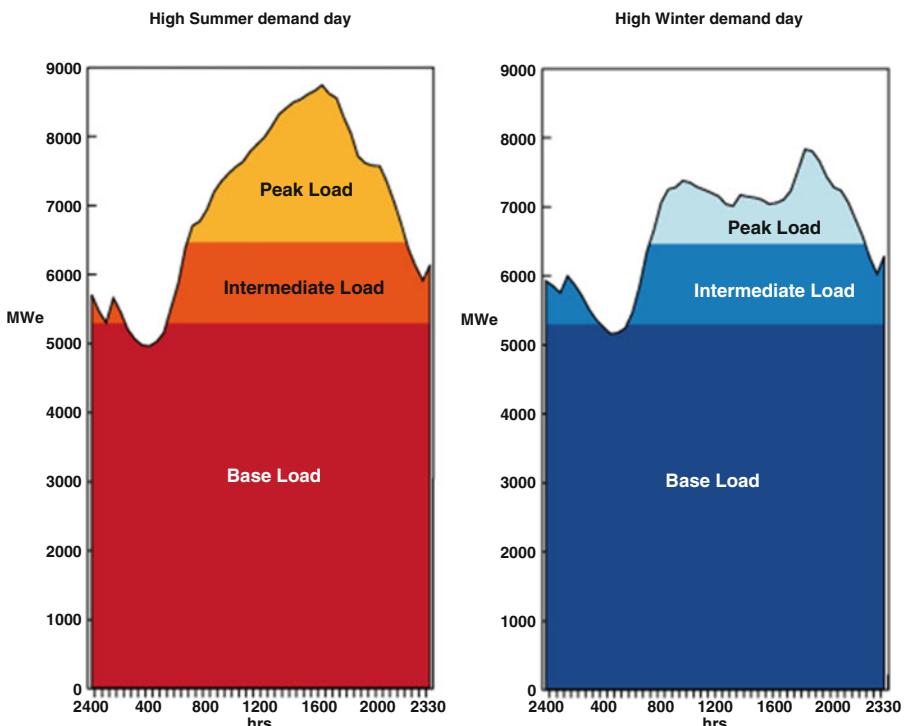


Fig. 3.8 Load curves for typical electricity grid (courtesy World Nuclear Association)

<sup>5</sup> <http://www.world-nuclear.org/info/Current-and-Future-Generation/World-Energy-Needs-and-Nuclear-Power/>

### 3.3 Hydrogen as a Source of Renewable Energy

Hydrogen is considered to be the main choice for storing renewable energy as it is easily transported and stored in large amounts. A major advantage of hydrolysis is that it produces hydrogen in a clean way. The problem is that it needs a source of electrical power in the first place. A new working project in Prenzlau, 75 miles North of Berlin in Germany, aims to combine the advantages of wind power and hydrogen to overcome the problems of both forms of power production and to embrace the advantages.<sup>6</sup>

The three wind turbines at the Prenzlau project can each produce 2 MW of power. Based on an estimated assumption that 1 MW can supply enough power for 240–500 households, WindUpBattery estimates that three turbines together should be able to supply enough energy to power between 720 and 1500 homes, assuming a constant wind supply. But the wind is not constant or reliable, so when it comes to future power companies working out how many homes should be powered by a certain number of wind turbines, the calculations need to take into consideration periods of low wind. This, combined with the fact that people do not use a set amount of electricity constantly but instead vary their demands during the day, means that there is always the possibility of differences between supply and demand.

Interestingly, according to Vattenfall, one of the energy companies participating in the Prenzlau project, currently there is no system within the renewable energy sector that is designed to compensate for supply and demand differences. Wind farms produce energy that is fed directly to the power grid, but the challenge is to develop and employ a way of storing energy when wind power production is greater than demand. The Prenzlau project enables a balance to be found in renewable energy production systems. Operating on 6 MW, this is the first full-scale European hybrid power plant to convert the variable nature of wind power into hydrogen for a reliable long-term renewable energy source for general electricity usage and for use in hydrogen fuel-cell-powered cars and other means of transport, as well as for heat to cofire the power plant itself.<sup>7</sup>

From the three 2 MW wind turbines, electric power can either be fed straight to the power grid or to an electrolysis unit that is used to produce hydrogen, which is then stored in the plant's hydrogen storage tanks. From there the hydrogen can then be fed along the system and mixed with biogas from a separate unit at the plant, and this mixture can be used to run two combined heat and power plants to produce both electricity for the power grid and district heating at times when high demand coincides with low wind power production (Fig. 3.9).

Alternatively the hydrogen from the storage tanks can be used at vehicle filling stations in certain locations and facilities that can be run by energy-related companies to supply fuel cell cars and other vehicles.

<sup>6</sup> <http://www.windupbattery.com/wind/hydrogen-hybrid-prenzlau.htm>

<sup>7</sup> <http://www.windupbattery.com/wind/hydrogen-hybrid-prenzlau.htm>

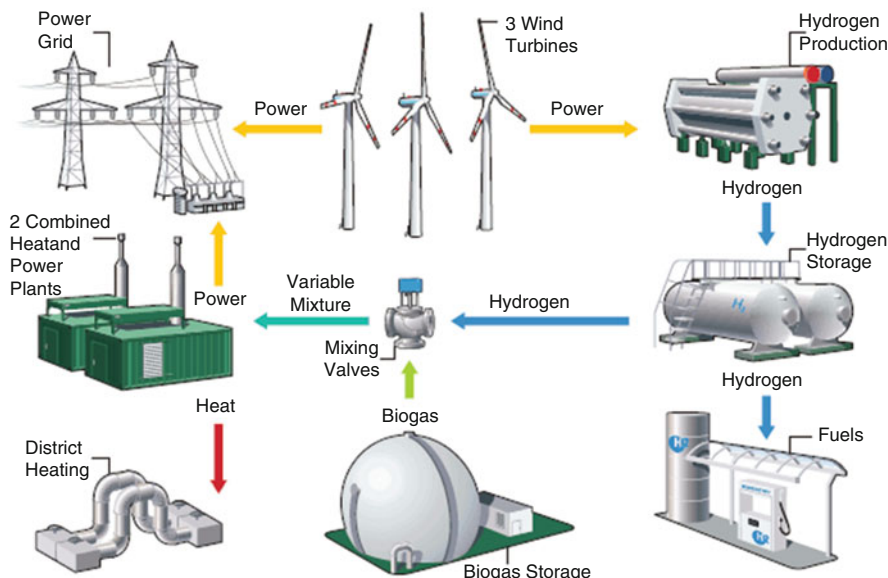


**Fig. 3.9** Hydrogen production plant based on wind energy (courtesy Prenzlau Corp.)

Hydrogen is a significant chemical product where about half of the annual production is used in making nitrogen fertilizers and about half to convert low-grade crude oils (especially from tar sands) into transport fuels.<sup>8</sup> Both uses are increasing significantly. Some is used for other chemical processes. World consumption in 2009 was about 70 million tonnes<sup>9</sup> per year, growing at about 7 % per annum. There has been considerable experience built up in connection with handling hydrogen on a large scale, though it is not entirely straightforward. About 96 % of hydrogen is made from fossil fuels: half from natural gas, 30 % from liquid hydrocarbons, and 18 % from coal. This gives rise to quantities of carbon dioxide emissions—each tonne produced gives rise to 11 tonnes of CO<sub>2</sub>. Electrolysis accounts for only 4 %.

### 3.3.1 Why Hydrogen as a Source of Renewable Energy Now?

At the rate at which we are burning fossil fuels owing to increasing demands on electricity driven by the growth of world population, there exists a looming specter of the exhaustion of fossil-based resources; therefore, many industrialized

<sup>8</sup> Eg (CH)<sub>n</sub> tar sands or (CH<sub>1.5</sub>)<sub>n</sub> heavy crude to (CH<sub>2</sub>)<sub>n</sub> transport fuel. Upgrading heavy crude oil and tar sands requires 3–4 kg of hydrogen per barrel (159 L) of product.

<sup>9</sup> In thermal terms @ 121 MJ/kg: 8470 PJ, equivalent to all of US nuclear electricity.

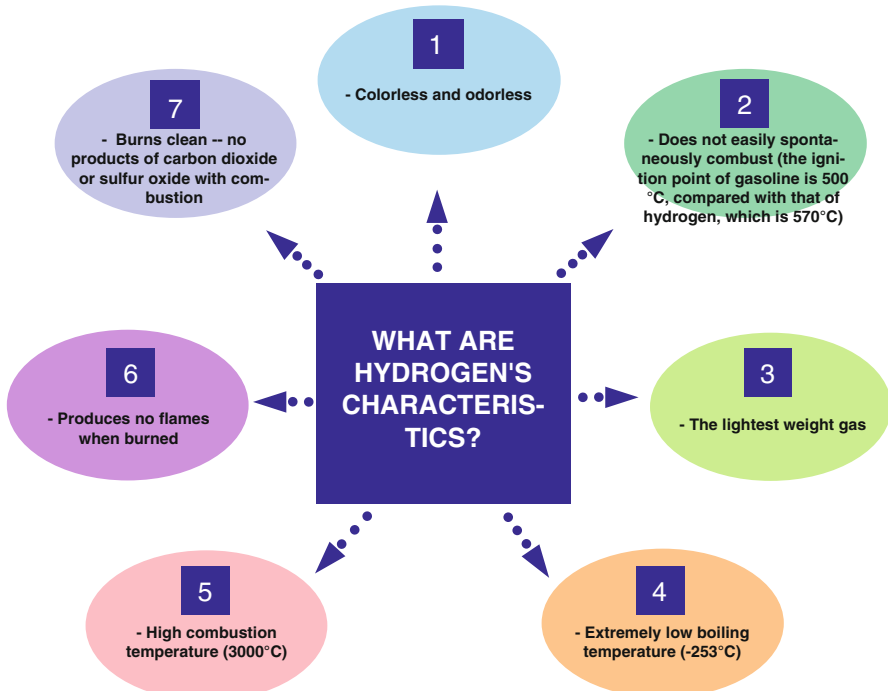


**Fig. 3.10** Hydrogen characteristics

countries, in their search for more electrical energy, are conducting intensive R&D on various kinds of new energy. Recent global environmental problems have made more urgent the need to use clean energy. Hydrogen seems to be an attractive source of energy because when it goes through a combustion process, water is produced. Up to now, almost all hydrogen produced for practical uses has been produced by fossil fuels.

Figure 3.10 depicts all the characteristics of hydrogen; if hydrogen could be produced by renewable energies, then energy use would truly become harmonized with the environment.

As a matter of fact, the Iwatani Corporation, with headquarters in Osaka and Tokyo, Japan, with capital of 20 billion yen, was the first company to produce liquid hydrogen at its Industrial Gases Corporation Chiba plant in Ichihara, Chiba, as a renewable source of energy to meet the increasing demands for liquid hydrogen nationwide and to improve the stability of the supply chain system. This plant has been in operation since July 2009 and is the first liquid hydrogen plant in eastern Japan, along with Hydro-Edge facilities in Sakai and Osaka, which started operations in April 2006 and has established a hydrogen supply chain system to improve manufacturing efficiency and supply stability, logistical efficiency, and the back-up system with two bases located in eastern and western Japan as part of its ongoing R&D program to move forward with HPPs (Fig. 3.11).



**Fig. 3.11** Liquid hydrogen facility in Japan (courtesy Iwatani Corporation)

Companies like Iwatani, with its plant that uses hydrogen byproduct produced by the adjacent factory in the industrial complex as material, has a liquid hydrogen manufacturing capability of 3000 L/h and a storage capacity of 300 kiloliter (kL).

### **3.3.2 Technical Development of Hydrogen Production**

As part of the process to produce hydrogen in particular in the liquid form, some manufacturers are using a solid polymer electrolyte membrane water electrolysis (SPE) approach as part of their production plan. The reasoning behind this is that SPE supposedly attains a higher current density and higher estimated energy efficiency, over 90 % compared to alkaline water electrolysis at current commercial market values.

Note that the SPE process is still in a premature stage of research, and technology must be focus on increasing its scale and life expectancy. Figure 3.12 is a snapshot of a conceptual production plant for the SPE process.

As part of producing hydrogen as a new source of energy, one should analyze the capital and operating costs associated with storing and transporting hydrogen if the production plant is not close to the end user facility. The storage techniques considered by industry center on liquid hydrogen, compressed gas, metal hydride, and underground storage facilities, and the transport of liquid hydrogen for delivery by truck, rail, and barge seems very feasible. Gaseous hydrogen delivery by truck, rail, and pipeline is another transport mode; finally, for metal hydride delivery, truck and rail can be considered [1].

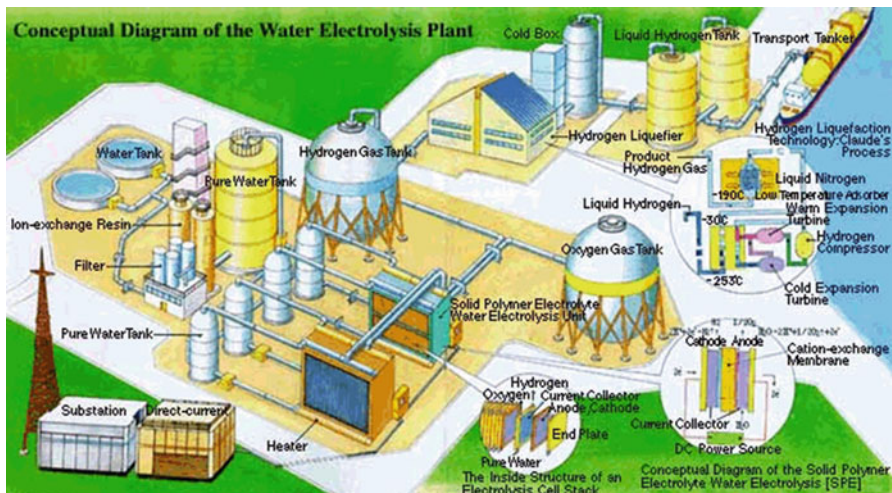


**Fig. 3.12** SPE conceptual of water electrolysis plant (courtesy World Energy Networking) (<https://www.enaa.or.jp/WE-NET/index.html>)

The optimum options for storing hydrogen are as follows:

1. Compressed gas,
2. As form of liquid,
3. Combined with metal hydride.

Underground storage might also be possible, although it is just a special case of compressed gas storage. Each option has pros and cons. For instance, liquid hydrogen has the highest storage density of any method, but it also requires an insulated storage container and an energy-intensive liquefaction process. Hydrogen can be liquefied by cooling the gas to form a liquid, and the process uses a combination of compressors, heat exchangers (a subject of this book), expansion engines, and throttle valves to achieve the desired cooling [2].

The simplest method for liquefaction is either a Linde cycle or a Joule–Thompson expansion cycle, where the hydrogen gas is at ambient pressure and then cooled in a heat exchanger before passing through a nozzle valve where it undergoes isenthalpic Joule–Thompson expansion, producing liquid. Flowcharts for both the Linde process and temperature-entropy techniques are shown in Figs. 3.13 and 3.14, respectively.

For further and more detailed information, the reader is encouraged to consult Flynn [2].

The Linde cycle works for gases, such as nitrogen, that cool upon expansion at room temperature. Hydrogen, however, warms upon expansion at room temperature. In order for hydrogen gas to cool upon expansion, its temperature must be below its inversion temperature of 202 K ( $-95^{\circ}\text{F}$ ). To reach the inversion temperature, modern hydrogen liquefaction processes use liquid nitrogen precooling to

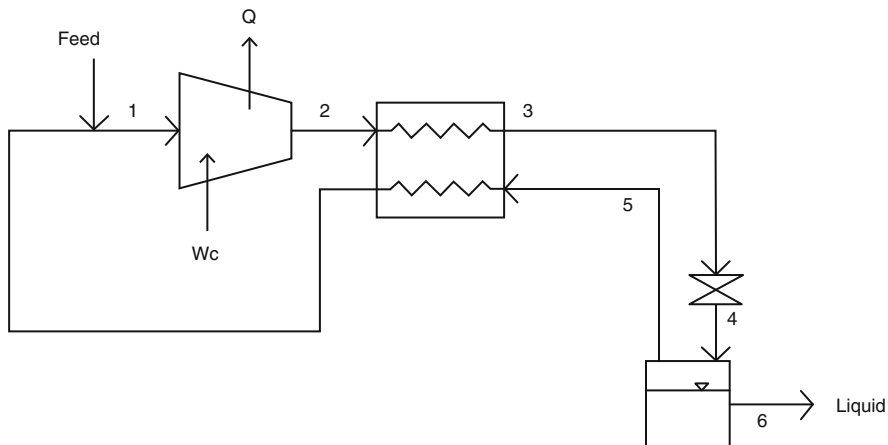


Fig. 3.13 Linde liquefaction process flowchart [1]

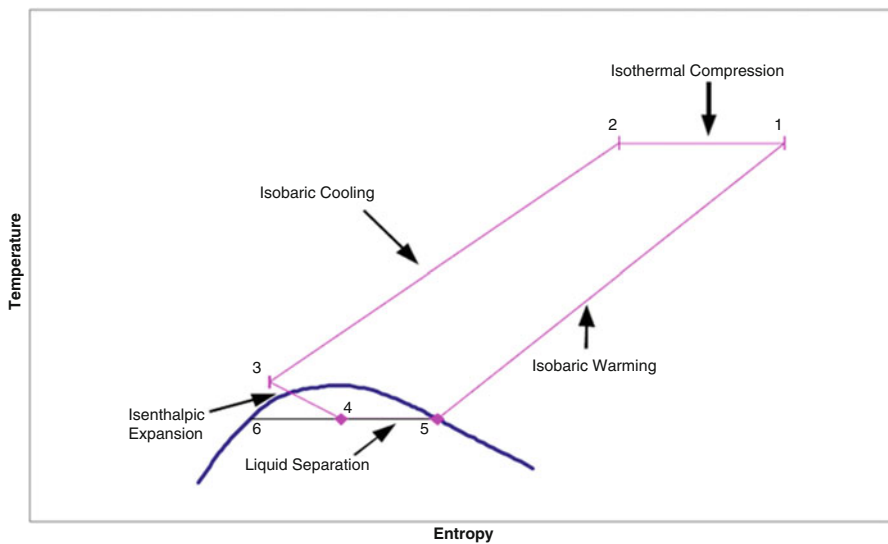
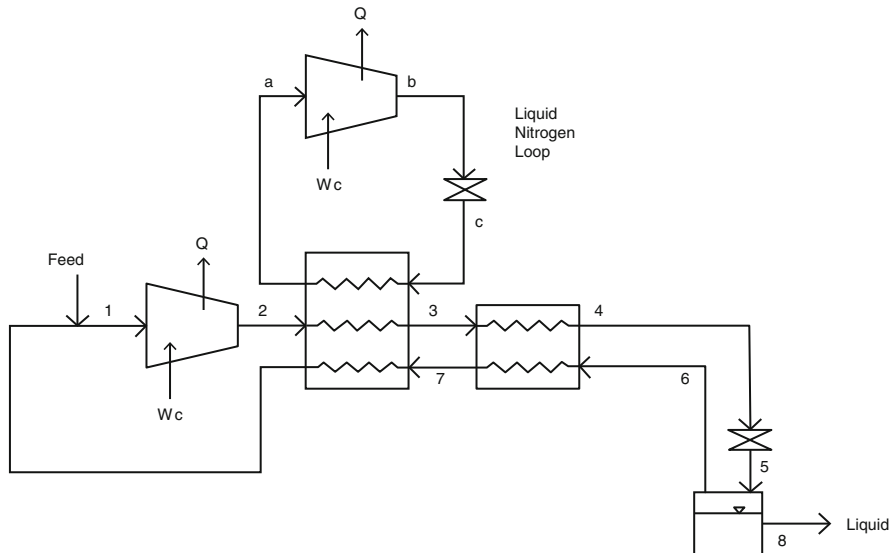


Fig. 3.14 Linde process temperature-entropy diagram [1]

lower the temperature of the hydrogen gas to 78 K ( $-319^{\circ}\text{F}$ ) before the first expansion valve. The nitrogen gas is recovered and recycled in a continuous refrigeration loop (Flynn [2]; Timmerhaus and Flynn [3]).

The precooled Linde process is shown in Fig. 3.15. Figure 3.16 is the associated temperature-entropy diagram for the process.

An alternative to the precooled Linde process is to pass the high-pressure gas through an expansion engine. An expansion engine, or turbine, will always cool a



**Fig. 3.15** Precooled liquefaction flowchart [1]

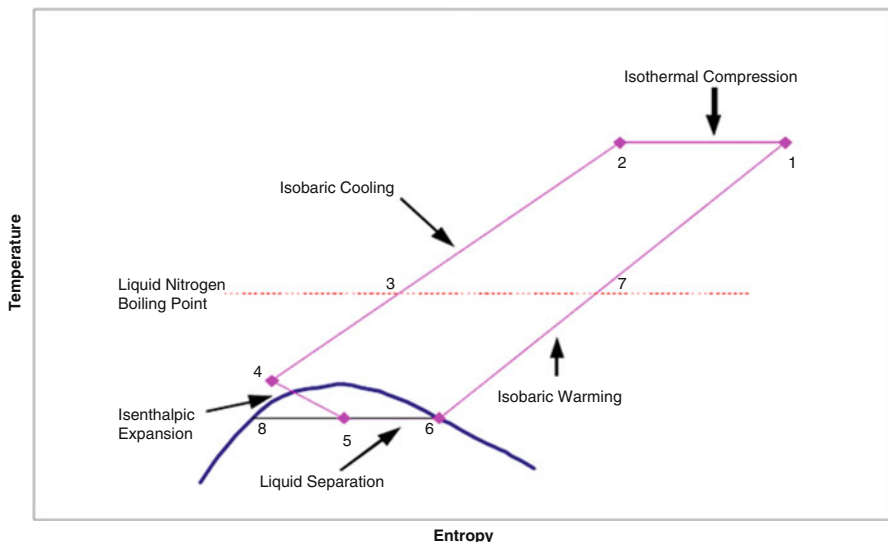


**Fig. 3.16** Precooled liquefaction temperature-entropy diagram [1]

gas, regardless of its inversion temperature (Flynn) [2]. The theoretical process referred to as ideal liquefaction uses a reversible expansion to reduce the energy required for liquefaction. It consists of an isothermal compressor followed by an isentropic expansion to cool the gas and produce a liquid.

Hydrogen liquefaction technology development will consist of system optimization, a large-scale compressor, and a large-scale expansion turbine.

### ***3.3.3 Technical Development for Hydrogen Product Transport and Storage***

For the purpose of transporting hydrogen products to end users and store them for further use later on by consumers, research will have to be done on hydrogen tankers for transport, storage systems, various related machinery and equipment (pumps, piping, valves, and so on) for liquid hydrogen, and metal hydride alloys to be used in distributed storage and transportation facilities. Based on this research, information concerning the transportation and storage of liquid hydrogen will be gathered. A structural material will be developed to withstand the extremely low temperature of liquid hydrogen ( $-253^{\circ}\text{C}$ ). In the previous section we expanded upon storage options and production of the hydrogen in liquid form and briefly discussed processes such liquefaction.

Compressed gas storage of hydrogen is the simplest storage solution– the only equipment required is a compressor and a pressure vessel (Schwarz and Amonkwah) [4]. The main problem with compressed gas storage is the low storage density, which depends on the storage pressure. Higher storage pressures result in higher capital and operating costs (Garret) [5]. Compressed gas storage, liquefaction, underground storage, and pipelines all require compressors; only metal hydride storage does not, although a compressor may also be used for hydrides depending on the hydride plateau pressure (Schwarz and Amonkwah) [4].

Underground storage depends on the local geology. Underground storage of hydrogen gas may be possible [6]. Underground storage of natural gas is common and underground storage of helium, which diffuses faster than hydrogen, has been done successfully in Texas [7].

Pipeline storage of hydrogen requires systems that are usually extended to several miles of piping and in some cases may be hundreds of miles long. Because of the great length, and therefore great volume, of these piping systems, a slight change in the operating pressure of a pipeline system can result in a large change in the amount of gas contained within the piping network. By making small changes in the operating pressure, the pipeline can be used to handle fluctuations in supply and demand, avoiding the cost of on-site storage (Hart 1997; Report to Congress 1995) [7].

Good details on the capital costs of these storage options are given by Wade A. Amos [1], and readers should refer to his report.

## **3.4 Development of a Hydrogen Combustion Turbine**

In connection with HPPs and in consideration of hydrogen as a renewable source of energy, it will be necessary to design some kind of hydrogen combustion turbine and do basic R&D on its optimum operation and cost-related issues.

A hydrogen combustion turbine is an extremely clean system for the environment. The system emits no carbon dioxide, sulfur oxide, or nitrogen oxide because the combustion process only uses hydrogen and oxygen. The energy efficiency of a hydrogen combustion turbine is expected to be 60 %, even at a temperature of 1200 °C at the entrance of the turbine, because there is no exhaust gas and therefore no exhaust gas loss. Concerning the hydrogen combustion turbine, as part of an overall project plan for its design the following items should be addressed in Phase I:

1. System optimization,
2. Combustion control technology,
3. Major components (turbine blade, rotor),
4. Major auxiliaries, and
5. Super-high-temperature materials.

These research results will eventually be applied to a hydrogen combustion turbine at a pilot or prototype plant. These items can also be considered in a feasibility study on hydrogen production at existing nuclear power plants (i.e., Generation III) or as part of Next Generation Nuclear Plants (NGNPs), (i.e., Generation IV), in which case an intermediate heat exchanger subsystem in the loop between the primary and secondary loop of a nuclear plant (discussed in this book) will have to be considered. Another common denominator is cycles such as the Brayton combined cycle to drive higher efficiency [8, 9] or nuclear air-Brayton combined cycle (NACC) [10], taking advantage of reactors such as a very-high-temperature reactor (VHTR) that operate at similar temperatures as part of a family of NGNPs and that require super-high-temperature materials. Figure 3.17 is a sketch of a conceptual model of a hydrogen combustion turbine.

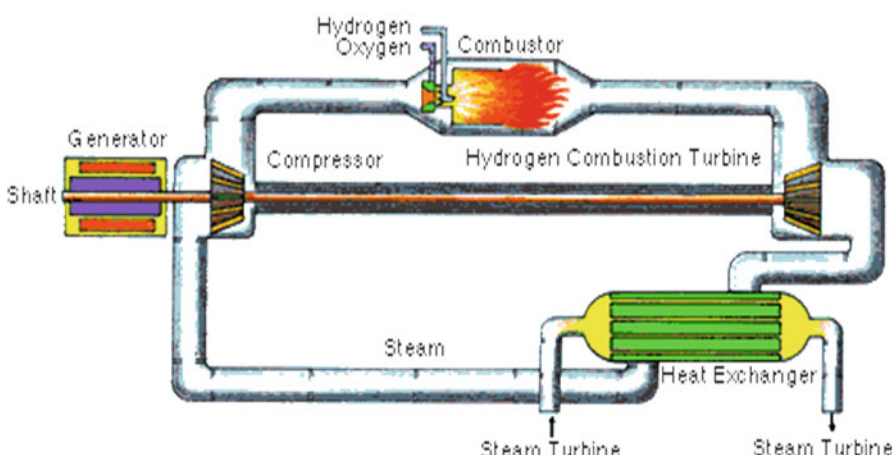


Fig. 3.17 Conceptual model of hydrogen combustion turbine

### 3.5 Feasibility Study on Hydrogen Energy Use

The use of hydrogen as a source of renewable energy requires estimating the level of hydrogen consumption in different sectors such as electric power, transportation, industry, and public welfare as depicted in Fig. 3.18. The utilization of liquid hydrogen for cryogenic energy will also need to be investigated and reviewed. If this source of energy can be realized and disseminated throughout the world early on in this century and the next, we will see hydrogen being used not only to run automobiles and fly aircraft, but also to power all appliances necessary for our day-to-day living (Fig. 3.19).

Hydrogen can be used and burned as fuel for transport, and it produces only water vapor, with no carbon dioxide or carbon monoxide. However, it is far from being an energy-dense fuel, and this limits its potential use for motor vehicles. By March 2014, there were 186 hydrogen refueling stations worldwide, 26 of them in Germany, and they were mainly used in trials of fuel cell vehicles; Japan has also been pushing for migration to fuel cell vehicles (FCVs) as well (Fig. 3.20).

Several automotive companies have developed demonstration hydrogen fuel cell vehicles (HFCVs). The Honda FCX Clarity, Chevy Equinox Fuel Cell, and others have been demonstrated. Other original equipment manufacturers (e.g., Toyota) have announced plans for FCVs. The rarity of the platinum currently used in fuel cells may be a problem for widespread adoption, along with the expense of the fuel

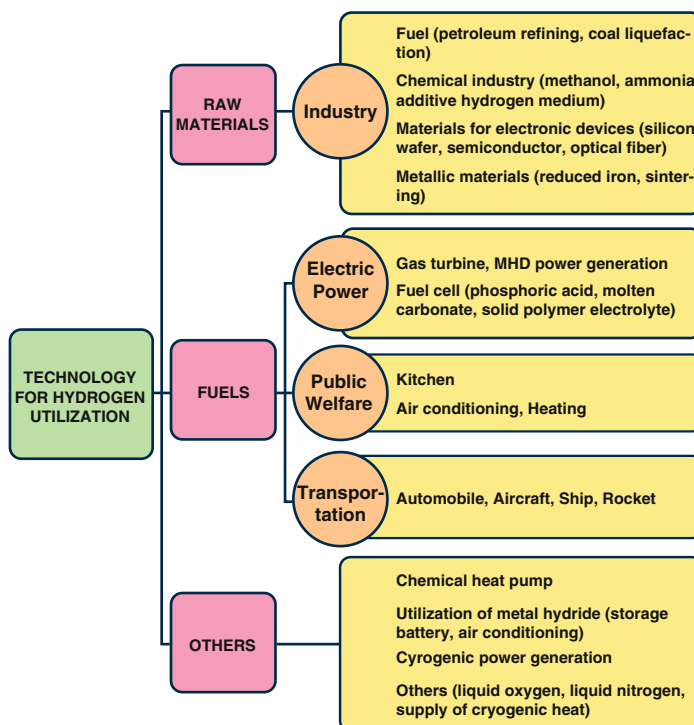


**Fig. 3.18** Forms of hydrogen utilization

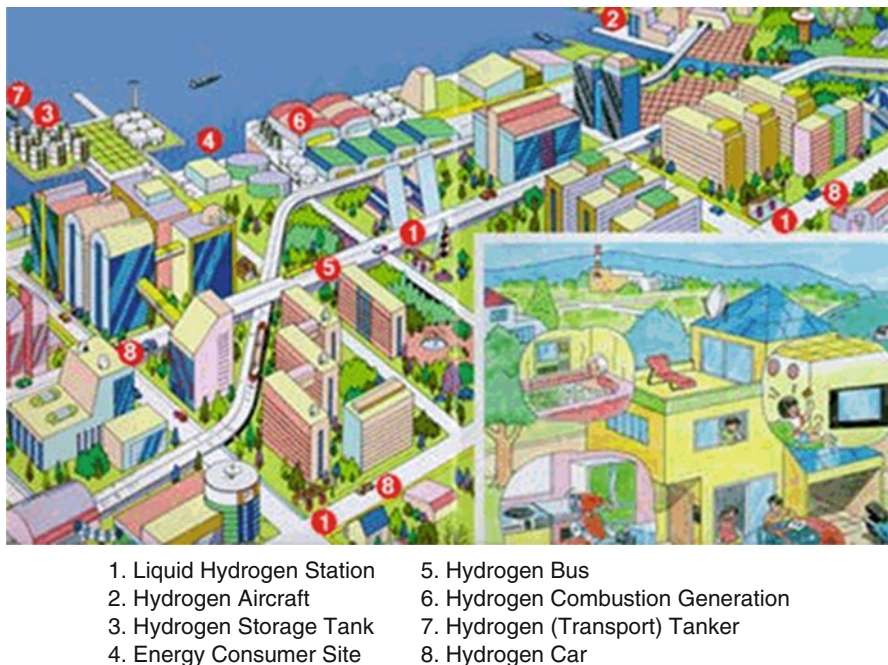


**Fig. 3.19** Utilization of hydrogen energy in twenty-first century and beyond



**Fig. 3.20** Honda FCX clarity and Silverado hydrogen internal combustion engine truck

cell itself. However, incentives and political focus can push development forward and prices down.

Hydrogen can be burned in a normal internal combustion engine, and some test cars are in operation. Trials in aircraft have also been carried out. In the immediate future the internal combustion engine is the only affordable technology available for using hydrogen. For instance, 100 BMW Hydrogen 7s have been built, and 25 were used in test programs in the USA. The cars covered more than 2 million kilometers in test programs around the globe. BMW is the only car manufacturer to have used hydrogen stored in its liquid state. The low energy density of 10.1 MJ/L is the limiting factor (cf. 3.5 times this for petrol), coupled with the need to cool the

170 L tank to  $-253^{\circ}\text{C}$ . BMW has abandoned this development and is collaborating with Toyota on FCVs, with a view to marketing a joint mid-sized platform and fuel cell stack by 2020.<sup>10</sup>

### 3.6 Hydrogen Production Using Nuclear Energy

Nuclear-generated hydrogen has important potential advantages over other sources that will be considered for a growing share of hydrogen in a future world energy economy. Still, there are technical uncertainties in nuclear hydrogen processes that need to be addressed through vigorous R&D efforts. Safety issues as well as hydrogen storage and distribution are important areas of research to be undertaken to support a successful hydrogen economy in the future.

The hydrogen economy is gaining higher visibility and stronger political support in several parts of the world. In recent years, the scope of the IAEA's program has been widened to include other more promising applications such as nuclear hydrogen production and higher-temperature process heat applications. The OECD (Organization for Economic Co-operation and Development) Nuclear Energy Agency, Euratom, and the Generation IV International Forum have also shown interest in the nonelectric applications of nuclear power based on future-generation advanced and innovative nuclear reactors.

Nuclear power already produces electricity as a major energy carrier. It is well placed, though beyond the capability of most current plants, to produce hydrogen if this becomes a major energy carrier.

The evolution of nuclear energy's role in hydrogen production over perhaps four decades has followed the following steps:

1. Electrolysis of water, using off-peak capacity;
2. Use of nuclear heat to assist steam reforming of natural gas;
3. High-temperature electrolysis of steam, using heat and electricity from nuclear reactors;
4. High-temperature thermochemical production using nuclear heat.

The first three are essentially cogeneration or known as combined heat and power (CHP). The last three are described in detail in the paper in this series "Nuclear process heat for industry." See also the 2013 I.E. technical report: *Hydrogen Production Using Nuclear Energy*.<sup>11</sup>

The projection of the European Commission High Level Group shown in Fig. 3.21 offers a realistic scenario of the hydrogen market and the application areas. The figure clearly shows that the largest near-term markets will be the

<sup>10</sup> <http://www.world-nuclear.org/info/Non-Power-Nuclear-Applications/Transport/Transport-and-the-Hydrogen-Economy/>

<sup>11</sup> [http://www-pub.iaea.org/MTCD/Publications/PDF/Pub1577\\_web.pdf](http://www-pub.iaea.org/MTCD/Publications/PDF/Pub1577_web.pdf)

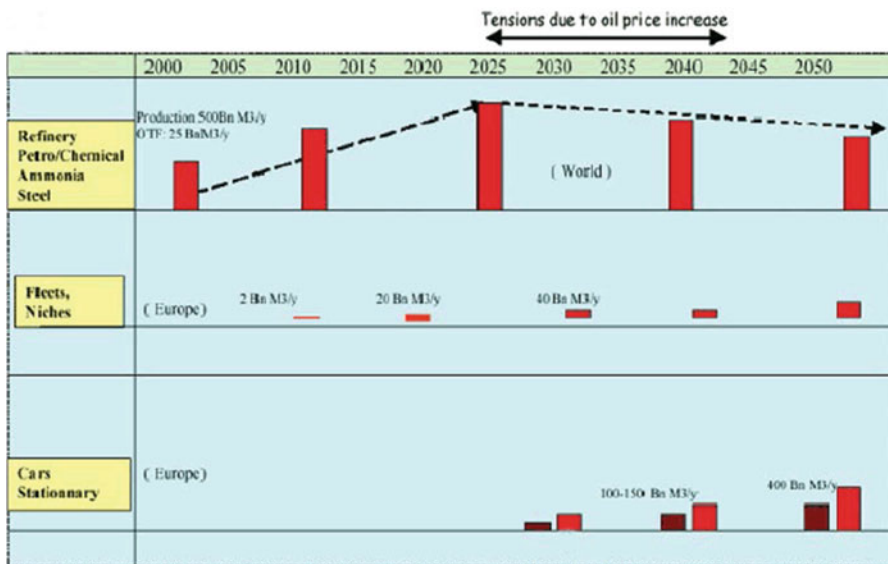


Fig. 3.21 Hydrogen production roadmap

petrochemical industry, requiring massive amounts of H<sub>2</sub> for the conversion of heavy oils, tar sands, and other low-grade hydrocarbons, as well as the fertilizer and steel industries.

Per our earlier discussion, hydrogen's main application as a source of fuel for transportation use is in fuel cells. Conceptually speaking, a fuel cell can be considered a refuelable battery, making electricity as a direct product of a chemical reaction, except that, whereas a normal battery has all the active chemical ingredients built in at the factory, fuel cells are supplied with fuel from an external source and oxygen from the air.

These fuel cells catalyze by converting the oxidation of hydrogen straight to electricity energy in cryogenic (relatively low temperatures) mode in a very efficient way. The claimed theoretical efficiency of converting chemical to electrical energy to power cars, according to Japanese scientists who have researched hydrogen as a renewable energy, is about 60 % or more. However, in practice about half that amount of efficiency has been demonstrated, except for high-temperature solid oxide fuel cells, which peaked at 46 %.

### Definition of Cogeneration

Cogeneration or CHP is the use of a heat engine or power station to generate electricity and useful heat at the same time. Trigeneration, or combined cooling, heat, and power (CCHP), refers to the simultaneous generation of electricity and useful heating and cooling from the combustion of a fuel or a solar heat collector. See Fig. 3.22 for the layout of a typical trigeneration power plant.

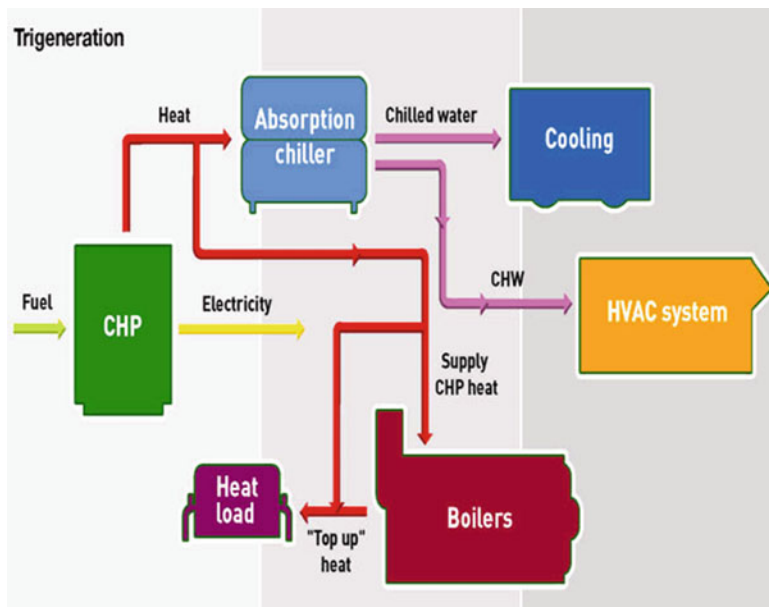


**Fig. 3.22** Diagram of typical trigeneration power plant

In terms of the advantages and disadvantages of hydrogen use in fuel cells, although combustion is a carbon-free process, and then distribution to consumers, on-board storage is a challenging problem for manufacturers of FCVs, where hydrogen will be used as a source of fuel. It is impossible to store hydrogen as simply as gasoline considering the compactness and simplicity of carrying a tank of gasoline or liquefied natural gas (LNG) on-board. To overcome this problem, it has been proposed that hydrogen be stored cryogenically at a very high pressure or chemically as hydrides. The latter seems like a more promising approach than the former, although from a refueling point of view it is not as straightforward as would be desired for use in FCVs.

Pressurized storage is the main currently available technology, and this means that at 345 times atmospheric pressure (34.5 MPa, 5000 psi), 10 times the volume is required as for an equivalent amount of petrol/gasoline. By 2010, however, 680 atm (70 MPa) was practical, and the weight penalty of a steel tank was reduced through the use of carbon fiber. Earlier, the tank was about 50 times heavier than the hydrogen it stored, but now it is only about 20 times as heavy, and the new target is to make it 10 times as heavy.

Another promising development for storage systems in the literature is the use of sodium borohydride ( $\text{NaBO}_2$ ) as an energy carrier. The  $\text{NaBO}_2$  is catalyzed to yield hydrogen, leaving a borate  $\text{NaBO}_2$  to be reprocessed.

Fuel cells are currently being used in electric forklift trucks, and this use is expected to increase steadily. They apparently are not very cost effective, about three times as much as batteries, but last twice as long (10,000 h) and have less

downtime; this might change if hydrogen could be produced at lower cost by optimizing its production capabilities at existing nuclear power plants or producing it as NGNPs in the near future. The first fuel cell electric cars running on hydrogen were expected to be on the fleet market soon after 2010, but 2015 is now the target. Fuel cell buses have clocked over 2 million km, and a fleet of 20 vehicles has been used in Vancouver. Another project has 3 Mercedes Citaro buses in each of 11 cities. Japan had a goal of five million FCVs on the road by 2020.

Current fuel cell design consists of bipolar electrode plates in a frame with electrolyte between, and the most common proton exchange membrane type and fuel cells using hydrogen can also be used for standalone small-scale stationary generating plants – where higher-temperature operation (e.g., of solid oxide fuel cells) and hydrogen storage may be less of a problem, or it may be reticulated like natural gas. Cogeneration fuel cell units for domestic power and heat are being deployed in Japan under a subsidy scheme that terminated in 2012, by which time unit costs were expected to drop from US\$ 50,000 to \$6000; the units need to last for a decade.<sup>12</sup>

But at present fuel cells are much more expensive to make than internal combustion engines (burning petrol/gasoline or natural gas). In the early 2000s, proton exchange membrane (PEM) units cost over \$1000 per kW, compared with \$100/kW for a conventional internal combustion engine. The target cost for a PEM fuel cell stack is below EUR100/kW, which will require reducing the amount of palladium catalyst.

### Proton Exchange Membrane Unit

Proton exchange membrane (PEM) fuel cells work with a polymer electrolyte in the form of a thin, permeable sheet. This membrane is small and light and works at low temperatures (about 80 °C, or about 175 °F). Other electrolytes require temperatures as high as 1000 °C.

PEM technology was invented at General Electric (GE) in the early 1960s, through the work of Thomas Grubb and Leonard Niedrach. GE announced initial success in mid-1960s when the company developed a small fuel cell for a program with the U.S. Navy's Bureau of Ships (Electronics Division) and the U.S. Army Signal Corps. The unit was fueled by hydrogen generated by mixing water and lithium hydride. This fuel mixture was contained in disposable canisters that could be easily supplied to personnel in the field. The cell was compact and portable, but its platinum catalysts were expensive.

Studies on the feasibility of hydrogen production at existing nuclear power plants have been conducted by most countries with nuclear capacities, with the USA having the most nuclear power from Generation III plants in production

<sup>12</sup> <http://www.world-nuclear.org/info/Non-Power-Nuclear-Applications/Transport/Transport-and-the-Hydrogen-Economy/>

supporting a network of electricity generators on a grid system. The Idaho National Laboratory (INL) is leading efforts in R&D on this matter (Idaho National Laboratory INL/EXT-09-16326) [11].

Although the INL report concentrated on existing nuclear power in line and the current design of plants based on Generation III configurations and specifications, it made no recommendations for producing hydrogen based on current designs of Generation IV plants or NGNPs. Currently, electrolysis equipment that is sized to produce 1 kg of hydrogen per second does not exist owing to a lack of demand for such plants, but demand for existing plants are increasing significantly owing to recent efforts to find a renewable source of energy to meet demand for electricity during peak hours.

As we have discussed so far, the cost of electricity is an important consideration in the economic feasibility of any hydrogen production facility. Prior to the release of the INL report, much of the discussion on keeping electrical costs low centered on the use of production facilities during off-peak hours when costs are generally lower. However, this study shows that off-peak use only results in higher breakeven hydrogen pricing because high-capital-cost plants are idle for many hours. Indeed there are times when on-peak electrical costs are lower than off-peak costs.

A need for such a feasibility study based on existing nuclear power plants should extend beyond Generation III in transition to Generation IV and should be included as part of the overall efforts in an R&D package on NGNPs as well.

Recent experiences with combined-cycle natural gas power plants have demonstrated efficiencies approaching 60 %. A combined-cycle molten salt (MS) nuclear Brayton-Rankine cycle appears to achieve efficiencies 5–10 % higher than a straight high-temperature Rankine cycle with peak coolant temperatures near 1000 K [8–10].

The key to achieving these efficiencies is a multiturbine, multiheat exchanger system that adds as much heat as possible near the peak output temperature of the MS coolant.

Since a nuclear heating system does not consume oxygen in a Brayton working fluid, it might be possible to build a hybrid system that burns the oxygen in the air after it has been heated by nuclear heat exchangers.

This would provide a topping capability for a hybrid nuclear plant that could use natural gas to expand its power output to meet peak demand above the base-load capability of the plant. If all that is required is to initiate injection of natural gas into the flow path of the nuclear Brayton cycle, the response time for adding significant power would be very short. The details of how this might be done are intriguing. Ignition of the injected gas should not be a problem as the working fluid would be at a high temperature.

In any gas turbine system that drives a rotating shaft (e.g., turboprop, turbo shaft), the turbine load is usually split between a gas generator turbine and a power turbine. The two turbines are not on the same shaft and usually rotate at different speeds. Normally it is desirable for the power turbine (connected to the drive shaft) to maintain control over the revolutions per minute separately from the level of torque delivered. The simplistic hybrid approach that has often been proposed

would have the natural gas injected after the gas generator turbine and before the power turbine.

This will be a problem as the pressure driving the gas through the turbine will not be strong enough to overcome the resistance of the higher-temperature gas to flow through the power turbine nozzles. Some of the flow could be bled off prior to arriving at the power turbine, but that would lower the efficiency of the injected combustible mixture by about 50 %.

The combustible gas will have to be injected before the gas generator turbine so that it can drive the pressure up and get the hotter working fluid through the power turbine nozzles.

This essentially requires a Brayton power system designed for two conditions.

The peak power with the combustion taking place will be the design condition and the base-load nuclear heating will be the off-design condition.

With support from the INL under its NUEP program among universities that are involved in the effort, including the University of New Mexico, with which the present author has an association, models are currently being built to address this combination of conditions – design and off-design to quantify the tradeoffs on both the high-temperature Brayton system and the bottoming Rankine cycle.

In the classic off-design problem, the machinery is designed to operate at a specific pressure temperature point and is then operated under a different set of conditions.

Off-design operation will affect system efficiency and performance. It is important to quantify the effects of this multiple-operating-point scenario.

A base-load nuclear-only system will probably become the off-design point, and if the effects of operating at this off-design point are severe, then the concept of a hybrid system may not be viable.

The variables associated with hydrogen production, including the storage and transportation, as discussed earlier, as well as variations in costs of electricity during on-peak and off-peak hourly and seasonal consumption makes the matter of production a challenging problem using existing technologies of hydrogen production. The cost variance also has an impact on the total cost of production, transportation, and storage.

A production process such as electrolysis requires large amounts of water, which has its own issues related both to locating reliable sources of water and the purification of water. In addition, water availability can vary from year to year; in some years drought is an issue for certain regions in a country.

Producing hydrogen via nuclear energy by combining hydrogen production with a new nuclear power plant has its own sets of rules and regulations regarding safety and licensing , which are currently not well defined. This includes the study of what would be involved to build such a facility next to a nuclear power plant facility, as well as an evaluation of how utilities would meet the needs of its customer base through the vicissitudes of daily and seasonal energy demands. Although there is tremendous movement toward securing renewable energy sources, and although policies and regulations are looking to impose every more stringent requirements for clean energy and encourage the use of renewable resources such as wind or

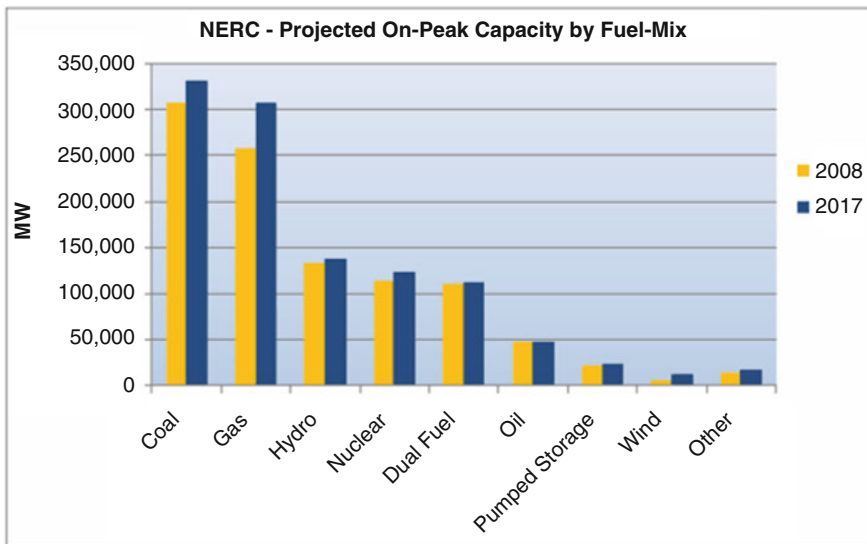


**Fig. 3.23** NERC current and projected generation capacity for electricity

solar, demands for electricity will not keep up with population growth, these two energy sources (wind and solar) will not be able to meet future energy demands, and so alternatives must be found. According to the North American Electric Reliability Corporation (NERC), which conducted an assessment of the reliability of most electric power systems in terms of continued delivery of power to meet future energy needs, , future power generation will have to include fuel mixes as sources of energy. To accomplish this, electrical utilities use various fuels, including nuclear, hydro, coal, gas, oil, wind, and solar, as energy sources for electricity generation. This diversity provides the electric utility industry independence from any single source of fuel [11].

The capability of the electric utility industry to utilize a variety of energy sources to generate electricity and to move quickly to the most economical fuel resource is an important factor in the planning of future generation resources (Fig. 3.23).

The projected growth in capacity is a response to increased demands for electricity per the NERC (Fig. 3.24); note that these graphs provide overall US capacity and demand, though the local picture might vary.

The National Renewable Energy Laboratory (NREL) published a report in 2004 based on the subject of *Hydrogen Demand* in which several sizes of production units were classified by the number of vehicles expected to use hydrogen as a source of fuel. Their finding was based on 12,000 miles/year (19,312 km/year) for the typical distance that will be driven by each hydrogen-fueled car, and each car will average 60 miles/kg (96.7 km/kg) of hydrogen consumption [i.e., 12,000 miles per year corresponds to about 32 miles (51.4 km) per day, which is close to that projected for each electric vehicle (EV)]. Therefore, each HFCV requires approximately 200 kg hydrogen per year. This is calculated based on the fact that 1 kg

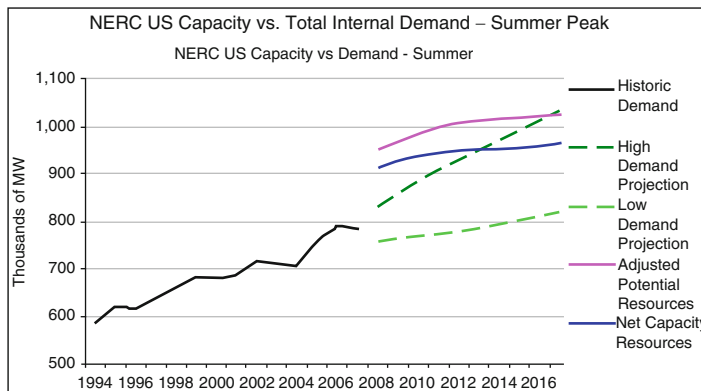


**Fig. 3.24** US capacity versus total demand

hydrogen contains approximately the same energy as 1 gal of gasoline; of course, different vehicles get different gas mileages, so this assumption just represents an average of all vehicles and so may not reflect the actual mileage of any particular vehicle, but it serves as a starting point to give an idea of the potential demand for hydrogen as a fuel cell.

On the other hand, if the average HFCV gets 45 miles per kilogram of hydrogen, then HPP designs will have to account for fewer than the five vehicle sizes identified here [12].

- The home size will serve the fuel needs of 1–5 cars with a hydrogen production rate of 200–1000 kg H<sub>2</sub>/year.
- The small neighborhood size will serve the fuel needs of 5–50 cars with a hydrogen production rate of 1000–10,000 kg H<sub>2</sub>/year.
- The neighborhood size will serve the fuel needs of 50–150 cars with a hydrogen production rate of 10,000–30,000 kg H<sub>2</sub>/year.
- The small forecourt (refueling station) size, which could be a single hydrogen pump at an existing station, will serve the fuel needs of 150–500 cars with a hydrogen production rate of 30,000–100,000 kg H<sub>2</sub>/year.
- A full hydrogen forecourt size will serve more than 500 cars per year with a hydrogen production rate greater than 100,000 kg H<sub>2</sub>/year.

Manufacturers of electrolytic hydrogen generators are sizing up their production equipment to meet demand and be able to deliver the needed quantities of hydrogen as discussed earlier, but if the production of HFCV and hydrogen internal combustion engine (HICE) rises, then the growth of hydrogen production should be justified accordingly – almost up to 1 kg/s for production facilities, which is equivalent to 86,400 kg/day leading to 31,500 tonnes/year or 0.032 million tonnes of hydrogen. Thus, production facilities of this magnitude will require being able to meet such projected demand for growth. Such a projection and demand are depicted in Figs. 3.25 and 3.26.

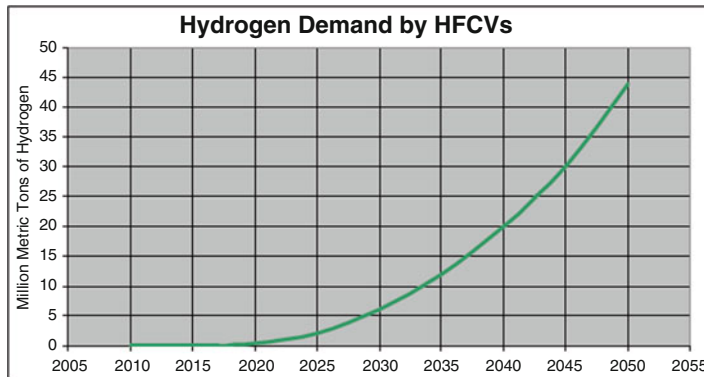


Fig. 3.25 Hydrogen demand in million tonnes per year [11]

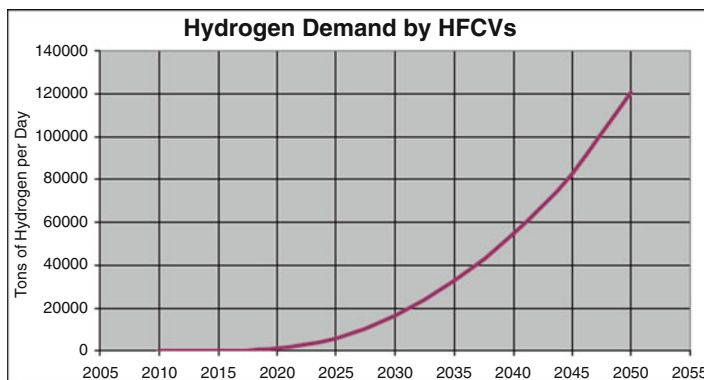


Fig. 3.26 Hydrogen demand in tons per day [12]

Market \ Penetration	1%	10%	30%	70%
<b>Small Urban</b>				
Population	100,000	100,000	100,000	100,000
Vehicles	116,000	116,000	116,000	116,000
H <sub>2</sub> fueled vehicles	1,160	11,600	34,800	81,200
H <sub>2</sub> fuel stations	12 <sup>a</sup>	6 <sup>b</sup>	17 <sup>b</sup>	39 <sup>b</sup>
H <sub>2</sub> demand (tpd)	1	8.3	2.5	58
<b>Large Urban</b>				
Population	1,000,000	1,000,000	1,000,000	1,000,000
Vehicles	890,000	890,000	890,000	890,000
H <sub>2</sub> fueled vehicles	8,900	89,000	267,000	623,000
H <sub>2</sub> fuel stations	86 <sup>a</sup>	43 <sup>b</sup>	128 <sup>b</sup>	298 <sup>b</sup>
H <sub>2</sub> demand (tpd)	9	83	250	580

a. 100 kg/d station (home size)

b. 1,500 kg/d station (small neighborhood)

Fig. 3.27 Key demand assumptions by market and penetration [13]

Demand for hydrogen will be driven by local users. Figure 3.27 shows the demand increase for various market sizes based on HFCV market penetration.

According to the Idaho National Laboratory report (INL/EXT-09-16326) 11, an analysis of existing gasoline stations in four major US cities shows that the general trend in station size and geographic distribution in each city is for stations of different sizes to be more or less uniformly distributed across urban areas. Although there is a slight trend for large stations to be located outside of downtown areas in three of the four cities, when normalized by average station size and total number of outlets in each city, relative station size distributions are nearly identical in each city.

This result is preserved in a cluster analysis, which simulates reduced station networks that might resemble early hydrogen station networks. The relative station size distributions for both existing gasoline networks and simulated early hydrogen networks suggest that around 10 % of stations will be at least twice as large as the average station size, and around 30 % of stations will be smaller than half the average station size [14].

The mix of home, neighborhood, and forecourt sizes will evolve as demand changes. The flexibility of a location to adapt to demand will be important as well. Other issues potentially limiting the siting and permitting of a hydrogen production facility include the so-called determination of need for hydrogen as required by state environmental reviews and water availability.

## 3.7 Constraints on Hydrogen Production Using Nuclear Energy

In conjunction with producing hydrogen from a nuclear power plant, certain constraints exist that need to be addressed and overcome in order to deal with the design and construction of large-scale hydrogen production facilities. These requirements relate to codes and standards and consideration of the regulatory, environmental, and licensing aspects of these facilities. The task becomes greater when considering colocating a hydrogen facility with an existing or new nuclear reactor or even locating the hydrogen facility adjacent to a nuclear site.

### 3.7.1 Safety: Hydrogen Generation

The US Department of Energy (DOE), through the Hydrogen, Fuel Cells, and Infrastructure Technologies (HFCIT) program, with the National Renewable Energy Laboratory (NREL), is coordinating a collaborative effort with leading standards-development organizations (SDOs), code-development organizations,

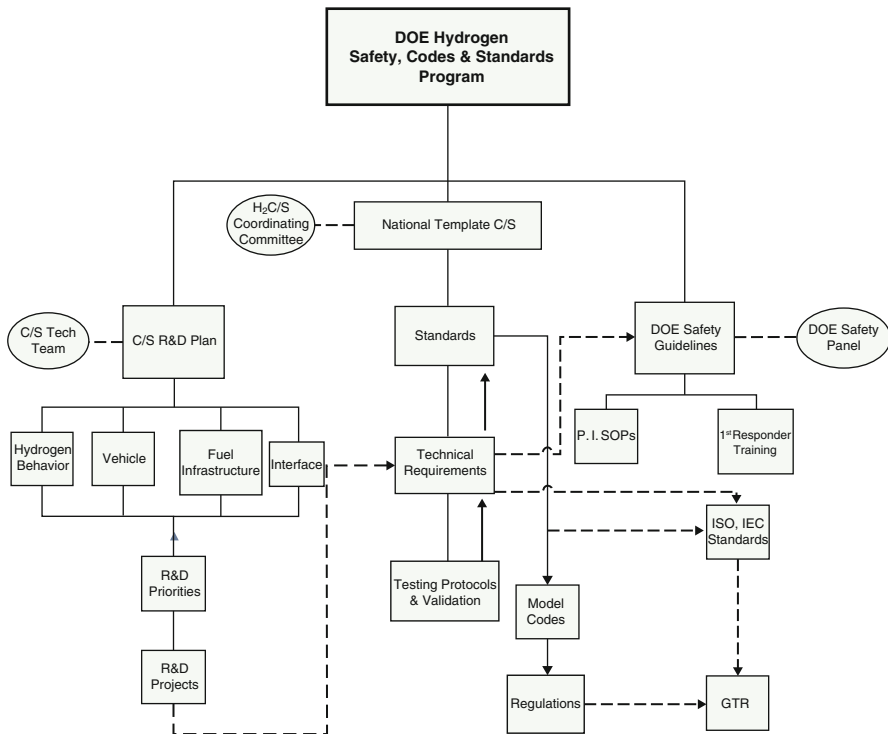


**Fig. 3.28** DOE hydrogen safety, codes, and standards program [15]

and other national laboratories “to prepare, review, and promulgate” hydrogen codes and standards needed to expedite hydrogen infrastructure development [15].

The development and promulgation of codes and standards are essential if hydrogen is to become a significant energy carrier and fuel because codes and standards are critical to establishing a market-receptive environment for commercializing hydrogen-based products and systems. The HFCIT program of the DOE and the NREL, with the help of the leading standards and model code development organizations, other national laboratories, and key stakeholders in the USA, are coordinating a collaborative government–industry effort to prepare, review, and promulgate hydrogen codes and standards needed to expedite hydrogen infrastructure development [15].

The DOE has undertaken a comprehensive program to support and facilitate the development of hydrogen codes and standards based on research, development, and testing (RD&T) needed to establish the scientific and technical foundation to meet the requirements embodied in the codes and standards. The overall structure of the program is shown in Fig. 3.28.

Over the past several years, a coordinated national agenda for hydrogen and fuel cell codes and standards has emerged through DOE leadership and the support and collaboration of industry and key SDOs and model code organizations [15].

The Research and Development (R&D) Roadmap provides a guide to the research, development, and demonstration activities needed to obtain data required for SDOs to develop performance-based codes and standards for a commercial hydrogen-fueled transportation sector in the USA.

Currently no large-scale, cost-effective, environmentally attractive hydrogen production process is available for commercialization, nor has such a process been identified. Our goal is to determine the potential for efficient, cost-effective, large-scale production of hydrogen utilizing high-temperature heat from an advanced nuclear power station. The benefits of this effort will include generation of a low-polluting transportable energy feedstock in a highly efficient method from an energy source that has little or no effect on greenhouse gas emissions and whose availability and sources are domestically controlled. This will help to ensure energy supply for a future transportation/energy infrastructure that is not influenced and controlled by foreign governments.

Conventional nuclear plants readily generate electric power, but fossil fuels are firmly entrenched in the transportation sector. Hydrogen is an environmentally attractive transportation fuel that has the potential to displace fossil fuels. Hydrogen will be particularly advantageous when coupled with fuel cells. Fuel cells have higher efficiency than conventional battery/internal combustion engine combinations and do not produce nitrogen oxides during low-temperature operation. Contemporary hydrogen production is primarily based on fossil fuels and more specifically on natural gas. When hydrogen is produced using energy derived from fossil fuels, there is little or no environmental advantage [16].

### ***3.7.2 Safety: Hydrogen Generation by Facility Location***

The public acceptance of nuclear energy is still greatly dependent on the risk of radiological consequences in case of severe accidents. Such consequences were recently emphasized with the Fukushima Daiichi accident in 2011. Nuclear power plants are among the safest and most secure industrial facilities in the United States. Multiple layers of physical security, together with high levels of operational performance, protect plant workers, the public, and the environment.

As a matter of fact, despite the highly efficient prevention measures adopted for current plants, some accident scenarios may, with low probability, result in a severe accident, potentially leading to core melting, plant damage, and dispersal of radioactive materials from the plant containment.

Even if the Japanese power station was not equipped with the newest devices for the prevention or mitigation of severe accidents, Fukushima, as well as the Three Mile Island accident in 1979, confirmed the key role of the containment barrier in the significant mitigation of radioactive releases.

Improvements in nuclear designs and the setup of adequate accident management strategies require confinement structures and emergency systems that are properly dimensioned (configuration, choice of materials, and cooling circuits) to

guarantee the integrity of the safety barriers and avoid the release of radioactive gases and aerosols to the external environment.

In this chapter, the schematics of typical nuclear power plants are preliminarily shown, together with the main concepts of nuclear reactions and the formation of radioactive isotopes.

The risk of radioactive release to the external environment because of accidents is then discussed in order to explain the reasons behind the safety criteria that characterize these kinds of installations. Attention is paid to the need to maintain the structural integrity of both cooling circuits and confinement structures. Seismic analyses are reported, as is the risk of containment building damage as a result of overpressurization in case of severe accidents.

US nuclear plants are well designed, operated by trained personnel, protected against attack, and prepared in the event of an emergency, and the following measures are in place:

1. **Emergency preparedness:** Every nuclear power plant in the country has a detailed plan for responding in the event of an emergency. Operators test that plan regularly, with the participation of local and state emergency response organizations.
2. **Operational safety:** Stringent federal regulation, automated and redundant safety systems, and industry commitment to comprehensive safety procedures keep nuclear power plants and their communities safe.
3. **Personnel training and screening:** Operators undergo rigorous training and must hold valid federal licenses. All nuclear power plant staff are subject to background and criminal history checks before they are granted access to a plant.
4. **Plant security:** Each nuclear power plant has extensive security measures in place to protect the facility from intruders. Since Sept. 11, 2001, the nuclear energy industry has substantially enhanced security at nuclear plants.

An illustration of the area of a nuclear power plant protected by armed guards, physical barriers, and surveillance equipment from a top-level point of view is given below (Fig. 3.29).

5. **Nuclear licensing:** All US nuclear power plant facilities that are currently operational are reviewed and granted operating licenses under licensing regulation 10 CFR Part 50 by the Nuclear Regulatory Commission (NRC), and by law, each particular nuclear facility is described in its Final Safety Analysis Report (FSAR). Included in the FSAR is a description of each facility's activities that take place at the site, "including the products and materials most likely to be processed, stored, or transported such as the preceding four points.<sup>13</sup> Therefore, the licensees prompt changes to the facilities and, pursuant to 10 CFR 50.59, each facility regulates itself. This includes all subsequent

---

<sup>13</sup> NUREG-0800, 2.2.1-2.2.2, Rev. 3, March 2007.

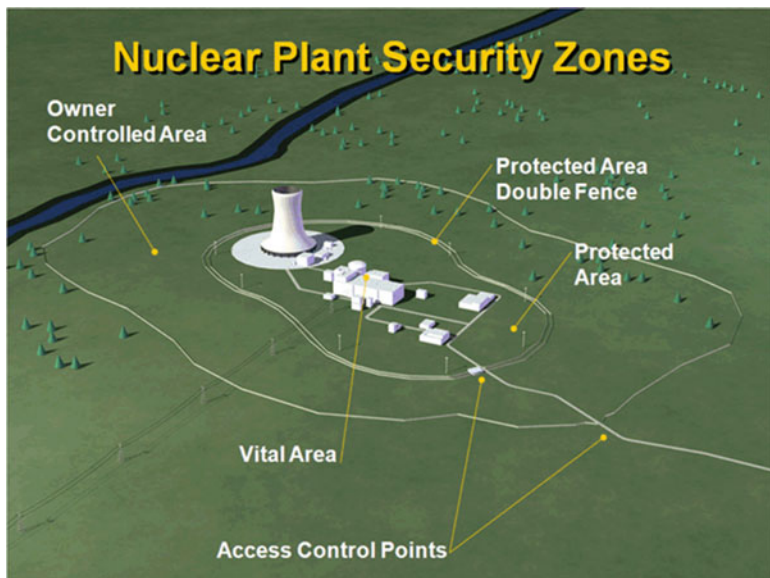


**Fig. 3.29** Nuclear plant security zones. *Source:* NEI

changes or modifications that a licensee wants to make in its operations at the facility.

6. **Nuclear liability insurance:** The NRC requires all owners of nuclear power plants to maintain financial protection through primary and secondary liability insurance coverage as mandated by the rules.
7. **Electrical system up-time and stability:** Preventive maintains nuclear power plants require in long term shutdown cooling requirements that consumed power and have very restrictive voltage and frequency limitations. The stability of the electrical system associated with a nuclear power plant that is not common in oil or gas and coal generating electricity. In terms of shutdowns for preventive maintenance, nuclear power plants have a different set of rules than traditional power plants. Even if a hydrogen production facility is powered from the grid, a shutdown or degraded operation could cause a grid disturbance, adversely impacting the nuclear plant load. The nature of hydrogen generation is that it can go very quickly from full production to zero. This type of load rejection is a feasible occurrence. Nuclear plants are currently designed and licensed for a loss-of-load event. However, depending on the power distribution provided to the hydrogen production facility (dedicated or off the grid) and the reliability and frequency of load disturbances, the licensee will likely need to review the electrical system stability. If it is determined that the frequency of a loss of external load event is increased, the licensee would need to evaluate the change under 10 CFR 50.59, as previously discussed, and request a license amendment from the NRC and approval, as required.
8. **Environmental review:** When issuing an amendment to a license it is necessary for the NRC to make a determination as to whether an environmental review is

required. An environmental review may be conducted in the form of an environmental assessment or an environmental impact statement.

### 3.8 Efficient Generation of Hydrogen Fuels Utilizing Nuclear Power

Currently, combustion processes from fissile fuel to provide power for transportation, electricity generation, heat for homes, and fuel for industry accounts for 86 % of the world's energy use [17, 18]. The disadvantages of utilizing fossil fuel include supply limitations, pollution, and emission of carbon dioxide ( $\text{CO}_2$ ), which is considered a factor in global warming and is now the subject of international treaties among countries [19, 20].

Hydrogen is an environmentally attractive transportation fuel that has the potential to displace fossil fuels. Hydrogen will be particularly advantageous when coupled with fuel cells. Fuel cells have higher efficiency than conventional battery/internal combustion engine combinations and do not produce nitrogen oxides during low-temperature operation. Contemporary hydrogen production is primarily based on fossil fuels and, more specifically, on natural gas. When hydrogen is produced using energy derived from fossil fuels, there is little or no environmental advantage [21].

Currently no large-scale, cost-effective, environmentally attractive hydrogen production process is available for commercialization, nor has such a process been identified.

To overcome these combined drawbacks, the search is on for a new source of renewable energy to replace fossil fuels in particular with a less-polluting process, primarily in parallel with nuclear energy coupled with an efficient HPP adjacent to it. This type of combination requires a nuclear power plant that can operate at very high-temperatures coupled with an efficient HPP via intermediate heat exchangers (IHXs) [16].

For example, the Japan Atomic Energy Agency (JAEA), under the concept of a small modular reactor (SMR) for a high-temperature test reactor (HTTR), has decided to couple a high-temperature gas reactor (HTGR) to a SMR using an IHX for the steam reforming process.

This approach has been applied in the Japanese HTTR project. A flow diagram of the hydrogen production system based on the SMR and its potential coupling to a HTTR is shown in Fig. 3.30. The total system is subdivided by the dotted line into the existing nuclear part on the left-hand side and the not yet existing chemical part on the right-hand side.

The requirements for a system with safe operation and high hydrogen production efficiency have spurred engineering design work on key components for the nuclear steam reforming process:

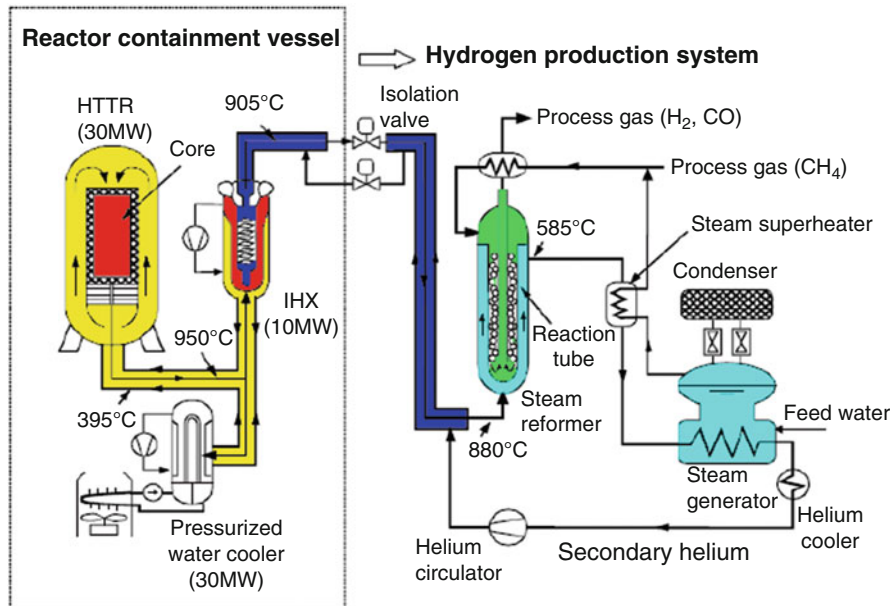


**Fig. 3.30** HTTR coupled to a hydrogen production plant based on SMR

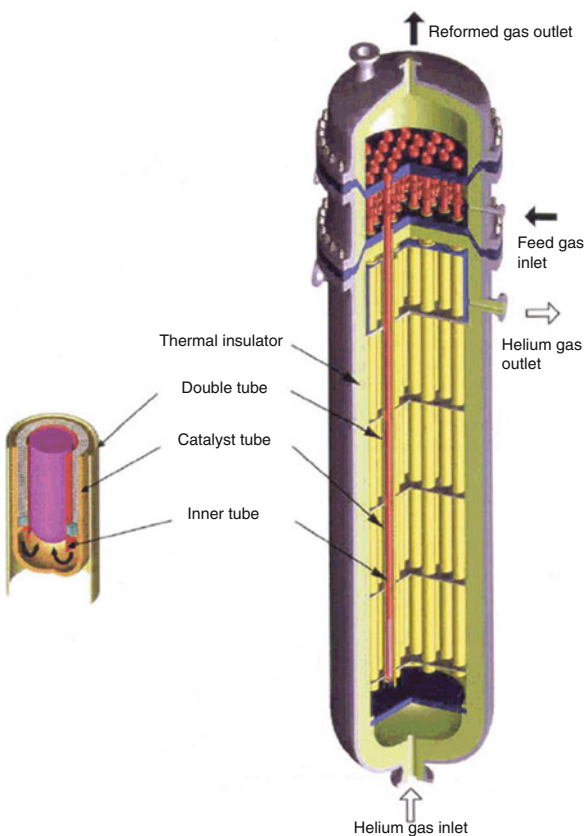
- A new concept steam reformer heated by helium gas from a nuclear reactor has been designed to achieve high hydrogen production performance and to be competitive with an economical, fossil-fuel-fired HPP.
- A natural convection type of steam generator will be used to achieve sufficient system controllability, accommodating the large difference in thermal dynamics between the nuclear reactor and the steam reformer.
- An air-cooled radiator will be connected to the steam generator to operate as a final heat sink during normal and anticipated operating conditions.

The separation of the primary circuit and the chemical process avoids the possibility of contamination in the steam reformer and reduces the permeation rates of hydrogen and tritium to negligible values. However, the heat fluxes in the steam reformer have values of around  $40 \text{ kW/m}^2$  if the same conditions as in the reforming process are met. The fabrication of the steam reformer and steam generator requires different standards than those of components that are directly integrated into the primary helium circuit [22].

For several years, steam reforming of methane has been considered the top candidate process in HTTRs for the world's first nuclear hydrogen power plant. A HTTR nuclear steam reforming system will therefore be taken as an example and described in more detail.

The HTTR steam reforming system was designed to provide about  $4200 \text{ Nm}^3/\text{h}$  of hydrogen using a Ni-based catalyst with 10 MW of thermal energy. A heat utilization ratio (defined as the ratio of output hydrogen energy to total input

**Fig. 3.31** Steam reformer component for connection to HTTR [22]



thermal energy) of 73 % is expected. This value is competitive with that of conventional systems, where the heat utilization ratio is around 80 %.

The HTTR can provide high-temperature helium gas at 905 °C at the outlet of the IHX and, owing to further heat loss from the hot gas duct between the IHX and the steam reformer, secondary helium at 880 °C at the inlet of the steam reformer. The steam reformer component is shown in Fig. 3.31 [22].

With the recent worldwide increased interest in hydrogen as a clean fuel of the future, Europe has also embarked on comprehensive research, development, and demonstration activities, with the main objective of moving from a carbon-based economy toward a CO<sub>2</sub>-emission-free energy structure. Because of the growing demand for hydrogen in the petrochemical, fertilizer, and refining industries, however, the near and medium terms will be characterized by a coexistence of hydrogen and hydrocarbons.

In Europe courtiers under the Framework Program (FP) and closer collaborations among them as part of their strategies are required to provide a balanced choice of energy supply technologies while achieving the principal objectives of

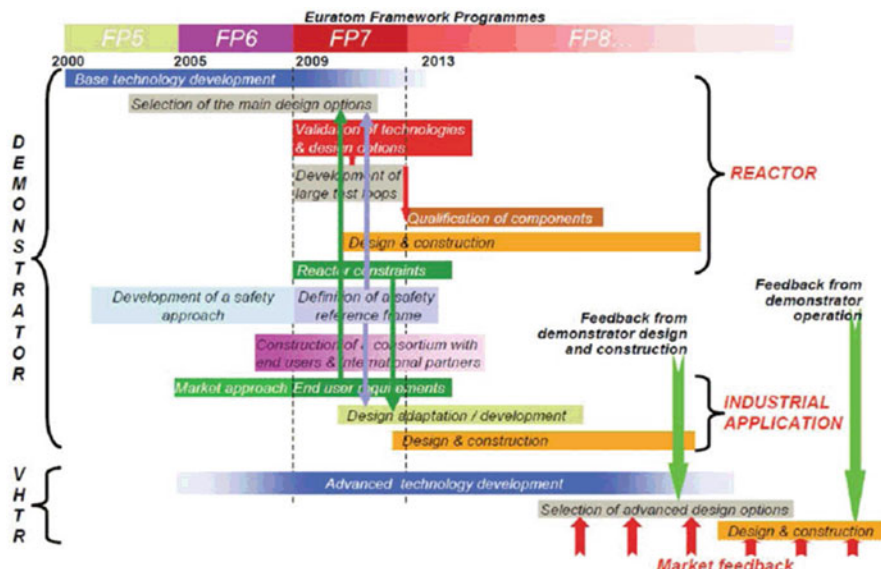


**Fig. 3.32** Suggested schedule for the development of a demonstrator HTR/VHTR for industrial process heat applications [22]

energy supply and continue for further developments with a Network of Excellence (NOE) with long-term joint planning and Integrated Project (IP).

For the demonstration of a HTR/VHTR, the coupling should involve a full-scale proven industrial process with high reliability of nuclear heat supply. A proposed schedule for the European demonstration HTR/VHTR is presented in Fig. 3.32.

Among the tasks of FP-6 and nuclear projects related to hydrogen, the most important is the IP and ReActor for Process heat, Hydrogen, And ELectricty generation (RAPHAEL) which start in 2005 and was terminated in 2010. This IP consisted of 33 partners from 10 European countries, with the objectives being, on the one hand, a study of advanced gas-cooled fast reactor (GFR) technologies needed for industrial reference designs, but concurring what benefits they are deriving from Japanese (HTR/VHTR) and Chinese (HTR-10) efforts in developing such technologies with their demonstrator projects in hand.

While RAPHAEL was fully focused on the development of a VHTR, five more activities were launched in the form of specific targeted research projects (STREPs) to deal with the other Generation IV reactor systems:

- RAPHAEL: Reactor for Process Heat, Hydrogen, and Electricity Generation (VHTR), 2005–2010;
- GCFR: Gas-Cooled Fast Reactor (GFR), 2005–2009;
- HPLWR: High-Performance Light Water Reactor (SCWR), 2006–2010;
- ELSY: European Lead-cooled SYstem (LFR), 2006–2010;

- EISOFAR: Road map for European Innovative SODium-cooled FAst Reactor (SFR), 2007–2008;
- ALISIA: Assessment of LIquid Salts for Innovative Applications (MSR), 2007.

Several years' joint research among European industrial companies that was dedicated to HTGR technologies in conjunction with hydrogen production using these power plants has led to the decision to build demonstration reactors using industrial process heat applications and it was concluded that such a collaboration requires a strong partnership with end user industries as well. Figure 3.32 present a schedule and timeline for the demonstration of HTR/VHTR types under the FP. The main objectives of the project are as follows:

- To identify the main applications for nuclear process heat;
- To determine the viability of combining a nuclear heat source with conventional industrial processes and CHP applications;
- To elaborate a program for the development of a coupled demonstrator between a VHTR and industrial processes that require a heat supply;
- To form a strategic alliance between the nuclear industry and process industries.

An essential prerequisite for the success of this project is the significant involvement of private companies in the form of industrial participation to develop and deploy innovative energy supply systems. As part of their effort on the hydrogen side of R&D, under a Hydrogen Network (HyNet) companies became active from 2001 to 2004 as a so-called thematic network with their FP-5 with 12 European contractors and more than 70 interested partners. Figure 3.33 shows the road map working on the development of strategies for the introduction of a European hydrogen fuel infrastructure.

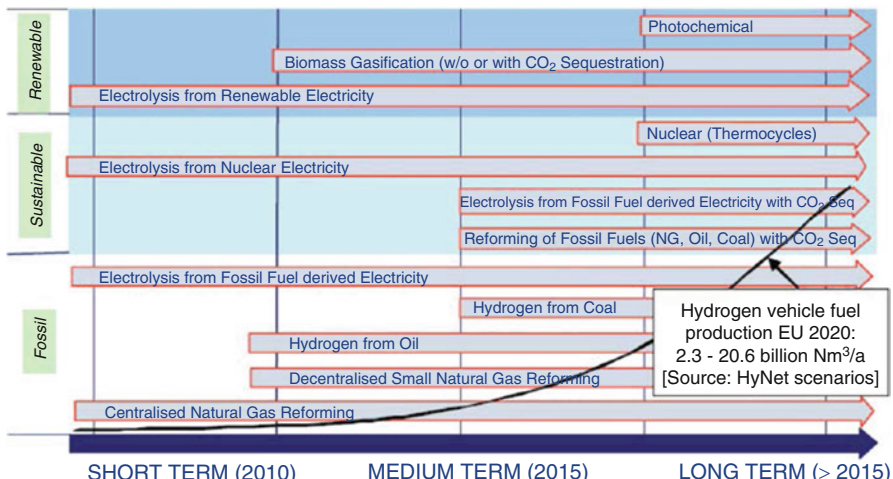


Fig. 3.33 HyNet timeline for hydrogen production technologies [22]

Hydrogen production is deemed a crucial element for the introduction of hydrogen into the energy sector in the form of renewable energy. Research efforts were to be concentrated on the further improvement of known reforming and gasification methods, also with regard to high-temperature primary energy systems such as Generation IV nuclear reactors and solar–thermal concentrating systems, on the development of CO<sub>2</sub> sequestration systems, on gas separation technologies, and on the efficiency improvement of hydrogen liquefaction technologies and system integration with hydrogen production facilities [22].

### 3.9 Thermal Characteristics for Coupling a Hydrogen Product Plant to HTR/VHTR

As part of the DOE’s effort to collaborate with universities and national laboratories under NUEP on R&D for employing the next generation high-temperature nuclear reactors a huge movement by these universities and industries around the world along with national labs, led by INL, has taken place. The use of high-temperature nuclear reactors to produce hydrogen utilizing either thermochemical cycles or high-temperature electrolysis is under way under the current budget of the DOE and NUEP.

Although the production of hydrogen using these types of processes in conjunction with next generation nuclear reactors coupled with HPPs is at its early stage of R&D, there are needs for the study of the coupling in either of these processes to high-temperature reactors both efficient heat transfer and adequate separation of these facilities to assure that facility safety and security during off-normal events in both plants do not impact each other.

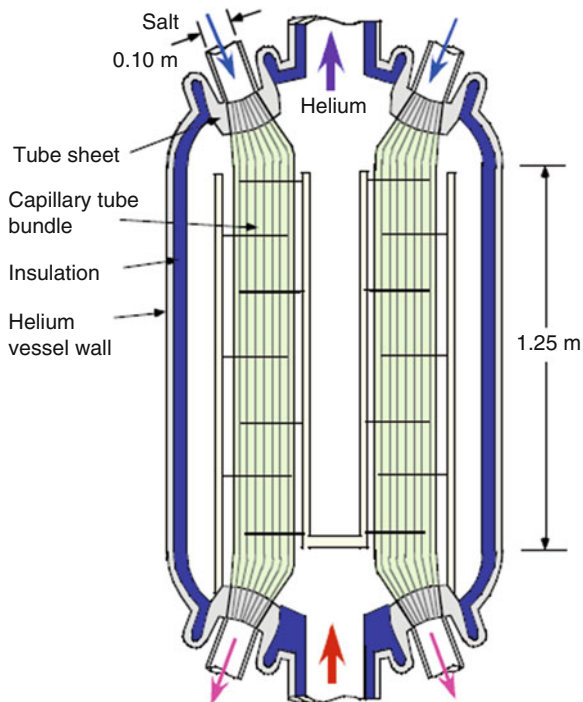
To prevent such events a need for implementing an intermediate heat transport loop such as IHX will be required to separate operations and safety between the two plants. The proposed investigation by the DOE to utilize high-temperature nuclear power plants to produce hydrogen as a source of renewable energy could be either: [21]

1. Single-purpose or
2. Dual-purpose.

Early plants, such as the proposed NGNP, may be dual-purpose facilities that capable of both hydrogen and efficient electrical generation. Later plants could be single-purpose facilities. At this stage of development, both single- and dual-purpose facilities need to be understood. Either way, both of the proposed plants should be studied and understood no matter regardless of which kind of plant is ultimately settled on.

Seven possible configurations for such an intermediate loop have been proposed by INL and they all are reported in the INL/EXT-05-00453 report [22], while other

**Fig. 3.34** IHX design proposed at UCB (UCBTH-07-003) [24]



researchers at universities have also reported new design configuration (Per Peterson) [23].

The one proposed by Peterson is depicted here in Fig. 3.34 and is designed based on the transport of heat from reactor to chemical processing plant, where the IHX will be used to couple these two plants. He suggested this design based on the following configuration:

- Small-diameter channels ( $D_0 = 3 \text{ mm}$ ,  $D_1 = 1 \text{ mm}$ ,  $L = 2 \text{ m}$ );
- Salt laminar flow regime ( $\text{Re} \sim 150$ );
- Linear heat rate of  $200 \text{ }^{\circ}\text{C/M}$ .

Peterson proposed a capillary tube and shell heat exchanger with the tube-bundle geometry formed by the diffusion bonding of multiple bundles of (approximately 2500) 3.0 mm diameter tubes with hexagonally tapered ends to form inlet and outlet tube sheets [23].

These types of IHXs are coupled between two production plants if they are adjacent to each other with a facility for removing heat from the reactor side of the intermediate loop and a process heat exchanger (PHX), where the high quantity of heat can then be utilized by a HPP to produce hydrogen using a process like thermochemical cycles or high-temperature electrolysis.

As was mentioned earlier, to take advantage of HTR/VHTR of the next generation to produce hydrogen as a new source of renewable energy, the acquisition of

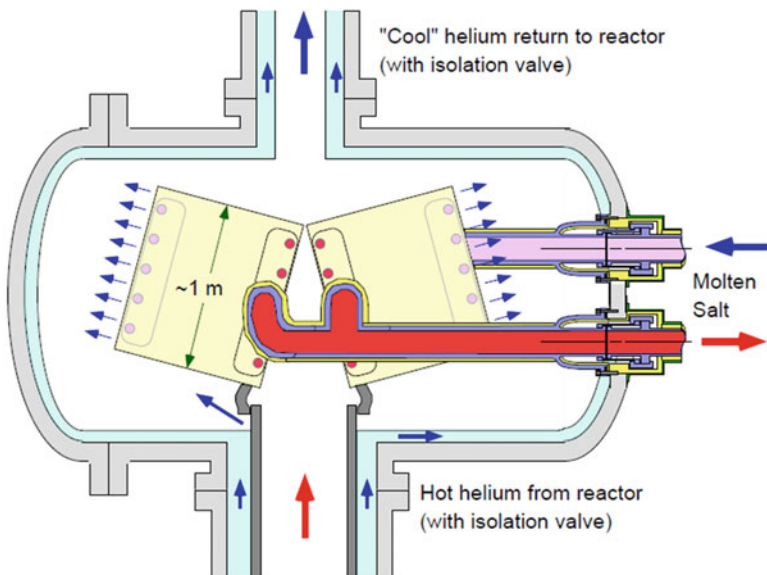


**Fig. 3.35** Preconceptual design for a 50 MW(t) intermediate heat exchanger in NGNP, based on a plate-type, compact high-temperature composite design [24]

such intermediate heat exchangers is required, and further studies should be conducted, both from a thermal-hydraulic point of view and to test the integrity of materials that these IHXs are built from to ensure that they can withstand the high temperature that NGNPs will demand for their operational optimum designs. Another example of a NGNP is the HTGR. It is expected that it will generate not just electricity but also hydrogen to charge up fuel cells for cars, trucks, and other mobile energy uses. INL engineers studied various heat-transfer working fluids – including helium and liquid salts – in seven different configurations. In computer simulations, serial configurations diverted some energy from the heated fluid flowing to the electric plant and HPP.

For these IHXs to be able act as intermediate loops between a liquid-salt (LS) or gas-cooled loop as a safety net or buffer to separate the reactor side from the hydrogen or chemical side of a plant combined within a facility of as such, we need these intermediate loops because by increasing the thermal inertia in the system with LS in the loop in particular, the intermediate loop midgets for the reduction of the sensitivity to temperature transient stresses.

Another proposed configuration of IHX by Peterson et al. (Report UCBTH-03-004) [24], who compare MS and high-pressure helium for the NGNP intermediate heat transfer fluid (Fig. 3.35).

These researchers propose that a base design of 50 MW(t) intermediate loops be used by NGNPs to transfer heat from the primary coolant to generate heat for the HPP using thermochemical and high-temperature electrolysis processes in order to

achieve an efficiency higher than 50 % where high temperatures are required for the baseline sulfur-iodine (SI) thermochemical process. The functional requirements for NGNP include a 1000 °C core outlet temperature for this proposed design.

The high temperature poses substantial technical challenges for IHXs and process heat exchangers, as well intermediate heat transfer loop components. They also believe that the two fluids for the NGNP intermediate loop for this approach be intermediate-pressure MS and high-pressure helium [24].

The best proposed approach for the thermal analysis of the design of such heat exchangers is the method of NTU effectiveness in a one-dimensional coordinate system by neglecting the longitudinal conduction in the  $x$ -direction for the main flow and then expanding it to a more accurate two-dimensional model to include cross-flow conduction of fluids as well as spatially varying both the longitudinal and latitudinal constraints. A finite-element method (FEM) can be employed to handle the computational analysis for each unit cell and can be built based on each region that captures the most important information of that particular region both in steady state initially and subsequently in transient mode for more accurate results. Utilization of dimensional analysis methods [25] is also recommended in order to deal with the complex form of fluid mechanics and fluid dynamics partial differential equations for thermal-hydraulic and heat transfer analysis.

As mentioned earlier, per INL/EXT-05-00453 [21], seven possible configurations for the high-temperature reactor primary coolant system and the intermediate heat transfer loop have been proposed, and the advantages and disadvantages of each, along with the working fluid [i.e., LiF-NaF-KF (Flinak) in the form of molar concentrations of 46.5 %, 11.5 %, and 42 %, respectively, as well as NaBF<sub>4</sub>-NaF in molar concentrations of 92 % and 8 %] for each of these suggested configurations, have been specified as well.

However, the recommendation of a specific design requires input from a variety of disciplines related to materials, thermal-hydraulics, economics, safety, and plant operability. This report also describes each of these intermediate heat transfer loop configurations and summarizes the thermal-hydraulic, structural, and efficiency calculations that have been done to characterize the advantages and issues associated with each configuration. The key issues that were taken into consideration are as follows:

- Configuration options;
- System parameters, such as temperature and pressure;
- Structural issues;
- Working fluid options and materials issues.

To perform this analysis this report (Davis) [21] has identified key requirements by picking two top-level high-temperature reactors from among NGNPs that fit into this calculation; a basic thermal-hydraulic analysis for interfacing and coupling between the nuclear power and HPP via an intermediate heat transfer loop is required.

Therefore for the purpose of any heat transfer and thermal-hydraulic analysis one needs to consider the following conditions:

1. Identify key requirements of the high-temperature reactor and the HPP that affect the choice of intermediate heat transport loop;
2. Identify and justify assumptions used in the evaluation;
3. Identify possible configurations of the intermediate heat transport loop along with the choice of fluids to be used for heat transfer media;
4. Perform preliminary stress evaluations to determine allowable materials for the intermediate heat transport loop to deal with the high temperature of base plants;
5. Estimate the size and thermal hydraulic performance of various components in the intermediate heat transport loop, including the heat exchangers and loop piping;
6. Estimate the overall cycle efficiency of each configuration;
7. Determine the sensitivity of the cycle efficiency to various parameters; and
8. Compare and contrast the different options to help in the selection of the configuration and working fluid together.

Another key requirement is the choice of nuclear reactor from among NGNPs, generation, based on its output of thermal power, and the coolant system to be used in that particular reactor. For example, small modular reactor (SMR) thermal power varies between 20 and 100 MW, such as the one going into production by the NuScale Corporation.<sup>14</sup> The choice of thermal power output impacts the nominal rise in fluid temperature across the core, based on plant design, and other variables, such as a pressure drop across the hot steam of the IHX, can be assumed that also drive the dependence on the pumping power associated with the pressure drop across the IHX.

All the aforementioned constraints play a huge rule in determining the separation distance between the nuclear and HPPs that are part of the safety factor and part of the licensing criteria. For example, for the Japanese HTTR this distance was calculated to be 300 m [26], while a similar distance for NGNPs, based on point design and other previously mentioned variables, was set to between 60 and 120 m [27].

Such a separation distance has a direct impact and affects the diameters and insulation requirements of the hot and cold legs in the heat transport loop, and the nominal temperature drop between the outlet of the NGNP and the maximum temperature delivered to the HPP is assumed to be 50 °C. This temperature drop imposes requirements on the effectiveness of the heat exchangers that connect the NGNP and production plant and the amount of heat loss that can be tolerated in the intermediate loop. To perform preliminary calculations, heat loss was assumed to cause the fluid temperature to drop 10 °C in the hot leg of the intermediate loop in nominal conditions [21].

The IHX can be a compact heat exchanger rather than one of shell and tube design; therefore, NTU-Effectiveness design should be taken into consideration (Dewson and Thonon) [28], while a process heat exchanger (PHX), which is a heat

---

<sup>14</sup> [www.nuscalepower.com](http://www.nuscalepower.com)

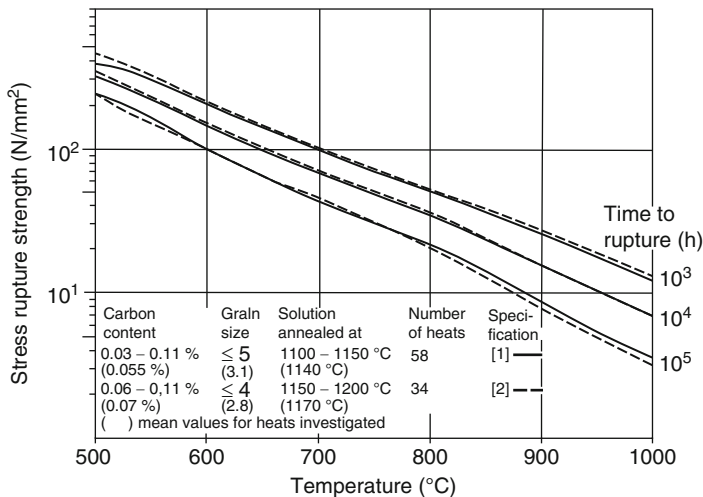


Fig. 3.36 Creep rupture strength of Alloy 800 (from Diehl and Bodman) [29]

exchanger (HX) that connects the heat transport loop to the HPP, can be a tube-in-shell type or a logarithmic mean temperature difference (LMTD) analysis may be done to design a heat exchanger like a PHX.

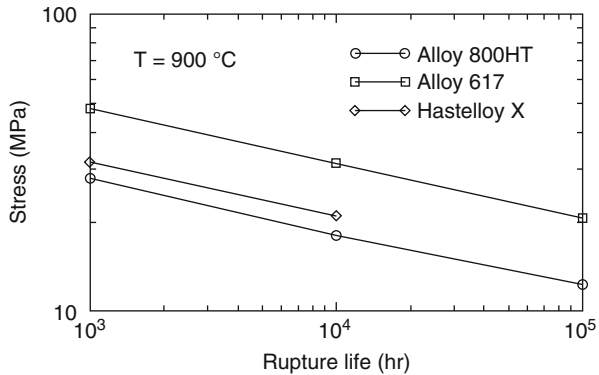
This type of shell-and-tube HX consists of tubes spirally wound into bundles and fitted into a shell. Because of the tube bundle geometry, a considerable amount of surface can be accommodated inside the shell. These HXs are used for gas-liquid heat transfer applications, primarily when the operating temperature or pressure is very high. The challenging part of this type of configuration is in preventive maintenance (PM) and cleaning associated with such PM.

Sizing of these IHXs as part of the thermal-hydraulic analysis is a function of the overall temperature difference between the outlet of the reactor core and the inlet on the cold side of the PHX and can be seen as tube-in-shell heat exchangers with the heat transport fluid flowing on the shell side. This configuration allows the tubes to contain the catalysts necessary for hydrogen production, which is judged to be the most convenient configuration. The tube side can be assumed to be at a low pressure (less than 1 MPa). The hot and cold legs of the intermediate loop may be assumed to be separate pipes, as opposed to an annular configuration [21].

For stress analysis a simplified approach can be taken for different components in any desired configuration based on points of design in order to determine the thickness requirement so that the circumferential stress can be allowed within optimum values and configurations as well. The creeping and rupture strength of materials also needs to be taken into consideration as part of the stress analysis; it depends on the operating time at a given temperature.

Figure 3.36 shows that the rupture strength of Alloy 800 decreases sharply with temperature. At an operating time of  $10^5$  h (about 11 years), the rupture strength is 240 MPa at 500 °C, but decreases to 8 MPa at 900 °C. The rupture strength also

**Fig. 3.37** Creep rupture strengths of candidate materials [21]



depends on the time at temperature. At 900 °C, the rupture strength increases from 8 to 16 MPa when the operating time decreases from 10<sup>5</sup> to 10<sup>4</sup> h. The data presented in Fig. 3.36 suggest that the mechanical design of the heat transport loop will be a challenge because of the desired high temperature and the long lifetime, both of which act to reduce the rupture strength.

The creep rupture strengths of three candidate materials for the heat transport loop are shown in Fig. 3.37 for a temperature of 900 °C. These three materials are Alloy 800HT, which is a high-temperature variation of Alloy 800 (Special Metals 2004a), Alloy 617 (Special Metals 2004b), and Hastelloy X (Haynes International 2005). Alloy 617 has the highest rupture strength of these three materials at 900 °C. The allowable stress will eventually be specified by an applicable code but will be less than the strengths shown in Fig. 3.37 to account for safety factors. For this analysis, the allowable stress was assumed to be half of the creep rupture strength.

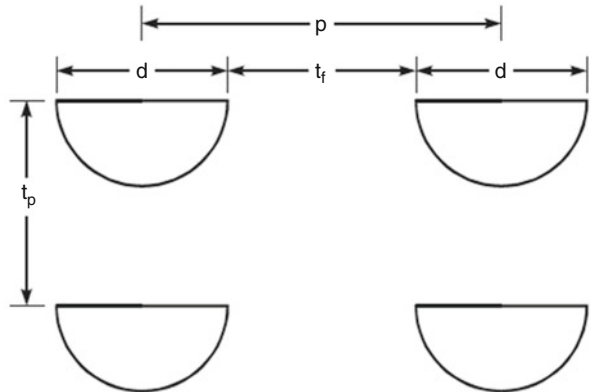
Crandall et al. [30] suggest using the following mathematical relationship to calculate the tangential stress  $\sigma$  for a thick wall:

$$\sigma = \frac{P_i \left[ (r_0/r)^2 + 1 \right] - P_0 \left[ (r_0/r_i)^2 + (r_0/r)^2 \right]}{(r_0/r_i)^2 - 1}, \quad (3.1)$$

where  $r$  is the radius,  $P$  the pressure, and subscripts  $i$  and  $o$  the inner and outer surfaces, respectively.

If the external pressure exceeds the internal pressure, then the stress is a negative value, but the maximum magnitude always occurs at the inner surface. The radius ratio that causes the maximum stress to be less than or equal to the allowable stress,  $\sigma_D$ , can be calculated from Eq. (3.1). For those cases where the internal pressure exceeds the external pressure, the limiting ratio is

**Fig. 3.38** Illustration of IHX channels



$$\frac{r_o}{r_i} \geq \sqrt{\frac{\sigma_D + P_i}{\sigma_D + 2P_o - P_i}}. \quad (3.2)$$

For cases where the external pressure exceeds the internal pressure, the maximum, absolute value of the stress will be less than or equal to the allowable stress when the radius ratio is

$$\frac{r_o}{r_i} \geq \sqrt{\frac{\sigma_D - P_i}{\sigma_D - 2P_o - P_i}}. \quad (3.3)$$

A simple stress analysis was also performed for the IHX assuming that it is a compact heat exchanger of the type designed by Heatic (Dewson and Thonon) [28]. The design of the heat exchanger channels is defined by the channel diameter,  $d$ , pitch,  $p$ , and plate thickness,  $t_p$ , as illustrated in Fig. 3.38. Each plate contains either hot or cold fluid, but not both. Adjacent plates contain the other fluid. Following the method used by Dostal et al. [31], the minimum wall thickness between channels,  $t_f$ , can be approximated as

$$t_f \geq \frac{p}{\frac{\sigma_D}{\Delta P} + 1}, \quad (3.4)$$

where  $\sigma_D$  is the allowable stress and  $\Delta P$  is the differential pressure between the hot and cold streams. Expressing Eq. (3.4) in terms of pitch-to-diameter ratio yields

$$\frac{p}{d} \geq 1 + \frac{\Delta P}{\sigma_D}. \quad (3.5)$$

The required plate thickness can also be calculated based on the method explained and reported by Dostal et al. [31]. The plate is assumed to be a thick-walled cylinder, with an inner radius of  $d/2$  and an outer radius of  $t_p$ . Equations (3.2)

and (3.5) can be used to calculate the thickness-to-diameter and pitch-to-diameter ratios for the IHX as a function of allowable stress and various pressures of the hot and cold streams. The allowable stress is assumed to be 10 MPa, which is approximately half of the rupture strength of Alloy 617 at 900 °C [21].

As part of thermal hydraulics and heat analysis, component sizing comes into play when we look at the nominal temperature drop between the outlet of a NGNP and the maximum temperature delivered to the HPP per design point assumption as a fixed rather than variable value. This temperature drop constrains the effectiveness of the heat exchangers that bridge the NGNP and the HPP and the amount of heat loss that would be tolerable in the intermediate loop. The distribution of the temperature drop between the heat exchangers and heat loss can be taken as a variable value. For example, if the heat loss can be reduced while the temperature drop across the heat exchanger can be increased, then a smaller or more compact heat exchanger can be used. As part of the analysis one can use the remaining temperature drop between the outlet of the NGNP and the maximum temperature delivered to the HPP and divide it evenly between the IHX and PHX and, if present, the secondary heat exchanger (SHX).

The effectiveness of a heat exchanger  $\epsilon$  can be written as Eq. (3.6), as suggested by Krieth [32], knowing that the temperature drop between the NGNP and the HPP drives the requirements for the heat exchanger:

$$\epsilon = \frac{(\dot{m} c_p)_{\text{hot}} [(T_{\text{hot}})_{\text{in}} - (T_{\text{hot}})_{\text{out}}]}{(\dot{m} c_p)_{\text{min}} [(T_{\text{hot}})_{\text{in}} - (T_{\text{cold}})_{\text{in}}]}, \quad (3.6)$$

where  $\dot{m} = v\rho$  ( $v$  is the flow rate and  $\rho$  the flow density) is the mass flow rate,  $c_p$  is the specific heat capacity at constant pressure and is assumed constant, and  $T_{\text{hot}}$  and  $T_{\text{cold}}$  are the temperatures for the hot and cold sides of the heat exchanger while the subscripts *in* and *out* refer to the inlet and outlet ends of the heat exchangers, and the subscript *min* refers to the minimum value for the hot and cold sides.

Equation (3.6) applies when a counterflow type of heat exchanger is chosen, which requires less surface area (i.e., more compact shape and presumably more cost effective from a production point of view) than is required by a parallel-flow type.

If we encounter the condition where the value of  $\dot{m}c_p$  is the same for the hot and cold flow streams, then the effectiveness temperature-wise just depends on the inlet and outlet temperature. An approximation can also be made to analyze the required heat transfer area  $A_{\text{ht}}$  in order to size the heat exchanger, where this is given by

$$A_{\text{ht}} = \frac{\epsilon (\dot{m} c_p)_{\text{min}} [(T_{\text{hot}})_{\text{in}} - (T_{\text{cold}})_{\text{in}}]}{U \Delta T}, \quad (3.7)$$

where  $U$  is the overall heat transfer coefficient and  $\Delta T$  is the logarithmic mean temperature difference (LMTD), which is calculated as follows:

$$\Delta T = \frac{\Delta T_a - \Delta T_b}{\ln(\Delta T_a / \Delta T_b)}, \quad (3.8)$$

where  $\Delta T_a$  is the temperature difference between the hot and cold fluid streams at one end of the heat exchanger and  $\Delta T_b$  is the temperature difference at the other end.

*Example 3.1* Calculate the heat transfer area for heat exchangers given the following values:

Flow Rate = 20,000 m/h

Density of Fluid = 1020 kg/m<sup>3</sup>

Specific Heat = 3.95 kJ/kg K

Overall Heat Transfer Coefficient = 5000 W/m<sup>2</sup> K

Temperature Change = 30 °C

Temperature Difference = 20.8 °C

Effectiveness = 1

**Solution** Using Eq. (3.7), we can calculate the heat transfer area as

$$A = \frac{1 \times 20,000 \times 1020 \times 3.95 \times 30}{3600 \times 20.8 \times 5000} = 6.5 \text{ m}^2.$$

The overall heat transfer coefficient is calculated from the heat transfer coefficients on both sides of the exchanger and the thermal conductivity and thickness of the metal. The heat transfer coefficients and the thermal conductivity are assumed constant over the length of the heat exchanger. For turbulent flow, the heat transfer coefficients are calculated using the Dittus-Boelter correlation, with a leading coefficient of 0.021 for gases and 0.023 for liquids (INEEL) [33]. For laminar flow, the heat transfer coefficients are calculated from the exact solution for fully developed flow with constant heating rate [34, 26]. The thermal conductivity of the metal is calculated assuming Alloy 800 and varies between 18 and 26 W/m K over the temperature range of interest.

Further analysis related to the subject of sizing of heat exchangers, including estimating the pumping power and efficiency evaluation, can be found in the next two chapters as well the books by Zohuri [8] and Zohuri and Fathi [25] or Zohuri and McDaniel [35].

The inner diameters of the hot and cold leg pipes in the heat transport loop are sized to produce a given pressure drop. The thickness of the piping is based on the results of the stress analysis. The heat loss is calculated using an overall heat transfer coefficient, which accounts for the thermal resistance of the heat transfer coefficient at the inner and outer surfaces, the pipe metal, and the insulation [36].

The pumping power  $Q_p$  is given by the following approximation analysis provided by Glasstone and Sesonske [37] as

$$Q_p = \frac{\dot{m} \Delta P}{\rho}, \quad (3.9)$$

where  $\dot{m}$  is the mass flow rate,  $\Delta P$  the pressure drop, and  $\rho$  the fluid density, which is based on the temperature at the inlet to the reactor for the hot stream of the IHX and on the temperature of the cold stream entering the IHX or the SHX for the intermediate and tertiary loops.

Further research, analysis, and development are required using concepts of NGNPs coupled with HPPs since NGNPs are still at the conceptual stage of design and their thermal efficiencies are constantly challenged (Zohuri) [8, 9]

### 3.10 Next Generation Nuclear Plant Intermediate Heat Exchanger Acquisition

As part of the strategy for acquiring the right IHX for NGNPs, first the right generation of nuclear power plant for the given purpose needs to be selected, and that plants needs to be able to deliver a quality product at sufficiently high temperatures. The DOE has selected the HTGR design for the NGNP project to be coupled with a HPP via an IHX and the subcomponents that are most efficient and cost effective.

The NGNP will demonstrate the use of nuclear power for electricity and hydrogen production. The reactor design will be a graphite-moderated, helium-

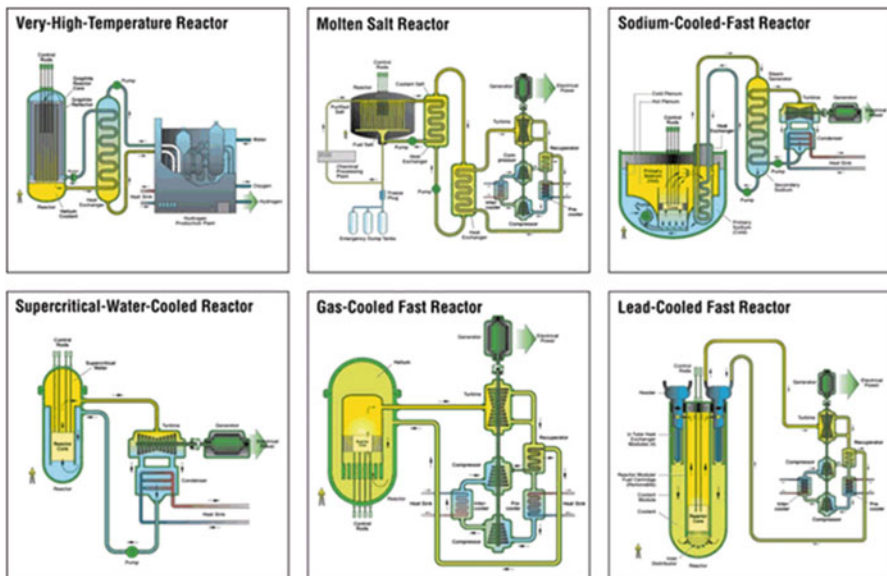
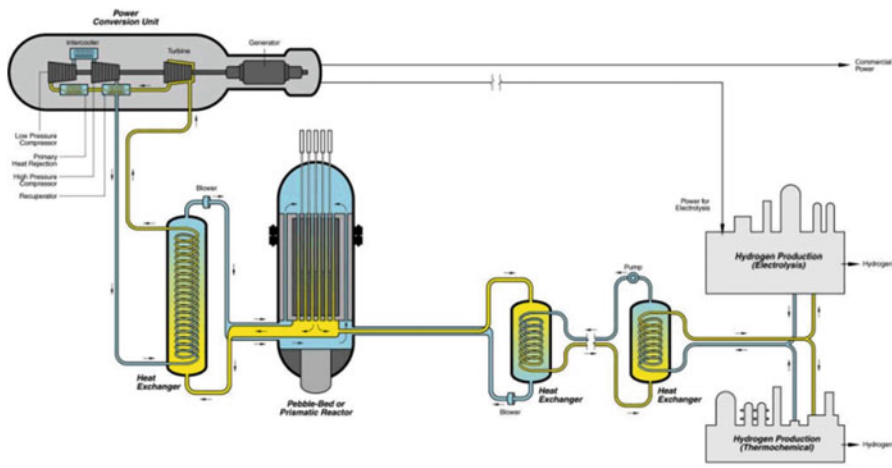


Fig. 3.39 Six proposed Generation IV systems



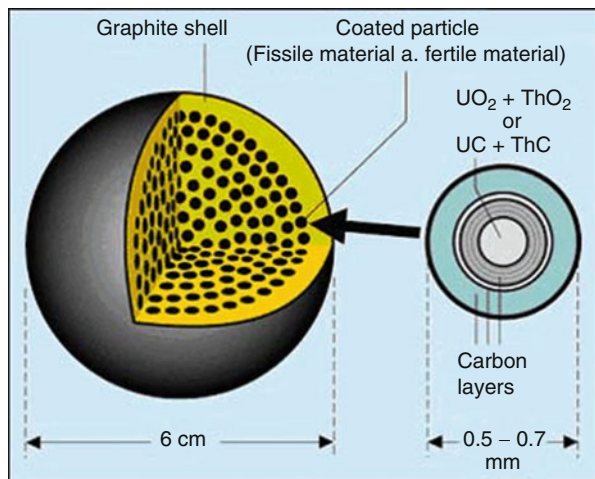
**Fig. 3.40** HTGR schematic, with optional hydrogen production plant attached ([https://daryanenergyblog.wordpress.com/ca/part-6\\_htgr/](https://daryanenergyblog.wordpress.com/ca/part-6_htgr/))

cooled, and prismatic or pebble-bed thermal-neutron spectrum reactor. The NGNPs will use very high-burn-up, low-enriched uranium, and tri-isotopic (TRISO)-coated fuel and have a projected plant design service life of 60 years. The HTGR concept is considered to be the nearest-term reactor design among all other six choices designated as Generation IV nuclear power plants and has the capability to efficiently produce hydrogen by being coupled to a hydrogen plant via a designated IHX set (Fig. 3.39). The plant size, reactor thermal power, and core configuration will ensure a passive decay heat removal system without fuel damage or radioactive material releases during accidents as part of safety net imposed on Generation IV reactors.

Figure 3.39 shows all the proposed six Generation IV systems that are on the table for consideration as part of the efforts by the Gen-IV International Forum (GIF) initiated in 2001. As can be seen from this figure, there are a total of six advanced nuclear power plant designs proposed, with the main desired aspects addressed in all of them – inherent safety, proliferation resistance, and, last but not least, efficiency and process heat capability.

Figure 3.40 is a conceptual illustration of a HTGR coupled with a HPP along with a power conversion unit (PCU). There are various iterations on this concept, most notably the concept proposed by the IAEA, which is the very-high-temperature reactor (VHTR) as part of the Generation IV family design (Fig. 3.40); all Generation IV reactors, including the pebble-bed reactor and the HTTR, share a number of common characteristics. They can all be grouped as HTGRs, and in principle all of them have a graphite-moderated reactor core using an inert gas, likely helium, as cooling fluid as a moderator.

As part of the core design and fuel options for HTGRs, the fuel would be either in the form of roughly 60 mm graphite spheres inside of which are suspended a

**Fig. 3.41** HTGR fuel pellet

matrix of silicon carbide and uranium dioxide particles, or stacks of prismatic blocks of a similar composition. By including thorium dioxide in the fuel mix, we can also partially utilize the thorium fuel cycle. However, because thorium has no naturally occurring fissile isotope, it must be used in a mixed mode with uranium (Fig. 3.41).

One of the key advantages of HTGRs is the high operating temperatures, ranging from a minimum of around 650 °C all the way up to 1000 °C. This has several useful advantages:

1. Firstly, we can now utilize the Brayton cycle, which can potentially allow for thermal efficiencies of up to 65 % (although 45–55 % is more typical) compared with a maximum of 47 % for the more conventional Rankine (with a typical range of 33–40 %) (Zohuri) [8, 9].
2. Alternatively, if the operating temperature can be maintained well below 800 °C, we can utilize the SI process to manufacture hydrogen directly using heat energy with a high level of energy efficiency (Zohuri) [8, 9].

The operating conditions for the NGNP represent a major departure from existing water-cooled reactor technologies. Few choices exist for metallic alloys for use at NGNP conditions, and the design lifetime considerations for the metallic components may restrict the maximum operating temperature. Qualification of materials for successful and long-life application in high-temperature conditions planned for the NGNP is a large portion of the effort in the NGNP materials R&D program [38].

Selection of the technology and design configuration for the NGNP must consider both the cost and risk profiles to ensure that the demonstration plant establishes a sound foundation for future commercial deployments. The NGNP challenge is to achieve a significant advancement in nuclear technology while at the

same time setting the stage for an economically viable deployment of the new technology in the commercial sector soon after 2020 [38].

Now that we have a better understanding of the VHTR concept and how such reactors operate, we can go back to our original topic of this section: a strategy for selecting the right IHX for this type of reactor to be used to couple the nuclear side with the hydrogen generating plant side. As we said, the major component of the NGNP driving a HPP is the IHX.

This component will transfer heat to secondary systems that will generate electricity or hydrogen. The IHX will be operated in flowing, impure helium on the primary and secondary sides at temperatures up to 950 °C. There are major high-temperature design, material availability, and fabrication issues that need to be addressed. The prospective materials are Alloys 617, 230, 800H, and XR, with Alloy 617 being the leading candidate for use at 950 °C.

Developing an acquisition strategy policy is part of the NGNP materials R&D Program. The objective of the NGNP materials R&D program is to provide the essential material studies and laboratory investigations needed to support the design and licensing of a reactor and balance of plant, excluding the hydrogen plant. The materials R&D program was initiated prior to the design effort to ensure that materials R&D activities are initiated early enough to support the design process. The thermal, environmental, and service life conditions of the NGNP will make selection and qualification of the high-temperature materials a significant challenge; thus, new materials and approaches may be required. The mission of the NGNP materials R&D program must support the objectives associated with the NGNP in the Energy Policy Act of 2005 and provide any materials-related support required during the development of the NGNP.

As a result of the Energy Policy Act, the selection of an IHX should take place based on certain assumptions [38]:

- The NGNP will be a full-sized reactor plant capable of electricity generation with a hydrogen demonstration unit of appropriate size.
- The reactor design will be a helium-cooled, graphite-moderated core design fueled with TRISO design fuel particles in carbon-based compacts or pebbles.
- The NGNP must demonstrate the capability to obtain a NRC operating license. The design, materials, and construction will need to meet appropriate quality assurance (QA) methods and criteria and other nationally recognized codes and standards.
- The demonstration plant will be designed to operate for a nominal 60 years.
- The NGNP program, including the materials program, will continue to be directed by the Idaho National Laboratory (INL) based on the guidelines given in the Energy Policy Act of 2005. The scope of work will be adjusted to reflect the level of congressional appropriations.
- Application for a NRC operating license and fabrication of the NGNP will occur with direct interaction and involvement of one or more commercial organizations.

Certain issues are arising owing to these assumptions that require some attention with respect to design efforts on NGNP-driven hydrogen generation plant and

associated IHX to perform such duty. These issues are listed here as general concerns [38]:

- The last HTGR design reactor built in the USA was the Fort St. Vrain (FSV) gas-cooled reactor [39], which was constructed in the early 1970s, generated the first power sent to the grid in 1976, and was taken out of service in 1989. The fact that there has been no HTGR construction in this country since then, along with the long gap in the construction of light water reactors (LWRs), means that, in connection with the NGNP, there is a lack of current industrial technical information and experience with regard to the materials of construction and fabrication practices associated with the NGNP designs currently under consideration.
- The design effort needs to be completed, which will include a final IHX design, so a material acquisition list can be developed. There needs to be new information developed as regards the primary metals producers who can produce high-temperature alloys in the required product forms specified for use in an IHX. For compact IHX designs joining and inspection R&D will be necessary.
- Another issue will be the identification of vessel fabrication vendors with the appropriate American Society of Mechanical Engineers (ASME) certifications to perform nuclear work. The number of these firms has declined over the last 20 years, and the NGNP will be competing for these services with resurgent orders for LWRs and chemical process facility components in a world market. There is significant competition for these fabrication resources.
- To meet the NGNP startup date of 2021, the IHXs must be delivered much earlier. The required delivery date must be identified and a schedule for materials acquisition and fabrication must be developed. For a given desired delivery date the following steps need to be completed with the appropriate completion dates:
  1. Place materials order with primary metal producer to obtain position in the melting schedule to secure material for fabrication.
  2. Finalize material shapes and sizes (tubing, sheet, forgings, plate) and choose the appropriate specifications for the intermediate product mill.
  3. Secure fabrication vendor services and ship material to vendor's facility.
  4. Set date for fabrication.
  5. Ship to Idaho.
  6. Install IHX and other major equipment to meet startup schedule.

Regarding the previously mentioned pros and cons, two alternative IHX designs were developed based on the printed circuit heat exchanger (PCHE) concept with one design developed by the Heatic Corp. and the second design developed by the Toshiba Corp. These designs consist of metal plates that are diffusion bonded together with flow channels that are chemically milled into the plate. The PCHE concept allows for simultaneous high-temperature and high-pressure operation with relatively thin wall thicknesses between the primary and secondary coolants. The PCHE designs are typically four to six times smaller than conventional shell-and-tube heat exchangers of equivalent duty, and designs have been developed with a

thermal effectiveness greater than 98 %. The description of a PCHE is presented throughout this book in various chapters; consult the index for page numbers.

An alternative design using a shell-and-tube, counterflow heat exchanger using a helically coiled tube was developed by Toshiba. For an equivalent heat-duty and LMTD, this type of heat exchanger is considerably larger than a PCHE. This design allows for in-service inspection (ISI) of the heat transfer tubes. This design has successfully operated in a HTTR [38, 39].

### 3.11 Applicability of Heat Exchanger to Process Heat Applications

The strategic goal of the advanced reactor concept program is to broaden the environmental and economic benefits of nuclear energy in the US economy from power production to meet energy needs and also demonstrate applicability to market sectors not being served by LWRs. The advanced high-temperature reactor (AHTR) offers unique advantages for a variety of markets beyond power production because of the high reactor outlet temperature (ROT) and because of the superior heat transport characteristics of molten salt. Increased ROT would expand the AHTR's applicability to many other applications [40].

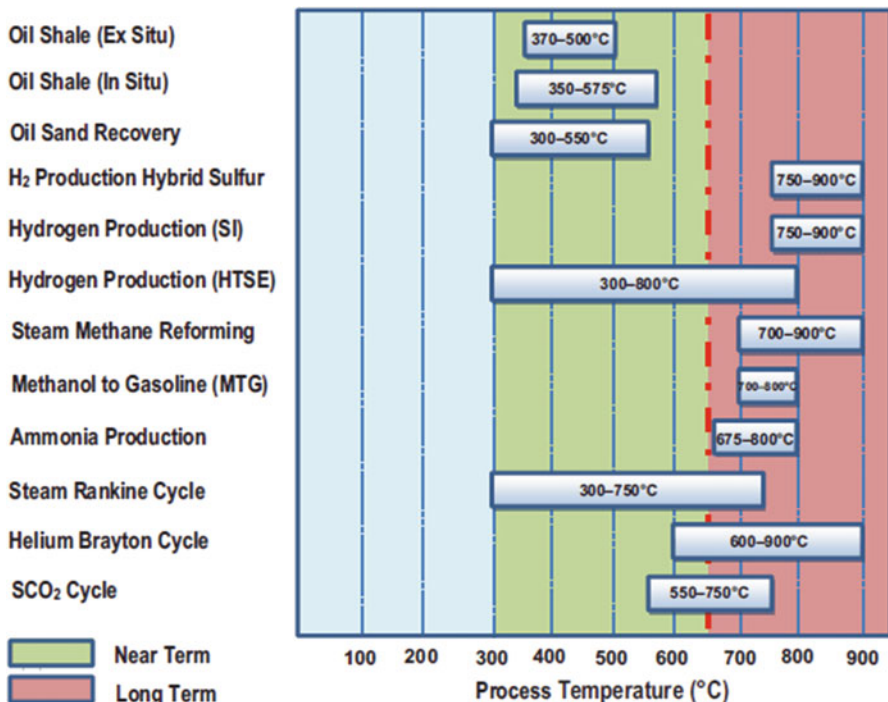
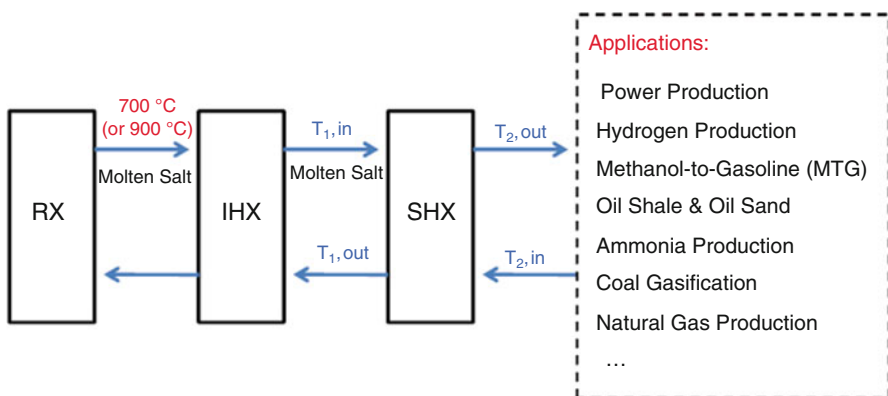


Fig. 3.42 Process applications for AHTR versus process-required temperature range [41]



**Fig. 3.43** Thermal energy transfer in AHTR for power or process application [41]

The integration of AHTR technology with conventional chemical industrial processes is presented in this section. The process heat industrial applications being considered are as follows: hydrogen production via steam methane reforming of natural gas and high-temperature steam electrolysis, substitute natural gas production, oil sands recovery via steam-assisted gravity drainage, coal-to-liquid production, natural gas-to-liquids production, methanol-to-gasoline production, ammonia production, ex situ oil shale, and in situ oil shale. The temperature ranges of applications that could be coupled to the AHTR with the current ROT (green band) and others that could potentially be coupled if the ROT was raised (red band) are shown in Fig. 3.42. These are representative and should not be considered inclusive of all potential applications.

### Situ Oil Definition

This relatively new method is mainly used to obtain bitumen in oil sand that is buried too deep below Earth's surface to be recovered with a truck and shovel. In situ technology injects steam deep beneath the Earth to separate the viscous bitumen from the sand and pump it up to the surface. The bitumen then goes through the same upgrading process as it would in a mining method.

Sabharwall et al.'s [40] report was based on heat from an AHTR that was transferred from the reactor core by the primary liquid-salt coolant to an intermediate heat-transfer loop through an IHX. The intermediate heat-transfer loop circulates intermediate liquid-salt coolant through a SHX to move the heat to a power conversion system or for processing industrial applications (Fig. 3.43).

The ROT is currently 704 °C and was reported by Sabharwall et al. [40], but will possibly increase to 900–1000 °C for the one of a kind. With its ability to provide higher ROT, the process heat application becomes an attractive option. Even

though the ROT for the AHTR is 700 °C (approximately 704 °C), the maximum allowable temperature for any process application is 650 °C, as shown by the dashed line in Fig. 3.43. Process heat applications are mentioned in this section, but details are given in TEV-1160, “AHTR Technical Evaluation” (Sabharwall and Kim) [41].

Sabharwall et al. [40] assumed the following conditions in the calculations for their analysis:

- The reactor outlet temperature for an AHTR is assumed to be 700 °C.
- An AHTR ROT should be much larger (approximately 50 °C) than the process application temperature requirement.
- Any power production/industrial application requiring greater than 650 °C is referred to as a long-term objective.
- The minimum AHTR heat exchanger temperature should be maintained high enough to avoid freezing of MS (>500 °C), which will provide an approximately 50 and 65 °C temperature threshold before fluoride salts, such as LiF-NaF-KF (FLiNaK), and chloride salts, such as KCl-MgCl<sub>2</sub>, freeze.
- The heat exchanger tube material should have sufficient mechanical integrity to sustain a pressure difference across the tube wall (which will depend on the application).

The process heat applications mentioned briefly in this section are discussed in greater detail in TEV-1160, “AHTR Technical Evaluation” (Sabharwall and Kim) [41]. With a ROT of 704 °C and maximum allowable temperature of 650 °C for process heat applications, the current AHTR could provide process heat for the following applications:

- Near-term integration (<650 °C):
  - Power production cycles (steam Rankine cycle, helium Brayton cycle, SCO<sub>2</sub> cycle);
  - Oil shale (in situ);
  - Oil shale (ex situ);
  - Oil sands.
- Long-term integration (>650 °C):
  - Hydrogen production via steam methane reforming,
  - Substitute natural gas production,
  - Coal-to-liquid production,
  - Natural gas-to-liquid production,
  - Methanol-to-gasoline production,
  - Ammonia production.

An AHTR, when compared to gas-cooled reactors for process heat applications, benefits from a higher reactor inlet temperature because the MS is a more efficient heat transport medium and can transfer all of the reactor’s heat with a smaller

temperature drop. This allows for the use of smaller and more efficient heat exchange equipment and produces smaller thermal stresses on the components.

## References

1. Wade A. Amos. (1998). Costs of storing and transporting hydrogen. National Renewable Energy Laboratory, US Department of Energy DE-AC36-83CH10093, November 1998.
2. Flynn, T. M. (1992). *A liquefaction of gases. McGraw-Hill encyclopedia of science & technology* (7th ed., Vol. 10, pp. 106–109). New York: McGraw-Hill.
3. Timmerhaus, C., & Flynn, T. M. (1989). *Cryogenic engineering*. New York: Plenum Press.
4. Schwarz, J. A., & Amonkwaah, K. A. G. (1993). *Hydrogen storage systems*. Washington, DC: U.S. Geological Survey.
5. Garret, D. E. (1989). *Chemical engineering economics*. New York: Von Nostrand Reinhold.
6. Zittel, W., & Wurster, R. (1996). *Hydrogen in the energy sector*. Ottobrunn: Ludwig-Bolkow-Systemtechnik GmbH.
7. Hart, D. (1997). *Hydrogen power: The commercial future of 'the Ultimate Fuel'*. London: Financial Times Energy Publishing.
8. Zohuri, B. (2015). *Combined cycle driven efficiency for next generation nuclear power plants: An innovative design approach*. Heidelberg: Springer.
9. Zohuri, B. (2014). *Innovative open air Brayton combined cycle systems for the next generation nuclear power plants*. Albuquerque, NM: University of New Mexico Publications.
10. Forsberg, C., McDaniel, P., & Zohuri, B. (2015). Variable electricity and steam from salt, helium, and sodium cooled base-load reactors with gas turbines and heat storage. Proceedings of ICAPP 2015 May 03-06, 2015, Nice, France. Paper 15115.
11. Feasibility study of hydrogen production at existing nuclear power plants, electric transportation applications. INL/EXT-09-16326.
12. Summary of electrolytic hydrogen production. National Renewable Energy Laboratory (NREL) Report, September 2004.
13. Mintz, M., & Gillette, J. (2005). H<sup>2</sup>A delivery scenario model and analysis. Argonne National Laboratory, February 8, 2005.
14. Melaina, M. W. (2005). Estimating relative station sizes in early hydrogen station networks. *Proceeding of the National Hydrogen Association (NHA) Annual Conference*, Washington, DC, March 2005.
15. Ohi, J. M. (2006). Hydrogen codes and standards: An overview of U.S. DOE activities, WHEC 16/13-16, June 2006, Lyon, France.
16. Besenbruch, G. E., Brown, L. C., Funk, J. F., Showalter, S. K. (2000). High efficiency generation of hydrogen fuels using nuclear power. GA Project 30047, September 2000.
17. International Energy Outlook 2000: DOE/EIA-0484 (2000). The Energy Information Administration of the Department of Energy ([www.eia.doe.gov](http://www.eia.doe.gov)).
18. Annual Energy Outlook 2000 with projections to 2020: DOE/EIA-0383 (2000). The Energy Information Administration of the Department of Energy ([www.eia.doe.gov](http://www.eia.doe.gov)).
19. Analysis of the Impacts of an Early Start for Compliance with the Kyoto Protocol: SR/OIAF/99-02. The Energy Information Administration of the Department of Energy ([www.eia.doe.gov](http://www.eia.doe.gov)).
20. Impacts of the Kyoto Protocol on U.S. Energy Markets and Economic Activity: SR/OIAF/98-03. The Energy Information Administration of the Department of Energy ([www.eia.doe.gov](http://www.eia.doe.gov)).
21. Davis, C. B., Barner, R. B., Sherman, S. R., & Wilson, D. F. (2005). Thermal-hydraulic analyses of heat transfer fluid requirements and characteristics for coupling a hydrogen product plant to a high-temperature nuclear reactor. The INL is a U.S. Department of Energy National Laboratory operated by Battelle Energy Alliance, June 2005.

22. Hydrogen production using nuclear energy. International Atomic Energy Agency (IAEA) Nuclear Energy Series No. NP-T-42 Report.
23. Peterson, P. F. (2007). Intermediate heat exchanger dynamic thermal response model. Eugenio Urquiza Fernández U.C. Berkeley Report UCBTH-07-006, August 31, 2007.
24. Peterson, P. F., Zhao, H., & Fukuda, G. (2003). U.C. Berkeley Report UCBTH-03-004, December 5, 2003.
25. Zohuri, B., & Fathi, N. (2015). *Thermal-hydraulic analysis of nuclear reactors*. Heidelberg: Springer.
26. Vernondern, K., & Nishihara, T. (2004). Valuation of the safety concept of the combined nuclear/chemical complex for hydrogen production with HTTR. JUEL-4135.
27. Smith, C., Beck, S., & Galyean, B. (2005). An engineering analysis for separation requirements of a hydrogen production plant and high-temperature nuclear reactor. INL/EXT-05-00137 Rev 0, March 2005.
28. Dewson, S. J., & Thonon, B. (2003). The development of high efficiency heat exchangers for helium gas cooled reactors. Paper 3213, ICAPP03.
29. Diehl, H., & Bodman, E. (1990). Alloy 800 specifications in compliance with component requirements. *Journal of Nuclear Materials*, 171, 63–70.
30. Crandall, S. H., Dahl, N. C., & Lardner, T. J. (1972). *An introduction to the mechanics of solids* (2nd ed.). New York: McGraw-Hill Book Company.
31. Dostal, V., Driscoll, M. J., & Hejzlar, P. (2004). A supercritical carbon dioxide cycle for next generation nuclear reactors. MIT-ANP-TR-100, March 2004.
32. Krieth, F. (1964). *Principles of heat transfer*. Scranton, PA: International Textbook Company.
33. INEEL. (2003a). RELAP5-3D code manual volume 4: Models and correlations. INEEL-98-00834, Revision 2.2, October 2003.
34. Kayes, W. M., & Crawford, M. E. (1980). *Convective heat and mass transfer* (2nd ed.). New York: McGraw-Hill Book Company.
35. Zohuri, B., & McDaniel, P. J. (2014). *Thermodynamics in nuclear power plant systems*. Heidelberg: Springer.
36. Bird, R. B., Stewart, W. E., & Lightfoot, E. N. (1960). *Transport phenomena*. New York: Wiley.
37. Glasstone, S., & Sesonske, A. (1967). *Nuclear reactor engineering*. Princeton, NJ: D. Van Nostrand Company, Inc.
38. Mizia, R. E. (2008). Next generation nuclear plant intermediate heat exchanger acquisition strategy. INL/EXT-08-14054, April 2008.
39. Copinger, D. A., & Moses, D. L. (2003). Fort Saint Vrain gas cooled reactor operational experience. Oak Ridge National Laboratory, NUREG/CR-6839 ORNL/TM-2003/223.
40. Sabharwall, P., Kim, E. S., McKellar, M., Anderson, N., & Patterson, M. (2011). Process heat exchanger options for the advanced high temperature reactor. Report INL/EXT-11-21584 Revision 1, Idaho National Laboratory, June 2011.
41. Sabharwall, P., & Kim, E. S. (2011). Fluoride high temperature reactor integration with industrial process applications. Idaho National Laboratory, TEV-1160.
42. General Atomics. (1996). Gas turbine-modular helium reactor (GT-MHR) conceptual design description report. GA Project No. 7658, 910720 Revision 1, July 1996.

# **Chapter 4**

## **A New Approach to Energy Conversion Technology**

A nuclear reactor produces and controls the release of energy from splitting the atoms of uranium. Uranium-fueled nuclear power is a clean and efficient way of boiling water to make the steam that drives turbine generators. Except for the reactor itself, a nuclear power station works like most coal- or gas-fired power stations.

### **4.1 Power Conversion Study and Technology Options Assessment**

In the USA, most reactor design and development for the generation of electrical power derived from early nuclear naval research, when it was realized that a compact nuclear power plant would have great advantages for submarine-driven nuclear propulsion systems. To have such a power plant on board would make possible long voyages across the oceans at high speeds without having to resurface at frequent intervals.

Operating temperatures of conventional light water reactors (LWRs), 280–320 °C, limit power conversion systems to producing pressurized steam that drives a condensing steam turbine. After employing thermal recovery measures, nuclear plants using this Rankine cycle see a net plant efficiency of around 32–34 %. Comparatively, gas turbines with turbine inlet temperatures of up to and greater than 1400 °C have simple cycle efficiencies of around 40 % that can be boosted to around 60 % in a combined cycle. The ability of the combined cycle or Brayton with recuperator cycle to drastically improve net plant efficiency is an especially appealing feature to employ with a nuclear power source, given the very low fuel costs for nuclear energy, but has previously been technically infeasible given the high operating temperature requirements of a combined cycle (Fig. 4.1).

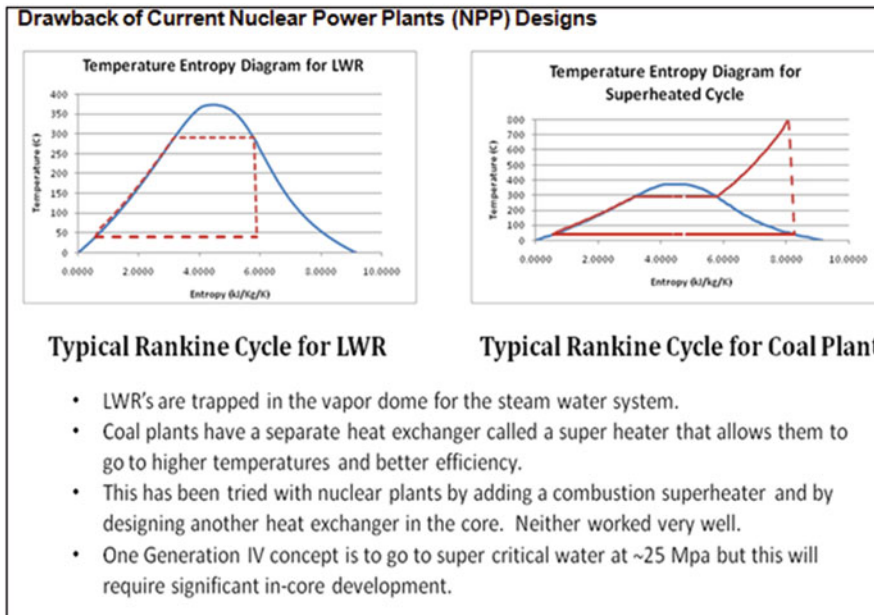


**Fig. 4.1** Drawback of current nuclear power plant (NPP) designs [1]

One of the differentiating features of fluoride salt HTRs is the operating temperature range of the primary coolant loop, 600–700 °C (reactor inlet and outlet temperatures, respectively). Although other advanced, HTRs have been developed, the high-temperature characteristics of the lithium fluoride and beryllium fluoride eutectic (FLiBe) molten salt primary coolant used in fluoride salt HTRs enable an operating temperature range that is uniquely suited to driving an open-air combined cycle that sees proportional increases in efficiency and power generation with elevated turbine inlet temperatures.

A study was conducted in September 2004 by a team of experts at the University of California at Berkeley, Nuclear Engineering Department. The executive summary shows that the electrical power conversion system (PCS) for Next Generation Nuclear Plants (NGNPs) will take advantage of a significantly higher reactor outlet temperature to provide greater efficiency than can be achieved by the current generation of LWRs. In anticipation of the design, development, and procurement of an advanced power conversion system for NGNPs, the study was initiated to identify the major design and technology options and the tradeoffs that must be considered in the evaluation of PCS options to support future research and procurement decisions. These PCS technology options affect cycle efficiency, capital cost, system reliability and maintainability, and technical risk and, therefore, the cost of electricity from Generation IV systems. A reliable evaluation and estimate of actual costs requires an optimized, integrated PCS design. In the early stages of

the NGNP project it was useful to identify the technology options that would be considered in the design of proposed PCS systems, identify the system performance and cost implications of these design options, and provide a general framework for evaluating the design choices and technology tradeoffs.

The ultimate measure of the value of power conversion options is the cost of electricity produced, which is a function of capital and operating cost recovery and the system efficiency and reliability. Evaluating cost is difficult to do without detailed integrated designs, but it is possible to identify the factors that influence component and system performance, cost, and technical risk. In this study, several existing Brayton conversion system designs were studied to illustrate and evaluate the implications of the major design choices to assess performance against the Generation IV economics and sustainability goals and to identify areas of technical incompleteness or weakness. Several reference system designs were considered to provide a semiquantitative basis for performing comparisons. The reference systems included the gas-turbine modular helium reactor (GT-MHR), pebble-bed modular reactor (PBMR), gas-turbine high-temperature reactor (GTHTR)-300, Framatome indirect cycle design, and advanced high-temperature reactor (AHTR) high-temperature Brayton cycle designs. Where appropriate, Generation II, III, and III+ LWRs [two 1970s designs, the European Pressurized Reactor (EPR) and the Economic Simplified Boiling Water Reactor (ESBWR)] were also considered.

The design choices and technology options considered relevant for the assessment of NGNP power conversion options included the cycle types and operational conditions, such as working fluid choices, direct vs. indirect, system pressure, and interstage cooling and heating options. The cost and maintainability of the PCS is also influenced by the PCS layout and configuration, including distributed vs. integrated PCS designs, single vs. multiple shafts, shaft orientation, and the implications for the pressure boundary.

From the summary given in Table 4.1 below, it is apparent that high-temperature gas reactor power conversion design efforts to date have resulted in very different design choices based on project-specific requirements and performance or technical risk requirements.

In the review of existing designs and the evaluation of the major technology options, it immediately becomes apparent that the optimized design involves a complex tradeoff of diverse factors, such as cost, efficiency, development time, maintainability, and technology growth path, that must be considered in an integrated PCS system context before final evaluation. General observations derived from the review of the reference systems, including comparisons with LWR systems where applicable, include the following:

- There are key PCS design choices that can have significant effects on PCS power density and nuclear island size, making careful and detailed analysis of design tradeoffs important in the comparison of PCS options.
- Considering the major construction inputs for nuclear plants – steel and concrete – HTRs appear to be able to break the economy-of-scale rules for LWRs and achieve similar material-input performance at much smaller unit sizes.

**Table 4.1** Summary of PCS design features for representative gas reactor systems

Feature	PBMR (horizontal)	GT-MHR	GTHTR300	Framatome indirect	AHTR-IT
Thermal power (MWt)	400	600	600	600	2400
Direct vs. indirect cycle	Direct	Direct	Direct	Indirect	Indirect
Recuperated vs. combined cycle	Recuperated	Recuperated	Recuperated	Combined	Recuperated
Intercooled vs. nonintercooled	Intercooled	Intercooled	Nonintercooled	Intercooled	Intercooled/ reheat
Integrated vs. distributed PCS	Distributed	Integrated	Distributed	Distributed	Distributed (modular)
Single vs. multiple TM shafts	Single (pre- viously multiple)	Single	Single	Single	Multiple (modular)
Synchronous vs. asynchronous	Reduction to synchronous	Asynchronous	Synchronous	Synchronous	Synchronous
Vertical vs. horizontal TM	Horizontal	Vertical	Horizontal	Horizontal	Vertical
Submerged vs. external generator	External	Submerged	Submerged	External	Submerged

- For HTRs, a much larger fraction of total construction inputs go into the nuclear island. To compete economically with LWRs, HTRs must find approaches to reduce the relative costs for nuclear-grade components and structures.

**PCS** technology options also include variations on the cycle operating conditions and the cycle type that can have an important impact on performance and cost. These options include the following:

- Working fluid choice – He, N<sub>2</sub>, CO<sub>2</sub>, and combinations thereof have been considered. Working fluid physical characteristics influence cycle efficiency and component design.
- System pressure – Higher pressures lead to moderate efficiency increases and smaller PCS components but increase the pressure boundary cost – particularly for the reactor vessel – which introduces a component-design and a system cost and performance tradeoff.
- Direct vs. indirect – Indirect cycles involve an intermediate heat exchanger (IHX) and a resulting efficiency reduction and more complex control requirements, but they facilitate maintenance.
- Interstage cooling (or heating) results in higher efficiency but greater complexity.

Some of the observations from this assessment of these factors include the following:

- Differences between He and N<sub>2</sub> working fluids were not considered critical for turbomachinery design because both involve similar differences from current combustion turbines, with the primary difference being in the heat exchanger (HX) size to compensate for the lower N<sub>2</sub> thermal conductivity.
- N<sub>2</sub> allows 3600-rpm compressor operation at thermal powers at and below 600 MW(t), while He compressors must operate at higher speeds requiring reduction gears, asynchronous generators, or multiple-shaft configurations. However, power-up ratings to approximately 800 MW(t) would permit 3600-rpm He compressor operation, providing a potentially attractive commercialization approach. Turbomachinery tolerances for He systems do not appear to be a key issue.
- Direct/indirect – Efficiency loss can be 2–4 %, depending on the design, and the IHX becomes a critical component at high temperatures. Direct cycles have an extended nuclear-grade pressure boundary. Maintainability is considered a key design issue for direct cycles.
- Interstage cooling, as well as bottoming cycles (Rankine), can result in significant efficiency improvements, but at a cost of complexity and lower temperature differences for heat rejection, affecting the potential for dry cooling and reduced environmental impact from heat rejection.

The PCS configuration and physical arrangement of the system components have important effects on the volume and material inputs into structures, on the pressure boundary volume and mass, on gas inventories and storage volume, on the uniformity of flow to HXs, on pressure losses, and on maintainability. The major factors considered in this study included the following:

- Distributed vs. integrated PCS design approach – PCS components can be located inside a single pressure vessel [e.g., Gas Turbine Modular Helium Reactor (GT-MHR)], or they can be divided between multiple pressure vessels [e.g., Pebble Bed Modular Reactor (PBMR), pebble bed high-temperature reactor (HTR)-300]. This is a major design choice, with important impacts in several areas of design and performance.
- Shaft orientation (vertical/horizontal) – Orientation affects the compactness of the system, the optimal design of ducting between turbomachinery and HXs. Vertical turbomachinery provides a reduced PCS footprint area and building volume and can simplify the ducting arrangement to modular recuperator and intercooler HXs.
- Single vs. multiple shafts – Single shafts may include flexible couplings or reduction gears. In multiple-shaft systems, turbocompressors are separated from synchronous turbogenerators, allowing the compressors to operate at higher speed and reducing the number of compressor stages required. Multiple shafts and flexible couplings reduce the weight of the individual turbomachines that bearings must support.

- Pressure boundary design – The pressure vessels that contain the PCS typically have the largest mass of any PCS components and provide a significant (~33 %) contribution to the total PCS cost.

## 4.2 Waste Heat Recovery

Waste heat is heat generated in a process by way of fuel combustion or chemical reaction, which is then “dumped” into the environment and not reused for useful or economic purposes. The essential fact is not the amount of heat, but rather its “value.” The mechanism to recover the unused heat depends on the temperature of the waste heat gases and the economics involved.

Large quantities of hot flue gases are generated from boilers, kilns, ovens, and furnaces. If some of the waste heat could be recovered, then a considerable amount of primary fuel could be saved. The energy lost in waste gases cannot be fully recovered. However, much of the heat could be recovered and adopting the following measures as outlined in this chapter can minimize losses.

### 4.2.1 *Advantages and Disadvantages of Waste Heat Recovery*

#### **Advantages:**

These systems have many benefits, which can be direct or indirect.

- Direct benefits:
  - The recovery process adds to the efficiency of the process and thus decreases the costs of fuel and energy consumption needed for that process.
- Indirect benefits:
  - Reduction in pollution: Thermal and air pollution dramatically decrease since less flue gases of high temperature are emitted from the plant since most of the energy is recycled.
  - Reduction in equipment size: As fuel consumption reduces, the control and security equipment for handling the fuel decreases. Also, filtering equipment for the gas is no longer needed in large sizes.
  - Reduction in auxiliary energy consumption: Reduction in equipment sizes means another reduction in the energy fed to those systems such as, for example, pumps, filters, and fans.

#### **Disadvantages:**

- Capital cost: The capital cost to implement a waste heat recovery system may outweigh the benefit gained in heat recovered. It is necessary to put a cost to the heat being offset.

- Quality of heat: Often waste heat is of low quality (temperature). It can be difficult to efficiently utilize the quantity of low-quality heat contained in a waste heat medium. HXs tend to be larger to recover significant quantities, which increases capital cost.
- Maintenance of equipment: Additional equipment requires additional maintenance costs.

## 4.3 Power Conversion System Components

The effectiveness or efficiency of the major PCS components, primarily the HXs and turbomachinery, is clearly a major factor in system cost and performance. An overall summary of each of these components is given in the following sections.

### 4.3.1 Heat Exchangers

A **heat exchanger** is a device built for efficient heat transfer from one medium to another, whether the media are separated by a solid wall, so that they never mix, or are in direct contact. They are widely used in space heating, refrigeration, air conditioning, power plants, chemical plants, petrochemical plants, petroleum refineries, and natural gas processing. One common example of a HX is the radiator in a car, in which a hot engine-cooling fluid, like antifreeze, transfers heat to air flowing through the radiator.

For efficiency, HXs are designed to maximize the surface area of the wall between the two fluids while minimizing resistance to fluid flow through the exchanger. The exchanger's performance can also be affected by the addition of fins or corrugations in one or both directions, which increase surface area and may channel fluid flow or induce turbulence.

As mentioned earlier, HXs transfer heat from one fluid to another and in particular at compact sizes is one of the important aspects of PCS components – if we want to rely on combined-cycle-driven efficiency of next generation nuclear power plants.

High heat transfer rates, modular construction, exotic alloys, low hold-up volume, and high internal turbulence all combine to improve efficiencies and process control, with longer maintenance cycles. The temperature difference at the pinch depends on the HX; in general, the smaller the temperature difference, the more expensive the HX [2].

Consider Fig. 4.2. The pinch point is defined as the point where the temperature difference is at a minimum. Taking as an example a temperature difference of 20 K, say, the combined cold stream can be moved from left to right on the diagram until the temperature difference at the pinch point is 20 K as shown in Fig. 4.2. It can then be seen that external heating of 90 kW and external cooling of 140 kW

**Fig. 4.2** Temperature against rate of enthalpy change for composite hot and cold streams

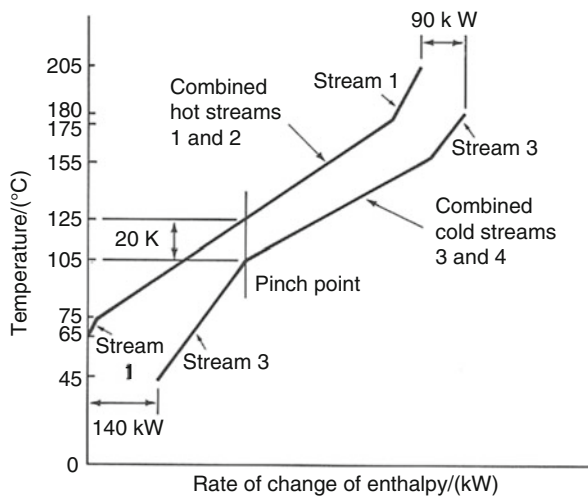


**Table 4.2** Data for four fluid streams

Stream number	Initial temp. (°C)	Final temp. (°C)	Mass flow rate (kg/s)	Specific heat capacity (kJ/kg K)	Heat cap rate (kW/K)	Rate of enthalpy increase (kW)
1	205	65	2.00	1.00	2.0	-280
2	175	75	3.20	1.25	4.0	-400
3	45	180	3.75	0.80	3.0	+405
4	105	155	3.00	1.50	4.5	+225
						50

are required; all other energy changes can be achieved by HXs between the various streams; the difference between the external heating and the external cooling is  $(90 - 140) = -50 \text{ kW}$ , the same as in Table 4.1. Note that the process in a boiler or condenser would appear as a horizontal line on a diagram such as Fig. 4.2. The data are given in Table 4.2.

As stated earlier, compact HXs have a vital role in producing higher efficiency if they are used in a combined gas-steam power cycle versus conventional shell-and-tube HXs.

They are available with standard connections in various diameters and in different lengths. Compact HXs can be designed in horizontal and vertical orientations and be used for a wide variety of applications including the following, among others:

- Compressed gas/water coolers,
- Water/water coolers,
- Oil/water coolers,
- Preheaters,
- Condensers and evaporators for chemical and technical processes of all kinds,

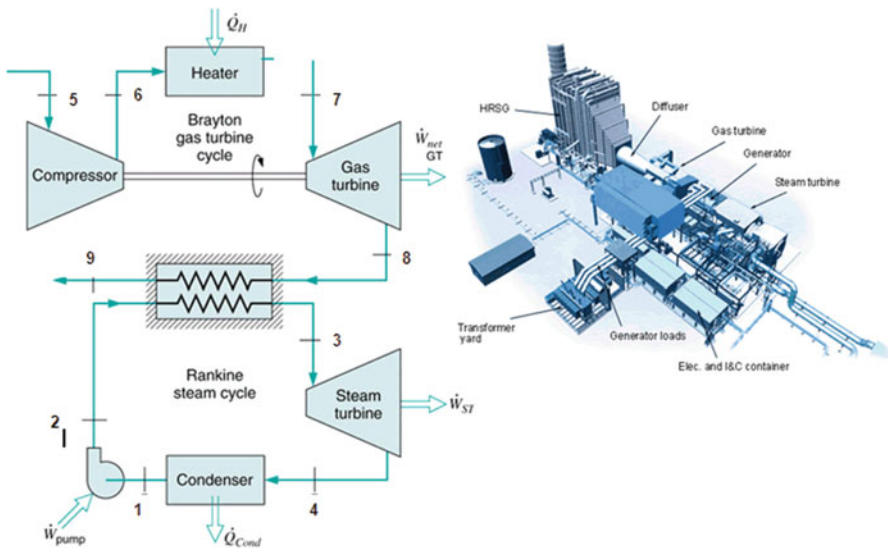


**Fig. 4.3** Combined gas (Brayton)-steam (Rankine) cycle

- Machine coolers,
- Oil coolers for hydraulic systems,
- Oil and water coolers for power machines.
- Refrigeration and air-conditioning units.

Consider a HX application in the case of combined gas-steam power cycles (Fig. 4.3), where the objective of this cycle is to combine a Brayton cycle with a Rankine cycle. This combination improves significantly the thermal efficiency of the power plant.

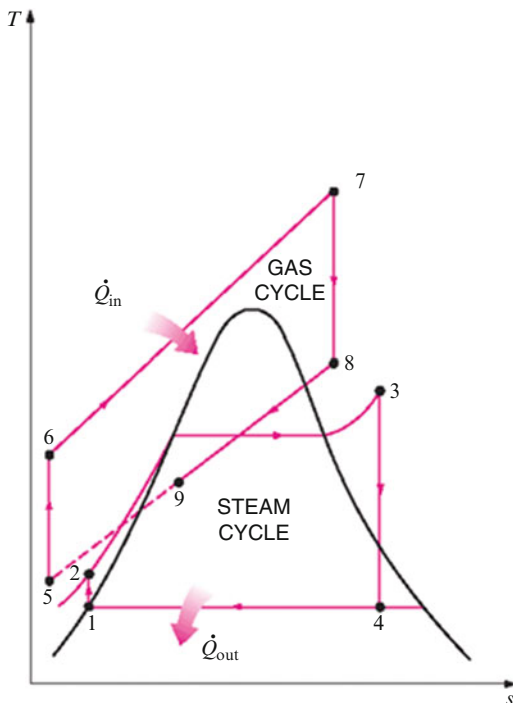
The idea behind a combined gas-steam power cycle is to use the high-temperature exhaust gases from the gas turbine to heat the steam within the boiler of the steam turbine.

If we consider such a combined cycle, the *T-s* diagram is presented in Fig. 4.4.

Heat exchanger components are defined and the required designs are summarized as follows:

- HX designs have significant impacts on both the efficiency and cost of the PCS. For a given HX type, higher efficiency must be balanced against the increased size or pressure drop implications. Using small passages increases HX surface area per unit volume, but those same small passages tend to reduce the heat transfer coefficient owing to laminar flow. Higher pressures may be utilized to force those flows back into the turbulent region, but those higher pressures force the construction of a more robust pressure boundary and increase the pumping power.
- The recuperator efficiency and total HX pressure drop have significant impacts on the cycle efficiency and there is significant leverage in optimizing the

**Fig. 4.4** *T-s* diagram of a combined gas (Brayton)–steam (Rankine) cycle



recuperator design for both high heat transfer efficiency and minimum pressure drop. For modular recuperators, careful attention must be paid to the module configuration and duct design to obtain equal flow rates for each module.

- Material limitations may limit the operating temperatures for many components, including the reactor vessel and HXs. But because of the large flexibility of the Brayton cycle, high-efficiency systems can still be designed within these limitations. Fabrication techniques will probably differ between intermediate, pre- and intercooler, and recuperator HXs because of their operating temperature ranges. It would appear that transients could be tolerated by most of these HX designs.

A HX is a device for transferring heat from one fluid to another. There are three main categories:

1. *Recuperative*: in which the two fluids are at all times separated by a solid wall;
2. *Regenerative*: in which each fluid transfers heat to or from a matrix of material;
3. *Evaporator*: in which the enthalpy of vaporization of the fluid is used to provide a cooling effect.

The most commonly used type is the recuperative HX, and it can be classified by flow arrangement, where numerous possibilities exist for flow arrangement in HXs.

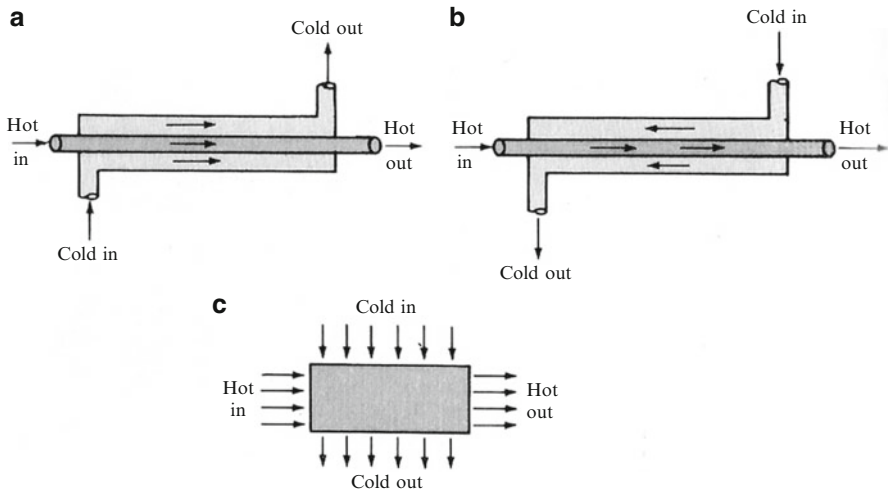


**Fig. 4.5** (a) Parallel flow, (b) Counterflow, and (c) Cross flow [4]

In this type of HX, the two fluids can flow [3–7]

1. In *parallel flow*,
2. In *counterflow*, or
3. In *cross flow*.

HXs may be classified according to their flow arrangement.

1. **Parallel flow:** In a parallel-flow HX configuration, the hot and cold fluids enter at the same end of the HX, flow through in the same direction (i.e., in parallel to one another to the other side), and leave together at the other end, as illustrated in Fig. 4.5a [5].
2. **Counter flow:** In a counterflow HX configuration, the hot and cold fluids enter at opposite ends of the HX and flow through in opposite directions, as illustrated in Fig. 4.5b [5].
3. **Cross flow:** In cross-flow HX configuration, the two fluids usually flow at right angles to each other, as illustrated in Fig. 4.5c [5]. In the cross-flow arrangement, the flow may be called *mixed* or *unmixed*, depending on the design. The countercurrent design is most efficient, in that it can transfer the most heat. In a cross-flow HX, the fluids travel roughly perpendicular to one another through the exchanger.

Figure 4.6a shows a simple arrangement in which both hot and cold fluids flow through individual channels formed by corrugation; therefore, the fluids are not free to move in the transverse direction. Then each fluid stream is said to be unmixed. Figure 4.6b illustrates a typical temperature profile for the outlet temperatures when both fluids are unmixed, as shown in Fig. 4.6a. The inlet temperatures for both fluids are assumed to be uniform, but the outlet temperatures exhibit variation transverse to the flow.

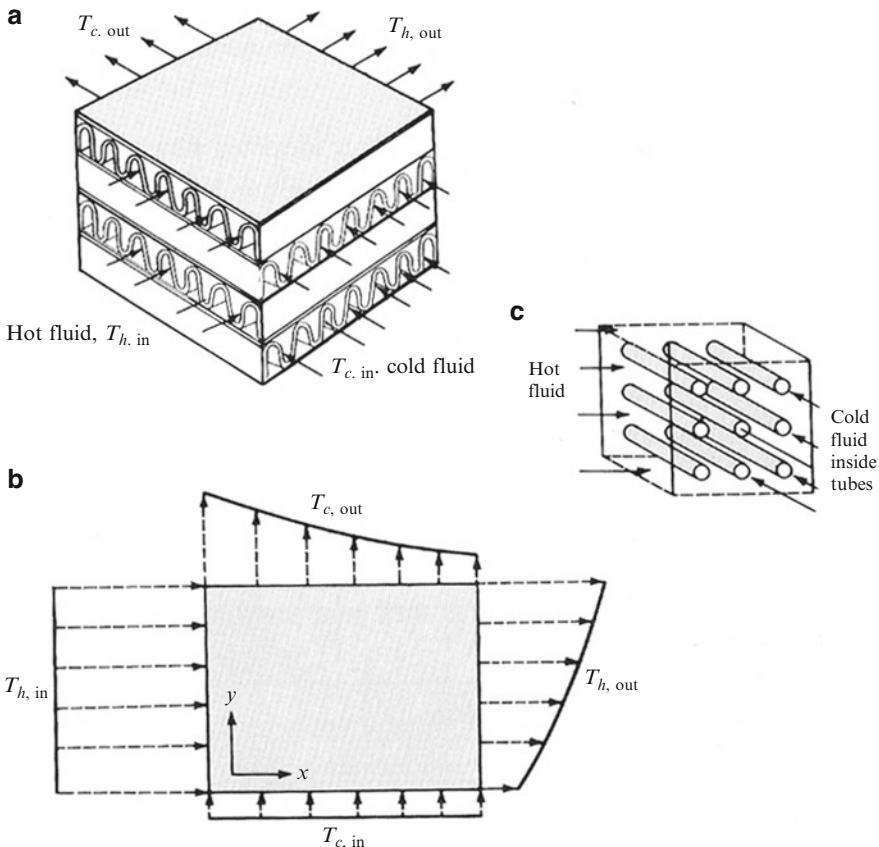


**Fig. 4.6** Cross-flow arrangements: (a) both fluids unmixed; (b) temperature profile when both fluids are unmixed; (c) cold fluid unmixed, hot fluid mixed [4]

In the flow arrangement shown in Fig. 4.6c, the cold fluid flows inside the tubes and so is not free to move in the transverse direction. Therefore, the cold fluid is said to be unmixed. However, the hot fluid flows over the tubes and is free to move in the transverse direction. Therefore, the hot fluid stream is said to be mixed. The mixing tends to make the fluid temperature uniform in the transverse direction; therefore, the exit temperature of a mixed stream exhibits negligible variation in the crosswise direction.

In general, in a cross-flow exchanger, three idealized flow arrangements are possible:

1. Both fluids are unmixed;
2. One fluid is mixed, the other unmixed; and
3. Both fluids are mixed.

The last arrangement is not commonly used.

In a shell-and-tube exchanger, the presence of a large number of baffles serves to “mix” the shell-side fluid in the sense discussed earlier; that is, its temperature tends to be uniform at any cross section.

The driving temperature across the heat transfer surface varies with position, but an appropriate mean temperature can be defined. In most simple systems this is the logarithmic mean temperature difference (LMTD). Sometimes direct knowledge of the LMTD is not available and the number of transfer units (NTU) method is used.

In summary, the NTU method is used to calculate the rate of heat transfer in HXs (especially countercurrent exchangers) when there is insufficient information to calculate the LMTD. In HX analysis, if the fluid inlet and outlet temperatures are specified or can be determined by the simple energy balance, the LMTD method can be used; but when these temperatures are not available, the NTU or *effectiveness method* is used.

We now summarize the principal HXs, as shown in Fig. 4.5a–c. The temperature variations of each type are shown in Fig. 4.5a–c. It can also be shown that for all three cases of Fig. 4.5 the true temperature difference is the LMTD, given by [5–7]

$$\text{LMTD} = \frac{(\Delta t_1 - \Delta t_2)}{\ln(\Delta t_1 / \Delta t_2)}. \quad (4.1)$$

On the other hand, in the case of the NTU or effectiveness method analysis, to define the efficiency of a HX, we need to find the maximum possible heat transfer that can be hypothetically achieved in a counterflow HX of infinite length. Therefore, one fluid will experience the maximum possible temperature difference, which is the difference  $T_{\text{hot,inlet}} - T_{\text{cold,inlet}}$  (the temperature difference between the inlet temperature of the hot stream  $T_{\text{hot,inlet}} = T_{\text{h,i}}$  and the inlet temperature of the cold stream  $T_{\text{cold,inlet}} = T_{\text{c,i}}$ ). The method proceeds by calculating the heat capacity rates (i.e., mass flow rate multiplied by the specific heat)  $C_h$  and  $C_c$  for the hot and cold fluids, respectively, and denoting the smaller one by  $C_{\min}$ . References such as Ozisik [5] or Incropera and DeWitt [6] and Incropera et al. [7] present detailed analyses of the NTU method; we simply write the result of finding the efficiency that is given in the form of Eq. (4.2) below:

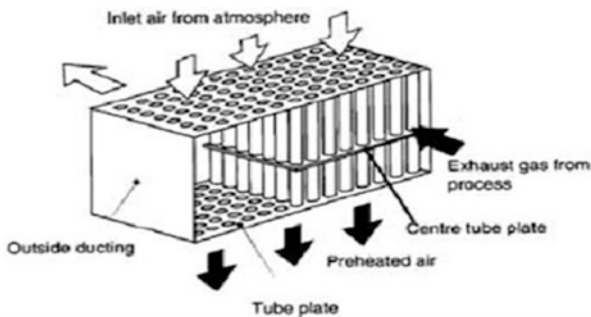
$$E = 1 - \exp[-\text{NTU}]. \quad (4.2)$$

As stated earlier, for a more detailed analysis of these two methods, the reader may consult the aforementioned classic textbooks.

### 4.3.1.1 Recuperative Heat Exchanger

Industrial process facilities recover, or “recuperate,” otherwise wasted heat energy using HXs, but on a much larger scale.

**Fig. 4.7** Waste heat recovery using recuperator



A recuperator is a special-purpose counterflow energy recovery HX positioned within the supply and exhaust air streams of an air-handling system, or in the exhaust gases of an industrial process, in order to recover waste heat.

In many types of processes, combustion is used to generate heat, and the recuperator serves to recuperate, or reclaim, this heat for reuse or recycling. The term *recuperator* refers as well to the liquid–liquid counterflow HXs used for heat recovery in the chemical and refinery industries and in closed processes such as ammonia–water or LiBr–water absorption refrigeration cycles.

Recuperators are often used in association with the burner portion of a heat engine to increase the overall efficiency. For example, in a gas-turbine engine, air is compressed and then mixed with fuel, which is subsequently burned and used to drive a turbine. The recuperator transfers some of the waste heat in the exhaust to the compressed air, thereby preheating it before it enters the fuel burner stage. Since the gases have been preheated, less fuel is needed to heat the gases up to the turbine inlet temperature. By recovering some of the energy usually lost as waste heat, the recuperator can make a heat engine or gas turbine significantly more efficient.

In a recuperator, heat exchange takes place between the flue gases and the air through metallic or ceramic walls. Ducts or tubes carry the air for combustion to be preheated; the other side contains the waste heat stream. A recuperator for recovering waste heat from flue gases is shown in Fig. 4.7.

There are different types of recuperators, and the choice of recuperator depends on the application. Descriptions of the different types of recuperator are presented in the following sections.

Figure 4.8 below is an illustration of various recuperators manufactured by various companies.

#### Metallic Radiation Recuperator

The simplest configuration for a recuperator is the metallic radiation recuperator, which consists of two concentric lengths of metal tubing, as shown in Fig. 4.9.

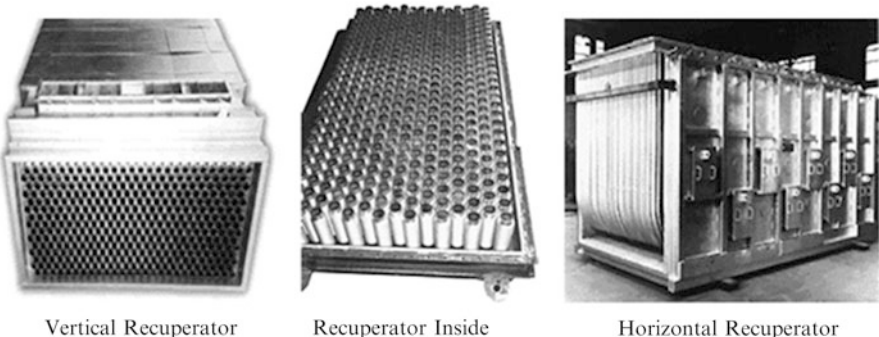
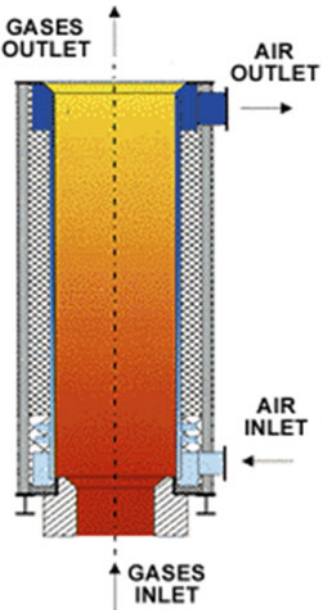


**Fig. 4.8** Different types of recuperator

**Fig. 4.9** Metallic radiation recuperator



The inner tube carries the hot exhaust gases while the external annulus carries the combustion air from the atmosphere to the air inlets of the furnace burners. The hot gases are cooled by the incoming combustion air, which now carries additional energy into the combustion chamber. This is the energy that does not have to be supplied by the fuel; consequently, less fuel is burned for a given furnace loading. The saving in fuel also means a decrease in combustion air, and therefore stack losses are decreased not only by lowering the stack gas temperatures but also by discharging smaller quantities of exhaust gas.

The radiation recuperator gets its name from the fact that a substantial portion of the heat transfer from the hot gases to the surface of the inner tube takes place by radiative heat transfer. The cold air in the annulus, however, is almost transparent to infrared radiation so that only convection heat transfer takes place with the incoming air. As shown in the diagram, the two gas flows are usually parallel, although the configuration would be simpler and the heat transfer more efficient if the flows were in opposite directions (or counterflow). The reason for the use of parallel flow is that recuperators frequently serve the additional function of cooling the duct carrying away the exhaust gases and consequently extending its service life.

### Convective Recuperator

A second common configuration for a recuperator is called the tube type or convective recuperator. As seen in Fig. 4.10 below, the hot gases are carried through a number of parallel small-diameter tubes, while the incoming air to be heated enters a shell surrounding the tubes and passes over the hot tubes one or more times in the direction normal to their axes.

If the tubes are baffled to allow the gas to pass over them twice, the HX is termed a two-pass recuperator; if two baffles are used, it is a three-pass recuperator, and so forth.

Although baffling increases both the cost of the exchanger and the pressure drop in the combustion air path, it increases the effectiveness of heat exchange. Shell-and-tube type recuperators are generally more compact and have a higher effectiveness than radiation recuperators because of the larger heat transfer area made possible through the use of multiple tubes and multiple passes of the gases.

Using steel plain tubes, in these recuperators the heat transfer between the primary and secondary fluid is made by means of convection (Fig. 4.11).

**Fig. 4.10** Convective recuperator

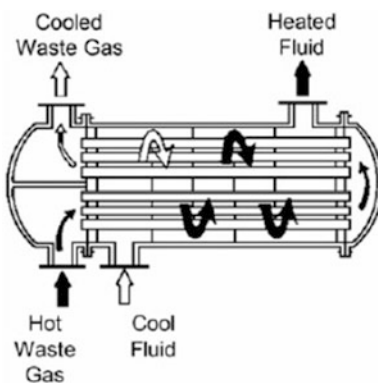
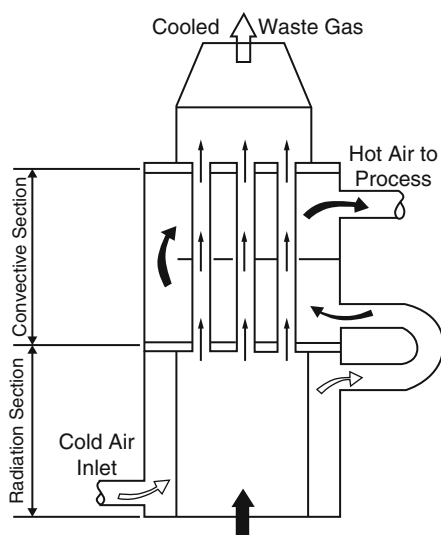


**Fig. 4.11** Typical commercial cross-flow convective recuperators



**Fig. 4.12** Hybrid recuperator

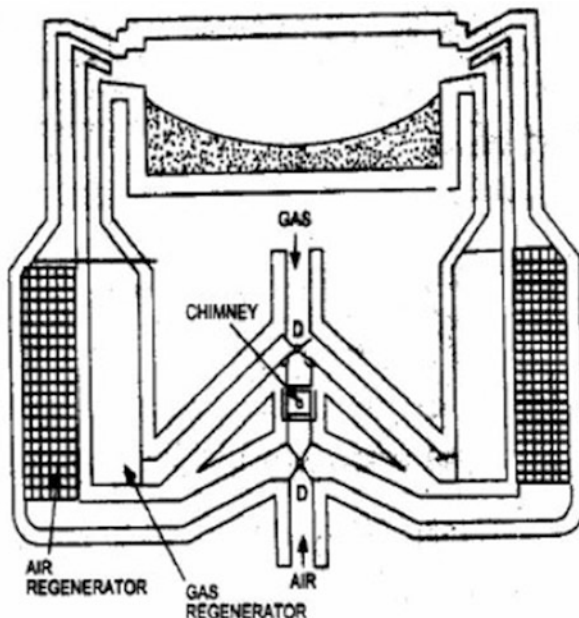


### Hybrid Recuperator

For maximum effectiveness of heat transfer, hybrid recuperators are used. These are combinations of radiation and convective designs, with a high-temperature radiation section followed by a convective section (Fig. 4.12).

These are more expensive than simple metallic radiation recuperators but less bulky.

**Fig. 4.13** Schematic of ceramic recuperator



### Ceramic Recuperator

The principal limitation on the heat recovery of metal recuperators is the reduced life of the liner at inlet temperatures exceeding 1100 °C. To overcome the temperature limitations of metal recuperators, ceramic tube recuperators have been developed whose materials allow operation on the gas side to be at 1550 °C and on the preheated air side 815 °C on a more or less practical basis. Early ceramic recuperators were built of tile and joined with furnace cement, and thermal cycling caused cracking of joints and rapid deterioration of the tubes. Later developments introduced various kinds of short silicon carbide tubes, which can be joined by flexible seals located in the air headers (Fig. 4.13).

Earlier designs experienced leakage rates of 8 to 60 %. The new designs are reported to last 2 years with air preheat temperatures as high as 700 °C, with much lower leakage rates.

#### 4.3.1.2 Regenerative Heat Exchanger

A regenerative HX, or more commonly a regenerator, is a type of HX where heat from the hot fluid is intermittently stored in a thermal storage medium before it is transferred to the cold fluid. To accomplish this, the hot fluid is brought into contact with the heat storage medium, then the fluid is displaced with the cold fluid, which absorbs the heat.

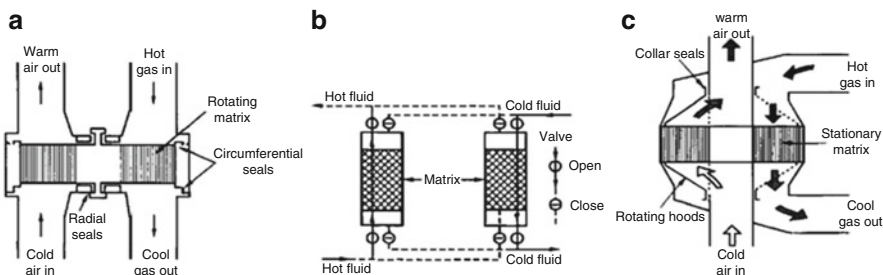
In regenerative HXs, the fluid on either side of the HX can be the same fluid. The fluid may go through an external processing step, and then it is flowed back through the HX in the opposite direction for further processing. Usually the application will use this process cyclically or repetitively.

The regenerator represents a class of HXs in which heat is alternately stored and removed from a surface. This heat transfer surface is usually referred to as the matrix of the regenerator, and for continuous operation the matrix must be moved into and out of the fixed hot and cold fluid streams. In this case, the regenerator is called a rotary regenerator. If, on the other hand, the hot and cold fluid streams are switched into and out of the matrix, the regenerator is referred to as a fixed matrix regenerator.

Figure 4.14 illustrates typical regenerator HXs; Fig. 4.14a–c shows rotary, fixed-matrix, and rotating-hoods HXs.

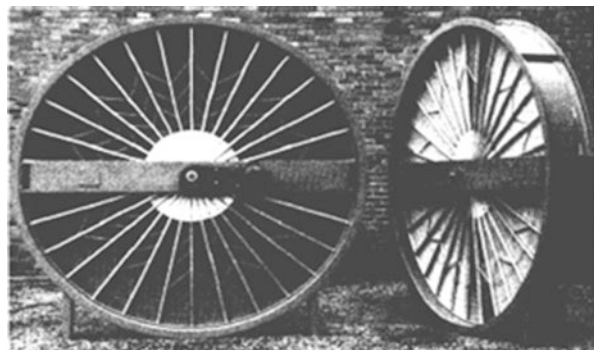
Typical rotary regenerators or heat wheels are shown in Fig. 4.15.

Further detailed analysis, including the advantages and disadvantages of this type of HX, is beyond the intended scope of this book; readers may conduct their own researches and investigations.



**Fig. 4.14** (a) Rotary, (b) fixed-matrix, and (c) rotating hoods

**Fig. 4.15** Typical rotary regenerators or heat wheels



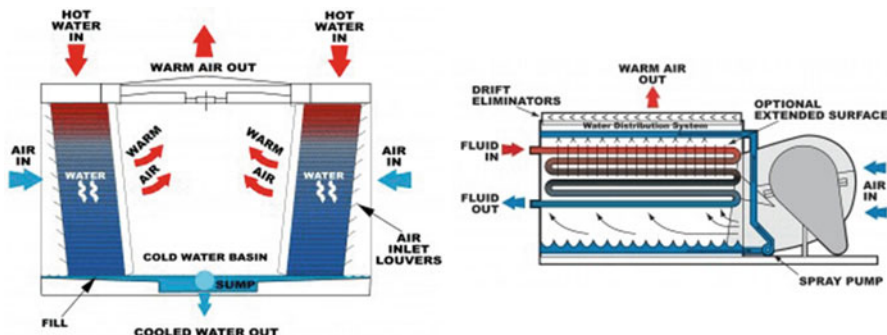


**Fig. 4.16** Cooling tower along with evaporative heat exchanger

#### 4.3.1.3 Evaporative Heat Exchanger

Normally this type of HX can be found in any cooling tower of power plants of all types and as the name of this HX suggests, it uses an evaporation process instead of a heat transfer processes.

In an open-circuit cooling tower, warm water from the heat source is evenly distributed via a gravity or pressurized nozzle system directly over a heat transfer surface called a fill or wet deck, while air is simultaneously forced or drawn through the tower, causing a small percentage of the water to evaporate. The evaporation process removes heat and cools the remaining water, which is collected in the tower's cold water basin and returned to the heat source (typically a water-cooled condenser or other HX). Figure 4.16 illustrates a cooling tower along with an evaporative HX.

Maintenance frequency will depend largely on the condition of the circulating water, the cleanliness of the ambient air used by the tower, and the environment in which the tower operates.

#### 4.3.2 Compact Heat Exchangers

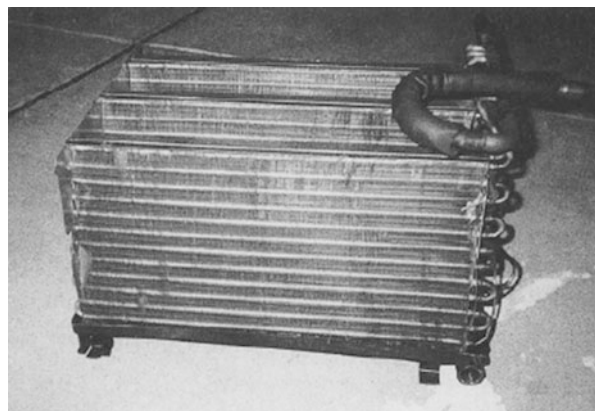
A type of HX that is specifically designed to achieve a larger heat transfer area per unit volume is known as a compact HX. Compact HXs are commonly used in gas-to-gas and gas-to-liquid (or liquid-to-gas) HXs to counteract the low heat transfer coefficient associated with gas flow with increased surface area.

Figure 4.17 illustrates the typical configuration and structure of a gas-to-liquid compact HX for a residential air-conditioning system.

Compact HXs are a class of HX that incorporate a large amount of heat transfer surface area per unit volume, where the area density  $\beta$  parameter comes into play.

The ratio of the heat transfer surface area of a HX to its volume is called the *area density*,  $\beta$ . A HX with  $\beta = 700 \text{ m}^2/\text{m}^3$  (or  $200 \text{ ft}^2/\text{ft}^3$ ) is classified as compact.

**Fig. 4.17** Residential gas-to-liquid compact heat exchangers



Examples of compact HXs are car radiators ( $1000 \text{ m}^2/\text{m}^3$ ), glass ceramic gas-turbine HXs ( $6000 \text{ m}^2/\text{m}^3$ ), the regenerator of a Stirling engine ( $15,000 \text{ m}^2/\text{m}^3$ ), and the human lung ( $20,000 \text{ m}^2/\text{m}^3$ ). A HX with  $\beta > 700 \text{ m}^2/\text{m}^3$  is classified as a compact HX.

Most automotive HXs fall into the compact HX category since space is an extreme constraint for automotive applications. By the same token, studies on open-air combined cycles have been conducted recently at the University of New Mexico by Zohuri and McDaniel and others [8–11] and on  $\text{CO}_2$  closed combined cycles by a team of engineers at Sandia National Laboratory [12–14], as well as by researchers at other universities and in industry utilizing the Brayton and Rankine cycles as a means of driving efficiencies in NGNPs (Generation IV) with small modular reactors (**SMRs**). The new approaches show promise for potential applications for these types of HX.

Compact HXs are categorized as follows [15, 16]:

- Tubular HX,
- Fin-plate HX,
- Tube-fin HX,
- Plate-frame HX,
- Regenerative HX.

Designing these types of HX is an easy task; the argument as to why it not that simple can be summarized as follows:

- Perform the required heat transfer AND
  - Minimize size and weight
  - Minimize pressure drop

- Meet required life
- Be resistant to fouling and contamination
- Minimize cost

Other important factors in designing these types of HX (compact), in particular in their application to high-temperature combined cycles for NGNPs, are the pinch point and imposed golden rules driven by pinch technology (Chap. 6), which makes them very expensive to manufacture.

A comparison of compact HXs with traditional shell-and-tube HXs can be summarized as follows:

- They occupy 80 % less space compared shell-and-tube HXs.
- The overall heat transfer coefficient is three or four times higher than shell-and-tube HX. This is very important advantages that are required by combined cycles in SMR to drive to higher thermal effectiveness out from cost of ownership to make them more desirable.
- They use low-pressure and low-temperature devices.

The limitations of compact HXs are as follows:

- Maximum design pressure: 25 bar.
- Maximum design temperature: 200 °C.
- It can only be used for clean fluids.

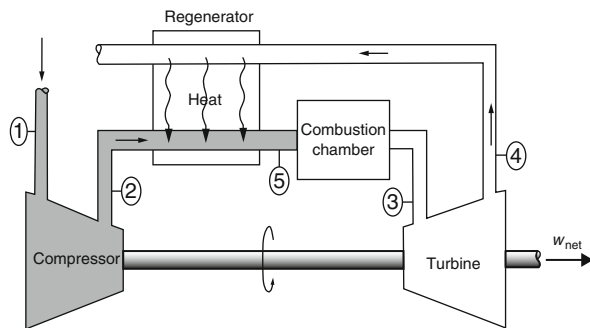
For further detailed information and related tables, as well as correlated experimental data, consult classic and well-known book by Kays and London [15], as well as the book edited by R. K. Shah [16].

## 4.4 Development of Gas Turbine

The gas turbine has experienced phenomenal progress and growth since its first successful development in the 1930s. The early gas turbines built in the 1940s and even 1950s had simple-cycle efficiencies of about 17 % because of the low compressor and turbine efficiencies and low turbine inlet temperatures due to metallurgical limitations of those times. Therefore, gas turbines found only limited use despite their versatility and their ability to burn a variety of fuels. Efforts to improve the cycle effectiveness concentrated in three areas:

1. Increasing the turbine inlet (or firing) temperatures.
2. Increasing the efficiencies of turbomachinery components.
3. Adding modifications to the basic cycle. The simple-cycle efficiencies of early gas turbines were practically doubled by incorporating intercooling, regeneration (or recuperation), and reheating. The back work ratio of a gas-turbine cycle improves as a result of intercooling and reheating. However, this does not mean that the thermal efficiency will also improve. Intercooling and reheating will always decrease the thermal efficiency unless they are accompanied by

**Fig. 4.18** *T-s diagram of a Brayton cycle with regeneration*



regeneration. This is because intercooling decreases the average temperature at which heat is added, and reheating increases the average temperature at which heat is rejected. Therefore, in gas-turbine power plants, intercooling and reheating are always used in conjunction with regeneration. These improvements, of course, come at the expense of increased initial and operating costs, and they cannot be justified unless the decrease in fuel costs offsets the increase in other costs. In the past, relatively low fuel prices, a general desire in the industry to minimize installation costs, and the tremendous increase in the simple-cycle efficiency due to the first figures figures [Fig. 4.18, *T-s diagram*] increased efficiency options to approximately 40 %, which left little desire for incorporating the modifications. With the continued expected rise in demand and cost of producing electricity, these options will play an important role in the future of gas-turbine power plants. The purpose of this book is to explore this third option of increasing cycle efficiency via intercooling, regeneration, and reheating.

Gas turbines installed until the mid-1970s suffered from low efficiency and poor reliability. In the past, large coal and nuclear power plants dominated the base-load electric power generation [Point 1 in Fig. 4.19]. Base-load units are on-line at full capacity or near full capacity almost all of the time. They are not easily or quickly adjusted for varying large amounts of load because of their characteristics of operation [17]. However, there has been a historic shift toward natural-gas-fired turbines because of their higher efficiencies, lower capital costs, shorter installation times, better emission characteristics, the abundance of natural gas supplies, and shorter startup times [Point 1 in Fig. 4.19]. Now electric utilities are using gas turbines for base-load power production as well as for peaking, meeting capacity at maximum load periods and in emergency situations because they are easily brought on-line or off-line [2 in Fig. 4.19]. The construction costs for gas-turbine power plants are roughly half those of comparable conventional fossil fuel steam power plants, which were the primary base-load power plants until the early 1980s, but peaking units are much higher in energy output costs. A recent gas turbine manufactured by General Electric uses a turbine inlet temperature of 1425 °C (2600 °F) and produces up to 282 MW while achieving a thermal efficiency of

**Fig. 4.19** A gas-turbine engine with recuperator

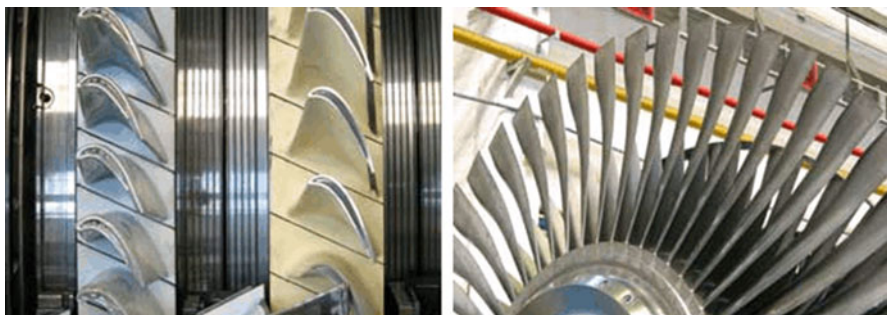
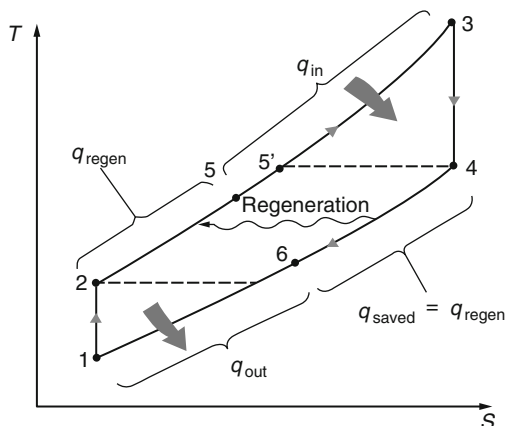


**Fig. 4.20** Difference between gas turbine (left) and steam turbine (right) blades

39.5 % in simple-cycle mode. Over half of all power plants to be installed in the foreseeable future are forecast to be gas turbine or combined gas-steam turbine types (Fig. 4.19).

An overall combined gas-steam power cycle was touched upon in the previous section (Sect. 4.3.1) of this chapter; and Fig. 4.20 shows the difference between gas and steam turbine blades.

Typical numerical examples for Brayton, Rankine, and combined cycles are presented below and are supported by computer code developed by Zohuri and McDaniel [1] at the University of New Mexico, Nuclear Engineering Department. The flowchart and overall capability of this code based on a static approach are explained in references [1] and [21] by Zohuri.

#### Numerical example:

- Simple Brayton efficiency: **36.8 %**
- Simple Rankine efficiency: **35 %**
- Combined Brayton and Rankine cycles: **56.4 %**

## 4.5 Turbomachinery

Thermal engines have been used widely since their invention in the seventeenth century. There are many kinds of this type of engine, and they are used in our everyday lives. The two types of turbomachinery encountered in nuclear plants are

1. Gas turbine,
2. Steam turbine.

Our main focus will be on gas turbines, where the Brayton cycle plays a big role, and we discuss it extensively in the next chapter (Chap. 5), a few points about it are worth making here.

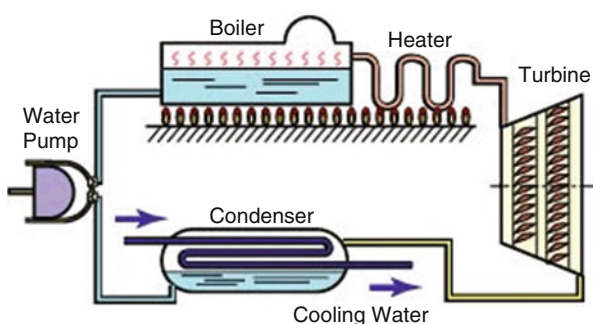
Figure 4.21 presents a simple steam turbine layout. The steam turbine has rotating blades instead of the piston and cylinder of the reciprocating steam engine. This engine is used as the power source in thermal and nuclear power plants. The steam turbine utilizes the dynamic pressure of the steam and converts thermal energy to mechanical energy, though the reciprocating steam engine utilizes the static pressure of the steam. Both engines use energy that is obtained upon expansion of the steam.

Turbomachinery that will be used in the next generation of nuclear power systems (Generation IV) will play a significant role in the future in commercial applications in the production of electricity.

In addition, as a general rule, anytime we talk about steam, we will be dealing with a Rankine cycle.

- First-order estimates of key turbine and compressor design and performance characteristics can be made with low-level analysis. For the reference systems, the key turbomachinery design parameters (speed, stages, stage diameters, blade heights, blade clearances) will be similar to those of current commercial gas-turbine engines.
- At lower reactor thermal powers He compressors will require greater than 3600 rpm operation to achieve efficiency goals [800 MW(t) allows 3600 rpm operation].

**Fig. 4.21** Schematic of steam turbine



- Maximum system temperatures in the reference designs are near the limit for uncooled turbines.
- For both direct and indirect designs, the seals, housing, and bearing components will be fundamentally different than in current gas turbines, requiring extensive development, with the associated costs and risk.

These observations illustrate the complex interactions of the many design choices that will be considered in the NGNP PCS. It is clear that detailed and integrated design efforts will have to be devoted to candidate designs before quantitative evaluations are possible. The assessment described in that study helped illuminate the critical design choices and the resulting implications for the cost and performance of the future NGNP PCS design.

## 4.6 Heat Transfer Analysis

Further analysis of heat transfer for any recuperative HX shows that the following governing equation is valid:

$$Q = \dot{m}_H c_H (t_{H1} - t_{H2}) = \dot{m}_C c_C (t_{C1} - t_{C2}) = UA_o (\text{LMTD})K, \quad (4.3)$$

where  $\dot{m}_H$  and  $\dot{m}_C$  are the mass flow rates of the hot and cold fluids, respectively;  $c_H$  and  $c_C$  are the specific heats of the hot and cold fluids, respectively;  $A_o$  is the outside area of the wall separating the two fluids;  $U$  is the overall heat transfer coefficient based on the outside area; and  $K$  is a multiplying factor for cross-flow and mixed-flow types ( $K = 1$  for counterflow and parallel flow).

The temperature variations, such as in Fig. 4.22a–c, can be shown for all three cases, where Fig. 4.22a shows temperature variations in counterflow with  $\dot{m}_C c_C > \dot{m}_H c_H$  and Fig. 4.22b indicates temperature variations in counterflow with  $\dot{m}_C c_C < \dot{m}_H c_H$ , while Fig. 4.22c illustrates the temperature variations in parallel flow.

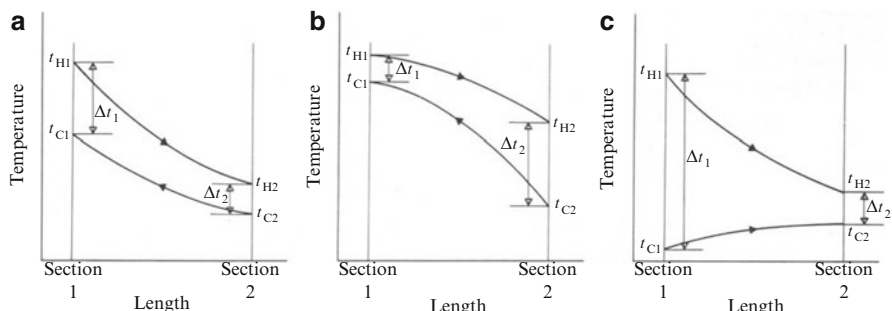


**Fig. 4.22** Temperature variations

Using the concept of thermal resistance in series we have

$$\frac{1}{UA_o} = \frac{1}{h_i A_i} + R_w + \frac{1}{h_o A_o} + F_i + F_o, \quad (4.4)$$

where subscripts  $o$  and  $i$  refer to the outside and inside surfaces of the separating wall, respectively;  $F$  represents the fouling factor by which, for most HXs, deposits of salts, oil, or other contaminant will gradually build up on the heat transfer surfaces. This is allowed in the design by using a *fouling factor*,  $F$ , in the form of an additional thermal resistance, as in Eq. (4.4). Cleaning of the HX takes place when the fouling reaches a design value. As part of fouling and treatment, for convenience in general, we can classify them under one of the following six headings, depending on the mechanism causing the deposition:

- Crystallization or precipitation fouling,
- Particulate fouling (silting),
- Biological fouling,
- Corrosion fouling,
- Chemical reaction fouling,
- Freezing or solidification fouling.

## 4.7 Combined-Cycle Power Plant

A combined-cycle gas-turbine power plant is essentially an electrical power plant in which a gas turbine and a steam turbine are used in combination to achieve greater efficiency than would be possible independently. The gas turbine drives an electrical generator while the gas-turbine exhaust is used to produce steam in a HX, called a heat recovery steam generator (**HRSG**), to supply a steam turbine whose output provides the means to generate more electricity. If the steam is used for heat, then the plant is referred to as a cogeneration plant.

It is important first to distinguish between a closed-cycle power plant (or heat engine) and an open-cycle power plant. In a closed cycle, fluid passes continuously around a closed circuit, through a thermodynamic cycle in which heat is received from a source at higher temperature, and heat is rejected to a sink at low temperature and work output is delivered usually to drive an electric generator.

A gas-turbine power plant may simply operate on a closed circuit, as shown in Fig. 4.23.

Most gas-turbine plants operate in an open circuit, with an internal combustion system, as shown in Fig. 4.24. Air fuel passes across the single control surface into the compressor and combustion chamber, and combustion products leave the control surface after expansion through the turbine.

The classical combined cycle for power production in a gas-turbine and steam plant are normally associated with the names Brayton and Rankine, respectively.

**Fig. 4.23** Closed-circuit gas-turbine plant

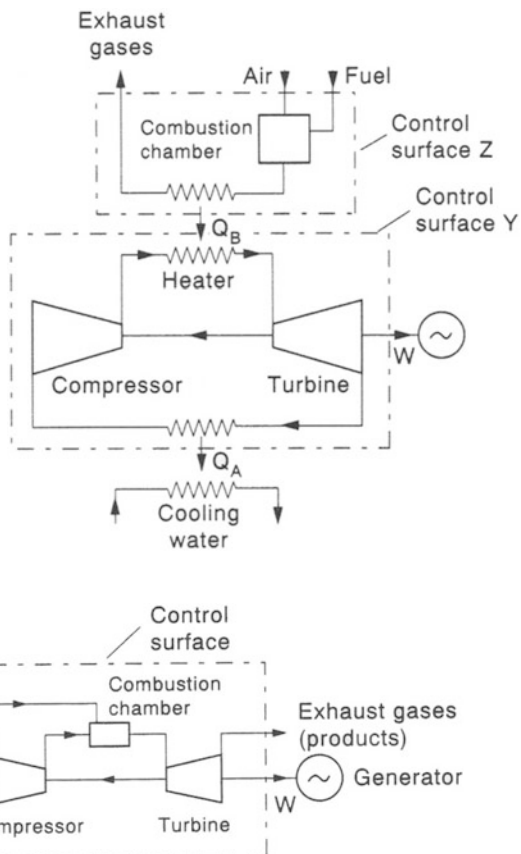


**Fig. 4.24** Open-circuit gas-turbine plant

Figure 4.25 below is a simple representation of a combined-cycle gas-turbine (CCGT) system. It demonstrates the fact that a CCGT system is comprised of two heat engines in a series. The upper engine is the gas turbine. The gas-turbine exhaust is the input to the lower engine (a steam turbine). The steam turbine emits heat as exhaust to a circulating water system that cools the steam condenser.

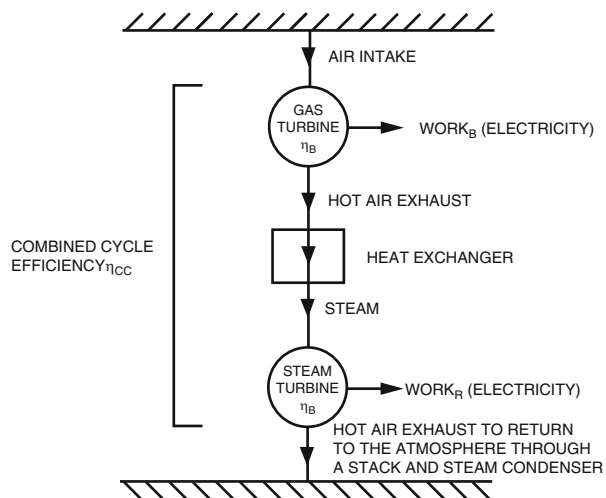
An approximate combined-cycle efficiency ( $\eta_{CC}$ ) is given by the equation

$$\eta_{CC} = \eta_B + \eta_R - (\eta_B \times \eta_R). \quad (4.5)$$

Equation (4.5) states that the sum of the individual efficiencies minus the product of the individual efficiencies equals the combined-cycle efficiency. This simple equation gives significant insight into why combined-cycle systems are successful.

For example, suppose the gas turbine's efficiency (Brayton)  $\eta_B$  is 40% (a reasonable value for modern gas turbines) and that the steam turbine efficiency (Rankine)  $\eta_R$  is 30% (a reasonable value for a Rankine cycle steam turbine).

**Fig. 4.25** Schematic of combined-cycle (CCGT) plant



Utilizing Eq. (4.5) would lead to the following conclusion:

$$\eta_{CC} = 0.4 + 0.3 - (0.4 \times 0.3),$$

$$\eta_{CC} = 0.58,$$

$$\eta_{CC} = 58\%.$$

The combined-cycle efficiency of 58 % is much greater than either that of the gas turbine or the steam turbine separately. The 58 % value is slightly misleading in that system losses were ignored. However, efficiency values in the 60 % range have been recorded for CCGT systems in the past few years [7].

CCGT power plants come in many different configurations. Some companies choose to treat the gas-turbine exhaust bypass stack as a commodity; others choose to incorporate a diverter damper into the turbine exhaust gas path. The diverter damper allows for the rapid configuration of the power plant as a combined-cycle or simple-cycle system. The initial cost of the diverter damper is much higher than the cost of treating the gas-turbine exhaust stack as a commodity. However, the diverter damper allows for the gas turbines to be operated in simple cycle when (HRSG) or steam turbine repair or maintenance is required.

## 4.8 Advanced Computational Materials Proposed for Generation IV Systems

Renewed interest in nuclear reactor technology has developed in recent years, in part as a result of international interest in sources of energy that do not produce CO<sub>2</sub> as a byproduct. One result of this interest was the establishment of the Generation IV International Forum, which is a group of international governmental entities whose goal is facilitating bilateral and multilateral cooperation related to the development of new nuclear energy systems.

Historically, both fusion and fission reactor programs have taken advantage of and built on research carried out by the other program. This leveraging can be expected to continue over the next 10 years as both experimental and modeling activities in support of the Generation IV program grow substantially. The Generation IV research will augment fusion studies (and vice versa) in areas where similar materials and exposure conditions are of interest. However, in addition to the concerns common to both fusion and advanced fission reactor programs, designers of a future DT fusion reactor will have the unique problem of anticipating the effects of the 14 MeV neutron source term. For example, advances in computing hardware and software should permit improved (and in some cases the first) descriptions of relevant properties in alloys based on ab initio calculations. Such calculations could provide the basis for realistic interatomic potentials for alloys, including alloy-He potentials that could be applied in classical molecular dynamics simulations. These potentials must have a more detailed description of many-body interactions than accounted for in the current generations, which are generally based on a simple embedding function. In addition, the potentials used under fusion reactor conditions (very high pKa energies) should account for the effects of local electronic excitation and electronic energy loss. The computational cost of using more complex potentials will also require the next generation of massively parallel computers. New results of ab initio and atomistic calculations can be coupled with ongoing advances in kinetic and phase field models to dramatically improve predictions of the nonequilibrium, radiation-induced evolution in alloys with unstable microstructures. This includes phase stability and the effects of helium on each microstructural component.

However, for all its promise, computational materials science is still a house under construction. As such, the current reach of the science is limited. Theory and modeling can be used to develop understanding of known critical physical phenomena, and computer experiments can, and have been used to, identify new phenomena and mechanisms, and to aid in alloy design. However, it is questionable whether the science will be sufficiently mature in the near future to provide a rigorous scientific basis for predicting critical materials' properties or for extrapolating well beyond the available validation database.

Two other issues remain even if the scientific questions appear to have been adequately answered. These are licensing and capital investment. Even a high degree of scientific confidence that a given alloy will perform as needed in a particular Generation IV or fusion environment is not necessarily transferable to the reactor licensing or capital market regimes. The philosophy, codes, and standards employed for reactor licensing are properly conservative with respect to design data requirements.

Experience with the US Nuclear Regulatory Commission suggests that only modeling results that are strongly supported by relevant, prototypical data will have an impact on the licensing process. In a similar way, it is expected that investment on the scale required to build a fusion power plant (several billion dollars) could be obtained only if a very high level of confidence existed that the plant would operate long and safely enough to return the investment.

These latter two concerns appear to dictate that an experimental facility capable of generating a sufficient, if limited, body of design data under essentially prototypical conditions (i.e., with ~14 MeV neutrons) will ultimately be required for the commercialization of fusion power. An aggressive theory and modeling effort will reduce the time and experimental investment required to develop the advanced materials that can perform in a DT fusion reactor environment. For example, the quantity of design data may be reduced to that required to confirm model predictions for key materials in critical exposure conditions. This will include some data at a substantial fraction of the anticipated end-of-life dose, which raises the issue of when such an experimental facility is required. Long lead times for the construction of complex facilities, coupled with several years' irradiation to reach the highest doses, imply that the decision to build any fusion-relevant irradiation facility must be made on the order of 10 years before the design data are needed.

Two related areas of research can be used as reference points for the expressed need to obtain experimental validation of model predictions. Among the lessons learned from ASCII, the importance of code validation and verification has been emphasized at workshops among the courtiers involved with such research.

Because of the significant challenges associated with structural materials applications in these advanced nuclear energy systems, the *Workshop on Advanced Computational Materials Science: Application to Fusion and Generation IV Fission Reactors* was convened by the US Department of Energy's Office of Science and the Office of Nuclear Energy, Science and Technology to ensure that research funded by these programs takes full advantage of ongoing advancements in computational science and the department's investment in computational facilities. In particular, participants in the workshop were asked to perform the following tasks:

1. Examine the role of high-end computing in the prediction of materials behavior under the full spectrum of radiation, temperature, and mechanical loading conditions anticipated for advanced structural materials that are required for future Generation IV fission and fusion reactor environments, and
2. Evaluate the potential for experimentally validated computational modeling and simulation to bridge the gap between data needed to support the design of these advanced nuclear technologies and both the available database and data that can be reasonably obtained in currently available irradiation facilities.

Like the requirements for advanced fusion reactors, the need to develop materials capable of performing in the severe operating environments expected in Generation IV reactors represents a significant challenge in materials science. There is a range of potential Generation IV fission reactor design concepts, and each concept has its own unique demands. Improved economic performance is a major goal of the Generation IV designs. As a result, most designs call for significantly higher operating temperatures than the current generation of LWRs to obtain higher thermal efficiencies. In many cases, the desired operating temperatures rule out the use of the structural alloys employed today. The very high operating temperature (up to 1000 °C) associated with NGNPs is a prime example of an attractive new system that will require the development of new structural materials.

The operating temperatures, neutron exposure levels, and thermomechanical stresses for the proposed Generation IV fission reactors are huge technological challenges among materials scientists and engineers. In addition, the transmutation products created in the structural materials by the high-energy neutrons produced in this generation of nuclear power reactors can profoundly influence the microstructural evolution and mechanical behavior of these materials.

## 4.9 Material Classes Proposed for Generation IV Systems

The types of materials that were proposed in a DOE workshop in March of 2004 are tabulated as follows (Table 4.3):

## 4.10 Generation IV Materials Challenges

A summary of these challenges for the NGNP are presented here. They are as follows:

- **Higher Temperature/Larger Temperature Ranges**
  - Examples
    - VHTR coolant outlet temperature near 1000 °C;
    - Gas-cooled faster reactor (GFR) transient temperatures to 1600–1800 °C, gradient across core of approximately 400 °C.
    - Lead-cooled faster reactor (LFR) to 800 °C steady-state outlet.
  - Issues
    - Creep,
    - Fatigue,
    - Toughness,
    - Corrosion/stress corrosion cracking (SCC).
- *Must drive modeling toward a predictive capability of materials properties in complex alloys across a wide temperature range.*
- **High flounce dose**
  - Examples
    - LFR, sodium-cooled faster reactor (SFR) cladding,
    - Supercritical water reactor core barrel,
    - Gas-cooled faster reactor FR matrix.
  - Issues

Table 4.3 Structural materials

System	Ferritic martensitic stainless steel alloys	Austenitic stainless steel alloys	Oxide-dispersed strengthened steels	Ni-based alloys	Graphite	Refractory alloys	Ceramics
GFR	P	P	P	P		P	P
LFR	P	P	S			S	S
MSR				P	P	S	S
SFR	P	P	P				
SCWR-thermal spectrum	P	P	S	S			
SCWR-fast spectrum	P	P	S	S			
VHTR	S			P	P	S	P

P primary, S secondary

Swelling  
Creep, stress relaxation

- *Must drive modeling toward a predictive capability of materials properties in complex alloys to large radiation dose.*

- **Unique Chemical Environments**

- Examples

- Pb and Pb-Bi eutectic,
    - Supercritical water,
    - High-temperature oxidation in gas-cooled systems,
    - Molten salts.

- Issues

- Corrosion,
    - SCC/irradiation-assisted SCC,
    - Liquid metal embrittlement.

- *Must drive modeling toward a predictive capability of chemical interactions in complex alloys to large radiation dose.*

## 4.11 Generation IV Materials Fundamental Issues

The coevolution of all components of the microstructure and their roles in the macroscopic response in terms of swelling, anisotropic growth, irradiation creep, and radiation-induced phase transformations should be studied within the science of complex systems (Fig. 4.26).

In summary, we can draw the following conclusions;

- Six concepts have been identified with the potential to meet Generation IV goals
- The concepts operate in more challenging environments than current LWRs and significant material development challenges must be met for any of the Generation IV systems to be viable.
- Experimental programs cannot cover the breadth of materials and irradiation conditions for the proposed Generation IV reactor designs.
- Modeling and microstructural analysis can provide the basis for a material selection that is performed based on an incomplete experimental database and that requires considerable judgment to carry out the necessary interpolation and extrapolation.

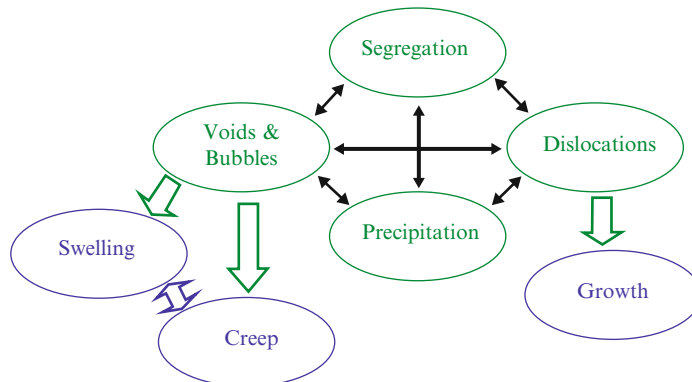


**Fig. 4.26** Flowchart of fundamental materials issues

## 4.12 Capital Cost of Proposed Generation IV Reactors

Different PCS design features may have substantial effects on the system capital cost. System optimization is typically complex because, for example, increased PCS cost can increase cycle efficiency, reducing reactor capital cost. The Generation IV Economic Modeling Working Group (EMWG 2004) recommends two methodologies for modeling economic costs: a top-down method based on scaling and detailed information about similar systems and a bottom-up method based on detailed accounting for all construction commodities, plant equipment, and labor hours. For top-down methods, the EMWG recommends the following (EMWG 2004):

The first task is to develop a reference design to which cost estimating techniques can be applied. The cost estimating part of this task generally is accomplished by considering the costs of equipment used for similar type projects and then scaling the equipment upwards or downwards. As an example, one might start cost estimating work on the very high temperature reactor (VHTR) by scaling reactor plant equipment from a project for which detailed estimates are available, such as the General Atomics HTGR.

For the purpose of system comparison, the top-down method was adopted to estimate PCS parameters that are important in scaling relative capital costs.

The measures selected were those typically calculated to provide input for system cost estimates and, thus, provide a basis for rough comparisons of system options. To provide an approximate baseline for comparison, where possible, comparisons were made with Generation II and Generation III+ LWR values. Figure 4.26 shows such a comparison, quantifying steel and concrete inputs for the reference systems considered in the study. Several insights can be drawn from Fig. 4.26. For example, the 1500 MWe passive ESBWR LWR has slightly smaller inputs than the 1970s LWRs, as well as the evolutionary environmental program requirements (EPRs).

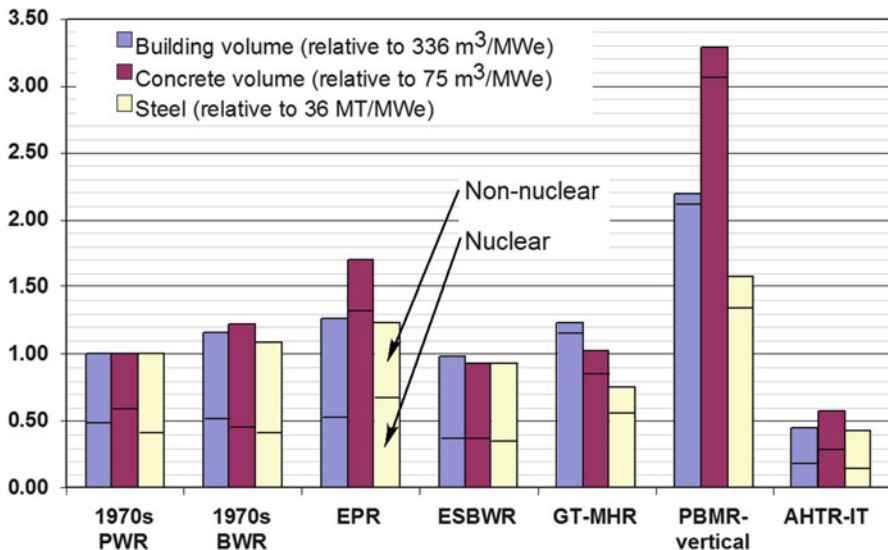


**Fig. 4.27** Comparison of total building volumes and total plant steel and concrete inputs for reference HTR and LWR systems considered

But Fig. 4.27 also shows that it is possible to build high-temperature gas-cooled reactors, for example, the 286 MWe GT-MHR, with smaller construction material inputs than for LWRs, owing to the higher thermodynamic efficiency and power density. This shows that it is possible, with high-temperature gas power cycle technology, to break the economic scaling of the large LWRs. This study also suggests that high-temperature, high-efficiency gas-cycle power conversion can be adapted to other advanced reactor systems. For example, the even smaller inputs for the high-temperature, liquid-cooled, 1235 MWe AHTR-IT show that economies of scale may exist for HTRs. However, the material inputs for HTRs can be sensitive to equipment design choices and configurations, as shown by the differences in Fig. 4.26 between the GT-MHR and the PBMR. Thus, careful attention to design tradeoffs is clearly important in the design of PCSs.

The selected capital costs that were calculated for the reference systems in the study and are presented in the report from the UC Berkeley team [18] in Chap. 2 in more detail and are based on the volumes of materials used:

- Structural costs:
  - Building volume ( $\text{m}^3/\text{MW(e)}_{\text{ave}}$ ) (nuclear/nonnuclear)
  - Concrete volume ( $\text{m}^3/\text{MW(e)}_{\text{ave}}$ ) (nuclear/nonnuclear)
- Reactor and PCS costs:
  - Reactor power density ( $\text{m}^3/\text{MW(e)}_{\text{ave}}$ ),
  - PCS power density ( $\text{m}^3/\text{MW(e)}_{\text{ave}}$ ) (nuclear/nonnuclear),
  - System-specific steel ( $\text{MT}/\text{MW(e)}_{\text{ave}}$ ) (nuclear/nonnuclear),

- Turbomachinery specific volume ( $\text{m}^3/\text{MW}(\text{e})_{\text{ave}}$ ),
- System-specific helium ( $\text{kg}/\text{MW}(\text{e})_{\text{ave}}$ ) (nuclear/nonnuclear) [nonrenewable resource, correlates with building volume (blow-down)]

For each of these figures of merit, the values for the nuclear and nonnuclear portions of the plant were estimated. This division recognizes the difference in costs for procuring and installing nuclear-grade materials. For example, for concrete and reinforcing steel, material costs are estimated to be 65 % greater for nuclear-grade materials and installation costs 30 % greater.

#### ***4.12.1 Economic and Technical Aspects of Combined-Cycle Performance***

The output and efficiency of combined-cycle plants can be increased during the design phase by selecting the following features [19]:

- Higher steam pressure and temperature,
- Multiple steam pressure levels,
- Reheat cycles.

Additional factors are considered if there is a need for peak power production. They include gas-turbine power augmentation by water or steam injection or a supplementary fired heat recovery steam generator (**HRSG**). If peak power demands occur on hot summer days, gas-turbine inlet evaporative cooling and chilling should be considered. Fuel heating is another technique that has been used to increase the efficiency of combined-cycle plants.

The ability of combined-cycle plants to generate additional power beyond their base capacity during peak periods has become an important design consideration. During the last decade, premiums were paid for power generated during peak summer periods. The cost of electricity during the peak periods can be 70 times more expensive than off-peak periods. Since the cost during the peak periods is much higher, most of a plant's profitability could be driven by the amount of power generated during these peak periods. Thus, plants that can generate large quantities of power during the peak periods can achieve the highest profits.

#### ***4.12.2 Economic Evaluation Technique***

Plant output and efficiency are carefully considered during the initial plant design because they impact the cost of electricity in combination with fuel costs, plant capital cost, cost of capital, and electricity sales. These factors will determine gas-turbine selection as well as the bottoming cycle design in combined-cycle operation.

As fuel costs increase, cycle selections typically include higher steam pressures, multiple steam pressure levels, reheat cycles, and higher steam temperatures. Once these selections have been made, other factors are addressed. Is there a need for peak power production with premiums paid for the resulting power? If so, gas-turbine power augmentation by way of water or steam injection or a supplementary fired HRSG may be the solution. Do peak power demands occur on a hot day (summer peaking)? This may suggest a potential benefit from some form of gas-turbine inlet evaporative cooling or chilling [20].

For existing plants, some performance enhancement options can also be economically retrofitted to boost power output and efficiency. Although this research's primary focus is on options that enhance output, a brief discussion of fuel gas heating, a technique used to enhance combined-cycle plant efficiency, is provided.

The ability of utilities and independent power producers (IPPs) to generate additional power beyond a plant's base capacity during summer peak power demand periods has become an important consideration in the design of combined-cycle plant configurations. In recent years, utilities and IPPs within the USA have received premiums for power generation capacity during summer peak power demand periods. The price of electricity varies greatly as a function of annual operating hours. The variation is also highly region dependent. With price-duration curves that are sharply peaked, implying a few hours annually with very high rates, the majority of a plant's profitability could be driven by the high peak energy rates that can be achieved over a relatively short period of time. Thus, a plant that can economically dispatch a large quantity of additional power could realize the largest profits.

While current market trends should be considered during the design and development phase of a combined-cycle facility, forecasts of future market trends and expectations are equally important and warrant design considerations.

One of the primary challenges facing developers of new combined-cycle plants, as well as owner/operators of existing plants, is the optimization of plant revenue streams. As a result of escalating peak energy rates and peak demand duration, significant emphasis has been placed on developing plant designs that maximize peak power generation capacity while allowing for cost-effective, efficient operation of the plant during nonpeak power demand periods.

In addition to maximizing plant profitability in the face of today's marketplace, expectations of future market trends must be considered. Therefore the goal is to determine which performance-enhancement options or combination of options can be applied to a new or existing combined-cycle plant to maximize total plant profits on a plant life-cycle basis.

With very few exceptions, the addition of power-enhancement techniques to a base plant configuration will negatively impact base-load performance and, hence, adversely affect a plant's net revenue generating capability during nonpeak periods [19].

In general, efficiency is the predominating economic driver during nonpeak generating periods, while capacity dominates economic evaluation during peak power demand periods. Thus, it is extremely important to develop an economic

model that considers both the cost of electricity (**COE**) during nonpeak periods while taking into consideration expectations of peak energy rates.

After having established baseline peak and nonpeak period performance levels for the various power-enhancement alternatives, a COE analysis technique is applied to determine alternatives that would afford the best overall life-cycle benefit. In addition to including both peak and nonpeak performance levels, the COE model includes the split between annual peak and nonpeak operating hours, the premium paid for peak power generation capacity, the cost of fuel, plant capital cost, the incremental capital cost of the enhancements, and the cost to operate and maintain the plant. This COE model can then be used to determine the sensitivity of a given power-enhancement alternative with respect to the economic parameters included within it [19].

Most peak power-enhancement opportunities exist in the topping cycle (gas turbine) as opposed to the bottoming cycle (HRSG/steam turbine). In general, with the exception of duct firing within a HRSG, few independent design enhancements can be made to a bottoming cycle that has already been fully optimized to achieve maximum plant performance. However, in general, performance enhancements to the gas turbines will carry with them an increase in bottoming cycle performance owing to an associated increase in gas-turbine exhaust energy [19].

### ***4.12.3 Output Enhancement***

The two major categories of plant output enhancements are

1. Gas-turbine inlet air cooling and
2. Power augmentation.

#### ***4.12.3.1 Gas-Turbine Inlet Air Cooling***

Industrial gas turbines operating at constant speed have a constant volumetric flow rate. Since the specific volume of air is directly proportional to temperature, cooler air has a higher mass flow rate. It generates more power in the turbine. Cooler air also requires less energy to be compressed to the same pressure as warmer air. Thus, gas turbines generate higher power output when the incoming air is cooler [21].

A gas-turbine inlet air cooling system is a good option for applications where electricity prices increase during warm months. It increases the power output by decreasing the temperature of the incoming air. In combined-cycle applications, it also results in improvements in thermal efficiency. A decrease in the inlet dry-bulb temperature by 10 °F (5.6 °C) will normally result in around a 2.7 % power increase of a combined cycle using heavy-duty gas turbines. The output of simple-cycle gas turbines is also increased by the same amount.

**Fig. 4.28** Combined-cycle system performance variation with ambient air temperature [19]

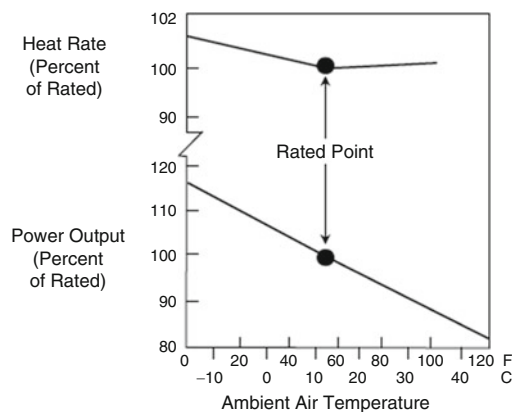


Figure 4.28 shows that a 10 °F (5.6 °C) reduction in gas-turbine inlet dry-bulb temperature for heavy-duty gas turbines improves combined-cycle output by about 2.7 %. The actual change is somewhat dependent on the method of steam turbine condenser cooling being used. Simple-cycle output is improved by a similar percentage.

Several methods are available for reducing gas-turbine inlet temperatures. There are two basic systems currently available for inlet cooling. The first and perhaps the most widely accepted system is evaporative cooling. Evaporative coolers make use of the evaporation of water to reduce the gas turbine's inlet air temperature. The second system employs various ways to chill the inlet air. In this system, the cooling medium (usually chilled water) flows through a HX located in the inlet duct to remove heat from the inlet air.

Evaporative cooling is limited by wet-bulb temperature. Chilling, however, can cool the inlet air to temperatures that are lower than the wet-bulb temperature, providing additional output, albeit at a significantly higher cost.

Depending on the combustion and control system, evaporative cooling may reduce NOx emissions; however, there is very little benefit to be gained from current dry low NOx technology. This is another avenue that requires further analysis and investigation as well as collaboration between scientific communities, national laboratories, and industry.

#### 4.12.3.2 Power Augmentation

Three basic methods are available for power augmentation: water or steam injection, HRSG supplementary firing, and peak firing.

These are the three methods that General Electric suggests, and they need to be investigated further by nuclear power manufacturers and the community involved with enhancing nuclear power energy efficiency [19] using combined-cycle technology.

Others aspects of the cost of producing electricity are generally expressed in US dollars per megawatt-hour or US cts/kWh, depending on the following parameters [21]:

- Capital cost of project,
- Fuel cost,
- Operation and maintenance cost.

The capital cost per unit of electricity for a given power plant depends on the following elements:

- Investment cost,
- Financing structure,
- Interest rate and return on equity,
- Load factor of plant (or equivalent utilization time).

The investment costs are the sum of the following items:

- Power plant contract prices(s);
- Interest during construction (depending on construction time);
- Owner's cost of project realization (e.g., project manager, owner's engineer, land cost).

The financing structure is defined by the debt-to-equity ratio of the financing, and the return on equity is the return expected by investors on their capital. Both are linked to project risks.

The load factor results from the type of application the plant is intended for: base, intermediate, or peak load operation and the availability and reliability of the power station.

Fuel costs per unit of electricity are proportional to the specific price of the fuel and inversely proportional to the average electrical efficiency of the installation. This average electrical efficiency must not be confused with the electrical efficiency at rated loads. It is defined as follows:

$$\bar{\eta} = \eta \times \eta_{\text{Oper}}, \quad (4.6)$$

where:

$\eta$  is the electrical net efficiency at rated load (this is the percentage of the fuel that is converted into electricity at a rated load for a new and clean condition);

$\eta_{\text{Oper}}$  is the operating efficiency, which takes into account the following losses:

- Startup and shutdown losses,
- Higher fuel consumption for partial load operation,
- Aging and fouling of plant.

## References

1. Zohuri, B. (2014). Innovative combined Brayton open cycle systems for the next generation nuclear power plants. PhD Dissertation, Nuclear Engineering Department, University of New Mexico.
2. Eastop, T. D., & Croft, D. R. (1990). *Energy efficiency*. New York: Longman.
3. Zohuri, B., & McDaniel, P. J. (2014). *Thermodynamics in nuclear power plant systems*. Heidelberg: Springer.
4. Zohuri, B., & Fathi, N. (2015). *Thermal-hydraulic analysis of nuclear reactors*. Heidelberg: Springer.
5. Necati Ozisik, M. (1985). *Heat transfer: A basic approach*. New York: McGraw-Hill.
6. Incropera, F. P., & DeWitt, D. P. (1990). *Fundamentals of heat and mass transfer* (3rd ed., pp. 658–660). New York: Wiley.
7. Incropera, F. P., DeWitt, D. P., Bergman, T. L., & Lavine, A. S. (2006). *Fundamentals of heat and mass transfer* (6th ed., pp. 686–688). New York: John Wiley & Sons.
8. Zohuri, B., McDaniel, P. J., & de Olivera, C. (2014). Air Brayton cycles for nuclear power plants. Submitted for Review.
9. Zohuri, B., McDaniel, P. J., & de Olivera, C. (2014). A comparison of a recuperated open cycle (Air) Brayton power conversion system with the traditional steam Rankine cycle for the next generation nuclear power plant. *ANS Transactions*, Reno, Nevada, June, 2014.
10. McDaniel, P. J., Zohuri, B., & de Olivera, C. (2014). A combined cycle power conversion system for small modular LMFBRs. *ANS Transactions*, Anaheim, California, November, 2014.
11. McDaniel, P. J., Zohuri, B., de Oliveira, C., & Cole, J. (2012). A combined cycle power conversion system for the next generation nuclear power plant. *ANS Transactions*, San Diego, California, November, 2012.
12. <http://energyfromthorium.com/2014/04/04/closed-loop-brayton-cycle-sandia-national-laboratory/>
13. Pasch, J., Conboy, T., Fleming, D., & Rochau, G. (2012). Supercritical CO<sub>2</sub> recompression Brayton cycle: Completed assembly description. SANDIA REPORT SAND2012-9546. Unlimited Release Printed, October 2012.
14. <http://www.netl.doe.gov/publications/proceedings/11/utsr/pdf/wed/Wright%20SCO2%20Power%20Cycle%20Summary%20UTSR%202011%20v2a.pdf>
15. Kays, W. M., & London, A. L. (1984). *Compact heat exchangers* (3rd ed.). New York: McGraw-Hill.
16. Shah, R. K. (Ed.). (1997). *Compact heat exchangers for the process industries*. New York: Begell House.
17. Pansini, A. J., & Smalling, K. D. (1991). *Guide to electric power generation*. Lilburn, GA: The Fairmont Press.
18. Peterson, P., Zhao, H., Ballinger, R., Fuller, R., Forsha, M., Nichols, B., Oh, C., & Vernon, M. E. (2004). Next generation nuclear plant power conversion study: Technology options assessment, September 1, 2004.
19. Jones, C., & Jacob, J., III. (2000). *Economic and technical considerations for combined-cycle performance-enhancement options*. GER-4200. Schenectady, NY: GE Power Systems.
20. Langston, L. S., & Opdyke, G. (1997). Introduction to gas turbine for non-engineers. *Global Gas Turbine News*, 37(2).
21. Zohuri, B. (2015). *Combined cycle driven efficiency for next generation nuclear power plants: An innovative design approach*. Heidelberg: Springer.

# **Chapter 5**

# **Evaluation of Next Generation Nuclear Plant Intermediate Heat Exchanger Operating Conditions**

An initial and preliminary analysis to determine the operating conditions for the Next Generation Nuclear Plant intermediate heat exchanger (IHX) that will transfer heat from the reactor primary system to demonstration hydrogen production plants was discussed in Chap. 3. In this chapter, we will expand on that point. The Department of Energy, under the leadership of the Idaho National Laboratory, is currently investigating two primary options for the production of hydrogen using a high-temperature reactor as the power source. These options are high-temperature electrolysis (HTE) and SI thermochemical hydrogen production processes. However, since the SI process relies entirely on process heat from the reactor, while the HTE process relies primarily on electrical energy, with only a small amount of process heat required, the design of the IHX is dictated by the SI process heat requirements. Therefore, the IHX operating conditions were defined assuming 50 MWt would be available for the production of hydrogen using the SI process.

## **5.1 Introduction**

In this chapter we will follow the preliminary evaluation by national laboratories under the auspices of the Department of Energy (DOE) and universities under the Nuclear Energy University Program (NEUP) to determine the conditions for Next Generation Nuclear Plant (NGNP) intermediate heat exchangers (IHXs) that will transfer heat from the reactor primary system to the demonstration hydrogen production plants (HPPs). This evaluation looks at two different scenarios as part of the options using nuclear power plants to couple with HPPs as part of their search for new sources of renewable energy and sources of fuel for transportation as part of industrial fuel cell programs nationwide and worldwide.

These options are the high-temperature electrolysis (HTE) and sulfur-iodine (SI) thermochemical production processes. However, since the SI process relies entirely on process heat from the reactor, while the HTE process relies primarily on

electrical energy with only a small amount of process heat required, the design of the IHX is dictated by the SI process heat requirements. Therefore, the IHX operating conditions are defined assuming a certain value (i.e., 50 MWt) is available for the production of hydrogen using the SI process. Then this heat is delivered to the hydrogen production process through an intermediate heat transport loop and possibly a tertiary loop to provide adequate separation between the reactor primary system and the hydrogen production process. This separation is needed to minimize the potential for tritium migration between the reactor primary system and hydrogen production process and to ensure that accident or upset conditions in the hydrogen production facility do not propagate to or impact the operation of the NGNP reactor.

As part of this effort, the DOE, along with other associated organizations such as the Nuclear Regulatory Commission (NRC), are calling for research and development (R&D) on a nuclear hydrogen initiative via national laboratories, such as the Idaho National Laboratory (INL) and their NEUP program, for the demonstration of hydrogen production technologies utilizing nuclear energy as a prototype. The goal was to demonstrate hydrogen production that is compatible with nuclear energy systems by way of scaled demonstrations and then to couple a commercial-sized demonstration plant with a Generation IV demonstration facility by approximately 2015. The process of producing the hydrogen from water is highly energy intensive, and the efficiency of the process depends on different factors for different processes. The HTE and the thermochemical cycles can produce hydrogen from water, and these processes are being developed, as discussed earlier.

For the demonstration of hydrogen generation using nuclear power, the INL in the USA and Korea Atomic Energy Research Institute (KAERI) in the Republic of Korea have proposed the development of a very-high-temperature reactor (VHTR) and a nuclear hydrogen development and demonstration (NHDD), respectively. The potential layouts of the VHTR and NHDD are shown in Figs. 5.1 and 5.2, respectively.

Both plants use the VHTR to supply the power, while they are designed to use two different hydrogen production processes: the HTE and the SI thermochemical process. The VHTR is used because the high temperature is essential in maximizing the hydrogen production efficiencies for both electrolysis and the thermochemical process [1].

To optimize the designs of such plant systems as VHTR and NHDD, it is necessary to be able to evaluate the operating parameters and production efficiencies of various design layouts. The presently proposed INL project aims to develop a computer program, HyPEP, to easily and quickly evaluate the efficiencies and operating parameters [1].

A conceptual design of a pebble-bed advanced high-temperature reactor (AHTR) with a power generation cycle suggested by Holcomb et al. [2] is also depicted in Fig. 5.3 here. This AHTR is part of the fluoride-salt-cooled high-temperature reactor (FHR) concept and is among the class of Generation IV proposed reactors that will produce a high outlet temperature of 704 °C using coated particle fuel in the form of pebbles and can potentially improve the attributes of other reactors.

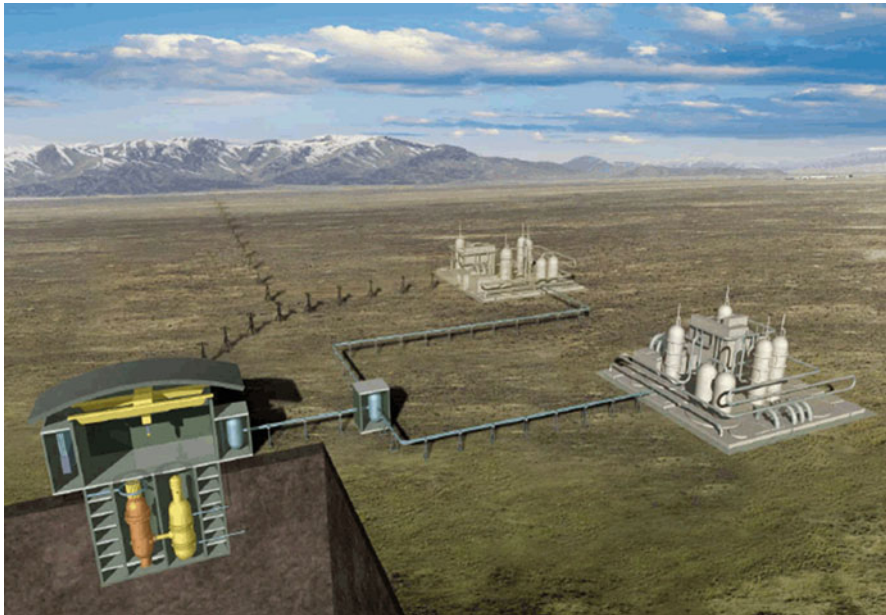


Fig. 5.1 Possible layout of VHTR for hydrogen production [1]

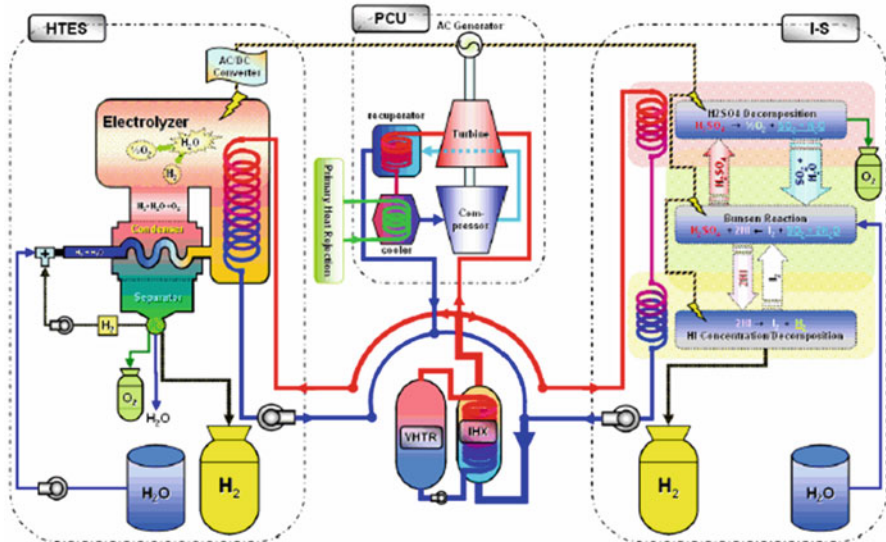
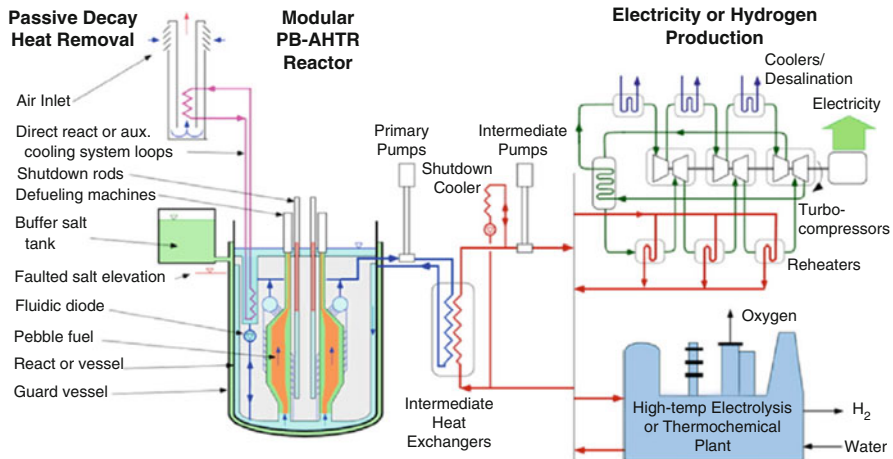


Fig. 5.2 Possible layout of proposed NHDD plant [1]



**Fig. 5.3** Conceptual design of pebble bed AHTR with power generation cycle [2]

As part of the evaluation of NGNP IHX operating conditions and depending on the design of such nuclear power plants, whether it is a direct or indirect power conversion cycle (PCU), the IHX will be required to provide heat for hydrogen production or for both hydrogen production and power conversion, as discussed at length in Chap. 3; therefore, a configuration can be picked as a base design that may be either direct or indirect power plant conversion type cycles, along with an integrated IHX either in parallel or series with the NGNP power conversion system. Consequently, the chosen efficiency configuration should be estimated using some kind of process optimization or running available commercial computer code used in the chemical or oil industry. The PCU efficiency  $\eta_{\text{PCU}}$  can be calculated using the following relationship:

$$\eta_{\text{PCU}} = \frac{\text{Electrical Power Output}}{\text{Reactor Thermal Power} - \text{H}_2 \text{ Process Power}} = \frac{\sum W_T - \sum W_C - W_S - \sum W_{\text{CIR}}}{Q_{\text{Th}} - Q_{\text{H}_2}}, \quad (5.1)$$

where:

$\Sigma W_T$  = total turbine workload;

$\Sigma W_C$  = total compressor workload;

$W_S$  = plant stationary load (for simplicity of analysis it can be neglected) but includes the power for the electrolysis for the HTE process or SI process;

$\Sigma W_{\text{CIR}}$  = circular workload in primary, intermediate, and, if present, tertiary loops;

$Q_{\text{Th}}$  = reactor thermal power;

$Q_{\text{H}_2}$  = power supplied through process heat exchanger (PHX) to HPP.

As stated in connection with the reference design evaluation that takes into consideration a high-temperature reactor of the next generation for coupling with HPPs that produce both electricity and hydrogen, the power conversion unit (PCU) utilizes an indirect electrical cycle based on the recommended base design point for such facilities. Less than 10 % of a nuclear reactor's thermal energy is dedicated to hydrogen production for any early expected demonstration or prototype plant given present R&D efforts for the coupling of NGNPs with hydrogen generation plants. As was mentioned earlier with respect to such an approach, an intermediate heat transport loop could be used to transfer heat from the nuclear reactor to the HPP and provide separation between the nuclear and hydrogen plants, and as part of the coolant system, helium could also be used as a working fluid in a gas-to-gas heat exchanger design process in the form a compact system, for the primary, secondary, and tertiary loops. Using Eq. (5.1) allows a best optimum PCU system to be selected for the best overall configuration via an examination process involved in a recuperated gas-Brayton cycle and recuperated combined bottom Rankine and Brayton cycle [3–10].

### Tertiary Loop

In a commercial pressurized nuclear power plant, heat transfer takes place between the reactor core and the circulating water, and the coolant is then pumped through the primary tube side of the steam generator by coolant pumps before returning to the reactor core. This is referred to as the primary loop. That water, which flows through the steam generator, boils water on the shell side (which is kept at a lower pressure than the primary side) to produce steam. This is referred to as the secondary loop. The secondary-side steam is delivered to the turbines to generate electricity. The steam is subsequently condensed via cooled water from a tertiary loop and returned to the steam generator to be heated once again. The *tertiary* cooling water may be recirculated to cooling towers, where it sheds waste heat before returning to condense more steam. Once-through tertiary cooling may otherwise be provided by a river, lake, or ocean. This primary–secondary–tertiary cooling scheme is the basis of a pressurized water reactor, which is the most common way to extract usable energy from a controlled nuclear reaction.

Another coolant system that can be considered is one based on molten salts in the primary and tertiary loops or CO<sub>2</sub> in the secondary and tertiary loops.

Bear in mind that the primary loop for a reference design can consist of a nuclear reactor, an IHX, and a circulator. The nuclear reactor may be assumed to be a high-temperature helium-cooled reactor or sodium-cooled reactor. Based on this assumption, one can impose thermal-hydraulic parameters (summarized in Table 5.1) that possibly will work with the suggested computer code HyPEP by the INL for the simplicity of analysis (Davis et al. [11])

**Table 5.1** Thermal-hydraulic parameters assumed for primary loop

Parameter	Value
Coolant	Helium
Pressure, MPa	7.0
Power, MW	600
Outlet temperature, °C	900
Temperature rise, °C	400
Differential pressure, MPa:	
Core	0.05
IHX	0.05

**Table 5.2** IHX and SHX parameters

Parameter	IHX	SHX
Nominal power, MW	600	50
Differential pressure (hot/cold), MPa	0.050/0.050	0.050/0.14
Heat exchanger width, m	4.77	1.51
Flow channels		
Diameter, mm	1.5	1.5
Pitch-to-diameter ratio	1.20	1.5
Thickness-to-diameter ratio	0.57	0.78
Length	2.26	1.11

Under these constraints, the secondary loop of the same reference base design then will consist of a PCU that is arranged in parallel with a secondary heat exchanger (SHX) that directs less than 10 % of the reactor power toward the hydrogen generation plant, as was mentioned earlier, and the PCU may consist of a recuperator, precooler, and another cooler placed between the low-pressure compressor (LPC) and the high-pressure compressor (HPC); and to improve the efficiency of the electrical cycle, two compressors and coolers can be utilized as well [11].

As part of a thermal hydraulic analysis, Davis et al. [11] suggest a certain width of the front face of the heat exchangers, which were assumed to be square, and channel length to obtain the desired pressure drop in the hot fluid and thermal performance. Table 5.2 presents a summary of IHX and SHX parameters based on thermodynamic states, which were also suggested as part of the design base reference and are depicted in Fig. 5.3.

As discussed earlier, in connection with the safety factor and licensing criteria, the intermediate heat transport loop transfers heat from the nuclear reactor to the HPP and provides physical separation between plants, which should make the nuclear plant easier to license.

Estimates for the required separation distance between the nuclear and hydrogen plants depend on the design and safety criteria applied and vary considerably.

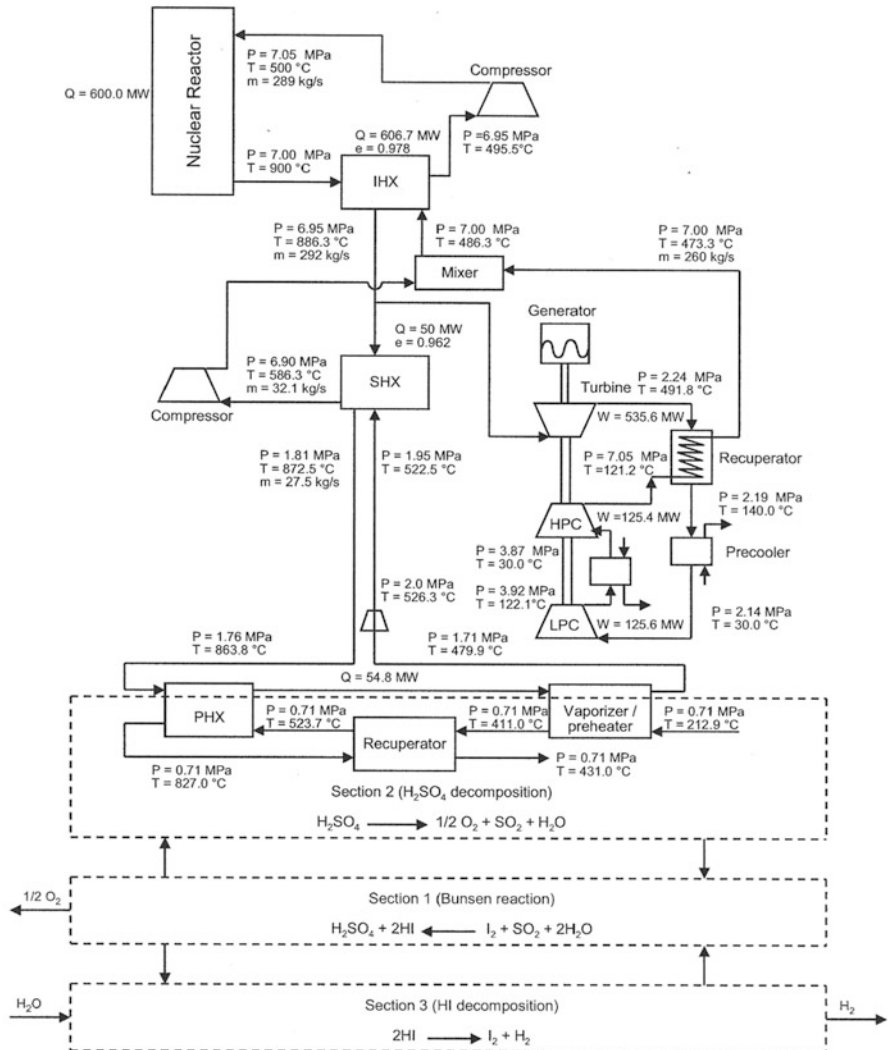


**Fig. 5.4** Schematic of reference design of integrated nuclear power and hydrogen generation plants

Also, an investigation by Oh et al. [1] on seven configuration options that pick and choose indicates that liquid salts for a coolant system are more efficient for transporting heat over long distances and are a better choice than helium and thus may ultimately be chosen as the working fluid (Fig. 5.4). The intermediate heat transport loop is assumed to be coupled to the HPP through two heat exchangers, where the first one goes through preheating and partial vaporization of the  $\text{H}_2\text{SO}_4/\text{H}_2\text{O}$  mixture, while the mixture, via a recuperator located as a whole within the hydrogen generation plant, enters a fully vaporized stage.

At this stage the PHX will drive the temporal mixture of its maximum temperature required by the referenced design point and limits by invoking the heat for this process from the intermediate heat transport loop. The thermodynamic conditions given in Fig. 5.4 on the hot side of the preheater/vaporizer and the PHX were taken from the values given by Davis et al. [11].

The thermodynamic conditions on the cold side of these heat exchangers were based on the values given by Brown et al. [12].

## 5.2 Hydrogen Production Plant Requirements

A HPP that needs to be coupled with a NGNP plant was extensively discussed in Chap. 3 of this book, along with the most important functional and technical requirements, were laid out as well. The process, detailed for such a reference design plant based on the thermochemical SI cycle, can be found in a report by Brown et al. [12]. In addition, General Atomics (San Diego, CA) has reported improving the cycle since they started working on the thermochemical cycle using their conceptual (GA-HTR) high-temperature nuclear plant as a source of heat for intermediate heat loops to generate hydrogen via this production plant that is coupled with a nuclear power plant.

The selection of the reference and alternative design as a roadmap to the finalized production plant imposes new sets of requirements, and any existing thermal-hydraulic computer codes or any other related computer codes, along with R&D, need to be capable of representing the combined nuclear, PCU, and, finally, hydrogen generating plant as part of the execution process of the code. The working fluids, components, stress analysis, heat transfer, and associated thermal analysis and other related phenomena for the intermediate heat transfer loop and IHX for the referenced design need to be identified and accounted for. The library of the code that forms part of the input parameters for the calculation needs to be updated constantly in order to accommodate new fact findings based on the results of new R&D on the application of the NGNP-driven HPP to produce hydrogen as a new source of renewable energy during off-peak periods of nuclear power plant.

Looking at the overall requirements for a hydrogen generating plant and its components from the top down, we need to include a nuclear reactor, heat exchangers, compressors, all the required pumping systems that are functional for given optimum design pressure points, turbines, generators, separators, chemical processing equipment, scrubbers, and other specialized equipment required to generate hydrogen as the final product of a hydrogen generating chemical plant.

### 5.2.1 Nuclear Reactor System

Nuclear reactor power plants with specific reference design/production configurations could be considered simply as a source for generating heat to drive hydrogen plants ultimately while producing electricity for a grid based on supply and demand. The effects of these components in the loop of a combined plant can drive the overall production efficiency of plant requirements both on nuclear side and hydrogen production side and need to be accounted for. Therefore, code must be developed to be able to handle such sets of requirements in particular to be standalone, and analyzing the thermodynamics aspects of analysis in transient mode is not an easy task and may require a need for a multidiscipline codes that are interoperable.

### 5.2.2 Turbomachinery System

The other important aspect of a hydrogen generation plant that one needs to take into consideration is the efficiency of the turbomachinery associated with the plant, so that it can perform to its optimum design point. Thus any computer code to be used should be able to handle such phenomena so that it can perform optimization analysis for the system, such as the compressor and turbine machines incorporated into the plant design both on the nuclear and hydrogen sides.

The overall PCU efficiency for the plant was defined by Eq. (5.1) and was denoted by  $\eta_{PCU}$ ; now we can elaborate on the efficiency of the turbomachinery of subsystems involved in the overall power plant on either side, nuclear or hydrogen, in the facility. Although more details can be found in the books by Zohuri [7] and Zohuri and McDaniel [13], we encourage readers to refer to articles written by these two authors that can be found in the reference section at the end of this chapter.

From a thermodynamics point of view, several cycles are used to generate electricity as part of a general consideration of power cycles, and the major difference between nuclear and nonnuclear power cycles is the source of heat. In a conventional plant the source of heat is driven by fossil fuels, while in the nuclear power plant the heat source rises from a nuclear fission or fusion process, and for the purposes of this book, when we talk about nuclear power plants we mean a fission process not fusion. Another difference in the cycles between these two types of plant is the type of cycle to consider – *open* or *closed cycles* [13] – and the efficiency of the turbomachinery utilized in these plants can either be calculated and analyzed based on either an open air-Brayton loop or closed CO<sub>2</sub> loop as a combined cycle in the case of nuclear power plants in order to determine the optimally efficient design for better thermal energy output (Zohuri) [7]. Some fossil fuel power cycles are open cycles in which the reacting gases are emitted into the atmosphere. But as we know, the primary task of a nuclear power plant is to generate electricity as part of a grid system.

Thermodynamically this can be depicted on a  $T$ - $s$  diagram for a simple power cycle, which consists of four stages:

1. **Heat addition,**
2. **Power generation through expansion,**
3. **Heat rejection, and**
4. **Compression.**

Figures 5.5 and 5.6 show two simple Brayton cycles (i.e., open and closed) respectively, that are used in gas turbines, such as jet engines. As shown in the figures, for any gas-turbine machine, the cycle consists of four steps [13]:

### 1. Step 1

Air is drawn in and compressed adiabatically.

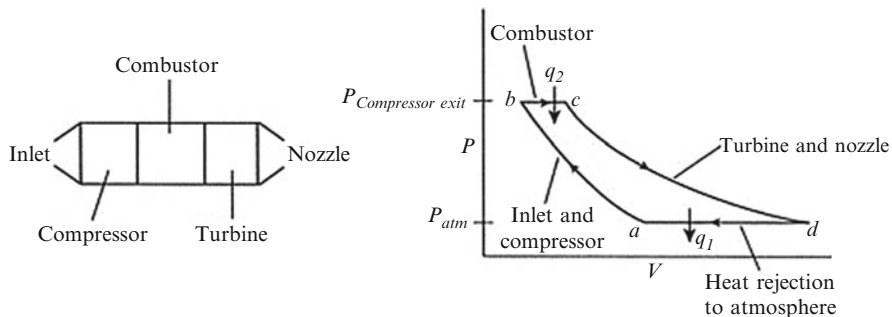


**Fig. 5.5** Steps of Brayton open cycle

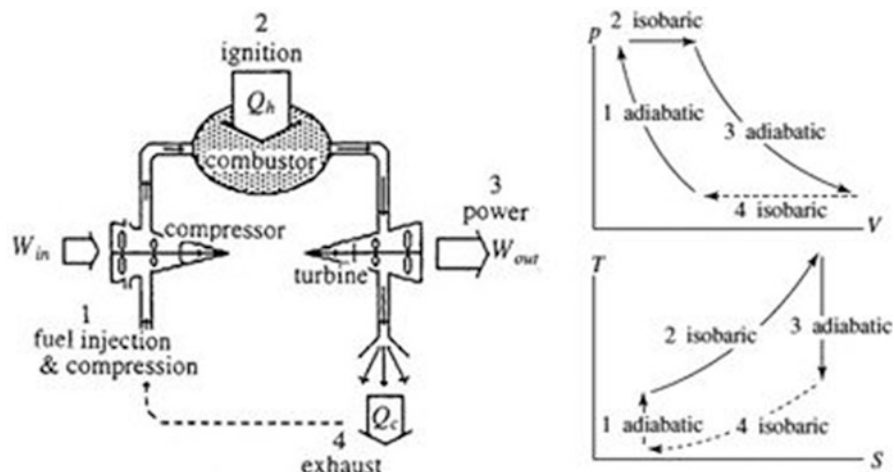


**Fig. 5.6** Steps of Brayton closed cycle

## 2. Step 2

The air is ignited where the fuel mixture in the combustion chamber expands isobarically.

## 3. Step 3

Work is harnessed by the engine, when gas enters the turbine and nozzle. The turbine blades direct the flow of gas through the nozzle. In the nozzle, the pressure decreases, the volume increases, and there is no change in heat or entropy – there is simply a change in the work.

## 4. Step 4

This step is isobaric, at a lower pressure. The gas is subsequently ejected.

In practice any turbine that is used in a nuclear generating power plant or HPP works on similar principles and the Brayton cycle can be divided into either *open* and *closed cycles*.

The open cycle, in which fuel is injected at the beginning and later ejected, is used in jet engines. The closed cycle, in which the fuel is recirculated through a closed loop, is commonly used in power generators.

Physical layouts of these two cycles are depicted in Fig. 5.7a, b.

Figure 5.8 is a general sketch of a thermodynamic model of a gas turbine engine cycle for power generation.

Thermodynamics allow the optimal performance of a cycle to be measured by its thermal efficiency, is defined as the ratio of the electrical power output to the heat input as

$$\eta_{\text{th}} = \frac{\dot{W}_{\text{elec}}}{\dot{Q}_{\text{in}}} \quad (5.2)$$

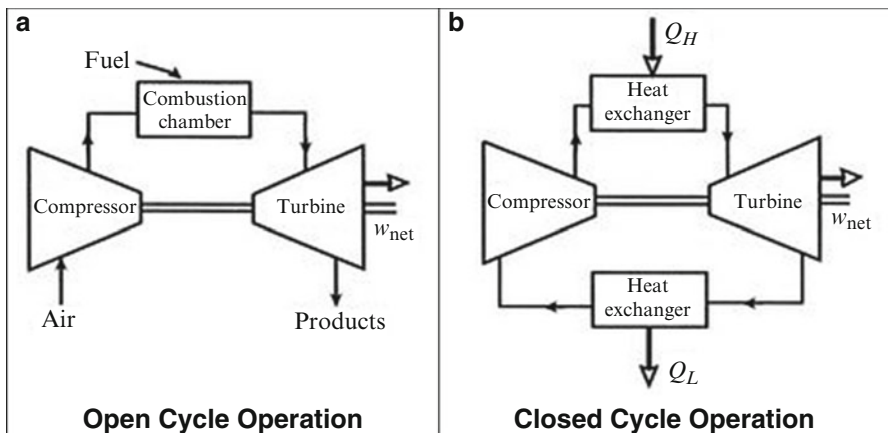


**Fig. 5.7** Options for operating Brayton cycle gas-turbine engine

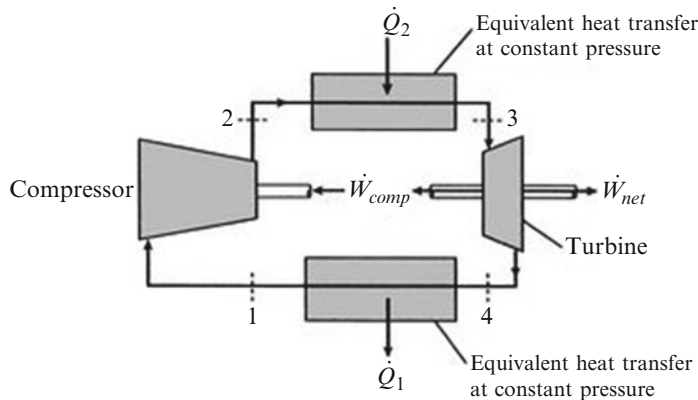
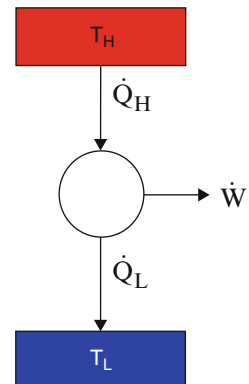


**Fig. 5.8** Thermodynamic model of gas turbine

**Fig. 5.9** Heat engine between hot source and cold sink



Hence a power cycle is based on the thermodynamic idea of a heat engine and may be produced from it by being placed between a high-temperature source and a low-temperature sink, as shown in Fig. 5.9. The work of the heat engine is then defined as

$$\dot{W} = \dot{Q}_H - \dot{Q}_L. \quad (5.3)$$

Analysis of Fig. 5.9 along with Eq. (5.3) indicates that heat is transferred from the high-temperature source to the heat engine and then heat is rejected from the heat engine to the low-temperature sink point, and thus the thermal efficiency of such a simple heat engine can be defined mathematically by Eq. (5.4) by substituting Eq. (5.3) into Eq. (5.2), so we have a new form for thermal efficiency:

$$\eta_{th} = \frac{\dot{Q}_H - \dot{Q}_L}{\dot{Q}_H} \quad (5.4)$$

In real life, a temperature difference is needed to transfer the heat from the heat source to the heat engine and consequently from the heat engine to the heat sink. However, in an ideal situation, if the differences approach a zero value, then the maximum efficiency is achieved and its value can be determined. Under these ideal conditions the maximum efficiency is called the *Carnot efficiency* ( $\eta_{\text{Carnot}}$ ) and is a function of heat source and sink temperatures under that ideal condition and can be defined mathematically as

$$\eta_{\text{Carnot}} = \frac{T_H - T_L}{T_H}. \quad (5.5)$$

Bear in mind that the efficiency of the hydrogen-production process increases with temperature. According to Argonne National Laboratory–West (ANLW) [14], the temperature supplied to the HPP should be at least 850 °C. The Independent Technology Review Group (ITRG) [15] claims that the current SI-based processes can operate at a minimum temperature of 800 °C. For this analysis, the maximum temperature supplied to the hydrogen plant is assumed to be 850 °C.

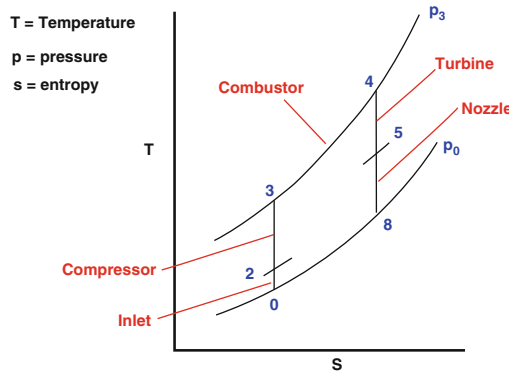
To provide estimates of the involved components and their performance, an assumption about the base configurations is required for the operating conditions of the NGNP, then it must be coupled to the HPP through an intermediate heat transport loop. To achieve this and for the purpose of conceptual study and research, one can, for example, consider a reactor such as the one depicted in Fig. 5.3 based on the FHR concept as proposed by Holcomb et al. [2] and developed at Oak Ridge National Laboratory (ORNL). The following assumptions can be made based on the design parameters for all cycles, such as Rankine supercritical and subcritical cycles, open air-Brayton cycle, helium Brayton-gas cycle, and a modified supercritical CO<sub>2</sub> Brayton cycle (e.g., the latter is being considered by Sandia National Laboratories as part of their research efforts in this area):

- Reactor heat output is 3400 MW(t),
- Reactor outlet temperature is 704 °C,
- Reactor inlet temperature is 600 °C,
- Turbines and compressors of the Brayton cycles have 90 % isentropic efficiencies,
- Circulators and pumps have 75 % isentropic efficiencies,
- IHXs and steam generators have minimum approach temperatures of 25 °C,
- All other heat exchangers in the Brayton cycles have minimum approach temperatures of 20 °C,
- The feedwater heaters in the Rankine cycles have minimum approach temperatures of 5.6 °C,
- Pressure drops across the components are 2 % of the inlet pressure to the component.

Taking the preceding base design parameters for a given FHR, the thermal efficiency for each of preceding power cycles can be analyzed and calculated. The reader may consult Sabharwall et al. [16].

**Fig. 5.10** Ideal Brayton cycle in *T-s* diagram

***Ideal Brayton Cycle***  
***T-s diagram***



In conclusion, if we look at simple gas turbine machinery as depicted in Fig. 5.8, based on thermodynamic modeling this cycle for power generation and for the drawing of the *T-s* diagram in Fig. 5.10 for this gas turbine, the Brayton cycle and its thermal efficiency can be written as follows:

$$\eta_{\text{th, Brayton}} = \frac{w_{\text{net}}}{q_{\text{in}}} = 1 - \frac{q_{\text{out}}}{q_{\text{in}}} = 1 - \frac{C_p(T_3 - T_2)}{C_p(T_4 - T_1)} = 1 - \frac{T_1 \left( \frac{T_4}{T_1} - 1 \right)}{T_2 \left( \frac{T_3}{T_2} - 1 \right)}, \quad (5.6)$$

$$\frac{T_2}{T_1} = \left( \frac{P_2}{P_1} \right)^{\frac{(k-1)}{k}} = \left( \frac{P_3}{P_4} \right)^{\frac{(k-1)}{k}} = \frac{T_3}{T_4}. \quad (5.7)$$

Now if use Fig. 5.10 and assume the following ideal situation:

- Ideal Brayton cycle under the cold air-standard assumptions
- Processes 1–2 and 3–4 are isentropic
- Pressure  $P_2 = P_3$  and  $P_4 = P_1$

Then substitution Eq. (5.7) into Eq. (5.6) yields

$$\eta_{\text{th, Brayton}} = 1 - \frac{1}{r_p^{\gamma}} = 1 - \frac{T_1}{T_2}, \quad \text{where } r_p = \frac{P_2}{P_1}. \quad (5.8)$$

As far as the advantages and related issues of this cycle are concerned, the following facts are established [7]:

- **Advantages**

- Open-cycle Brayton systems are a well-developed technology – e.g., gas-turbine plants, jet engines, marine propulsion.
- Higher operating temperatures make them more competitive versus steam plants (LWRs).
- Several hundred thousand systems have been built and installed worldwide.
- Systems are simple and compact and use no cooling water as a heat sink.

- **Brayton System Issues**

- Combustion Brayton systems operate at very high temperatures approaching stoichiometric.
- Since the heat generation is in the fluid, the walls and mechanical components can be, and are, cooled to avoid these high temperatures.
- For a reactor-driven Brayton system, the heat is generated in the solid reactor core and every component in its path to the working fluid sits atop the peak temperature in the fluid.
- One method to overcome this lower temperature limit is to use multiple reheat cycles. Multiple reheat cycles allow most of the heat to be input near the peak temperature of the cycle.
- The pressure drops in a heat exchanger can be significantly less than the nominal 5 % of a combustion chamber, easily in the 1 % or less range.
- Two other design options were also considered as methods of improving system efficiency.
- Recuperators are gas-to-gas heat exchangers that heat the compressed gas with exhaust from the turbines. However, since the hot side operates near atmospheric pressure, they tend to be quite large to achieve high effectiveness.
- With a combined cycle, there may be a modest amount of cooling available for an intercooler to improve the efficiency of the Brayton cycle part of the system.

Two efficiency improvements are often made to the simple Brayton cycle, as follows [7]:

1. A recuperator heat exchanger can be added to use the exhaust heat to preheat the inlet air recovering as much as 95 % of the exhaust heat.
2. A bottoming steam (Rankine) cycle can be added to use the exhaust heat to boil water and drive turbines. This is called a combined cycle and has produced the most efficient electricity generating power plants known.

### **5.2.3 Overall Efficiency of Plants**

Further analysis of plant efficiency requires looking at the overall efficiency and being able to calculate that as

$$\eta_{\text{overall}} = \frac{\sum W_T - \sum W_C - W_S - \sum W_{\text{CIR}} + Q_{H_2}}{Q_{\text{th}}}, \quad (5.9)$$

where again:

$\Sigma W_T$  = total turbine workload;

$\Sigma W_C$  = total compressor workload;

$W_S$  = plant stationary load (for simplicity of analysis it can be neglected), which includes the power for the electrolysis for HTE process or SI process;

$\Sigma W_{CIR}$  = circular workload in primary, intermediate, and, if present, tertiary loops;

$Q_{Th}$  = reactor thermal power;

$Q_{H_2}$  = hydrogen production mass flow rate times the specific energy content of the hydrogen.

To calculate the polytropic efficiency rather than the isentropic efficiency for the efficiency of turbomachinery (Zohuri and McDaniel) [13], we follow the following procedure. The equations for the expansion and compression processes in a perfect gas are taken from Saravanamuttoo et al. [17]. Therefore, for an expansion, the efficiency is calculated from

$$\frac{T_{0,\text{exit}}}{T_{0,\text{inlet}}} = \left( \frac{P_{0,\text{exit}}}{P_{0,\text{inlet}}} \right)^{\left( \frac{R}{c_p} \eta_{p,e} \right)}, \quad (5.10)$$

where:

$R$  = gas constant,

$c_p$  = specific heat at constant pressure,

$\eta_{p,e}$  = turbine polytropic efficiency,

$P_{0,\text{exit}}$  = stagnation pressure at exit point,

$P_{0,\text{inlet}}$  = stagnation pressure at inlet point,

$T_{0,\text{exit}}$  = exit gas temperature at stagnation stage,

$T_{0,\text{inlet}}$  = inlet gas temperature at stagnation stage.

Subscript 0 refers to the stagnation point for both temperature and pressure in this equation. For a compression, the efficiency is calculated from

$$\frac{T_{0,\text{exit}}}{T_{0,\text{inlet}}} = \left( \frac{P_{0,\text{exit}}}{P_{0,\text{inlet}}} \right)^{\left[ \left( \frac{R}{c_p} \right) \left( \frac{1}{\eta_{p,e}} \right) \right]}. \quad (5.11)$$

The adiabatic and polytropic efficiencies are included in the compressor calculations. An isentropic flash ( $P_{in}$  and  $\text{Entropy}_{in}$ ) is performed internally to obtain the ideal (isentropic) properties:

$$\begin{aligned} \text{Adiabatic Efficiency} &= \frac{\text{Work Required}_{(\text{ideal})}}{\text{Work Required}_{(\text{actual})}} \\ &= \frac{(H_{out} - H_{in})_{\text{ideal}}}{(H_{out} - H_{in})_{\text{Actual}}} \end{aligned} \quad (5.12)$$

and

$$\text{Polytropic Efficiency} = \frac{\left[ \left( \frac{P_{\text{out}}}{P_{\text{in}}} \right)^{\left( \frac{n-1}{n} \right)} \right] \times \left[ \left( \frac{n}{n-1} \right) \times \left( \frac{k-1}{k} \right) \right]}{\left[ \left( \frac{P_{\text{out}}}{P_{\text{in}}} \right)^{\left( \frac{k-1}{k} \right)} - 1 \right]} \times \text{Adiabatic Efficiency.} \quad (5.13)$$

In Eq. (5.13) variables  $n$  and  $k$  are defined as follows:

$$n = \frac{\log \left( \frac{P_{\text{out}}}{P_{\text{in}}} \right)}{\log \left( \frac{P_{\text{out, actual}}}{P_{\text{in}}} \right)} \quad \text{and} \quad k = \frac{\log \left( \frac{P_{\text{out}}}{P_{\text{in}}} \right)}{\log \left( \frac{P_{\text{out, ideal}}}{P_{\text{in}}} \right)}, \quad (5.14)$$

where ideal is isentropic (100 % efficiency), actual is a given efficiency,  $H$  is mass enthalpy, out is product stream (discharge), in is a feed stream (suction),  $P$  is pressure, MW is molecular weight,  $\rho$  is mass density,  $n$  is a polytropic exponent, and  $k$  is an isentropic exponent. Through this analysis we need to be concerned with another parameter known as the *compressibility factor* for both ideal and actual (real) gases denoted by  $z$ .

To close the loop of this analysis and have a better understanding of compressibility fact  $z$ , we go back to Eq. (5.10), and we can see that it has a dependency on the universal gas constant  $R$  and pressure  $P$  as well as temperature  $T$  both at stagnation point. But the science of thermodynamics allows us to define and ideal-gas equation of state that relates the pressure, temperature, and specific volume  $v$  of a substance as follows:

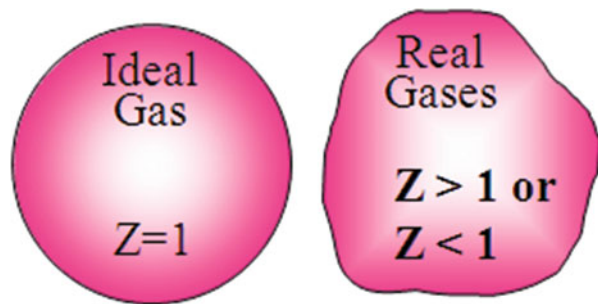
$$Pv = RT. \quad (5.15)$$

But as a word of caution, we should be careful in using this relation (Eq. 5.15) since *an ideal gas is a fictitious substance and real gases exhibit an ideal-gas behavior at relatively low pressures and high temperatures* and it would be a good approximation from a thermodynamic point of view to say that P-v-T behaviors are of a real gas at low densities. Air, nitrogen, oxygen, hydrogen, argon, neon, and carbon dioxide fall into this category with less than 1 % margin of error.

However, the deviation from an ideal-gas behavior can be properly accounted for by bringing the compressibility factor  $z$  into play and defining it furthermore by the following relationships, where this compressibility factor is represented by the specific volume ratios of actual (or real) gas  $v_{\text{actual}}$  and ideal gas  $v_{\text{ideal}}$ , respectively, as

$$z = \frac{Pv}{RT} \quad \text{or} \quad z = \frac{v_{\text{actual}}}{v_{\text{ideal}}}. \quad (5.16)$$

**Fig. 5.11** Compressibility factor



So the having the relationship established in Eq. (5.16) raises the following question:

***Under what conditions is it appropriate to apply the ideal-gas equation of state?***

The answer was given earlier by the science of thermodynamics for P-v-T behaviors of an ideal gas:

***At low pressure and high temperature at low densities.***

And further elaboration on this matter reveals that the *compressibility factor* accounts mainly for two things:

1. Molecular structure of the gas,
2. Intermolecular attractive forces.

And we can say that for real gases,  $z < 1$  or  $z > 1$ , and, consequently, for an ideal gas the compressibility factor is  $z = 1$ , as shown in Fig. 5.11.

In summary, the compressibility factor  $z$  is approximately the same for all gases at the same reduced temperature and reduced pressure, which is the *principle of corresponding states* and is mathematically represented as

$$z = z(P_{\text{Reduced}}, T_{\text{Reduced}}) \quad \text{for all gases.} \quad (5.17)$$

As one can see from Eq. (5.17),  $P_{\text{Reduced}}$  and  $T_{\text{Reduced}}$  are the *reduced pressure* and *reduced temperature*, respectively, and are defined as

$$P_{\text{Reduced}} = \frac{P}{P_{\text{Critical}}} \quad \text{and} \quad T_{\text{Reduced}} = \frac{T}{T_{\text{Critical}}}, \quad (5.18)$$

where  $P_{\text{Critical}}$  and  $T_{\text{Critical}}$  are the critical pressure and critical temperature properties, while  $P$  and  $T$  are the stagnation pressure and temperature, respectively. Figure 5.12 is an illustration of the *compressibility factor* for ten substances.

Now continuing with our analysis of overall plant efficiency, we can see that the adiabatic and polytropic efficiencies are parts of the expander calculations. An isentropic flash ( $P_{\text{in}}$  and  $\text{Entropy}_{\text{in}}$ ) is performed to obtain the ideal (isentropic) properties. The flash is done internally on the expander fluid, and then we can write

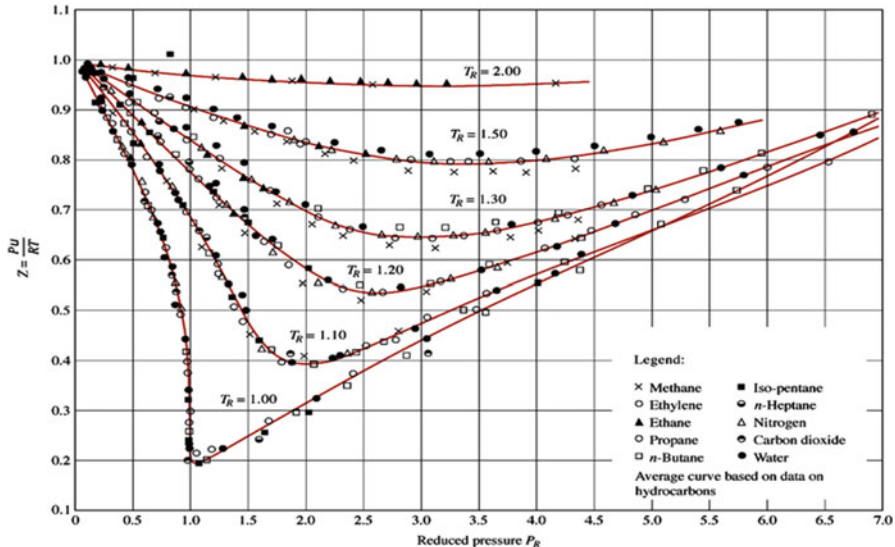


Fig. 5.12 Compressibility factor for ten substances (Moran and Shapiro) [18]

$$\text{Polytropic Efficiency} = \frac{\left[ \left( \frac{P_{\text{out}}}{P_{\text{in}}} \right)^{\left( \frac{k-1}{k} \right)} \right]}{\left[ \left( \frac{P_{\text{out}}}{P_{\text{in}}} \right)^{\left( \frac{n-1}{n} \right)} - 1 \right] \times \left[ \left( \frac{n}{n-1} \right) \times \left( \frac{k-1}{k} \right) \right]} \times \text{Adiabatic Efficiency.} \quad (5.19)$$

To calculate the pressure and temperature at the exit of a polytropic expansion or compression process, pressure-enthalpy ( $P$ - $h$ ) data from the National Institute of Standards and Technology (NIST) database (NIST version 7.) can be used. The procedure is described below and depicted in graphical form in Fig. 5.13:

1. Starting point 1: follow the line of constant entropy to the required discharge pressure of  $P_2$ , locating the isentropic discharge state point  $2_{\text{in}}$ .
2. With these two points located, the differential isentropic enthalpy can be calculated from the following equation:

$$\Delta h_{\text{isentropic}} = h_{2_{\text{in}}} - h_1. \quad (5.20)$$

3. Calculate the real discharge enthalpy of point 2 using

$$h_2 = \frac{\Delta h_{\text{isentropic}}}{\eta_{\text{isentropic}}} + h_1, \quad (5.21)$$

where  $\eta_{\text{isentropic}}$  is the isentropic process efficiency.

**Fig. 5.13** Pressure-enthalpy ( $P-h$ ) diagram

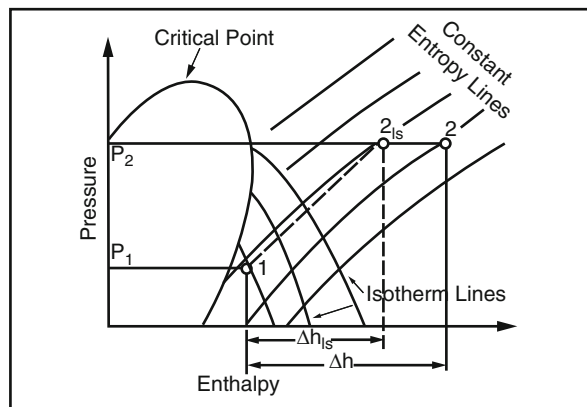
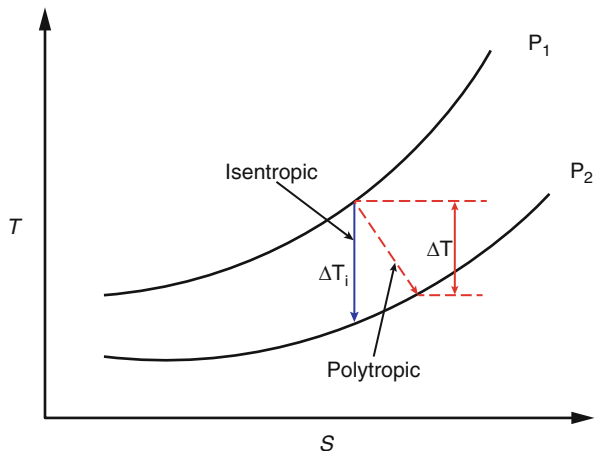


**Fig. 5.14**  $T-s$  diagram for isentropic and polytropic (real) compression



Point 2 is on the same pressure  $P_2$  line shown in Fig. 5.14. At point 2, the temperature can be obtained on the same temperature isotherm line as in Fig. 5.13.

The actual discharge temperature can now be obtained from the  $P-h$  diagram (GPSA) [19] or  $P-h$  database. The properties of the working fluid can be incorporated as a property lookup table. Pressure–temperature–enthalpy data from the NIST database can be used.

The use of pressure–enthalpy data from the NIST will eliminate problems associated with the nonconstant heat capacity term defined in Eqs. (5.10) and (5.11) for a nonideal gas such as carbon dioxide in critical conditions [1].

The pressure ratio, defined as the outlet pressure from the high pressure compressor (HPC) divided by the inlet pressure to the low pressure compressor (LPC), will be varied to optimize the overall cycle efficiency. Cooling was applied between compressors to reduce the power consumed by the HPC. Cooler components will be

used to simulate the heat loss and differential pressure along the hot and cold legs of the intermediate heat transport loop. To identify the location of the LPC and HPC in a HPP, refer to Fig. 5.4 of this chapter.

### 5.2.4 Heat Exchanger System

Choosing the right heat exchanger to account for their footprints and compactness yet be efficient enough to meet the demands imposed on them is another important parameter and tool associated with the requirements for hydrogen generating power plants. This process also is not very straight since the choice of working fluid along with the type of heat exchanger and related configuration associated with thermal-hydraulic and stress analysis makes the process very difficult given the accuracy needed to ensure these reference design heat exchangers work properly, and the results again require transient analysis computer code rather than steady-state code for final optimal design.

One type of heat exchanger that has been proposed is the printed circuit heat exchanger (PCHE) in gas-to-gas form with either a cross-flow or counterflow compact structure, so the model should be able to take the effects of wavy channels in the PCHE into consideration to compensate for the heat transfer and pressure drop as well as flow conditions (either laminar or turbulent) through these channels. Although more details can be found in Chaps. 6 and 7 about heat exchangers and their types as well as their configurations, here, a typical compact heat exchanger of the PCHE type is illustrated in Fig. 5.15.

Among the strategy parameters for IHX acquisition is the coolant fluid for heat transfer as a selection criterion, and there are a variety of heat transfer fluids that can be used in high-temperature heat exchangers to meet the demands heat requires for

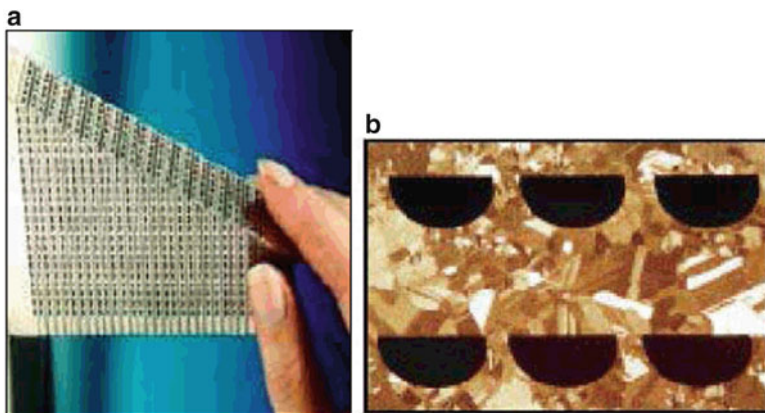


**Fig. 5.15** Printed circuit heat exchanger (Heatric homepage 2011). (a) Photo of PCHE. (b) Cross-sectional view of PHCE

the nuclear side of a plant to couple with the hydrogen side; they include, for example, gases, liquid metals, and molten salts. The following list shows some general characteristics required for heat transfer fluids:

- Low pumping power to improve efficiency through less stringent pump requirements.
- High heat transfer performance to achieve high efficiency.
- Low coolant volume for greater efficiency.
- Low structural materials volume for greater efficiency.
- Low heat loss for greater efficiency.
- Low temperature drop for greater efficiency.

The characteristics of heat transfer fluids have been extensively investigated by Kim et al. [20] for high-temperature applications based on the following figures-of-merit (FOMs):

- $FOM_{ht}$  represents the heat transfer performance of the coolant. It measures the heat transfer rate per unit of pumping power for a given geometry.
- $FOM_p$  represents the pumping power of the coolant. It measures the pumping power required to transport the same energy for a given geometry.
- $FOM_{cv}$  represents the volume of the coolant. It measures the coolant volume required for transferring heat with the same heat and pumping power.
- $FOM_{ccv}$  represents the volume of the structural materials. It measures the volume of the coolant structural materials required for transferring heat with the same heat duty and pumping power under given operating conditions ( $T$  and  $P$ ).
- $FOM_{hl}$  represents the heat loss of the coolant. It measures the heat loss of the coolant when it is transported the same distance with the same heat duty and pumping power.
- $FOM_{dt}$  represents the temperature drop in the coolant while transferring thermal energy with a given heat duty and pumping power.

Table 5.3 shows comparisons of the thermal-hydraulic characteristics of the various coolants based on the estimated FOMs (Kim et al.) [20].

In this estimation, water at 25 °C and 0.1 MPa was selected to be the reference coolant. The following summarizes the results:

- A higher  $FOM_{ht}$  is preferred for better heat transfer performance. According to the comparisons, sodium shows the highest value (=19.05) and argon the lowest (0.05). Overall,  $FOM_{ht}$  is the highest in liquid metal followed by liquid water, molten salt, and gases.
- A lower  $FOM_p$  is preferred for greater efficiency and economics. According to the comparisons, liquid water has the lowest value (=1.0) and argon the highest value (=72,592). Overall,  $FOM_p$  is the lowest in molten salt followed by liquid metals and gases.
- A lower  $FOM_{cv}$  is preferred because it requires a lower coolant volume to achieve the same heat transfer performance under the same pumping power. According to the comparisons, liquid water has the lowest value (=1.0) and

**Table 5.3** Principal features of several types of heat exchangers (Shah and Sekulic) [21]

	Coolant	FOM <sub>ht</sub>	FOM <sub>P</sub>	FORM <sub>cv</sub>	FORM <sub>ccv</sub>	FORM <sub>hl</sub>	FORM <sub>dt</sub>
Reference	Water (25 °C, 1 atm)	1.00	1.00	1.00	1.00	1.00	1.00
Gas (700 °C, 7 MPa)	He	0.12	25,407.41	67.74	4741.80	0.40	0.40
	Air	0.07	40,096.15	80.10	5607.14	0.26	0.26
	CO <sub>2</sub>	0.11	11,390.17	47.19	3303.46	0.32	0.32
	H <sub>2</sub> O (Steam)	0.11	10,012.63	45.10	3157.12	0.32	0.32
	Ar	0.05	72,592.09	101.44	7100.53	0.20	0.20
Molten salt (700 °C)	LiF-NaF-KF	0.80	2.87	1.57	1.57	0.92	0.92
	NaF-ZrF <sub>4</sub>	0.45	5.02	1.98	1.98	0.56	0.56
	KF-ZrF <sub>4</sub>	0.38	8.69	2.49	2.49	0.51	0.51
	LiF-NaF-ZrF <sub>4</sub>	0.40	5.36	2.05	2.05	0.50	0.50
	LiCl-KC1	0.55	14.99	3.07	3.07	0.76	0.76
	LiCl-RbC1	0.47	23.03	3.66	3.66	0.70	0.70
	NaCl-MgCl <sub>2</sub>	0.58	16.26	3.18	3.18	0.81	0.81
	KC1-MgCl <sub>2</sub>	0.50	14.30	3.02	3.02	0.70	0.70
	NaF-NaBF <sub>4</sub>	0.71	5.66	2.04	2.04	0.88	0.88
	KF-KBF <sub>4</sub>	0.64	8.98	2.47	2.47	0.84	0.84
	RbF-RbF <sub>4</sub>	0.54	14.61	3.01	3.01	0.75	0.75
	Sodium	19.05	33.62	4.19	4.19	28.91	28.91
Liquid metal (700 °C)	Lead	6.05	111.64	6.90	6.90	10.82	10.82
	Bismuth	6.61	100.69	6.60	6.60	11.66	11.66
	Lead-Bismuth	4.86	142.94	7.65	7.65	8.95	8.95

argon the highest (=101.44). Overall, FOM<sub>cv</sub> is the lowest in molten salt followed by liquid metals and gases.

- A lower FOM<sub>ccv</sub> is preferred because it requires less structural material volume for both heat transfer pipes and components. Overall, the same result was obtained as with FOM<sub>cv</sub>. The FOM<sub>ccv</sub> is lowest in molten salt followed by liquid metals and gases.
- A lower FOM<sub>hl</sub> is preferred because it requires less insulation for preventing heat loss. According to the comparisons, argon has the lowest value (0.2) and sodium the highest (28.9). Overall, FOM<sub>hl</sub> is the lowest in gases followed by molten salt and liquid metal.
- A lower FOM<sub>dt</sub> is preferred because more thermal energy can be transferred long distances without much of a temperature drop. The same values were obtained for FOM<sub>dt</sub> as for FOM<sub>hl</sub>.

The heat transfer coefficient is one of the important parameters when designing a heat exchanger, simply because it determines overall heat exchanger sizes and performance. A list of some coolant types and the ranges of their heat transfer coefficients are listed in Table 5.4 (Kakac and Liu) [22]. As can be seen, water exhibits the highest heat transfer coefficient in dropwise condensation, and gases exhibit the lowest in natural circulation.

**Table 5.4** Order of magnitude of heat transfer coefficient (Kakac and Liu) [22]

Fluid	$H$ (W/m <sup>2</sup> K)
Gases (natural convection)	3–25
Engine oil (natural convection)	30–60
Flowing liquids (nonmetal)	100–10,000
Flowing liquid metal	5000–25,000
Boiling heat transfer	
Water, pressure < 5 bars, $dT < 25$ K	5000–10,000
Water, pressure 5–100, $dT = 20$ K	4000–15,000
Film boiling	300–400
Condensing heat transfer	
Film condensation on horizontal tubes	9000–25,000
Film condensation on vertical surface	4000–11,000
Dropwise condensation	60,000–120,000

### 5.2.5 Heat Exchanger Design Configuration

As stated earlier, a heat exchanger that thermally connects a NGNP to a heat transport loop can be designed in such a way as to fit into the category of compact heat exchangers, and Dewson and Thonon [42] also proposed an approach, where this heat exchanger couples the heat transport loop to the hydrogen generation plant, and this loop can be designed to be a tube-in-shell class of heat exchanger with the heat transport fluid flowing on the shell side. Using such a configuration allows the tubes to contain the catalysts for the hydrogen production process, and the tube side is assumed to be on a low pressure (less than 1 MPa) side simply because the efficiency of the hydrogen generating process decreases at higher pressures. As an additional assumption, the hot and cold legs of the intermediate loop could be separate pipes, as opposed to an annular configuration.

For the purposes of design convenience, we can assume the following convention and definition relative to heat exchangers that are involved with a NGNP-driven HPP.

The first heat exchanger downstream of the **NGNP** outlet is referred to as the **IHX**. The heat exchanger that connects the intermediate heat transport loop to the HPP is referred to as the **PHX**. The third heat exchanger, which if present is located between the IHX and the PHX, is referred to as the **SHX**.

The configuration of connectivity of both nuclear and HPPs may be either a direct or indirect electrical cycle with serial or parallel heat exchanger options. There may be additional options to include the SHX as well; they are all discussed in what follows (Davis) [23].

In the serial option IHX could be located between the nuclear reactor outlet and PCU, where the IHX removes less than 10 % of the nuclear reactor's thermal energy and directs it toward the HPP (Fig. 5.16). Under this condition and configuration, the HPP receives a higher temperature fluid than the PCU equipment. Although this

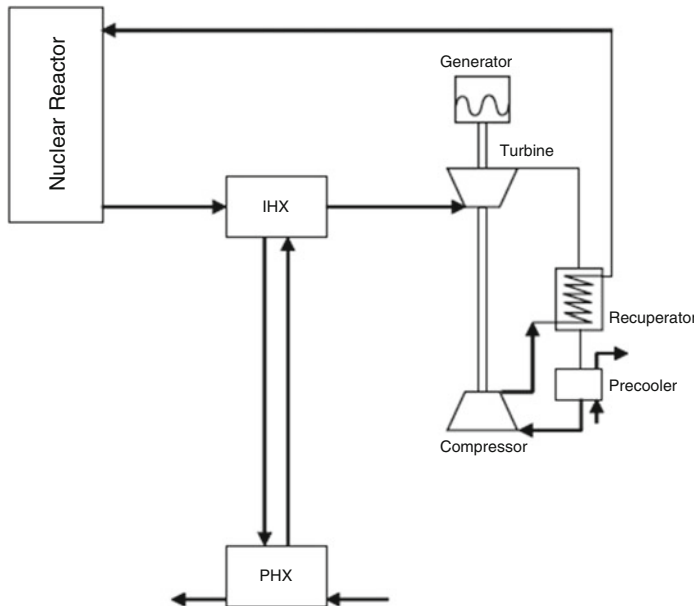


**Fig. 5.16** Direct electrical cycle and serial IHX [23]

configuration relatively speaking is a very simple layout and in particular makes it feasible for a hydrogen power plant to coexist with a nuclear plant, the overall efficiency of the electrical production process will be reduced as was argued earlier at the beginning of this section.

The option of a parallel configuration is a more complicated one, but its advantage is that it results in a higher overall efficiency because both the electrical and HPPs see the maximum possible temperature. Under this condition and configuration, the hottest fluid is divided, with most of it going to the PCU while the remainder of it is directed toward the HPP. With these options, a small compressor or blower is required to compensate for the pressure loss across the IHX and allow the fluid streams to mix downstream of the recuperator (Fig. 5.17).

As a third option, one can include a SHX, and this option provides greater safety because it increases the separation distance between the nuclear power plant and HPP. In this way, the safety of the facility increases and may boost the operational licensing of a nuclear power plant as part of this process. However, the downside of this option is that it requires more capital investment from total cost of ownership (TCO) point of view and lowers the overall efficiency of the plant (Fig. 5.18).

For further configurations and other optional design layouts between nuclear and hydrogen generating plants, the reader may consult the report INL/EXT-05-00228 by Davis [23].

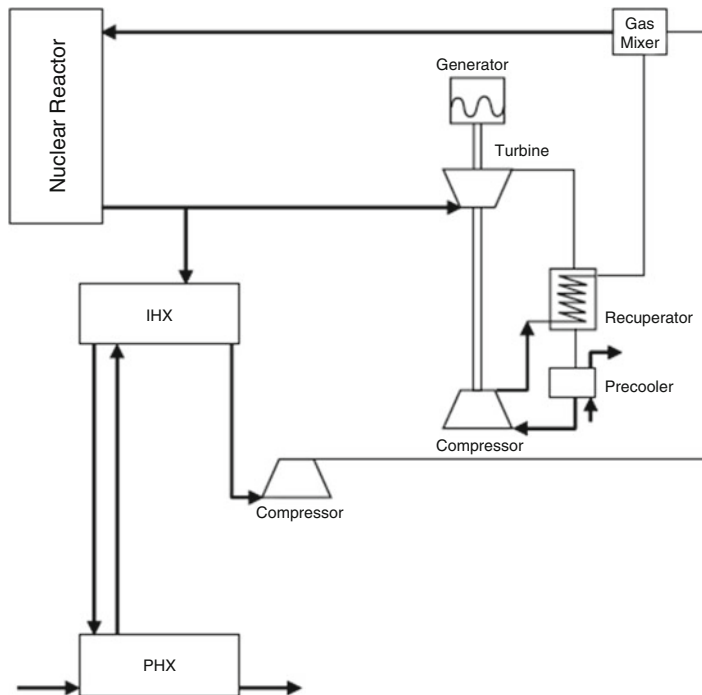


**Fig. 5.17** Direct electrical cycle and a parallel IHX [23]

### 5.2.6 *Intermediate Heat Exchanger Stress Analysis*

As mentioned earlier, the current concept of NGNP utilization is to drive a hydrogen generation plant coupled through a PCHE to an IHX and be able to interface with an intermediate heat transport loop (IHTL).

Heatric is the manufacturer of this type of heat exchanger, which uses laminated plates (Fig. 5.19), which have chemically etched semicircular channels between each diffusion-bonded layer, as illustrated in Fig. 5.15b.

This type of heat exchanger is compact, efficient, and capable of withstanding high pressures, all of which are attractive to the NGNP program. However, a stress analysis is necessary to verify that the PCHE is operating in an acceptable range because of the high operating temperature.

A simplified stress analysis on this type of heat exchanger was performed by Davis et al. [24], which yielded fluid channel configurations based on the pressure differential between the primary coolant of the nuclear reactor and the fluid of the IHTL. More details can be found in Lillo et al. [25].

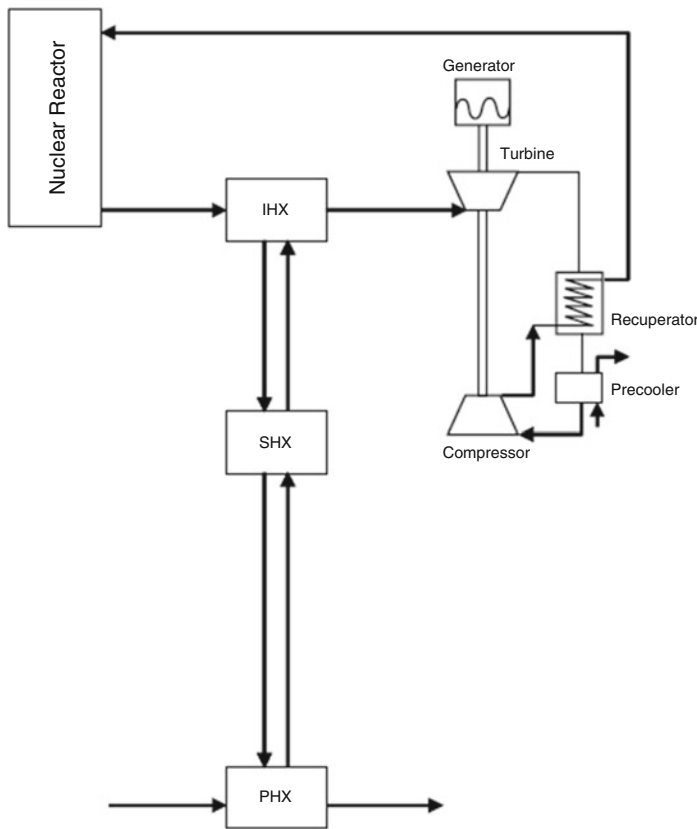


**Fig. 5.18** Direct electrical cycle, serial IHX, and SHX [23]

### 5.2.7 Heat Exchanger Materials and Comparisons

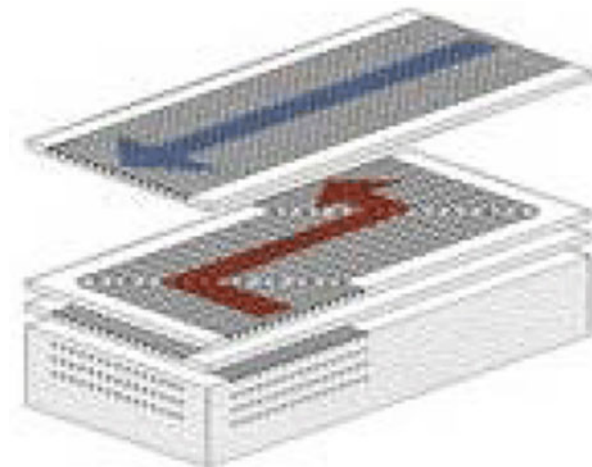
In the process of manufacturing heat exchangers that have good operational performance and durability and that have a longer life cycle in high-temperature conditions produced by a nuclear reactor source of energy, the selection of the right materials is one of the most challenging steps for meeting the operational temperature requirements according to the design criteria.

There are three main classes of high-temperature materials, as reported by Sunden [26], that we must take into consideration; these materials are very promising candidates for a variety of applications at high temperatures. They are as follows:

#### 1. High-temperature nickel-based alloy (e.g., Hastelloy)

This is a good material and may be compatible with helium and molten salt applications and tolerates temperatures in a range of 750 °C. This material also has good potential for use in sulfuric acid thermal decomposition.

**Fig. 5.19** Diffusion bonded layers in a Heatic heat exchanger



## 2. High-temperature ferritic steels (particularly oxide-dispersion ferritic steels)

There is a good possibility that these steels will be compatible with lead/bismuth under proper chemistry control conditions and with molten salts. Silica-bearing steels may be candidate materials for sulfuric acid thermal decomposition.

## 3. Advanced carbon and silicon composite

This material offers excellent mechanical strength and thermal stress performance beyond 1000 °C. The material is now used in high-temperature rocket booster nozzles to eliminate the need for cooling these nozzles to maintain the integrity of the materials that are used in such cooling and for the reentry nose of space shuttles and the leading edges of their wings.

According to Sundén [26], the best materials in terms of endurance and ability to withstand thermal stress to meet the design requirements for IHXs used in the coupling of VHTRs with HPPs is  $\text{SiC}_p/\text{Al}_2\text{O}_3$ , which has a particle-reinforcing phase-based material property. However, note that this material is still in the R&D process to the point that the numerical values of the properties are indicative and much more characterization effort is required.

Ohadi and Buckley [27] created Table 5.5, which is presented below; it includes nickel-based alloy, ceramic materials, and a carbon and SiC composite. In conjunction with this table, Fig. 5.20, provided by Brent [28], is an illustration of the specific strength versus temperature for various composite materials. One worthy note here is that ceramic packaging of integrated circuits was considered over 20 years ago by researchers in the aerospace industry because it can withstand any type of radiation (i.e., neutron rays, gamma rays), either artificial or natural in space, that may impose a latch up in IC and cause structural damage to substrates used in PNP junctions. For further information and discussion, please refer to Chap. 7, under Sect. 7.4.

**Table 5.5** Selected properties of most commonly used high-temperature materials and fabrication technologies [27]

High-temperature material/ fabrication technology	Metallic Ni alloys (Inconel 718)	Ceramics oxides of Al, Si, Sr, Ti, Y, Be, Zr, N and SiN, AlN, B4C, BN, WC94/C06	Carbon-carbon composite	Carbon fiber SiC composite
Temperature range	1200–1250 °C	1500–2500 °C	3300 °C (inert environment)	1400–1650 °C
			1400–1650 °C (with SiC layer)	
Density	8.19 g/cm <sup>3</sup>	1.8–14.95 g/cm <sup>3</sup>	2.25 g/cm <sup>3</sup>	1.7–2.2 g/cm <sup>3</sup>
Hardness	250–410 (Brinell)	400–3000 kgf/mm <sup>2</sup> (V)	0.5–1.0 (Mohs)	2400–3500 (V)
Elongation	<15 %	N/A	N/A	–
Tensile strength	800–1300 MPa	48–2000 MPa	33 (Bulk mod.)	1400–4500 MPa
Tensile modules	50 GPa	140–600 GPa	4.8 GPa	140–720 GPa
Strength of HX	Adequate, but limited owing to creep and thermal exp	Inadequate, low mechanical parameters for stress; good thermal and electrical parameters	Poor, oxidation starts at 300 °C	Highest because of carbon fiber and SiC
Electrical conductivity	125 μΩ cm	2E–06–1E +18 Ω cm	1275 μΩ cm	1275 μΩ cm
Thermal conductivity	11.2 W/m K	0.05–300 W/m K	80–240 W/m K	1200 W/m K
Thermal expansion	13E–06 K <sup>-1</sup>	0.54–10E–06 K <sup>-1</sup>	0.6–4.3E–06 K <sup>-1</sup>	–
Comments	Metallic expansion joints are weak link	Often very expensive fabrication cost for conventional application; technology proprietary for the most part; technologically hard to produce	Lifetime is low even protected by SiC (adhesion is poor)	Comparatively less expensive; successful proprietary fabrication technologies available

More interesting materials and chemistry-related problems need more research in connection with applications where the control of these problems is imposing complicated conditions by neutron transmutation (e.g., fission neutron effects) and where any related contamination issues need to be addressed; this includes debris from fission products for molten-salt transmutation.

Further investigation was carried out by Dewson and Li [29] on selecting a material for VHTR IHXs, which is summarized in Table 5.6.

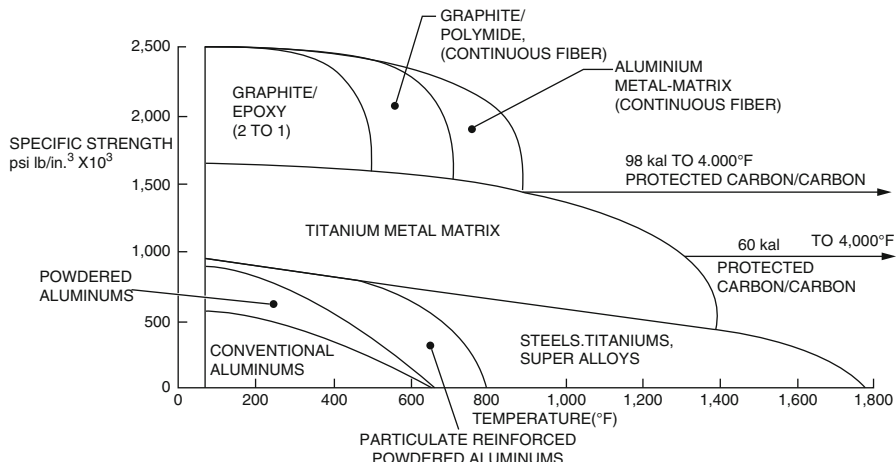


Fig. 5.20 Specific strength versus temperature [28]

Table 5.6 Candidate materials for VHTR IHXs [29]

Alloys	UNS Number	$T_{\max}$ (°C)	$S^{898^{\circ}\text{C}}$ (MPa)	UTS (MPa)	0.2 % PS (MPa)	EI (%)	Nominal composition (wt%)
617	N06617	982	12.4	655	240	30	52Ni-22Cr-13Co-9Mo-1.2Al
556	R30556	898	11.0	690	310	40	21Ni-30Fe-22Cr-18Co-3Mo-3W-0.3Al
800 HT	N08811	898	6.3	450	170	30	33Ni-42Fe-21Cr
800 H	N08810	898	5.9	450	170	30	33Ni-42Fe-21Cr
330	N08330	898	3.3	483	207	30	Fe-35Ni-19Cr-1.25Si
230	N06230	898	10.3	760	310	40	57Ni-22Cr-14W-2Mo-0.3Al-0.05La
HX	N06002	898	8.3	655	240	35	47Ni-22Cr-9Mo-18Fe
253 MA	S30815	898	4.9	600	310	40	Fe-21Cr-11Ni-0.2N

The researchers selected and compared the following eight candidate materials that are shown in Table 5.6 that based on ASME VIII (boiler and pressure vessel code) and they: Alloy 617, Alloy 556, Alloy 800H, Alloy 880HT, Alloy 330, Alloy 230, Alloy HX, and 253MA.

Table 5.6 lists the allowable design stress ( $S$ ) at  $898^{\circ}\text{C}$ , the minimum required mechanical properties (ultimate tensile stress [UTS]), 0.2 % proof stress (PS), and elongation (EI) at room temperature, together with the nominal compositions of the alloys. The researchers extensively compared the mechanical properties, physical properties, and corrosion resistance of the candidate materials and concluded that Alloys 617 and 230 are the most suitable materials for an IHX [30].

### 5.2.8 *Sizing of Components*

The sizing of heat exchangers and the carrying out of thermal-hydraulic analyses of their ability to process heat application duty for the right fluid as coolant based designed heat transfer fluid requirements and characteristics for coupling a hydrogen production to a high-temperature nuclear reactor or any high-temperature reactor of the NGNP family is an important step for the design of such plants, and series iteration of a thermal-hydraulic analysis should be conducted to determine the optimum point of efficiency [31]. Also, some other analyses were given by Davis et al. [11] based on the geometry required to be inputted for a choice of compact heat exchanger of a PCHE type.

For this PCHE, the basic geometry and related analysis, the diameter of the semicircular flow channel, the pitch-to-diameter aspect ratio of channels, and the thickness of the plates need to be taken into consideration. See Figs. 3.37, 5.15a, b of this chapter as well as Fig. 7.7 of Chap. 7.

Extensive analyses and the related thermo-mechanical relationship for heat exchanger effectiveness were shown in Chap. 3 (Eq. 3.6) and pipe components to be sized to produce the desired amount of pressure drop for the given length, flow rate, and thermodynamic conditions in the pipe.

Turbomachinery size can be estimated from the power produced or consumed by the component. Schlenker [32], using cost function analysis for a high-temperature reactor in a direct-cycle connectivity of component mode, suggests that the cost of new turbomachinery can be scaled from the cost of existing machines if the changes in power and operating pressure and temperature are known. While Dostal et al. [32], based on a design for supercritical carbon dioxide (S-CO<sub>2</sub>) for next generation nuclear reactors, used this method to estimate the cost for turbomachinery in a Brayton cycle utilizing a CO<sub>2</sub> closed cycle, which is the same approach as that used by a team of researchers at Sandia National Laboratories. Thus, the power and operating conditions should also provide an indication of component size.

As part of the effect of temperature on cost, the Brayton cycle recuperator and the reactor-to-power cycle IHX are large, expensive components. For our nominal 300 MWe unit, the S-CO<sub>2</sub> recuperator (which has a thermal duty 2.5 times that of the reactor core) would cost about \$16/kWe. The IHX would then cost \$6.4/kWe, provided the steel (Type 347) can withstand the higher temperature service. If, for example (as in a He-cooled counterpart), the INCOLOY 800 at 1000 °C had to be used, an increase in cost by a factor of seven has been projected by Wang [33].

Sizing assessment has a direct impact on the cost of heat exchangers given the task of heat transfer assigned to them as part of the base design configuration, and the choice of fluid will drive this cost to higher levels. For example, in the case of supercritical carbon dioxide (S-CO<sub>2</sub>), one of the key enabling features behind the revival of S-CO<sub>2</sub> as a serious contender in NGNPs is the extreme compactness of the PCHE design and the compactness of the equipment manufactured by Heatric as early as 1990. These components are currently specified for use in IHXs, recuperators, and precoolers in the power cycle. Hence their cost is an important aspect of total S-CO<sub>2</sub> plant costs and they were considered by INL and SNL

**Table 5.7** Material cost factors

	Material	Cost multiplier
Carbon	Steel	1.0
304L	SS	1.8
316L	SS	2.2
Ti		2.8
Incoloy	825	3.0
Inconel	625	5.0
Hastelloy	C-276	5.9
Zirconium		7.7

National Laboratories' research team as part of their study and feasibility of utilizing such techniques in their IHXs.

Table 5.7 also provides relative cost factors for heat exchangers constructed of various materials. This was based on a study reported by Argonne National Laboratory for materials such as SS-316-L in general service in S-CO<sub>2</sub> and, hence, also as a base case material for the purpose of coupling a nuclear plant with a hydrogen generating plant via these types of IHX using PCHEs owing to their compactness and overall sizing and their footprint on the land required for such facilities.

Another point worth noting is that only in the past 2 years, Heatic has developed an improved design, designated MP (for multiported), which provides true counterflow (as opposed to the Z-flow in earlier designs). This permits a further reduction in size/weight/cost/pressure drop – up to 50 % according to Heatic – and naturally the more compact the heat exchanger geometry is, the more expensive the manufacturing process will be, particularly if the pinch point gets reduced to its minimum temperature differential. Naturally, preventive maintenance during the offline period will not be cheap, either.

As part of a sizing and cost analysis, Dostal [34] compared S-CO<sub>2</sub> and steam cycle (SC) efficiencies (Fig. 5.21).

As illustrated in Fig. 5.21, above around 550 °C, S-CO<sub>2</sub> we recognize and efficiency advantages, which increases with temperature if we make plausible extrapolations for steam. Since S-CO<sub>2</sub> has a lower capital cost, above 550 °C we can predict a growing cost-of-energy advantage. Thus our final economic assessment will hinge on what turbine inlet temperature is assumed, and this is a function of IHX performance capabilities and, consequently, the choice of high-temperature NGNP reactor type to couple with the HPP.

The preceding considerations and observations suggest that we should focus on a limited number of specific applications in our future work. Since the VHTR has top priority in US programs and likewise for similar HTGRs worldwide, this would appear to be a natural path to take. This also drives the issues under study by this author and others to look at combined cycles and the feasibility of utilizing a Rankine vs. Brayton cycle or a combination of both (Zohuri) [7]. This consideration further drives the cost reduction perspective by selecting the right PCU per choice of nuclear reactor plant, which would also further reduce the total direct cost (TDC), maybe by few percent folds.

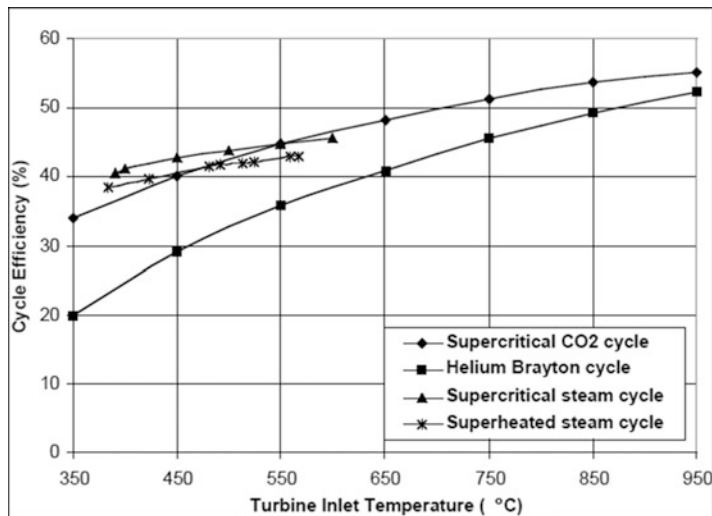


**Fig. 5.21** Cycle efficiency comparison of advanced power cycles [34]

### 5.2.9 Heat Exchanger Cost Analysis

Sabharwall and Kim [30] report on this aspect of IHXs for the NGNP acquisition and design selection process, although generally, manufacturers have their own methods of cost estimation. They use a simple heat exchanger costing methodology based on empirical cost data of the Engineering Sciences Data Unit (ESDU) [35] for various feasible heat exchanger types [21]. Detailed costs will depend on the operating conditions and materials used. The decision variable in this method is the cost of a heat exchanger per unit of its thermal size defined by

$$C_{UA} = \frac{\text{cost}}{\frac{q}{\Delta T_m}}, \quad (5.22)$$

where:

cost = cost of heat exchanger,

$q$  = thermal duty,

$\Delta T_m$  = mean temperature.

Table 5.8 shows a sample of the cost data represented by the values of  $C_{UA}$  (Shah and Sekulic) [21]. This table was prepared for an application using gas as hot fluid at a medium pressure of about 2 MPa and cold fluid as treated water. An extensive set of  $C_{UA}$  data for various heat exchangers can be found in ESDU [35].

**Table 5.8** Cost data  $C_{UA}$  versus  $UA$  for various heat exchanger types [21, 35]

$q/\Delta T_m$	$C_{UA}$ (\$/(W/K))				Welded plate	
	Shell-and-tube	Double tube	Printed circuit	Plate-fin	$U$ (W/m <sup>2</sup> K)	$C_{UA}$ (\$/(W/K))
	$U = 484$ (W/m <sup>2</sup> K)	$U = 484$ (W/m <sup>2</sup> K)	$U = 1621$ (W/m <sup>2</sup> K)	$U = 1621$ (W/m <sup>2</sup> K)		
$10^3$	3.98	2.5	12	—	349	4.9
$5 \times 10^3$	1.00	0.75	2.4	3.1	1187	1.22
$3 \times 10^4$	0.29	0.31	0.6	0.513	1068	0.41
$10^5$	0.17	0.31	0.42	0.210	1112	0.28
$10^6$	0.106	0.31	0.28	0.115	1173	0.22

Original cost data in ESDU are approximated to US dollar value in 2000

### 5.3 Reactor and Power Conversion Unit

As part of any modeling process, the reactor and PCU should be modeled and assembled on the basis of information on basic components that form part of the overall plant, such as the reactor core and turbomachinery in the loop, including the compressor, heat exchanger, pump, junction, and piping systems. In developing models for each of these components one must choose from among ideal versus real gas treatment, polytropic versus isentropic process treatment, and spatially lumped versus discretized treatment of heat transfer and pressure drop. Among all these components some are implicit and some explicit functions of coolant fluid involved in part of the base design. For helium at NGNP conditions a reasonable selection is ideal gas, polytropic process, and spatial lumping. For supercritical carbon dioxide the variation in properties with pressure and temperature is far from ideal so one must use real gas, isentropic efficiency, and spatial discretization for heat transfer. Generic characteristic curves for turbomachinery are probably acceptable, and preferably for optimization of a particular design option and choice, real gas, isentropic process, and spatial discretization is more acceptable than any other conditions.

For the purpose of developing a computer code whether steady-state or transient time-dependent mode for turbomachines in the loop, stage-by-stage calculation of characteristic curves for the actual coolant using a line code is most preferable, hence this way one can identify key design parameters for the turbine and compressor necessary to achieve the highest possible state-of-the-art efficiency utilizing the best single or combined cycle (i.e., Rankine, Brayton, or combined). This way it is possible to determine the number of stages, stage diameters, and stage blade heights that are necessary to achieve the desired efficiency as well as how the recuperator or reheating stage can meet that efficiency.

The best way to achieve such a goal from a thermal-hydraulic point of view is to apply dimensional analysis (Zohuri) [36] for all aspects of the coolant fluid by identifying all the nondimensional parameters such as the Reynolds number to

differentiate between laminar and turbulent flow, specific speed ( $N_s$ ), and specific diameter ( $D_s$ ), so a correlation of  $N_s-D_s$  would be possible to determine the number of stages and so forth to meet the highest possible efficiencies.

Some of these parameters and their relationships are identified as follows:

$$N_s = \frac{N \cdot \dot{V}^5}{h^{0.75}}, \quad D_s = \frac{D \cdot h^{0.25}}{\dot{V}^5}, \quad (5.23)$$

where:

$N$  = shaft speed;

$\dot{V}$  = actual volume flow rate measured at each stage of inlet and outlet conditions for compressor and turbine, respectively;

$h$  = isentropic enthalpy change;

$D$  = blade tip diameter.

It should be noted that for the purpose of this analysis involving turbomachinery, including the turbine or compressor, there are several types of efficiencies that are dealt with and discussed in most works in the literature. Two of the most important ones that we need to deal with are the overall *isentropic efficiency*, which refers to the turbomachinery performance, and the other is the polytropic or small-stage efficiency. Any computer code developed around these sorts of numbers should be able to discriminate between these two. For example, if we talk about the pressure ratios of the base design, then an overall compressor efficiency of, say, 85 % corresponds to a polytropic efficiency of 95 %. Another efficiency that we can take into consideration is the total-to-static efficiency between the total inlet state and the static exit state, which is different than the total-to-total efficiency. By using total-to-static efficiencies, turbine and compressor exit losses are accounted for. Consult Balje [37] for a detailed discussion of the different types of turbomachinery efficiencies.

## 5.4 Thermochemical Hydrogen Production

The SI water splitting cycle is a promising candidate for thermochemical hydrogen production. It consists of three chemical reactions that sum up to the processes of water dissociation, as follows:

1.  $H_2SO_4 \rightarrow SO_2 + H_2O + (\frac{1}{2})O_2$ ,
2.  $xI_2 + SO_2 + 2H_2O \rightarrow 2HI_x + H_2SO_4$ ,
3.  $2HI_x \rightarrow xI_2 + H_2$ .

The SI process cycle is divided into three sections and illustrated in Fig. 5.22, as follows:

Recall that according to the basic chemistry of a thermochemical hydrogen generating process, sulfuric acid, when heated to about 830 °C, decomposes into

**Fig. 5.22** Three reactions in sulfur-iodine (SI) process

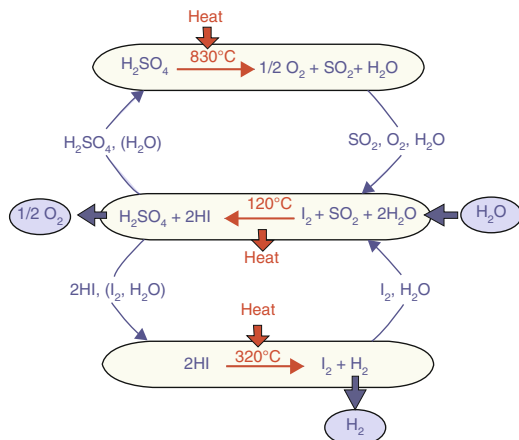
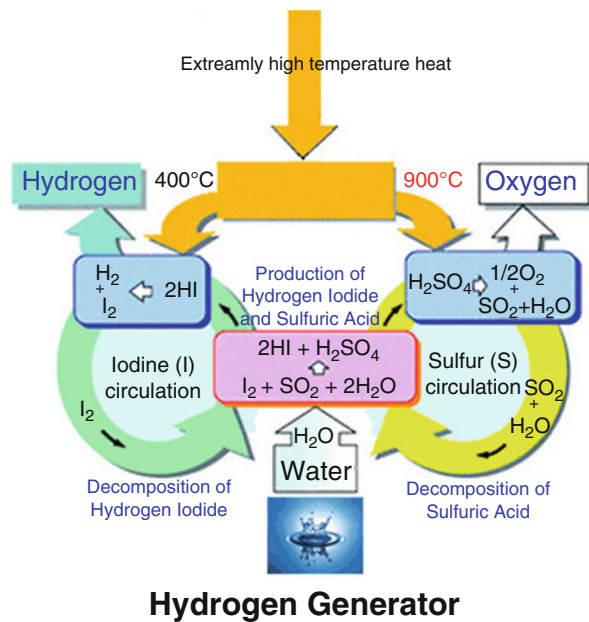


**Fig. 5.23** Chemistry of thermochemical hydrogen generator



water ( $\text{H}_2\text{O}$ ), oxygen ( $\text{O}_2$ ), and sulfur dioxide ( $\text{SO}_2$ ). The oxygen is removed, the  $\text{SO}_2$  and water are cooled, and the sulfur dioxide reacts with water and iodine to form sulfuric acid and hydrogen iodide. The sulfuric acid is separated and removed, and the hydrogen iodide is heated to  $300^\circ\text{C}$ , where it breaks down into hydrogen and iodine. The net result is hydrogen and oxygen produced from water. The hydrogen can be separated and purified. The sulfuric acid and iodine are recycled and used to repeat the process that fits into the aforementioned chemical reaction (Fig. 5.23).

See Oh et al. [1] for a detailed discussion of the different types of thermochemical hydrogen generation coupled with a nuclear reactor.

## 5.5 High-Temperature Electrolysis

A schematic of a nuclear hydrogen plant using HTE is shown in Fig. 5.24. The VHTR supplies thermal energy to drive the PCU and to heat steam for the electrolysis process. The high-temperature heat exchanger supplies superheated steam to the cells at a temperature of approximate 850 °C and a pressure of 5 MPa (725 psi). The input gas contains both steam and hydrogen in order to maintain reducing conditions in the electrolyte conditions.

To deal with this layout and approach to HTE, one needs to model a simulation process based on the reference design of a coupling nuclear reactor with HPP and incorporate many of the systems and components so that the simulator code can eventually handle all aspects of the process, and performance will fairly reflect the eventual best optimum design point for all systems in the plant. The simulation model should ultimately be able to handle every aspect of heat transfer and thermal-hydraulic analysis of plant design based on a dynamic model (i.e., transient analysis) rather than static (i.e., steady state) for its final version.

The HTE process is simpler than the SI cycle from the standpoint of phenomena and flow-sheet complexity. In place of multiple nonlinear chemical equilibrium there is a single chemical reaction involving water and a solid-state electrolyte. While the electrode chemistry may be complex, the integral behavior is relatively simple.

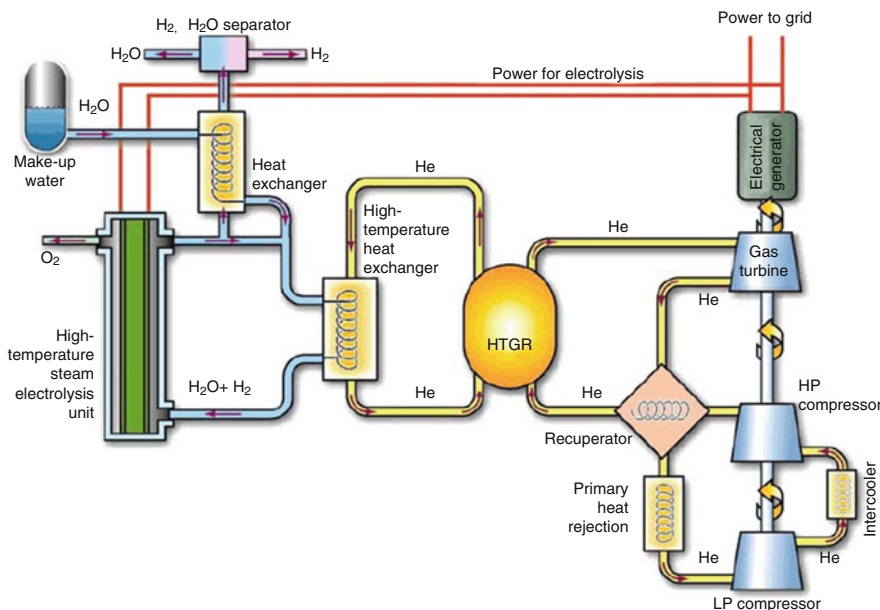


**Fig. 5.24** System coupled with very-high-temperature reactor [1]

The stability of the coupled nuclear and chemical plants will be a factor in how well temperatures can be regulated during load changes or upsets. Some insight into the type of model needed is obtained by examining the phenomena that give rise to dynamic behavior. Mass and energy storage giving rise to large time constants coupled with energy production that is temperature or pressure dependent can potentially create oscillatory behavior [1].

Within the HTE process a significant source of mass and energy to be stored is the subcooled water that undergoes a phase change upstream of the electrolytic cell. Process heat loops from the reactor to the hydrogen plant will have large time constants. Combined with electrolysis, where the rate of electrical energy consumption has a pressure and temperature dependence, there is the potential for oscillatory behavior. A model capable of predicting such behavior is needed to represent these phenomena [1].

## 5.6 System Thermal Transfer for Process Heat Application

Recent interest in new sources of renewable energy, along with technological development associated with the development of Generation IV reactors as steps toward the NGNP, has raised strong interest among scientists, researchers at universities, and industrial communities in collaboration with national laboratories to take advantage of the high temperatures generated by some of these types of nuclear power plants. VHTRs, such as the gas-cooled fast reactor (GFR) or gas-turbine high-temperature reactor (GTHTR) and others, show promise as a source of thermal energy that can be transported via IHXs coupled with HPPs. This will result in the use of the hydrogen produced in industries and emerge as a new source of renewable energy to meet demand during electricity during peak periods, in parallel with the production of the electricity duty required of them.

Process heat is not restricted to hydrogen production but is also envisioned for various other processes, such as the extraction of iron ore, coal gasification, and enhanced oil recovery. To utilize process heat, a thermal device is needed to transfer the thermal energy from the NGNP to the hydrogen plant in the most efficient way possible. However, the existence of these two plants side by side or near each other introduces new safety issues that will require new sets of rules and regulations in accordance with licensing criteria enforced by the relevant regulatory agencies in charge.

A few options are being studied by researchers involved in this area of technology to transfer thermal energy generated by a nuclear reactor of the new type in an efficient way, in particular, in cases where there exists a considerable distance between two plants. One simple option is to use a wiring net between two plants so electrical energy can be transferred from the nuclear to the hydrogen side of a plant

and then convert the electrical energy to heat on the principle of energy conservation in order to produce the required heat source for chemical hydrogen production.

However, this approach is not very cost effective or efficient and results in energy losses of 60–70 % because of the steps involved in converting thermal to electrical energy, even in a manner inherent in the Brayton cycle. Thus we need to look at other options, such as a single-phase forced convection loop where a hot fluid is mechanically pumped between heat exchangers stationed between the nuclear and hydrogen plants. But the transport of these hot fluids and the high-temperature process impose their own unique thermodynamics and physical problems on the basis of both a thermal-hydraulic analysis of thermal energy transport and materials and physical thermal stress imposed on the subsystem and attached components such as piping and pumping elements.

Although single-phase forced convection along with low-pressure helium seems an attractive choice among the options under consideration for NGNPs coupled with HPPs, it suffers from its own deficiency of not being suitable for such facilities simply because low-pressure helium requires higher pumping power, so the process is not cost effective or efficient at producing hydrogen.

A third option could be two-phase heat transfer, where one can take advantage of high-temperature thermosyphon conditions where thermal energy transport takes place between evaporator and condenser via evaporation and condensation processes and the influence of gravity causes the circulation of fluid between two elements. Heat pipe devices are a very good example of such a process. They are considered a passive system requiring no mechanical pumping in thermal energy transport [38].

Thermosyphon devices have the capability to transport very large amounts of heat in virtually isothermal conditions with a minimum loss of heat at high rates over considerable distances in a passive mode, without any requirement for external pumping devices. As discussed earlier as part of the licensing constraints for safety, a proper distance must be maintained between the nuclear power plant and HPP, and heat pipes and thermosyphons would easily satisfy this requirement in a very cost-effective and efficient way. For a discussion of the design and a further understanding of such devices, the reader may consult Zohuri [38].

A simple schematic of a heat pipe and a controllable thermosyphon device are depicted in Figs. 5.25 and 5.26.

In both devices the heat input governs the rate of evaporation within the evaporator and consequently the rate of heat transfer in them. The shape and form of the condenser (variable or fixed type) can regulate the rate of condensation and the rate of thermal energy, and heat transfer exchange can be controlled over a spectrum of conditions from “off-mode” to “fully on” situations, hence the term controllable heat pipe or thermosyphon stick.

The choice of working fluid as a form of thermal energy transport depends on the temperature and pressure of operation; hence a favorable working fluid can be identified. For example, mercury or any alkaline metal may be suitable choices for handling the process heat transfer duty in these devices, simply because they have the following physical and chemical characteristics:

**Fig. 5.25** Schematic of simple heat pipe device (Zohuri) [38]

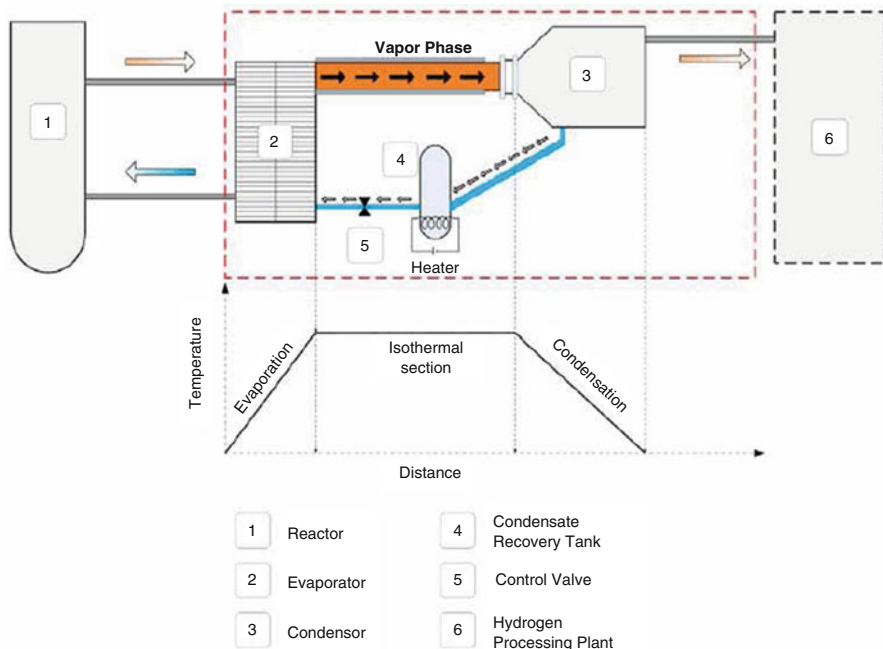
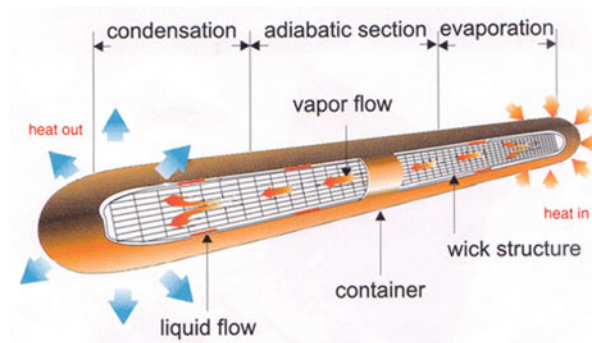


**Fig. 5.26** Schematic of simple controllable thermosyphon (Sabharwall and Kim) [30]

- High boiling temperature,
- Availability and cost effectiveness,
- Good heat transfer properties (latent and specific heat are both high),
- Typically good chemical compatibility (except Li).

More suitable working fluids than alkali metals may exist, such as molten salts (Sohal et al.) [39]. Corrosive behavior at high temperatures or lack of high-temperature thermodynamic properties, especially for superheated vapors, rule out fundamental analysis of many possible thermosyphon working fluids.

## 5.7 System Stress Analysis Model

A simplified version of stress analysis was presented in Sect. 3.9 of Chap. 3 in this book for different components in various configurations. The analysis determined the thickness required so that the circumferential stress is less than or equal to an assumed allowable value for a base design. The use of consistent stresses will allow identification of limiting components. A fair comparison between different configurations and further information can be found in Davis [23] and Diehl and Bodman [40].

## 5.8 System Cost Analysis Model

Earlier in this chapter a cost analysis was discussed with respect to IHXs and other major systems in plant and facilities of NGNPs driving hydrogen generating plants. But one needs to develop a model that can deal with capital costs and component costs of design configurations and be able to determine a so-called true cost for an actual production plant.

This model should also be able to handle all the steps of design and the collection of all categories for various major components and systems that would be interoperable with the rest of the modeling that would be responsible for dynamically handling, for example, heat transfer and thermal-hydraulic analysis or efficiency optimization for turbomachinery and their operational performance during on- or off-peak periods. An online search will identify many open sources with respect to this matter, in particular articles published by NRC, DOE, and the International Atomic Energy Agency (IAEA) as posted on their Web sites.

## 5.9 Verification and Validation Model

Many people many countries around the globe and here in the USA are involved in the effort to create a common NHDD project, and they are all pushing for common ground for modeling a cost-effective and efficient method of producing hydrogen via NGNPs, either as a new source of renewable energy or for transportation in the form of fuel cells in the near future. Some of these efforts are being led by countries like Japan under the Japan Hydrogen and Fuel Cell project, which is a program led by their Ministry of Economy, or the Republic of Korea as part of its Ministry of Science Technology (MOST). Thus, there exists huge momentum behind the commercialization of fuel cells as a path to hydrogen production, and it is an inexorable trend.

Any effort toward the commercialization of the next generation of nuclear power plants to drive the production of hydrogen goes beyond just the pure R&D of such

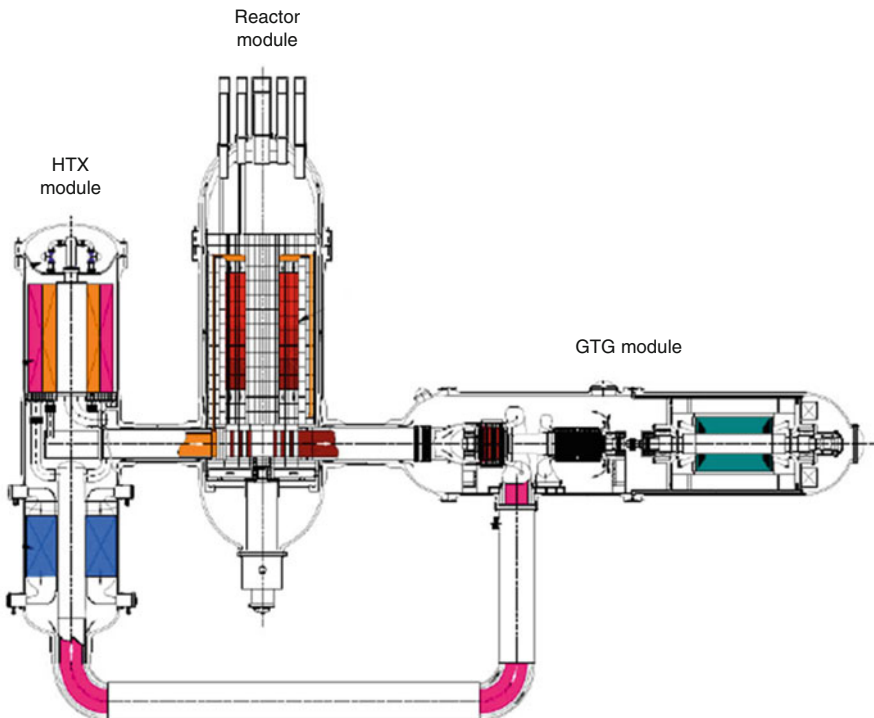


**Fig. 5.27** GTHTR 300 reactor and power conversion system [1]

facilities. Also essential is the verification and validation (V&V) of the developed plants to assure their operation, safety, and efficiency. Providing a model for such a V&V process becomes more and more a matter of verifying and validating numerical tools, following design cases. One candidate for the V&V is the GTHTR 300 design as part of the NGNP proposed by Yen et al. [41], who take into account the cost and performance design for a power conversion system using this particular reactor.

Their verification and validation of the GTHTR 300 is based on a direct-cycle gas-cooled reactor that incorporates a distributed power conversion system with horizontal turbomachinery such as a turbine, compressor, and pumping as well as heat exchangers located in separate housing vessels that are needed to couple with the hydrogen generating plant. Such a top-level configuration is illustrated in Fig. 5.27.

Figure 5.28 shows a schematic of the GTHTR 300 reactor, and Fig. 5.29 shows the cycle efficiency calculated a design value and a range of parameters that were varied.

In addition to the previously described V&V, the discharge temperature from the expander and compressor based on analysis and calculations could be compared with the pressure-enthalpy ( $P-h$ ) diagram presented in Figs. 5.13 and 5.14 (Oh et al.) [1].

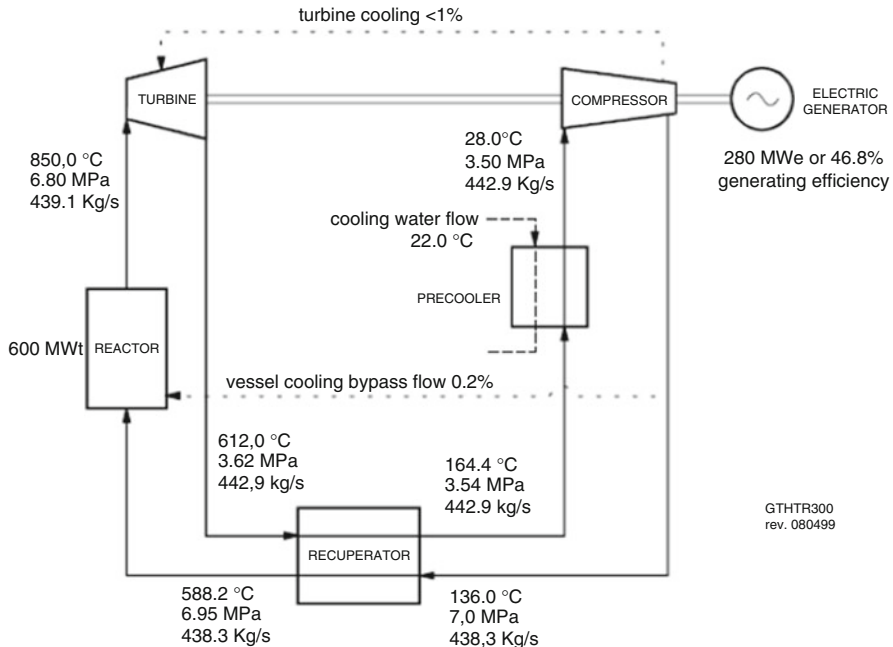
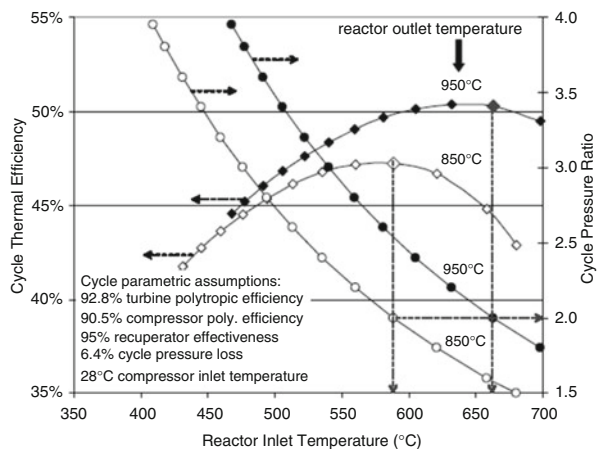


**Fig. 5.28** Schematic of GTHTR 300 design [1]

**Fig. 5.29** Cycle efficiency as a function of reactor inlet temperature [1]



## 5.10 System Integration

Last but not least is the task of integrating all the major elements of a facility for production purposes, which would be the coupling of the VHTR, PCU, and HPP through the intermediate heat transfer loop (IHETL). This integration would call for

Activity Description	Year 1	Year 2	Year 3
Formulation of modular program structure	→		
Basic equation setup	→		
TH property routine setup	→		
Numerical scheme setup	→		
Component model development		→	
Code Verification & Validation		→	
Cost model development		→	
Optimization scheme development		→	
Sample application to NHDD		→	→
Final Report			→

**Fig. 5.30** Illustration of top-level project plan

a proper project plan to monitor and control all the planning from concept to R&D, manufacture of a subsystem and prototype of a conceptual reference design as well as V&V steps to make sure all the components and subsystems are able to perform to the expected base design parameters and, consequently, go to full commercial production plant.

The project plant should be able to measure all the steps of progress through either a bar chart or a Gantt chart, along with the monitoring of budgets and resources allocated to such projects, along with a measurement of milestones to make sure the project is on time and within budget through its timeline functionality. A top-level project plan for a 3 year plan is illustrated in Fig. 5.30.

## References

1. Oh, C. H., Davis, C. B., Sherman, S. R., Vilim, R., Lee, Y. J., & Lee, W. J. (2006). *Development of HyPEP, A hydrogen production plant efficiency calculation program*. Idaho Falls, ID: Idaho National Laboratory.
2. Holcomb, D. E., Cetiner, S. M., Flanagan, G. F., Pertz, F. J., & Yoder, G. L. (2009). An analysis of testing requirements for fluoride salt-cooled high temperature reactor components. ORNL/TM-2009/297, November 2009.
3. Zohuri, B., McDaniel, P. J., & de Oliveira, C. (2014). Air Brayton cycles for nuclear power plants. Submitted for Review.
4. Zohuri, B., McDaniel, P. J., & de Oliveira, C. (2014). A comparison of a recuperated open cycle (Air) Brayton power conversion system with the traditional steam Rankine cycle for the next generation nuclear power plant. *ANS Transactions*, Reno, Nevada, June, 2014.
5. McDaniel, P. J., Zohuri, B., & de Oliveira, C. (2014). A combined cycle power conversion system for small modular LMFBRs. *ANS Transactions*, Anaheim, California, November, 2014.
6. McDaniel, P. J., Zohuri, B., de Oliveira, C., & Cole, J. (2012). A combined cycle power conversion system for the next generation nuclear power plant. *ANS Transactions*, San Diego, California, November, 2012.
7. Zohuri, B. (2015). *Combined cycle driven efficiency for next generation nuclear power plants: An innovative design approach*. Heidelberg: Springer.

8. Zohuri, B. (2014). *Innovative open air Brayton combined cycle systems for the next generation nuclear power plants*. Albuquerque, NM: University of New Mexico Publications.
9. Forsberg, C., McDaniel, P., & Zohuri, B. (2015). Variable electricity and steam from salt, helium, and sodium cooled base-load reactors with gas turbines and heat storage. Proceedings of ICAPP 2015 May 03-06, 2015, Nice, France. Paper 15115.
10. Jones, C., & Jacob, J., III. (2000). *Economic and technical considerations for combined-cycle performance-enhancement options*. GER-4200. Schenectady, NY: GE Power Systems.
11. Davis, C. B., Barner, R. B., Sherman, S. R., & Wilson, D. F. (2005). Thermal-hydraulic analyses of heat transfer fluid requirements and characteristics for coupling a hydrogen product plant to a high-temperature nuclear reactor. INL/EXT-05-00453, June 2005.
12. Brown, L. C., Besenbruch, G. E., Lentsch, R. D., Schultz, K. R., Funk, J. F., Pickard, P. S., Marshall, A. C., & Showalter, S. K. (2003). High efficiency generation of hydrogen fuels using nuclear power. Final technical report for the period August 1, 1999 through September, 30, 2002, GA-A24285, June 2003.
13. Zohuri, B., & McDaniel, P. (2015). *Thermodynamics in nuclear power plant*. Heidelberg: Springer.
14. ANLW. (2004). Reactor/process interface requirements. ANL W7500-0001-ES-00, Revision 0, July.
15. Independent Technology Review Group. (2004). Design features and technology uncertainties for the next generation nuclear plant. INEEL/EXT-04-01816, June.
16. Sabharwall, P., Kim, E. S., McKellar, M., Anderson, N., & Patterson, M. (2011). Process heat exchanger options for the advanced high temperature reactor. Report INL/EXT-11-21584 Revision 1, Idaho National Laboratory, June 2011.
17. Saravanamuttoo, H. I. H., Rogers, G. F. C., Cohen, H., & Straznicky, P. (2008). *Gas turbine theory* (6th ed.). Harlow: Pearson Publisher Company.
18. Moran, M. J., & Shapiro, H. N. (2010). *Fundamentals of engineering thermodynamics* (7th ed.). New York: Wiley.
19. GPSA (Gas Processors Suppliers Association). (1998). *Engineering data book* (11th ed.). Tulsa, OK: GPSA.
20. Kim, E. S., Sabharwall, P., & Anderson, N. (2011). Development of figure of merits (FOMs) for intermediate coolant characterization and selection. *ANS Annual Meeting*, Hollywood Florida, USA, June 25–30, 2011.
21. Shah, R. K., & Sekulic, S. P. (2003). *Fundamentals of heat exchanger design*. New York: John Wiley and Sons.
22. Kakac, S., & Liu, H. (2002). *Heat exchangers: Selection, rating and thermal design* (2nd ed.). Boca Raton, FL: CRC Press. ISBN 0849309026.
23. Davis, C. B. (2005). Analysis methods and desired outcomes of system interface heat transfer fluid requirements and characteristics analyses. Idaho National Laboratory Report INL/EXT-05-00228, April 2005.
24. Davis, C. B., Oh, C. H., Barner, R. B., & Wilson, D. F. (2005). Thermal-hydraulic analyses of heat transfer fluid requirements and characteristics for coupling a hydrogen production plant to a high-temperature nuclear reactor. INL/EXT-05-00453, June 2005.
25. Lillo, T. M., Williamson, R. L., Reed, T. R., Davis, C. B., & Ginosar, D. M. (2005). Engineering analysis of intermediate loop and process heat exchanger requirements to include configuration analysis and materials needs. Idaho National Laboratory Report INL/EXT-05-00690, September 2005.
26. Sundén, B. (2005). High temperature heat exchangers (HTHE). *Proceedings of Fifth International conference on Enhanced, Compact and Ultra-Compact Heat Exchangers: Science, Engineering and Technology*, Hoboken, NJ, USA, September 2005.
27. Ohadi, M. M., & Buckley, S. G. (2001). High temperature heat exchangers and microscale combustion systems: Applications to thermal system miniaturization. *Experimental Thermal and Fluid Science*, 25, 207–217.

28. Brent, A. (1989). *Fundamentals of composites manufacturing materials methods and applications*. Dearborn, MI: SME.
29. Dewson, S., & Li, X. (2005). Selection criteria for the high temperature reactor intermediate heat exchanger. Proceedings of ICAPP'05, Seoul, Korea, May 15–19, 2005.
30. P. Sabharwall, and E. S. Kim. (2011). High temperature thermal devices for nuclear process heat transfer applications, developments in heat transfer, Dr. Marco Aurelio Dos Santos Bernardes (Ed.), Rijeka, Croatia: InTech, ISBN: 978-953-307-569-3. Available from: <http://www.intechopen.com/books/developments-in-heattransfer/high-temperature-thermal-devices-for-nuclear-process-heat-transfer-applications>
31. Zohuri, B. (2016). *Application of compact heat exchanger for combined cycle driven efficiency in next generation of nuclear power plants a novel approach*. New York: Springer.
32. Schlenker, H. V. (1974). Cost functions for HTR-direct-cycle components. *Atomkenergie (ATKE)*, 22(4), 226–235.
33. Wang, C. (2003). Design, analysis and optimization of the power conversion system for the modular pebble bed reactor system. Ph.D. Thesis, MIT Nuclear Engineering Dept., Aug. 2003.
34. Dostal, V., Driscoll, M. J., & Hejzlar, P. (2004). A supercritical carbon dioxide cycle for next generation nuclear reactors. MIT-ANP-TR-100, March 10, 2004.
35. ESDU. (1994). *Selection and costing of heat exchangers. Engineering science data. Item 92013*. London: ESDU, Int.
36. Zohuri, B. (2015). *Dimensional analysis and self-similarity methods for engineering and scientist*. New York: Springer.
37. Balje, O. E. (1981). *Turbomachines: A guide to design, selection and theory* (1st ed.). New York: John Wiley & Sons.
38. Zohuri, B. (2011). *Heat pipe design and technology: A practical approach*. Boca Raton, FL: CRC Press.
39. Sohal, M., Ebner, M., Sabharwall, P., & Sharpe, P. (2010). Engineering database of liquid salt thermo-physical and thermo-chemical properties. INL/EXT-10-18297, Idaho National Laboratory, Idaho, March 2010.
40. Diehl, H., & Bodman, E. (1990). Alloy 800 specifications in compliance with component requirements. *Journal of Nuclear Materials*, 171, 63–70.
41. Yan, X., et al. (2003). Cost and performance design approach for GT-HTR300 power conversion system. *Nuclear Engineering and Design*, 226, 351–373.
42. Dewson, S. J., & Thonon, B. (2003). The development of high efficiency heat exchangers for helium gas cooled reactors, Paper 3213, ICAPP03.

# **Chapter 6**

## **Heat Exchangers**

A number of technologies are being investigated for the Next Generation Nuclear Plant (NGNP) that will produce heated fluids at significantly higher temperatures than current-generation power plants. The higher temperatures offer the opportunity to significantly improve the thermodynamic efficiency of the energy conversion cycle. One of the concepts currently under study is the molten salt reactor. The coolant from a molten salt reactor may be available at temperatures as high as 800–1000 °C. At these temperatures, an open Brayton cycle combined with a Rankine bottoming cycle appears to have some strong advantages. Thermodynamic efficiencies approaching 50 % appear possible. Requirements for circulating cooling water will be significantly reduced. However, to realistically estimate the efficiencies achievable, it is essential to have good models for the heat exchangers involved as well as the appropriate turbomachinery. This study concentrates on modeling all power conversion equipment from the fluid exiting the reactor to the energy released to the environment.

### **6.1 Heat Exchanger Types**

A heat exchanger is a heat-transfer device that exchanges heat between two or more process fluids. Heat exchangers have widespread industrial and domestic applications. Many types of heat exchanger have been developed for use in steam power plants, chemical processing plants, building heat and air conditioning systems, transportation power systems, and refrigeration units.

The actual design of heat exchangers is a complicated problem. It involves more than heat-transfer analysis alone. The cost of fabrication and installation, weight, and size play important roles in the selection of the final design from a total cost of ownership point of view. In many cases, although cost is an important consideration, size and footprint often tend to be the dominant factors in choosing a design.

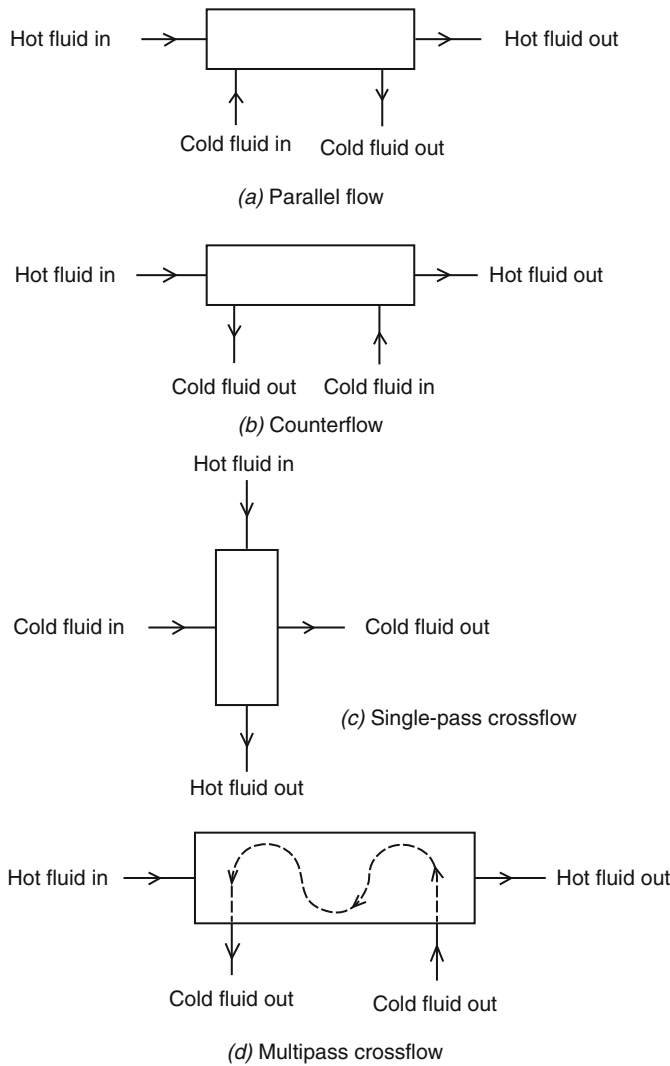


**Fig. 6.1** Types of flow path configuration through heat exchanger

Most heat exchangers may be classified as one of several basic types. The four most common types, based on flow-path configuration, are illustrated in Fig. 6.1 below [1].

1. In *concurrent*, or *parallel-flow*, units the two fluid streams enter together at one end, flow through in the same direction, and leave together at the other end.
2. In *countercurrent*, or *counterflow*, units the two streams move in opposite directions.

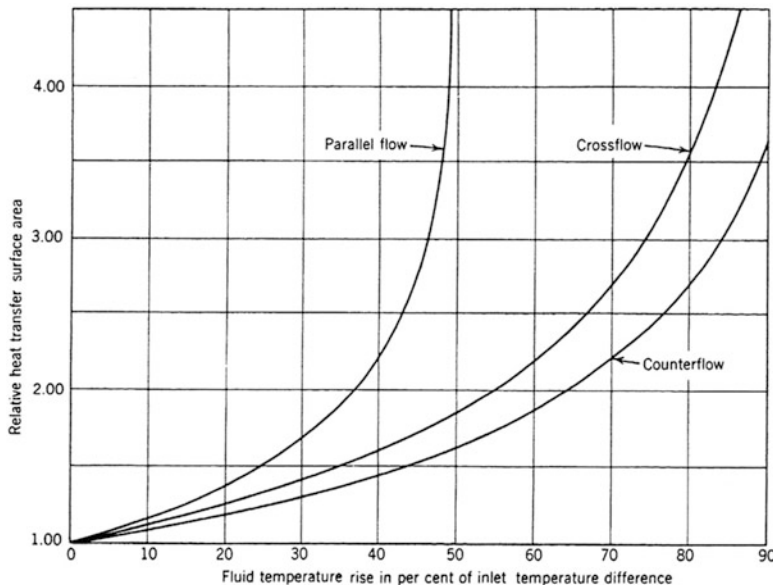


**Fig. 6.2** Required relative heat-transfer surface area as a function of the ratio of the temperature rise (or drop) in the fluid stream having a greater change in temperature than the difference in temperature between the inlet streams

3. In *single-pass, cross-flow* units one fluid moves through the heat-transfer matrix at right angles to the flow path of the other fluid.
4. In *multipass cross-flow* units one fluid stream shuttles back and forth across the flow path of the other fluid stream, usually giving a cross-flow approximation to the counterflow.

The most important difference between these four basic types of heat exchanger lies in the relative amounts of heat-transfer surface area required to transfer the desired amount of heat between the two fluids.

Figure 6.2 below shows the relative area required for each type as a function of the change in temperature of the fluid with the largest temperature change requirement for a typical set of conditions. In the region in which the fluid temperature change across the heat exchanger is a small percentage of the difference in temperature between the two entering fluid streams, all the units require roughly the same area. The parallel-flow heat exchanger is of interest primarily for applications in this region. Cross-flow units have a somewhat broader range of application and are particularly suited to some types of heat-exchanger construction that have special advantages. The counterflow heat exchanger requires the least area. Furthermore, it is the only type that can be employed in regions where the temperature change in one or both of the fluid streams closely approaches the temperature difference between the entering fluid streams.

In addition, heat exchangers may be classified as direct contact or indirect contact. In the direct-contact type, heat transfer takes place between two immiscible fluids, such as a gas and a liquid, coming into direct contact. For example, cooling towers, jet condensers for water vapor, and other vapors utilizing water spray are typical examples of direct-contact exchangers.

***Immiscible fluids are incapable of being mixed or blended together. Immiscible liquids that are shaken together eventually separate into layers. Oil and water are typical immiscible fluids.***

In the indirect-contact type of heat exchanger, such as automobile radiators, the hot and cold fluids are separated by an impervious surface, and they are referred to as *surface heat exchangers*. There is no mixing of the two fluids.

## 6.2 Classification According to Transfer Processes

Heat exchangers are classified according to transfer processes into indirect- and direct-contact types.

### 6.2.1 *Indirect-Contact Heat Exchangers*

In an indirect-contact heat exchanger, the fluid streams remain separate and the heat transfers continuously through an impervious dividing wall or into and out of a wall in a transient manner. Thus, ideally, there is no direct contact between thermally interacting fluids. This type of heat exchanger is also referred to as a surface heat exchanger and can be further classified into direct-transfer type, storage type, and fluidized-bed exchangers.

### 6.2.2 *Direct-Contact Heat Exchangers*

In this type, heat transfers continuously from the hot fluid to the cold fluid through a dividing wall. Although a simultaneous flow of two (or more) fluids is required in the exchanger, there is no direct mixing of the two (or more) fluids because each fluid flows in separate fluid passages. In general, there are no moving parts in most such heat exchangers. This type of exchanger is known as a recuperative heat exchanger or, simply, a recuperator. Some examples of direct-transfer heat exchangers are tubular, plate-type, and extended-surface exchangers.

Note that the term *recuperator* is not commonly used in the process industry for shell-and-tube and plate heat exchangers, although they are also considered recuperators. Recuperators are further subclassified as prime surface exchangers

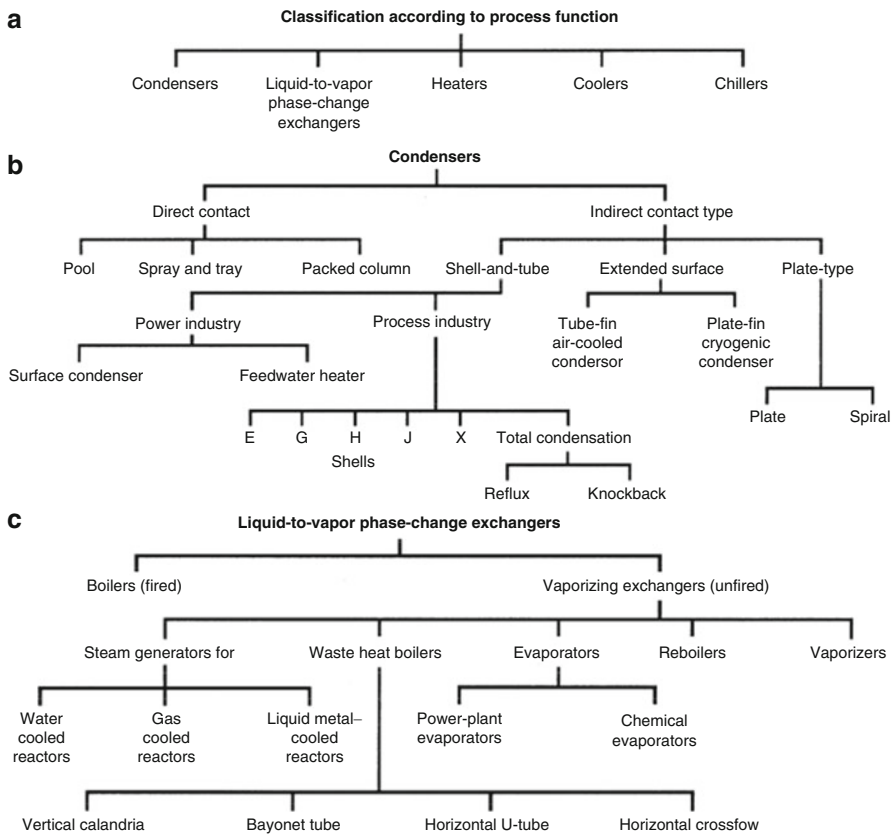


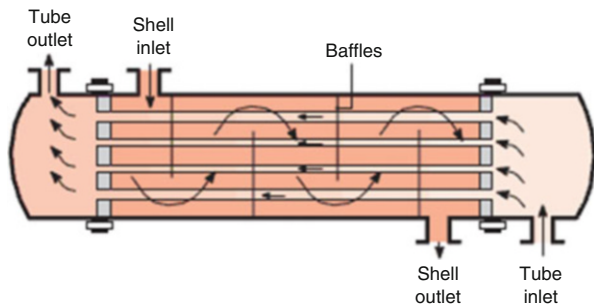
**Fig. 6.3 (a)** Classification according to process function; **(b)** classification of condensers; **(c)** classification of liquid-to-vapor phase-change exchangers

and extended-surface exchangers. Prime surface exchangers do not employ fins or extended surfaces on any fluid side. Plain tubular exchangers, shell-and-tube exchangers with plain tubes, and plate exchangers are good examples of prime surface exchangers. Recuperators constitute the vast majority of all heat exchangers (Fig. 6.3).

## 6.3 Classification of Heat Exchanger by Construction Type

Heat exchangers can also be classified according to their construction features. For example, there are tubular, plate, plate-fin, tube-fin, and regenerative exchangers. An important performance factor for all heat exchangers is the amount of heat-transfer surface area within the volume of the heat exchanger. This is called its *compactness factor* and is measured in square meters per cubic meter.

**Fig. 6.4** A shell-and-tube heat exchanger; one shell pass and one tube pass [2]



### 6.3.1 Tubular Heat Exchangers

Tubular exchangers are widely used and are manufactured in many sizes, flow arrangements, and types. They can accommodate a wide range of operating pressures and temperatures. The ease of manufacture and their relatively low cost have been the principal reasons for their widespread use in engineering applications. A commonly used design, called the *shell-and-tube* exchanger, consists of round tubes mounted on a cylindrical shell with their axes parallel to that of the shell.

Figure 6.4 illustrates the main features of a shell-and-tube exchanger having one fluid flowing inside the tubes and the other flowing outside the tubes. The principal components of this type of heat exchanger are the tube bundle, shell, front and rear end headers, and baffles. The baffles are used to support the tubes, to direct the fluid flow approximately normal to the tubes, and to increase the turbulence of the shell fluid. There are various types of baffles, and the choice of baffle type, spacing, and geometry depends on the flow-rate-allowable shell-side pressure drop, tube support requirement, and flow-induced vibrations. Many variations of the shell-and-tube exchanger are available; the differences lie in the arrangement of flow configurations and in the details of construction.

Baffled heat exchangers with one shell pass and two tube passes and with two shell passes and four tube passes are shown in Fig. 6.5a, b, respectively [3].

The character of the fluids may be *liquid-to-liquid*, *liquid-to-gas*, or *gas-to-gas*. Liquid-to-liquid exchangers have the most common applications. Both fluids are pumped through the exchangers; hence, the heat transfer on both the tube side and the shell side is by forced convection. Since the heat-transfer coefficient is high with the liquid flow, generally there is no need to use fins [2].

The liquid-to-gas arrangement is also commonly used; in such cases, the fins are usually added on the gas side of the tubes, where the heat-transfer coefficient is low.

Gas-to-gas exchangers are used in exhaust-gas and air-preheating recuperators for gas gas-turbine systems, cryogenic gas-liquefaction systems, and steel furnaces. Internal and external fins generally are used in the tubes to enhance heat transfer.

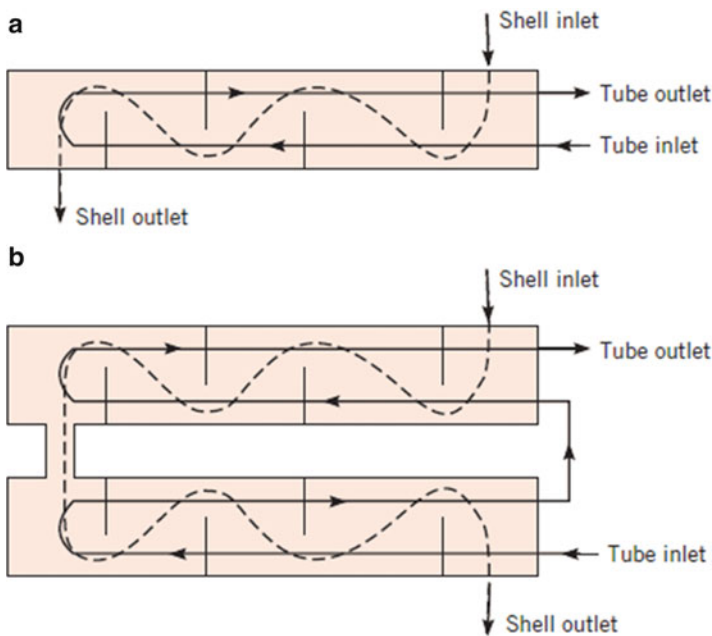


**Fig. 6.5** Shell-and-tube heat exchangers. (a) One shell pass and two tube passes. (b) Two shell passes and four tube passes [3]

### 6.3.2 Plate Heat Exchangers

As the name implies, plate heat exchangers usually are constructed of thin plates. The plates may be smooth or have some form of corrugation. Since the plate geometry cannot accommodate as high pressure or temperature differentials as a circular tube, this type of exchanger is generally designated for moderate temperature or pressure differentials of the compactness factor for plate exchangers ranges from about  $120\text{--}230 \text{ m}^2/\text{m}^3$ .

### 6.3.3 Plate-Fin Heat Exchangers

The compactness factor can be significantly improved (i.e., up to about  $6000 \text{ m}^2/\text{m}^3$ ) by using the plate-fin type of heat exchanger. Figure 6.6 illustrates typical plate-fin configurations. Flat plates separate louvered or corrugated fins. Cross-flow, counterflow, or parallel-flow arrangements can be obtained readily by properly arranging the fins on each side of the plate. Plate-fin exchangers are generally used for gas-to-gas applications, but they are used for low-pressure applications not exceeding about 10 atm. (that is, 1000 kPa). The maximum operating temperatures are limited to about  $800^\circ\text{C}$ . Plate-fin heat exchangers have also been used for cryogenic applications.

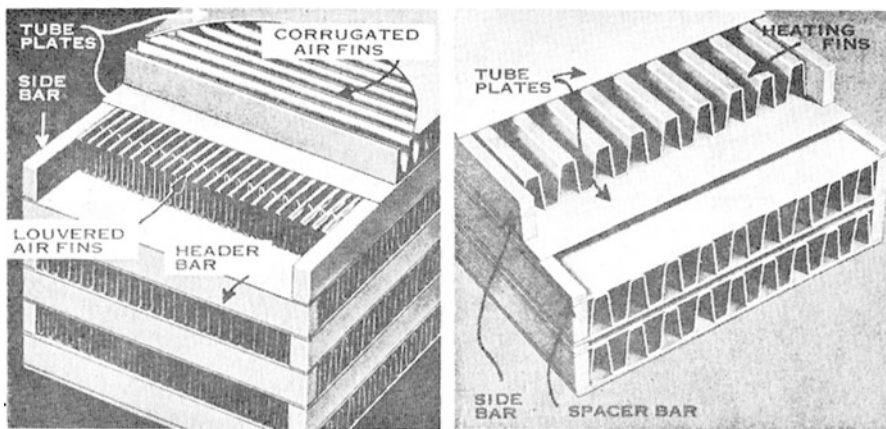


**Fig. 6.6** Plate-fin heat exchangers (courtesy Harrison Radiator Division of General Motors Corporation)

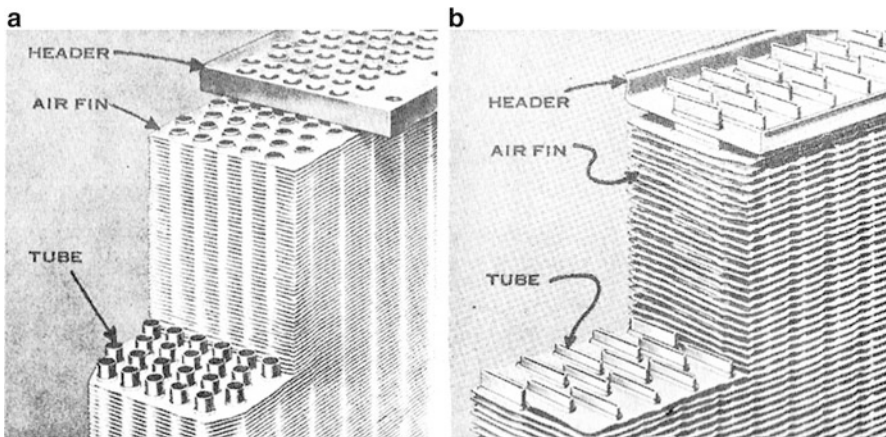


**Fig. 6.7** Tube-fin heat exchangers. (a) Round tube and fin. (b) Flat tube and fin (courtesy Harrison Radiator Division of General Motors Corporation)

### 6.3.4 *Tube-Fin Heat Exchangers*

When a high operating pressure or an extended surface is needed on one side, tube-fin exchangers are used. Figure 6.7 illustrates two typical configurations, one with round tubes and the other with flat tubes. Tube-fin exchangers can be used for a wide range of tube fluid operating pressures not exceeding about 30 atm and operating temperatures from low cryogenic applications to about 870 °C. The maximum compactness ratio is somewhat less than that obtainable with plate-fin exchangers.

Tube-fin heat exchangers are used in gas-turbine, nuclear, fuel cell, automobile, airplane, heat pump, refrigeration, electronics, cryogenics, air conditioning, and many other applications.

### 6.3.5 Regenerative Heat Exchangers

Regenerative heat exchangers use a heat-transfer matrix that is heated by one fluid and then cooled by a second fluid. The flow over the matrix is switched as a function of time, with both fluids flowing over the same surfaces of the matrix. They have seen little use in fixed station power plants and will not be emphasized here.

## 6.4 Condensers

Condensers are used for such varied applications as steam power plants, chemical processing plants, and nuclear electric plants for space vehicles. The major types include the *surface condensers*, *jet condensers*, and *evaporative condensers*. The most common type is the surface condenser, which has a feedwater system [5]. Figure 6.8 shows a section through a typical two-pass surface condenser for a large steam turbine

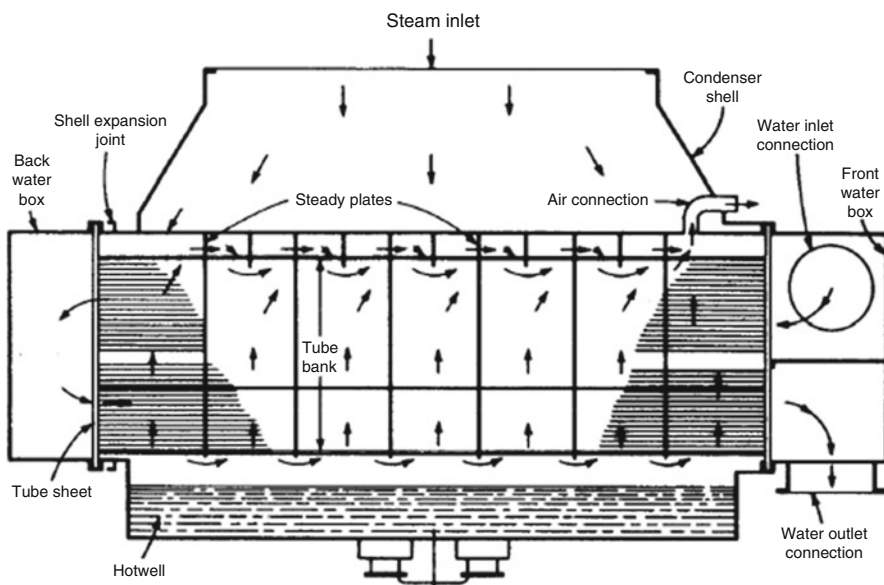


**Fig. 6.8** Section through a typical two-pass surface condenser for a large plant (courtesy Allis-Chalmers Manufacturing Company)

in a power plant. Since the steam pressure at the turbine exit is only 1.0–2.0 in Hg absolute, the steam density is very low and the volume rate of flow is extremely large. To minimize the pressure loss in transferring steam from the turbine to the condenser, the condenser is normally mounted beneath and attached to the turbine. Cooling water flows horizontally inside the tubes, while the steam flows vertically downward from the large opening at the top and passes transversely over the tubes. Note that provision is made to aspirate cool air from the regions just above the center of the hot well. This is important because the presence of noncondensable gas in the steam reduces the heat-transfer coefficient for condensation.

## 6.5 Boilers

Steam boilers are one of the earliest applications of heat exchangers. The term *steam generator* is often applied to boilers in which the heat source is a hot fluid stream rather than the products of combustion.

An enormous variety of boiler types exist, ranging from small units for house heating applications to huge, complex, expensive units for modern power stations.

## 6.6 Classification According to Compactness

The ratio of the heat-transfer surface area on one side of the heat exchanger to the volume can be used as a measure of the compactness of a heat exchanger. A heat exchanger having a surface area density on any one side greater than around  $700 \text{ m}^2/\text{m}^3$  quite arbitrarily is referred to as a compact heat exchanger regardless of its structural design. For example, automobile radiators having an area density of approximately  $1100 \text{ m}^2/\text{m}^3$  and the glass ceramic heat exchangers for some vehicular gas-turbine engines having an area density of approximately  $6600 \text{ m}^2/\text{m}^3$  are compact heat exchangers. The human lungs, with an area density of about  $20,000 \text{ m}^2/\text{m}^3$ , are the most compact heat-and-mass exchangers. The very fine matrix regenerator for the Stirling engine has an area density approaching that of the human lung.

On the other extreme of the compactness scale, plane tubular and shell-and-tube type exchangers, having an area density in the range of  $70\text{--}500 \text{ m}^2/\text{m}^3$ , are not considered compact [2].

The incentive for using compact heat exchangers lies in the fact that a high value of compactness reduces the volume for a specified heat exchanger performance.

When heat exchangers are to be employed for automobiles, marine uses, aircraft, aerospace vehicles, cryogenic systems, and refrigeration and air conditioning, the weight and size – hence the compactness – become important. To increase the

effectiveness or the compactness of heat exchangers, fins are used. In a gas-to-liquid heat exchanger, for example, the heat-transfer coefficient on the gas side is an order of magnitude lower than for the liquid side. Therefore, fins are used on the gas side to obtain a balanced design; the heat-transfer surface on the gas side becomes much more compact.

## 6.7 Types of Applications

Heat exchangers are often classified based on the application for which they are intended, and special terms are employed for major types. These terms include *boiler, steam generator, condenser, radiator, evaporator, cooling tower, regenerator, recuperator, heater, and cooler*. The specialized requirements of the various applications have led to the development of many types of construction, some of which are unique to particular applications [4].

## 6.8 Cooling Towers

In locations where the supply of water is limited, heat may be released into the atmosphere very effectively by means of cooling towers such as that Fig. 6.9a–c here. A fraction of the water sprayed into these towers evaporates, cooling the balance. Because of the high heat of vaporization of water, the water consumption

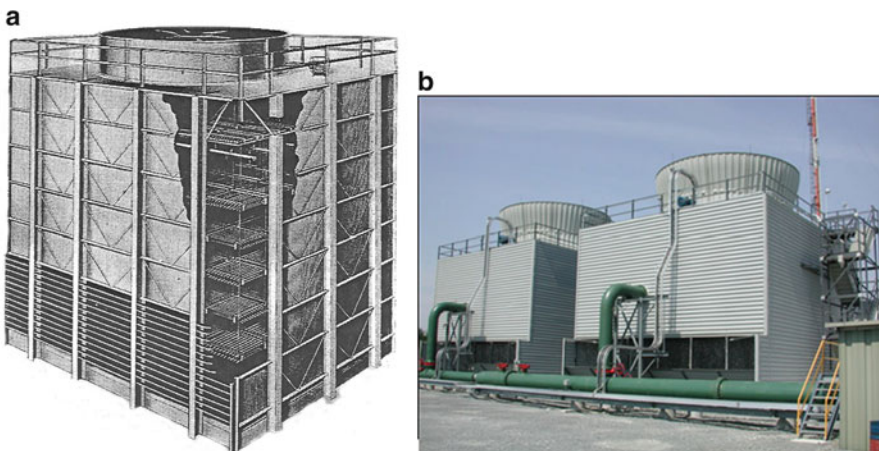


**Fig. 6.9** (a) Vertical induced draft-cooling tower (courtesy Foster Wheeler Corp.) [1]. (b) Schematic of cooling tower. (c) Forced convection cooling tower with draft induced by a fan [1]

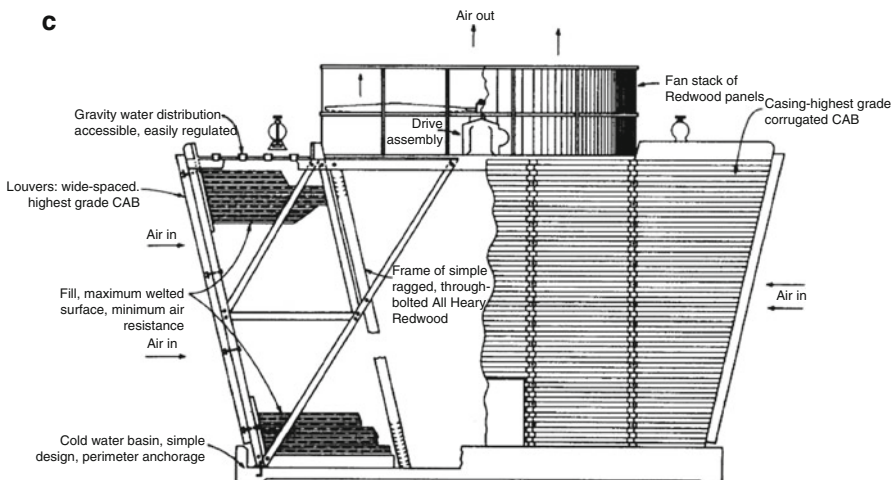


**Fig. 6.9 (continued)**

is only about 1 % as much as would be the case if water were taken from a lake or a stream and heated 10 or 20 °F.

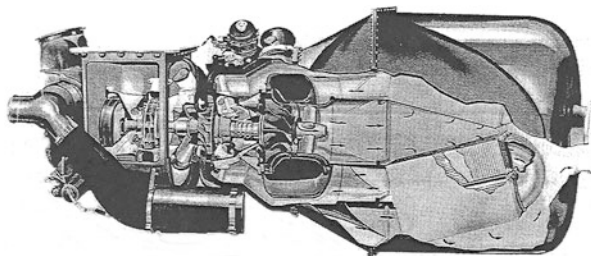
Cooling towers may be designed so that the air moves through them by thermal convection, or fans may be employed to provide forced air circulation. To avoid contamination of the process water, shell-and-tube heat exchangers are sometimes employed to transmit heat from the process water to the water recirculated through the cooling tower.

## 6.9 Regenerators and Recuperators

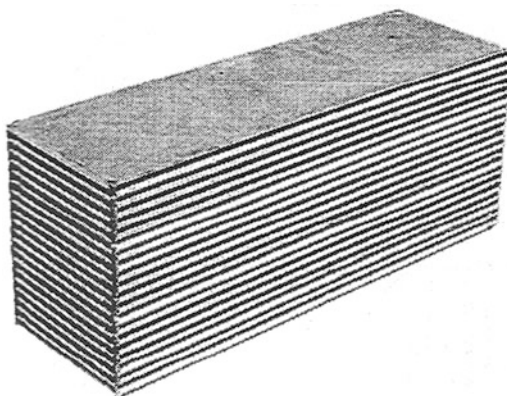
The thermal efficiency of gas-turbine power plants can be greatly increased if heat can be extracted from the hot gases that are leaving the gas turbine and added to the air being supplied to the combustion chamber. For a major gain in thermal efficiency, it is necessary to employ a very large amount of heat-transfer surface area. This is particularly noticeable in gas-turbine plants, where even with counterflow the size of the heat exchanger required for good performance tends to be large compared to the size of the turbine and compressor. This characteristic can be observed even in a small, portable gas turbine [about 3 ft (0.91 m) in diameter] shown in Fig. 6.10. Note that in this device the hot combination gases leave the radial in-flow turbine wheel at the right end of the shaft and enter a set of heat exchanger cores arranged in parallel around the central axis.

Figure 6.10 shows a close-up view of one of these cores. In each core, the hot gases from the turbine flow roughly radially outward through one set of gas passages. Air from the centrifugal compressor wheel, which is at the center of the

**Fig. 6.10** A small gas-turbine power plant fitted with a recuperator to improve the fuel economy (courtesy of AiResearch Manufacturing Company) [4]



**Fig. 6.11** A brazed plate-fin recuperator core for the gas turbine of Fig. 6.9 (courtesy of AiResearch Manufacturing) [4]



shaft, flows to the right through the space just inside the outer casing and axially into the other set of gas passages through the core. The air being heated makes two passes, flowing first to the right in the outer portion of the core and then back to the left through the inner portion, thus giving a two-pass cross-flow approximation to the counterflow. (The flow passages through the combustion chamber are not shown in this view.)

As can be seen in Fig. 6.11, the heat exchanger core is constructed of alternate layers of flat and corrugated sheets. The flat sheets separate the hot and cold fluid streams, while the corrugated sheets act as fins that roughly triple the heat-transfer surface area per unit of volume. Note also that the axis of the corrugations is at right angles in alternate layers to provide a cross-flow pattern for the two fluid streams.

One of several recuperator units to be mounted in parallel in much larger gas-turbine plants is shown in Fig. 6.12. The hot exhaust gas from the turbine enters vertically at the bottom, flows upward through the heat-transfer matrix, and discharges vertically from the top. The air from the compressor enters a large circular port at the top at the right end, flows vertically downward in pure counterflow, and leaves a second circular port at the bottom to flow to the combustion chamber. The hot exhaust gas passages are formed by corrugated sheets sandwiched between flat plates that extend all the way from the bottom to the top of the unit. The air to be heated flows horizontally from the long plenum at the top into the spaces between the walls of the exhaust gas passages. Curved space strips

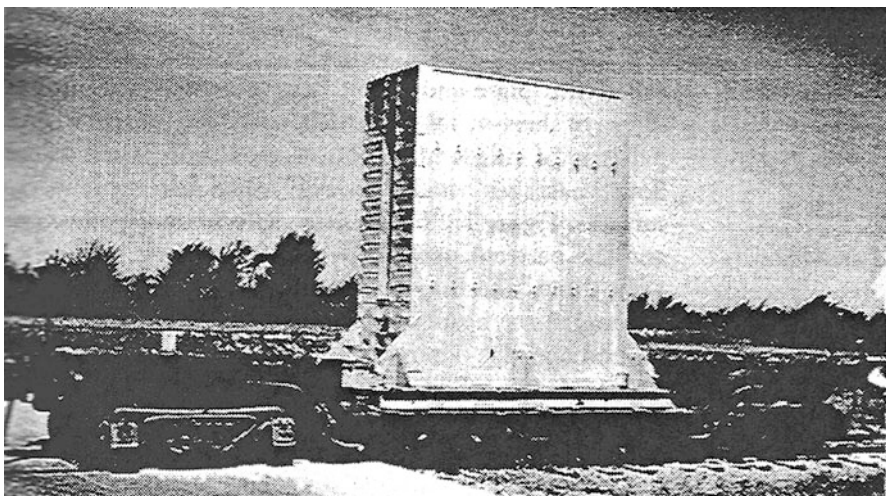


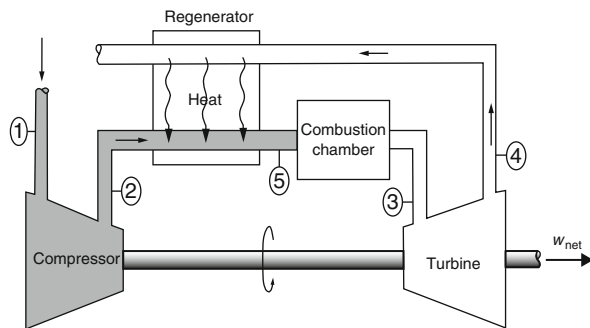
Fig. 6.12 A welded steel recuperator for a large gas-turbine power plant (courtesy Harrison Radiator Division, General Motors Corp) [4]

guide the air through a  $90^\circ$  bend and then downward between the heated walls. A similar header arrangement is used at the bottom. Note that both the flow passage area and the heat-transfer surface area for the hot exhaust gas are about three times as great as the corresponding values for the air being heated. This comes about because the two fluid streams differ in density by a factor of about 4.

The air preheaters in steam power plants are usually quite different from the units just described for gas turbines. Rotary regenerators are often used. These consist of a cylindrical drum filled with a heat-transfer matrix made of alternately flat and corrugated sheets. The drum is mounted so that the hot gas heats a portion of the matrix as it passes from the furnace to the stack. The balance of the matrix gives up its stored heat to the fresh air en route from the forced draft fans to the furnace. The ducts are arranged so that the two gas streams move through the drum in counterflow fashion while it is rotated, so that the temperature of any given element of the metal matrix fluctuates relatively little as it is cycled from the hot to the cold gas streams.

In the steam- and gas-turbine power plant fields, a distinction is sometimes made between air preheaters that involve a conventional heat-transfer matrix with continuous flow on both sides of a stationary heat-transfer surface and those through which fluids flow periodically. The hot fluid is heating one section of the matrix, while the cold fluid is removing heat from another section. Where this distinction is made, the term *regenerator* is applied to the periodic-flow type of heat exchanger, since this term has long been applied to units of this type employed for blast furnaces and steel furnaces, whereas the term *recuperator* is applied to units through which the flow is continuous.

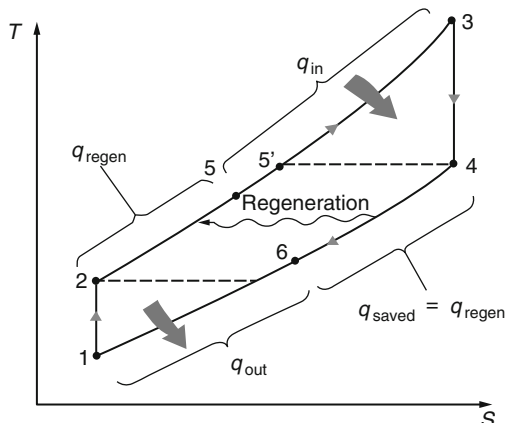
**Fig. 6.13** A gas-turbine engine with recuperator



Recuperators are used for gas turbines, but the gas turbines installed until the mid-1970s suffered from low efficiency and poor reliability. In the past, large coal and nuclear power plants dominated base-load electric power generation (Point 1 in Fig. 6.13). Base-load units are on line at full capacity or near full capacity almost all of the time. They are not easily or quickly adjusted for varying large amounts of load because of their characteristics of operation [6]. However, there has been a historic shift toward natural-gas-fired turbines because of their higher efficiencies, lower capital costs, shorter installation times, better emission characteristics, the abundance of natural gas supplies, and shorter startup times (Point 1 in Fig. 6.13). Now electric utilities use gas turbines for base-load power production as well as for peaking, making capacity at maximum load periods, and in emergency situations because they are easily brought on line or off line (Point 2 in Fig. 6.13). The construction costs for gas-turbine power plants are roughly half that of comparable conventional fossil fuel steam power plants, which were the primary base-load power plants until the early 1980s, but peaking units have much higher energy output costs. A recent gas turbine manufactured by General Electric uses a turbine inlet temperature of 1425 °C (2600 °F) and produces up to 282 MW while achieving a thermal efficiency of 39.5 % in the simple-cycle mode. Over half of all power plants to be installed in the near future are forecast to be gas-turbine or combined gas–steam turbine types (Fig. 6.13).

In gas-turbine engines with a Brayton cycle that includes a recuperator, the temperature of the exhaust gas leaving the turbine is often considerably higher than the temperature of the air leaving the compressor. Therefore, the high-pressure air leaving the compressor can be heated by transferring heat to it from the hot exhaust gases in a counterflow heat exchanger, which is also known as a regenerator or recuperator (Point 1 in Fig. 6.14). Gas-turbine regenerators are usually constructed as shell-and-tube type heat exchangers using very small-diameter tubes, with the high-pressure air inside the tubes and low-pressure exhaust gas in multiple passes outside the tubes [7]. The thermal efficiency of the Brayton cycle increases as a result of regeneration since the portion of energy of the exhaust gases that is normally released into the surroundings is now used to preheat the air entering the combustion chamber. This in turn decreases the heat input (and, thus, fuel) requirements for the same net work output. Note, however, that the use of a

**Fig. 6.14** T-s diagram of a Brayton cycle with regeneration



regenerator is recommended only when the turbine exhaust temperature is higher than the compressor exit temperature. Otherwise, heat will flow in the reverse direction (to the exhaust gases), decreasing the efficiency. This situation is encountered in gas turbines operating at very high-pressure ratios (Point 1 in Fig. 6.14).

The highest temperature occurring within the regenerator is the temperature of the exhaust gases leaving the turbine and entering the regenerator (Point 1 in Fig. 6.14). The gas turbine recuperator receives air from the turbine compressor at pressures ranging from 73.5 to 117 psia and temperatures from 350 to 450 °F (Point 3 in Fig. 6.14). Under no conditions can the air be preheated in the regenerator to a temperature above this value. In the limiting (ideal) case, the air will exit the regenerator at the inlet temperature of the exhaust gases. Air normally leaves the regenerator at a lower temperature (Point 1 in Fig. 6.14). Gas-turbine exhaust gas passes over the other side of the recuperator at exhaust temperatures ranging from 750 to 1000 °F. Compressor air temperatures are now raised to higher temperatures up to about 750–900 °F as the air enters the combustor. Turbine exhaust gases are then reduced to between 500 and 650 °F from the original 750–1000 °F. This heat recovery contributes appreciably to the turbine fuel rate reduction and increase in efficiency (Point 3 in Fig. 6.14). The regenerator is well insulated, and any changes in kinetic and potential energies are neglected.

A regenerator with a higher effectiveness will save a greater amount of fuel since it will preheat the air to a higher temperature prior to combustion (Point 1 on Fig. 6.14). However, achieving a higher effectiveness requires the use of a larger regenerator, which carries a higher price tag and causes a larger pressure drop because shaft horsepower is reduced. Pressure drop through the regenerator or recuperator is important and should be kept as low as practical on both sides. Generally, the air pressure drop on the high-pressure side should be held below 2 % of the compressor total discharge pressure. The gas pressure drop on the exhaust side (hot side) should be held below 4 in. of water. Therefore, the use of a regenerator with a very high effectiveness cannot be justified economically unless

the savings from the fuel costs exceed the additional expenses involved. The effectiveness of most regenerators used in practice is below 0.85. The thermal efficiency of an ideal Brayton cycle with regeneration depends on the ratio of the minimum to maximum temperatures as well as the pressure ratio. Regeneration is most effective at lower pressure ratios and low minimum-to-maximum temperature ratios.

Gas-to-air recuperators (or regenerators) are also used on marine type industrial and utility open-cycle gas-turbine applications. In this application, the recuperator receives air from the turbine compressor at pressures and temperatures ranging as described earlier, where gas-turbine exhaust gas passes over the other side of the recuperator at the exhaust temperature, depending on the turbine. The air side (high-pressure side) of the recuperator is in the system between the compressor and the combustor, and the compressor air is raised to a higher temperature up to that mentioned earlier as it enters the combustor. Obviously, a pressure drop through the regenerator or recuperator is important and should be kept as low as practical on both sides.

## 6.10 Heat Exchanger Analysis: Use of LMTD

Utilizing the log mean temperature difference (LMTD) method is one way of designing or predicting the performance of a heat exchanger; it is essential to relate the total heat-transfer rate to measurable quantities such as the inlet and outlet fluid temperatures, the overall heat-transfer coefficient, and the total surface area for heat transfer. Two such relations may readily be obtained by applying overall energy balances to the hot and cold fluids, as shown in Fig. 6.15. In particular, if  $q$  is the total rate of heat transfer between the hot and cold fluids and there is negligible heat transfer between the exchanger and its surroundings, as well as negligible potential and kinetic energy changes, application of the steady flow energy equation gives

$$q_{\text{total}} = \dot{m}_h (h_{h,i} - h_{h,o}) \quad (6.1a)$$

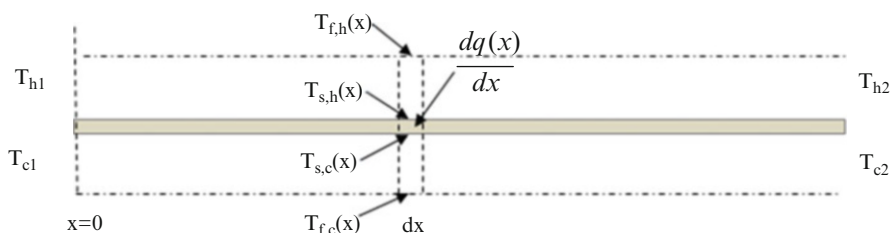


**Fig. 6.15** Heat transfer between two moving fluids separated by a solid boundary

and

$$q_{\text{total}} = \dot{m}_c (h_{c,o} - h_{c,i}), \quad (6.1b)$$

where  $h$  is the fluid enthalpy, the subscripts  $h$  and  $c$  refer to the hot and cold fluids, respectively, and the subscripts  $i$  and  $o$  designate the fluid inlet and outlet conditions, respectively. If the fluids are not undergoing a phase change and constant specific heats are assumed, these expressions reduce to

$$q_{\text{total}} = \dot{m}_h c_{p,h} (T_{h,i} - T_{h,o}) \quad (6.2a)$$

and

$$q_{\text{total}} = \dot{m}_c c_{p,c} (T_{c,o} - T_{c,i}), \quad (6.2b)$$

where the temperatures appearing in the expressions refer to the *mean* fluid temperatures at the designated locations. Note that Eqs. (6.1a), (6.1b), (6.2a), and (6.2b) are independent of the flow arrangement and heat exchanger type.

Now consider the heat transfer at a particular point,  $x$ , on the heat-transfer surface. At  $x$  there will be a bulk hot fluid temperature given by  $T_{f,h}(x)$ , a wall surface temperature on the hot fluid side given by  $T_{s,h}(x)$ , a wall surface temperature on the cold fluid side given by  $T_{s,c}(x)$ , and a cold fluid bulk temperature given by  $T_{f,c}(x)$ . The total temperature drop from the hot fluid at  $x$  to the cold fluid at  $x$  is given by

$$\begin{aligned} \Delta T &= T_{f,h}(x) - T_{f,c}(x) \\ &= T_{f,h}(x) - T_{s,h}(x) + T_{s,h}(x) - T_{s,c}(x) + T_{s,c}(x) - T_{f,c}(x) \\ &= \Delta T_{f,h} + \Delta T_s + \Delta T_{f,c}. \end{aligned}$$

Then the heat flux leaving the hot fluid is given by

$$\frac{dq(x)}{dx} = h_{f,h} A_{f,h} (T_{f,h}(x) - T_{s,h}(x)) = h_{f,h} dA_{f,h} \Delta T_{f,h}(x), \quad \Delta T_{f,h}(x) = \frac{\frac{dq(x)}{dx}}{h_{f,h} dA_{f,h}}.$$

The heat flux crossing the wall between the two fluids is given by

$$\frac{dq(x)}{dx} = \frac{k_s}{\delta_s} dA_s (T_{s,h}(x) - T_{s,c}(x)) = \frac{k_s}{\delta_s} dA_s \Delta T_s(x), \quad \Delta T_s(x) = \frac{\frac{dq(x)}{dx}}{\frac{k_s}{\delta_s} dA_s}.$$

And the heat flux into the cold fluid is given by

$$\frac{dq(x)}{dx} = h_{f,c} dA_{f,c} (T_{s,c}(x) - T_{f,c}(x)) = h_{f,c} dA_{f,c} \Delta T_{f,c}(x), \quad \Delta T_{f,c}(x) = \frac{\frac{dq(x)}{dx}}{h_{f,c} dA_{f,c}}.$$

Then the difference in the bulk temperatures of the two fluids can be written

$$\begin{aligned} T_{f,h}(x) - T_{f,c}(x) &= \frac{\frac{dq(x)}{dx}}{h_{f,h}dA_{f,h}} + \frac{\frac{dq(x)}{dx}}{\frac{k_s}{\delta_s}dA_s} + \frac{\frac{dq(x)}{dx}}{h_{f,c}dA_{f,c}} \\ &= \frac{dq(x)}{dx} \left[ \frac{1}{h_{f,h}dA_{f,h}} + \frac{\delta_s}{k_s dA_s} + \frac{1}{h_{f,c}dA_{f,c}} \right]. \end{aligned} \quad (6.3)$$

Note that  $\delta_s$  will depend on the geometry. For slab or plate geometry

$$\delta_s = \Delta t \quad \text{the wall thickness.}$$

For cylindrical geometry typical of tubes

$$\delta_s = r_{in} \ln \left( \frac{r_{out}}{r_{in}} \right) \quad r_{out} - r_{in} = \text{tube wall thickness.}$$

Also note that the differential areas do not all have to be equal. There will be a slight difference if the bounding surface is a tube, but the addition of fins to either the hot or the cold side could change the effective area significantly, and that is the area that must be used in Eq. (6.3). Also, note that the areas are per unit length. That is why they have been written as  $dA$ :

$$\begin{aligned} T_{f,h}(x) - T_{f,c}(x) &= \frac{dq(x)}{dx} \left( \frac{1}{U \frac{dA}{dx}} \right) \quad \frac{1}{U \frac{dA}{dx}} = \frac{1}{h_{f,h}dA_{f,h}} + \frac{\delta_s}{k_s dA_s} + \frac{1}{h_{f,c}dA_{f,c}}, \\ \frac{dq(x)}{dx} &= U \frac{dA}{dx} (T_{f,h} - T_{f,c}). \end{aligned}$$

Then the heat lost by the hot fluid is given by

$$\frac{dq(x)}{dx} = -\dot{m}_{f,h} C_{p,h} \frac{dT_{f,h}(x)}{dx}, \quad (6.4)$$

and the heat gained by the cold fluid is given by

$$\frac{dq(x)}{dx} = \dot{m}_{f,c} C_{p,c} \frac{dT_{f,c}(x)}{dx}. \quad (6.5)$$

Combining these two equations gives

$$\frac{dT_{f,h}(x)}{dx} - \frac{dT_{f,c}(x)}{dx} = -\frac{dq(x)}{dx} \left( \frac{1}{m_h C_{p,h}} + \frac{1}{m_c C_{p,c}} \right) = -U \frac{dA}{dx} (T_{f,h} - T_{f,c}),$$

$$\Delta T(x) = T_{f,h}(x) - T_{f,c}(x),$$

$$\frac{d\Delta T(x)}{dx} = -U \frac{dA}{dx} \Delta T \left( \frac{1}{m_h C_{p,h}} + \frac{1}{m_c C_{p,c}} \right),$$

$$\frac{d\Delta T(x)}{\Delta T(x)} = -U \left( \frac{1}{m_h C_{p,h}} + \frac{1}{m_c C_{p,c}} \right) dA - \frac{dA}{dx} dx = dA.$$

Integrating gives

$$\ln \left( \frac{\Delta T_2}{\Delta T_1} \right) = -UA \left( \frac{1}{m_h C_{p,h}} + \frac{1}{m_c C_{p,c}} \right). \quad (6.6)$$

Now for the hot fluid flowing from left to right, Eq. (6.2a) becomes

$$q_{\text{total}} = \dot{m}_h C_{p,h} (T_{f,h,1} - T_{f,h,2}) - \frac{1}{\dot{m}_h C_{p,h}} = \frac{(T_{f,h,1} - T_{f,h,2})}{q_{\text{total}}}.$$

In addition, for the cold fluid also flowing from left to right (parallel flow), Eq. (6.2b) becomes

$$q_{\text{total}} = \dot{m}_c C_{p,c} (T_{f,c,2} - T_{f,c,1}), \quad \frac{1}{\dot{m}_c C_{p,c}} = \frac{(T_{f,c,2} - T_{f,c,1})}{q_{\text{total}}}.$$

Plugging these into Eq. (6.3) gives

$$\begin{aligned} \ln \left( \frac{\Delta T_2}{\Delta T_1} \right) &= -UA \left( \frac{T_{f,h,1} - T_{f,h,2}}{q_{\text{total}}} + \frac{T_{f,c,2} - T_{f,c,1}}{q_{\text{total}}} \right) = \frac{UA}{q_{\text{total}}} (T_{f,h,2} - T_{f,c,2} - T_{f,h,1} + T_{f,c,1}), \\ \ln \left( \frac{\Delta T_2}{\Delta T_1} \right) &= \frac{UA}{q_{\text{total}}} (\Delta T_2 - \Delta T_1) \quad q_{\text{total}} = UA \frac{(\Delta T_2 - \Delta T_1)}{\ln \left( \frac{\Delta T_2}{\Delta T_1} \right)}, \\ q_{\text{total}} &= UA \Delta T_{\text{lm}} \quad \Delta T_{\text{lm}} = \frac{(\Delta T_2 - \Delta T_1)}{\ln \left( \frac{\Delta T_2}{\Delta T_1} \right)}. \end{aligned} \quad (6.7)$$

This looks a lot like Newton's law of cooling, with  $\Delta T_{\text{lm}}$  playing the role of the standard  $\Delta T$ .  $\Delta T_{\text{lm}}$  is called the log-mean temperature difference.

Now consider the counterflow arrangement. In this case Eq. (6.5) becomes

$$\frac{dq(x)}{dx} = -\dot{m}_{f,c} C_{p,c} \frac{dT_{f,c}(x)}{dx}.$$

Moreover, Eq. (6.6) becomes

$$\ln\left(\frac{\Delta T_2}{\Delta T_1}\right) = -UA\left(\frac{1}{\dot{m}_h C_{p,h}} - \frac{1}{\dot{m}_c C_{p,c}}\right).$$

Then Eq. (6.2b) becomes

$$q_{\text{total}} = \dot{m}_c c_{p,c} (T_{f,c,1} - T_{f,c,2}).$$

This gives

$$\begin{aligned} \ln\left(\frac{\Delta T_2}{\Delta T_1}\right) &= -UA\left(\frac{T_{f,h,1} - T_{f,h,2}}{q_{\text{total}}} - \frac{T_{f,c,1} - T_{f,c,2}}{q_{\text{total}}}\right) = \frac{UA}{q_{\text{total}}} (T_{f,h,2} - T_{f,c,2} - T_{f,h,1} + T_{f,c,1}), \\ \ln\left(\frac{\Delta T_2}{\Delta T_1}\right) &= \frac{UA}{q_{\text{total}}} (\Delta T_2 - \Delta T_1), \quad q_{\text{total}} = UA \frac{(\Delta T_2 - \Delta T_1)}{\ln\left(\frac{\Delta T_2}{\Delta T_1}\right)} \end{aligned}$$

which are the identical equations for the parallel-flow heat exchanger. It is important to remember how the  $\Delta T$  are defined.

$$\text{Parallel Flow : } \Delta T_1 = T_{f,h,\text{in}} - T_{f,c,\text{in}} \quad \Delta T_2 = T_{f,h,\text{out}} - T_{f,c,\text{out}},$$

$$\text{Counterflow : } \Delta T_1 = T_{f,h,\text{in}} - T_{f,c,\text{out}} \quad \Delta T_2 = T_{f,h,\text{out}} - T_{f,c,\text{in}}.$$

*Example 6.1* A counterflow, concentric-tube heat exchanger is used to cool the lubricating oil for a large industrial gas-turbine engine. The flow rate of cooling water through the inner tube ( $D_i = 25 \text{ mm}$ ) is  $0.2 \text{ kg/s}$ , while the flow rate of oil through the outer annulus ( $D_o = 45 \text{ mm}$ ) is  $0.1 \text{ kg/s}$ . The oil and water enter at temperatures of  $100^\circ\text{C}$  and  $30^\circ\text{C}$ , respectively. How long must the tube be made if the outlet temperature of the oil is to be  $60^\circ\text{C}$ ? (the steel tube that separates the two flows is so thin that the temperature drop across it may be neglected) (Fig. 6.16).

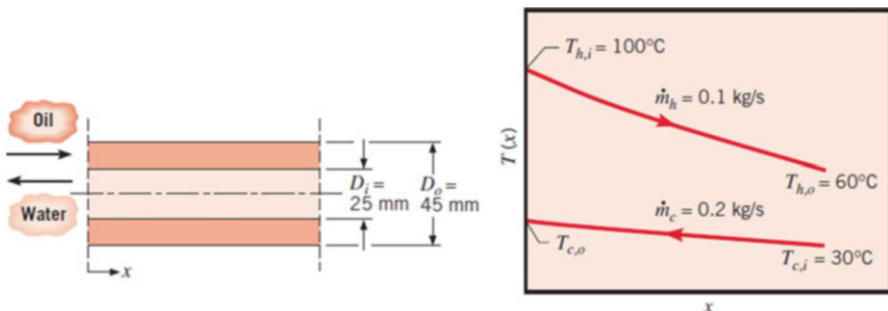


**Fig. 6.16** Schematic of Example 6.1 (Incropera, F., D. Dewitt, T. Bergman, A. Lavine, ‘Fundamentals of Heat and Mass Transfer’, 7th Edition, 2011)

**Solution**

**Known:** Fluid flow rates and the inlet temperature for a counterflow, concentric-tube heat exchanger of prescribed inner and outer diameter

**Find:** Tube length to achieve a desired hot fluid outlet temperature.

**Assumptions:**

1. Negligible heat loss to the surroundings.
2. Negligible kinetic and potential energy changes.
3. Constant properties.
4. Negligible tube wall thermal resistance and fouling factors.
5. Fully developed conditions for the water and oil ( $U$  independent of  $x$ ).

**Properties:**

Table A.5, unused engine oil ( $\bar{T}_h = 80^\circ\text{C} = 353\text{ K}$ ):

$$c_p = 2131 \text{ J/kg K}, \mu = 3.25 \times 10^{-2} \text{ N s/m}^2, k = 0.138 \text{ W/m K}.$$

Table A.6, water ( $T_c \approx 35^\circ\text{C} = 308\text{ K}$ ):

$$c_p = 4178 \text{ J/kg K}, \mu = 725 \times 10^{-6} \text{ N s/m}^2, k = 0.625 \text{ W/m K}, \text{Pr} = 4.85.$$

**Analysis:**

The required heat-transfer rate may be obtained from the overall energy balance for the hot fluid, Eq. (6.1a):

$$q = \dot{m}_h c_{p,h} (T_{h,i} - T_{h,o}),$$

$$q = 0.1 \text{ kg/s} \times 2131 \text{ J/kg K} (100 - 60)^\circ\text{C} = 8524 \text{ W}.$$

Applying Eq. (6.2b), the water outlet temperature is

$$T_{c,o} = \frac{q}{\dot{m}_c c_{p,c}} + T_{c,i},$$

$$T_{c,o} = \frac{8524 \text{ W}}{0.2 \text{ kg/s} \times 2131 \text{ J/kg K}} + 30^\circ\text{C} = 40.2^\circ\text{C}.$$

Accordingly, use of  $\bar{T}_c = 35^\circ\text{C}$  to evaluate the water properties was a good choice. The required heat-exchanger length may now be obtained from Eq. (6.7):

$$q = UA\Delta T_{lm},$$

where  $A = \pi D_i L$ ,

$$\Delta T_{lm} = \frac{(T_{h,i} - T_{c,o}) - (T_{h,o} - T_{c,i})}{\ln[(T_{h,i} - T_{c,o})/(T_{h,o} - T_{c,i})]} = \frac{59.8 - 30}{\ln(59.8/30)} = 43.2^\circ\text{C}.$$

The overall heat-transfer coefficient is

$$U = \frac{1}{(1/h_i) + (1/h_o)}.$$

For water flow through the tube,

$$\dot{m} = \rho A V \frac{\dot{m}}{A} = \rho V$$

$$Re_D = \frac{\dot{m}_c D_i}{A \mu} = \frac{4\dot{m}}{\pi D_i \mu} = \frac{4 \times 0.2 \text{ kg/s}}{\pi (0.025 \text{ m}) 725 \times 10^{-6} \text{ N s/m}^2} = 14,050.$$

Accordingly, the flow is turbulent and the convection coefficient may be computed from the following equations:

$$Nu_D = 0.023 Re_D^{4/5} Pr^{0.4},$$

$$Nu_D = 0.023(14,050)^{4/5}(4.85)^{0.4} = 90.$$

Hence,

$$h_i = Nu_D \frac{k}{D_i} = \frac{90 \times 0.625 \text{ W/m K}}{0.025 \text{ m}} = 2250 \text{ W/m}^2 \text{ K}.$$

For the flow of oil through the annulus, the hydraulic diameter is

$$D_h = \frac{4A}{P} = \frac{4(\pi r_o^2 - \pi r_i^2)}{2\pi(r_o - r_i)} = 2(r_o - r_i) = D_o - D_i$$

and the Reynolds number is

$$Re_D = \frac{\rho u_m D_h}{\mu} = \frac{\dot{m} (D_o - D_i)}{A \mu} = \frac{\dot{m} (D_o - D_i)}{\mu \pi (D_o^2 - D_i^2)/4},$$

$$Re_D = \frac{4\dot{m}}{\pi(D_o + D_i)\mu} = \frac{4(0.1 \text{ kg/s})}{\pi(0.045 + 0.025)3.25 \times 10^{-2} \text{ kg/sm}} = 56.0.$$

The annular flow is therefore laminar. For a constant heat flux the laminar correlation is given by the following equation:

$$Nu_i = \frac{h_o D_h}{k} = 4.36$$

and

$$h_o = 4.36 \frac{0.138 \text{ W/m K}}{0.020 \text{ m}} = 30.1 \text{ W/m}^2 \text{ K}.$$

The overall convection coefficient is then

$$U = \frac{1}{(1/2250 \text{ W/m}^2\text{K}) + (1/30.1 \text{ W/m}^2\text{K})} = 29.7 \text{ W/m}^2\text{K},$$

and from the rate equation it follows that

$$L = \frac{q}{U\pi D_i \Delta T_{lm}} = \frac{8524 \text{ W}}{29.7 \text{ W/m}^2\text{K}\pi(0.025 \text{ m})(43.2^\circ\text{C})} = 84.6 \text{ m.}$$

**Comments:**

1. The hot-side convection coefficient controls the rate of heat transfer between the two fluids, and the low value of  $h_o$  is responsible for the large value of  $L$ .
2. Because  $h_i \gg h_o$ , the tube-wall temperature will follow closely that of the coolant water.

Many heat exchangers have been designed based on a log-mean temperature difference. However, there are some problems with proceeding based on the log-mean temperature difference equation. First, it says nothing about cross-flow heat exchangers, which are very common owing to the ease of construction of this type of exchanger. Second, it often requires iterative calculations for a design if not all of the inlet and exit temperatures are known a priori. In the preceding example, the outlet temperature of the oil was not specified, and an iterative solution would have been required. Iterative solutions can certainly be accurate, but they often require more work. Third, the log-mean temperature difference method does not provide a feel for the maximum heat transfer possible given the entering conditions of the fluids. Sometimes this is an important parameter to understand if the design is to be optimized.

## 6.11 Effectiveness-NTU Method for Heat-Exchanger Design

A better method has been developed for heat-exchanger design that uses some of the preceding analysis. This method is called the effectiveness-number of transfer unit (NTU) method.<sup>1</sup> It starts by considering the fluid heat-transfer capacity rates defined as

---

<sup>1</sup> Kays, W. M., & London, A. L. (1998). Compact heat exchangers (3rd Ed.). Malabar FL: Krieger Publishing Company.

$$\begin{aligned} \text{Cold Fluid Capacity Rate } C_c &= \dot{m}_c C_{p,c} \text{ W/K,} \\ \text{Cold Fluid Capacity Rate } C_h &= \dot{m}_h C_{p,h} \text{ W/K.} \end{aligned} \quad (6.8)$$

Then the maximum amount of heat that can be transferred between the two fluids is the minimum fluid capacity rate times the difference in temperature of the hot fluid entering the exchanger and the cold fluid entering the exchanger, or

$$\begin{aligned} C_{\min} &= \min(C_c, C_h), \\ q_{\max} &= C_{\min}(T_{h,in} - T_{c,in}). \end{aligned} \quad (6.9)$$

Then the heat-exchanger effectiveness is defined as

$$\epsilon = \frac{q_{\text{act}}}{q_{\max}} = \frac{C_h(T_{h,in} - T_{h,out})}{C_{\min}(T_{h,in} - T_{c,in})} = \frac{C_c(T_{c,in} - T_{c,out})}{C_{\min}(T_{h,in} - T_{c,in})}. \quad (6.10)$$

The number of heat-exchanger transfer units is then defined as

$$\text{NTU} = \frac{UA}{C_{\min}}, \quad (6.11)$$

where  $U$  and  $A$  are defined as previously. The heat capacity-rate ratio is defined as

$$C_r = \frac{C_{\min}}{C_{\max}}. \quad (6.12)$$

Then in general it is possible to express the effectiveness as

$$\epsilon = \epsilon(\text{NTU}, C_r, \text{Flow Arrangement}).$$

Different functions for  $\epsilon$  have been developed for many flow arrangements.<sup>2</sup> The three main flow arrangements of interest are parallel flow, counterflow, and cross flow.

#### Parallel Flow:

For parallel flow the expression is

$$\epsilon = \frac{1 - e^{-\text{NTU}(1+C_r)}}{1 + C_r}. \quad (6.13)$$

---

<sup>2</sup>Kays and London, Op. Cit.

There are two interesting limits:

$$\begin{aligned} C_r \rightarrow 0 & \quad \epsilon = 1 - e^{-NTU}, \\ C_r \rightarrow 1 & \quad \epsilon = \frac{1}{2}. \end{aligned} \quad (6.14)$$

The  $C_r=0$  limit corresponds to one fluid vaporizing or condensing, and the heat capacity rate for this fluid becomes immense. The other limit,  $C_r=1.0$ , corresponds to both fluids having the same heat capacity rate.

Counterflow:

$$\epsilon = \frac{1 - e^{-NTU(1-C_r)}}{1 - C_r e^{-NTU(1-C_r)}}. \quad (6.15)$$

Addressing the same two limits:

$$\begin{aligned} C_r \rightarrow 0 & \quad \epsilon = 1 - e^{-NTU}, \\ C_r \rightarrow 1 & \quad \epsilon = \frac{NTU}{1 + NTU}. \end{aligned} \quad (6.16)$$

The  $C_r=0$  limit is the same, but the  $C_r=1$  limit is twice as effective for large values of NTU. This essentially is the known performance advantage of counterflow heat exchangers.

Cross Flow: Cross flow must be broken down into three different types. The performance is different depending on whether or not the fluids are allowed to mix as they move through the exchanger. A typical tube-and-shell exchanger would have the fluid moving through the tubes described as unmixed and the fluid moving through the shell would be mixed.

**Cross Flow – Both Fluids Unmixed**

This case requires a series numerical solution and the curves for values of various  $C_r$  values are given in Kays and London. For the case of  $C_r=0$ , the solution is the same as for counterflow and parallel flow:

$$C_r = 0 \quad \epsilon = 1 - e^{-NTU}.$$

However, all of the curves for any value of  $C_r$  asymptotically approach 1.0, like the counterflow exchanger. For all  $C_r > 0$  the effectiveness is less than for a counterflow exchanger with the same  $C_r$ .

**Cross Flow – One Fluid Mixed**

For the case of

$$\begin{aligned} C_{\max} &= C_{\text{unmixed}} & C_{\min} &= C_{\text{mixed}} \\ \epsilon &= 1 - e^{-\Gamma/C_r} & \Gamma &= 1 - e^{-NTUC_r} \end{aligned} \quad (6.17)$$

And for the case of

$$\begin{aligned} C_{\max} &= C_{\text{mixed}} & C_{\min} &= C_{\text{unmixed}} \\ \epsilon &= \frac{1 - e^{-\Gamma' C_r}}{C_r} & \Gamma' &= 1 - e^{-\text{NTU}} \end{aligned} \quad (6.18)$$

Once again, for  $C_r = 0$ , this gives the same behavior as a counterflow heat exchanger. For  $C_r = 1.0$ , it gets complicated, but it is important to note that if a choice is possible, it is better to have the fluid with the smaller heat capacity rate be the mixed fluid (Eq. 6.17).

#### Cross Flow – Both Fluids Mixed

The closed form solution is

$$\epsilon = \frac{\text{NTU}}{\frac{\text{NTU}}{(1-e^{-\text{NTU}})} + \frac{C_r \text{NTU}}{1-e^{-\text{NTU} C_r}} - 1}. \quad (6.19)$$

As always, for the case of  $C_r = 0$ , the results are the same as for the counterflow exchanger.

For  $C_r = 1.0$  as NTU becomes large, the effectiveness goes to 1/2. However, this is the only case where better effectiveness can be obtained at a lower NTU. The effectiveness actually decreases after a NTU of around 3–5.

There are many other configurations reported by Kays and London, but these three are the most important. The availability of solutions for the common cross-flow case of one fluid mixed makes this technique very useful.

*Example 16.2* Consider a gas-to-gas recuperator of a shell-and-tube design.

The tubes are 2 cm in diameter spaced on 4 cm centers with a 2 mm thickness made of aluminum. The flow cross section is a  $2 \times 2$  m square. The pressure ratio for the compressor is 20. Both fluids are air and the cold fluid is in the tubes. The hot fluid enters at 783 K and exits at 670 K and is atmospheric pressure. The cold fluid enters at 655 K and exits at 768 K and is at 20 atm. The flow rate is 2.5E + 5 kg/h for a 10 MW power plant.

#### Solution

Start with the hot fluid – calculate Reynolds number:

$$N \text{ tubes} = 2401, A_{\text{flow}} = 2^2 - 2401 \times \pi(0.012)^2 = 2.9138 \text{ m}^2,$$

$$\dot{m} = \rho A V \quad \rho V = \frac{\dot{m}}{A} = \frac{69.44 \text{ kg/s}}{2.9138} = 23.8 \text{ kg/s/m}^2,$$

$$\mu = 3.65E - 5 \quad D = \frac{4(0.04^2 - \pi 0.012^2)}{2\pi 0.012} = 0.0609 \text{ m},$$

$$\text{Re} = \frac{23.8 \times 0.0609}{3.7E - 05} = 39,789.2.$$

This is clearly in the turbulent range.

Using the same equations, the cold fluid  $\text{Re} = 56,731.1$ ,

$$\text{Pr}_{\text{hot}} = C_p m/k = 1078.8 \times 3.65E - 5 / 0.0564 = 0.697,$$

$$\text{Pr}_{\text{cold}} = C_p m/k = 1076.7 \times 3.25E - 5 / 0.050 = 0.700,$$

$$\text{Nu}_{\text{hot}} = 0.023 \times 39,789.2^{0.8} \times 0.697^{0.3} = 98.7,$$

$$h_{\text{hot}} = 98.7 \times 0.0564 / 0.0609 = 91.5 \text{ W/m}^2/\text{K},$$

$$\text{Nu}_{\text{cold}} = 0.023 \times 56,731.1^{0.8} \times 0.700^{0.4} = 127.0,$$

$$h_{\text{cold}} = 127.0 \times 0.0500 / 0.02 = 316.0 \text{ W/m}^2/\text{K}.$$

This allows us to calculate  $UA$  as a function of  $L$ :

$$A_{\text{hot}} = 2\pi(0.012) \times 2401 \times L = 724.8 \times L \text{ m}^2,$$

$$A_{\text{cold}} = 2\pi(0.01) \times 2401 \times L = 603.4 \times L \text{ m}^2,$$

$$A_{\text{tube}} = 2\pi(0.011) \times 2401 \times L = 663.74 \times L \text{ m}^2,$$

$$\begin{aligned} \frac{1}{UA} &= \left( \frac{1}{h_{\text{hot}} A} + \frac{t}{kA} + \frac{1}{h_{\text{cold}} A} \right) \\ &= \frac{1}{91.5(724.8)L} + \frac{0.002}{218(663.74)L} + \frac{1}{316(603.4)L} \\ &= (1.508E - 5 + 1.38E - 8 + 5.25E - 6)/L = \frac{2.03E - 5}{L} \text{ W/K}, \end{aligned}$$

$$\dot{Q} = 8.46E + 6W, \quad \Delta T_{\text{in}} = 15 \text{ K}, \quad \Delta T_{\text{out}} = 15 \text{ K},$$

$$\Delta T_{\text{lmm}} = 15 \text{ K}, \quad \dot{Q} = \left( \frac{UA}{L} \right) L \Delta T_{\text{lmm}}, \quad L = \frac{\dot{Q}}{(UA/L) \Delta T_{\text{lmm}}},$$

$$L = \frac{8.46E + 6}{4.92E + 4 \times 15} = 11.5 \text{ m}.$$

Now try the effectiveness-NTU method:

$$C_{\text{hot}} = 2.5E + 5 / 3600 \times 1078.8 = 7.49E + 04,$$

$$C_{\text{cold}} = 2.5E + 5 / 3600 \times 1076.7 = 7.48E + 04 = C_{\min},$$

$$C_r = 0.998 \sim 1.0 \quad \epsilon = \text{NTU}/(\text{NTU} + 1) \quad \text{NTU} = \epsilon/(1 - \epsilon),$$

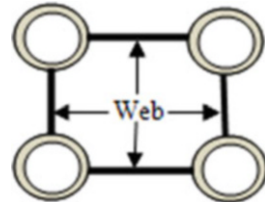
$$\epsilon = \frac{C_{\text{hot}}(T_{\text{h,in}} - T_{\text{h,out}})}{C_{\min}(T_{\text{h,in}} - T_{\text{c,in}})} = \frac{7.49E + 4 \times (783 - 670)}{7.48E + 4 \times (783 - 655)} = 0.8846,$$

$$\text{NTU} = 7.67, \quad \frac{\text{NTU}}{L} = \frac{UA/L}{C_{\min}} = 0.6576, \quad L = \frac{7.67}{0.6576} = 11.6 \text{ m}.$$

Note that the largest resistance to heat transfer was in the hot-side convection, and the resistance of the tube wall was negligible.

So add fins to the hot-side channel by putting a 2 mm thick web between the tubes (Fig. 6.17).

First, recalculate the hydraulic diameter for the hot side.

**Fig. 6.17** Web channel

Treating the web as a wetted perimeter gives a new  $D_h = 0.0329$  m.  
This gives a new

$$Re = 21,521.3,$$

$$Nu = 60.4,$$

$$h = 104.0.$$

Dividing the web in half for a fin for each tube yields

$$w = 0.01, t = 0.002, P = 0.02, A = 0.00002, m = 21.79, L = 0.008,$$

$$mL = 0.1743, h_{\text{fin}} = 0.9899, h_o = 0.9915, A_{\text{tot}} = 0.1394,$$

$$h_o \times A_{\text{tot}} = 0.1382, A_{\text{hot}}/A_{\text{cold}} = 2.1997, A_{\text{hot}}/L = 1,327.3.$$

The cold side and tube resistances do not change, so

$$\frac{1}{UA} = \frac{1}{1.25E - 5 \times L}, \quad L = \frac{\dot{Q}}{v_A / L \Delta T_{lmn}} = \frac{8.47E + 6}{7.98E + 4 \times 15} = 7.1 \text{ m}.$$

Now to obtain the pressure drops,

$$C_{f,\text{hot}} = 0.046Re^{-0.2} = 0.046 \times 21,521.3^{-0.2} = 6.25E - 3,$$

$$C_{f,\text{cold}} = 0.046Re^{-0.2} = 0.046 \times 56,731.1^{-0.2} = 5.15E - 3.$$

This gives

$$\tau_{\text{hot}} = 6.25E - 3 \times \frac{1}{2} \rho V^2 = \frac{3.13E - 3}{\rho_{\text{hot}}} \left( \frac{\dot{m}}{A} \right)_{\text{hot}}^2,$$

$$\tau_{\text{cold}} = 5.15E - 3 \times \frac{1}{2} \rho V^2 = \frac{2.58E - 3}{\rho_{\text{cold}}} \left( \frac{\dot{m}}{A} \right)_{\text{cold}}^2,$$

$$\rho_{\text{hot}} = \frac{101,325 \times 28.9669}{8314.4 \times 783} = 0.451 \text{ kg/m}^3, \quad \rho_{\text{cold}} = \frac{20 \times 101,325 \times 28.9669}{768 \times 8314.4} 9.193 \text{ kg/m}^3,$$

$$\tau_{\text{hot}} = \frac{3.13E - 3}{0.451} (23.83)_{\text{hot}}^2 = 3.941 \text{ Pascals},$$

$$\tau_{\text{cold}} = \frac{2.58E - 3}{9.193} (92.1)_{\text{cold}}^2 = 2.38 \text{ Pascals}.$$

Clearly these pressure drops are negligible compared to atmospheric pressure. This says that the heat exchanger could be made a lot more compact by adding more surface area per unit volume –  $\text{m}^2/\text{m}^3$ .

## 6.12 Special Operating Conditions

It is useful to note certain special conditions under which heat exchangers may be operated. Figure 6.18a shows temperature distributions for a heat exchanger in which the hot fluid has a heat capacity rate,  $C_h \equiv \dot{m}_h C_{p,h}$ , which is much larger than that of the cold fluid,  $C_c \equiv \dot{m}_c C_{p,c}$ .

For this case the temperature of the hot fluid remains approximately constant throughout the heat exchanger, while the temperature of the cold fluid increases. The same condition is achieved if the hot fluid is a condensing vapor. Condensation occurs at constant temperature, and, for all practical purposes,  $C_h \rightarrow \infty$ . Conversely, in an evaporator or a boiler (Fig. 6.18b), it is the cold fluid that experiences a change in phase and remains at a nearly uniform temperature ( $C_c \rightarrow \infty$ ). The same effect is achieved without phase change if  $C_h \ll C_c$ . Note that, with condensation or evaporation, the heat rate is given by Eq. (6.1a) or (6.1b), respectively. Conditions illustrated in Fig. 6.18a or b also characterize an internal tube flow (or *single-stream heat exchanger*) exchanging heat with a surface at constant temperature or an external fluid at constant temperature.

The third special case (Fig. 6.18c) involves a counterflow heat exchanger for which the heat capacity rates are equal ( $C_h = C_c$ ). The temperature difference  $\Delta T$  must then be constant throughout the exchanger, in which case  $\Delta T_1 = \Delta T_2 = \Delta T_{lm}$ .

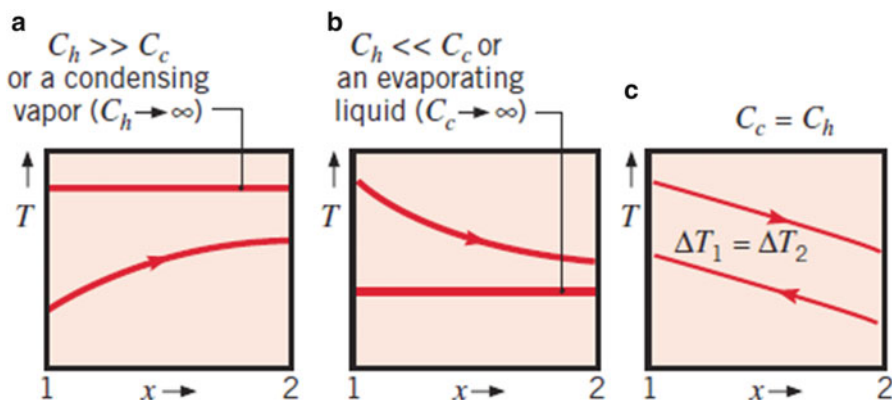


**Fig. 6.18** Special heat-exchanger conditions. (a)  $C_h \gg C_c$  or a condensing vapor. (b) An evaporating liquid or  $C_h \ll C_c$ . (c) A counterflow heat exchanger with equivalent fluid heat capacities  $C_h = C_c$  (Incropera, F., D. Dewitt, T. Bergman, A. Lavine, ‘Fundamentals of Heat and Mass Transfer’, 7th Edition, 2011)

## 6.13 Compact Heat Exchangers and Their Classifications

A heat exchanger is quite arbitrarily referred to as a *compact heat exchanger*, provided it has a surface area density greater than  $700 \text{ m}^2/\text{m}^3$ , which is characterized for the ratio of their surface area per unit volume of the exchanger. Such a ratio is quite arbitrarily referred to as a compact heat exchanger. By a large heat-transfer surface area per unit volume of the exchanger, resulting in reduced space, weight, support structure and footprint, energy requirements, and cost, as well as improved process design and plant layout and processing conditions, together with low fluid inventory. This is done by increasing the heat-transfer surface area via fins per unit volume ( $\text{m}^2/\text{m}^3$ ) and there many variations (Fig. 6.19a–c).

A special and important class of heat exchangers is used to achieve a very large ( $\geq 400 \text{ m}^2/\text{m}^3$  for liquids such as liquid-to-gas type exchangers and  $\geq 700 \text{ m}^2/\text{m}^3$  for gases such as gas-to-gas exchangers) heat-transfer surface area per unit volume. Called *compact heat exchangers*, these devices have dense arrays of finned tubes or plates and are typically used when at least one of the fluids is a gas and, hence, is characterized by a small convection coefficient. The tubes may be flat or circular, as in Fig. 6.19a and b, c, respectively, and the fins may be a plate or circular, as in Fig. 6.19a, b, and c, respectively. Parallel-plate heat exchangers may be finned or corrugated and may be used in single-pass (Fig. 6.19d) or multipass (Fig. 6.19e) modes of operation. Flow passages associated with compact heat exchangers are

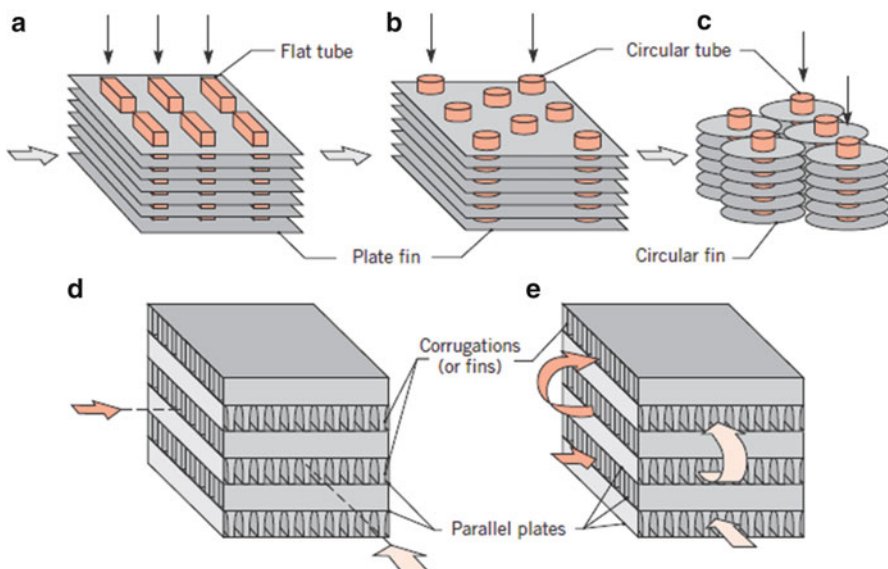


**Fig. 6.19** Compact heat-exchanger cores. (a) Fin-tube (flat tubes, continuous plate fins). (b) Fin-tube (circular tubes, continuous plate fins). (c) Fin-tube (circular tubes, circular fins). (d) Plate-fin (single pass). (e) Plate-fin (multipass). (Incropera, F., D. Dewitt, T. Bergman, A. Lavine, 'Fundamentals of Heat and Mass Transfer', 7th Edition, 2011)

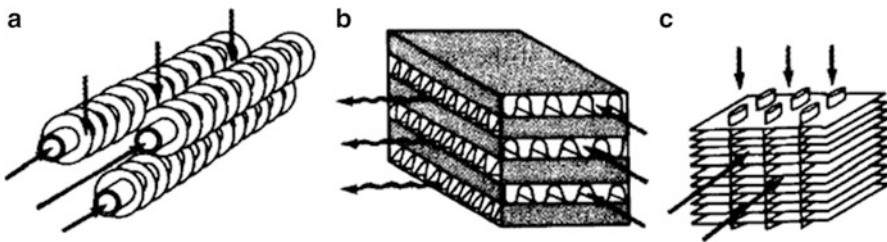


**Fig. 6.20** Typical heat-transfer matrices for compact heat exchangers: (a) Circular finned-tube matrix; (b) plain plate-fin matrix; (c) finned flat-tube matrix [4]

typically small ( $D_h \leq 5$  mm), where  $D_h$  is the magnitude of the *hydraulic diameter* and the flow is often laminar. Many of the geometries are far too complicated to apply deterministic methods to predict their performance. Thus, many of these compact heat exchangers have had their performance determined experimentally.

Kays and London [5] have studied a wide variety of configurations for heat-transfer matrices and cataloged their heat-transfer and pressure-drop characteristics. Figure 6.20 shows typical heat-transfer materials for compact heat exchangers [4]. Figure 6.20a shows a *circular finned-tube array* with fins on individual tubes; Fig. 6.20b shows a *plain plate-fin matrix* formed by corrugation, and Fig. 6.20c shows a *finned flat-tube matrix* [4].

The heat-transfer and pressure-drop characteristics of such configurations for use as compact heat exchangers have been determined experimentally as explained earlier. Figures 6.21, 6.22, and 6.23 show typical heat-transfer and friction-factor data for three different configurations.

Note that the principal dimensionless groups governing these correlations are the Stanton, Prandtl, and Reynolds numbers [4]:

$$\text{St} = \frac{h}{Gc_p}, \quad \text{Pr} = \frac{c_p\mu}{k}, \quad \text{Re} = \frac{GD_h}{\mu}. \quad (6.20)$$

Here  $G$  is the *mass velocity* defined as

$$G = \frac{m}{A_{\min}} \text{ kg}/(\text{m}^2 \text{s}), \quad (6.21)$$

where  $m$  = total mass flow rate of fluid (kg/s) and  $A_{\min}$  = minimum free-flow cross-sectional area ( $\text{m}^2$ ) regardless of where this minimum occurs.

The magnitude of the *hydraulic diameter*  $D_h$  for each configuration is specified in Figs. 6.21, 6.22, and 6.23. The hydraulic diameter  $D_h$  is defined as

$$D_h = 4 \frac{LA_{\min}}{A}, \quad (6.22)$$

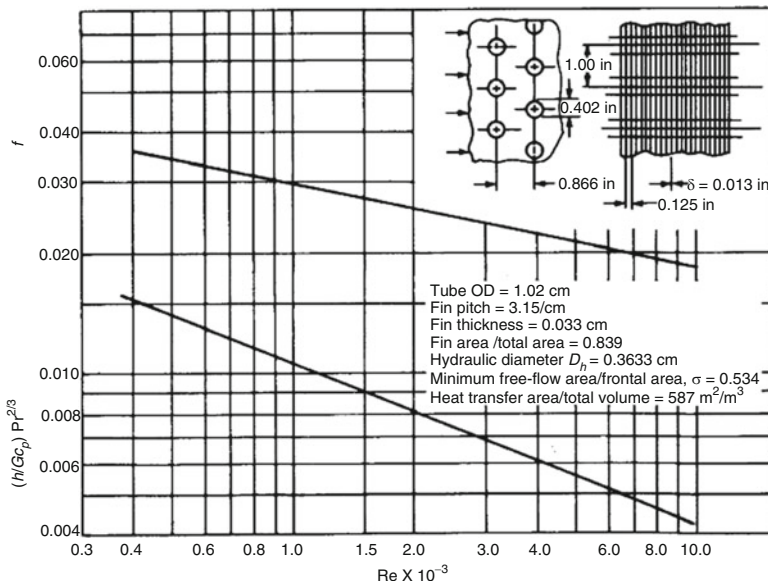


**Fig. 6.21** Heat transfer and friction factor for flow across plate-fin circular tube matrix (courtesy Kays and London)

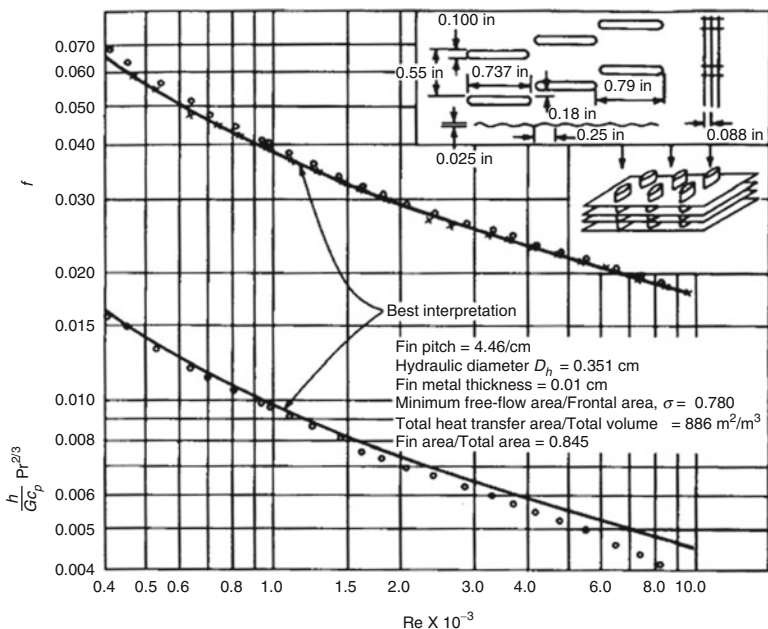


**Fig. 6.22** Heat transfer and friction factor for flow across finned flat-tube matrix (courtesy Kays and London)

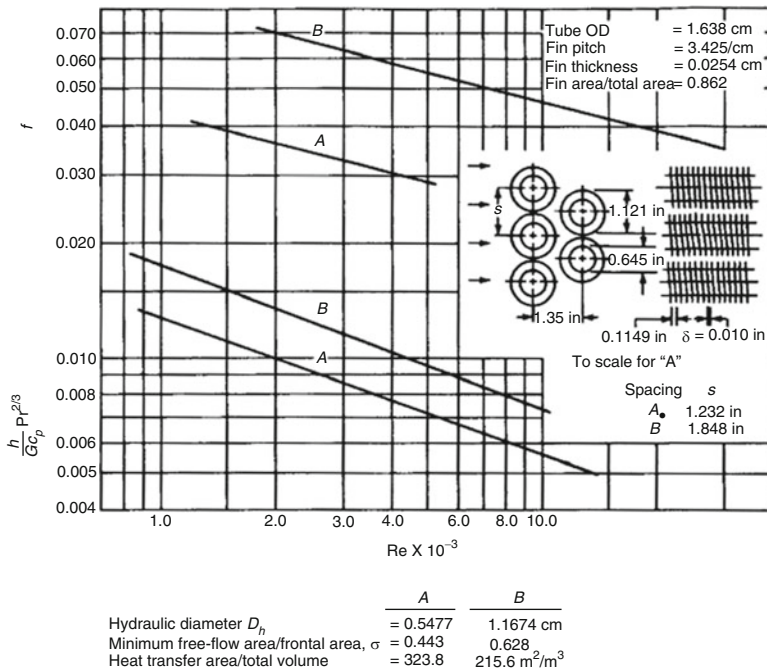


**Fig. 6.23** Heat transfer and friction factor for flow across circular finned-tube matrix (courtesy Kays and London)

where  $A$  is the total heat-transfer area and the quantity  $LA_{\min}$  can be regarded as the minimum free-flow passage volume since  $L$  is the flow length of the heat-exchanger matrix.

Thus, once the heat-transfer and the friction-factor charts such as those shown in Figs. 6.20, 6.21, 6.22, and 6.23 are available for a specified matrix, and the Reynolds number  $Re$  for the flow is given, the heat-transfer coefficient  $h$  and the friction  $f$  for flow across the matrix can be evaluated. Then the rating and sizing problem associated with the heat-exchanger matrix can be performed by utilizing either the LMTD or the effectiveness-NTU method of analysis.

## References

1. Fraas, A. P. (1989). *Heat exchanger design* (2nd ed.). New York, NY: Wiley Interscience.
2. Nenadi Ozisik, M. (1985). *Heat transfer: a basic approach*. New York, NY: McGraw-Hill.
3. Incropera, F., Dewitt, D., Bergman, T., & Lavine, A. (2007). *Introduction to heat transfer* (5th ed.). New York, NY: John Wiley & Sons.
4. Incropera, F., Dewitt, D., Bergman, T., & Lavine, A. (2011). *Fundamentals of heat and mass transfer* (7th ed.). New York, NY: Wiley.

5. Kays, W. M., & London, A. L. (1964). *Compact heat exchangers* (2nd ed.). New York, NY: McGraw-Hill.
6. Pansini, A. J., & Smalling, K. D. (1991). *Guide to electric power generation*. Liburn, GA: The Fairmont Press.
7. Boyen, J. L. (1975). *Practical heat recovery*. New York, NY: John Wiley & Sons.

# Chapter 7

## Effective Design of Compact Heat Exchangers for Next Generation Nuclear Plants

A number of technologies are being investigated for the Next Generation Nuclear Plant (NGNP) that will produce heated fluids at significantly higher temperatures than current generation power plants. The higher temperatures offer the opportunity to significantly improve the thermodynamic efficiency of the energy conversion cycle. Selection of the technology and design configuration for the NGNP must consider both the cost and risk profiles to ensure that the demonstration plant establishes a sound foundation for future commercial deployments. The NGNP challenge is to achieve a significant advancement in nuclear technology while at the same time setting the stage for an economically viable deployment of the new technology in the commercial sector soon after 2020. Energy is the elixir of life for the world's economy and for individual prosperity. Efforts being made for greater energy efficiency – especially in industrial countries – have indeed proved effective, as evidenced by the fact that energy consumption throughout the world is growing slower than gross domestic products. At the same time, however, the hunger for energy in quickly growing economies is leading to shifts in energy mixes – which drives undesired CO<sub>2</sub> emissions upward. In the conversion of primary energy to final and useful energy, technology from universities and national laboratories plus industry toward the design of the NGNP has made key contributions to the efficient handling of the resources of our planet.

### 7.1 Introduction

As stated in previous chapters, for a nuclear system to take advantage of combined-cycle technology, there are a number of changes to the plant components that have to be made. The most significant, of course, is that the combustion chamber must be replaced by a **heat exchanger** in which the working fluid from the nuclear reactor secondary loop is used to heat the air (Fig. 7.1). The normal Brayton cycle is an internal combustion one where the working fluid is heated by the combustion of the

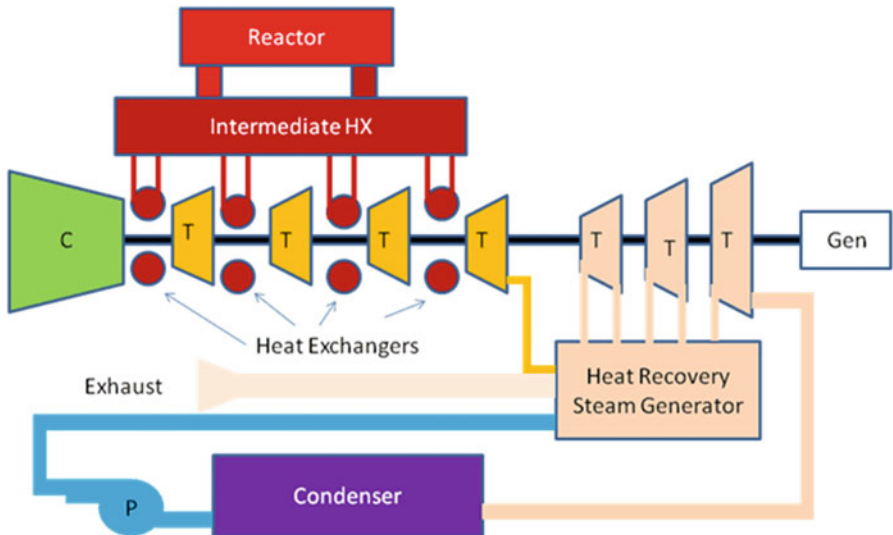


**Fig. 7.1** Layout for four-turbine combined cycle with intermediate heat exchanger

fuel with the air in the combustion chamber. The walls of the combustion chamber can be cooled and peak temperatures in the working fluid can be significantly above the temperature that the walls of the chamber can tolerate for any length of time.

For a nuclear reactor system the heat transfer is in the opposite direction. All reactor components and fluids in the primary and secondary loops must be at a higher temperature than the peak temperature of the gas exiting the heat exchanger. This severely restricts the peak temperature that can be achieved for air entering the turbine.

Out of six Generation IV configurations that the US Department of Energy (DOE) has selected, the high-temperature gas-cooled reactor (HTGR) design for the Next Generation Nuclear Plant (NGNP) project is a frontrunner for such an innovative approach. The NGNP will demonstrate the use of nuclear power for electricity and hydrogen production. It will have an outlet gas temperature in the range of 850–950 °C and a plant design service life of 60 years [1]. As part of our studies, we have also shown that in the air-Brayton combined-cycle (BCC) power system [2–8] and nuclear air-Brayton combined-cycle (NACC) power systems [9], the higher temperature for outlet gas, the better the chances of increasing the overall thermal efficiency of the power plant. This would make it more cost effective and more compatible with natural gas plants costwise, from both a total cost of ownership (TCO) and return on investment (ROI) point of view. The reactor design will be a graphite-moderated, helium-cooled, and prismatic or pebble-bed reactor and use low-enriched uranium, Tristructural-isotropic (TRISO)-coated fuel. The plant size, reactor thermal power, and core configuration will ensure passive decay heat removal without fuel damage or radioactive material releases during accidents. The NGNP material research and development (R&D) is responsible for

performing R&D on likely NGNP materials in support of the NGNP design, licensing, and construction activities.

As part of an IHX acquisition strategy, as well as its application in NGNPs, compact designs are attractive because they minimize the capital investment in materials, thereby yielding overall capital savings in footprint, volume, and structural support costs; however, they represent a significant technical risk at this stage of their development. Qualification of diffusion bonding methods and development of in-service inspection methods represent significant schedule risks.

Compact heat exchangers (CHEs) will lead to substantial capital savings, in connection with footprint, volume, and structural support costs, of up to 85 % over traditional technologies, such as shell-and-tube designs. Significant cost savings will be generated in the following areas:

- Reduced deck and skid volume required for implementation and installation,
- Reduced structural support requirements,
- Reduced pipe-work runs and sizing,
- Improved access for maintenance,
- Reduced relief and flare systems,
- Topside craneage for installation and maintenance.

CHEs would allow for an exceptionally high heat-transfer efficiency-to-volume ratio using methods such as printed circuit heat exchangers. Also, plate heat exchangers improve thermal management and economy in both fossil-fuel-fired and nuclear stations. The compact size, high-quality products, and ease of maintenance make them an attractive choice for new construction, retrofits, or capacity expansions. CHEs are a perfect fit in heating/condensing, liquid, gas, or two-phase operations where reliability, safety, and uptime are important considerations.

The definition of compactness is rather arbitrary [10]. The ratio of the heat-transfer surface area on one side of the heat exchanger to the volume can be used as a measure of the compactness of heat exchangers. A heat exchanger having a surface area density on any one side greater than around  $700 \text{ m}^2/\text{m}^3$  quite arbitrarily is referred to as a CHE regardless of its structural design. For example, automobile radiators having an area density on the order of  $1100 \text{ m}^2/\text{m}^3$  and the glass ceramic heat exchangers used in some vehicular gas-turbine engines having an area density on the order of  $6600 \text{ m}^2/\text{m}^3$  are CHEs. Human lungs, with an area density of about  $20,000 \text{ m}^2/\text{m}^3$ , are the most compact heat-and-mass exchangers. The very fine matrix regenerator for the Stirling engine has an area density approaching that of the human lung.

On the other extreme of the compactness scale, plane tubular and shell-and-tube type exchangers, having an area density in the range of  $70\text{--}500 \text{ m}^2/\text{m}^3$ , are not considered compact [10]. The incentive for using CHEs lies in the fact that a high value of compactness reduces the volume for a specified heat-exchanger performance.

When heat exchangers are to be employed in automobiles, marine uses, aircraft, aerospace vehicles, nuclear power plants, or any other power-generating plants, such as gas- or fossil-fuel-based plants, cryogenic systems, or refrigeration and air

conditioning systems, the weight, size, and, hence, the compactness become important. To increase the effectiveness or the compactness of heat exchangers, fins are used. In a gas-to-liquid heat exchanger, for example, the heat-transfer coefficient on the gas side is an order of magnitude lower than on the liquid side. Therefore, fins are used on the gas side to obtain a balanced design; the heat-transfer surface on the gas side becomes much more compact.

To obtain such a balanced design for heat transfer between two sides, we have to be concerned about pinch points. A pinch point is defined as a point where the temperature difference is at a minimum. The temperature difference at the pinch depends on the type of heat exchanger; in general, the smaller the temperature difference, the more expensive the heat exchanger.

If the simple Brayton cycle is modified to include a recuperator (which will transfer heat from the turbine exhaust to preheat compressed high-pressure air before going to the combustion chamber), less fuel will be required to obtain the desired turbine inlet temperature of the compressed air, and the optimum pressure ratio (for either the compressor or turbine) will be reduced to typically 3–4. This improves the thermal efficiency of the cycle. Alternatively, a regenerator can also be used replacing a recuperator. A number of regenerative cycles are presented by McDonald and Wilson [11].

## 7.2 Classification of Heat Exchangers

As we have learned so far, heat exchangers are devices that are designed to exchange heat. This constitutes a very broad category of devices, so first we need to focus our attention on heat exchangers that exchange heat between two fluids. These fluids can be gases or liquids. Even with this constraint, it is still difficult to provide an overview, and a classification needs to be made. It is possible to classify heat exchangers in a number of ways.

1. The first classification of heat exchangers depends on the basic path of the fluid as it goes through the heat exchanger. Thus, the differences in the fluids paths, as per our previous chapter, are identified as follows:
  - Parallel flow,
  - Counterflow, and
  - Cross flow.

Each of these categories was described in Chap. 6 and will be briefly described here as a refresher. Parallel-flow exchangers are those devices in which the warmed and cooled fluids flow past each other in the same direction, in contrast with the counterflow exchangers, where these two flow in the opposite direction. In the case of a cross flow, fluids flows pass at right angles to each other.

2. The second classification made depends on the state of the medium in the heat exchanger.
  - Liquid-to-liquid exchangers are those in which two liquids interact. Also in this group are gas-to-gas heat exchangers like air preheaters in steam plants and helium-cooled reactor gas-turbine plants. These devices operate with heat-transfer coefficients that are between 10 and 100 times lower than the coefficients of liquid-to-liquid exchangers.
  - Gas-to-gas exchangers are generally much larger and heavier if the same amount of transferred heat is demanded.
  - A third type is the liquid-to-gas heat exchanger (or vice versa), in which usually water and air are used, for instance in automotive radiators. Because of the lower heat-transfer coefficients on the gas side, fins are usually placed on the exchanging surfaces.
3. A third classification method is based on the purpose of the heat exchanger. Unlike the other classifications, this is not a designer's choice but a direct demand to fulfill the need for, say, an evaporator. So any demand based on this classification is generally a starting point from which the designer needs to make decisions about the other classifications, like the choice between counter-flows or cross flow.

Other examples of purpose classification are based on the cooler, which cools liquids or gases by means of water, the chiller, which cools a fluid with a refrigerant such as Freon to below a temperature that would be obtainable if water was used, and the condenser that condenses a vapor, often in the presence of a noncondensable gas (only shell-tube condensers; this is a classification based on where condensation occurs: horizontal in-shell, vertical in-shell, horizontal in-tube, and vertical in-tube).
4. The last classification is actually the most important choice of the designer of a heat-exchange system. This is the choice of what kind of construction will be used. In what follows are discussed the two most common options: double-pipe heat exchangers and shell-and-tube heat exchangers.

In summary all these classifications of heat exchangers are depicted in Figs. 7.2, 7.3, and 7.4.

Notice that in Fig. 7.2 the parameter  $\beta$  designates compactness or surface area density for heat exchangers. This quantitative parameter arbitrarily defines a compact heat exchange surface as one that has an area density greater than  $700 \text{ m}^2/\text{m}^3$  ( $213 \text{ ft}^2/\text{ft}^3$ ). The range of surface area density and hydraulic diameter for various types of CHE and heat-exchange surfaces can be found in Kay and London's book [17].

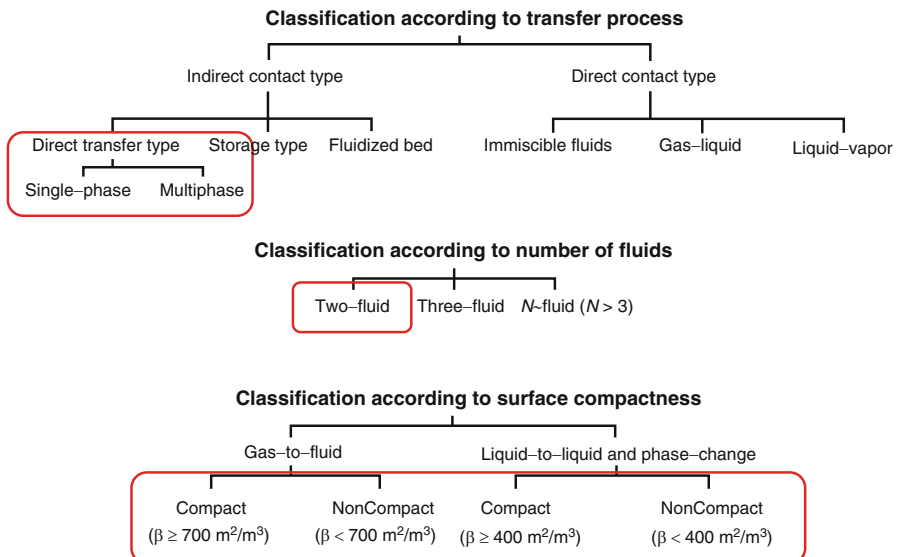


Fig. 7.2 Classification of heat exchangers according to transfer process

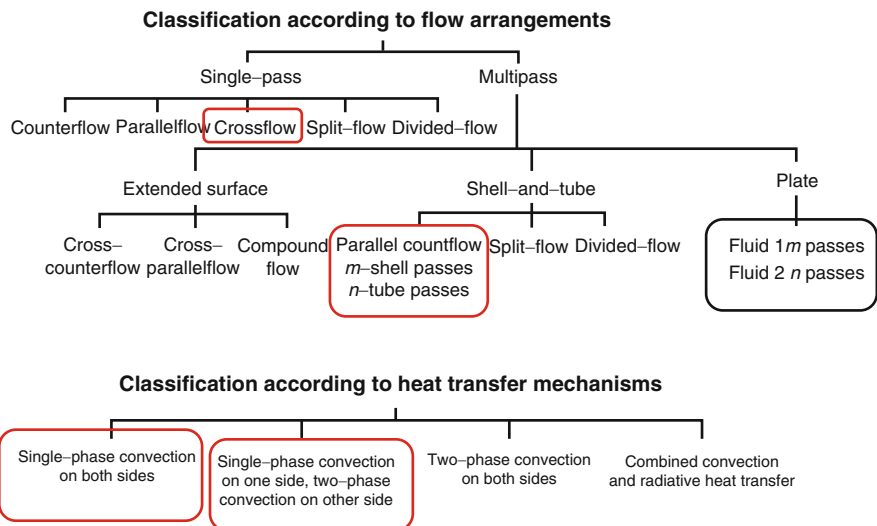
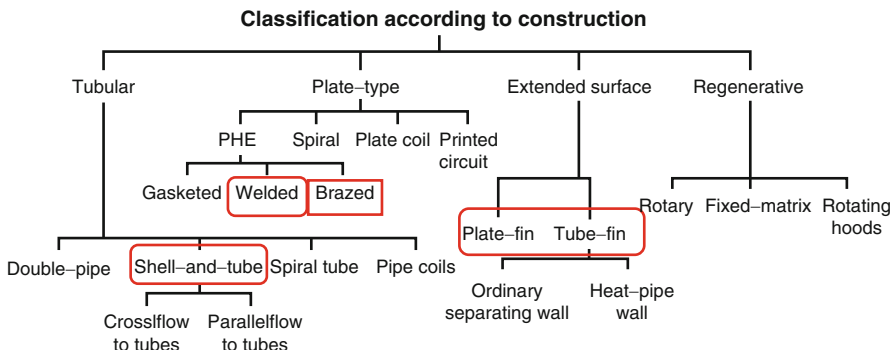


Fig. 7.3 Classification of heat exchangers according to flow arrangement



**Fig. 7.4** Classification of heat exchangers according to construction

### 7.3 Compact-Heat-Exchanger-Driven Efficiencies in Brayton Cycle

As we analyzed and demonstrated the modeling of computer code in Chap. 5 via a steady-state approach (i.e., transient analysis should be considered for greater accuracy sooner rather than later), if the simple Brayton cycle is modified to include a recuperator (which will transfer heat from the turbine exhaust to preheat compressed high-pressure air before going to the combustion chamber), it will require less fuel to obtain the desired turbine inlet temperature of compressed air, and the optimum pressure ratio (either for compressor or turbine) will be reduced to typically 3–4. This improves the thermal efficiency of the cycle. Alternatively, a regenerator can also be used, replacing the recuperator.

With a distributed power generation market, and renewed interest in nuclear power plants, in particular next generation and small modular reactors (SMRs), one of the most economical solutions today is to generate power through small gas-turbine systems in the form of a Brayton cycle combined with these reactors. These gas turbines can be arbitrarily categorized as microturbines (with output of 5–200 kW) and miniturbines (with output of 200–500 kW). The thermal efficiency of microturbines is about 20 % or less if no recuperator is used in the system. Using a recuperator (a regenerator can also be considered but it has a number of problems) operating at 87 % effectiveness, the efficiency of the gas-turbine system increases to around 30 %, a substantial performance improvement. However, the cost of the recuperator is around 25–30 % of the total power plant, so the TCO and ROI are not well justified.

This means that the heat exchanger or recuperator must be designed to yield high performance at minimum cost. While the offset strip fin geometry is one of the highest performing surfaces, it is also quite expensive to manufacture. This necessitates the use of all prime surface heat exchangers with no brazing as part of the heat-exchanger design and acquisition process.

As shown in Chap. 6, CHEs transfer more energy in a cost-effective manner than other heat exchangers and save more energy compared to standard technology. CHEs transfer heat from one fluid, either gas or liquid, to another. CHEs have a significantly greater surface area per unit volume than conventional types of heat exchangers. In terms of energy efficiency performance and capacity scheme, also known as the enhanced capital allowance (ECA) scheme, a CHE is defined as a heat exchanger with a surface-to-volume ratio greater than  $200 \text{ m}^2/\text{m}^3$ .

### **Energy Efficiency Performance and Capacity Scheme Also Known As Enhanced Capital Allowance Scheme**

The scheme calls for manufacturers and importers of refrigeration equipment to establish that their products conform to certain requirements on energy efficiency, performance, and capacity. Such equipment is then “ECA Registered” and appears on what is known as the Energy Technology List. Anyone purchasing equipment from the list will be entitled to 100 % tax relief on their investment in the first year.

The scheme was developed by the Internal Revenue and DEFRA (Department for Environment, Food and Rural Affairs) and is managed by the Carbon Trust.

To meet the requirements of the new ECA scheme, manufacturers must have their refrigeration equipment tested to prove that it conforms to various requirements on energy efficiency, performance, and capacity.

CHEs are characterized by a high surface area per unit volume, which can result in a higher efficiency than conventional heat exchangers; at a significantly smaller volume [typically CHEs can achieve efficiencies of over 95 % CF (cubic feet), 80 % noncompact heat exchangers].

CHEs transfer more energy in a cost-effective manner than other heat exchangers and save more energy compared to standard technology. Investments in CHEs can only qualify for enhanced capital allowances if the specific product appears on the Energy Technology Product list.

Four types of CHE are covered by the ECA scheme:

1. Plate heat exchangers,
2. Plate-finned heat exchangers,
3. Printed circuit heat exchangers,
4. CHEs with precision formed surfaces.

Each of these CHEs is briefly described in what follows.

#### **1. Plate Heat Exchangers**

A plate type heat exchanger is a type of heat exchanger that uses metal plates to transfer heat between two fluids. This has a major advantage over a conventional heat exchanger in that the fluids are exposed to a much larger surface area because



**Fig. 7.5** Typical schematic of plate heat exchangers (courtesy United Heat Exchanger Company, India) <http://www.heatexchanger.co.in/plate-heat-exchanger.html>

the fluids spread out over the plates. This facilitates the transfer of heat and greatly increases the speed of temperature change. It is not as common to see plate heat exchangers because they need well-sealed gaskets to prevent fluids from escaping, although modern manufacturing processes have made them feasible (Fig. 7.5).

The concept behind a heat exchanger is the use of pipes or other containment vessels to heat or cool one fluid by transferring heat between it and another fluid. In most cases, the exchanger consists of a coiled pipe containing one fluid that passes through a chamber containing another fluid. The walls of the pipe are usually made of metal or another substance with a high thermal conductivity to facilitate interchange, whereas the outer casing of the larger chamber is made of a plastic or coated with thermal insulation to discourage heat from escaping from the exchanger. The plate heat exchanger (PHE) was invented by Dr. Richard Seligman in 1923 and revolutionized methods of indirect heating and cooling of fluids.

A plate type heat exchanger is composed of multiple thin, slightly separated plates that have very large surface areas and fluid-flow passages for heat transfer. This stacked-plate arrangement can be more effective, in a given space, than a shell-and-tube heat exchanger. Advances in gasket and brazing technology have made the plate type heat exchanger increasingly practical. In HVAC applications, large heat exchangers of this type are called plate-and-frame; when used in open loops, these heat exchangers are normally of the gasket type to allow periodic disassembly, cleaning, and inspection. There are many types of permanently bonded plate heat exchangers, such as dip-brazed and vacuum-brazed plate varieties, and they are often specified for closed-loop applications such as refrigeration. PHEs also differ in the type of plate used and in the configurations of those plates. Some plates may be stamped with a chevron or other patterns, where others may have machined fins or grooves.

As part of the manufacturer specifications one can make the following observations:

- Liquid foods, such as milk, fruit juices, beer, wine, and liquid eggs, are pasteurized using PHEs.
- Wine and fruit juices are normally desiccated prior to pasteurization in order to remove oxygen and minimize oxidative deterioration of the products.
- PHEs consist of a large number of thin, vertical steel plates that are clamped together in a frame.

Their applications include the following:

- Plates produce an extremely large surface area, which allows for the fastest possible transfer.
- Making each chamber thin ensures that the majority of the volume of the liquid contacts the plate, again aiding exchange.
- Troughs also create and maintain a turbulent flow in the liquid to maximize heat transfer in the exchanger.
- A high degree of turbulence can be obtained at low flow rates, and a high heat-transfer coefficient can then be achieved.

A few advantages worth mentioning for this type of CHE are as follows:

- Easy maintenance and suitable for clean-in-place (CIP), and easily accessible plate pack;
- High heat-transfer coefficients;
- Flexibility to change plate arrangement and to add or remove plate;
- No mixing of product;
- Compact construction;
- Optimized heat recovery.

The disadvantages of PHEs are as follows:

- A bonding material between plates limits the operating temperature of the cooler.
- Overtightening of the clamping bolts results in an increased pressure drop across the cooler.
- The initial cost is high since titanium plates are expensive and titanium is a noble metal; other parts of the cooling system are susceptible to corrosion.
- With PHEs, careful dismantling and assembly are essential.

## 2. Plate–Fin Heat Exchangers

A plate–fin heat exchanger is made of layers of corrugated sheets separated by flat metal plates, typically aluminum, to create a series of finned chambers. Separate hot and cold fluid streams flow through alternating layers of the heat exchanger and are enclosed at the edges by side bars. Heat is transferred from one stream through the fin interface to the separator plate and through the next set of fins into the adjacent fluid.

The fins also serve to increase the structural integrity of the heat exchanger and allow it to withstand high pressures while providing an extended surface area for heat transfer (Fig. 7.6).

A high degree of flexibility is present in plate–fin heat exchanger designs as they can operate with any combination of gas, liquid, and two-phase fluids. Heat transfer between multiple process streams is also accommodated, with a variety of fin heights and types as different entry and exit points available for each stream.

This is a type of heat exchanger design that uses plates and finned chambers to transfer heat between fluids. It is often categorized as a CHE to emphasize its



**Fig. 7.6** Typical schematic of plate finned heat exchangers (courtesy United Heat Exchanger Company, India) <http://www.heatexchanger.co.in/plate-heat-exchanger.html>

relatively high heat-transfer surface-area-to-volume ratio. The plate-fin heat exchanger is widely used in many industries, including the aerospace industry, owing to its compact size and lightweight properties, as well as in cryogenics, where its ability to facilitate heat transfer with small temperature differences is an advantage. Plate-fin heat exchangers are generally used in industries where the fluids have little chance of fouling.

The following are manufacturer specifications of this type of exchanger:

- The four main types of fins are as follows: plain, which refers to simple straight-finned triangular or rectangular designs; herringbone, where the fins are placed sideways to provide a zigzag path; and serrated and perforated, which refer to cuts and perforations in the fins to augment flow distribution and improve heat transfer.

This type of heat exchanger has the following types of applications:

- Natural gas liquefaction,
- Cryogenic air separation,
- Ammonia production,
- Offshore processing,
- Nuclear engineering,
- Syngas production.

Advantages of this type of CHE:

- High thermal effectiveness and close temperature approach. (A temperature approach as low as 3 K between single-phase fluid streams and 1 K between boiling and condensing fluids is fairly common.)
- Large heat-transfer surface area per unit volume (typically  $1000 \text{ m}^2/\text{m}^3$ ).
- Low weight.
- Multistream operation (up to ten process streams can exchange heat in a single heat exchanger).
- True counterflow operation (unlike the shell-and-tube heat exchanger, where the shell side flow is usually a mixture of cross and counterflow).

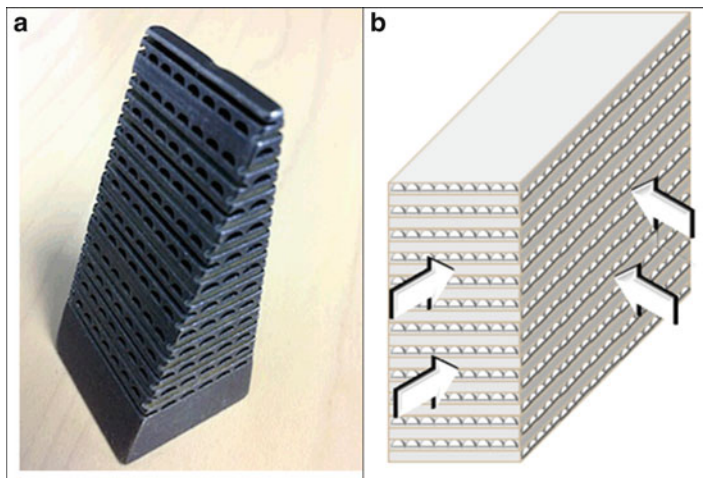


**Fig. 7.7** Example of typical PCHE block

### 3. Printed Circuit Heat Exchangers

This new type of exchanger was developed by Heatic Pty Ltd over the last 7 years (Johnston,<sup>1</sup> Johnston,<sup>2</sup> Reay<sup>3</sup>). Flat plates are photochemically etched with heat-transfer passages and then diffusion bonded together to form a solid block. The exchanger is illustrated in Fig. 7.7a, b, and a schematic cross section is shown in the figure. It is clear that the heat-transfer surface is effectively all primary. Entry and exit ports may be formed within the block, or alternatively headers may be welded onto the edges as with plate-fin exchangers.

The printed circuit heat exchanger (PCHE) is a compact type of heat exchanger and is an alternative to shell-and-tube heat exchangers. Its name is derived from the procedure used to manufacture the flat metal plates that form the core of the heat exchanger, which is done by chemical milling. These plates are then stacked and diffusion bonded, converting the plates into a solid metal block containing precisely engineered fluid flow passages. These channels are typically semicircular in cross section with a depth of 1.5–3 mm. PCHEs are typically built from stainless steels and can operate at temperatures from cryogenic to 800 °C (1500 °F).

<sup>1</sup> Johnston, A. et al. (1985). *Printed circuit heat exchangers for energy conservation*. End of Grant Report No 519, National Energy Research, Development and Demonstration Program, Australia.

<sup>2</sup> Johnston, A. et al. (1986, December). Miniaturized heat exchangers for chemical processing. *The Chemical Engineer*.

<sup>3</sup> Reay, D. A. (1990). *Novel techniques in heat exchanger design including printed circuit units*. Symposium on Advanced Heat Exchanger Design, Inst. Chem. Engr., Leeds, UK.

**Advantages of PCHEs:**

- Channels are optimized for countercurrent flow;
- High heat-transfer surface area per unit volume of the exchanger, resulting in reduced weight, space, and supporting structure;
- Used for temperature ranges of  $-200$  to  $900\text{ }^{\circ}\text{C}$ ;
- High pressure drops in excess of 600 bar;
- Reduced energy requirement and cost;
- Improved process design, plant layout, and processing conditions;
- Low fluid inventory compared to conventional designs such as shell-and-tube exchanger;
- Four to six times smaller and lighter than conventional designs such as shell-and-tube exchanger;
- Extremely high heat-transfer coefficients with small-hydraulic-diameter flow passages;
- Used for gases, liquids, and two-phase flows.

**Disadvantages:**

- Expensive compared to shell-and-tube units;
- Fluid needs to be extremely clean;
- Blockages can occur easily because of the fine channels ( $0.5$ – $2$  mm);
- Blockages can be avoided by fine filtration (typically  $300\text{ }\mu\text{m}$ ), but this will incur additional costs;
- Filters need to be cleaned regularly;
- Blockages require chemical cleaning, which can be difficult in some installations, and the system needs to be designed for this;
- Galvanic compatibility with the piping material can be an issue; an insulation kit or coated spool piece may be needed.

#### 4. CHEs with Precision Formed Surfaces

Among compact, efficient, and economical heat exchangers, those like Tranter<sup>4</sup> heat exchangers have one thing in common – heat transfer occurs through plates instead of tubes. As part of the precision formed surface, their spiral heat exchanger transfers heat through two spirally wound plates. Turbulent flow at low velocity produces high heat-transfer efficiency and low fouling. The result is compact units with small heat-transfer areas compared to conventional shell-and-tube exchangers. Plate exchangers conserve both materials and labor resources, reducing up-front costs and future operational costs. The prime surface heat exchangers have a configuration known as PLATECOIL, which looks like a tank, vessel, or reactor unit, and what is called IPF – Infinite PLATECOIL Flexibility. They come in various shapes, including tangent bends, pancakes, dished heads, cones, and

---

<sup>4</sup> <http://www.tranter.com/Pages/products/prime-surface/configurations.aspx>

bends around curves, all with precision and dimensional stability unequaled by dimpled sheet or pipe fabrications (see Figs. 7.8 and 7.9 below).

Though compact and light in weight, PLATECOIL panels can attain surprisingly high jacket operating pressure ratings. And because they deliver higher flow velocities than other technologies, heat transfer is improved and fouling reduced.

**Fig. 7.8** Single-embossed, curved PLATECOIL panels are fabricated into pressure reactors offering uniform and controlled heat distribution



**Fig. 7.9** Different angle view of PLATECOIL. (a) Single-embossed, curved PLATECOIL panels are fabricated into pressure reactors offering uniform and controlled heat distribution, though they are compact and lightweight. (b) PLATECOIL cone fabrication used to heat a viscous product for economical and efficient handling. (c) PLATECOIL clamp-on panels can be fabricated to bend around the corners of rectangular vats (courtesy Tranter Company, Wichita Falls, Texas)

### Fouling Factor

Fouling is a generic term for the deposition of foreign matter on a heat-transfer surface. Deposits accumulating in the small channels of a CHE affect both heat transfer and fluid flow. Fouling deposits constricting passages in a CHE are likely to increase the pressure drop and therefore reduce the flow rate. Reduced flow rate may be a process constraint; it reduces efficiency and increases the associated energy use and running costs. Maintenance costs will also increase. Fouling remains the area of greatest concern for those considering the installation of CHEs.

Fouling problems cannot be avoided in many heat exchanger operations, and it is necessary to introduce defensive measures to minimize fouling and the cost of cleaning. The fouling control measures used during either design or operation must be subjected to a thorough economic analysis, taking into consideration all the costs of the fouling control measures and their projected benefits in reducing costs due to fouling. Under some conditions, nearly asymptotic fouling resistances can be obtained, and this suggests a somewhat different approach to the economics.

The widespread installation of CHEs has been hindered by the perception that the small passages are more strongly affected by the formation of deposits.

For further information refer to the paper by Masoud Asadi and Ramin Haghighi Khoshkhoos\*.

\*Investigation into fouling factor in CHE, International Journal of Innovation and Applied Studies, Volume 2, Issue 3, March 2013, Pages 238–249

Vessel sides can be easily designed with two or more zones to efficiently satisfy diverse process requirements. Also, panels can be configured as internal baffles or mixers with heat exchanger surfaces for reduced cycle time. Heavy-gauge materials and special reinforcing features effectively withstand agitation forces.

Specially configured curved PLATECOIL panels are an economical means of converting existing unjacketed vessels to heated reactors, or of upgrading the thermal capacity of existing reactors. Standard units are available in 7 widths and 12 lengths, or in customized variations.

- Jacketed tanks and vessels
- Clamp-on upgrades
- Cryogenic shrouds
- Drum warmers
- Pipe coolers
- Gas cylinder heaters
- Heavy wall vessels and platens

CHEs are employed in many different applications because of their high surface area density. Plate-fin heat exchangers in particular are well suited for gas-to-gas and air-to-air recuperators and heat recovery units, among many other applications. In this chapter, fully or periodically developed laminar flows of air ( $\text{Pr} = 0.72$ ) inside a variety of different interfin channels of plate-fin heat exchangers, a constant property, are studied computationally, with the goal of achieving a better understanding of plate-fin heat exchangers and providing new designs with performance superior to the existing ones.

The majority of plate-fin channels have rectangular, trapezoidal, or triangular cross-sectional shapes. Their convective behavior for air flows is investigated and solutions and polynomial equations to predict the Nusselt number are provided. Besides the limiting cases of a perfectly conducting and insulated fin, the actual conduction in the fin is also considered by applying a conjugate conduction-convection boundary condition at the fin surface between partition plates. For the latter, new sets of solutions and charts to determine the heat-transfer coefficient based on the fin materials, channel aspect ratio, and fin density are presented.

Furthermore, while a large fin density increases the heat-transfer surface area, the convection coefficient can be increased by geometrical modification of the fins. To this end, two different novel plate-fin configurations are proposed by Huzayyin [13] and their convective behavior is investigated here. These include:

1. Slotted plate-fins with trapezoidal converging-diverging corrugations.
2. Offset-strip fins with in-phase sinusoidal corrugations.

The enhanced heat-transfer performance of the plate-fin compact core with perforated fin walls of symmetric, trapezoidally profiled, converging-diverging corrugations is modeled computationally. Airflow rates in the range  $10 \leq \text{Re} \leq 1000$  are considered in a two-dimensional duct geometry described by the trapezoid inclination angle, the convergent-divergent amplitude ratio, the dimensionless corrugation pitch, and a surface porosity  $\beta$  of 10 %. The fin-wall flow transpiration is seen to promote enhanced heat transfer by inducing cross-stream mixing and periodic disruption and restarting of boundary layers. With uniform heat flux  $H_I$  at the fin walls, an unusual performance is obtained where a higher Nusselt number is accompanied by a reduction in the corresponding friction factor, relative to a nonslotted geometry of the same dimensions.

In the case of sinusoidal wavy offset-strip channels, Huzayyin [13] showed that the performance enhancement could be evaluated for airflows in the range  $10 \leq \text{Re} \leq 1000$ , with fins at constant wall temperature  $T$ , and the effect of the wavy-fin amplitude, interfin spacing, and fin-offset position on the thermal-hydraulic performance is reported. It is generally seen that S-shaped offset channels perform better than C-shaped ones. An average of 400 % reduction in the volume of a plate-fin heat exchanger can be achieved with S-shaped offset fins when compared to that with plain parallel fins [13].

The use of CHEs for both single- and two-phase applications in the process industries is being actively encouraged. In this chapter the benefits of CHEs, as well

as their limitations, will be briefly reviewed; this will be followed by a description of a number of types of CHE, some well-established and others relative newcomers to the market.

## 7.4 Thermal Energy Transfer for Process Heat Application in Enhanced Mode

Recent technological developments in next generation nuclear reactors have created renewed interest in nuclear process heat for industrial applications. The NGNP will most likely produce electricity and process heat for hydrogen production. Process heat is not restricted to hydrogen production but is also envisioned for various other technologies such as the extraction of iron ore, coal gasification, and enhanced oil recovery. To utilize process heat, a thermal device is needed to transfer the thermal energy from the NGNP to the hydrogen plant in the most efficient way possible. There are several options for transferring multimegawatt thermal power over such a distance. One option is simply to produce only electricity, transfer it by wire to the hydrogen plant, and then reconvert the electrical energy to heat via Joule or induction heating. Electrical transport, however, suffers energy losses of 60–70 % because of the thermal-to-electric conversion inherent in the Brayton cycle. A second option is to transport thermal energy via a single-phase forced convection loop where a fluid is mechanically pumped between heat exchangers at the nuclear and hydrogen plants. High temperatures, however, present unique challenges for materials and pumping. Single-phase, low-pressure helium is an attractive option for NGNP but not suitable for a single-purpose facility dedicated to hydrogen production because low-pressure helium requires higher pumping power and makes the process very inefficient. A third option is two-phase heat transfer utilizing a high-temperature *thermosyphon*. Heat transport occurs via evaporation and condensation, and the heat transport fluid is recirculated by gravitational force. Thermosyphons have the ability to transport heat at high rates over appreciable distances, virtually isothermally, and without any requirement for external pumping devices.<sup>5</sup>

Heat pipes and thermosyphons have the ability to transport very large quantities of heat over relatively long distances with small temperature losses [12]. Applications of heat pipes and thermosyphons require heat sources for heating and heat sinks for cooling. The development of the heat pipe and thermosyphon was originally directed toward space applications. However, the recent emphasis on energy conservation has promoted the use of heat pipes and thermosyphons as components in terrestrial heat recovery units and solar energy systems. Thermosyphons have less thermal resistance, wider operating limits (the integrity of the wick material might not hold in heat pipes at very high temperatures), and

---

<sup>5</sup> [www.intechopen.com](http://www.intechopen.com)

lower fabrication costs than capillary heat pipes, which makes a thermosyphon a better heat recovery thermal device.

Perhaps the most important aspect of thermosyphon technology is that it can easily be turned off when required, whereas a heat pipe cannot be turned off. This safety feature makes the licensing of NGNP process heat-transfer systems comparatively easier. This section describes a thermosyphon system and the potential benefits of using it in order to transfer process heat from the nuclear plant to the hydrogen production plant.

For hot fluid inlet temperatures of less than around 675 °C, stainless steel material can be used for the heat exchanger, which has a reasonable cost. However, for higher inlet temperatures in heat exchangers associated with higher turbine inlet temperatures, superalloys are essential, which alone increases the material cost of the exchanger by a factor of 4 to 5.

Power generation is generally measured in megawatts. There is a need for low power generation in remote areas, greater grid power availability, emergency power, uninterrupted power, and other reasons. With the decentralization of power generation services, distributed power generation is becoming more widespread. The common mode is to generate power by a diesel engine. This is a costly method of power generation. The alternative is to generate electricity using a gas turbine in a simple Brayton cycle. Gas-turbine technology has advanced considerably over the last 60 years, and power generation on a large scale (in megawatts) is common, particularly in hydro and thermal power plants. Though gas-turbine technology for smaller power ranges (5–500 kW) has developed, it is very costly [14].

Gas turbines generating power in the 5–200 kW range are referred to as *microturbines* and those in the 200–500 kW range are called *miniturbines* (McDonald).<sup>6</sup> We will now briefly summarize microturbine technology.

### **Definition of Microturbine**

A microturbine implies a small compact gas-turbine-based power system and includes a turbocompressor (a turbine and compressor on a single shaft), a combustion chamber, and a generator, with a recuperator as an optional component. However, almost all microturbines require recuperators to achieve desirable system thermodynamic efficiency.

As stated in Chap. 5, if the simple Brayton cycle is employed and modified to include a recuperator (which will transfer heat from the turbine exhaust to preheat compressed high-pressure air before going to the combustion chamber), it will require less fuel to obtain the desired turbine inlet temperature of the compressed air, and the optimum pressure ratio (for either the compressor or turbine) will be reduced to typically 3–4. This improves the thermal efficiency of the cycle [14].

---

<sup>6</sup> McDonald, C. F. (2003). Recuperator considerations for future higher efficiency microturbines. *Applied Thermal Engineering* 23, 1463–1487.

Alternatively, a regenerator can also be used replacing a recuperator. A number of regenerative cycles are presented by McDonald and Wilson [11]. However, the durability and air-to-gas leakage problems are serious enough that the recuperator is not being considered after over 50 years of development. Regenerator development also started after the Second World War. Very high-performance brazed plate-fin type recuperators have been developed and are being used in large systems today. Owing to cost pressures, the modern recuperator designs for microturbine systems use prime surfaces on both fluid sides with no brazing, just stacking, and welded at the side edges to form airflow passages to prevent leaks and the mixing of the fluids. This allows high heat-transfer performance with a low pressure drop, an essential design requirement today. Since both fluids are gases (compressed air and turbine exhaust gas) in the heat exchanger, the design of inlet and outlet manifolds to ensure good flow distribution through the core on both fluid sides is a challenging task [14].

### Brazing Process

Brazing is a metal-joining process whereby a filler metal is heated above the melting point and distributed between two or more close-fitting parts by capillary action. The filler metal is brought slightly above its melting (liquid) temperature while being protected by a suitable atmosphere, usually a flux. It then flows over the base metal (known as wetting) and is then cooled to join the work pieces together. It is similar to soldering, except the temperatures used to melt the filler metal are higher for brazing.

When using a recuperator in a microturbine, the recuperator cost is around 25–30 % of the microturbine system. When a significant cost reduction is necessary, a brazed plate-fin type costly recuperator is not acceptable. The alternative is to use a high-performance prime surface recuperator without brazing. This avoids costly fin manufacturing and brazing, reducing the cost of the recuperator without performance reduction [14].

As part of the design criteria for such a recuperator one should follow the major steps in the design and development of a gas-to-gas recuperator of a CHE (R. K. Shah) [14] as follows:

- Determine the approximate core size using prior empirical data and finite-difference tools.
- Manufacture a heat-transfer surface and test to determine  $j$  (Colburn factor  $j = StPr^{2/3}$ ) and  $f$  (Fanning friction factor; some textbooks show this as  $f_c$ ) nodes vs. Reynolds (Re) number design data. The basic performance data for an enhanced surface are shown as curves of the Colburn factor  $j$ , and the Fanning friction factor  $f$ , plotted versus Reynolds number Re. Kays and London [17] present  $j$  and  $f$  vs. Re for a large number of compact surfaces, in one of the first comprehensive collections of data on enhanced surfaces for CHEs.
- Determine core size and tool sample plates for manufacturing development and test cores.

- Analyze the flow and temperature in the core using computational fluid dynamics (CFD) to predict the flow and temperature distribution and to verify performance.
- Compute thermal stresses using transient temperature distribution models input into a finite-element analysis program. If the thermal stresses are not acceptable, modify appropriately the heat-transfer surface design.
- Build, instrument, and test cores to verify thermal models.
- Refine the design to mitigate risks brought to light by analysis and test results.

Some of the materials used for CHEs (recuperator) include 300 series stainless steel (AISI 347 SS) for temperatures below around 675 °C, Inconel 625, Inconel 803, Haynes 120, Haynes 214, and PM2000 materials up to around 900 °C. For a 50 kW microturbine, the recuperator should weigh around 40 kg, and the thin-foil stainless steel should cost about \$12/kg. Thus, in round figures the recuperator material should cost around \$500 (McDonald) [15, 16].

While the plate-fin recuperator technology and manufacturing processes are known, there is good design flexibility and the recuperator should be lightweight. There are some important limitations on the plate-fin design: high material and capital costs, long braze cycle, potential for high repair rate, limited material flexibility, complex assembly, and difficult automated manufacturing. Thus the current emphasis is on the development of a recuperator using a primary surface only with the following attributes (R. K. Shah) [14]:

- The basic core construction consists of a laser-welded stack of stamped plates (one or two parts).
- The simple construction leads to a highly robust design.
- A fully automated laser welding process is possible to seal side edges and form flow passages on one fluid side. Laser welding eliminates the high cost of nickel braze materials that are traditionally used in high-temperature heat exchangers.

In order for a combined cycle in the form of a Brayton cycle configuration to be economically viable, the recuperator or heat exchanger used in it as a component of the system must be cost effective and compact for applications that require compact packaging. One such application is a hybrid engine with a microturbine generating electricity at the maximum efficiency and a hybrid vehicle then running on the electricity or direct-drive vehicles. For an automotive application with an engine power rating of 65–100 kW and cost of \$25/kW, the recuperator should be manufactured for about \$150. Such an exchanger should operate at high temperatures, involve low-cost manufacturing methods, and be easy to replace or maintain (McDonald and Wilson) [11].

In summary, in the search for a special surface geometry to enhance heat transfer in an industrial heat exchanger application, in particular for NGNPs, there are many options. Now the question is:

## How can one compare the performance improvement from various enhanced surfaces?

Certainly, one can judge the relative heat-transfer enhancement for selected geometries by comparing the heat-transfer coefficients or dimensionless heat-transfer parameters (e.g., Nusselt number, Stanton number) yielded by each enhanced surface. But this will only give a partial indication of performance [18, 19].

Enhanced surfaces do provide a greater heat-transfer coefficient, but they also lead to increased fluid flow friction and pressure drop. Sometimes, the benefits gained from heat-transfer enhancement are not great enough to offset the increased friction losses. Clearly, then, the performance goal is to gain maximum enhancement of heat transfer with minimum penalty on pumping power. However, this balance is difficult to quantify in a manner that allows straightforward comparisons between various enhanced surface geometries.

Generally speaking, heat-transfer surfaces can be used for three purposes:

1. To make heat exchangers more compact in order to reduce their overall volume and, possibly, their cost;
2. To reduce the pumping power required for a given heat-transfer process; or
3. To increase the overall *UA* value of the heat exchanger.

### Heat Exchanger value of UA

Nearly all heat-transfer equipment can be analyzed from the following basic design equation:

$$q = UA\Delta T, \quad (1)$$

which relates the heat flow rate or duty ( $q$ ) to the driving force or temperature difference ( $\Delta T$ ) by a proportionality constant ( $UA$ ), where  $U$  is a coefficient and  $A$  is the heat-transfer area. Heat exchanger analyses usually involve the process of determining the  $UA$  required for the process to operate and comparing that to the  $UA$  available.

The  $UA$  required is normally determined based only on thermodynamics. The  $UA$  available is calculated from the heat exchanger geometry and the transport properties of the fluid.

A higher  $UA$  value can be exploited in one of two ways:

1. To obtain an increased heat exchange rate for fixed fluid inlet temperatures or
2. To reduce the mean temperature difference for the heat exchange; this increases the thermodynamic process efficiency, which can result in a saving of operating costs.

Enhancement techniques can be separated into two categories [20]:

#### 1. Passive:

Passive methods require no direct application of external power. Instead, passive techniques employ special surface geometries or fluid additives that cause heat-transfer enhancement;

## 2. Active:

On the other hand, active schemes, such as electromagnetic fields and surface vibration, do require external power for operation.

The majority of commercially interesting enhancement techniques are passive ones. Active techniques have attracted little commercial interest because of the costs involved and the problems associated with vibration or acoustic noise [21].

Special surface geometries provide enhancement by establishing a higher  $hA$  per unit base surface area, where  $h$  is the heat-transfer coefficient and  $A$  is the heat-transfer surface area on the same fluid side for which value of  $h$  is mentioned.

Clearly, there are three basic ways of accomplishing this [21]:

1. Increase the effective heat-transfer surface area ( $A$ ) per unit volume without appreciably changing the heat-transfer coefficient ( $h$ ). Plain fin surfaces enhance heat transfer in this manner.
2. Increase  $h$  without appreciably changing  $A$ . This is accomplished by using a special channel shape, such as a wavy or corrugated channel, which provides mixing owing to secondary flows and boundary-layer separation within the channel. Vortex generators also increase  $h$  without a significant area increase by creating longitudinally spiraling vortex exchange fluid between the wall and core regions of the flow, resulting in increased heat transfer.
3. Increase both  $h$  and  $A$ . Interrupted fins (i.e., offset strip and louvered fins) act in this way. These surfaces increase the effective surface area and enhance heat transfer through repeated growth and destruction of the boundary layers.

In forced-convection heat transfer between a gas and a liquid, the heat-transfer coefficient of the gas may be 10–50 times smaller than that of the liquid. The use of specially configured surfaces can be used to reduce the gas-side thermal resistance. For heat transfer between two gases, the difficulty in inducing the desired heat exchange is even more pronounced. In this case especially, the use of enhanced surfaces can substantially reduce heat exchanger size. This is the motivation behind the design of a category of heat exchangers with reduced size and greatly enhanced gas-side heat transfer, which are referred to as *compact*.

A CHE is generally defined as one that incorporates a heat-transfer surface having a high area density. In other words, it possesses a high ratio of heat-transfer surface area to volume. This does not necessarily mean that a CHE is of small mass or volume.

Figure 7.10 shows a spectrum of surface area density for heat exchangers. The range of surface area density and hydraulic diameter is given for various types of heat exchange surfaces, with the dividing line for compactness clearly marked.

Compact surfaces are utilized to yield a specified heat exchanger performance  $q/\Delta T_{\text{mean}}$ , within acceptable mass and volume constraints, where is calculated by using Eqs. (7.1a) and (7.1b) as follows:

$$\frac{q}{\Delta T_{\text{mean}}} = U\beta V \quad (7.1a)$$

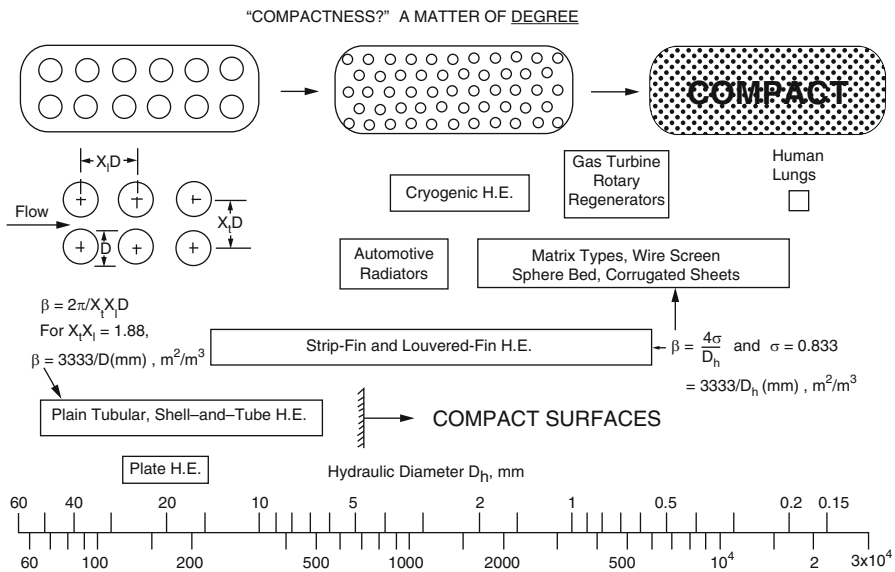


Fig. 7.10 Heat-transfer surface area density ( $\beta$  m<sup>2</sup>/m<sup>3</sup>)

or

$$\frac{q}{\Delta T_{\text{mean}} \beta} = UV \quad (7.1b)$$

Analyzing Eq. (7.1b), it is obvious that a high  $\beta$  decreases the volume. Furthermore, compact surfaces generally result in higher overall conductance,  $U$ . And since compact surfaces can achieve structural strength and stability with thinner sections, the reduction in heat exchanger mass is even more pronounced than the reduction in volume [22].

Various techniques can be used to make heat exchangers more compact. Figure 7.11 shows three general types of extended-surface geometries that can be used to increase gas-side heat-transfer coefficients.

These include:

- A finned-tube heat exchanger with flat fins,
- A finned-tube heat exchanger with individually finned tubes, and
- A plate-fin heat exchanger.

This paper focuses on various types of plate-fin geometries.

A typical element of a plate-fin heat exchanger consists of a die-formed **fin** (type of material) plate sandwiched between flat metal separator plates, as shown in Fig. 7.12.

These heat exchangers are widely used in cryogenic applications because of their low cost, small size, light weight, high thermal capacity, and effectiveness relative to other types of heat exchangers. The result of the improved effectiveness is the achievement of true countercurrent flow where there is an increase in the temperature spread and a closer approach to the ideal. This means that the refrigerant cooling curve is closer to the natural gas cooling curve [19].

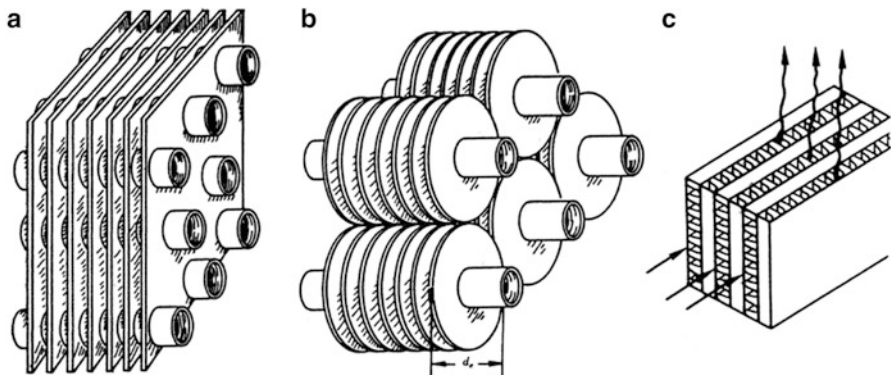


**Fig. 7.11** (a) Finned-tube heat exchanger with flat fins, (b) individually finned tubes, (c) plate-fin heat exchanger [17]

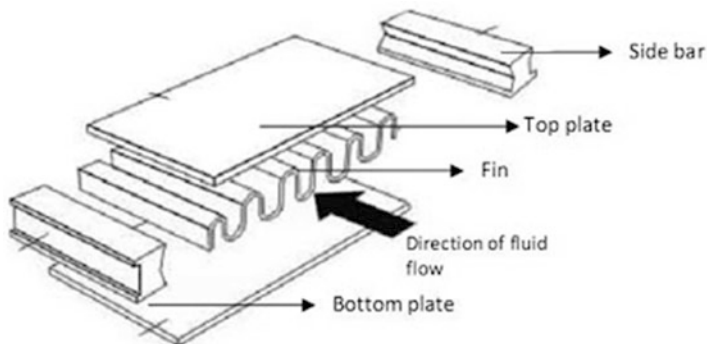


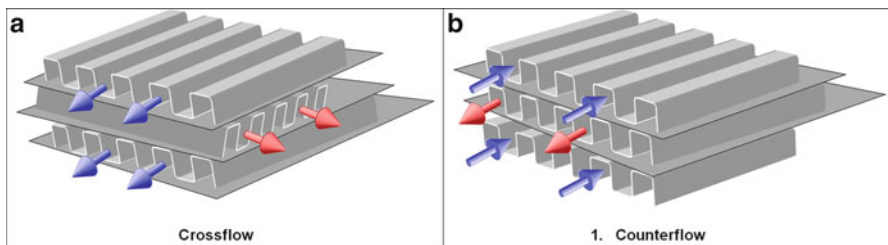
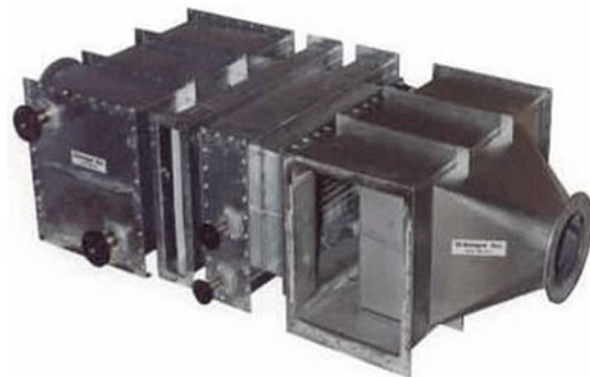
**Fig. 7.12** Construction details of a typical single-element plate-fin heat exchanger

The exchanger is made up of manifolds or headers that consist of elements. A manifold and an element are shown in Figs. 7.6 and 7.13 respectively. An element is made up of a corrugated die-formed fin plate placed between flat metal separator plates. There are side bars along the outside of the fin sections. A stack of the elements is welded to form a rigid matrix and can be designed to meet any configuration and size requirements. The stacks are welded onto the manifolds. Depending on the application, a number of manifolds can be assembled to form the heat exchanger.

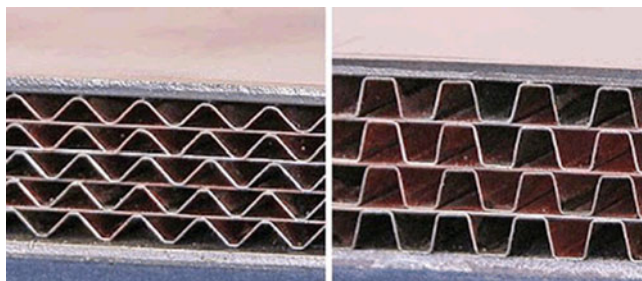
The wavy configuration of the fin promotes (Fig. 7.11) turbulence and therefore improves heat transfer. This increase in heat transfer is accompanied by an increase in pressure drop. This is a problem with low-density fluids like gases because of the extra work required to surmount the pressure drop.

Figure 7.14a, b shows the side bars located along the outer edges of the **fin** sections, while Fig. 7.15 shows the installed stack of these manifold headers.

**Fig. 7.13** Manifold or header (courtesy xchanger.com)



**Fig. 7.14** (a) Cross-flow and (b) counterflow arrangements of plate-fin heat exchangers



**Fig. 7.15** Fin configurations

This work is often much higher than the increase in heat transfer acquired from the fins. For applications where any fin configuration other than the simplest is proposed, a thorough analysis of the effect on the system should be conducted.

In designing a plate-fin heat exchanger, it is possible to have different heights of the alternating fin plates. There is no requirement to have the same height or spacing of separator plates. This is a useful freedom to have in situations where the difference in density of the hot and cold fluids is large. In cryogenic systems, the refrigerant stream entering the expander has a higher density than the stream

coming out of the expander. In this kind of situation, it is necessary to use a greater height for the lower-density stream so that a common Reynolds number and, therefore, heat-transfer coefficient,  $U$ , can be attained.

Aluminum is the usual material of construction in plate-fin heat exchangers for cryogenic applications.

Stacks of such elements are then welded or dip-brazed to form large heat-exchange devices like those in Fig. 7.16. A wide variety of plate-fin geometries have been used to obtain enhanced heat transfer, and engineers are constantly working to develop new and more effective enhanced surfaces [19].

Six commonly used plate-fin geometries are shown in Fig. 7.17.

**Fig. 7.16** Large matrix of plate-fin heat exchanger elements [19]

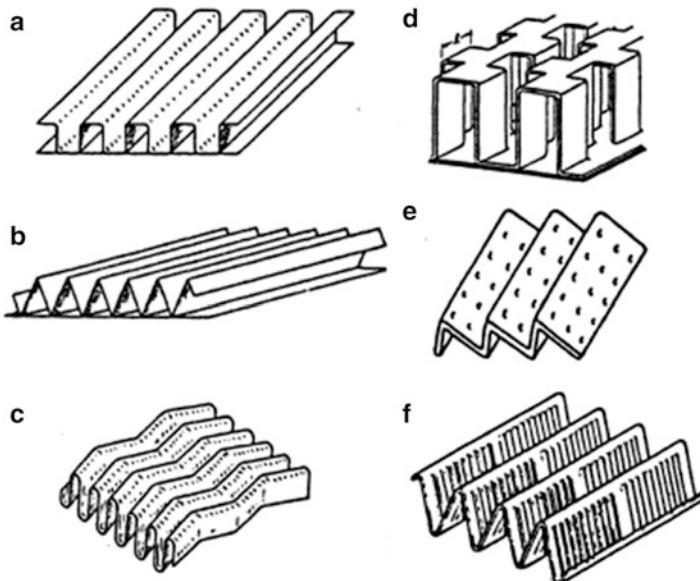
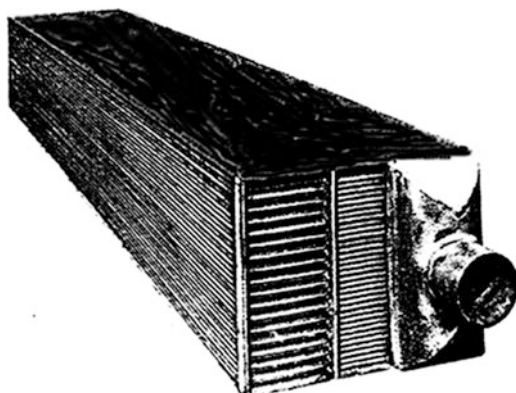


**Fig. 7.17** (a) Plain rectangular fins, (b) plain triangular fins, (c) wavy fins, (d) offset strip fins, (e) perforated fins, (f) louvered fins [19]

Typical fin spacings are 300–800 fins/m. Because of their small hydraulic diameter and the low density of gases, these surfaces are usually operated in a Reynolds number range of  $500 < \text{Re} < 1500$ . As a result, plate-fin enhancement geometries must be effective in the low-Reynolds-number regime. For example, surface roughness has been shown to promote heat transfer in the turbulent regime, but it does not provide appreciable enhancement in the lower-Reynolds-number range [19].

## 7.5 Design Criteria for Process Heat Exchangers

There are some criteria that a process heat exchanger must satisfy; they are easily enough stated if we confine ourselves to a certain process. The criteria are as follows.

The heat exchanger must meet the process requirements. This means that it must effect the desired change in the thermal condition of the process stream within the allowable pressure drops. At the same time, it must continue doing this until the next scheduled shutdown for maintenance.

The heat exchanger must withstand the service conditions of the environment of the plant, which includes the mechanical stresses of installation, startup, shutdown, normal operation, emergencies, and maintenance. In addition, the heat exchanger must also resist corrosion by the environment, processes, and streams. This is mainly a matter of choosing the right construction materials, but mechanical design does have some effect.

The heat exchanger must be maintainable, which usually implies choosing a configuration that permits cleaning and replacement. To do this, the limitations are the positioning of the exchanger and providing clear space around it. Replacement usually involves tubes and other components that may be especially vulnerable to corrosion, erosion, or vibration.

The cost of the heat exchanger should be consistent with requirements. Meaning of the cost here implement to the cost of installation. Operation cost and cost of lost production due to exchanger malfunction or lack of availability should be considered early on in the design process.

The limitations of the heat exchanger relate to length, diameter, weight and tube specifications due to plant requirements and process flow.

As part of the design methodology, we need to look at design in terms of an activity aimed at providing complete descriptions of an engineering system such as, in our case, a combined cycle of an open air-Brayton cycle or part of a system or just of a single system component. By identifying a well-defined design methodology, we can clear a path to specify the system/components and their structure, size, and performance, as well as other characteristics that are important for manufacturing and utilization, such as the next generation of nuclear power plants. This is a

very important point of departure for any combined-cycle drive efficiency upward for either an open or closed cycle.<sup>7</sup>

In considering the scope and formulation of these activities, one must understand that the design methodology must be applicable to a very complex structure. Furthermore, a design methodology for a heat exchanger as a subcomponent of a system must be consistent with the *life-cycle design* of the system, which includes the following stages [23]:

- Problem formulation including interaction with end user;
- Concept development, such as the selection of preliminary and workable designs;
- Detailed exchanger design that includes design calculations and other important pertinent considerations;
- Manufacturing and cost effectiveness;
- Utilization considerations, such as operation, life cycle, phase-out, and final disposal;

These various quantitative and qualitative design aspects and their interaction and interdependence allow us to arrive at an optimum heat-exchanger design. Figure 7.18 illustrates a methodology for designing a new single heat exchanger from a holistic point of view and can be characterized as a *one-time case study* method that includes [23]:

- Process and design specifications;
- Thermal and hydraulic design;
- Mechanical design;
- Manufacturing considerations and costs, both total cost of ownership and return on investment;
- Tradeoff factors and system-based optimization.

These design considerations are usually not sequential; there could be strong interactions and feedback among the aforementioned considerations, as indicated by the double-sided arrows in Fig. 7.17, and may require a number of iterations before the design is finalized.

As part of the augmentation of the previously described design methodology, based on the problem of specifications and experience, the heat exchanger construction type and flow arrangement constitute the first line of selection criteria for such a subsystem of a larger system. For example, in the case of an open air-Brayton cycle, as part of enhancing its overall output efficiency (Chap. 5), a cross-flow or counterflow pattern for a CHE subsystem was the most promising, according to the computer code generated and related analysis and calculations.

---

<sup>7</sup> While the Department of Nuclear Engineering of the University of New Mexico, under the leadership of Dr. McDaniel, together with the present author, studied open air-Brayton cycles, Sandia National Laboratories is investigating CO<sub>2</sub> closed-loop cycles.

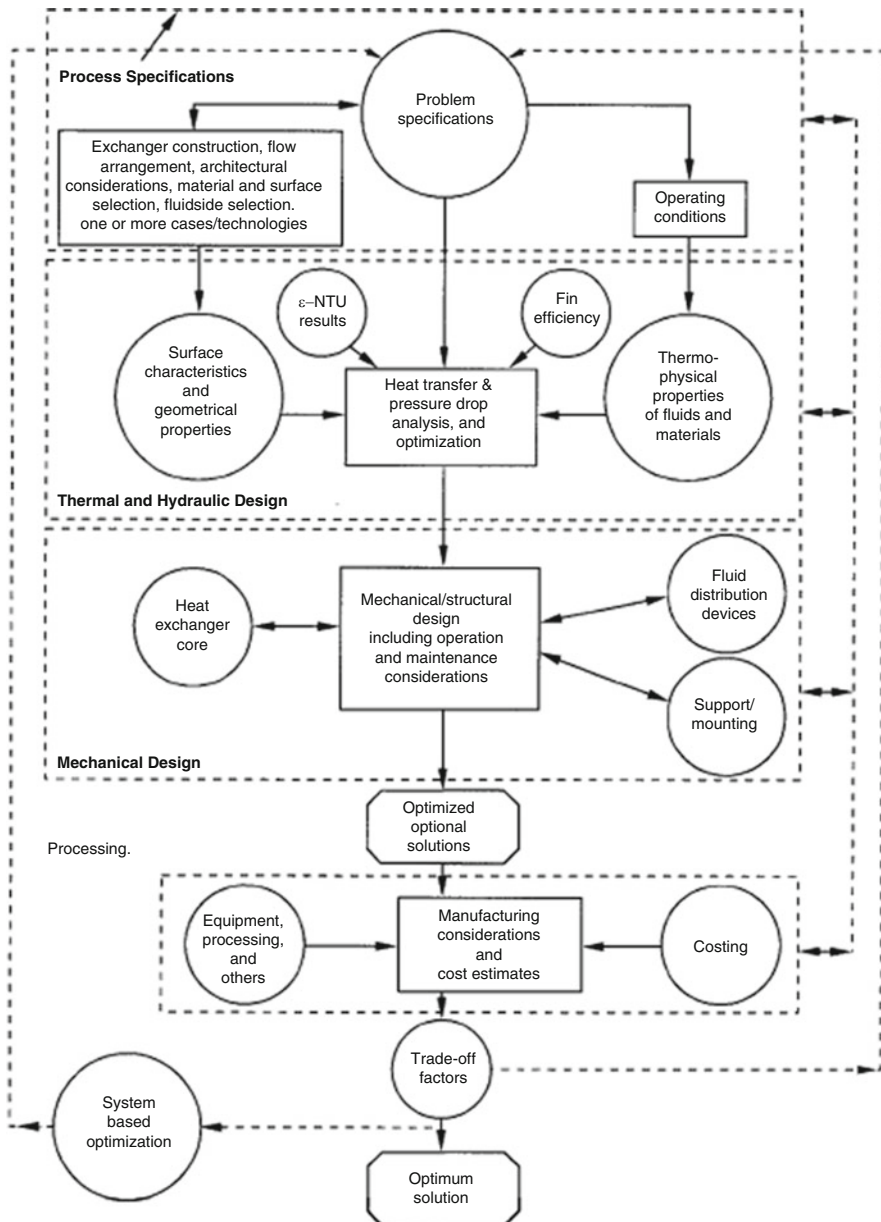


**Fig. 7.18** Heat exchanger design methodology (modified from Shah, 1982; Taborek, 1988; and Kays and London, 1998) [23]

As stated earlier, the analysis was done on the basis of the steady-state case and the code was developed for this infrastructure.

In summary the selection criteria and construction type depend on the following parameters:

1. Fluids (gas, liquids, or condensation/evaporation) used on each side of a two-fluid heat exchanger,
2. Operating pressure and temperature,
3. Fouling,
4. Surface selection to enhance the mode of efficient heat transfer,
5. Whether or not leakage or contamination of one fluid to the other is permitted,
6. Cost and available heat exchanger manufacture technology for production and commercial purposes not R&D and prototype,
7. Preventive maintenance (PM) and intended life cycle.

As part of the design methodology, one can also use the following chart, in particular for the design of a CHE, so one can go through processes faster (Fig. 7.19).

Factors that influence the surface selection include, for example, the operating pressure, fouling, maintenance requirements, erosion, fabrication, and cost.

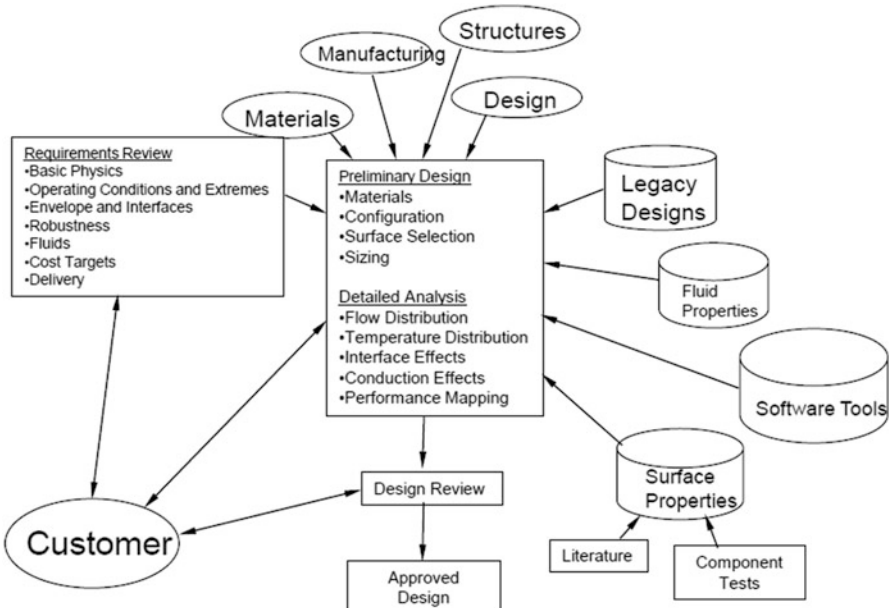


**Fig. 7.19** Compact heat exchanger design methodology steps and process

## 7.6 Thermal and Hydraulic Design

Heat exchanger thermal and hydraulic design and analysis involves a complex analysis and quantitative heat transfer and pressure drop (in case of transient analysis rather than steady-state) or exchanger size. So in today's modern computer capabilities most of thermodynamics design method and iteration of processes to find the most efficient gain and optimization are done via Computational Fluid Dynamics (CFD) and design methods and inputs to these analysis are summarized as follows, which depends on the type of exchanger:

- **Basic Thermohydraulic Design Methods:**

P-NTU, log mean temperature difference (LMTD),  $\varepsilon$ -NTU, or  $\psi$ -P methods .

- **Thermophysical Properties:**

For any analysis of pressure drop and heat transfer, the following thermophysical fluid properties (gas-to-gas or gas-to-fluid as media for heat exchange) are needed; they are defined as follows:

- $\mu$  = dynamic viscosity,
- $c_p$  = specific heat at constant pressure,
- $k$  = thermal conductivity,
- $\gamma$  = surface tension.

Note that for the conduction wall, thermal conductivity is needed.

- **Surface Geometrical Properties:**

For the purpose of pressure-drop and heat-transfer analysis, at a minimum the following surface geometrical properties are required on each side of a two-fluid heat exchanger:

- $A$  = heat-transfer area, which includes both primary and secondary surface area, if any;
- $A_{fr}$  = core frontal area;
- $A_a$  = minimum free flow area;
- $D_h$  = hydraulic diameter;
- $L$  = flow length;
- $V$  = core volume;
- $T, W$  = fin thickness and fin conduction length;
- $L_1, L_2, L_3$  = core dimensions.

These quantities are obtained from a computation of the basic dimensional layout of the core and heat-transfer surface. In the case of shell-and-tube type heat exchangers, one should take into consideration various leakage and bypass flow areas as well.

- **Surface Characteristics:**

For the purpose of characterizing the surface, heat transfer  $j$  and flow friction  $f$  are key inputs for the exchanger heat transfer and pressure-drop analysis, respectively [18]. Experimental results for a variety of CHEs are presented in

Kays and London [17]. More references on  $j$  and  $f$  factor are furnished in Shah and Sekulic [23], Chap. 4.

- **Heat Exchanger Specification Sheet:**

A heat exchanger specification sheet is an important fact sheet to help you with the design methodology of your choice and the type of heat exchanger for the intended application. Many Microsoft Excel Sheet templates can be found on the Internet and are downloadable free of charge.<sup>8</sup> A sample sheet is shown here in Fig. 7.20.

### 7.6.1 Equations and Parameters

The heat exchanger design equation can be used to calculate the required heat-transfer surface area for a variety of specified fluids, inlet and outlet temperatures, and types and configurations of heat exchangers, including counterflow or parallel flow. A value is needed for the overall heat-transfer coefficient for the given heat exchanger, fluids, and temperatures. Heat-exchanger calculations can be made for the required heat-transfer area or the rate of heat transfer for a heat exchanger of area that is given.

Heat-exchanger theory leads to the basic heat exchanger design equation:

$$q = UA\Delta T_m, \quad (7.2)$$

where  $q$  is the rate of heat transfer between the two fluids in the heat exchanger (Btu/h),  $U$  is the overall heat-transfer coefficient (Btu/h ft<sup>2</sup> °F),  $A$  is the heat-transfer surface area (ft<sup>2</sup>), and  $\Delta T_m$  is the LMTD (°F), calculated from the inlet and outlet temperatures of both fluids. Note that the product of  $UA$  is the overall heat-transfer coefficient and reference surface area.<sup>9</sup> This product is often called the heat-transfer conductance.

For the design of heat exchangers, the basic heat-exchanger design equation can be used to calculate the required heat-exchanger area for known or estimated values of the other three parameters,  $q$ ,  $U$ , and  $\Delta T_m$ . Each of those parameters will now be discussed in the following sections, but before we jump into these parameters we need to have some understanding of how to assess the basic concept and initial sizing of the intended heat exchanger based on its application within the system where this exchanger will be used. Thus, the next section will describe basic concepts and initial size assessment [24].

---

<sup>8</sup> [http://www.brighthubengineering.com/hvac/89972-preliminary-heat-exchanger-design-calculations-involved/#imgn\\_0](http://www.brighthubengineering.com/hvac/89972-preliminary-heat-exchanger-design-calculations-involved/#imgn_0)

<sup>9</sup> Note that any such value of the overall coefficient  $U$  must be uniquely associated with its reference surface area  $A$ , but the product  $UA$  is independent of reference area, having dimensions W/K or kW/K in metric or KMS.

	A	B	C	D	E	F	G	H	I
<b>1 Preliminary Heat Exchanger Design (U.S. units)</b>									
<b>2 Estimation of Heat Transfer Area Needed</b>									
<b>3</b>									
<b>4 Inputs</b>					<b>Calculations</b>				
<b>5</b>									
<b>6</b>	Fluid <sub>1</sub> mass flow				Heat Transfer Rate, Q =	<u>925,000</u>	Btu/hr		
<b>7</b>	rate, m <sub>1</sub> =	<u>25,000</u>	lb/hr						
<b>8</b>					Log Mean Temp	<u>79.58</u>	°F		
<b>9</b>	Fluid <sub>1</sub> temp. in, T <sub>1in</sub> =	<u>190</u>	°F		Diff, ΔT <sub>lm</sub> =				
<b>10</b>									
<b>11</b>	Fluid <sub>1</sub> temp. out, T <sub>1out</sub> =	<u>140</u>	°F		Heat Transfer Area, A =	<u>96.86</u>	ft <sup>2</sup>		
<b>12</b>									
<b>13</b>	Fluid <sub>1</sub> sp. heat, C <sub>p1</sub> =	<u>0.74</u>	Btu/lb-°F		Fluid <sub>2</sub> mass flow				
<b>14</b>					rate, m <sub>2</sub> =	<u>55,000</u>	lb/hr		
<b>15</b>	Fluid <sub>2</sub> temp. in, T <sub>2in</sub> =	<u>50</u>	°F						
<b>16</b>									
<b>17</b>	Fluid <sub>2</sub> temp. out, T <sub>2out</sub> =	<u>120</u>	°F						
<b>18</b>									
<b>19</b>	Fluid <sub>2</sub> sp. heat, C <sub>p2</sub> =	<u>1.0</u>	Btu/lb-°F						
<b>20</b>									
<b>21</b>	Overall heat transf.								
<b>22</b>	coeff. estim., U =	<u>120.0</u>	Btu/1hr-ft <sup>2</sup> -°F						
<b>23</b>									
<b>24</b>	<b>Equations used for calculations:</b>								
<b>25</b>									
<b>26</b>	Q = ± (m <sub>1</sub> )(C <sub>p1</sub> )(T <sub>1in</sub> - T <sub>1out</sub> )								
<b>27</b>									
<b>28</b>	Q = ± (m <sub>2</sub> )(C <sub>p2</sub> )(T <sub>2in</sub> - T <sub>2out</sub> )								
<b>29</b>									
<b>30</b>	ΔT <sub>lm</sub> = [(T <sub>1in</sub> - T <sub>2out</sub> ) - (T <sub>1out</sub> - T <sub>2in</sub> )]/[ln[(T <sub>1in</sub> - T <sub>2out</sub> )/(T <sub>1out</sub> - T <sub>2in</sub> )]]								
<b>31</b>									
<b>32</b>	Q = U A ΔT <sub>lm</sub>								

Fig. 7.20 Heat exchanger specification sample sheet

### 7.6.1.1 Basic Concept and Initial Size Assessment as Part of the Design Process

As part of the design methodology and design process, we have to have a basic concept of the initial sizing of the exchanger according to its application, and for that, when the pressure drop and thermal (i.e., heat transfer) specification has been fixed, then it is possible to do a quick analysis to determine the most appropriate heat exchanger type based on the flow configuration, which will be either cross flow or counterflow or, often, multipass overall counterflow arrangements (i.e., compact shell-and-tube exchanger). For this we need first to settle on an effectiveness design or method approach, and then the LMTD method (Chap. 6).

Earlier, in Chap. 4 of this book, we touched upon the effectiveness method also known as number of transfer units (NTU) as a design parameter for heat exchangers. We will now evaluate this parameter further in the context of our design methodology for a CHE as part of our subsystem for the NGNP.

Heat exchangers are usually analyzed using either the LMTD or the effectiveness–NTU ( $\epsilon$ -NTU) method. The LMTD method is convenient for determining the overall heat-transfer coefficient based on the measured inlet and outlet fluid temperatures. The  $\epsilon$ -NTU method is more convenient for predicting the outlet fluid temperatures if the heat-transfer coefficient and the inlet temperatures are known.

The analysis presented below assumes certain constraints:

1. There is no energy loss to the environment.
2. The heat exchanger is in steady state.
3. There are no phase changes in the fluids.
4. The heat capacities of the fluids are independent of temperature.
5. The overall heat-transfer coefficient is independent of the fluid temperature and position within the heat exchanger.

Since all heat exchangers considered in this experiment have a single pass for both the hot and cold fluids, the discussion that follows is limited to single-pass heat exchangers. The qualitative dependence of the fluid temperature on position inside a single-pass heat exchanger is shown in Fig. 7.21. Although Fig. 7.21b shows a situation for parallel flow, our main target for the intended CHE for driven combined-cycle efficiency for the NGNP focuses on either a cross-flow or counterflow type of classification of exchanger. This has been backed up by computer code and analysis that are presented in Chap. 5 of this book. The presentation of parallel flow is a matter of compression for the purpose of effectiveness analysis only.

We can analyze the total heat-transfer rate  $q$  as follows:

$$q = \int_1^2 dq', \quad (7.3)$$

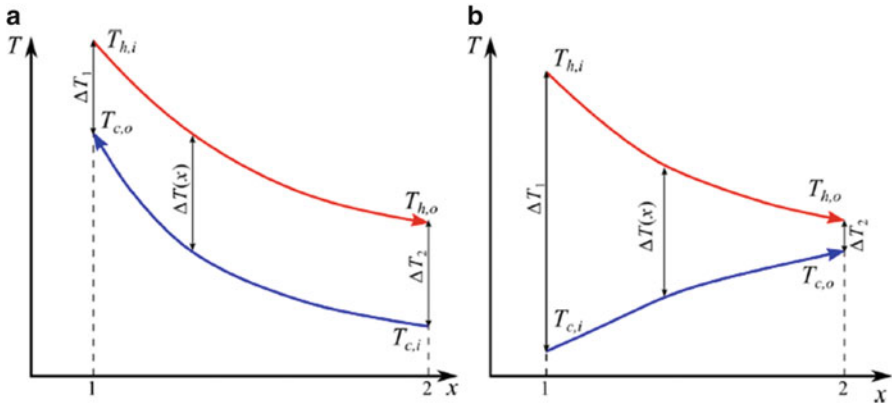
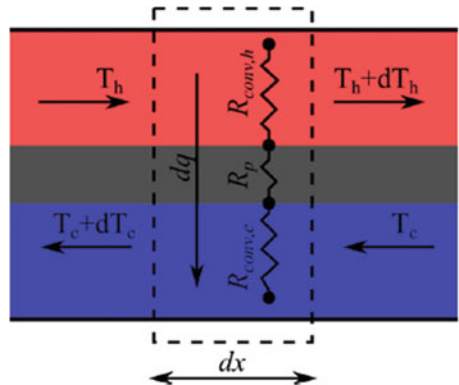


**Fig. 7.21** Temperature profiles in (a) counterflow and (b) parallel-flow single-pass heat exchangers. Note that in a counterflow heat exchanger the outlet temperature of the cold fluid can exceed the outlet temperature of the hot fluid, but this cannot happen in a parallel-flow system

**Fig. 7.22** Energy balance in a differential element of a single-pass heat exchanger operated in counterflow regime



where  $dq'$  is some aspect of the differential form of Eq. (7.2) for a segment of a single-pass flow heat exchanger from point 1 to point 2, shown schematically in Fig. 7.22, in order to present the overall heat-transfer coefficient  $U$ . Equation (7.4) represents the overall heat-transfer coefficient  $U$  in this segment:

$$dq'(x) = U\Delta T(x)dA(x), \quad (7.4)$$

where  $U$  is the overall heat-transfer coefficient,  $\Delta T(x)$  is the local temperature difference between the hot and cold fluids within this segment, and  $dA(x)$  is the contact area in the differential segment.

Note that red, blue, and gray colors represent the hot fluid, cold fluid, and the partition between the fluids, respectively. The dashed rectangle shows a differential segment corresponding to the energy balance Eq. (7.4). Three resistances

( $R_{\text{conv,h}}$ ,  $R_p$ , and  $R_{\text{conv,c}}$ ) contributing to the total resistance to the heat transfer are indicated schematically. Therefore, for the overall heat-transfer coefficient  $U$  we can write

$$U = \frac{1}{R_{\text{Total}}} = \frac{1}{R_{\text{conv,h}} + R_p + R_{\text{conv,c}}} \quad (7.5)$$

where:

$R_{\text{conv,h}}$  = convective heat transfer, which is resistant to the convective heat transfer and inversely proportional to the convective heat-transfer coefficient,  $h = 1/R_{\text{conv,h}}$ . The convective heat-transfer coefficient depends on the fluid properties, flow geometry, and flow rate. It is convenient to describe this dependence using several dimensionless numbers, namely, the Reynolds number

$$\text{Re} = \frac{L\nu\rho}{\mu}, \quad (7.6)$$

the Prandtl number

$$\text{Pr} = \frac{c_p\mu}{k}, \quad (7.7)$$

and finally the Nusselt number by

$$\text{Nu} = \frac{hL}{k}. \quad (7.8)$$

Here,  $\rho$ ,  $\mu$ ,  $k$ , and  $c_p$  are the density, viscosity, thermal conductivity, and heat capacity of the fluid, respectively,  $\nu$  is the flow velocity, and  $L$  is the characteristic length. The choice of  $L$  depends on the system geometry. For example, for a flow in a circular pipe,  $L$  is the pipe diameter.

The relationship between  $\text{Re}$ ,  $\text{Pr}$ , and  $\text{Nu}$  depends on the system geometry and whether the flow is laminar or turbulent. For example, for a turbulent flow inside a pipe with a circular cross section of diameter  $D$ ,

$$\text{Nu} = 0.027\text{Re}^{0.8}\text{Pr}^{1/3}. \quad (7.9)$$

$R_p$  = conductive heat transfer, which is the resistance  $R_p$  to heat transfer through the partition, which depends on the system geometry. In the current experiment, you will need to consider heat conduction in the radial direction of a cylindrical tube and heat conduction across a thin plate. Resistances in both of these cases can be obtained analytically by solving the heat diffusion equation.

However, it is possible to obtain  $Q$  by combining Eq. (7.4) with energy balance in differential segments of the heat exchanger as

$$dq = -C_{p,h}dT_h = C_{p,c}dT_c = C_{p,k}dT_k. \quad (7.10)$$

Here,  $dT_k$  is the temperature change of fluid k ( $k = c$  or  $h$ ) in the interval under consideration, and  $C_{p,k}$  is the heat capacity rate of fluid k under constant pressure, given as

$$C_{p,k} = \dot{m}_k c_k \text{ for } k = c \text{ or } h, \quad (7.11)$$

where  $\dot{m}_k$  and  $c_k$  are the mass flow rate and heat capacity of fluid k, respectively. This analysis yields

$$q = UA\Delta T_m. \quad (7.12)$$

This is the exact equation we introduced previously and is identified as Eq. (7.2), where  $A$  is the total contact area and  $\Delta T_m$  the LMTD, which is the subject of the next section.

### 7.6.1.2 Logarithmic Mean Temperature Difference

The driving force for any heat-transfer process is a temperature difference. For heat exchangers, there are two fluids involved, with the temperatures of both changing as they pass through the heat exchanger, so some type of average temperature difference is needed. Many heat-transfer textbooks have a derivation showing that the LGMT is the right average temperature to use for heat-exchanger calculations. In the case of compact shell-and-tube heat exchangers (Fig. 7.23), the mathematical relationship is as follows.

The log mean temperature is defined in terms of temperature differences, as shown in Eq. (7.13).  $T_{h,in}$  and  $T_{h,out}$  are the inlet and outlet temperatures of the hot

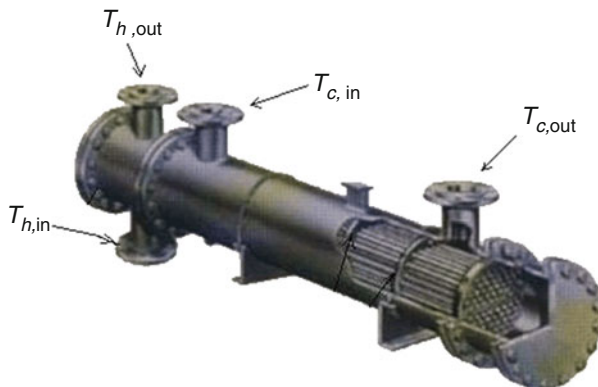


**Fig. 7.23** Straight-tube, two-pass shell-and-tube compact heat exchanger

fluid and  $T_{c, \text{in}}$  and  $T_{c, \text{out}}$  are the inlet and outlet temperatures of the cold fluid. Those four temperatures are shown in the diagram on the left for a straight-tube, two-pass shell-and-tube heat exchanger with the cold fluid as the shell-side fluid and the hot fluid as the tube-side fluid:

$$\Delta T_m = \frac{(T_{h, \text{in}} - T_{c, \text{out}}) - (T_{h, \text{out}} - T_{c, \text{in}})}{\ln\left(\frac{(T_{h, \text{in}} - T_{c, \text{out}})}{(T_{h, \text{out}} - T_{c, \text{in}})}\right)}. \quad (7.13)$$

In general form Eq. (7.13) can be written

$$\Delta T_m = \frac{\Delta T_1 - \Delta T_2}{\ln(\Delta T_1 / \Delta T_2)}. \quad (7.14)$$

Here, we can define a new term,  $\Delta T_k$ , which refers to the temperature difference of the hot and cold fluids at point k ( $k = c$  or  $h$ ), i.e.,

$$\Delta T_1 = T_{h, \text{in}} - T_{c, \text{out}} \text{ and } \Delta T_2 = T_{h, \text{out}} - T_{c, \text{in}}, \quad (7.15)$$

or the counterflow current, and for parallel flow it yields the following form:

$$\Delta T_1 = T_{h, \text{in}} - T_{c, \text{in}} \text{ and } \Delta T_2 = T_{h, \text{out}} - T_{c, \text{out}}. \quad (7.16)$$

### Note that:

1. If the heat capacity rates of the cold and hot fluids are the same and the heat exchanger is operated in the counterflow regime, then  $\Delta T$  is independent of position in the heat exchanger. In this case Eqs. (7.12) and (7.14) are not applicable and the total heat-transfer rate  $Q$  should be obtained by direct integration of Eq. (7.4).
2. This result holds for single-pass heat exchangers only. However, the LMTD method can be extended to more complex heat-exchanger designs (e.g., multipass and cross-flow systems) using a correction factor (see [25]).

Now that we have a better understanding of LMTD methodology, we can see that this method is very useful for determining the overall heat-transfer coefficient  $U$  based on the experimental values of the inlet and outlet temperatures and the fluid flow rates. However, this method is not very convenient for the prediction of outlet temperatures if the inlet temperatures and  $U$  are known. In this case, one has to solve a nonlinear system of two equations [see Eq. (7.12) and the overall energy balance] for two unknowns ( $T_{h, \text{out}}$  and  $T_{c, \text{out}}$ ). This solution requires application of an iterative approach.

A more convenient method for predicting outlet temperatures is the effectiveness method, known as the NTU method and sometimes written  $e$ -NTU. This method can be derived from the LMTD method without introducing any additional assumptions. Therefore, the effectiveness-NTU and LMTD methods are equivalent.

An advantage of the effectiveness-NTU method is its ability to predict outlet temperatures without resorting to a numerical iterative solution of a system of nonlinear equations.

### 7.6.1.3 Effectiveness-NTU Method

Now that we have a better understanding of LMTD, we will define the heat-exchanger effectiveness  $\epsilon$  as

$$\epsilon = \frac{q}{q_{\max}} = \frac{C_h(T_{h, \text{in}} - T_{h, \text{out}})}{C_{\min}(T_{h, \text{in}} - T_{c, \text{in}})} = \frac{C_c(T_{c, \text{in}} - T_{c, \text{out}})}{C_{\min}(T_{h, \text{in}} - T_{c, \text{in}})}, \quad (7.17)$$

where  $Q$  is the actual rate of heat transfer from hot to cold fluid and  $Q_{\max}$  is the maximum possible rate of heat transfer for given temperatures of the fluids as

$$q_{\max} = C_{\min}(T_{h, \text{in}} - T_{c, \text{in}}). \quad (7.18)$$

In this equation  $C_{\min}$  represents the smaller of the two heat capacity rates between  $C_c$  and  $C_h$ , where  $C_c$  and  $C_h$  are the cold stream and hot stream heat capacity rates, respectively, one of which will be  $C_{\min}$  unless the exchanger is balanced. This allows the effectiveness of the exchanger to be designed, and it can be determined directly from the terminal temperatures if these temperatures are known and so the stream parameters are known as well. As stated earlier, besides this criterion the other major relationship that will be needed for the design is given by Eq. (7.12).

If the heat-exchanger effectiveness is known, one can readily obtain  $Q$  from Eqs. (7.17) and (7.18) by solving these two equations simultaneously. After that, the outlet temperatures can be obtained from the energy balance.

The efficiency  $\epsilon$  depends on the heat-exchanger geometry, flow pattern (i.e., parallel flow, counterflow, cross flow), and the NTU.

Now we define the NTU for the exchanger as

$$\text{NTU} = \frac{UA}{C_{\min}}. \quad (7.19)$$

The relationships between the effectiveness and NTU have been established for a large variety of heat-exchanger configurations. Most of these relationships involve the *ratio of stream capacity rates* denoted by  $C_r = C_{\min}/C_{\max}$  of the smaller and larger heat capacity rates  $C_c$  and  $C_h$ . For example, for a single-pass heat exchanger in a parallel-flow regime the effectiveness is

$$\epsilon = \frac{1 - \exp[-\text{NTU}(1 + C_r)]}{1 + C_r}. \quad (7.20)$$

For a single-pass heat exchanger in the counterflow regime, the effectiveness is expressed as

$$\begin{cases} \varepsilon = \frac{1 - \exp[-\text{NTU}(1 + C_r)]}{1 + C_r \exp[-\text{NTU}(1 - C_r)]} & \rightarrow \quad \text{if } C_r < 1, \\ \varepsilon = \frac{\text{NTU}}{1 + \text{NTU}} & \rightarrow \quad \text{if } C_r < 1. \end{cases} \quad (7.21)$$

Similarly, for a cross-flow regime, we can define the effectiveness as

$$\varepsilon = \frac{1}{C_r} [1 - \exp\{-C_r[1 - \exp(-\text{NTU})]\}]. \quad (7.22)$$

Nowadays, designing a heat exchanger is made much easier by tools such as computer-aided design (CAD) and computer-aided manufacturing (CAM), along with some mathematical and algebraic relationships among all the previously discussed parameters; these tools facilitate the process of choosing the right heat exchanger for the right application and make the design process easier than would hand calculations. For most commonly used configurations, Table 7.1 was proposed by Kays and London [17] and Hesselgreaves [24].

Typical temperatures for common arrangements are depicted in Fig. 7.24.

Equation (7.22) shows an idealized performance with infinite surface area, and Fig. 7.25 shows an idealized temperature distribution diagram [24].

**HHH = Hot fluid has Highest heat capacity rate. Hot end pinch point**  
**CHC = Cold fluid has Highest heat capacity rate. Cold end Pinch Point**

These acronyms allow us to remember the location of a pinch point at either end of a heat exchanger.

Figure 7.25 clearly shows that the maximum heat transferred is obtained when the stream of lowest heat capacity rate has an outlet temperature equal to the inlet temperature (for a counterflow configuration) of the other stream. For a parallel-flow arrangement, that state is reached when both streams attain the same temperature at the outlet and the pinch point is the point of equal temperature. Note that per this idealized situation, the pinch point corresponds to a zero temperature difference.

Further analysis of the NTU is illustrated graphically in Fig. 7.26, which reveals the product of the required area and heat-transfer coefficient  $UA$  based on Eq. (7.2) or (7.12), which relates these two parameters to the effectiveness, determined by the specified temperatures, and the stream capacity rates ratio  $C_r$ .

From Fig. 7.25 for various heat exchanger types, it is obvious that the configuration creates some differences in the value of effectiveness for low  $C_r$  (i.e.,  $C_r < 0.25$ ), or NTU of less than 1 (i.e.,  $\text{NTU} < 1$ ). For this range of  $\text{NTU} < 1$ , we can see that the effectiveness is low as well. Now analyzing the given mathematical relationships for effectiveness of heat exchangers of different types (Table 7.1), it is

**Table 7.1** Effectiveness–NTU relationships [24]

<b>Counterflow:</b> $\epsilon = \frac{1 - \exp[-\text{NTU}(1 + C_r)]}{1 + C_r \exp[-\text{NTU}(1 - C_r)]}$
Asymptotic value = 1 as $\text{NTU} \rightarrow \infty$ , for all $C_r$
<b>Unmixed cross flow</b> (approximation from Kays and Crawford) [26]
$\epsilon = 1 - \exp \left\{ \frac{(\exp(-\text{NTU}^{0.78} C_r) - 1) \text{NTU}^{0.22}}{C_r} \right\}$
Asymptotic value = 1 as $\text{NTU} \rightarrow \infty$ , for all $C_r$
<b>Parallel or cocurrent flow:</b> $\epsilon = \frac{1 - \exp(-\text{NTU}(1 + C_r))}{1 + C_r}$
Asymptotic value = $1/(1 + C_r)$ , for all $C_r$
<b>Cross flow, <math>C_{\min}</math> unmixed:</b> $\epsilon = \frac{1}{C_r} \{1 - \exp[-C_r(1 - \exp(-\text{NTU}))]\}$
Asymptotic value = $[1 - \exp(-C_r)]/C_r$ as $\text{NTU} \rightarrow \infty$
<b>Cross flow, <math>C_{\max}</math> unmixed:</b> $\epsilon = 1 - \exp \left\{ -\frac{1}{C_r} [1 - \exp(-\text{NTU} C_r)] \right\}$
Asymptotic value = $[1 - \exp(1 - C_r)]$ as $\text{NTU} \rightarrow \infty$
<b>Cross flow, both fluids mixed:</b> $\epsilon = \frac{1}{\frac{\text{NTU}}{1 - \exp(-\text{NTU})} + \frac{\text{NTU} C_r}{1 - \exp(-\text{NTU} C_r)} - 1}$
Asymptotic value = $1/(1 + C_r)$ , for all $C_r$
<b>Multipass overall counterflow, fluid mixed between passes</b>
$\epsilon = \frac{\left( \frac{1 - \epsilon_p C_r}{1 - \epsilon_p} \right)^n}{\left( \frac{1 - \epsilon_p C_r}{1 - \epsilon_p} \right)^n - C_r}$
with $\epsilon_p$ = effectiveness of each pass [as a function of $\text{NTU}_p = (\text{NTU}/n)$ ] $n$ = number of identical passes (i.e., each pass having the same $\epsilon_p$ ) and
$\epsilon_p = \frac{\left( \frac{1 - \epsilon C_r}{1 - \epsilon} \right)^{1/n} - 1}{\left( \frac{1 - \epsilon C_r}{1 - \epsilon} \right)^{1/n} - C_r}$
Limiting value = $\epsilon_{\text{counterflow}}$ , as $n \rightarrow \infty$
<b>Multipass overall parallel flow, fluids mixed between passes:</b>
$\epsilon = \frac{1}{1 + C_r} \{1 - [1 - (1 + C_r) \epsilon_p]^n\}$
All configurations, $C_r = 0$ for pure condensation and evaporation:
$\epsilon = 1 - \exp(-\text{NTU})$

also clear for the purpose of CAD/CAM design, a cross-flow type exchanger is most appropriate due to the simplicity of its relationship, as shown in this table, which most often applies to liquid/gas CHEs and their application to enhancing the overall efficiency of NGNPs that are driven by combined cycles such as an open air-Brayton cycle. This choice in particular applies to the case of exchangers for which the gas-side heat-transfer coefficient is low and dominates the overall conductance of the  $UA$  product. On the other hand, if  $C_r$  is higher than 0.25, and particularly if the required effectiveness is higher than 0.80 (i.e.,  $\epsilon > 0.80$ ), then a

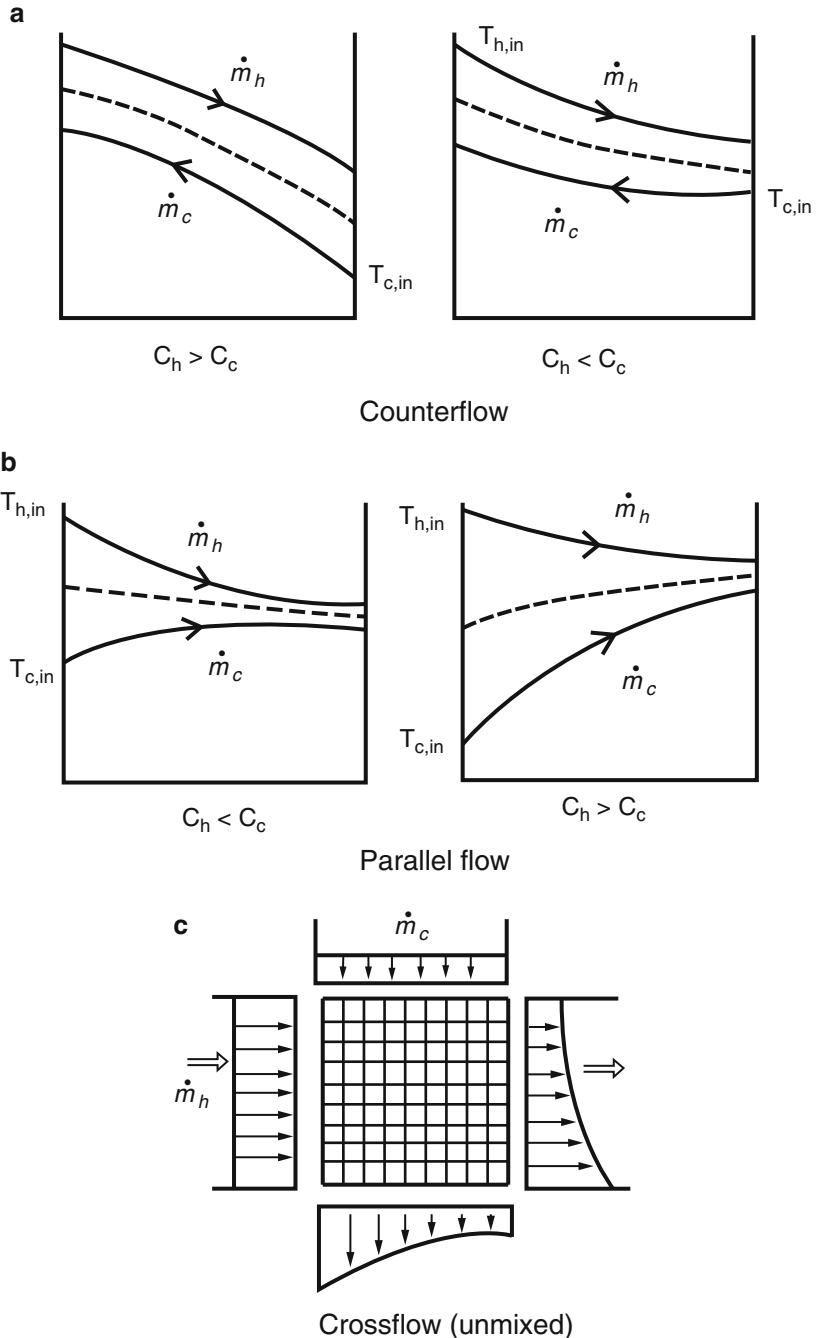


**Fig. 7.24** Typical temperature distributions in heat exchangers [24]

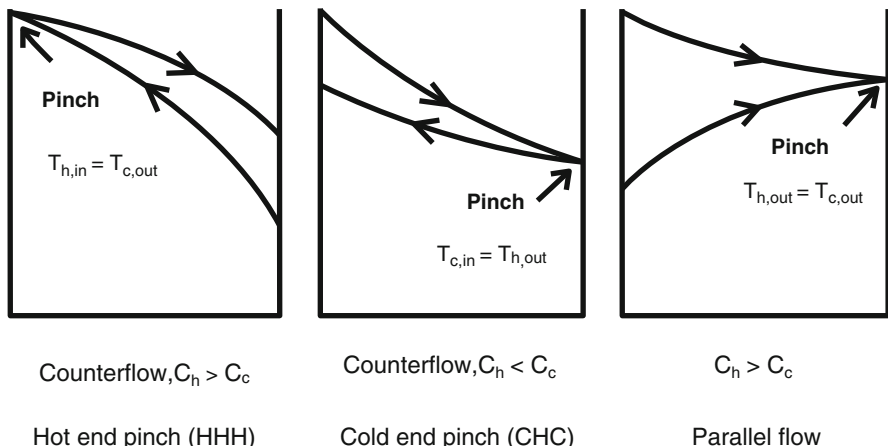


**Fig. 7.25** Idealized temperature distributions showing pinch point [24]

counterflow configuration would be a better choice and usually provide the most economical design. Figure 7.26c shows that for multipass cross-counterflow the pure counterflow value of effectiveness is closely approached for three or more passes, which is preferred more often over the pure counterflow configuration because porting involves an easier and cheaper design.

For better computer coding utilizing any CAD tool and the scope of calculations where the terminal temperatures are often specified, it is better to have NTU as a function of effectiveness  $\epsilon$ , where this parameter can be determined directly.

Therefore, it is better to create another table such as Table 7.2 to explicitly define NTU in terms of  $\epsilon$ . This then gives the overall conductance  $UA$  and is directly equivalent to the LMTD method discussed earlier.

A further aspect strongly affecting counterflow versus cross flow is that of pressure drop. These points are further explored in the subsequent discussion on mass velocity equation, but before we continue with the mass velocity equation we need to start our discussion with pressure-drop phenomena first.

#### 7.6.1.4 Pressure Drop

For the application of CHE in NGNPs, it is necessary to have accurate design tools for predicting heat transfer and pressure drop. Until recently, this type of heat exchanger had not been well studied, and in the scientific literature there were large discrepancies between results reported by different investigators.

A fundamental requirement during heat exchanger design is the ability to predict heat-transfer coefficients and pressure drops under the conditions of interest. Studies in the literature reporting on single- and two-phase fluid flow and heat transfer in CHEs are relatively rare. However, extensive applications in process

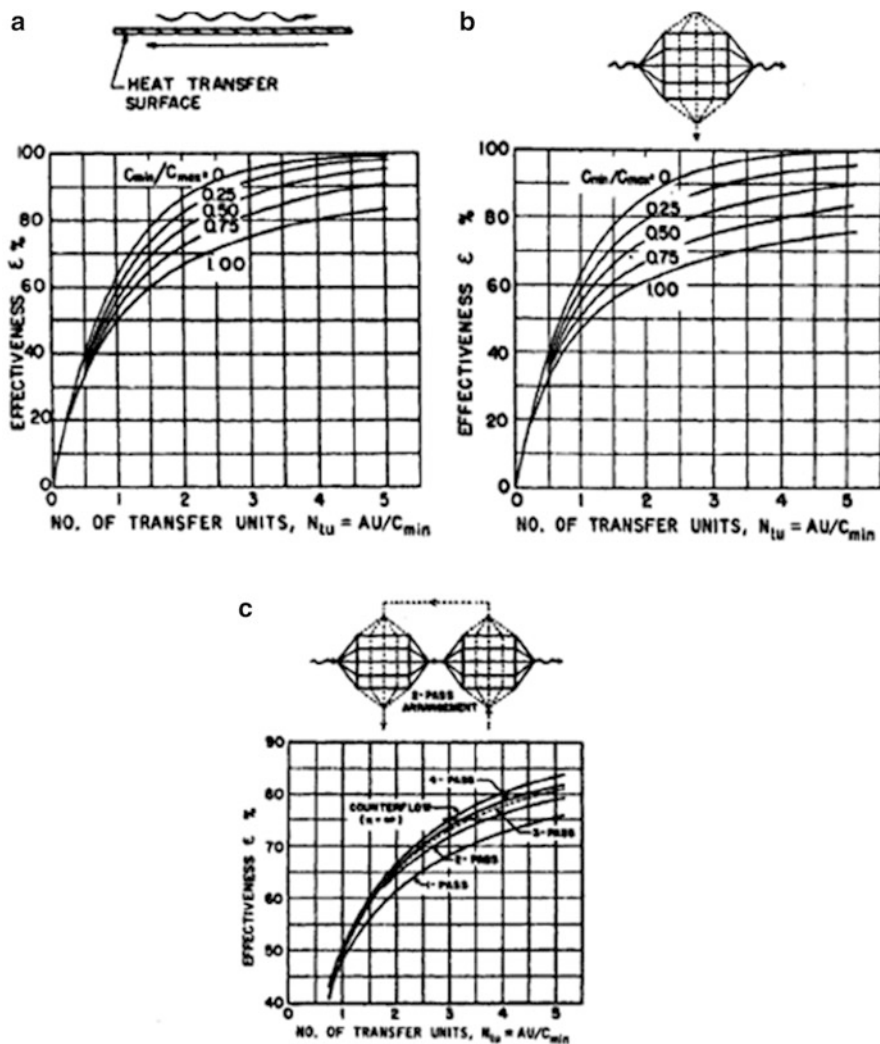


**Fig. 7.26** Effectiveness versus NTU curves for simple configurations. (a) Effectiveness of counterflow. (b) Effectiveness of cross flow (both streams unmixed). (c) Effectiveness of multipass cross-counterflow,  $C_r = 1$ , unmixed streams within passes, both streams mixed between passes [17]

industries exist where the heat is transferred utilizing flows via confined spaces, which can provide more compact design and better performance.

Several features make CHEs attractive in industrial applications where energy conservation, space and weight constraints, and cost are important considerations. These features include high thermal effectiveness (ratio of actual heat transferred to the theoretical maximum heat that can be transferred), large heat-transfer surface-to-volume ratio (surface area density), low weight per heat-transfer duty,

**Table 7.2** Inverse (NTU- $\epsilon$ ) relationships

---

<b>Counterflow:</b> NTU = $\frac{1}{C_r - 1} \ln\left(\frac{\epsilon - 1}{C_r(\epsilon - 1)}\right)$
<b>Cross flow (<math>C_r = 1</math>):</b> NTU = $\frac{\epsilon}{1 - \epsilon}$
<b>Parallel flow:</b> NTU = $\frac{-\ln[1 - (1 + C_r)\epsilon]}{1 + C_r}$
<b>Cross flow:</b>
<b><math>C_{\max}</math> mixed, <math>C_{\min}</math> unmixed:</b> NTU = $-\ln\left[1 + \frac{1}{C_r} \ln(1 - C_r\epsilon)\right]$
<b><math>C_{\max}</math> unmixed, <math>C_{\min}</math> mixed:</b> NTU = $\frac{-1}{C_r} \ln[1 + \ln(1 - \epsilon)]$
<b>All configurations, <math>C_r = 0</math>:</b> NTU = $-\ln(1 - \epsilon)$

---

opportunity for true counterflow operation, close temperature approach (as a result of the ability to design for true counterflow), design flexibility, and reduced fluid inventory. Flow maldistribution and the design of headers to minimize maldistribution remain inherent problems in the application of such heat exchangers, especially in the case of phase-change heat transfer. The potential for fouling of small flow passages represents a major disadvantage in the use of CHEs. However, fouling should not be a problem in applications that involve clean fluids.

The pressure drop  $\Delta p$  of fluid through a surface can be calculated as a function of the Darcy friction factor  $f$  (some textbooks show this as  $f_d$  or  $f_D$ , so do not be confused by the Fanning friction factor  $f_c$  or  $C_f$ ) using Eq. (7.23), neglecting for practical purposes the relatively small contributions of entry and exit losses and flow acceleration:

$$\Delta p = \frac{1}{2} \rho u^2 \frac{4L}{d_h} f, \quad (7.23)$$

where

$u$  = flow velocity, and with the mass flow rate  $\dot{m}$ , it is equal to

$$u = \frac{\dot{m}}{\rho A_c}; \quad (7.24)$$

$\rho$  = flow density;

$d_h$  = hydraulic diameter;

$L$  = flow length;

$A_c$  = flow area, which varies with flow length.

Substituting Eq. (7.24) into (7.23) for velocity  $u$ , we have

$$\frac{2\rho\Delta p}{\dot{m}^2} = f \frac{4L}{d_h A_c} = \text{constant for given conditions}, \quad (7.25)$$

and if we consider two surfaces denoted by 1 and 2, with a given pressure drop, we can write

$$\frac{(A_c^2)_1}{(A_c^2)_2} = \frac{f_1 L_1(d_h)_2}{f_2 L_2(d_h)_1}. \quad (7.26a)$$

Therefore, if the thermal performance is ignored, the flow areas for the two surfaces 1 and 2 with similar friction factors are the same if the  $L/d_h$  ratios are the same.

And for given conditions the product  $\text{Pr}^{2/3}N$  is fixed, so to compare the two surfaces 1 and 2, we write

$$\frac{L_1}{L_2} = \frac{d_{h,1}j_2}{d_{h,2}j_1}. \quad (7.26b)$$

Equation (7.26b) shows that the flow length is directly proportional to the hydraulic diameter and inversely proportional to the  $j$  factor, which is Reynolds number dependent.

If we consider the dimensionless  $j$  or the Colburn factor in terms of the Nusselt number  $\text{Nu} = \frac{\alpha d_h}{\lambda}$ , Reynolds number  $\text{Re}$  and Prandtl number  $\text{Pr}$  as previously (Chap. 6), then we can again write

$$j = \frac{\text{Nu}}{\text{Re}\text{Pr}^{1/3}} = \text{St}\text{Pr}^{2/3}, \quad (7.27)$$

where  $\text{St} = \frac{\alpha}{Gc_p}$  is the Stanton number, in which  $\alpha$  is nondimensionalized in terms of mass velocity  $G$ . Note that for a fixed  $G$ ,  $j$  is proportional to  $\alpha$ . If we substitute the value of the Nusselt number into Eq. (7.27) in terms of  $\alpha$  then the equation reduces to

$$\begin{cases} \frac{\alpha d_h}{\lambda} = \frac{\alpha d_n}{v} j \text{Pr}^{1/3} \\ \text{and} \\ \alpha = \frac{\dot{m}}{\rho v} \lambda \text{Pr}^{1/3} \frac{j}{A_c}. \end{cases} \quad (7.28)$$

Assuming the specified load  $q$  is given by the heat-transfer and rate equations for either side of the exchanger analogous to Eq. (7.12), then we can write

$$q = \alpha A \overline{\Delta T} = \dot{m} c_p (T_2 - T_1). \quad (7.29)$$

Manipulating Eqs. (7.29) and (7.28) and given the value for the Nusselt number, we obtain the following relationship:

$$j = \frac{A_c}{A} \text{Pr}^{2/3} N, \quad (7.30)$$

where  $N = \text{NTU}$ .

Recall the relationship for the hydraulic diameter  $d_h$ :

$$d_h = \frac{4A_c L}{A}. \quad (7.31)$$

Then we have an alternative equation form for Eq. (7.30):

$$j = \frac{d_h}{4L} \Pr^{2/3} N. \quad (7.32)$$

Now combining Eqs. (7.25) and (7.32), we produce the *core mass velocity equation*, which can be written

$$\begin{cases} \frac{2\rho\Delta p}{\dot{m}^2} = \frac{f\Pr^{2/3}N}{jA_c^2} \\ \text{and} \\ \frac{G^2}{2\rho\Delta p} = \frac{j/f}{\Pr^{2/3}N}. \end{cases} \quad (7.33)$$

Here,  $G$  is the mass velocity as per Eq. (6.13)  $\dot{m}/A_c$ . As mentioned,  $G$  and, therefore, the flow area  $A_c$  can be closely estimated based on the design specification methodology, and this equation, with the assumption of a typical value  $j/f$  ( $f$  is the Fanning friction factor), is often used as a starting point for preliminary sizing, as stated earlier [23].

Note that the basic elements of the effect of the surface on thermal design, as embodied in the previously given Eqs. (7.32) and (7.33), are as follows:

- The flow length decreases as the hydraulic diameter decreases;
- The flow area is largely independent of the hydraulic diameter.

Thus, if performance specifications include a pressure drop, as is normally the case, then increasing compactness only implies the reduction of flow length, with a change of shape, or aspect ratio, of the active block. In practice, this reduction in flow length can make longitudinal conduction a problem to be taken into account. In terms of comparing surfaces 1 and 2, based on Eqs. (7.25) and (7.26b), we can deduce the following equation:

$$\frac{(A_c)_1}{(A_c)_2} = \left[ \frac{f_1}{f_2} \cdot \frac{j_2}{j_1} \right]^{1/2} = \left( \frac{j_2/f_2}{j_1/f_1} \right)^{1/2}. \quad (7.34)$$

The form of Eq. (7.34) gives rise to the description of the ratio  $j/f$  as the *flow area goodness factor* (London) [26].

By now, you are getting a fair idea about one of the design criteria in Sect. 7.4 of this chapter; as part of the thermal energy transfer for the process of heat application in enhanced mode, we need information provided by Eq. (7.30) to be able to

manufacture a heat-transfer surface and test the collected correlation data in order to determine the basic performance of an enhanced surface for heat transfer in a CHE.

### 7.6.1.5 Core Mass Velocity Equation

In summary, the core mass velocity equation based on the discussion in the previous section can be summarized here, assuming the sides are chosen and we drop the suffix h for the hot side and c for the cold side, and the  $N$  are given in the following form:

$$\frac{2\rho\Delta p}{\dot{m}^2} = \frac{f\Pr^{2/3}N}{jA_c^2} \quad \text{and} \quad \frac{G^2}{2\rho\Delta p} = \frac{j/f}{\Pr^{2/3}N}. \quad (7.35)$$

All the parameters that are used in these equations are defined as previously. For laminar flows, these equations yield the following form:

$$\frac{2\rho\Delta p}{\dot{m}^2} = \frac{N\Pr}{A_c^2} \frac{k}{\text{Nu}} \quad \text{and} \quad \frac{G^2}{2\rho\Delta p} = \frac{\text{Nu}/k}{\Pr N}, \quad (7.36)$$

where the friction factor  $f$  is given by  $f = k/\text{Re}$ .

Note that, for given conditions of  $\Pr$ ,  $N$ ,  $p$ , and  $\Delta p$ , it is clear that  $G$  is only a function of  $j/f$ , or  $\text{Nu}/k$ , and most importantly is independent of the hydraulic diameter of the surface. The ratio  $j/f$  ( $f$  is the Fanning friction factor) is only a weak function of the Reynolds number, being of the order of 0.2–0.3 for most compact surfaces. Thus  $G$ , and hence flow area  $A_c$ , can be closely estimated from the design specification [24].

The operating Reynolds number, of which  $j/f$  is a weak function and  $j$  is a strong function for most surfaces, is, in terms of the prescribed side NTU and pressure drop,

$$\frac{\text{Re}}{d_h(j/f)^{1/2}} = \frac{1}{\eta} \left( \frac{2\rho\Delta p}{\Pr^{2/3}N} \right)^{1/2}, \quad (7.37)$$

and for laminar flow Eq. (7.37) results in

$$\frac{\text{Re}}{d_h(\text{Nu}/k)^{1/2}} = \frac{1}{\eta} \left( \frac{2\rho\Delta p}{\Pr N} \right)^{1/2}. \quad (7.38)$$

If  $G$  has already been calculated and accounted for as earlier, we can simply write

$$\text{Re} = \frac{Gd_h}{\mu}, \quad (7.39)$$

where  $\mu$  is the dynamic viscosity of the fluid.

Note that this estimation of  $G$  effectively determines the through-flow velocity, which is also reflected in Eq. (7.38), since this velocity is proportional to  $\text{Re}/d_h$ . The velocity is, in addition, responsible for determining the controllable entropy generation rate and features in economic optimization (Martin) [32].

## 7.7 Overall Heat Exchanger Design Process

The design of heat exchangers is an iterative (trial and error) process. Here is a set of steps for the process:

1. Calculate the required heat-transfer rate,  $q$ , in Btu/h from specified information about fluid flow rates and temperatures.
2. Make an initial estimate of the overall heat-transfer coefficient,  $U$ , based on the fluids involved.
3. Calculate the logarithmic mean temperature difference,  $\Delta T_m$ , from the inlet and outlet temperatures of the two fluids.
4. Calculate the estimated heat-transfer area required using  $A = q/U\Delta T_m$ .
5. Select a preliminary heat-exchanger configuration.
6. Make a more detailed estimate of the overall heat-transfer coefficient,  $U$ , based on the preliminary heat-exchanger configuration.

### 7.7.1 Input Information Needed

To start the heat-exchanger design process, several items of information are needed:

1. The two fluids involved need to be identified.
2. The heat capacity of each fluid is needed.
3. The required initial and final temperatures for one of the fluids are needed.
4. The design value of the initial temperature for the other fluid is needed.
5. An initial estimate for the value of the overall heat-transfer coefficient,  $U$ , is needed.

Knowing the first four items makes it possible to determine the required heat-transfer rate,  $q$ , and the inlet and outlet temperatures of both fluids, thereby allowing calculation of the LMTD,  $\Delta T_m$ . With values now available for  $q$ ,  $U$ , and  $\Delta T_m$ , an

initial estimate for the required heat-transfer area can be calculated from the equation,

For the design of heat exchangers, the basic heat-exchanger design equation can be used to calculate the required heat-exchanger area for known or estimated values of the other three parameters,  $q$ ,  $U$ , and  $\Delta T_m$ . Each of those parameters will now be discussed briefly.

### 1. LMTD, $\Delta T_m$

The driving force for any heat-transfer process is a temperature difference. For heat exchangers, two fluids are involved, with the temperatures of both changing as they pass through the heat exchanger, so some type of average temperature difference is needed. Many heat-transfer textbooks have a derivation showing that the LMTD is the right average temperature to use for heat-exchanger calculations. The log mean temperature is defined in terms of the temperature differences, as shown in the equation at the right.  $T_{h_{in}}$  and  $T_{h_{out}}$  are the inlet and outlet temperatures of the hot fluid and  $T_{c_{in}}$  and  $T_{c_{out}}$  are the inlet and outlet temperatures of the cold fluid. Those four temperatures are shown in the diagram at the left for a straight-tube, two-pass shell-and-tube heat exchanger with the cold fluid as the shell-side fluid and the hot fluid as the tube-side fluid (see Fig. 7.23 as well):

$$\Delta T_m = \frac{(T_{h_{in}} - T_{c_{out}}) - (T_{h_{out}} - T_{c_{in}})}{\ln \left\{ \frac{(T_{h_{in}} - T_{c_{out}})}{(T_{h_{out}} - T_{c_{in}})} \right\}}. \quad (7.40)$$

### 2. Heat-transfer Rate $q$

Heat-transfer Rate  $q$  can be calculated based on above design rules. This information can be found by Eq. (7.12) and then an initial estimate for the required heat-transfer area can be calculated from the relationship of  $A = q/U\Delta T_m$ .

Heat exchanger calculations with the heat exchanger design equation require a value for the heat-transfer rate,  $q$ , which can be calculated from the known flow rate of one of the fluids, its heat capacity, and the required temperature change. The following equation should be used:

$$q = \dot{m}_h c_{p_h} (T_{h_{in}} - T_{h_{out}}) = \dot{m}_c c_{p_c} (T_{c_{out}} - T_{c_{in}}),$$

where (units are given in the British system and can easily be given in the MKS system as well):

$\dot{m}_h$  = mass flow rate of hot fluid (slug/h),

$c_{p_h}$  = heat capacity of hot fluid at constant pressure (BTU/slug °F),

$\dot{m}_c$  = mass flow rate of cold fluid (slug/h),

$c_{p_c}$  = heat capacity of cold fluid at constant pressure (BTU/slug °F),

and the temperatures are as defined in the previous section.

**Table 7.3** Typical value of heat-transfer coefficient

Typical ranges of values of $U$ for shell-and-tube heat exchangers		
Hot fluid	Cold fluid	$U$ (Btu/h ft <sup>2</sup> °F)
Water	Water	140–260
Steam	Water	260–700
Light oils	Water	62–159
Gases	Water	3–50
Water	Light organics	35–53

The required heat-transfer rate can be determined from known flow rate, heat capacity, and temperature change for either the hot fluid or the cold fluid. Then either the flow rate of the other fluid for a specified temperature change or the outlet temperature for a known flow rate and inlet temperature can be calculated.

### 3. Overall Heat-transfer Coefficient, $U$

The overall heat-transfer coefficient,  $U$ , depends on the conductivity through the heat-transfer wall separating the two fluids and the convection coefficients on both sides of the heat-transfer wall. For a shell-and-tube heat exchanger, for example, there would be an inside convective coefficient for the tube-side fluid and an outside convective coefficient for the shell-side fluid. The heat-transfer coefficient for a given heat exchanger is often determined empirically by measuring all of the other parameters in the basic heat-exchange equation and calculating  $U$ . Typical ranges of  $U$  values for various heat-exchanger/fluid combinations are available in textbooks, handbooks, and on Web sites for other types of heat exchanger, such as our intended CHE (London and Kays) [17]. A sampling is given in Table 7.3 for shell-and-tube heat exchangers.

## 7.8 Design Summary

As part of the design process and methodology for CHEs, they generally fall within scope of certain constraints, which include:

1. Implementation of basic heat-exchange equation;
2. Flow frontal entrance area;
3. Volume, weight, and size;
4. Pressure drop.

With these constraints in mind, different heat-transfer surfaces may be analyzed and plotted on graphs as part of specification Excel sheets for comparison purposes and for making a decision as to the selection of the application exchanger.

### 1. Basic Heat-Transfer or Exchange Equation

A preliminary heat-exchanger design to estimate the required heat-exchanger surface area can be made using the basic heat-exchange equation,  $q = UA\Delta T_m$ , if values are known or can be estimated for  $q$ ,  $A$  and  $\Delta T_m$ . Heat-exchange theory tells us that  $\Delta T_m$  is the right average temperature difference to use. So we need the following basic heat-transfer equation:

$$q = UA\Delta T_m, \quad (7.41)$$

where the estimated heat-transfer area required, using  $A = q/U\Delta T_m$  and LMTD, is given by Eq. (7.40).

### 2. Flow Area

Using the mass velocity  $G \propto (\text{St}/f)^{1/2}$  for a given pressure drop, we can write the following flow area relationship:

$$\text{StPr}^{2/3}/f \text{ versus Re.} \quad (7.42)$$

Further investigation of Eq. (7.42) indicates that a higher  $(\text{StPr}^{2/3}/f)$  surface characteristic implies a smaller flow frontal entrance area ( $A_c$ ) for a given  $\Delta p/p$ . Again,  $f$  is the Fanning friction factor.

### 3. Exchanger Volume, Weight, and Size

A useful comparison of exchanger volume, weight, and size is made as follows:

$$h_{\text{std}} \text{ versus } E_{\text{std}}, \quad (7.43)$$

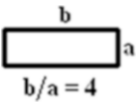
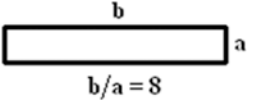
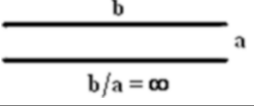
where  $E_{\text{std}}$  is the friction power per unfit area in  $\text{hp}/\text{ft}^2$ . Here the subscript std indicates an evaluation of the reference fluid properties (i.e., air at 500 °F and 1 atm) [33].

Equation (7.43) implies that a surface with a higher  $h_{\text{std}}$  vs.  $E_{\text{std}}$  characteristic will tend to have the smallest core volume as a result of better compactness. Hence, these surface goodness factors are not infallible and are usually indicative of the relative performance of the surfaces. For heat-exchanger surfaces operating at lower Reynolds numbers near laminar flow (London [33] and Zohuri and Fathi) [18], classical analyses for laminar flow solutions for fully developed flow in cylindrical passages are very worthwhile. These analyses could be used as a benchmark for several different types of surfaces to be looked at as part of a comparison helping in the final selection of exchangers for all intended purposes and application (i.e., open air-Brayton cycle-driven efficiency for NGNPs) [2].

Table 7.4 provides a comparison for different cross sections of these passages at near laminar flow. Some noteworthy points are given in what follows [2, 33]:

1. The convective heat-transfer coefficient for constant flux conditions  $q$  (BTU/h ft), with constant flow length, is 9–28 % higher than for a constant or uniform wall

**Table 7.4** Laminar flow solution comparison of laminar-flow solutions for different cross sections

Cross section	$(\text{Nu})_T$	$\frac{(\text{Nu})_q}{(\text{Nu})_T}$	$f\text{Re}$	$\{\text{StPr}^{2/3}\}/f = \frac{1.15 (\text{Nu})_T}{f\text{Re}}$
	2.35	1.28	13.33	0.203
	3.66	1.19	16.0	0.264
	2.89	1.26	14.2	0.234
 $b/a = 4$	4.65	1.15	18.3	0.292
 $b/a = 8$	5.95	1.09	20.5	0.334
 $b/a = \infty$	7.54	1.09	24.0	0.361

Note: (a) For  $L/4r_h > 100$

(b) For  $\text{Pr} = 0.66$

where  $r_h$  is the hydraulic radius

temperature (known as a *T-boundary condition*) boundary condition. The smallest difference is for a rectangular passage with a large aspect ratio and the largest for the triangular passage. See Table 7.4 in this book; for more detailed information refer to the book by Zohuri and Fathi [2], Chap. 5.

2. The ratio  $\text{StPr}^{2/3}/f$  is constant for a given surface irrespective of  $\text{Re}$ .
3. Rectangular passages of large aspect ratio tend to have smaller frontal area requirements by about one-third relative to the triangular passage.

Note that the rectangular cross section with high aspect ratio ( $b/a$ ) long and narrow offers the least frontal area. If we use a given number from Table 7.4 to form  $h_{\text{STD}}$  vs.  $E_{\text{STD}}$ , we produce results for the surfaces all with a common magnitude of  $4r_h = 2 \times 10^{-3}$  ft (for a surface density  $\beta$  of  $1200 < \beta < 1800 \text{ ft}^2/\text{ft}^3$ ). Clearly, we can see that there exist large differences between surfaces, with the large-aspect-ratio rectangular passages again being superior to the triangular passages in a rather spectacular fashion, as shown in Fig. 7.27, and that represents a 3.2–1.0 higher heat-transfer coefficient [26].

**Fig. 7.27** Heat-transfer power versus friction power for fully developed laminar flow. Note again the superiority of the high-aspect-ratio rectangular section

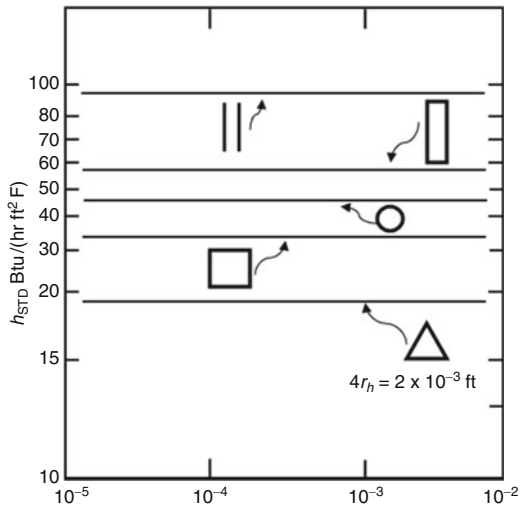


Figure 7.17 shows some of these passages that go with the data from Table 7.4, and it is interesting to compare these surfaces with each other and to reference them to Fig. 7.27 and Table 7.4.

It is also important to make some preliminary points on the importance of obtaining accurate geometrical dimensions, both for test data reduction purposes and in the comparison of different surface geometries as part of design methodology; these will form the basis for measuring the actual surfaces of the exchanger that is ultimately selected. Bear in mind that for the surface geometrical factors three parameters are of primary interest:

1. Porosity,  $p$ ;
2. Hydraulic radius,  $r_h$ ; and
3. Area density,  $\beta$ .

Note that only two of these parameters are independent, per Eq. (7.44) as shown below:

$$\beta = \frac{p}{r_h}. \quad (7.44)$$

The definitions of these parameters are important because they specify the geometrical measurements that must be made:

$$\begin{aligned} p &= \frac{A(\text{flow})}{A_c(\text{frontal})}, \\ p &= \frac{A(\text{flow}) \times L}{A(\text{heat transfer})}, \\ \beta &= \frac{A(\text{heat transfer})}{A_c(\text{frontal}) \times L}. \end{aligned} \quad (7.45)$$

Out of any test measurement of different geometries (Fig. 7.17) of flow passage,  $A_c$ (frontal) and  $L$  of the test core can be measured with good accuracy; however,  $A$  (flow) and  $A$ (heat transfer) are not easily established.

In the test data reduction processes, it can be shown that

$$\begin{aligned} \text{Re} &\propto 1/\beta, \\ \text{St} &\propto p/\beta, \\ f &\propto p^3/\beta. \end{aligned} \quad (7.46)$$

For surface comparisons, presented by Eqs. (7.42) and (7.43), it may be shown that

$$\begin{aligned} \text{StPr}^{2/3}/f &\propto p^2, \\ h_{\text{std}} &\propto p/\beta^2, \\ E_{\text{std}} &\propto p^3/\beta^4. \end{aligned} \quad (7.47)$$

#### 4. Pressure Drop for Fully Developed Flow

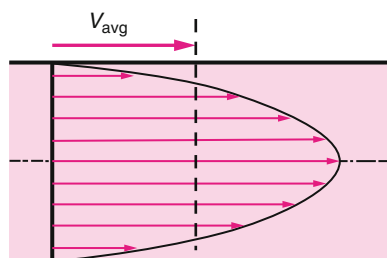
Although we have talked about a pressure drop  $\Delta p$  as a quantity of interest in the design methodology for a CHE, we will expand upon this from the point of view of a fully developed laminar flow solution for different cross-section passages. Analysis of the pressure drop for flow within a pipe has a direct impact on maintaining consistent fluid flow. To satisfy this requirement of consistency, we note that  $(dp/dx) = \text{constant}$ , and integrating from  $x = x_1$  where the pressure is  $p_1$  to  $x = x_1 + L$  where the pressure is  $p_2$  gives

$$\frac{dp}{dx} = \frac{p_2 - p_1}{L}. \quad (7.48)$$

Now, taking another value known as the average velocity  $V_{\text{avg}}$  into account for a laminar flow profile as shown in Fig. 7.28, we can calculate this value at some streamwise cross section determined from the requirement that the *conservation of mass* principle from fluid mechanics must be satisfied:

**Fig. 7.28** Average velocity

$V_{\text{avg}}$  is defined as the average speed through a cross section



$$\dot{m} = \rho V_{\text{avg}} A_c = \int_{A_c} \rho u(r) dA_c, \quad (7.49)$$

where:

$\dot{m}$  = mass flow rate,

$\rho$  = fluid density,

$A_c$  = cross-sectional area, and

$u(r)$  = velocity profile.

Hence, the average velocity for incompressible flow in a circular pipe of radius  $R$  can be expressed as

$$V_{\text{avg}} = \frac{\int_{A_c} \rho u(r) dA_c}{\rho A_c} = \frac{\int_{r=0}^{r=R} \rho u(r) 2\pi r dr}{\rho \pi R^2} = \frac{2}{R^2} \int_{r=0}^{r=R} u(r) r dr. \quad (7.50)$$

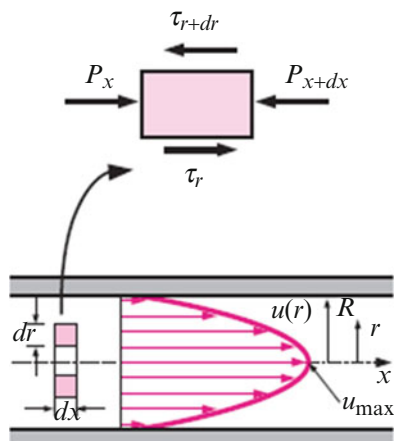
Note that for fully developed laminar pipe flow,  $V_{\text{avg}}$  is half the maximum velocity.

Now consider the steady laminar flow of an incompressible fluid with constant properties in the fully developed region of a straight circular pipe. We can obtain the momentum equation by applying a momentum balance to a differential volume element, as shown in Fig. 7.29.

Figure 7.29 is a depiction of a free-body diagram of a ring-shaped differential fluid element of radius  $r$ , thickness  $dr$ , and length  $dx$  oriented coaxially with a horizontal pipe in fully developed laminar flow. In this demonstration, the volume element involves only pressure ( $p$ ) and viscous effects ( $\mu$ ) and therefore the pressure and shear force  $\tau$  must balance each other in given  $x$ - and  $r$ -directions (i.e., the cylindrical coordinate and everything around the azimuth angle  $\theta$  is symmetrical;  $x$  is the axial direction):

$$(2\pi r dr p)_x - (2\pi r dr p)_{x+dx} + (2\pi r dx \tau)_r - (2\pi r dx \tau)_{r+dr} = 0. \quad (7.51)$$

**Fig. 7.29** Free-body diagram of a ring-shaped differential fluid element



Equation (7.51) is established based on the fact that the pressure force acting on a submerged plane surface is the product of the pressure at the centroid of the surface and surface area  $A$  and the force balance is given by this equation on the volume element in the flow direction, as shown in Fig. 7.29, which is an indication of fully developed flow in a horizontal pipe.

Dividing both sides of Eq. (7.51) by  $2\pi r dr dx$  and rearranging algebraically, this equation reduces to the following form as Eq. (7.52):

$$r \frac{p_{x+dx} - p_x}{dx} + \frac{(r\tau)_{r+dr} - (r\tau)_r}{dr} = 0. \quad (7.52)$$

Taking the limit as  $dr, dx \rightarrow 0$  yields

$$r \frac{dp}{dx} + \frac{d(r\tau)}{dr} = 0. \quad (7.53)$$

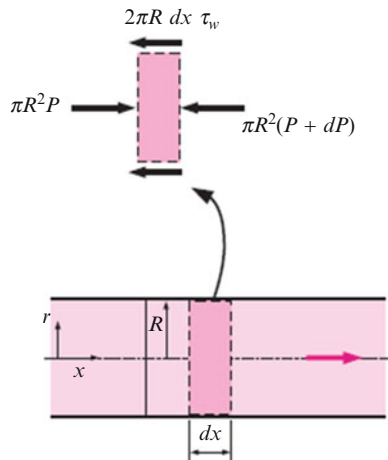
Now substituting  $\tau = -\mu(du/dr)$  and taking  $\mu = \text{constant}$  provides the desired two-dimensional linear partial differential equation (PDEs) Eq. (7.54):

$$\frac{\mu}{r} \frac{d}{dr} \left( r \frac{du}{dr} \right) = \frac{dp}{dx}. \quad (7.54)$$

Note that the quantity  $du/dr$  is negative in pipe flow, and the negative sign is included to obtain positive values for  $\tau$  [i.e.,  $(du/dr) = -(du/dy)$  since  $y = R - r$ ].

Utilizing Fig. 7.30 (which is a free-body diagram of a fluid disk element of radius  $R$  and length  $dx$  in fully developed laminar flow in a horizontal pipe) allows us to justify a solution for partial differential Eq. (7.54) using separation-of-variable methods, with the given boundary conditions

**Fig. 7.30** Free-body diagram of a fluid disk element



$$\text{Boundary Conditions} \quad \begin{cases} (\frac{du}{dr}) = 0 & \text{at } r = 0, \\ u = 0 & \text{at } r = R. \end{cases} \quad (7.55)$$

Note that as part of justification, we can claim that the left-hand side of Eq. (7.54) is a function of  $r$ , and the right-hand side is a function of  $x$ . The equality must hold for any value of  $r$  and  $x$ , and an equality of the form  $f(r) = g(r)$  can be satisfied only if both  $f(r)$  and  $g(r)$  are equal to the same constant. Thus we conclude that  $(dp/dx) = \text{constant}$ . This can be verified by writing a force balance on a volume element of radius  $R$  and thickness  $dx$  (a slice of the pipe), which gives (Fig. 7.30).

The general solution of such a problem is given as

$$u(r) = \frac{r^2}{4\mu} \left( \frac{dp}{dx} \right) + C_1 \ln r + C_2. \quad (7.56)$$

Applying the boundary conditions provided by Eq. (7.55) sets causes Eq. (7.56) to reduce to the following form:

$$u(r) = -\frac{R^2}{4\mu} \left( \frac{dp}{dx} \right) \left( 1 - \frac{r^2}{R^2} \right). \quad (7.57)$$

Now substitution of Eq. (7.57) into Eq. (7.50) and doing the proper calculus yields the final form for the average velocity  $V_{\text{avg}}$ :

$$\begin{aligned} V_{\text{avg}} &= \frac{2}{R^2} \int_0^R u(r) dr \\ &= -\frac{2}{R^2} \int_0^R \frac{R^2}{4\mu} \left( \frac{dp}{dr} \right) \left( 1 - \frac{r^2}{R^2} \right) r dr \\ &= -\frac{2}{8\mu} \left( \frac{dp}{dr} \right). \end{aligned} \quad (7.58)$$

Based on the result of Eq. (7.58), the profile velocity  $u(r)$  as the final form of the solution to Eq. (7.57) can also be written

$$u(r) = 2V_{\text{avg}} \left( 1 - \frac{r^2}{R^2} \right) \quad (7.59)$$

and the maximum velocity at the centerline of a horizontal pipe for a fully developed laminar flow can be derived as  $u(r)|_{\text{max}} = 2V_{\text{avg}}$ , which supports the observation made earlier that  $V_{\text{avg}} = (1/2)u_{\text{max}}$ .

Now that we have established the preceding results, we can go back to finalizing the analysis of the pressure drop or head loss for a fully developed laminar fluid as part of our CHE design methodology by paying attention to Eq. (7.48) and substituting this equation into Eq. (7.58); then the pressure drop can be expressed as

$$\text{Laminar flow} \quad \Delta p = p_1 - p_2 = \frac{8\mu LV_{\text{avg}}}{R^2} = \frac{32\mu LV_{\text{avg}}}{D^2}. \quad (7.60)$$

Note that  $D = D_h = d_h$  is known as the hydraulic diameter.

Examination of Eq. (7.60) indicates that the pressure drop is proportional to the viscosity  $\mu$  of the fluid, and  $\Delta p$  would be zero if there were no friction. Therefore, the drop in pressure from  $p_1$  to  $p_2$  in this case is due entirely to viscous effects, and this equation represents the pressure loss  $\Delta p_L$  when a fluid of viscosity  $\mu$  flows through a pipe of constant diameter  $D$  and length  $L$  at average velocity  $V_{\text{avg}}$ .

A pressure drop due to viscous effects represents an irreversible pressure loss, and it is called pressure loss  $\Delta p_L$  to emphasize that it is a loss, just like the head loss  $h_L$ , which is proportional to it.

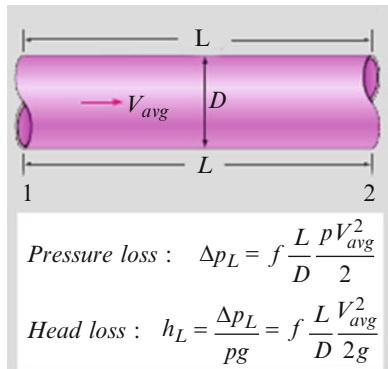
In practice, it is convenient to express the pressure loss for all types of fully developed internal flows (laminar or turbulent flows, circular or noncircular pipes, smooth or rough surfaces, horizontal or inclined pipes) as Fig. 7.31.

Hence a pressure drop (loss) for such circumstances can be summarized as

$$\text{Pressure loss : } \Delta p_L = f \frac{L}{D} \frac{\rho V_{\text{avg}}^2}{2}, \quad (7.61)$$

where  $\rho V_{\text{avg}}^2/2$  is the *dynamic pressure* and  $f$  the *Darcy friction factor*.

**Fig. 7.31** Relation for pressure and head loss, valid for laminar and turbulent flows, both circular and noncircular pipes



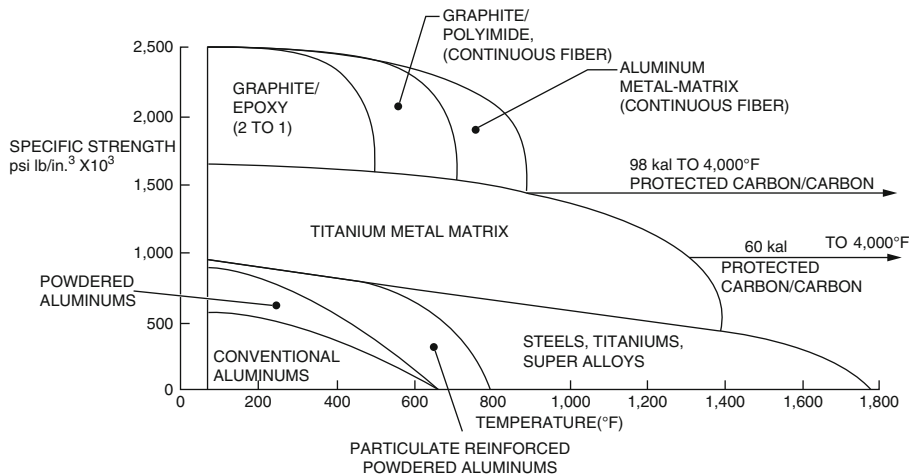


Fig. 7.32 Specific strength vs. temperature [29]

### Note that

the Darcy friction factor  $f$  (some textbooks denote it by  $f_d$ ) should not be confused with the *friction coefficient*  $f_c$  (denoted in some textbooks by  $C_f$ ), which is known as the *Fanning friction factor* and defined as

$$\text{Fanning friction factor : } C_f = f_c = \frac{2\tau_w}{\rho V_{\text{avg}}^2} = \frac{f}{4},$$

where  $\tau_w$  is the internal wall shear stress of the passage or pipe:

$$f = \frac{8\tau_w}{\rho V_{\text{avg}}^2}. \quad (7.62)$$

This friction is also called the Darcy–Weisbach friction factor, named after the Frenchman Henry Darcy (1803–1858) and the German Julius Weisbach (1806–1871).

Setting Eqs. (7.60) and (7.61) equal to each other and solving for  $f$  gives the friction factor for fully developed laminar flow in a circular pipe as

$$\text{Circular pipe, laminar : } f = \frac{64\mu}{\rho DV_{\text{avg}}} = \frac{64}{\text{Re}}. \quad (7.63)$$

Equation (7.63) shows that *in laminar flow, the friction factor is a function of the Reynolds number only and is independent of the roughness of the pipe surface.*

In the analysis of piping or passages on either side of CHE systems, pressure losses are commonly expressed in terms of the *equivalent fluid column height*, called the head loss and symbolically shown as  $h_L$ . Noting from fluid statics that  $\Delta p = \rho gh$  and thus a pressure difference of  $\Delta p$  corresponds to a fluid height of  $h = \Delta p / \rho g$ , we obtain the pipe head loss by dividing  $\Delta p_L$  by  $\rho g$  to give

$$\text{Head loss : } h_L = \frac{\Delta p_L}{\rho g} = f \frac{L}{D} \frac{V_{\text{avg}}^2}{2g}. \quad (7.64)$$

Again, note that  $D = D_h = d_h$  is known as the hydraulic diameter.

The head loss  $h_L$  represents the additional height that the fluid needs to be raised to by a pump in order to overcome the frictional losses in the pipe. The head loss is caused by viscosity, and it is directly related to the wall shear stress. Equations (7.61) and (7.64) are valid for both laminar and turbulent flows in both circular and noncircular pipes, but Eq. (7.64) is valid only for fully developed laminar flow in circular pipes.

Finally, as part of the design methodology process it is best to have Excel spreadsheet templates that can be downloaded to make preliminary heat-exchanger design calculations; see “Excel Spreadsheet Templates for Preliminary Heat Exchanger Design” in Fig. 7.20.

## 7.9 CHEs in Practice

Factors that ultimately affect the deployment of CHEs for use in open air-Brayton combined cycles to support enhancement of NGNP overall efficiency in order to make these reactors more cost effective are discussed by Hesselgreaves [24].

The choice of heat exchanger for the intended application (i.e., combined cycle; also see Chap. 5) and the exercise of selecting a design methodology and analysis, fabrication, and eventual installation of the unit must be carried out, including putting in place all guidelines for future preventive maintenance (PM) to increase the unit’s life cycle; moreover, it should be carried out from the point of view of that the heat exchanger is a subsystem of the big picture (i.e., an operational power plant). Reay and Hesselgreaves [24] have a good chapter on this subject, and the reader is referred to that reference.

## 7.10 Heat-Exchanger Materials and Comparisons

Material selection is one of the most important tasks in high-temperature applications [31]. There are four main categories of high-temperature materials: high-temperature nickel-based alloy, high-temperature ferritic steels, advanced carbon and silicon carbide composite, and ceramics (Sunden) [27].

Ohadi and Buckley [28] extensively reviewed materials for high-temperature applications. High-temperature nickel-based material has good potential for helium and molten salts up to 750 °C. High-temperature ferritic steel shows good performance under fusion and fission neutron irradiation to around 750 °C. Advanced carbon and silicon carbide composite has excellent mechanical strength at temperatures exceeding 1000 °C. It is currently used for high-temperature rocket nozzles to eliminate the need for nozzle cooling and for thermal protection of the space shuttle nose and wing leading edges. Many options are available that involve a trade between fabrication flexibility and cost, neutron irradiation performance, and coolant compatibility. Table 7.5 compares the properties of the most commonly used high-temperature materials (Ohadi and Buckley) [28]. It includes nickel-based alloy, ceramic materials, and carbon and SiC composites. Figure 7.27 shows the specific strength vs. temperature for various composite materials.

Dewson and Li [30] carried out a material selection study of very-high-temperature reactor (VHTR) IHXs; these materials can be regarded as and used for similar practical purposes and applications as CHEs for NGNPs as well.

Dewson and Li selected and compared the following eight candidate materials based on ASME VIII (boiler and pressure vessel code): Alloy 617, Alloy 556, Alloy 800H, Alloy 880HT, Alloy 330, Alloy 230, Alloy HX, and 253MA.

Table 7.6 lists the allowable design stress ( $S$ ) at 898 °C, the minimum required mechanical properties (ultimate tensile stress [UTS]), 0.2 % proof stress (PS), and elongation (El) at room temperature, together with the nominal compositions of the alloys. The researchers extensively compared the mechanical properties, physical properties, and corrosion resistance for the candidate materials and ultimately concluded that Alloys 617 and 230 are the most suitable materials for an IHX.

## 7.11 Guide to CHEs

As part of our conclusion on the subject of CHEs, we summarize for a generic process the advantages and limitations of these exchangers' design, which is applicable to all technologies, such as general advantages and limitations of compact exchanger designs, common applications, fouling, energy efficiency, heat-transfer enhancement, exchanger selection and types, specification and operation, process intensification, and, last but not least, software programs.

In general, the final selection of heat exchanger design, which will be unique for each intended function and application. In appropriate applications, compact designs offer substantial advantages over more conventional exchanger designs, usually shell-and-tube heat exchangers.

Of course, in recent years, the benefits of using CHE designs have only been realized in appropriate applications in connection with combined-cycle-driven efficiency as part of the NGNP (Zohuri) [2, 4], and researchers from universities, national laboratories, and industry are heavily involved with both aspects of this combined-cycle approach (Open or Closed cycle).

**Table 7.5** Selected properties of most commonly used high-temperature materials and fabrication technologies [29]

High-temperature material/fabrication technology	Metallic Ni alloys (Inconel 718)	Ceramic oxides of Al, Si, Sr, Ti, Y, Be, Zr, B and Si <sub>3</sub> N <sub>4</sub> , AlN, B4C, BN, WC94/C96	Carbon–carbon composite	Carbon fiber–SiC composite
Temperature range	1200–1250 °C	1500–2500 °C	3300 °C (inert environment) 1400–1650 °C (with SiC layer)	1400–1650 °C
Density	8.19 g/cm <sup>3</sup>	1.8–14.95 g/cm <sup>3</sup>	2.25 g/cm <sup>3</sup>	1.7–2.2 g/cm <sup>3</sup>
Hardness	250–410 (Brinell)	400–3000 kgf/mm <sup>2</sup> (V)	0.5–1.0 (Mohs)	2400–3500 (V)
Elongation	<15 %	N/A	N/A	–
Tensile strength	800–1300 MPa	48–2000 MPa	33 (Bulk Mod.)	1400–4500 MPa
Tensile modulus	50 GPa	140–600 GPa	4.8 GPa	140–720 GPa
Strength of heat exchanger	Strength adequate but limited owing to creep and thermal expansion	Strength not adequate, low mechanical parameters for stress; good thermal and electrical parameters	Strength poor, oxidation starts at 300 °C	Highest owing to carbon fiber and SiC
Electrical conductivity	12.5 µΩ cm	2E – 06 – 1E + 18 Ωcm	1275 µΩ cm	1275 µΩ cm
Thermal conductivity	11.2 W/m K	0.05–300 W/m K	80–240 W/m K	1200 W/m K
Thermal expansion	13E – 06 K <sup>-1</sup>	0.54–10E – 06 K <sup>-1</sup>	0.6–4.3E – 06 K <sup>-1</sup>	–
Comments	Metallic expansion joints are the weak link	Often very high fabrication costs for conventional applications Technology proprietary for the most part Technologically hard to produce	Life time is short even when protected by SiC (adhesion is poor)	Comparatively less expensive, successful proprietary fabrication technologies available

**Table 7.6** Candidate materials for very-high-temperature reactor intermediate heat exchangers [31]

Alloy	UNS number	Tmax (°C)	S898°C (MPa)	UTS (MPa)	0.2 % PS (MPa)	EI (%)	Nominal composition (wt%)
617	N06617	982	12.4	655	240	30	52Ni-22Cr-13Co-9Mo-1.2Al
556	R30556	898	11.0	690	310	40	21Ni-30Fe-22Cr-18Co-3Mo-3W-0.3Al
800HT	N08811	898	6.3	450	170	30	33Ni-42Fe-21Cr
800H	N08810	898	5.9	450	170	30	33Ni-42Fe-21Cr
330	N08330	898	3.3	483	207	30	Fe-35Ni-19Cr-1.25Si
230	N06230	898	10.3	760	310	40	57Ni-22Cr-14W-2Mo-0.3Al-0.05La
HX	N06002	898	8.3	655	240	35	47Ni-22Cr-9Mo-18Fe
253MA	S30815	898	4.9	600	310	40	Fe-21Cr-11Ni-0.2N

The requirement in most heat-transfer applications is to maximize the amount of heat transferred, subject to capital-cost and pressure-drop constraints. Both cost and heat-transfer performance generally increase in proportion to exchange surface area, as discussed in detail earlier.

### 7.11.1 Generic Advantages of Compact Design

The main benefits of using CHEs are as follows:

- Improved heat exchanger thermal effectiveness,
- Closed approach temperatures,
- High heat-transfer coefficients and transfer areas per exchanger volume,
- Small size,
- Multistream and multipass configurations,
- Tighter temperature control,
- Energy savings,
- Reduced inventory volume and hazard risk,
- Process intensification using combined reactor/exchangers.

These technological advantages can be converted into reduced operation and capital costs (ROI and TCO) and greater energy savings compared to shell-and-tube units. The performance characteristics of CHEs have particular relevance in process integration, for example, in composite process heating and cooling curves. Most details of the preceding points can be found in different sections of this chapter as well as in the publication by Energy Efficiency [33] and other references given at the end of this chapter.

## References

1. Mizia, R. E. (2008, April). *Next generation nuclear plant intermediate heat exchanger acquisition strategy*. INL/EXT-08-14054.
2. Zohuri, B. (2015). *Combined cycle driven efficiency for next generation nuclear power plants: An innovative design approach*. New York, NY: Springer Publishing Company.
3. Zohuri, B., & McDaniel, P. (2015). *Thermodynamics in nuclear power plant*. New York, NY: Springer Publishing Company.
4. Zohuri, B. (2014). *Innovative open air Brayton combined cycle systems for the next generation nuclear power plants*. Albuquerque, NM: University of New Mexico Publications.
5. Zohuri, B., & McDaniel, P. (2015). *A comparison of a recuperated open cycle (air) Brayton power conversion system with the traditional steam Rankine cycle for the next generation nuclear power plant*. Nuclear Science.
6. McDaniel, P. J., Zohuri, B., & de Oliveira, C. R. E. (2014, September). *A combined cycle power conversion system for small modular LMFBRs*. ANS Transactions.
7. Zohuri, B., McDaniel, P., & de Oliveira, C. R. E. (2014, June). *A comparison of a recuperated open cycle (air) Brayton power conversion system with the traditional steam Rankine cycle for the next generation nuclear power plant*. ANS Transactions.
8. McDaniel, P. J., de Oliveira, C. R. E., Zohuri, B., & Cole, J. (2012, November). *A combined cycle power conversion system for the next generation nuclear power plant*. ANS Transactions.
9. Forsberg, C., McDaniel, P., & Zohuri, B. (2015). *Variable Electricity and Steam from Salt, Helium, and Sodium Cooled Base-Load Reactors with Gas Turbines and Heat Storage*. Proceedings of ICAPP 2015, May 03–06, Nice (France) Paper 15115.
10. Nencti Ozisik, M. (1985). *Heat transfer: A basic approach*. New York, NY: McGraw-Hill.
11. McDonald, C. F., & Wilson, D. G. (1996). The utilization of recuperated and regenerated engine cycles for high-efficiency gas turbines in the 21st century. *Applied Thermal Engineering*, 16, 635–653.
12. Zohuri, B. (2011). *Heat pipe design and technology: a practical approach*. Boca Raton, FL: CRC Press.
13. Huzayyin, O. A. S. (2011). *Computational Modeling of Convective Heat Transfer in Compact and Enhanced Heat Exchangers*. University of Cincinnati, 193 pages, 3475151.
14. Shah, R. K. (2005). *Compact heat exchangers for microturbines*. Rochester, NY: Rochester Institute of Technology Dept. of Mechanical Engineering.
15. McDonald, C. F. (2000). *Low cost recuperator concept for microturbine applications* (ASME Paper No. 2000-GT-167). New York, NY: ASME.
16. McDonald, C. F. (2000). Low-cost compact primary surface recuperator concept for microturbines. *Applied Thermal Engineering*, 20, 471–497.
17. Kays, W. M., & London, A. L. (1984). *Compact heat exchangers* (3rd ed.). New York, NY: McGraw-Hill.
18. Zohuri, B., & Fathi, N. (2015). *Thermal hydraulic analysis of nuclear reactors*. New York, NY: Springer Publishing Company.
19. Stone, K. (1996). *Review of literature on heat transfer enhancement in compact heat exchangers*. Urbana, IL: Air Conditioning & Refrigeration Center Mechanical & Industrial Engineering Dept., University of Illinois.
20. Bergles, A. E., Webb, R. L., & Junkan, G. H. (1979). Energy conservation via heat transfer enhancement. *Energy*, 4, 193–200.
21. Webb, R. L. (1987). Enhancement of single-phase heat transfer. In S. Kakac, R. K. Shah, & A. E. Bergles (Eds.), *Enhancement of single-phase heat transfer* (p. 17-1-62). New York, NY: Wiley.
22. Shah, R. K. (1983). Classification of heat exchangers. In S. Kakac, R. K. Shah, & A. E. Bergles (Eds.), *Low Reynolds number flow heat exchangers* (pp. 9–14). Washington, DC: Hemisphere Publishing Corporation.

23. Shah, R. K., & Sekulic, D. P. (2003). *Fundaments of heat exchangers design*. New York, NY: John Wiley & Sons.
24. Hesselgreaves, J. E. (2001). *Compact heat exchangers, selection, design and operation*. New York, NY: Pergamon Publication.
25. Kays, W. M., & Crawford, M. E. (1993). *Convective heat and mass transfer* (3rd ed.). New York, NY: McGraw Hill.
26. London, A. L. (1964). Compact heat exchangers: Part 2 — Surface geometry. *Mechanical Engineering*, 86, 31–34.
27. Sundén, B., (2005). High Temperature Heat Exchangers (HTHE). *Proceedings of Fifth International conference on Enhanced, Compact and Ultra-Compact Heat Exchangers: Science, Engineering and Technology*, Hoboken, NJ, USA, September 2005.
28. Ohadi, M. M., & Buckley, S. G. (2001). High temperature heat exchangers and microscale combustion systems: Applications to thermal system miniaturization. *Experimental Thermal and Fluid Science*, 25, 207–217.
29. Brent, A. (1989). *Fundamentals of composites manufacturing materials methods and applications*. Dearborn, MI: SME.
30. Dewson, S., & Li, X., (2005). *Selection Criteria for the High Temperature Reactor Intermediate Heat Exchanger*. Proceedings of ICAPP'05, Seoul, Korea, May 15–19, 2005.
31. Sabharwall, P., & Kim, E. S. (2011). *High temperature thermal devices for nuclear process heat transfer applications*. Idaho: Idaho National Laboratory United States of America.
32. Martin, H. (1999). Economic Optimization of Compact Heat Exchangers. *Proceedings of the International Conference on Compact Heat Exchangers and Enhancement Technology for the Process Industries*, Banff, Begell House, New York.
33. Compact Heat Exchangers—Module 4.1. (2000, September). Energy Efficiency, GIR.

## Appendix A: Table and Graph Compilations

The following tables provide samples of engineering data for materials of interest to thermodynamics. For any detailed design work, more extensive handbooks should be consulted. The thermophysical property data for water, carbon dioxide, and sodium were generated for this book. They represent the best fit to the latest physical measurements. More extensive tables are available from the National Institutes of Standards and Technology (NIST).

## A.1 Physical Constants

Acceleration of Gravity	$g = 9.80665 \text{ m/sec}^2$ or $32.174 \text{ ft/sec}^2$
Sea Level Atmospheric Pressure	$p_{SL} = 101.325 \text{ kPa}$ $= 1.01325 \text{ bar}$ $= 14.696 \text{ psia}$ $= 760 \text{ mm Hg (0}^\circ\text{C)}$ $= 29.9213 \text{ in Hg (32}^\circ\text{F)}$ $= 10.3323 \text{ m H}_2\text{O (4}^\circ\text{C)}$
Boltzman's Constant	$k = 1.3806503 \times 10^{-23} \text{ joule/K}$
Avogadro's Number	$N_a = 6.02214199 \times 10^{23} \text{ 1/gm mole}$
Electronic Charge	$q_e = 1.60217646 \times 10^{-19} \text{ coulomb}$
Electron Volt	$\varepsilon = 1.60217646 \times 10^{-19} \text{ joules}$
Atomic Mass Unit	$amu = 1.6605402 \times 10^{-27} \text{ kg}$ $= 931.49432 \text{ MeV/c}^2$
Plank's Constant	$h = 6.62606876 \times 10^{-34} \text{ joule-sec}$ $\hbar = h/2\pi = 1.054571596 \times 10^{-34} \text{ joule-sec}$
Stefan Boltzman Constant	$\sigma = 0.17123 \times 10^{-8} \text{ Btu/(h-ft}^2\text{-}{}^\circ\text{R}^4)$ $\sigma = 5.670400 \times 10^{-8} \text{ w/(m}^2\text{-K}^4)$
Speed of Light in Vacuum	$c = 2.99792458 \times 10^8 \text{ meters/sec}$
Solar constant	$q_{solar} = 429 \text{ Btu/(h-ft}^2)$ $q^{solar} = 1,353 \text{ W/m}^2$
Universal Gas Constant	$\mathcal{R} = 8.31447 \text{ kj/(kgmol-K)}$ $= 8.31447 \text{ kPa-m}^3\text{/(kgmol-K)}$ $= 0.0831447 \text{ bar-m}^3\text{/(kgmol-K)}$ $= 82.05 \text{ L-atm/(kgmol-K)}$ $= 1.98583 \text{ Btu/(lbmol-}{}^\circ\text{R)}$ $= 1545.37 \text{ ft-lbf/(lbmol-}{}^\circ\text{R)}$ $= 10.73 \text{ psia-ft}^3\text{/(lbmol-}{}^\circ\text{R)}$

## A.2 Conversion Factors

Distance

<u>To Convert</u>	<u>To</u>	<u>Multiply By</u>
millimeters	meters	$10^{-3}$
centimeters	meters	$10^{-2}$
kilometers	meters	$10^3$
inches	feet	1/12
feet	yards	1/3
feet	miles	1/5,280
yards	miles	1/1,760
inches	centimeters	2.54
feet	meters	0.3048

Area

<u>To Convert</u>	<u>To</u>	<u>Multiply By</u>
millimeters <sup>2</sup>	meters <sup>2</sup>	$10^{-6}$
centimeters <sup>2</sup>	meters <sup>2</sup>	$10^{-4}$
kilometers <sup>2</sup>	meters <sup>2</sup>	$10^6$
inches <sup>2</sup>	feet <sup>2</sup>	1/144
inches <sup>2</sup>	centimeters <sup>2</sup>	6.4516
centimeters <sup>2</sup>	inches <sup>2</sup>	0.1550
feet <sup>2</sup>	meters <sup>2</sup>	0.092903
meters <sup>2</sup>	feet <sup>2</sup>	10.7639

Volume

<u>To Convert</u>	<u>To</u>	<u>Multiply By</u>
millimeters <sup>3</sup>	meters <sup>3</sup>	$10^{-9}$
centimeters <sup>3</sup>	meters <sup>3</sup>	$10^{-6}$
liters	meters <sup>3</sup>	$10^{-3}$
kilometers <sup>3</sup>	meters <sup>3</sup>	$10^9$
inches <sup>3</sup>	centimeters <sup>3</sup>	16.3871
centimeters <sup>3</sup>	inches <sup>3</sup>	0.061024
feet <sup>3</sup>	meters <sup>3</sup>	0.0283168
meters <sup>3</sup>	feet <sup>3</sup>	35.3147

Force

<u>To Convert</u>	<u>To</u>	<u>Multiply By</u>
kg-m/sec <sup>2</sup>	newtons	1.0
pound-mass-ft/sec <sup>2</sup>	pounds-force	1/32.1745
newtons	pounds-force	4.4482
pounds-force	newtons	0.2248

Mass and Density

<u>To Convert</u>	<u>To</u>	<u>Multiply By</u>
grams	kilograms	$10^{-3}$
metric tonnes	kilograms	$10^3$
ounces	pounds-mass	1/16
tons	pounds-mass	2000

	grams	ounces	1/28.35
	ounces	grams	28.35
	pounds-mass	kilograms	0.4536
	kilograms	pounds-mass	2.2046
	tons	metric tonnes	0.9072
	metric tonnes	tons	1.1023
	grams/cc	lbm/ft <sup>3</sup>	62.427
	grams/cc	kg/m <sup>3</sup>	10 <sup>3</sup>
	lb/ft <sup>3</sup>	kg/m <sup>3</sup>	16.0187
Pressure			
	<u>To Convert</u>	<u>To</u>	<u>Multiply By</u>
	psi	in Hg	2.036
	psi	in H <sub>2</sub> O	27.7
	atm	in Hg	29.92
	atm	ft H <sub>2</sub> O	33.93
	atm	Pa	101,320
	atm	bar	1.0133
	atm	psi	14.69
	kPa	psi	0.145
	psi	kPa	6.895
Energy			
	<u>To Convert</u>	<u>To</u>	<u>Multiply By</u>
	joules	ergs	107
	lbf-ft	joules	1.356
	Btu	joules	1055
	Btu	ft-lbf	778
	Cal	Btu	0.003968
	Cal	ft-lbf	3.088
	Btu	W-hr	0.2930
	kW-hr	Btu	3412
	Cal	joules	4.1868
	kJ/kg	Btu/lbm	0.4992
	Btu/lbm	kJ/kg	2.3260
	Cal/gm	Btu/lbm	1.8000
Power			
	<u>To Convert</u>	<u>To</u>	<u>Multiply By</u>
	hp	ft-lbf/s	550
	hp	Btu/hr	2545
	hp	kW	0.7455
	W	Btu/hr	3.412
	kW	hp	1.341
	ton	Btu/hr	12,000
	ton	kW	3.517
Heat Transfer			
	<u>To Convert</u>	<u>To</u>	<u>Multiply By</u>
	W/m/K	Btu/hr/ft/R	0.57779

kcal/h/m/K	W/m/K	1.1630
kcal/h/m/K	Btu/h/ft/R	0.67197
Btu/h/ft/R	W/m/K	1.7307
W/m <sup>2</sup> /K	Btu/h/ft <sup>2</sup> /R	0.17611
Btu/hr/ft <sup>2</sup> /R	W/m <sup>2</sup> /K	5.6783

## Fluid Flow

To Convert	To	Multiply By
m <sup>3</sup> /s	ft <sup>3</sup> /s	35.3147
g/cm/sec (poise)	lbf-sec/ft <sup>2</sup>	0.002088
lbf-sec/ft <sup>2</sup>	g/cm/sec	478.96
lbf-sec/ft <sup>2</sup>	kg/m/hr	172,400
lbm/ft/sec	gm/cm/sec	14.882
m <sup>2</sup> /sec	ft <sup>2</sup> /sec	10.7639
cm <sup>2</sup> /sec	ft <sup>2</sup> /hr	3.875
ft <sup>2</sup> /sec	m <sup>2</sup> /hr	334.45

## A.3 Standard Atmosphere

Table A3.1: SI Units

$$p_{SL} = 101325 \text{ Pas}$$

$$T_{SL} = 288.2 \text{ K}$$

$$\rho_{SL} = 1.225 \text{ kg/m}^3$$

Altitude (km)	P/P <sub>SL</sub>	T/T <sub>SL</sub>	$\rho/\rho_{SL}$
0	1	1	1
1	0.887	0.9774	0.9075
2	0.7846	0.9549	0.8217
3	0.692	0.9324	0.7423
4	0.6085	0.9098	0.6689
5	0.5334	0.8873	0.6012
6	0.466	0.8648	0.5389
7	0.4057	0.8423	0.4817
8	0.3519	0.8198	0.4292
9	0.304	0.7973	0.3813
10	0.2615	0.7748	0.3376
11	0.224	0.7523	0.2978
12	0.1915	0.7519	0.2546
13	0.1636	0.7519	0.2176
14	0.1399	0.7519	0.186
15	0.1195	0.7519	0.159
16	0.1022	0.7519	0.1359

$$p_{SL} = 2116 \text{ lbf/ft}^3$$

$$T_{SL} = 518.7^\circ R$$

$$\rho_{SL} = 0.07647 \text{ lbm/ft}^3$$

<u>Altitude (kft)</u>	<u>P/P<sub>SL</sub></u>	<u>T/T<sub>SL</sub></u>	<u>&lt;math&gt;\rho/\rho_{SL}&lt;/math&gt;</u>
0	1.0	1.0	1.0
2	0.9298	0.9863	0.9428
4	0.8637	0.9725	0.8881
6	0.8014	0.9588	0.8359
8	0.7429	0.945	0.7861
10	0.6878	0.9313	0.7386
12	0.6362	0.9175	0.6933
14	0.5877	0.9038	0.6502
16	0.5422	0.8901	0.6092
18	0.4997	0.8763	0.5702
20	0.4599	0.8626	0.5332
22	0.4227	0.8489	0.498
24	0.388	0.8352	0.4646
26	0.3557	0.8215	0.433
28	0.3256	0.8077	0.4031
30	0.2975	0.794	0.3747
32	0.2715	0.7803	0.348
34	0.2474	0.7666	0.3227
36	0.225	0.7529	0.2988
38	0.2044	0.7519	0.2719
40	0.1858	0.7519	0.2471
42	0.1688	0.7519	0.2245
44	0.1534	0.7519	0.204
46	0.1394	0.7519	0.1854
48	0.1267	0.7519	0.1685
50	0.1151	0.7519	0.1531

## A.4 Critical State Properties of Gases

		Molar Mass	P <sub>crit</sub> MPa	T <sub>crit</sub> K	P <sub>crit</sub> atm	T <sub>crit</sub>	V <sub>crit</sub>	Z <sub>crit</sub>
Air		28.996	3.77	133.0	37.21	239.0	88.3	0.300
Ammonia	NH <sub>3</sub>	17.031	11.28	405.5	111.32	729.8	72.5	0.243
Argon	Ar	39.950	4.86	151.0	47.96	272.0	75.2	0.291
Carbon Dioxide	CO <sub>2</sub>	44.010	7.39	304.2	72.93	547.5	94.0	0.293
Carbon Monoxide	CO	28.010	3.50	133.0	34.54	240.0	93.1	0.294
Chlorine	Cl <sub>2</sub>	70.906	7.99	416.9	78.87	750.4	124.0	0.276
Helium	He	4.003	0.23	5.3	2.27	9.5	57.5	0.303
Hydrogen	H <sub>2</sub>	2.016	1.30	33.3	12.83	59.9	65.0	0.304
Iodine	I <sub>2</sub>	253.809	11.70	819.0	115.47	1474.2	167.0	0.287
Krypton	Kr	83.800	5.50	209.4	54.28	376.9	92.2	0.291
Lithium	Li	6.941	67.00	3223.0	661.24	5801.4	120.0	0.300
Mercury	Hg	200.590	150.97	1763.2	1490.0	3173.7	29.1	0.300
Methane	CH <sub>4</sub>	16.043	4.64	191.1	45.79	343.9	99.0	0.290
Neon	Ne	20.180	2.73	44.5	26.94	227.1	41.7	0.307
Nitrogen	N <sub>2</sub>	28.013	3.39	126.2	33.46	227.1	90.1	0.291
Oxygen	O <sub>2</sub>	31.999	5.08	154.8	50.14	278.6	73.4	0.288
Potassium	K	39.098	16.42	2105.9	162.02	3790.7	320.0	0.300
Propane	C <sub>3</sub> H <sub>8</sub>	44.097	4.26	370.0	42.04	665.9	200.0	0.277
Sodium	Na	22.990	25.60	2503.9	252.65	4507.0	244.0	0.300
Water	H <sub>2</sub> O	18.015	22.10	647.4	218.11	1165.3	56.0	0.230
Water (Heavy)	D <sub>2</sub> O	20.023	21.72	644.7	214.36	1160.4	54.9	0.222
Xenon	Xe	131.290	5.84	289.8	57.65	521.6	118.8	0.290

## A.5 Constants for van der Waals Equation of State

<u>Substance</u>	Molar		a kPa-m <sup>6</sup> / kmol <sup>2</sup>	b m <sup>3</sup> /kmol	atm- ft <sup>6</sup> /lbmol <sup>2</sup>	a atm-ft <sup>3</sup> /lbmol	b ft <sup>3</sup> /lbmol
	Mass						
Air	28.996		136.83	0.03666	345.21	0.58621	
Ammonia	NH <sub>3</sub>	17.031	425.09	0.03736	1075.80	0.59826	
Argon	Ar	39.95	136.81	0.03229	346.85	0.51752	
Carbon Dioxide	CO <sub>2</sub>	44.0098	365.16	0.04278	924.18	0.68507	
Carbon Monoxide	CO	28.0104	147.38	0.03949	374.96	0.63407	
Chlorine	Cl <sub>2</sub>	70.906	634.26	0.05422	1605.62	0.86835	
Helium	He	4.0026	3.56	0.02395	8.94	0.38193	
Hydrogen	H <sub>2</sub>	2.0158	24.87	0.02662	62.88	0.42607	
Iodine	I <sub>2</sub>	253.809	1671.81	0.07275	4232.15	1.16510	
Krypton	Kr	83.8	232.51	0.03957	588.59	0.63372	
Lithium	Li	6.941	4521.16	0.04999	11445.24	0.80067	
Mercury	Hg	200.59	600.48	0.01214	1520.11	0.19439	
Methane	CH <sub>4</sub>	16.043	229.51	0.04280	580.74	0.68534	
Neon	Ne	20.1797	21.15	0.01694	430.43	0.76922	
Nitrogen	N <sub>2</sub>	28.0134	137.00	0.03869	346.63	0.61946	
Oxygen	O <sub>2</sub>	31.9988	137.56	0.03167	348.12	0.50712	
Potassium	K	39.0983	7877.53	0.13331	19942.70	2.13513	
	C <sub>3</sub> H						
Propane	<sub>8</sub>	44.097	937.13	0.09026	2371.61	1.44542	
Sodium	Na	22.9898	7141.57	0.10165	18078.79	1.62795	
Water	H <sub>2</sub> O	18.0152	553.04	0.03044	1399.97	0.48757	
Water (Heavy)	D <sub>2</sub> O	20.023	557.95	0.03084	1412.43	0.49400	
Xenon	Xe	131.29	419.20	0.05156	1061.20	0.82572	

$$R = 8314 \text{ J/kmol/K} = 1545 \text{ ft-lbf/lbmol/R} = 0.73023 \text{ atm-ft}^3/\text{lbmol/R}$$

## A.6 Constants for Redlich–Kwong Equation of State

<u>Substance</u>		Molar Mass	a kPa-m <sup>6</sup> - K <sup>1/2</sup> /kmol <sup>2</sup>	b m <sup>3</sup> /kmol	atm-ft <sup>6</sup> -R <sup>1/2</sup> / lbmol <sup>2</sup>	a ft <sup>3</sup> /lbmol	b
Air		28.996		1598.9	0.02541	5407.8	0.40631
Ammonia	NH <sub>3</sub>	17.031		8673.7	0.02589	29448.7	0.41466
Argon	Ar	39.95		1703.5	0.02238	5796.3	0.35870
Carbon Dioxide	CO <sub>2</sub>	44.0098		6453.4	0.02965	21912.0	0.47483
Carbon Monoxide	CO	28.0104		1722.3	0.02737	5886.1	0.43949
Chlorine	Cl <sub>2</sub>	70.906		13122.4	0.03758	44568.3	0.60187
Helium	He	4.0026		8.3	0.01660	27.9	0.26473
Hydrogen	H <sub>2</sub>	2.0158		145.4	0.01845	493.2	0.29531
Iodine	I <sub>2</sub>	253.809		48479.7	0.05042	164653.6	0.80756
Krypton	Kr	83.8		3409.3	0.02743	11579.2	0.43925
Lithium	Li	6.941		260082.9	0.03465	883330.7	0.55496
Mercury	Hg	200.59		25549.3	0.00841	86774.1	0.13473
Methane	CH <sub>4</sub>	16.043		3214.9	0.02967	10912.6	0.47502
Neon	Ne	20.1797		143.0	0.01174	6572.7	0.53316
Nitrogen	N <sub>2</sub>	28.0134		1559.5	0.02682	5293.1	0.42936
Oxygen	O <sub>2</sub>	31.9988		1734.2	0.02195	5887.8	0.35150
Potassium	K	39.0983		366303.6	0.09240	1244158.2	1.47990
Propane	C <sub>3</sub> H <sub>8</sub>	44.097		18265.5	0.06256	62012.5	1.00185
Sodium	Na	22.9898		362104.2	0.07045	1229829.9	1.12836
Water	H <sub>2</sub> O	18.0152		14258.5	0.02110	48424.8	0.33795
Water (Heavy)	D <sub>2</sub> O	20.023		14354.4	0.02138	48752.6	0.34240
Xenon	Xe	131.29		7230.7	0.03574	24558.0	0.57232

$$R = 8314 \text{ J/kmol/K} = 1545 \text{ ft-lbf/lbmol/R} = 0.73023 \text{ atm-ft}^3/\text{lbmol/R}$$

## A.7 Constants for the Peng–Robinson Equation of State

<u>Substance</u>	Mass	Molar	a	b	a	b	$\omega$
			kPa-m <sup>6</sup> /kmol <sup>2</sup>	m <sup>3</sup> /kmol	atm-ft <sup>6</sup> /lbmol <sup>2</sup>	ft <sup>3</sup> /lbmol	
Air	28.996		148.29	0.02282	374.15	0.36484	0.032
Ammonia	NH <sub>3</sub>	17.031	460.72	0.02325	1165.97	0.37234	0.252
Argon	Ar	39.95	148.28	0.02010	375.92	0.32209	-0.004
Carbon Dioxide	CO <sub>2</sub>	44.0098	395.76	0.02662	1001.65	0.42636	0.225
Carbon Monoxide	CO	28.0104	159.73	0.02458	406.39	0.39462	0.049
Chlorine	Cl <sub>2</sub>	70.906	687.42	0.03374	1740.20	0.54044	0.073
Helium	He	4.0026	3.86	0.01490	9.69	0.23770	0
Hydrogen	H <sub>2</sub>	2.0158	26.96	0.01657	68.16	0.26517	-0.215
Iodine	I <sub>2</sub>	253.809	1811.93	0.04528	4586.88	0.72512	0.07
Krypton	Kr	83.8	252.00	0.02463	637.92	0.39441	0.001
Lithium	Li	6.941	4900.11	0.03111	12404.55	0.49831	-0.153
Mercury	Hg	200.59	650.81	0.00755	1647.52	0.12098	-0.139
Methane	CH <sub>4</sub>	16.043	248.75	0.02664	629.41	0.42654	0.008
Neon	Ne	20.1797	22.93	0.01054	466.51	0.47874	-0.041
Nitrogen	N <sub>2</sub>	28.0134	148.48	0.02408	375.69	0.38553	0.04
Oxygen	O <sub>2</sub>	31.9988	149.09	0.01971	377.30	0.31562	0.021
Potassium	K	39.0983	8537.81	0.08297	21614.24	1.32884	-0.031
Propane	C <sub>3</sub> H <sub>8</sub>	44.097	1015.67	0.05618	2570.39	0.89958	0.152
Sodium	Na	22.9898	7740.16	0.06326	19594.10	1.01318	-0.076
Water	H <sub>2</sub> O	18.0152	599.40	0.01895	1517.31	0.30345	0.344
Water(Heavy)	D <sub>2</sub> O	20.023	604.71	0.01920	1530.82	0.30745	0.361
Xenon	Xe	131.29	454.34	0.03209	1150.15	0.51390	0.012

$$R = 8314 \text{ J/kmol/K} = 1545 \text{ ft-lbf/lbmol/R} = 0.73023 \text{ atm-ft}^3/\text{lbmol/R}$$

## A.8 Thermophysical Properties of Solids

Material	Melting Point (K)	Density	(Cp in J/kg/K)		(k in W/m/K)						
			T(K)		200	300	400	600	800	1000	1200
Aluminum(Pure)	933	2702	k	237	237	240	231	218			
			C <sub>p</sub>	798	903	949	1033	1146			
Aluminum (2024-T6)	775	2770	k	163	177	186	186				
			C <sub>p</sub>	787	875	925	1042				
Beryllium	1550	1850	k	301	200	161	126	106	90.8	78.7	
			C <sub>p</sub>	1114	1825	2191	2604	2823	3018	3227	3519
Bismuth	545	9780	k	9.69	7.86	7.04					
			C <sub>p</sub>	120	122	127					
Boron	2573	2500	k	55.5	27	16.8	10.6	9.6	9.85		
			C <sub>p</sub>	600	1107	1463	1892	2160	2338		
Cadmium	594	8650	k	99.3	96.8	94.7					
			C <sub>p</sub>	222	231	242					
Chromium	2118	7160	k	111	93.7	90.9	80.7	71.3	65.4	61.9	57.2
			C <sub>p</sub>	384	449	484	542	581	616	682	779
Copper (Pure)	1358	8933	k	413	401	393	379	366	352	339	
			C <sub>p</sub>	356	385	397	417	433	451	480	
Iron (Pure)	1810	7870	k	94	80.2	69.5	54.7	43.3	32.8	28.3	32.1
			C <sub>p</sub>	384	447	490	574	680	975	609	654
Carbon Steel		7854	k		60.5	56.7	48	39.2	31.3		
			C <sub>p</sub>		434	487	559	685	1169		
302 Stainless		8055	k		15.1	17.3	20	22.8	25.4		
			C <sub>p</sub>		480	512	559	585	606		
304 Stainless	1670	7900	k	12.6	14.9	16.6	19.8	22.6	25.4	28	31.7
			C <sub>p</sub>	402	477	515	557	582	611	640	682
316 Stainless		8238	k		13.4	15.2	18.3	21.3	24.2		
			C <sub>p</sub>		468	504	550	576	602		
347 Stainless		7978	k		14.2	15.8	18.9	21.9	24.7		
			C <sub>p</sub>		480	513	559	585	606		
Lead	601	11340	k	36.7	35.3	34	31.4				
			C <sub>p</sub>	125	129	132	142				
Lithium	454	534	k		84.8						
			C <sub>p</sub>		3580						
Magnesium	923	1740	k	159	156	153	149	146			
			C <sub>p</sub>	934	1024	1074	1170	1267			
Molybdenum	2894	10240	k	143	138	134	126	118	112	105	98
			C <sub>p</sub>	224	251	261	275	285	295	308	330
Nickel (Pure)	1728	8900	k	107	90.7	80.2	65.6	67.6	71.8	76.2	82.6

			$C_p$	383	444	485	592	530	562	594	616
Inconel X-750	1665	8510	k	10.3	11.7	13.5	17	20.5	24	27.6	33
			$C_p$	372	439	473	510	546	626		
Niobium	2741	8570	k	52.6	53.7	55.2	58.2	61.3	64.4	67.5	72.1
			$C_p$	249	265	274	283	292	301	310	324
Palladium	1827	12020	k	71.6	71.8	73.6	79.7	86.9	94.2	102	110
			$C_p$	227	244	251	261	271	281	291	307
Platinum (Pure)	2045	21450	k	72.6	71.6	71.8	73.2	75.6	78.7	82.6	89.5
			$C_p$	125	133	136	141	146	152	157	165
60%Pt-40%Rh	1800	16630	k		47	52	59	65	69	73	76
			$C_p$		162						
Plutonium	913	19860	k		25.1						
			$C_p$		104.4						
Potassium	337	862	k		102.5						
			$C_p$		757.1						
Rhenium	3453	21100	k	51	47.9	46.1	44.2	44.1	44.6	45.7	47.8
			$C_p$	127	136	139	145	151	156	162	171
Rhodium	2236	12450	k	154	150	146	136	127	121	116	110
			$C_p$	220	243	253	274	293	311	327	349
Silver	1235	10500	k	430	429	425	412	396	379	361	
			$C_p$	225	235	239	250	2623	277	292	
Sodium	371	986	k		142						
			$C_p$		1084						
Tantalum	3269	16600	k	57.5	57.5	57.8	58.6	59.4	60.2	61	62.2
			$C_p$	133	140	144	146	149	152	155	160
Thorium	2023	11700	k	54.6	54	54.5	55.8	56.9	56.9	58.7	
			$C_p$	112	118	124	134	145	156	167	
Tin	505	7310	k	73.3	66.6	62.2					
			$C_p$	215	227	243					
Titanium	1953	4500	k	24.5	21.9	20.4	19.4	19.7	20.7	22	24.5
			$C_p$	465	522	551	591	633	675	620	686
Tungsten	3660	19300	k	186	174	159	137	125	118	113	107
			$C_p$	122	132	137	142	145	148	152	157
Uranium	1406	19070	k	25.1	27.6	29.6	34	38.8	43.9	49	
			$C_p$	108	116	125	146	176	180	161	
Vanadium	2192	6100	k	31.3	30.7	31.3	33.3	35.7	38.2	40.8	44.6
			$C_p$	430	489	515	540	563	597	645	714
Zinc	693	7140	k	118	116	111	103				
			$C_p$	367	389	402	436				
Zirconium	2125	6570	k	25.2	22.7	21.6	20.7	21.6	23.7	26	28.8
			$C_p$	264	278	300	322	342	362	344	344

Beryllium Oxide	2725	3000	k		272	196	111	70	47	33	21.5
			C <sub>p</sub>		1030	1350	1690	1865	1975	2055	2145
Carbon	1500	1950	k	1.18	1.6	1.89	2.19	2.37	2.53	2.84	3.48
Amorphous			C <sub>p</sub>		509						
Graphite	2273	2210	k		5.7	16.8	9.23	4.09	2.68	2.01	1.6
Pyrolytic			C <sub>p</sub>	411	709	992	1406	1650	1793	1890	1974
Silicon Carbide	3100	3160	k		490				87	58	30
			C <sub>p</sub>		675	880	1050	1135	1195	1243	1310
Silicon Dioxide	1883	2220	k	1.14	1.38	1,51	1.75	2.17	2.87	4	
			C <sub>p</sub>		745	905	1040	1105	1155	1195	
Silicon Nitride	2173	2400	k		16	13.9	11.3	9.88	8.76	8	7.16
			C <sub>p</sub>	578	691	778	937	1063	1155	1226	1306
Thorium Dioxide	3573	9110	k		13	10.2	6.6	4.7	3.68	3.12	2.73
			C <sub>p</sub>		235	255	274	285	295	303	315
Uranium Dioxide	3138	10980	k	13.1	10.05	8.17	5.95	4.67	3.849	3.27	2.67
			C <sub>p</sub>	278	277.4	277.3	277	277	277.2	277	277
Plutonium	2673	11460	k	16.3	11.17	8.489	5.73	4.33	3.477	2.91	2.33
Dioxide			C <sub>p</sub>		276.1						
Concrete		2300	k			1.4					
			C <sub>p</sub>		880						
Glass		2500	k			1.4					
			C <sub>p</sub>		750						
Ice	273	920	k	2.03	1.88						
			C <sub>p</sub>	1945	2040						
Paraffin		900	k			0.24					
			C <sub>p</sub>		2890						
Paper		930	k			0.18					
			C <sub>p</sub>		1340						
Sand		1515	k			0.27					
			C <sub>p</sub>		800						
Soil		2050	k			0.52					
			C <sub>p</sub>		1840						

## A.9 Thermophysical Properties of Liquids

	<u>Temp</u>	<u>273</u>	<u>280</u>	<u>300</u>	<u>320</u>	<u>340</u>	<u>360</u>	<u>400</u>
Engine Oil	$\rho$ ( $\text{kg}/\text{m}^3$ )	899.1	895.3	884.1	871.8	859.9	847.8	825.1
	$C_p$ ( $\text{J}/\text{kg}/\text{K}$ )	1796	1827	1909	1993	2076	2161	2337
	$\mu$ ( $\text{N}\cdot\text{s}/\text{m}^2$ )	3.85	2.17	0.486	0.141	0.00531	0.00252	0.00087
	$k$ ( $\text{W}/\text{m}/\text{K}$ )	0.147	0.144	0.145	0.143	0.139	0.138	0.134
	<u>Temp</u>	<u>273</u>	<u>300</u>	<u>350</u>	<u>400</u>	<u>450</u>	<u>500</u>	<u>600</u>
Water (liquid)	$\rho$ ( $\text{kg}/\text{m}^3$ )	1000.0	997.0	973.7	937.2	890.5	831.3	648.9
	$C_p$ ( $\text{J}/\text{kg}/\text{K}$ )	4217.0	4179.0	4195.0	4256.0	4400.0	4660.0	7000.0
$T_m = 273$	$\mu$ ( $\text{N}\cdot\text{s}/\text{m}^2$ )	1.75E-03	8.55E-04	3.43E-04	2.17E-04	1.52E-04	1.18E-04	8.10E-05
	$k$ ( $\text{W}/\text{m}/\text{K}$ )	0.569	0.613	0.668	0.688	0.678	0.642	0.497
	<u>Temp</u>	<u>273</u>	<u>300</u>	<u>350</u>	<u>400</u>	<u>450</u>	<u>500</u>	<u>600</u>
Water (vapor)	$\rho$ ( $\text{kg}/\text{m}^3$ )	0.0048	0.0256	0.2600	1.3680	4.8077	13.05	72.99
	$C_p$ ( $\text{J}/\text{kg}/\text{K}$ )	1854	1872	1954	2158	2560	3270	8750
$T_b = 373$	$\mu$ ( $\text{N}\cdot\text{s}/\text{m}^2$ )	8.02E-06	9.09E-06	1.11E-05	1.31E-05	1.49E-05	1.66E-05	2.27E-05
	$k$ ( $\text{W}/\text{m}/\text{K}$ )	0.0182	0.0196	0.023	0.0272	0.0331	0.0423	0.103
Heavy	<u>Temp</u>	<u>273</u>	<u>353</u>					
Water (liquid)	$\rho$ ( $\text{kg}/\text{m}^3$ )	1105.4	1078.2					
	$C_p$ ( $\text{J}/\text{kg}/\text{K}$ )	4207.7	4178.4					
$T_m = 277$	$\mu$ ( $\text{N}\cdot\text{s}/\text{m}^2$ )							
	$k$ ( $\text{W}/\text{m}/\text{K}$ )	0.5931	0.632					
Heavy	<u>Temp</u>	<u>313.2</u>	<u>300</u>	<u>350</u>	<u>400</u>	<u>450</u>	<u>500</u>	<u>600</u>
Water (vapor)	$\rho$ ( $\text{kg}/\text{m}^3$ )	0.0058	0.0250	0.2717	1.4771	5.2966	14.75	83.96
	$C_p$ ( $\text{J}/\text{kg}/\text{K}$ )	1694.8	1712	1743.4	1779.4	1817.1	1856.4	1938.9
$T_b = 376$	$\mu$ ( $\text{N}\cdot\text{s}/\text{m}^2$ )							
	$k$ ( $\text{W}/\text{m}/\text{K}$ )	0.0187	0.0202	0.0237	0.02884	0.0309	0.0371	0.0482
Lithium	<u>Temp</u>	<u>473</u>	<u>673</u>	<u>873</u>	<u>1073</u>	<u>1273</u>		
$T_m = 452$ K	$\rho$ ( $\text{kg}/\text{m}^3$ )	508.9	491.2	475.1	457.5	441.4		
	$C_p$ ( $\text{kJ}/\text{kg}/\text{K}$ )	5861.5	4563.6	3810	3056.4	2302.7		
$T_b = 1590$ K	$\mu$ ( $\text{N}\cdot\text{s}/\text{m}^2$ )	5.65E-04	4.56E-04	4.56E-04	4.56E-04	4.56E-04		
	$k$ ( $\text{W}/\text{m}/\text{K}$ )	46.33	39.49	25.93	11.12	10.38		

	<u>Temp</u>	<u>477.8</u>	<u>588.9</u>	<u>700.0</u>	<u>811.1</u>	<u>922.2</u>	<u>1033.3</u>	<u>1154.8</u>
Sodium	$\rho$ ( $\text{kg}/\text{m}^3$ )	904.4	878.1	851.6	824.9	798.1	771.1	741.6
$T_m=371$	$C_p$ (J/kg/K)	1.338	1.300	1.274	1.259	1.255	1.263	1.284
$T_b = 1156 \text{ K}$	$\mu$ ( $\text{N}\cdot\text{s}/\text{m}^2$ )	4.52E-04	3.33E-04	2.66E-04	2.26E-04	1.97E-04	1.74E-04	1.57E-04
	$k$ (W/m/K)	81.52	75.81	70.27	65.08	60.23	55.56	50.88
	<u>Temp</u>	<u>600</u>	<u>800</u>	<u>1000</u>	<u>1200</u>	<u>1392.6</u>	<u>1400</u>	<u>1800</u>
		588.9	700.0	811.1	922.2	1029.2	1033.3	1255.6
Potassium	$\rho$ ( $\text{kg}/\text{m}^3$ )	771.9	745.8	719.1	692.0	665.4	664.2	607.7
$T_m=337$	$C_p$ (J/kg/K)	0.783	0.791	0.804	0.825	0.854	0.854	0.934
$T_b = 1033 \text{ K}$	$\mu$ ( $\text{N}\cdot\text{s}/\text{m}^2$ )	2.54E-04	2.06E-04	1.71E-04	1.47E-04	1.31E-04	1.31E-04	1.09E-04
	$k$ (W/m/K)	43.61	39.98	36.69	33.75	30.81	30.81	25.10
	<u>Temp</u>	<u>366</u>	<u>644</u>	<u>977</u>				
NaK (45/50)	$\rho$ ( $\text{kg}/\text{m}^3$ )	887.4	821.7	740.1				
$T_m=292 \text{ K}$	$C_p$ (J/kg/K)	1130	1055	1043				
$T_b = 1098 \text{ K}$	$\mu$ ( $\text{N}\cdot\text{s}/\text{m}^2$ )	5.79E-04	2.36E-04	1.61E-04				
	$k$ (W/m/K)	25.6	27.5	28.9				
	<u>Temp</u>	<u>366</u>	<u>672</u>	<u>1033</u>				
NaK(22/78)	$\rho$ ( $\text{kg}/\text{m}^3$ )	849	775.3	690.4				
$T_m=262 \text{ K}$	$C_p$ (J/kg/K)	946	879	883				
$T_b = 1057 \text{ K}$	$\mu$ ( $\text{N}\cdot\text{s}/\text{m}^2$ )	4.92E-04	2.07E-04	1.46E-04				
	$k$ (W/m/K)	24.4	26.7	29.4				
	<u>Temp</u>	<u>644</u>	<u>755</u>	<u>977</u>				
Lead	$\rho$ ( $\text{kg}/\text{m}^3$ )	10540	10412	10140				
$T_m=600 \text{ K}$	$C_p$ (J/kg/K)	159	155	151				
$T_b = 2010 \text{ K}$	$\mu$ ( $\text{N}\cdot\text{s}/\text{m}^2$ )	2.39E-03	1.93E-03	1.37E-03				
	$k$ (W/m/K)	16.1	15.6	14.9				
	<u>Temp</u>	<u>273</u>	<u>300</u>	<u>350</u>	<u>400</u>	<u>450</u>	<u>500</u>	<u>600</u>
Mercury	$\rho$ ( $\text{kg}/\text{m}^3$ )	13595	13529	13407	13287	13167	13048	12809
$T_m=234 \text{ K}$	$C_p$ (J/kg/K)	140.4	139.3	137.7	136.5	135.7	135.3	135.5
$T_b = 630 \text{ K}$	$\mu$ ( $\text{N}\cdot\text{s}/\text{m}^2$ )	1.69E-03	1.52E-03	1.31E-03	1.17E-03	1.08E-03	1.01E-03	9.11E-04
	$k$ (W/m/K)	8.18	8.54	9.18	9.8	10.4	10.95	11.95
	<u>Temp</u>	<u>589</u>	<u>811</u>	<u>1033</u>				
Bismuth	$\rho$ ( $\text{kg}/\text{m}^3$ )	10011	9739	9467				
$T_m=544 \text{ K}$	$C_p$ (J/kg/K)	144.4	154.5	164.5				
$T_b = 1750 \text{ K}$	$\mu$ ( $\text{N}\cdot\text{s}/\text{m}^2$ )	1.62E-03	1.10E-03	7.90E-04				
	$k$ (W/m/K)	16.4	15.6	15.6				
	<u>Temp</u>	<u>422</u>	<u>644</u>	<u>922</u>				
PbBi(44.5/55.5)	$\rho$ ( $\text{kg}/\text{m}^3$ )	10524	10236	9835				
$T_m=398 \text{ K}$	$C_p$ (J/kg/K)	147	147	147				
$T_b = 1943 \text{ K}$	$\mu$ ( $\text{N}\cdot\text{s}/\text{m}^2$ )	1.85E-03	1.53E-03	1.15E-03				
	$k$ (W/m/K)	9.05	11.86	15.3788				

## A.10 Thermophysical Properties of Gases

	Temp (K)	250	300	500	650	800	1000	1200	1400	1600	1800	
	$\mu$ (N·s/m <sup>2</sup> )	1.60E-05	2.08E-05	2.70E-05	3.23E-05	3.70E-05	4.24E-05	4.73E-05	5.30E-05	5.84E-05	6.37E-05	
	k (W/m/K)	0.0223	0.0300	0.0407	0.0497	0.0573	0.0667	0.0763	0.0910	0.1060	0.1200	
Carbon Dioxide	Temp (K)	280	300	350	400	450	500	550	600	650	700	
Carbon Dioxide	$\mu$ (N·s/m <sup>2</sup> )	1.40E-05	1.49E-05	1.69E-05	1.90E-05	2.10E-05	2.31E-05	2.51E-05	2.70E-05	2.88E-05	3.05E-05	
Carbon Dioxide	k (W/m/K)	0.0152	0.0166	0.0205	0.0243	0.0283	0.0325	0.0366	0.0407	0.0445	0.0481	
Carbon Monoxide	Temp (K)	250	300	350	400	450	500	550	600	650	700	
Carbon Monoxide	$\mu$ (N·s/m <sup>2</sup> )	1.52E-05	1.75E-05	1.98E-05	2.18E-05	2.37E-05	2.54E-05	2.71E-05	2.86E-05	3.01E-05	3.15E-05	
Carbon Monoxide	k (W/m/K)	0.0214	0.0250	0.0285	0.0318	0.0350	0.0381	0.0411	0.0440	0.0470	0.0500	
Helium	Temp (K)	250	300	350	400	450	500	600	700	800	900	
Helium	$\mu$ (N·s/m <sup>2</sup> )	1.70E-05	1.99E-05	2.21E-05	2.43E-05	2.63E-05	2.83E-05	3.20E-05	3.50E-05	3.82E-05	4.14E-05	
Helium	k (W/m/K)	0.1335	0.1520	0.1700	0.1870	0.2040	0.2200	0.2520	0.2780	0.3040	0.3300	
Hydrogen	Temp (K)	250	300	350	400	450	500	600	800	1000	1200	1400
Hydrogen	$\mu$ (N·s/m <sup>2</sup> )	7.89E-06	8.96E-06	9.88E-06	1.08E-05	1.26E-05	1.42E-05	1.72E-05	2.01E-05	2.26E-05	2.51E-05	2.81E-05
Hydrogen	k (W/m/K)	0.1570	0.1830	0.2040	0.2260	0.2660	0.3050	0.3780	0.4480	0.5280	0.6100	
Nitrogen	Temp (K)	250	300	350	400	500	600	700	800	900	1100	
Nitrogen	$\mu$ (N·s/m <sup>2</sup> )	1.55E-05	1.78E-05	2.00E-05	2.22E-05	2.58E-05	2.91E-05	3.21E-05	3.49E-05	3.75E-05	4.23E-05	
Nitrogen	k (W/m/K)	0.0222	0.0259	0.0293	0.0327	0.0389	0.0446	0.0499	0.0548	0.0597	0.0700	
Oxygen	Temp (K)	250	300	350	400	500	600	700	800	900	1100	
Oxygen	$\mu$ (N·s/m <sup>2</sup> )	1.79E-05	2.07E-05	2.34E-05	2.58E-05	3.03E-05	3.44E-05	3.81E-05	4.15E-05	4.47E-05	5.06E-05	
Oxygen	k (W/m/K)	0.0226	0.0268	0.0296	0.0330	0.0412	0.0473	0.0528	0.0589	0.0649	0.0758	
Water	Temp (K)	380	400	450	500	550	600	650	700	750	800	
Water	$\mu$ (N·s/m <sup>2</sup> )	1.27E-05	1.34E-05	1.53E-05	1.70E-05	1.88E-05	2.07E-05	2.25E-05	2.43E-05	2.60E-05	2.79E-05	
Water	k (W/m/K)	0.0246	0.0261	0.0299	0.0339	0.0379	0.0422	0.0464	0.0505	0.0549	0.0592	

## A.11 Ideal Gas Heat Capacities for Selected Gases

	$\tau$	$C_0^*$	$C_1$	$C_2$	$C_3$	$C_4$	Range (K)	Range (°R)	Max Error
Air	0.0140	9.0761	-3.4743	1.7804	-0.3134	0.0188	100-6200	56-3444	0.77%
100% Air + CP(CH <sub>1</sub> )	0.0400	9.5147	-3.9901	2.1908	-0.3898	0.0229	300-4000	167-2222	0.32%
100% Air + CP(CH <sub>2</sub> )	0.0400	9.7159	-4.0842	2.1394	-0.3635	0.0202	300-4000	167-2222	0.35%
100% Air + CP(CH <sub>3</sub> )	0.0400	9.8608	-4.1581	2.1088	-0.3464	0.0184	300-4000	167-2222	0.37%
Carbon Dioxide	1.0000	-5.8291	12.0893	-2.7155	0.2747	-0.0102	300-5800	167-3222	0.18%
Carbon Monoxide	0.0750	12.1297	-7.2191	3.4222	-0.6162	0.0387	300-5800	167-3222	0.36%
Hydrogen	0.5000	12.2786	-4.7650	1.4175	-0.1407	0.0037	300-5800	167-3222	0.48%
Nitrogen	0.1000	12.2568	-7.0276	3.1766	-0.5465	0.0328	300-6400	167-3556	0.38%
Oxygen	0.0005	8.5200	-3.1865	1.9424	-0.3855	0.0261	300-6400	167-3556	0.98%
Water	0.1500	15.8257	-10.0486	4.3395	-0.6669	0.0355	300-6400	167-3556	0.28%
Hydroxyl Ion	0.0025	11.4039	-4.7972	1.7247	-0.2252	0.0099	540-6300	300-3500	0.62%
Nitrous Oxide	7.5500	-21.2671	28.5044	-9.0836	1.2789	-0.0676	540-6300	300-3500	0.71%
Nitrogen Dioxide	1.5000	-16.0807	21.1941	-5.8523	0.7382	-0.0356	540-6300	300-3500	0.81%
Methane	2.8500	-21.3124	17.0304	-1.4849	-0.0505	0.0043	540-6300	300-3500	0.20%

The ideal gas constant pressure specific heat is given by

$$\theta = \left( \frac{T(\text{K})}{100} \right) = \left( \frac{T(\text{^{\circ}R})}{180} \right) \quad C_p = \sum_{i=0}^{i=4} C_i(\theta)^{\frac{1}{2}} = \frac{\text{kcal}}{\text{kgmol} - \text{K}} = \frac{\text{Btu}}{\text{lbm} - \text{^{\circ}R}} \quad C_0 = C_0^* \left( \frac{\theta^2}{\theta^2 + \tau} \right).$$

25°C (77°F), 1 atm							
		h <sub>f</sub> kj/kmol	g <sub>f</sub> kj/kmol	s° kj/kmol/K	h <sub>f</sub> Btu/lbmol	g <sub>f</sub> Btu/lbmol	s° Btu/lbmol/R
Carbon	C(s)	0	0	5.74	0	0	1.371
Hydrogen	H <sub>2</sub> (g)	0	0	130.68	0	0	31.215
Nitrogen	N <sub>2</sub> (g)	0	0	191.61	0	0	45.768
Oxygen	O <sub>2</sub> (g)	0	0	205.04	0	0	48.976
Carbon Monoxide	CO(g)	-110,530	-137,150	197.65	-47523	-58968	47.211
Carbon Dioxide	CO <sub>2</sub> (g)	-393,520	-394,360	213.8	-169195	-169556	51.069
Steam	H <sub>2</sub> O(g)	-241,820	-228,590	188.83	-103971	-98283	45.104
Water	H <sub>2</sub> O(l)	-285,830	-237,180	69.92	-122893	-101976	16.701
Ammonia	NH <sub>3</sub> (g)	-46,190	-16,590	192.33	-19860	-7133	45.940
Methane	CH <sub>4</sub> (g)	-74,850	-50,790	186.16	-32182	-21837	44.467
Propane	C <sub>3</sub> H <sub>8</sub> (g)	-103,850	-23,490	269.91	-44651	-10100	64.471
n-Octane	C <sub>8</sub> H <sub>18</sub> (g)	-208,450	16,530	466.73	-89624	7107	111.484
n-Octane	C <sub>8</sub> H <sub>18</sub> (l)	-249,950	6,610	360.79	-107467	2842	86.179
Methyl Alcohol	CH <sub>3</sub> OH(g)	-200,670	-162,000	239.7	-86279	-69652	57.255
Methyl Alcohol	CH <sub>3</sub> OH(l)	-277,690	-166,360	126.8	-119394	-71527	30.288
Monatomic Oxygen	O(g)	249,190	231,770	161.06	107140	99650	38.471
Monatomic Hydrogen	H(g)	218,000	203,290	114.72	93730	87405	27.402
Monatomic Nitrogen	N(g)	472,650	455,510	153.3	203217	195848	36.618
Hydroxyl Ion	OH(g)	39,460	34,280	183.7	16966	14739	43.879
		h <sub>fg</sub> kj/kmol	C <sub>p</sub> kj/kmol/K	h <sub>fg</sub> Btu/lbmol	C <sub>p</sub> Btu/lbmol/R		
Water		44,010	35.3	18922	8.43		
Propane		15,060	122.2	6475	29.18		
n-Octane		41,460	254.7	17826	60.84		
Methyl Alcohol		37,900	83.5	16295	19.95		
Sodium		100819	29.9	43347	7.14		
Potassium		83934	30.6	36088	7.31		
Mercury		61303	27.9	26358	6.66		

## **Appendix B: Gas Property Tables for Selected Gases**

### **B.1 Air Properties (SI Units)**

Temperature		<i>h</i>	<i>u</i>	<i>Pr</i>	<i>Vr</i>	<i>s<sub>o</sub></i>	Gamma
K	C	kg/kgmol	kJ/kgmol			kJ/kgmol/K	
100	-173.1	1604.8	1142.6	0.03	6018.5	23.8878	1.400
125	-148.1	2331.0	1663.3	0.07	1916.6	30.3695	1.401
150	-123.1	3056.4	2182.4	0.12	1217.2	35.6598	1.402
175	-98.1	3781.8	2701.0	0.21	829.17	40.1327	1.401
200	-73.1	4507.5	3219.7	0.34	594.50	44.0087	1.401
225	-48.1	5233.5	3738.5	0.51	443.22	47.4293	1.401
250	-23.1	5959.9	4257.7	0.73	340.76	50.4908	1.401
275	1.9	6686.9	4777.2	1.02	268.59	53.2620	1.400
300	26.9	7414.4	5297.2	1.39	216.07	55.7943	1.400
325	51.9	8142.9	5818.2	1.84	176.81	58.1266	1.399
350	76.9	8872.6	6340.2	2.38	146.79	60.2895	1.398
375	101.9	9603.7	6863.8	3.04	123.39	62.3073	1.396
400	126.9	10336.8	7389.2	3.82	104.82	64.1997	1.395
425	151.9	11072.0	7916.7	4.73	89.874	65.9826	1.393
450	176.9	11809.8	8446.8	5.79	77.685	67.6695	1.391
475	201.9	12550.5	8979.8	7.02	67.631	69.2711	1.389
500	226.9	13294.2	9515.8	8.44	59.253	70.7971	1.387
525	251.9	14041.4	10055.3	10.06	52.205	72.2555	1.384
550	276.9	14792.3	10598.4	11.90	46.231	73.6525	1.381
575	301.9	15547.0	11145.4	13.98	41.128	74.9945	1.379
600	326.9	16305.7	11696.3	16.33	36.742	76.2859	1.376
625	351.9	17068.5	12251.4	18.97	32.948	77.5314	1.373
650	376.9	17835.5	12810.7	21.92	29.648	78.7349	1.370
675	401.9	18606.9	13374.1	25.22	26.765	79.8992	1.367
700	426.9	19382.6	13942.1	28.89	24.233	81.0276	1.365
725	451.9	20162.6	14514.4	32.95	22.002	82.1225	1.362
750	476.9	20946.8	15090.8	37.45	20.027	83.1861	1.359
775	501.9	21735.5	15671.7	42.41	18.274	84.2203	1.357
800	526.8	22528.4	16256.8	47.87	16.711	85.2274	1.354
825	551.8	23325.6	16846.1	53.87	15.315	86.2087	1.351
850	576.8	24126.8	17439.7	60.44	14.064	87.1653	1.349
875	601.8	24932.1	18037.2	67.62	12.940	88.0990	1.347
900	626.8	25741.4	18638.5	75.46	11.926	89.0111	1.344
925	651.8	26554.5	19243.9	84.00	11.012	89.9020	1.342
950	676.8	27371.3	19852.8	93.28	10.184	90.7733	1.340
975	701.8	28191.9	20465.7	103.36	9.433	91.6261	1.338
1000	726.8	29016.1	21082.2	114.27	8.751	92.4606	1.336
1025	751.8	29843.6	21701.8	126.08	8.130	93.2783	1.334
1050	776.8	30674.4	22324.6	138.83	7.563	94.0789	1.333
1075	801.8	31508.7	22951.0	152.57	7.046	94.8638	1.331
1100	826.8	32346.0	23580.6	167.37	6.572	95.6337	1.329
1125	851.8	33186.2	24212.8	183.29	6.138	96.3890	1.328
1150	876.8	34029.3	24848.2	200.39	5.739	97.1304	1.326
1175	901.8	34875.2	25486.4	218.70	5.373	97.8575	1.325
1200	926.8	35723.9	26127.4	238.35	5.035	98.5727	1.324
1225	951.8	36574.9	26770.7	259.35	4.723	99.2747	1.322
1250	976.8	37428.9	27416.6	281.80	4.436	99.9647	1.321

1275	1001.8	38285.6	28065.2	305.76	4.170	100.6433	1.320
1300	1026.8	39143.5	28715.8	331.30	3.924	101.3101	1.319
1325	1051.8	40004.7	29369.0	358.49	3.696	101.9659	1.318
1350	1076.8	40868.0	30024.6	387.42	3.485	102.6112	1.317
1375	1101.8	41733.0	30681.8	418.17	3.288	103.2462	1.316
1400	1126.8	42600.6	31341.7	450.85	3.105	103.8718	1.315
1425	1151.8	43470.4	32003.0	485.52	2.935	104.4876	1.314
1450	1176.8	44340.9	32665.9	522.22	2.777	105.0935	1.313
1475	1201.8	45214.2	33331.4	561.10	2.629	105.6904	1.312
1500	1226.8	46089.4	33999.0	602.25	2.491	106.2789	1.311
1525	1251.8	46966.6	34668.5	645.68	2.362	106.8578	1.310
1550	1276.8	47845.5	35339.7	691.69	2.241	107.4300	1.309
1575	1301.8	48726.2	36011.9	740.16	2.128	107.9931	1.309
1600	1326.8	49607.8	36685.8	791.40	2.022	108.5495	1.308
1625	1351.8	50491.7	37362.0	845.22	1.923	109.0966	1.307
1650	1376.8	51376.2	38038.9	902.11	1.829	109.6381	1.306
1675	1401.8	52262.5	38717.5	961.77	1.742	110.1705	1.306
1700	1426.8	53152.0	39397.5	1024.76	1.659	110.6979	1.305
1725	1451.8	54042.3	40080.2	1090.79	1.581	111.2171	1.304
1750	1476.8	54932.8	40763.0	1160.12	1.508	111.7294	1.304
1775	1501.8	55825.3	41449.4	1233.09	1.439	112.2365	1.303
1800	1526.8	56720.1	42134.9	1309.56	1.375	112.7367	1.303
1825	1551.8	57613.3	42820.4	1389.69	1.313	113.2305	1.302
1850	1576.8	58509.4	43508.9	1473.67	1.255	113.7182	1.302
1875	1601.8	59409.7	44201.5	1561.58	1.201	114.2000	1.301
1900	1626.8	60306.9	44891.0	1653.65	1.149	114.6762	1.300
1925	1651.8	61207.5	45582.2	1749.90	1.100	115.1466	1.300
1950	1676.8	62110.5	46279.2	1850.59	1.054	115.6117	1.299
1975	1701.8	63012.8	46972.2	1955.91	1.010	116.0718	1.299
2000	1726.8	63915.9	47669.2	2066.18	0.968	116.5278	1.298
2025	1751.8	64819.8	48365.4	2181.02	0.928	116.9775	1.298
2050	1776.8	65726.4	49062.8	2300.86	0.891	117.4222	1.298
2075	1801.8	66632.6	49762.9	2425.62	0.855	117.8612	1.297
2100	1826.8	67543.5	50464.5	2555.79	0.822	118.2958	1.297
2125	1851.8	68450.4	51165.3	2691.76	0.789	118.7267	1.296
2150	1876.8	69360.0	51865.6	2833.21	0.759	119.1525	1.296
2175	1901.8	70272.1	52568.3	2979.99	0.730	119.5725	1.295
2200	1926.8	71182.2	53272.4	3133.78	0.702	119.9908	1.295
2225	1951.8	72097.2	53978.1	3293.20	0.676	120.4033	1.295
2250	1976.8	73011.9	54686.7	3458.58	0.651	120.8107	1.294
2275	2001.8	73923.4	55388.9	3630.89	0.627	121.2149	1.294
2300	2026.8	74842.5	56098.7	3809.81	0.604	121.6148	1.294
2325	2051.9	75754.3	56804.4	3995.67	0.582	122.0108	1.293
2350	2076.9	76674.1	57518.2	4189.73	0.561	122.4051	1.293
2375	2101.9	77592.9	58227.6	4389.97	0.541	122.7932	1.293
2400	2126.9	78507.2	58935.8	4597.72	0.522	123.1776	1.292
2425	2151.9	79426.7	59646.1	4813.26	0.504	123.5585	1.292
2450	2176.9	80349.7	60363.0	5037.23	0.486	123.9366	1.292
2475	2201.9	81273.4	61077.4	5270.24	0.470	124.3125	1.291
2500	2226.9	82192.5	61790.4	5509.22	0.454	124.6812	1.291
2525	2251.9	83114.8	62506.7	5757.86	0.439	125.0482	1.291
2550	2276.9	84041.1	63223.6	6015.53	0.424	125.4122	1.290

2575	2301.9	84969.4	63942.5	6280.78	0.410	125.7709	1.290
2600	2326.9	85886.2	64650.1	6557.81	0.396	126.1298	1.290
2625	2351.9	86807.6	65368.9	6844.26	0.384	126.4852	1.289
2650	2376.9	87741.2	66093.0	7139.73	0.371	126.8366	1.289
2675	2401.9	88664.3	66806.7	7447.82	0.359	127.1878	1.289
2700	2426.9	89596.2	67529.3	7761.68	0.348	127.5310	1.289
2725	2451.9	90518.9	68249.2	8089.94	0.337	127.8753	1.288
2750	2476.9	91450.9	68965.3	8423.94	0.326	128.2117	1.288
2775	2501.9	92381.9	69687.0	8769.42	0.316	128.5458	1.288
2800	2526.9	93311.9	70414.3	9131.02	0.307	128.8818	1.288
2825	2551.9	94248.4	71141.4	9502.36	0.297	129.2132	1.287
2850	2576.9	95182.0	71865.7	9888.05	0.288	129.5439	1.287
2875	2601.9	96115.2	72589.6	10282.3	0.280	129.8690	1.287
2900	2626.9	97050.2	73321.8	10686.3	0.271	130.1894	1.286
2925	2651.9	97967.6	74029.8	11103.6	0.263	130.5078	1.286
2950	2676.9	98908.9	74761.9	11543.9	0.256	130.8311	1.286
2975	2701.9	99845.8	75489.4	11986.1	0.248	131.1437	1.286
3000	2726.9	100781.8	76216.1	12444.3	0.241	131.4555	1.285
3025	2751.9	101706.6	76944.6	12933.0	0.234	131.7758	1.285
3050	2776.9	102662.5	77678.1	13408.5	0.227	132.0760	1.285
3075	2801.9	103596.5	78402.8	13907.1	0.221	132.3795	1.285
3100	2826.9	104539.8	79149.9	14431.7	0.215	132.6873	1.284
3125	2851.9	105465.8	79866.5	14965.8	0.209	132.9895	1.284
3150	2876.9	106407.4	80611.9	15519.7	0.203	133.2916	1.284
3175	2901.9	107353.1	81348.2	16072.2	0.198	133.5824	1.284
3200	2926.9	108280.3	82053.1	16655.2	0.192	133.8786	1.284
3225	2951.9	109232.0	82808.5	17257.4	0.187	134.1739	1.283
3250	2976.9	110178.3	83545.5	17879.8	0.182	134.4685	1.283
3275	3001.9	111123.2	84267.9	18497.0	0.177	134.7506	1.283
3300	3026.9	112069.4	85004.8	19152.7	0.172	135.0402	1.283
3325	3051.9	113008.3	85747.5	19806.8	0.168	135.3194	1.283
3350	3076.9	113938.4	86468.3	20500.1	0.163	135.6055	1.283
3375	3101.9	114883.0	87203.5	21213.6	0.159	135.8899	1.282
3400	3126.9	115838.3	87949.5	21938.6	0.155	136.1693	1.283

## B.2 Air Properties (English Units)

Temperature		h	u	Pr	Vr	S <sub>o</sub>	Gamma
R	F	Btu/lbmol	Btu/lbmol			Btu/lbmol/R	
100	-359.7	690.0	491.3	0.004	26215.8	5.7059	1.402
140	-319.7	968.4	692.7	0.012	11288.7	8.0473	1.399
180	-279.7	1246.6	892.9	0.030	6018.51	9.7953	1.400
220	-239.7	1524.1	1091.9	0.060	3648.55	11.1878	1.401
260	-199.7	1801.4	1290.4	0.108	2406.77	12.3457	1.402
300	-159.7	2078.6	1488.6	0.178	1685.34	13.3375	1.402
340	-119.7	2355.9	1686.8	0.276	1233.92	14.2051	1.401
380	-79.7	2633.3	1885.1	0.406	935.173	14.9765	1.401
420	-39.7	2910.8	2083.4	0.576	728.608	15.6709	1.401
460	0.3	3188.5	2281.8	0.792	580.625	16.3024	1.401
500	40.3	3466.4	2480.4	1.061	471.455	16.8816	1.400
540	80.3	3744.5	2679.2	1.388	388.917	17.4166	1.400
580	120.3	4022.8	2878.2	1.784	325.178	17.9140	1.399
620	160.3	4301.6	3077.7	2.254	275.068	18.3788	1.398
660	200.3	4580.9	3277.6	2.808	235.036	18.8153	1.397
700	240.3	4860.7	3478.1	3.455	202.608	19.2269	1.396
740	280.3	5141.3	3679.3	4.204	176.016	19.6167	1.394
780	320.3	5422.6	3881.3	5.066	153.972	19.9869	1.393
820	360.3	5704.9	4084.2	6.051	135.513	20.3398	1.391
860	400.3	5988.1	4288.0	7.171	119.925	20.6771	1.389
900	440.3	6272.5	4493.0	8.438	106.655	21.0003	1.387
940	480.3	6558.0	4699.1	9.866	95.277	21.3106	1.384
980	520.3	6844.7	4906.4	11.468	85.459	21.6094	1.382
1020	560.3	7132.7	5115.0	13.257	76.939	21.8974	1.380
1060	600.3	7422.1	5325.0	15.252	69.500	22.1757	1.377
1100	640.3	7712.8	5536.3	17.466	62.978	22.4449	1.375
1140	680.3	8004.9	5749.1	19.918	57.234	22.7058	1.372
1180	720.3	8298.6	5963.3	22.626	52.152	22.9589	1.370
1220	760.3	8593.7	6178.9	25.609	47.640	23.2048	1.367
1260	800.3	8890.2	6396.0	28.886	43.620	23.4439	1.365
1300	840.3	9188.2	6614.7	32.479	40.025	23.6768	1.362
1340	880.3	9487.6	6834.7	36.411	36.802	23.9037	1.360
1380	920.3	9788.6	7056.3	40.703	33.904	24.1250	1.357
1420	960.3	10091.0	7279.2	45.382	31.290	24.3410	1.355
1460	1000.3	10394.8	7503.7	50.467	28.930	24.5520	1.353
1500	1040.3	10700.1	7729.5	55.993	26.789	24.7583	1.351
1540	1080.3	11006.8	7956.8	61.980	24.847	24.9600	1.349
1580	1120.3	11314.8	8185.4	68.460	23.079	25.1575	1.346
1620	1160.3	11624.2	8415.3	75.463	21.468	25.3509	1.344
1660	1200.3	11934.8	8646.5	83.016	19.996	25.5403	1.343
1700	1240.3	12246.8	8879.1	91.154	18.650	25.7260	1.341
1740	1280.3	12560.0	9112.8	99.909	17.416	25.9082	1.339
1780	1320.3	12874.3	9347.9	109.313	16.283	26.0868	1.337
1820	1360.3	13190.1	9584.1	119.404	15.242	26.2621	1.336
1860	1400.3	13506.8	9821.5	130.218	14.284	26.4343	1.334
1900	1440.3	13824.8	10059.9	141.791	13.400	26.6034	1.332
1940	1480.3	14143.7	10299.3	154.172	12.583	26.7696	1.331
1980	1520.3	14463.8	10540.2	167.374	11.830	26.9328	1.329
2020	1560.3	14784.7	10781.6	181.464	11.132	27.0933	1.328
2060	1600.3	15106.9	11024.3	196.483	10.484	27.2512	1.327
2100	1640.3	15429.8	11267.8	212.465	9.884	27.4065	1.325

2140	1680.3	15753.9	11512.5	229.464	9.326	27.5594	1.324
2180	1720.3	16078.8	11757.9	247.495	8.808	27.7096	1.323
2220	1760.3	16404.3	12004.1	266.670	8.325	27.8578	1.322
2260	1800.3	16731.0	12251.4	286.998	7.875	28.0036	1.321
2300	1840.3	17058.3	12499.3	308.512	7.455	28.1472	1.320
2340	1880.3	17386.4	12748.0	331.296	7.063	28.2887	1.319
2380	1920.3	17715.5	12997.7	355.367	6.697	28.4280	1.318
2420	1960.3	18045.4	13247.9	380.859	6.354	28.5655	1.317
2460	2000.3	18375.8	13498.9	407.717	6.034	28.7009	1.316
2500	2040.3	18706.8	13750.4	436.076	5.733	28.8344	1.315
2540	2080.3	19038.8	14003.3	465.990	5.451	28.9661	1.314
2580	2120.3	19371.5	14256.2	497.469	5.186	29.0960	1.313
2620	2160.3	19704.9	14510.2	530.594	4.938	29.2240	1.313
2660	2200.3	20038.5	14764.7	565.557	4.703	29.3507	1.312
2700	2240.3	20372.8	15019.5	602.250	4.483	29.4755	1.311
2740	2280.3	20708.4	15275.7	640.811	4.276	29.5988	1.310
2780	2320.3	21044.0	15531.8	681.229	4.081	29.7202	1.310
2820	2360.3	21380.2	15788.6	723.753	3.896	29.8405	1.309
2860	2400.3	21716.9	16045.9	768.283	3.723	29.9591	1.308
2900	2440.3	22054.3	16303.8	814.954	3.558	30.0762	1.308
2940	2480.3	22392.2	16562.5	863.846	3.403	30.1919	1.307
2980	2520.3	22730.5	16821.4	915.164	3.256	30.3065	1.306
3020	2560.3	23069.5	17080.2	968.642	3.118	30.4192	1.306
3060	2600.3	23409.4	17340.7	1024.76	2.986	30.5311	1.305
3100	2640.3	23749.1	17601.7	1083.25	2.862	30.6413	1.305
3140	2680.3	24090.0	17863.1	1144.37	2.744	30.7503	1.304
3180	2720.3	24430.2	18123.9	1208.42	2.632	30.8585	1.303
3220	2760.3	24772.7	18386.8	1275.04	2.525	30.9650	1.303
3260	2800.3	25113.9	18647.9	1344.65	2.424	31.0706	1.302
3300	2840.3	25456.2	18911.5	1417.230	2.328	31.1750	1.302
3340	2880.3	25799.0	19174.8	1492.974	2.237	31.2784	1.301
3380	2920.3	26141.9	19438.3	1571.546	2.151	31.3802	1.301
3420	2960.3	26485.7	19702.6	1653.649	2.068	31.4814	1.300
3460	3000.3	26829.7	19967.2	1739.133	1.989	31.5814	1.300
3500	3040.3	27175.2	20233.2	1828.024	1.915	31.6804	1.300
3540	3080.3	27519.7	20498.2	1920.853	1.843	31.7788	1.299
3580	3120.3	27863.3	20762.4	2016.791	1.775	31.8756	1.299
3620	3160.3	28210.6	21030.3	2116.627	1.710	31.9715	1.298
3660	3200.3	28555.4	21295.6	2220.483	1.648	32.0667	1.298
3700	3240.3	28902.8	21563.5	2327.995	1.589	32.1606	1.297
3740	3280.3	29248.9	21830.9	2439.306	1.533	32.2533	1.297
3780	3320.3	29597.1	22098.9	2555.792	1.479	32.3459	1.297
3820	3360.3	29943.8	22366.9	2675.917	1.428	32.4371	1.296
3860	3400.3	30290.4	22633.4	2801.559	1.378	32.5283	1.296
3900	3440.3	30640.2	22904.4	2930.566	1.331	32.6177	1.295
3940	3480.3	30986.3	23170.4	3064.678	1.286	32.7065	1.295
3980	3520.3	31337.5	23442.8	3203.413	1.242	32.7944	1.295
4020	3560.3	31685.2	23710.3	3347.464	1.201	32.8818	1.295
4060	3600.3	32034.6	23981.0	3496.259	1.161	32.9682	1.294
4100	3640.3	32384.9	24251.2	3650.195	1.123	33.0537	1.294
4140	3680.3	32735.3	24521.4	3809.811	1.087	33.1387	1.294
4180	3720.3	33082.6	24791.3	3975.642	1.051	33.2233	1.293
4220	3760.3	33434.7	25063.3	4144.901	1.018	33.3061	1.293

4260	3800.3	33783.8	25333.7	4322.743	0.985	33.3895	1.293
4300	3840.3	34136.5	25606.2	4503.871	0.955	33.4711	1.292
4340	3880.3	34488.3	25877.8	4692.876	0.925	33.5527	1.292
4380	3920.3	34839.6	26150.3	4886.152	0.896	33.6328	1.292
4420	3960.3	35191.0	26421.6	5089.733	0.868	33.7139	1.291
4460	4000.3	35543.2	26695.1	5296.056	0.842	33.7928	1.291
4500	4040.3	35895.4	26968.5	5509.218	0.817	33.8712	1.291
4540	4080.3	36248.5	27241.5	5729.551	0.792	33.9491	1.291
4580	4120.3	36602.1	27513.4	5957.094	0.769	34.0264	1.290
4620	4160.3	36952.2	27787.6	6193.744	0.746	34.1038	1.290
4660	4200.3	37307.9	28061.8	6433.935	0.724	34.1793	1.290
4700	4240.3	37662.5	28337.6	6686.213	0.703	34.2557	1.290
4740	4280.3	38016.2	28612.6	6939.447	0.683	34.3295	1.289
4780	4320.3	38370.7	28885.5	7206.479	0.663	34.4045	1.289
4820	4360.3	38721.3	29157.4	7476.027	0.645	34.4774	1.289
4860	4400.3	39078.7	29436.0	7761.679	0.626	34.5519	1.289
4900	4440.3	39433.7	29712.2	8050.20	0.609	34.6244	1.288
4940	4480.3	39787.4	29987.2	8348.87	0.592	34.6967	1.288
4980	4520.3	40143.3	30264.4	8651.44	0.576	34.7674	1.288
5020	4560.3	40499.7	30539.2	8967.89	0.560	34.8387	1.288
5060	4600.3	40853.1	30813.9	9294.72	0.544	34.9098	1.287
5100	4640.3	41209.2	31091.2	9628.23	0.530	34.9798	1.287
5140	4680.3	41569.5	31369.9	9975.90	0.515	35.0503	1.287
5180	4720.3	41920.0	31641.7	10326.3	0.502	35.1188	1.287
5220	4760.3	42283.6	31926.5	10686.3	0.488	35.1869	1.286
5260	4800.3	42634.6	32198.8	11058.6	0.476	35.2549	1.286
5300	4840.3	42998.2	32480.8	11436.7	0.463	35.3216	1.286
5340	4880.3	43352.6	32753.6	11837.8	0.451	35.3901	1.286
5380	4920.3	43707.3	33029.6	12237.7	0.440	35.4561	1.285
5420	4960.3	44063.5	33307.1	12652.2	0.428	35.5222	1.285
5460	5000.3	44425.7	33590.6	13080.4	0.417	35.5883	1.285
5500	5040.3	44778.9	33864.9	13523.8	0.407	35.6545	1.285
5540	5080.3	45140.7	34148.0	13970.3	0.397	35.7190	1.285
5580	5120.3	45503.7	34432.3	14431.7	0.387	35.7835	1.284
5620	5160.3	45860.1	34704.3	14902.8	0.377	35.8473	1.284
5660	5200.3	46219.4	34984.8	15386.9	0.368	35.9108	1.284
5700	5240.3	46574.9	35261.6	15895.4	0.359	35.9754	1.284
5740	5280.3	46937.0	35550.6	16402.2	0.350	36.0377	1.284
5780	5320.3	47297.3	35826.5	16926.3	0.341	36.1002	1.283
5820	5360.3	47652.4	36102.9	17458.6	0.333	36.1617	1.283
5860	5400.3	48016.0	36387.7	18015.0	0.325	36.2240	1.283
5900	5440.3	48376.2	36669.2	18567.9	0.318	36.2840	1.283
5940	5480.3	48741.1	36949.6	19152.7	0.310	36.3456	1.283
5980	5520.3	49098.1	37233.5	19748.3	0.303	36.4064	1.283
6020	5560.3	49454.6	37511.3	20352.3	0.296	36.4662	1.282
6060	5600.3	49816.3	37794.3	20969.2	0.289	36.5255	1.283
6100	5640.3	50180.0	38073.6	21615.6	0.282	36.5858	1.282
6140	5680.3	50540.0	38354.8	22238.5	0.276	36.6422	1.282
6180	5720.3	50901.3	38637.4	22929.3	0.270	36.7030	1.282

### B.3 H<sub>2</sub>O Properties (SI Units)

Temperature K	h kJ/kgmol	u kJ/kgmol	Pr	Vr	S <sub>o</sub> kJ/kgmol/K	Gamma
200	-73.1	5510.1	4124.4	0.290	1259.160	169.2769
225	-48.1	6344.3	4757.4	0.460	490.529	173.2069
250	-23.1	7179.1	5389.8	0.700	356.982	176.7249
275	1.9	8015.2	6022.5	1.030	267.626	179.9124
300	26.9	8853.5	6656.6	1.460	205.544	182.8300
325	51.9	9694.8	7293.2	2.020	161.051	185.5235
350	76.9	10539.8	7933.1	2.730	128.322	188.0283
375	101.9	11389.1	8576.9	3.620	103.711	190.3722
400	126.9	12243.3	9225.3	4.710	84.853	192.5772
425	151.9	13102.8	9878.8	6.060	70.166	194.6613
450	176.9	13967.9	10537.7	7.680	58.563	196.6392
475	201.9	14838.9	11202.3	9.640	49.284	198.5230
500	226.9	15716.2	11873.1	11.970	41.779	200.3229
525	251.9	16600.0	12550.2	14.730	35.649	202.0476
550	276.9	17490.4	13233.8	17.970	30.599	203.7044
575	301.9	18387.7	13924.2	21.780	26.404	205.2997
600	326.9	19291.9	14621.5	26.210	22.895	206.8390
625	351.9	20203.2	15325.8	31.340	19.941	208.3270
650	376.9	21121.8	16037.4	37.280	17.438	209.7682
675	401.9	22047.9	16756.2	44.100	15.306	211.1660
700	426.9	22981.3	17482.5	51.930	13.481	212.5239
725	451.9	23922.3	18216.3	60.870	11.911	213.8447
750	476.9	24870.9	18957.7	71.050	10.556	215.1311
775	501.9	25827.4	19706.8	82.620	9.380	216.3855
800	526.8	26791.6	20463.6	95.730	8.357	217.6099
825	551.8	27763.5	21228.2	110.550	7.463	218.8063
850	576.8	28743.5	22000.8	127.260	6.679	219.9765
875	601.8	29731.3	22781.2	146.060	5.991	221.1218
900	626.8	30727.1	23569.5	167.160	5.384	222.2440
925	651.8	31731.0	24365.9	190.810	4.848	223.3439
950	676.8	32742.7	25170.1	217.260	4.373	224.4232
975	701.8	33762.4	25982.4	246.790	3.951	225.4828
1000	726.8	34790.1	26802.5	279.710	3.575	226.5235
1025	751.8	35825.8	27630.7	316.320	3.240	227.5464
1050	776.8	36869.4	28466.6	357.010	2.941	228.5522
1075	801.8	37920.9	29310.7	402.140	2.673	229.5419
1100	826.8	38980.1	30162.4	452.140	2.433	230.5162
1125	851.8	40047.3	31022.0	507.430	2.217	231.4753
1150	876.8	41122.3	31889.3	568.520	2.023	232.4204
1175	901.8	42204.8	32764.1	635.900	1.848	233.3515
1200	926.8	43294.8	33646.7	710.130	1.690	234.2695
1225	951.8	44392.7	34536.8	791.850	1.547	235.1750
1250	976.8	45497.7	35434.4	881.630	1.418	236.0679
1275	1002	46610.2	36338.9	980.230	1.301	236.9493
1300	1027	47729.9	37251.2	1088.310	1.195	237.8188
1325	1052	48856.9	38170.4	1206.690	1.098	238.6773
1350	1077	49991.0	39096.9	1336.320	1.010	239.5256
1375	1102	51131.9	40030.1	1477.870	0.930	240.3626
1400	1127	52279.6	40969.9	1632.520	0.858	241.1900
1425	1152	53434.1	41916.8	1801.100	0.791	242.0070
1450	1177	54595.2	42870.1	1984.990	0.730	242.8153
1475	1202	55762.9	43830.1	2185.000	0.675	243.6134

1500	1227	56936.6	44796.6	2402.600	0.624	244.4027	1.214
1525	1252	58116.8	45768.6	2638.960	0.578	245.1828	1.213
1550	1277	59302.9	46747.5	2895.720	0.535	245.9547	1.212
1575	1302	60495.3	47732.2	3174.180	0.496	246.7180	1.210
1600	1327	61693.9	48722.7	3475.590	0.460	247.4722	1.209
1625	1352	62898.1	49719.2	3802.260	0.427	248.2190	1.208
1650	1377	64107.6	50721.0	4155.830	0.397	248.9582	1.207
1675	1402	65323.3	51729.0	4537.600	0.369	249.6889	1.206
1700	1427	66543.8	52741.4	4950.400	0.343	250.4128	1.205
1725	1452	67769.7	53760.0	5395.200	0.320	251.1281	1.204
1750	1477	69000.6	54783.2	5875.270	0.298	251.8368	1.203
1775	1502	70237.3	55811.5	6392.490	0.278	252.5382	1.202
1800	1527	71478.6	56845.0	6949.430	0.259	253.2327	1.201
1825	1552	72724.0	57883.6	7548.220	0.242	253.9198	1.200
1850	1577	73975.0	58926.9	8192.660	0.226	254.6010	1.199
1875	1602	75230.7	59974.9	8884.150	0.211	255.2746	1.198
1900	1627	76490.6	61026.3	9627.270	0.197	255.9425	1.197
1925	1652	77754.6	62083.5	10424.460	0.185	256.6039	1.196
1950	1677	79024.1	63144.5	11278.480	0.173	257.2585	1.195
1975	1702	80296.8	64209.4	12194.130	0.162	257.9074	1.195
2000	1727	81574.7	65279.6	13173.870	0.152	258.5499	1.194
2025	1752	82855.8	66353.0	14222.670	0.142	259.1868	1.193
2050	1777	84140.9	67430.4	15346.000	0.134	259.8188	1.193
2075	1802	85430.3	68512.2	16540.930	0.125	260.4421	1.192
2100	1827	86723.8	69598.0	17823.400	0.118	261.0630	1.191
2125	1852	88019.4	70685.9	19185.650	0.111	261.6753	1.191
2150	1877	89320.2	71778.9	20643.450	0.104	262.2841	1.190
2175	1902	90626.4	72875.9	22198.160	0.098	262.8878	1.189
2200	1927	91933.1	73976.5	23853.41	0.092	263.4857	1.189
2225	1952	93244.3	75078.4	25619.01	0.087	264.0793	1.188
2250	1977	94559.1	76185.5	27490.67	0.082	264.6656	1.188
2275	2002	95876.4	77295.1	29486.28	0.077	265.2482	1.187
2300	2027	97196.6	78407.7	31609.24	0.073	265.8262	1.186
2325	2052	98522.0	79526.9	33860.18	0.069	266.3981	1.186
2350	2077	99849.5	80646.8	36256.23	0.065	266.9665	1.185
2375	2102	101181.8	81769.7	38795.49	0.061	267.5293	1.185
2400	2127	102514.1	82894.4	41493.24	0.058	268.0882	1.184
2425	2152	103850.5	84023.1	44350.89	0.055	268.6419	1.184
2450	2177	105189.8	85154.6	47387.27	0.052	269.1924	1.183
2475	2202	106531.3	86288.5	50591.75	0.049	269.7364	1.183
2500	2227	107878.4	87427.9	53995.10	0.046	270.2777	1.183
2525	2252	109226.4	88568.2	57590.81	0.044	270.8137	1.182
2550	2277	110576.9	89711.0	61398.02	0.042	271.3459	1.182
2575	2302	111929.5	90855.9	65430.73	0.039	271.8747	1.181
2600	2327	113285.2	92005.5	69692.74	0.037	272.3994	1.181
2625	2352	114646.5	93157.5	74183.61	0.035	272.9185	1.180
2650	2377	116004.6	94309.6	78938.94	0.034	273.4351	1.180
2675	2402	117370.5	95466.2	83955.33	0.032	273.9473	1.180
2700	2427	118734.1	96623.8	89240.35	0.030	274.4548	1.179
2725	2452	120104.6	97784.9	94835.10	0.029	274.9603	1.179
2750	2477	121475.6	98946.5	100725.1	0.027	275.4613	1.178

2775	2502	122851.6	100113.2	106929.9	0.026	275.9583	1.178
2800	2527	124226.5	101282.1	113469.0	0.025	276.4517	1.178
2825	2552	125603.7	102449.9	120392.1	0.023	276.9441	1.177
2850	2577	126984.2	103624.4	127621.4	0.022	277.4289	1.177
2875	2602	128364.0	104798.1	135249.5	0.021	277.9115	1.177
2900	2627	129749.0	105973.8	143271.5	0.020	278.3906	1.176
2925	2652	131137.9	107153.4	151752.6	0.019	278.8687	1.176
2950	2677	132529.4	108338.8	160597.6	0.018	279.3397	1.176
2975	2702	133916.9	109520.3	169925.2	0.018	279.8090	1.176
3000	2727	135309.9	110704.0	179739.8	0.017	280.2758	1.175
3025	2752	136707.7	111892.5	190023.6	0.016	280.7384	1.175
3050	2777	138101.4	113080.1	200807.2	0.015	281.1973	1.175
3075	2802	139504.2	114270.3	212141.3	0.014	281.6538	1.174
3100	2827	140902.4	115465.7	224116.0	0.014	282.1103	1.174
3125	2852	142306.1	116666.6	236620.6	0.013	282.5617	1.174
3150	2877	143714.6	117859.2	249705.6	0.013	283.0092	1.173
3175	2902	145122.6	119057.9	263395.2	0.012	283.4529	1.173
3200	2927	146534.1	120260.1	277801.660	0.012	283.8956	1.173

## B.4 H<sub>2</sub>O Properties (English Units)

Temperature R	Temperature F	h Btu/lbmol	u Btu/lbmol	Pr	Vr	so Btu/lbmol/R	Gamma
300	-159.7	2369.1	1773.3	0.138	2180.3	40.4340	1.332
340	-119.7	2687.7	2016.1	0.227	1495.8	41.4308	1.332
380	-79.7	3006.4	2258.2	0.355	1069.9	42.3172	1.332
420	-39.7	3325.3	2500.0	0.531	791.26	43.1150	1.332
460	0.3	3644.4	2741.7	0.765	601.31	43.8408	1.331
500	40.3	3964.1	2983.5	1.070	467.29	44.5071	1.330
540	80.3	4284.5	3226.0	1.460	369.98	45.1236	1.329
580	120.3	4606.0	3469.2	1.949	297.60	45.6979	1.327
620	160.3	4928.7	3713.5	2.555	242.62	46.2359	1.326
660	200.3	5252.8	3959.1	3.298	200.12	46.7425	1.324
700	240.3	5578.5	4206.2	4.198	166.75	47.2216	1.321
740	280.3	5905.9	4455.0	5.279	140.19	47.6765	1.319
780	320.3	6235.2	4705.5	6.566	118.80	48.1098	1.317
820	360.3	6566.5	4957.9	8.088	101.38	48.5240	1.314
860	400.3	6899.8	5212.3	9.877	87.07	48.9208	1.312
900	440.3	7235.2	5468.8	11.968	75.20	49.3020	1.309
940	480.3	7572.8	5727.4	14.397	65.29	49.6690	1.306
980	520.3	7912.7	5988.3	17.207	56.95	50.0231	1.304
1020	560.3	8254.8	6251.4	20.444	49.89	50.3653	1.301
1060	600.3	8599.4	6516.8	24.155	43.88	50.6966	1.298
1100	640.3	8946.3	6784.7	28.397	38.74	51.0179	1.296
1140	680.3	9295.7	7054.9	33.228	34.31	51.3299	1.293
1180	720.3	9647.5	7327.6	38.712	30.48	51.6332	1.290
1220	760.3	10001.9	7602.8	44.919	27.16	51.9285	1.288
1260	800.3	10358.8	7880.6	51.925	24.27	52.2164	1.285
1300	840.3	10718.3	8160.8	59.814	21.73	52.4972	1.282
1340	880.3	11080.3	8443.7	68.674	19.51	52.7716	1.280
1380	920.3	11445.0	8729.1	78.604	17.56	53.0397	1.277
1420	960.3	11812.3	9017.2	89.707	15.83	53.3021	1.275
1460	1000.3	12182.4	9308.0	102.10	14.30	53.5591	1.272
1500	1040.3	12555.0	9601.4	115.90	12.94	53.8109	1.270
1540	1080.3	12930.4	9897.5	131.25	11.73	54.0578	1.267
1580	1120.3	13308.4	10196.2	148.29	10.66	54.3002	1.265
1620	1160.3	13689.1	10497.7	167.16	9.69	54.5382	1.262
1660	1200.3	14072.6	10801.9	188.05	8.83	54.7719	1.260
1700	1240.3	14458.7	11108.7	211.13	8.05	55.0019	1.258
1740	1280.3	14847.6	11418.3	236.59	7.35	55.2280	1.256
1780	1320.3	15239.2	11730.6	264.64	6.73	55.4504	1.253
1820	1360.3	15633.5	12045.6	295.50	6.16	55.6695	1.251
1860	1400.3	16030.5	12363.2	329.42	5.65	55.8852	1.249
1900	1440.3	16430.2	12683.6	366.64	5.182	56.0979	1.247
1940	1480.3	16832.6	13006.6	407.45	4.761	56.3074	1.245
1980	1520.3	17237.5	13332.3	452.14	4.379	56.5141	1.243
2020	1560.3	17645.2	13660.6	501.01	4.032	56.7179	1.241
2060	1600.3	18055.5	13991.6	554.41	3.716	56.9190	1.239
2100	1640.3	18468.5	14325.1	612.69	3.428	57.1175	1.237
2140	1680.3	18883.9	14661.4	676.25	3.165	57.3135	1.235
2180	1720.3	19302.0	15000.1	745.49	2.924	57.5071	1.234
2220	1760.3	19722.6	15341.4	820.84	2.705	57.6983	1.232
2260	1800.3	20145.8	15685.2	902.78	2.503	57.8873	1.230
2300	1840.3	20571.4	16031.4	991.74	2.319	58.0739	1.229
2340	1880.3	20999.5	16380.1	1088.31	2.150	58.2584	1.227

2380	1920.3	21430.1	16731.3	1193.04	1.995	58.4409	1.225
2420	1960.3	21863.0	17084.8	1306.48	1.852	58.6213	1.224
2460	2000.3	22298.3	17440.8	1429.28	1.721	58.7997	1.222
2500	2040.3	22735.9	17799.0	1562.15	1.600	58.9762	1.221
2540	2080.3	23175.9	18159.7	1705.67	1.489	59.1507	1.220
2580	2120.3	23618.1	18522.4	1860.70	1.387	59.3235	1.218
2620	2160.3	24062.5	18887.5	2027.89	1.292	59.4944	1.217
2660	2200.3	24509.1	19254.7	2208.25	1.205	59.6636	1.216
2700	2240.3	24958.0	19624.3	2402.60	1.124	59.8311	1.214
2740	2280.3	25408.8	19995.7	2611.83	1.049	59.9969	1.213
2780	2320.3	25861.9	20369.3	2836.81	0.980	60.1610	1.212
2820	2360.3	26316.9	20745.1	3078.89	0.916	60.3236	1.211
2860	2400.3	26774.0	21122.7	3338.68	0.857	60.4844	1.210
2900	2440.3	27233.1	21502.4	3617.71	0.802	60.6438	1.209
2940	2480.3	27694.1	21884.1	3917.13	0.751	60.8017	1.208
2980	2520.3	28157.1	22267.6	4238.07	0.703	60.9581	1.207
3020	2560.3	28621.8	22652.9	4581.75	0.659	61.1130	1.206
3060	2600.3	29088.6	23040.2	4950.40	0.618	61.2666	1.205
3100	2640.3	29556.9	23429.2	5344.50	0.580	61.4188	1.204
3140	2680.3	30027.3	23820.2	5765.36	0.545	61.5693	1.203
3180	2720.3	30498.9	24212.7	6216.06	0.512	61.7188	1.202
3220	2760.3	30972.8	24607.1	6696.83	0.481	61.8667	1.201
3260	2800.3	31447.9	25002.8	7210.55	0.452	62.0135	1.200
3300	2840.3	31925.1	25400.5	7758.22	0.425	62.1589	1.199
3340	2880.3	32403.6	25799.5	8342.94	0.400	62.3031	1.199
3380	2920.3	32883.8	26200.3	8964.83	0.377	62.4459	1.198
3420	2960.3	33365.2	26602.3	9627.27	0.355	62.5875	1.197
3460	3000.3	33848.5	27006.1	10332.8	0.335	62.7279	1.196
3500	3040.3	34333.3	27411.5	11083.4	0.316	62.8672	1.196
3540	3080.3	34819.3	27818.0	11881.8	0.298	63.0053	1.195
3580	3120.3	35307.1	28226.7	12730.8	0.281	63.1424	1.194
3620	3160.3	35795.5	28635.7	13632.1	0.266	63.2782	1.194
3660	3200.3	36286.0	29046.7	14587.9	0.251	63.4128	1.193
3700	3240.3	36777.7	29459.3	15603.8	0.237	63.5465	1.192
3740	3280.3	37270.8	29872.9	16681.3	0.224	63.6791	1.192
3780	3320.3	37765.0	30287.7	17823.4	0.212	63.8106	1.191
3820	3360.3	38260.4	30703.7	19031.2	0.201	63.9408	1.191
3860	3400.3	38757.5	31121.3	20314.7	0.190	64.0704	1.190
3900	3440.3	39256.3	31540.6	21672.0	0.180	64.1988	1.189
3940	3480.3	39754.2	31959.8	23104.2	0.171	64.3259	1.189
3980	3520.3	40254.5	32380.6	24626.0	0.162	64.4526	1.188
4020	3560.3	40756.8	32802.8	26228.5	0.153	64.5778	1.188
4060	3600.3	41259.2	33225.7	27925.1	0.145	64.7022	1.187
4100	3640.3	41763.0	33650.8	29712.9	0.138	64.8255	1.187
4140	3680.3	42267.9	34075.5	31609.3	0.131	64.9483	1.186
4180	3720.3	42774.2	34502.4	33603.3	0.124	65.0698	1.186
4220	3760.3	43281.6	34930.3	35710.0	0.118	65.1906	1.185
4260	3800.3	43789.6	35358.9	37931.6	0.112	65.3104	1.185
4300	3840.3	44299.2	35789.0	40277.3	0.107	65.4296	1.185
4340	3880.3	44809.7	36220.1	42746.5	0.102	65.5477	1.184
4380	3920.3	45320.6	36652.2	45340.8	0.097	65.6647	1.184

## B.5 CO<sub>2</sub> Properties (SI Units)

Temperature		<i>h</i>	<i>u</i>	<i>Pr</i>	<i>Vr</i>	<i>s<sub>o</sub></i>	Gamma
K	C	kJ/kgmol	kJ/kgmol			kJ/kgmol/K	
200	-73.1	4898.9	3513.4	0.28	1292.15	194.0903	1.345
225	-48.1	5723.6	4168.1	0.44	506.17	197.9744	1.329
250	-23.1	6579.3	4847.3	0.69	364.53	201.5795	1.313
275	1.9	7465.7	5552.2	1.03	267.07	204.9580	1.300
300	26.9	8382.0	6283.1	1.51	198.55	208.1462	1.288
325	51.9	9326.8	7039.4	2.17	149.50	211.1705	1.277
350	76.9	10298.7	7820.2	3.07	113.86	214.0510	1.267
375	101.9	11296.2	8624.6	4.28	87.607	216.8035	1.259
400	126.9	12318.0	9451.5	5.88	68.045	219.4409	1.252
425	151.9	13362.7	10299.9	7.97	53.308	221.9741	1.245
450	176.9	14429.0	11168.8	10.69	42.099	224.4118	1.239
475	201.9	15516.0	12057.2	14.18	33.493	226.7625	1.234
500	226.9	16622.5	12964.2	18.63	26.832	229.0325	1.229
525	251.9	17747.4	13889.0	24.27	21.635	231.2279	1.224
550	276.9	18890.0	14830.6	31.34	17.551	233.3538	1.220
575	301.9	20049.4	15788.5	40.15	14.320	235.4150	1.217
600	326.9	21224.9	16762.0	51.08	11.746	237.4160	1.213
625	351.9	22415.5	17750.2	64.54	9.684	239.3600	1.210
650	376.9	23620.8	18752.7	81.02	8.023	241.2508	1.207
675	401.9	24840.1	19768.7	101.10	6.677	243.0914	1.204
700	426.9	26072.5	20797.6	125.43	5.581	244.8847	1.202
725	451.9	27317.8	21839.1	154.78	4.684	246.6325	1.199
750	476.9	28575.4	22892.7	190.02	3.947	248.3377	1.197
775	501.9	29844.5	23957.4	232.14	3.339	250.0022	1.195
800	526.8	31124.9	25033.3	282.27	2.834	251.6279	1.193
825	551.8	32415.8	26119.5	341.74	2.414	253.2172	1.191
850	576.8	33717.0	27215.8	411.95	2.063	254.7706	1.189
875	601.8	35027.9	28321.6	494.59	1.769	256.2906	1.188
900	626.8	36348.2	29436.6	591.50	1.522	257.7783	1.186
925	651.8	37677.6	30560.6	704.80	1.312	259.2352	1.185
950	676.8	39015.2	31692.8	836.76	1.135	260.6620	1.183
975	701.8	40361.3	32833.2	990.10	0.985	262.0610	1.182
1000	726.8	41715.3	33981.6	1167.6	0.856	263.4322	1.181
1025	751.8	43076.4	35137.1	1372.6	0.747	264.7767	1.180
1050	776.8	44445.2	36299.4	1608.6	0.653	266.0959	1.179
1075	801.8	45820.7	37468.8	1879.7	0.572	267.3905	1.178
1100	826.8	47202.7	38644.7	2190.0	0.502	268.6610	1.177
1125	851.8	48591.4	39827.4	2544.8	0.442	269.9092	1.176
1150	876.8	49985.1	41015.0	2949.0	0.390	271.1346	1.175
1175	901.8	51385.5	42209.0	3408.9	0.345	272.3395	1.174
1200	926.8	52791.4	43408.4	3930.4	0.305	273.5230	1.173
1225	951.8	54201.5	44612.9	4521.0	0.271	274.6868	1.172
1250	976.8	55618.1	45822.6	5188.2	0.241	275.8313	1.172
1275	1001.8	57039.4	47037.0	5940.2	0.215	276.9566	1.171
1300	1026.8	58464.9	48255.7	6786.6	0.192	278.0639	1.170
1325	1051.8	59895.8	49479.7	7737.8	0.171	279.1545	1.170
1350	1076.8	61329.7	50707.6	8803.1	0.153	280.2268	1.169
1375	1101.8	62768.5	51939.5	9994.9	0.138	281.2824	1.169
1400	1126.8	64211.8	53175.9	11326.2	0.124	282.3220	1.168
1425	1151.8	65658.4	54415.7	12812.8	0.111	283.3473	1.168
1450	1176.8	67108.3	55658.6	14466.2	0.100	284.3563	1.167
1475	1201.8	68563.2	56906.7	16304.6	0.090	285.3509	1.167

1500	1226.8	70020.9	58157.6	18344.6	0.082	286.3310	1.166
1525	1251.8	71481.7	59410.6	20600.9	0.074	287.2954	1.166
1550	1276.8	72945.4	60668.3	23101.9	0.067	288.2480	1.165
1575	1301.8	74412.2	61927.4	25868.1	0.061	289.1882	1.165
1600	1326.8	75883.0	63192.1	28916.1	0.055	290.1142	1.164
1625	1351.8	77355.4	64456.8	32270.5	0.050	291.0267	1.164
1650	1376.8	78831.3	65726.7	35969.4	0.046	291.9289	1.164
1675	1401.8	80312.5	67000.2	40024.4	0.042	292.8169	1.163
1700	1426.8	81791.3	68272.9	44496.2	0.038	293.6975	1.163
1725	1451.8	83278.7	69551.0	49369.3	0.035	294.5615	1.163
1750	1476.8	84762.2	70828.5	54730.5	0.032	295.4185	1.162
1775	1501.8	86252.2	72110.8	60579.4	0.029	296.2627	1.162
1800	1526.8	87742.6	73395.1	66965.8	0.027	297.0959	1.162
1825	1551.8	89235.2	74680.0	73954.8	0.025	297.9212	1.162
1850	1576.8	90731.9	75972.3	81574.9	0.023	298.7365	1.161
1875	1601.8	92231.5	77262.6	89849.9	0.021	299.5398	1.161
1900	1626.8	93730.0	78555.0	98864.0	0.019	300.3346	1.161
1925	1651.8	95230.1	79845.8	108640.8	0.018	301.1186	1.160
1950	1676.8	96736.7	81146.4	119300.4	0.016	301.8968	1.160
1975	1701.8	98244.5	82444.8	130839.1	0.015	302.6643	1.160
2000	1726.8	99751.9	83746.2	143305.3	0.014	303.4209	1.160
2025	1751.8	101259.1	85044.1	156882.2	0.013	304.1735	1.160
2050	1776.8	102767.9	86346.8	171483.8	0.012	304.9133	1.159
2075	1801.8	104283.4	87653.0	187278.1	0.011	305.6458	1.159
2100	1826.8	105797.3	88960.8	204390.5	0.010	306.3727	1.159
2125	1851.8	107314.4	90271.8	222790.0	0.010	307.0894	1.159
2150	1876.8	108833.1	91581.2	242630.1	0.009	307.7986	1.159
2175	1901.8	110353.8	92895.8	264062.5	0.008	308.5023	1.158
2200	1926.8	111871.4	94204.1	287095.1	0.008	309.1976	1.158
2225	1951.8	113391.6	95521.6	311872.0	0.007	309.8858	1.158
2250	1976.8	114915.7	96836.3	338455.4	0.007	310.5658	1.158
2275	2001.8	116442.1	98153.4	367187.4	0.006	311.2432	1.158
2300	2026.8	117966.3	99471.5	397703.9	0.006	311.9070	1.158
2325	2051.9	119491.0	100793.5	430530.6	0.005	312.5663	1.157
2350	2076.9	121023.1	102109.7	465834.2	0.005	313.2215	1.157
2375	2101.9	122555.9	103439.7	503490.9	0.005	313.8678	1.157
2400	2126.9	124083.5	104758.0	544061.8	0.004	314.5121	1.157
2425	2151.9	125613.1	106078.3	587250.6	0.004	315.1472	1.157
2450	2176.9	127156.1	107418.5	633421.1	0.004	315.7764	1.157
2475	2201.9	128681.3	108734.4	682687.7	0.004	316.3991	1.157
2500	2226.9	130225.1	110068.8	735216.5	0.003	317.0154	1.156
2525	2251.9	131764.7	111399.1	791136.3	0.003	317.6248	1.156
2550	2276.9	133298.1	112723.1	851306.1	0.003	318.2342	1.156
2575	2301.9	134830.4	114052.7	914842.4	0.003	318.8326	1.156
2600	2326.9	136372.1	115385.0	982925.9	0.003	319.4294	1.156
2625	2351.9	137910.9	116721.1	1054793.8	0.002	320.0161	1.156
2650	2376.9	139455.6	118056.4	1132149.1	0.002	320.6044	1.156
2675	2401.9	140996.3	119387.8	1213719.6	0.002	321.1828	1.156
2700	2426.9	142542.7	120731.5	1299797.3	0.002	321.7525	1.155
2725	2451.9	144091.2	122070.6	1393380.3	0.002	322.3305	1.155
2750	2476.9	145633.1	123403.2	1491186.5	0.002	322.8945	1.155

2775	2501.9	147180.6	124741.3	1594517.1	0.002	323.4515	1.155
2800	2526.9	148735.4	126086.8	1705346.0	0.002	324.0101	1.155
2825	2551.9	150272.8	127428.0	1821001.6	0.002	324.5557	1.155
2850	2576.9	151831.0	128776.9	1945136.3	0.001	325.1039	1.155
2875	2601.9	153381.2	130104.7	2077527.0	0.001	325.6513	1.155
2900	2626.9	154935.0	131462.2	2215282.5	0.001	326.1851	1.155
2925	2651.9	156479.4	132797.3	2363265.3	0.001	326.7227	1.155
2950	2676.9	158032.4	134141.0	2516307.0	0.001	327.2444	1.154
2975	2701.9	159594.8	135494.0	2681335.5	0.001	327.7725	1.154
3000	2726.9	161139.8	136842.8	2854293.8	0.001	328.2921	1.154
3025	2751.9	162703.6	138197.3	3035087.0	0.001	328.8027	1.154
3050	2776.9	164262.6	139533.9	3231907.8	0.001	329.3251	1.154
3075	2801.9	165809.9	140884.9	3433278.0	0.001	329.8276	1.154
3100	2826.9	167368.2	142233.9	3647235.0	0.001	330.3302	1.154
3125	2851.9	168937.7	143594.1	3874568.3	0.001	330.8329	1.154
3150	2876.9	170504.6	144951.7	4115300.8	0.001	331.3340	1.154
3175	2901.9	172053.7	146304.5	4366548.0	0.001	331.8267	1.154
3200	2926.9	173619.6	147648.0	4633662.0	0.001	332.3203	1.154

## B.6 CO<sub>2</sub> Properties (English Units)

Temperature		<i>h</i>	<i>u</i>	<i>Pr</i>	<i>Vr</i>	<i>s<sub>o</sub></i>	Gamma
R	F	Btu/lbmol	Btu/lbmol			Btu/lbmol/R	
300	-159.7	2106.3	1510.6	0.139	2152.4	46.3610	1.369
340	-119.7	2405.9	1749.9	0.223	1521.8	47.2980	1.353
380	-79.7	2715.2	1995.7	0.345	1103.0	48.1580	1.338
420	-39.7	3035.0	2249.4	0.515	814.94	48.9579	1.323
460	0.3	3365.3	2511.7	0.752	611.48	49.7090	1.310
500	40.3	3706.0	2782.8	1.076	464.84	50.4190	1.298
540	80.3	4056.8	3062.7	1.511	357.39	51.0939	1.288
580	120.3	4417.3	3351.2	2.090	277.56	51.7378	1.278
620	160.3	4787.1	3648.1	2.850	217.53	52.3541	1.269
660	200.3	5165.6	3953.0	3.839	171.90	52.9458	1.262
700	240.3	5552.6	4265.8	5.114	136.89	53.5150	1.255
740	280.3	5947.6	4586.0	6.741	109.78	54.0636	1.249
780	320.3	6350.1	4913.3	8.802	88.62	54.5933	1.243
820	360.3	6759.9	5247.5	11.392	71.98	55.1057	1.238
860	400.3	7176.6	5588.2	14.626	58.80	55.6018	1.233
900	440.3	7599.8	5935.3	18.635	48.30	56.0828	1.229
940	480.3	8029.4	6288.3	23.574	39.87	56.5498	1.225
980	520.3	8465.0	6647.1	29.626	33.08	57.0036	1.221
1020	560.3	8906.3	7011.6	37.001	27.57	57.4450	1.218
1060	600.3	9353.2	7381.3	45.939	23.07	57.8746	1.215
1100	640.3	9805.3	7756.2	56.722	19.39	58.2933	1.212
1140	680.3	10262.6	8136.0	69.673	16.36	58.7017	1.209
1180	720.3	10724.8	8520.6	85.149	13.86	59.1001	1.206
1220	760.3	11191.6	8909.7	103.578	11.78	59.4891	1.204
1260	800.3	11662.9	9303.3	125.433	10.05	59.8693	1.202
1300	840.3	12138.6	9701.1	151.242	8.596	60.2409	1.199
1340	880.3	12618.4	10102.9	181.629	7.378	60.6045	1.197
1380	920.3	13102.2	10508.7	217.266	6.352	60.9602	1.195
1420	960.3	13589.9	10918.2	258.923	5.484	61.3086	1.194
1460	1000.3	14081.3	11331.3	307.466	4.748	61.6498	1.192
1500	1040.3	14576.3	11748.0	363.861	4.122	61.9842	1.190
1540	1080.3	15074.6	12168.0	429.178	3.588	62.3121	1.189
1580	1120.3	15576.2	12591.3	504.618	3.131	62.6336	1.187
1620	1160.3	16080.9	13017.6	591.502	2.739	62.9491	1.186
1660	1200.3	16588.8	13447.0	691.365	2.401	63.2589	1.185
1700	1240.3	17099.6	13879.2	805.734	2.110	63.5629	1.184
1740	1280.3	17613.1	14314.1	936.428	1.858	63.8614	1.182
1780	1320.3	18129.4	14751.8	1085.49	1.640	64.1548	1.181
1820	1360.3	18648.2	15192.0	1255.08	1.450	64.4430	1.180
1860	1400.3	19169.6	15634.8	1447.55	1.285	64.7264	1.179
1900	1440.3	19693.5	16079.8	1665.6	1.141	65.0049	1.178
1940	1480.3	20219.4	16527.1	1912.1	1.015	65.2791	1.177
1980	1520.3	20747.9	16976.7	2190.0	0.904	65.5486	1.177
2020	1560.3	21278.2	17428.2	2503.0	0.807	65.8138	1.176
2060	1600.3	21810.7	17882.0	2854.7	0.722	66.0749	1.175
2100	1640.3	22345.2	18337.8	3248.9	0.646	66.3318	1.174
2140	1680.3	22881.5	18795.1	3690.6	0.58	66.5849	1.173
2180	1720.3	23420.2	19254.7	4183.8	0.521	66.8340	1.173
2220	1760.3	23959.9	19715.7	4734.5	0.469	67.0796	1.172
2260	1800.3	24501.8	20178.5	5347.8	0.423	67.3215	1.172
2300	1840.3	25045.1	20643.0	6029.7	0.381	67.5598	1.171
2340	1880.3	25590.1	21108.9	6786.6	0.345	67.7946	1.170

2380	1920.3	26136.7	21576.7	7626.4	0.312	68.0263	1.170
2420	1960.3	26684.6	22045.6	8555.0	0.283	68.2545	1.169
2460	2000.3	27234.1	22515.9	9583.4	0.257	68.4799	1.169
2500	2040.3	27785.2	22988.0	10716.0	0.233	68.7017	1.168
2540	2080.3	28337.1	23461.1	11966.3	0.212	68.9209	1.168
2580	2120.3	28890.4	23935.0	13342.3	0.193	69.1370	1.167
2620	2160.3	29445.2	24411.0	14855.7	0.176	69.3504	1.167
2660	2200.3	30001.2	24887.9	16518.6	0.161	69.5611	1.166
2700	2240.3	30558.6	25366.2	18344.6	0.147	69.7693	1.166
2740	2280.3	31116.4	25845.2	20339.8	0.135	69.9743	1.166
2780	2320.3	31676.4	26325.8	22525.3	0.123	70.1770	1.165
2820	2360.3	32236.2	26806.9	24913.5	0.113	70.3771	1.165
2860	2400.3	32797.9	27289.1	27520.3	0.104	70.5747	1.165
2900	2440.3	33360.1	27772.5	30363.9	0.096	70.7700	1.164
2940	2480.3	33923.7	28256.7	33463.0	0.088	70.9630	1.164
2980	2520.3	34488.2	28742.4	36840.5	0.081	71.1540	1.164
3020	2560.3	35053.5	29228.3	40502.2	0.075	71.3421	1.163
3060	2600.3	35619.3	29715.4	44496.3	0.069	71.5289	1.163
3100	2640.3	36186.2	30202.8	48807.2	0.064	71.7125	1.163
3140	2680.3	36754.6	30691.8	53499.3	0.059	71.8948	1.162
3180	2720.3	37323.8	31182.2	58565.9	0.054	72.0745	1.162
3220	2760.3	37894.3	31673.2	64062.9	0.05	72.2526	1.162
3260	2800.3	38464.2	32163.7	70006.4	0.047	72.4288	1.162
3300	2840.3	39035.2	32655.3	76418.2	0.043	72.6029	1.161
3340	2880.3	39606.3	33147.6	83339.1	0.04	72.7750	1.161
3380	2920.3	40180.1	33642.6	90818.4	0.037	72.9457	1.161
3420	2960.3	40752.4	34136.2	98864.0	0.035	73.1143	1.161
3460	3000.3	41326.5	34630.1	107520.6	0.032	73.2809	1.161
3500	3040.3	41900.9	35125.8	116863.0	0.030	73.4464	1.160
3540	3080.3	42476.5	35622.6	126858.2	0.028	73.6094	1.160
3580	3120.3	43051.5	36117.4	137653.7	0.026	73.7716	1.160
3620	3160.3	43629.7	36616.9	149204.5	0.024	73.9316	1.160
3660	3200.3	44205.8	37112.8	161585.4	0.023	74.0899	1.160
3700	3240.3	44783.2	37611.5	174927.8	0.021	74.2474	1.159
3740	3280.3	45361.9	38111.4	189169.0	0.020	74.4029	1.159
3780	3320.3	45940.8	38610.2	204391.3	0.018	74.5565	1.159
3820	3360.3	46519.2	39109.8	220690.0	0.017	74.7089	1.159
3860	3400.3	47100.7	39611.2	238098.2	0.016	74.8597	1.159
3900	3440.3	47680.2	40112.0	256730.5	0.015	75.0093	1.158
3940	3480.3	48261.0	40614.0	276623.2	0.014	75.1575	1.158
3980	3520.3	48843.2	41117.5	297891.2	0.013	75.3046	1.158
4020	3560.3	49423.9	41617.9	320487.7	0.013	75.4498	1.158
4060	3600.3	50007.8	42123.1	344603.6	0.012	75.5939	1.158
4100	3640.3	50588.8	42624.0	370381.8	0.011	75.7371	1.158
4140	3680.3	51172.8	43129.3	397704.7	0.010	75.8785	1.158
4180	3720.3	51756.2	43633.9	426811.9	0.010	76.0187	1.157
4220	3760.3	52341.1	44140.0	457729.2	0.009	76.1576	1.157
4260	3800.3	52925.3	44642.7	490688.2	0.009	76.2957	1.157
4300	3840.3	53509.1	45150.5	525804.1	0.008	76.4329	1.157
4340	3880.3	54095.4	45655.2	562836.0	0.008	76.5681	1.157
4380	3920.3	54680.1	46161.2	602004.0	0.007	76.7017	1.157

4420	3960.3	55268.8	46668.4	644330.8	0.007	76.8366	1.157
4460	4000.3	55853.4	47174.2	688207.0	0.006	76.9675	1.157
4500	4040.3	56443.5	47685.6	735215.0	0.006	77.0987	1.156
4540	4080.3	57030.7	48194.0	785035.6	0.006	77.2289	1.156
4580	4120.3	57616.4	48700.9	837485.5	0.005	77.3573	1.156
4620	4160.3	58205.2	49208.2	893302.4	0.005	77.4854	1.156
4660	4200.3	58793.7	49717.9	952144.0	0.005	77.6121	1.156
4700	4240.3	59383.1	50228.6	1014058.7	0.005	77.7372	1.156
4740	4280.3	59971.4	50738.1	1080090.8	0.004	77.8625	1.156
4780	4320.3	60560.5	51248.5	1149724.5	0.004	77.9866	1.156
4820	4360.3	61147.8	51757.1	1223372.8	0.004	78.1099	1.156
4860	4400.3	61739.5	52270.0	1299799.6	0.004	78.2302	1.155
4900	4440.3	62331.9	52783.6	1382923.1	0.004	78.3533	1.155
4940	4480.3	62921.9	53292.1	1468143.8	0.003	78.4720	1.155
4980	4520.3	63513.1	53807.4	1559496.6	0.003	78.5919	1.155
5020	4560.3	64102.9	54312.8	1655452.1	0.003	78.7105	1.155
5060	4600.3	64698.0	54829.1	1755773.1	0.003	78.8273	1.155
5100	4640.3	65286.3	55338.7	1862446	0.003	78.9445	1.155
5140	4680.3	65878.2	55851.9	1973642	0.003	79.0596	1.155
5180	4720.3	66474.8	56369.7	2091677	0.002	79.1750	1.155
5220	4760.3	67067.6	56883.7	2215282	0.002	79.2890	1.155
5260	4800.3	67664.1	57401.5	2345174	0.002	79.4021	1.154
5300	4840.3	68253.5	57912.1	2480459	0.002	79.5135	1.154
5340	4880.3	68847.6	58427.5	2625082	0.002	79.6260	1.154
5380	4920.3	69441.6	58937.1	2776344	0.002	79.7373	1.154
5420	4960.3	70032.3	59449.0	2934292	0.002	79.8472	1.154
5460	5000.3	70626.9	59964.9	3101107	0.002	79.9570	1.154
5500	5040.3	71225.6	60490.4	3274133	0.002	80.0648	1.154
5540	5080.3	71821.0	61001.5	3457955	0.002	80.1733	1.154
5580	5120.3	72413.3	61515.0	3647232	0.002	80.2791	1.154
5620	5160.3	73007.7	62030.7	3851144	0.001	80.3871	1.154
5660	5200.3	73615.6	62554.3	4063894	0.001	80.4939	1.154
5700	5240.3	74205.5	63071.0	4279592	0.001	80.5966	1.154
5740	5280.3	74808.4	63589.5	4513548	0.001	80.7023	1.154
5780	5320.3	75401.4	64103.8	4753843	0.001	80.8053	1.153

## B.7 Nitrogen Properties (SI Units)

Temperature K	Temperature C	h kJ/kgmol		Pr	Vr	S <sub>o</sub> kJ/kgmol/K	Gamma
		u kJ/kgmol	Pr				
200	-73.1	4842.2	3456.7	0.34	1072.9	174.5226	1.399
225	-48.1	5570.4	3981.6	0.51	443.82	177.9535	1.399
250	-23.1	6298.6	4505.5	0.73	340.92	181.0223	1.400
275	1.9	7026.5	5028.6	1.02	268.58	183.7977	1.400
300	26.9	7754.4	5551.2	1.39	216.03	186.3310	1.400
325	51.9	8482.4	6073.4	1.84	176.82	188.6617	1.400
350	76.9	9210.7	6595.7	2.38	146.87	190.8208	1.399
375	101.9	9939.8	7118.5	3.04	123.53	192.8329	1.398
400	126.9	10670.1	7642.3	3.81	105.04	194.7179	1.397
425	151.9	11401.8	8167.4	4.71	90.150	196.4925	1.396
450	176.9	12135.5	8694.3	5.77	78.014	198.1698	1.394
475	201.9	12871.4	9223.4	6.99	68.000	199.7613	1.393
500	226.9	13609.9	9754.9	8.38	59.654	201.2764	1.391
525	251.9	14351.2	10289.2	9.97	52.632	202.7233	1.388
550	276.9	15095.7	10826.5	11.78	46.675	204.1086	1.386
575	301.9	15843.5	11367.2	13.83	41.584	205.4382	1.384
600	326.9	16594.9	11911.4	16.13	37.204	206.7174	1.381
625	351.9	17350.1	12459.2	18.71	33.413	207.9503	1.378
650	376.9	18109.0	13010.8	21.59	30.112	209.1411	1.376
675	401.9	18872.0	13566.4	24.79	27.225	210.2928	1.373
700	426.9	19639.0	14126.0	28.35	24.688	211.4086	1.370
725	451.9	20410.0	14689.6	32.30	22.448	212.4909	1.368
750	476.9	21185.3	15257.4	36.65	20.464	213.5421	1.365
775	501.9	21964.7	15829.3	41.44	18.700	214.5643	1.362
800	526.8	22748.2	16405.3	46.71	17.125	215.5594	1.360
825	551.8	23535.9	16985.5	52.49	15.717	216.5289	1.357
850	576.8	24327.7	17569.7	58.81	14.452	217.4743	1.355
875	601.8	25123.5	18158.0	65.72	13.314	218.3971	1.352
900	626.8	25923.4	18750.3	73.24	12.288	219.2984	1.350
925	651.8	26727.3	19346.6	81.43	11.359	220.1794	1.348
950	676.8	27534.9	19946.6	90.32	10.518	221.0410	1.345
975	701.8	28346.4	20550.5	99.96	9.754	221.8840	1.343
1000	726.8	29161.6	21158.1	110.40	9.058	222.7097	1.341
1025	751.8	29980.4	21769.3	121.68	8.424	223.5184	1.339
1050	776.8	30802.9	22384.0	133.85	7.844	224.3111	1.337
1075	801.8	31628.7	23002.2	146.97	7.314	225.0885	1.335
1100	826.8	32458.0	23623.8	161.09	6.828	225.8510	1.334
1125	851.8	33290.4	24248.6	176.26	6.383	226.5993	1.332
1150	876.8	34126.0	24876.5	192.54	5.973	227.3338	1.330
1175	901.8	34964.7	25507.5	210.00	5.595	228.0554	1.329
1200	926.8	35806.4	26141.4	228.69	5.247	228.7641	1.327
1225	951.8	36650.9	26778.3	248.67	4.926	229.4606	1.326
1250	976.8	37498.2	27417.9	270.02	4.629	230.1453	1.324
1275	1002	38348.2	28060.2	292.80	4.355	230.8186	1.323
1300	1027	39200.7	28704.9	317.08	4.100	231.4809	1.322
1325	1052	40055.8	29352.3	342.93	3.864	232.1324	1.321
1350	1077	40913.3	30002.1	370.42	3.645	232.7735	1.319
1375	1102	41773.1	30654.2	399.63	3.441	233.4045	1.318
1400	1127	42635.2	31308.5	430.64	3.251	234.0258	1.317
1425	1152	43499.3	31964.9	463.53	3.074	234.6377	1.316
1450	1177	44365.7	32623.6	498.38	2.909	235.2404	1.315
1475	1202	45234.0	33284.2	535.27	2.756	235.8341	1.314

1500	1227	46104.4	33946.7	574.30	2.612	236.4192	1.313
1525	1252	46976.4	34611.0	615.54	2.477	236.9958	1.312
1550	1277	47850.4	35277.3	659.11	2.352	237.5643	1.312
1575	1302	48726.0	35945.2	705.07	2.234	238.1247	1.311
1600	1327	49603.5	36614.8	753.54	2.123	238.6775	1.310
1625	1352	50482.5	37285.9	804.59	2.020	239.2224	1.309
1650	1377	51363.2	37958.9	858.34	1.922	239.7601	1.309
1675	1402	52245.1	38633.2	914.92	1.831	240.2907	1.308
1700	1427	53128.6	39308.8	974.39	1.745	240.8144	1.307
1725	1452	54013.4	39985.9	1036.90	1.664	241.3313	1.307
1750	1477	54899.8	40664.5	1102.50	1.587	241.8413	1.306
1775	1502	55787.6	41344.7	1171.36	1.515	242.3450	1.305
1800	1527	56676.6	42025.8	1243.57	1.447	242.8423	1.305
1825	1552	57566.8	42708.1	1319.26	1.383	243.3335	1.304
1850	1577	58458.1	43391.7	1398.50	1.323	243.8184	1.304
1875	1602	59350.7	44076.7	1481.52	1.266	244.2979	1.303
1900	1627	60244.3	44762.3	1568.34	1.211	244.7713	1.303
1925	1652	61139.2	45449.6	1659.15	1.160	245.2393	1.302
1950	1677	62035.0	46137.7	1754.00	1.112	245.7015	1.302
1975	1702	62932.4	46827.0	1853.15	1.066	246.1586	1.301
2000	1727	63830.5	47517.4	1956.68	1.022	246.6106	1.301
2025	1752	64729.4	48208.6	2064.67	0.981	247.0572	1.300
2050	1777	65629.4	48900.8	2177.38	0.942	247.4991	1.300
2075	1802	66530.4	49593.8	2294.82	0.904	247.9358	1.300
2100	1827	67432.2	50287.9	2417.25	0.869	248.3679	1.299
2125	1852	68335.2	50983.2	2544.70	0.835	248.7951	1.299
2150	1877	69238.7	51679.0	2677.57	0.803	249.2182	1.298
2175	1902	70143.8	52376.0	2815.68	0.772	249.6364	1.298
2200	1927	71049.1	53073.7	2959.36	0.743	250.0501	1.298
2225	1952	71955.4	53772.2	3108.89	0.716	250.4599	1.297
2250	1977	72862.1	54471.2	3264.18	0.689	250.8652	1.297
2275	2002	73770.2	55171.6	3425.64	0.664	251.2666	1.297
2300	2027	74679.0	55872.4	3593.33	0.640	251.6639	1.296
2325	2052	75588.3	56574.0	3767.45	0.617	252.0573	1.296
2350	2077	76498.6	57276.6	3948.23	0.595	252.4469	1.296
2375	2102	77409.8	57979.6	4135.53	0.574	252.8322	1.295
2400	2127	78321.5	58683.6	4329.93	0.554	253.2141	1.295
2425	2152	79233.6	59388.1	4531.69	0.535	253.5928	1.295
2450	2177	80147.2	60093.6	4740.30	0.517	253.9669	1.295
2475	2202	81061.3	60799.6	4956.64	0.499	254.3380	1.294
2500	2227	81974.9	61506.3	5180.90	0.483	254.7058	1.294
2525	2252	82889.7	62213.5	5412.57	0.467	255.0695	1.294
2550	2277	83806.5	62921.7	5653.13	0.451	255.4310	1.293
2575	2302	84722.2	63629.7	5901.50	0.436	255.7885	1.293
2600	2327	85639.7	64339.5	6158.56	0.422	256.1430	1.293
2625	2352	86557.4	65048.8	6424.15	0.409	256.4940	1.293
2650	2377	87474.6	65759.0	6698.76	0.396	256.8420	1.292
2675	2402	88394.1	66470.0	6982.77	0.383	257.1872	1.292
2700	2427	89313.6	67181.9	7276.13	0.371	257.5293	1.292
2725	2452	90232.9	67893.5	7579.28	0.360	257.8687	1.292
2750	2477	91153.4	68606.3	7891.81	0.348	258.2046	1.292

2775	2502	92074.3	69318.7	8214.82	0.338	258.5381	1.291
2800	2527	92995.6	70033.0	8547.82	0.328	258.8685	1.291
2825	2552	93917.5	70746.5	8891.44	0.318	259.1961	1.291
2850	2577	94840.0	71461.3	9246.23	0.308	259.5214	1.291
2875	2602	95762.3	72176.7	9612.03	0.299	259.8440	1.291
2900	2627	96685.2	72891.1	9988.31	0.290	260.1632	1.290
2925	2652	97609.5	73607.7	10376.35	0.282	260.4801	1.290
2950	2677	98533.2	74323.8	10777.49	0.274	260.7954	1.290
2975	2702	99457.2	75039.2	11188.71	0.266	261.1068	1.290
3000	2727	100382.7	75757.0	11613.83	0.258	261.4168	1.290
3025	2752	101307.1	76473.7	12049.96	0.251	261.7233	1.290
3050	2777	102233.1	77192.0	12500.42	0.244	262.0284	1.290
3075	2802	103158.5	77909.7	12963.57	0.237	262.3308	1.289
3100	2827	104084.9	78628.4	13439.74	0.231	262.6307	1.289
3125	2852	105011.0	79346.8	13930.07	0.224	262.9286	1.289
3150	2877	105937.8	80065.2	14434.00	0.218	263.2241	1.289
3175	2902	106865.5	80786.8	14951.77	0.212	263.5171	1.289
3200	2927	107793.2	81505.2	15484.30	0.207	263.8080	1.289
3225	2952	108720.8	82225.1	16030.68	0.201	264.0963	1.289
3250	2977	109649.0	82945.6	16593.23	0.196	264.3831	1.289
3275	3002	110577.2	83666.1	17171.93	0.191	264.6681	1.288
3300	3027	111504.7	84386.0	17764.55	0.186	264.9502	1.288
3325	3052	112434.6	85108.1	18374.79	0.181	265.2310	1.288
3350	3077	113363.7	85829.6	18999.02	0.176	265.5087	1.288
3375	3102	114292.6	86550.8	19643.30	0.172	265.7859	1.288
3400	3127	115224.0	87272.8	20301.83	0.167	266.0601	1.288
3425	3152	116154.8	87995.9	20979.58	0.163	266.3331	1.288
3450	3177	117084.1	88719.2	21673.51	0.159	266.6036	1.287
3475	3202	118014.7	89442.1	22386.46	0.155	266.8727	1.287
3500	3227	118947.9	90166.0	23118.61	0.151	267.1403	1.287
3525	3252	119880.8	90891.2	23867.95	0.148	267.4055	1.287
3550	3277	120813.0	91615.7	24637.25	0.144	267.6692	1.287

## B.8 Nitrogen Properties (English Units)

Temperature		<i>h</i>	<i>u</i>	<i>Pr</i>	<i>Vr</i>	<i>S<sub>o</sub></i>	Gamma
R	F	Btu/lbmol	Btu/lbmol			Btu/lbmol/R	
300	-159.7	2081.9	1486.2	0.177	1692.8	41.6870	1.400
340	-119.7	2360.0	1687.3	0.275	1237.9	42.5571	1.400
380	-79.7	2638.2	1888.1	0.406	937.06	43.3308	1.399
420	-39.7	2916.5	2088.5	0.576	729.35	44.0272	1.399
460	0.3	3194.8	2288.7	0.792	580.81	44.6601	1.400
500	40.3	3473.0	2488.5	1.061	471.43	45.2400	1.400
540	80.3	3751.2	2688.2	1.389	388.86	45.7752	1.400
580	120.3	4029.4	2887.8	1.784	325.19	46.2722	1.400
620	160.3	4307.7	3087.4	2.253	275.18	46.7363	1.399
660	200.3	4586.3	3287.2	2.805	235.26	47.1717	1.399
700	240.3	4865.2	3487.2	3.449	202.95	47.5819	1.398
740	280.3	5144.5	3687.6	4.194	176.46	47.9700	1.397
780	320.3	5424.5	3888.5	5.048	154.50	48.3384	1.396
820	360.3	5705.1	4090.1	6.024	136.12	48.6893	1.394
860	400.3	5986.5	4292.4	7.131	120.60	49.0243	1.392
900	440.3	6268.8	4495.6	8.382	107.38	49.3451	1.391
940	480.3	6552.0	4699.8	9.788	96.040	49.6531	1.389
980	520.3	6836.4	4904.9	11.362	86.252	49.9493	1.387
1020	560.3	7121.8	5111.2	13.119	77.752	50.2348	1.384
1060	600.3	7408.4	5318.6	15.072	70.330	50.5104	1.382
1100	640.3	7696.3	5527.3	17.237	63.815	50.7770	1.380
1140	680.3	7985.5	5737.2	19.631	58.073	51.0352	1.378
1180	720.3	8275.9	5948.5	22.269	52.988	51.2856	1.375
1220	760.3	8567.8	6161.0	25.171	48.469	51.5288	1.373
1260	800.3	8861.0	6375.0	28.354	44.438	51.7653	1.370
1300	840.3	9155.6	6590.3	31.839	40.831	51.9955	1.368
1340	880.3	9451.6	6807.1	35.645	37.593	52.2198	1.366
1380	920.3	9749.0	7025.2	39.795	34.677	52.4385	1.363
1420	960.3	10047.9	7244.7	44.312	32.046	52.6520	1.361
1460	1000.3	10348.1	7465.6	49.217	29.664	52.8605	1.359
1500	1040.3	10649.8	7688.0	54.537	27.504	53.0643	1.356
1540	1080.3	10952.8	7911.7	60.297	25.540	53.2637	1.354
1580	1120.3	11257.2	8136.8	66.523	23.751	53.4588	1.352
1620	1160.3	11563.0	8363.2	73.244	22.118	53.6499	1.350
1660	1200.3	11870.1	8591.0	80.487	20.624	53.8372	1.348
1700	1240.3	12178.6	8820.1	88.285	19.256	54.0208	1.346
1740	1280.3	12488.3	9050.5	96.664	18.001	54.2009	1.344
1780	1320.3	12799.3	9282.2	105.660	16.846	54.3776	1.342
1820	1360.3	13111.6	9515.1	115.308	15.784	54.5511	1.340
1860	1400.3	13425.1	9749.2	125.636	14.805	54.7215	1.339
1900	1440.3	13739.7	9984.5	136.685	13.901	54.8889	1.337
1940	1480.3	14055.5	10221.0	148.490	13.065	55.0534	1.335
1980	1520.3	14372.5	10458.6	161.090	12.291	55.2151	1.334
2020	1560.3	14690.6	10697.3	174.521	11.575	55.3741	1.332
2060	1600.3	15009.8	10937.1	188.827	10.909	55.5306	1.331
2100	1640.3	15330.0	11177.9	204.048	10.292	55.6845	1.329
2140	1680.3	15651.2	11419.8	220.229	9.717	55.8361	1.328
2180	1720.3	15973.4	11662.6	237.408	9.183	55.9852	1.327
2220	1760.3	16296.6	11906.4	255.635	8.684	56.1321	1.325
2260	1800.3	16620.7	12151.2	274.959	8.219	56.2768	1.324
2300	1840.3	16945.7	12396.7	295.426	7.785	56.4194	1.323
2340	1880.3	17271.6	12643.3	317.078	7.380	56.5599	1.322

2380	1920.3	17598.4	12890.6	339.970	7.001	56.6983	1.321
2420	1960.3	17925.9	13138.8	364.158	6.645	56.8348	1.320
2460	2000.3	18254.3	13387.8	389.695	6.313	56.9694	1.319
2500	2040.3	18583.4	13637.5	416.625	6.001	57.1021	1.318
2540	2080.3	18913.3	13888.0	445.019	5.708	57.2330	1.317
2580	2120.3	19243.9	14139.2	474.922	5.432	57.3622	1.316
2620	2160.3	19575.2	14391.1	506.397	5.174	57.4896	1.315
2660	2200.3	19907.2	14643.7	539.497	4.931	57.6153	1.314
2700	2240.3	20239.9	14897.0	574.296	4.701	57.7395	1.313
2740	2280.3	20573.1	15150.8	610.851	4.486	57.8620	1.313
2780	2320.3	20907.0	15405.4	649.229	4.282	57.9830	1.312
2820	2360.3	21241.5	15660.4	689.473	4.090	58.1024	1.311
2860	2400.3	21576.5	15916.1	731.685	3.909	58.2204	1.310
2900	2440.3	21912.2	16172.2	775.912	3.738	58.3370	1.310
2940	2480.3	22248.3	16429.0	822.200	3.576	58.4520	1.309
2980	2520.3	22585.0	16686.3	870.690	3.423	58.5658	1.308
3020	2560.3	22922.3	16944.2	921.370	3.278	58.6782	1.308
3060	2600.3	23260.0	17202.4	974.393	3.140	58.7893	1.307
3100	2640.3	23598.0	17461.2	1029.80	3.010	58.8991	1.307
3140	2680.3	23936.7	17720.4	1087.65	2.887	59.0077	1.306
3180	2720.3	24275.9	17980.2	1148.04	2.770	59.1150	1.306
3220	2760.3	24615.5	18240.3	1211.08	2.659	59.2211	1.305
3260	2800.3	24955.4	18500.9	1276.77	2.553	59.3260	1.305
3300	2840.3	25295.9	18761.9	1345.29	2.453	59.4298	1.304
3340	2880.3	25636.7	19023.3	1416.60	2.358	59.5324	1.304
3380	2920.3	25977.8	19285.1	1490.97	2.267	59.6340	1.303
3420	2960.3	26319.4	19547.2	1568.34	2.181	59.7345	1.303
3460	3000.3	26661.4	19809.7	1648.83	2.098	59.8339	1.302
3500	3040.3	27003.8	20072.7	1732.57	2.020	59.9322	1.302
3540	3080.3	27346.5	20336.0	1819.63	1.945	60.0296	1.302
3580	3120.3	27689.5	20599.7	1910.11	1.874	60.1260	1.301
3620	3160.3	28032.8	20863.5	2004.12	1.806	60.2214	1.301
3660	3200.3	28376.6	21127.9	2101.77	1.741	60.3158	1.300
3700	3240.3	28720.7	21392.7	2203.02	1.680	60.4093	1.300
3740	3280.3	29065.2	21657.7	2308.13	1.620	60.5018	1.300
3780	3320.3	29409.8	21922.9	2417.25	1.564	60.5936	1.299
3820	3360.3	29754.8	22188.4	2530.38	1.510	60.6844	1.299
3860	3400.3	30100.3	22454.5	2647.55	1.458	60.7743	1.299
3900	3440.3	30445.8	22720.7	2769.04	1.408	60.8634	1.298
3940	3480.3	30791.8	22987.2	2894.83	1.361	60.9516	1.298
3980	3520.3	31137.9	23253.9	3025.20	1.316	61.0391	1.298
4020	3560.3	31484.6	23521.1	3159.98	1.272	61.1256	1.297
4060	3600.3	31831.1	23788.4	3299.54	1.230	61.2115	1.297
4100	3640.3	32178.1	24055.9	3443.92	1.191	61.2965	1.297
4140	3680.3	32525.6	24324.0	3593.33	1.152	61.3808	1.296
4180	3720.3	32873.0	24591.9	3747.78	1.115	61.4644	1.296
4220	3760.3	33220.9	24860.3	3907.33	1.080	61.5472	1.296
4260	3800.3	33569.1	25129.1	4072.25	1.046	61.6293	1.296
4300	3840.3	33917.3	25398.0	4242.58	1.014	61.7107	1.295
4340	3880.3	34266.0	25667.3	4418.55	0.982	61.7914	1.295
4380	3920.3	34614.7	25936.5	4600.30	0.952	61.8714	1.295
4420	3960.3	34963.6	26206.0	4787.81	0.923	61.9508	1.294
4460	4000.3	35313.2	26476.1	4981.34	0.895	62.0295	1.294

4500	4040.3	35662.5	26746.3	5180.90	0.869	62.1075	1.294
4540	4080.3	36012.3	27016.7	5386.68	0.843	62.1848	1.294
4580	4120.3	36362.4	27287.3	5598.82	0.818	62.2615	1.294
4620	4160.3	36712.3	27557.7	5817.90	0.794	62.3377	1.293
4660	4200.3	37062.9	27828.8	6043.10	0.771	62.4132	1.293
4700	4240.3	37413.4	28099.9	6275.62	0.749	62.4881	1.293
4740	4280.3	37764.0	28371.1	6514.80	0.728	62.5624	1.293
4780	4320.3	38115.1	28642.7	6761.13	0.707	62.6361	1.292
4820	4360.3	38466.5	28914.7	7015.17	0.687	62.7094	1.292
4860	4400.3	38817.8	29186.5	7276.14	0.668	62.7819	1.292
4900	4440.3	39169.1	29458.4	7544.44	0.649	62.8538	1.292
4940	4480.3	39520.6	29730.4	7821.43	0.632	62.9254	1.292
4980	4520.3	39873.0	30003.4	8105.91	0.614	62.9963	1.291
5020	4560.3	40224.8	30275.7	8398.19	0.598	63.0667	1.291
5060	4600.3	40577.1	30548.5	8699.26	0.582	63.1366	1.291
5100	4640.3	40929.5	30821.5	9008.12	0.566	63.2059	1.291
5140	4680.3	41281.6	31094.5	9326.59	0.551	63.2749	1.291
5180	4720.3	41634.7	31368.2	9653.38	0.537	63.3433	1.291
5220	4760.3	41987.2	31641.2	9988.32	0.523	63.4110	1.290
5260	4800.3	42340.2	31914.7	10333.02	0.509	63.4784	1.290
5300	4840.3	42693.8	32188.9	10686.94	0.496	63.5453	1.290
5340	4880.3	43046.5	32462.5	11050.74	0.483	63.6118	1.290
5380	4920.3	43399.9	32736.1	11423.45	0.471	63.6776	1.290
5420	4960.3	43753.4	33010.2	11806.61	0.459	63.7432	1.290
5460	5000.3	44107.0	33284.6	12198.95	0.448	63.8081	1.290
5500	5040.3	44460.7	33558.8	12602.40	0.436	63.8727	1.290
5540	5080.3	44814.5	33832.9	13015.39	0.426	63.9367	1.289
5580	5120.3	45168.7	34108.0	13439.72	0.415	64.0004	1.289
5620	5160.3	45522.8	34382.3	13874.76	0.405	64.0637	1.289
5660	5200.3	45876.8	34657.2	14319.60	0.395	64.1264	1.289
5700	5240.3	46231.2	34931.8	14777.22	0.386	64.1888	1.289
5740	5280.3	46586.3	35207.4	15245.71	0.376	64.2508	1.289
5780	5320.3	46940.0	35482.3	15725.32	0.368	64.3123	1.289
5820	5360.3	47294.6	35757.5	16217.27	0.359	64.3735	1.289
5860	5400.3	47648.8	36032.3	16721.14	0.350	64.4342	1.288
5900	5440.3	48004.0	36308.0	17236.29	0.342	64.4945	1.288
5940	5480.3	48358.9	36583.4	17764.58	0.334	64.5545	1.288
5980	5520.3	48714.6	36859.7	18306.96	0.327	64.6142	1.288
6020	5560.3	49069.8	37135.4	18859.23	0.319	64.6732	1.288
6060	5600.3	49424.7	37410.9	19427.11	0.312	64.7321	1.288
6100	5640.3	49780.2	37687.0	20007.33	0.305	64.7906	1.288
6140	5680.3	50135.4	37962.7	20600.29	0.298	64.8486	1.288
6180	5720.3	50491.1	38238.9	21209.51	0.291	64.9064	1.288
6220	5760.3	50847.7	38516.1	21830.38	0.285	64.9637	1.287
6260	5800.3	51202.9	38791.8	22466.66	0.279	65.0208	1.287
6300	5840.3	51559.1	39068.6	23118.64	0.273	65.0776	1.287
6340	5880.3	51915.2	39345.2	23782.05	0.267	65.1338	1.287
6380	5920.3	52271.8	39622.4	24462.81	0.261	65.1898	1.287

## B.9 Oxygen Properties (SI Units)

Temperature		h	u	Pr	Vr	S <sub>o</sub>	Gamma
K	C	kJ/kgmol	kJ/kgmol			kJ/kgmol/K	
200	-73.1	4844.7	3459.2	0.330	1074.6	188.0074	1.399
225	-48.1	5573.2	3979.9	0.510	444.49	191.4393	1.399
250	-23.1	6302.3	4501.1	0.730	341.27	194.5121	1.398
275	1.9	7032.8	5023.8	1.020	268.54	197.2970	1.397
300	26.9	7765.6	5548.8	1.390	215.56	199.8474	1.395
325	51.9	8501.6	6077.0	1.850	175.89	202.2038	1.392
350	76.9	9241.6	6609.2	2.410	145.49	204.3974	1.389
375	101.9	9986.3	7146.0	3.080	121.74	206.4524	1.385
400	126.9	10736.2	7688.1	3.890	102.89	208.3882	1.381
425	151.9	11491.8	8235.9	4.850	87.693	210.2205	1.377
450	176.9	12253.4	8789.6	5.980	75.307	211.9616	1.373
475	201.9	13021.2	9349.5	7.300	65.100	213.6220	1.369
500	226.9	13795.1	9915.7	8.830	56.611	215.2100	1.365
525	251.9	14575.5	10488.2	10.610	49.493	216.7328	1.361
550	276.9	15362.2	11067.0	12.650	43.479	218.1965	1.357
575	301.9	16155.0	11652.1	14.990	38.366	219.6063	1.353
600	326.9	16954.0	12243.2	17.650	33.992	220.9665	1.350
625	351.9	17759.0	12840.3	20.670	30.230	222.2808	1.346
650	376.9	18569.7	13443.2	24.090	26.980	223.5526	1.343
675	401.9	19386.0	14051.6	27.940	24.158	224.7849	1.340
700	426.9	20207.7	14665.5	32.260	21.697	225.9803	1.337
725	451.9	21034.5	15284.5	37.100	19.544	227.1409	1.334
750	476.9	21866.4	15908.5	42.490	17.653	228.2688	1.332
775	501.9	22702.9	16537.2	48.480	15.986	229.3661	1.329
800	526.8	23544.0	17170.5	55.130	14.512	230.4342	1.327
825	551.8	24389.3	17807.9	62.470	13.206	231.4744	1.325
850	576.8	25238.9	18449.7	70.580	12.043	232.4888	1.323
875	601.8	26092.4	19095.3	79.500	11.006	233.4786	1.321
900	626.8	26949.3	19744.4	89.300	10.079	234.4443	1.319
925	651.8	27810.0	20397.4	100.030	9.248	235.3876	1.318
950	676.8	28674.0	21053.5	111.750	8.501	236.3092	1.316
975	701.8	29541.2	21712.9	124.550	7.828	237.2105	1.314
1000	726.8	30411.7	22375.4	138.470	7.222	238.0915	1.313
1025	751.8	31284.8	23040.8	153.610	6.673	238.9542	1.312
1050	776.8	32160.9	23708.9	170.030	6.175	239.7984	1.310
1075	801.8	33039.5	24379.7	187.820	5.723	240.6257	1.309
1100	826.8	33921.0	25053.3	207.050	5.313	241.4361	1.308
1125	851.8	34804.5	25729.1	227.810	4.938	242.2303	1.307
1150	876.8	35690.4	26407.2	250.190	4.597	243.0094	1.306
1175	901.8	36578.8	27087.6	274.280	4.284	243.7737	1.305
1200	926.8	37469.3	27770.3	300.160	3.998	244.5233	1.304
1225	951.8	38362.2	28455.3	327.960	3.735	245.2596	1.303
1250	976.8	39256.8	29142.2	357.750	3.494	245.9826	1.302
1275	1002	40153.4	29830.7	389.660	3.272	246.6929	1.301
1300	1027	41051.8	30521.4	423.800	3.068	247.3910	1.300
1325	1052	41952.2	31214.1	460.240	2.879	248.0768	1.300
1350	1077	42854.5	31908.4	499.160	2.705	248.7517	1.299
1375	1102	43758.2	32604.3	540.600	2.543	249.4148	1.298
1400	1127	44664.2	33302.6	584.770	2.394	250.0678	1.297
1425	1152	45572.1	34002.5	631.780	2.256	250.7106	1.297
1450	1177	46480.9	34703.6	681.690	2.127	251.3426	1.296

1475	1202	47391.8	35406.7	734.760	2.007	251.9659	1.295
1500	1227	48304.3	36111.1	791.040	1.896	252.5795	1.295
1525	1252	49218.7	36817.5	850.640	1.793	253.1835	1.294
1550	1277	50133.9	37525.4	913.810	1.696	253.7789	1.293
1575	1302	51051.3	38234.7	980.670	1.606	254.3660	1.293
1600	1327	51970.3	38946.0	1051.430	1.522	254.9453	1.292
1625	1352	52890.2	39657.4	1126.040	1.443	255.5152	1.291
1650	1377	53811.9	40372.2	1205.050	1.369	256.0790	1.291
1675	1402	54735.2	41087.9	1288.250	1.300	256.6340	1.290
1700	1427	55660.0	41804.1	1375.960	1.236	257.1816	1.290
1725	1452	56586.7	42523.1	1468.570	1.175	257.7232	1.289
1750	1477	57513.6	43242.3	1565.810	1.118	258.2562	1.288
1775	1502	58444.0	43964.2	1668.390	1.064	258.7838	1.288
1800	1527	59374.3	44687.6	1776.380	1.013	259.3051	1.287
1825	1552	60306.7	45412.4	1889.640	0.966	259.8190	1.287
1850	1577	61239.9	46137.1	2008.650	0.921	260.3268	1.286
1875	1602	62175.3	46864.8	2133.750	0.879	260.8291	1.286
1900	1627	63111.9	47593.7	2264.990	0.839	261.3253	1.285
1925	1652	64050.0	48323.3	2402.790	0.801	261.8163	1.284
1950	1677	64989.3	49054.8	2547.020	0.766	262.3010	1.284
1975	1702	65929.9	49786.9	2697.750	0.732	262.7790	1.283
2000	1727	66870.6	50521.6	2856.260	0.700	263.2536	1.283
2025	1752	67815.3	51258.6	3021.750	0.670	263.7219	1.282
2050	1777	68759.6	51993.6	3195.660	0.641	264.1871	1.282
2075	1802	69706.0	52732.3	3376.570	0.615	264.6449	1.281
2100	1827	70653.6	53472.2	3565.950	0.589	265.0986	1.281
2125	1852	71602.0	54212.9	3763.990	0.565	265.5479	1.280
2150	1877	72552.5	54955.7	3970.630	0.541	265.9922	1.280
2175	1902	73505.1	55699.0	4186.520	0.520	266.4324	1.279
2200	1927	74456.5	56444.3	4412.320	0.499	266.8691	1.279
2225	1952	75410.8	57190.9	4646.560	0.479	267.2992	1.278
2250	1977	76366.4	57938.9	4892.130	0.460	267.7273	1.278
2275	2002	77324.9	58688.0	5147.180	0.442	268.1498	1.277
2300	2027	78282.5	59439.6	5413.640	0.425	268.5695	1.277
2325	2052	79242.9	60190.7	5690.300	0.409	268.9838	1.276
2350	2077	80202.2	60942.3	5978.470	0.393	269.3945	1.276
2375	2102	81165.1	61697.5	6278.510	0.378	269.8016	1.275
2400	2127	82128.8	62451.9	6591.310	0.364	270.2058	1.275
2425	2152	83092.6	63209.4	6915.330	0.351	270.6048	1.274
2450	2177	84060.2	63967.9	7253.860	0.338	271.0021	1.274
2475	2202	85028.5	64726.9	7605.280	0.325	271.3954	1.273
2500	2227	85997.5	65489.8	7969.600	0.314	271.7845	1.273
2525	2252	86964.4	66250.6	8348.850	0.302	272.1710	1.273
2550	2277	87935.4	67015.6	8740.540	0.292	272.5521	1.272
2575	2302	88909.4	67780.3	9149.560	0.281	272.9323	1.272
2600	2327	89883.7	68545.3	9573.050	0.272	273.3085	1.271
2625	2352	90857.1	69312.6	10011.66	0.262	273.6809	1.271
2650	2377	91831.8	70077.9	10468.70	0.253	274.0521	1.270
2675	2402	92811.6	70851.8	10942.12	0.244	274.4198	1.270
2700	2427	93788.0	71618.8	11430.69	0.236	274.7829	1.269
2725	2452	94769.9	72391.4	11939.27	0.228	275.1448	1.269

2750	2477	95754.4	73166.6	12466.23	0.221	275.5039	1.269
2775	2502	96733.4	73939.4	13008.47	0.213	275.8579	1.268
2800	2527	97720.0	74716.8	13570.96	0.206	276.2098	1.268
2825	2552	98698.0	75492.0	14159.12	0.200	276.5625	1.267
2850	2577	99688.5	76269.9	14760.84	0.193	276.9085	1.267
2875	2602	100674.1	77052.6	15385.88	0.187	277.2533	1.267
2900	2627	101660.0	77829.3	16033.14	0.181	277.5959	1.266
2925	2652	102649.4	78609.3	16702.24	0.175	277.9358	1.266
2950	2677	103642.2	79392.9	17392.24	0.170	278.2724	1.265
2975	2702	104632.1	80176.6	18109.35	0.164	278.6083	1.265
3000	2727	105629.1	80964.3	18842.33	0.159	278.9381	1.265
3025	2752	106618.5	81747.7	19605.69	0.154	279.2683	1.264
3050	2777	107617.3	82537.1	20394.44	0.150	279.5962	1.264
3075	2802	108613.8	83324.3	21208.77	0.145	279.9217	1.264
3100	2827	109604.7	84112.4	22050.11	0.141	280.2451	1.263
3125	2852	110603.4	84901.8	22912.96	0.136	280.5643	1.263
3150	2877	111600.9	85690.0	23813.95	0.132	280.8849	1.263
3175	2902	112598.4	86484.7	24740.19	0.128	281.2021	1.262
3200	2927	113599.7	87276.7	25688.12	0.125	281.5147	1.262
3225	2952	114600.5	88068.1	26669.83	0.121	281.8265	1.262
3250	2977	115604.2	88862.5	27674.83	0.117	282.1341	1.261
3275	3002	116609.5	89658.5	28729.51	0.114	282.4450	1.261
3300	3027	117612.1	90458.3	29793.74	0.111	282.7474	1.261
3325	3052	118627.2	91257.6	30908.52	0.108	283.0528	1.260
3350	3077	119629.9	92057.5	32048.53	0.105	283.3539	1.260
3375	3102	120639.1	92857.4	33222.66	0.102	283.6530	1.260
3400	3127	121644.6	93653.5	34440.44	0.099	283.9523	1.259
3425	3152	122653.0	94459.1	35676.52	0.096	284.2455	1.259
3450	3177	123666.0	95262.8	36961.71	0.093	284.5397	1.259
3475	3202	124674.9	96062.4	38297.42	0.091	284.8348	1.259
3500	3227	125690.8	96869.0	39663.05	0.088	285.1261	1.258
3525	3252	126703.0	97671.8	41036.38	0.086	285.4091	1.258
3550	3277	127718.6	98484.7	42482.84	0.084	285.6971	1.258

## B.10 Oxygen Properties (English Units)

Temperature R	Temperature F	h		Pr	Vr	$S_o$ Btu/lbmol/R	Gamma
		Btu/lbmol	Btu/lbmol				
300	-159.7	2083.0	1487.3	0.177	1696.0	44.9080	1.400
340	-119.7	2361.2	1686.1	0.274	1240.0	45.7784	1.399
380	-79.7	2639.5	1885.0	0.405	938.55	46.5524	1.399
420	-39.7	2918.0	2084.0	0.575	730.37	47.2491	1.399
460	0.3	3196.7	2283.4	0.791	581.31	47.8831	1.398
500	40.3	3476.1	2483.2	1.061	471.30	48.4653	1.397
540	80.3	3756.2	2683.9	1.392	388.01	49.0043	1.395
580	120.3	4037.4	2885.7	1.792	323.61	49.5066	1.392
620	160.3	4319.9	3088.8	2.272	272.87	49.9777	1.390
660	200.3	4604.0	3293.5	2.841	232.28	50.4217	1.387
700	240.3	4889.8	3499.8	3.511	199.35	50.8421	1.383
740	280.3	5177.5	3708.1	4.294	172.33	51.2418	1.380
780	320.3	5467.1	3918.3	5.203	149.92	51.6229	1.376
820	360.3	5758.8	4130.6	6.252	131.17	51.9876	1.372
860	400.3	6052.6	4344.9	7.456	115.34	52.3375	1.369
900	440.3	6348.6	4561.5	8.832	101.90	52.6738	1.365
940	480.3	6646.7	4780.1	10.398	90.403	52.9979	1.361
980	520.3	6946.9	5001.0	12.171	80.517	53.3106	1.358
1020	560.3	7249.3	5223.9	14.174	71.965	53.6131	1.355
1060	600.3	7553.8	5448.9	16.425	64.536	53.9058	1.351
1100	640.3	7860.3	5676.0	18.949	58.052	54.1897	1.348
1140	680.3	8168.8	5905.1	21.768	52.371	54.4651	1.345
1180	720.3	8479.2	6136.0	24.909	47.372	54.7328	1.342
1220	760.3	8791.5	6368.9	28.397	42.962	54.9931	1.340
1260	800.3	9105.7	6603.7	32.262	39.055	55.2465	1.337
1300	840.3	9421.6	6840.1	36.531	35.586	55.4932	1.335
1340	880.3	9739.2	7078.3	41.237	32.495	55.7339	1.332
1380	920.3	10058.4	7318.1	46.411	29.734	55.9686	1.330
1420	960.3	10379.2	7559.4	52.088	27.262	56.1977	1.328
1460	1000.3	10701.4	7802.3	58.302	25.042	56.4216	1.326
1500	1040.3	11025.2	8046.6	65.092	23.044	56.6403	1.324
1540	1080.3	11350.2	8292.2	72.494	21.243	56.8542	1.322
1580	1120.3	11676.6	8539.1	80.549	19.615	57.0634	1.321
1620	1160.3	12004.2	8787.4	89.298	18.142	57.2682	1.319
1660	1200.3	12333.1	9036.8	98.787	16.804	57.4687	1.318
1700	1240.3	12663.1	9287.3	109.057	15.588	57.6651	1.316
1740	1280.3	12994.2	9539.1	120.159	14.481	57.8577	1.315
1780	1320.3	13326.4	9791.8	132.140	13.471	58.0464	1.314
1820	1360.3	13659.6	10045.5	145.054	12.547	58.2316	1.312
1860	1400.3	13993.7	10300.2	158.939	11.703	58.4131	1.311
1900	1440.3	14328.8	10555.9	173.867	10.928	58.5914	1.310
1940	1480.3	14664.9	10812.5	189.878	10.217	58.7663	1.309
1980	1520.3	15001.7	11069.9	207.053	9.563	58.9383	1.308
2020	1560.3	15339.4	11328.1	225.424	8.961	59.1071	1.307
2060	1600.3	15677.9	11587.3	245.068	8.406	59.2730	1.306
2100	1640.3	16017.1	11847.0	266.042	7.893	59.4361	1.305
2140	1680.3	16357.1	12107.6	288.437	7.419	59.5966	1.304
2180	1720.3	16697.9	12368.9	312.265	6.981	59.7542	1.304
2220	1760.3	17039.2	12630.9	337.650	6.575	59.9094	1.303
2260	1800.3	17381.4	12893.6	364.668	6.197	60.0623	1.302
2300	1840.3	17724.2	13157.0	393.349	5.847	60.2126	1.301
2340	1880.3	18067.6	13420.9	423.798	5.522	60.3607	1.300

2380	1920.3	18411.9	13685.7	456.060	5.219	60.5064	1.300
2420	1960.3	18756.6	13951.0	490.289	4.936	60.6501	1.299
2460	2000.3	19101.8	14216.9	526.500	4.672	60.7916	1.298
2500	2040.3	19447.6	14483.3	564.786	4.426	60.9310	1.298
2540	2080.3	19794.1	14750.4	605.319	4.196	61.0686	1.297
2580	2120.3	20141.4	15017.9	648.093	3.981	61.2042	1.296
2620	2160.3	20489.0	15286.3	693.189	3.780	61.3378	1.296
2660	2200.3	20837.0	15554.9	740.793	3.591	61.4697	1.295
2700	2240.3	21185.9	15824.3	791.037	3.413	61.6000	1.295
2740	2280.3	21535.4	16094.4	843.836	3.247	61.7283	1.294
2780	2320.3	21885.1	16364.7	899.451	3.091	61.8551	1.293
2820	2360.3	22235.5	16635.4	957.983	2.944	61.9803	1.293
2860	2400.3	22586.5	16907.2	1019.44	2.805	62.1038	1.292
2900	2440.3	22938.1	17179.4	1084.06	2.675	62.2258	1.292
2940	2480.3	23290.0	17451.8	1151.88	2.552	62.3463	1.291
2980	2520.3	23642.0	17724.4	1223.12	2.436	62.4655	1.291
3020	2560.3	23994.9	17997.9	1297.84	2.327	62.5832	1.290
3060	2600.3	24348.5	18272.0	1375.96	2.224	62.6993	1.290
3100	2640.3	24702.3	18546.3	1458.02	2.126	62.8143	1.289
3140	2680.3	25057.2	18821.8	1543.78	2.034	62.9278	1.289
3180	2720.3	25412.4	19097.5	1633.68	1.947	63.0402	1.288
3220	2760.3	25767.9	19373.6	1727.83	1.864	63.1515	1.287
3260	2800.3	26123.7	19649.9	1826.07	1.785	63.2613	1.287
3300	2840.3	26480.3	19927.1	1928.68	1.711	63.3699	1.286
3340	2880.3	26836.9	20204.6	2036.13	1.640	63.4776	1.286
3380	2920.3	27194.4	20482.6	2147.96	1.574	63.5837	1.285
3420	2960.3	27552.4	20761.2	2264.99	1.510	63.6891	1.285
3460	3000.3	27910.7	21039.7	2387.13	1.449	63.7934	1.285
3500	3040.3	28269.7	21319.2	2514.14	1.392	63.8963	1.284
3540	3080.3	28629.2	21599.6	2646.86	1.337	63.9985	1.284
3580	3120.3	28988.8	21879.8	2785.34	1.285	64.0997	1.283
3620	3160.3	29348.9	22160.4	2929.13	1.236	64.1997	1.283
3660	3200.3	29710.1	22442.2	3078.65	1.189	64.2986	1.282
3700	3240.3	30071.2	22723.8	3235.02	1.144	64.3970	1.282
3740	3280.3	30433.1	23006.3	3397.46	1.101	64.4942	1.281
3780	3320.3	30795.0	23288.7	3565.94	1.060	64.5904	1.281
3820	3360.3	31157.5	23571.8	3741.25	1.021	64.6857	1.280
3860	3400.3	31520.6	23855.4	3924.16	0.984	64.7805	1.280
3900	3440.3	31884.3	24139.6	4114.02	0.948	64.8743	1.279
3940	3480.3	32247.9	24424.7	4310.84	0.914	64.9671	1.279
3980	3520.3	32612.7	24709.1	4515.11	0.881	65.0590	1.278
4020	3560.3	32978.3	24995.2	4727.45	0.850	65.1503	1.278
4060	3600.3	33343.0	25280.5	4947.04	0.821	65.2404	1.278
4100	3640.3	33708.5	25566.6	5175.92	0.792	65.3303	1.277
4140	3680.3	34075.1	25854.4	5413.64	0.765	65.4194	1.277
4180	3720.3	34441.8	26141.0	5659.10	0.739	65.5075	1.276
4220	3760.3	34809.4	26429.1	5914.01	0.714	65.5950	1.276
4260	3800.3	35176.7	26717.0	6177.31	0.690	65.6815	1.275
4300	3840.3	35545.1	27005.9	6450.56	0.667	65.7674	1.275
4340	3880.3	35913.5	27294.8	6734.85	0.644	65.8531	1.275
4380	3920.3	36282.0	27584.6	7026.65	0.623	65.9373	1.274
4420	3960.3	36650.8	27874.7	7330.08	0.603	66.0213	1.274
4460	4000.3	37021.3	28163.6	7644.56	0.583	66.1047	1.273

4500	4040.3	37392.1	28455.7	7969.59	0.565	66.1874	1.273
4540	4080.3	37762.7	28746.1	8305.63	0.547	66.2694	1.273
4580	4120.3	38133.7	29038.3	8653.25	0.529	66.3508	1.272
4620	4160.3	38504.2	29330.1	9013.26	0.513	66.4318	1.272
4660	4200.3	38876.5	29623.7	9383.72	0.497	66.5117	1.271
4700	4240.3	39249.3	29916.3	9767.59	0.481	66.5914	1.271
4740	4280.3	39622.2	30210.4	10162.9	0.466	66.6702	1.271
4780	4320.3	39995.4	30503.5	10573.0	0.452	66.7487	1.270
4820	4360.3	40369.8	30797.7	10995.9	0.438	66.8266	1.270
4860	4400.3	40741.7	31090.9	11430.7	0.425	66.9036	1.269
4900	4440.3	41117.8	31386.8	11879.5	0.412	66.9801	1.269
4940	4480.3	41492.4	31682.7	12343.5	0.400	67.0562	1.269
4980	4520.3	41867.4	31977.5	12823.6	0.388	67.1319	1.268
5020	4560.3	42244.0	32275.3	13321.3	0.377	67.2076	1.268
5060	4600.3	42619.0	32570.2	13831.8	0.366	67.2822	1.268
5100	4640.3	42995.1	32867.5	14356.2	0.355	67.3561	1.267
5140	4680.3	43373.6	33165.5	14897.9	0.345	67.4297	1.267
5180	4720.3	43750.6	33464.1	15455.8	0.335	67.5027	1.267
5220	4760.3	44126.3	33761.1	16033.1	0.326	67.5755	1.266
5260	4800.3	44505.8	34060.4	16624.9	0.316	67.6475	1.266
5300	4840.3	44883.6	34359.5	17240.2	0.307	67.7197	1.265
5340	4880.3	45262.6	34658.3	17867.5	0.299	67.7906	1.265
5380	4920.3	45641.6	34958.6	18513.8	0.291	67.8612	1.265
5420	4960.3	46019.8	35258.0	19178.5	0.283	67.9312	1.265
5460	5000.3	46400.1	35556.8	19868.9	0.275	68.0015	1.264
5500	5040.3	46779.6	35860.3	20578.2	0.267	68.0711	1.264
5540	5080.3	47162.7	36159.1	21300.1	0.260	68.1396	1.264
5580	5120.3	47542.1	36462.5	22050.1	0.253	68.2083	1.263
5620	5160.3	47924.1	36762.9	22821.5	0.246	68.2766	1.263
5660	5200.3	48306.8	37066.9	23609.7	0.240	68.3440	1.263
5700	5240.3	48689.4	37370.7	24424.0	0.233	68.4114	1.262
5740	5280.3	49071.1	37670.9	25258.6	0.227	68.4781	1.262
5780	5320.3	49452.4	37973.4	26122.2	0.221	68.5449	1.262
5820	5360.3	49836.4	38278.6	27005.5	0.216	68.6109	1.262
5860	5400.3	50219.4	38583.0	27911.8	0.210	68.6765	1.261
5900	5440.3	50604.0	38886.0	28843.0	0.205	68.7416	1.261
5940	5480.3	50984.9	39190.9	29793.6	0.199	68.8060	1.261
5980	5520.3	51369.0	39496.3	30780.5	0.194	68.8707	1.260
6020	5560.3	51755.9	39801.7	31791.3	0.189	68.9349	1.260
6060	5600.3	52142.4	40106.5	32828.2	0.185	68.9986	1.260
6100	5640.3	52526.9	40412.4	33889.5	0.180	69.0618	1.260
6140	5680.3	52910.4	40717.1	34992.4	0.175	69.1254	1.259
6180	5720.3	53295.7	41023.6	36107.9	0.171	69.1877	1.259
6220	5760.3	53684.3	41333.4	37269.0	0.167	69.2506	1.259
6260	5800.3	54071.3	41638.9	38424.6	0.163	69.3112	1.259
6300	5840.3	54458.4	41947.2	39662.9	0.159	69.3742	1.258
6340	5880.3	54843.1	42253.2	40889.6	0.155	69.4347	1.258
6380	5920.3	55229.9	42561.3	42160.0	0.151	69.4955	1.258

## B.11 Hydrogen Properties (SI Units)

Temperature K	h kJ/kgmol	u kJ/kgmol	Pr	Vr	s <sub>o</sub> kJ/kgmol/K	Gamma
200	-73.1	4805.7	3420.1	0.350	1029.2	114.446
225	-48.1	5495.8	3924.5	0.520	435.08	117.697
250	-23.1	6198.6	4437.6	0.740	338.55	120.659
275	1.9	6910.5	4956.6	1.020	268.69	123.373
300	26.9	7628.8	5479.7	1.380	216.99	125.873
325	51.9	8351.6	6005.5	1.830	177.96	128.187
350	76.9	9077.5	6532.9	2.370	147.95	130.338
375	101.9	9805.5	7061.1	3.010	124.49	132.347
400	126.9	10534.8	7589.8	3.780	105.88	134.230
425	151.9	11265.0	8118.5	4.670	90.912	136.001
450	176.9	11995.8	8647.1	5.720	78.734	137.672
475	201.9	12727.0	9175.5	6.910	68.713	139.253
500	226.9	13458.4	9703.7	8.280	60.384	140.754
525	251.9	14190.1	10231.7	9.830	53.397	142.182
550	276.9	14922.0	10759.6	11.580	47.487	143.544
575	301.9	15654.3	11287.4	13.550	42.449	144.846
600	326.9	16386.9	11815.4	15.740	38.124	146.093
625	351.9	17120.1	12343.6	18.180	34.387	147.290
650	376.9	17853.8	12872.2	20.870	31.138	148.441
675	401.9	18588.3	13401.3	23.850	28.299	149.550
700	426.9	19323.5	13931.1	27.130	25.804	150.619
725	451.9	20059.8	14461.6	30.720	23.601	151.653
750	476.9	20797.1	14993.2	34.640	21.649	152.653
775	501.9	21535.7	15525.8	38.930	19.910	153.621
800	526.8	22275.6	16059.6	43.580	18.356	154.561
825	551.8	23016.8	16594.8	48.640	16.962	155.473
850	576.8	23759.7	17131.3	54.120	15.707	156.360
875	601.8	24504.3	17669.5	60.040	14.575	157.224
900	626.8	25250.5	18209.4	66.430	13.549	158.065
925	651.8	25998.7	18751.0	73.310	12.617	158.884
950	676.8	26748.8	19294.5	80.720	11.769	159.685
975	701.8	27500.9	19840.0	88.670	10.995	160.466
1000	726.8	28255.2	20387.5	97.210	10.287	161.230
1025	751.8	29011.6	20937.1	106.340	9.638	161.977
1050	776.8	29770.2	21489.0	116.120	9.042	162.708
1075	801.8	30531.1	22043.0	126.570	8.493	163.425
1100	826.8	31294.6	22599.6	137.720	7.987	164.126
1125	851.8	32060.3	23158.3	149.620	7.519	164.815
1150	876.8	32828.6	23719.8	162.280	7.087	165.490
1175	901.8	33599.4	24283.3	175.750	6.686	166.153
1200	926.8	34372.8	24849.8	190.080	6.313	166.8049
1225	951.8	35148.7	25418.6	205.290	5.967	167.4448
1250	976.8	35927.5	25990.4	221.430	5.645	168.0741
1275	1001.8	36708.8	26564.4	238.530	5.345	168.6927
1300	1026.8	37493.0	27141.3	256.670	5.065	169.3019
1325	1051.8	38279.6	27720.8	275.850	4.803	169.9012
1350	1076.8	39068.9	28303.0	296.150	4.559	170.4915
1375	1101.8	39861.4	28888.0	317.590	4.329	171.0727
1400	1126.8	40656.2	29475.7	340.260	4.115	171.6458
1425	1151.8	41453.9	30066.2	364.180	3.913	172.2106
1450	1176.8	42254.3	30659.3	389.400	3.724	172.7673
1475	1201.8	43057.5	31254.8	415.990	3.546	173.3165

1500	1226.8	43863.2	31853.6	444.010	3.378	173.8584	1.347
1525	1251.8	44671.7	32454.5	473.490	3.221	174.3928	1.345
1550	1276.8	45483.5	33058.9	504.510	3.072	174.9204	1.344
1575	1301.8	46297.5	33665.3	537.150	2.932	175.4416	1.342
1600	1326.8	47113.8	34274.7	571.450	2.800	175.9562	1.341
1625	1351.8	47933.5	34886.7	607.450	2.675	176.4641	1.339
1650	1376.8	48755.8	35501.8	645.290	2.557	176.9665	1.338
1675	1401.8	49580.5	36118.8	684.920	2.446	177.4620	1.336
1700	1426.8	50407.3	36738.3	726.580	2.340	177.9529	1.335
1725	1451.8	51237.3	37361.0	770.150	2.240	178.4370	1.333
1750	1476.8	52069.7	37985.7	815.840	2.145	178.9162	1.332
1775	1501.8	52903.8	38612.9	863.700	2.055	179.3901	1.331
1800	1526.8	53740.8	39241.4	913.720	1.970	179.8581	1.330
1825	1551.8	54581.4	39875.1	966.120	1.889	180.3218	1.328
1850	1576.8	55424.0	40510.0	1020.85	1.812	180.7799	1.327
1875	1601.8	56267.7	41146.0	1078.02	1.739	181.2329	1.326
1900	1626.8	57114.5	41785.2	1137.85	1.670	181.6819	1.325
1925	1651.8	57963.9	42427.7	1200.31	1.604	182.1262	1.324
1950	1676.8	58816.2	43072.4	1265.35	1.541	182.5649	1.322
1975	1701.8	59669.1	43717.5	1333.32	1.481	183.0000	1.321
2000	1726.8	60524.9	44365.6	1404.24	1.424	183.4308	1.320
2025	1751.8	61382.1	45016.0	1478.15	1.370	183.8572	1.319
2050	1776.8	62242.3	45667.7	1555.15	1.318	184.2794	1.318
2075	1801.8	63105.5	46323.1	1635.33	1.269	184.6973	1.317
2100	1826.8	63969.2	46979.2	1718.79	1.222	185.1112	1.316
2125	1851.8	64836.1	47638.4	1805.64	1.177	185.5210	1.315
2150	1876.8	65704.2	48300.4	1896.32	1.134	185.9284	1.314
2175	1901.8	66575.0	48963.5	1990.34	1.093	186.3307	1.313
2200	1926.8	67446.9	49627.8	2088.08	1.054	186.729	1.312
2225	1951.8	68324.0	50295.5	2189.74	1.016	187.124	1.311
2250	1976.8	69197.7	50963.2	2295.26	0.980	187.516	1.310
2275	2001.8	70077.9	51634.0	2405.30	0.946	187.905	1.310
2300	2026.8	70956.1	52304.6	2519.14	0.913	188.290	1.309
2325	2051.9	71839.3	52980.1	2637.34	0.882	188.671	1.308
2350	2076.9	72722.6	53657.3	2759.89	0.851	189.048	1.307
2375	2101.9	73608.8	54335.9	2887.56	0.822	189.424	1.306
2400	2126.9	74496.5	55015.8	3019.41	0.795	189.795	1.305
2425	2151.9	75383.7	55697.0	3156.42	0.768	190.164	1.305
2450	2176.9	76275.0	56378.9	3298.22	0.743	190.530	1.304
2475	2201.9	77168.5	57063.2	3444.71	0.718	190.891	1.303
2500	2226.9	78065.4	57754.0	3597.46	0.695	191.252	1.302
2525	2251.9	78958.7	58441.2	3755.16	0.672	191.608	1.302
2550	2276.9	79858.3	59131.5	3918.30	0.651	191.962	1.301
2575	2301.9	80757.3	59824.4	4087.42	0.630	192.313	1.300
2600	2326.9	81660.9	60518.7	4262.98	0.610	192.663	1.299
2625	2351.9	82562.7	61211.2	4443.41	0.591	193.008	1.299
2650	2376.9	83468.5	61911.0	4630.75	0.572	193.351	1.298
2675	2401.9	84374.3	62607.4	4824.38	0.554	193.691	1.297
2700	2426.9	85280.6	63307.7	5023.60	0.537	194.028	1.297
2725	2451.9	86190.2	64007.9	5230.92	0.521	194.364	1.296
2750	2476.9	87100.1	64711.8	5444.85	0.505	194.697	1.295

2775	2501.9	88012.9	65418.5	5666.24	0.490	195.029	1.295
2800	2526.9	88928.4	66124.7	5893.76	0.475	195.356	1.294
2825	2551.9	89842.6	66829.6	6130.21	0.461	195.683	1.293
2850	2576.9	90761.3	67545.5	6370.52	0.447	196.003	1.293
2875	2601.9	91678.1	68252.9	6621.13	0.434	196.323	1.292
2900	2626.9	92599.3	68964.8	6879.94	0.422	196.642	1.291
2925	2651.9	93523.4	69679.6	7146.94	0.409	196.959	1.291
2950	2676.9	94447.0	70393.8	7424.87	0.397	197.276	1.290
2975	2701.9	95365.3	71109.4	7707.28	0.386	197.586	1.290
3000	2726.9	96299.9	71828.1	8001.78	0.375	197.898	1.289
3025	2751.9	97225.9	72551.3	8304.25	0.364	198.206	1.289
3050	2776.9	98155.4	73271.5	8614.29	0.354	198.511	1.288
3075	2801.9	99082.3	73989.1	8934.31	0.344	198.814	1.287
3100	2826.9	100015.5	74712.9	9264.16	0.335	199.116	1.287
3125	2851.9	100948.4	75443.1	9604.56	0.325	199.416	1.286
3150	2876.9	101874.6	76160.0	9951.58	0.317	199.711	1.286
3175	2901.9	102824.7	76900.7	10313.1	0.308	200.008	1.285
3200	2926.9	103754.9	77628.2	10687.4	0.299	200.3040	1.284

## B.12 Hydrogen Properties (English Units)

Temperature R	Temperature F	h		u		Pr	Vr	S <sub>o</sub> Btu/lbmol/R	Gamma
		Btu/lbmol	Btu/lbmol	Btu/lbmol	Btu/lbmol				
300	-159.7	2066.2	1470.5	0.195	1541.3	27.3370	1.467		
340	-119.7	2319.9	1656.3	0.290	1171.3	28.1307	1.446		
380	-79.7	2580.6	1847.0	0.418	908.85	28.8554	1.432		
420	-39.7	2846.5	2041.2	0.584	718.63	29.5205	1.421		
460	0.3	3116.2	2238.0	0.796	577.94	30.1338	1.414		
500	40.3	3388.7	2436.7	1.060	471.90	30.7019	1.409		
540	80.3	3663.4	2636.7	1.383	390.58	31.2303	1.405		
580	120.3	3939.5	2837.6	1.772	327.23	31.7236	1.403		
620	160.3	4216.8	3039.0	2.237	277.16	32.1859	1.401		
660	200.3	4494.8	3240.8	2.784	237.05	32.6204	1.399		
700	240.3	4773.4	3442.8	3.422	204.54	33.0302	1.398		
740	280.3	5052.3	3644.9	4.160	177.90	33.4177	1.398		
780	320.3	5331.5	3847.0	5.005	155.84	33.7851	1.397		
820	360.3	5610.8	4049.0	5.968	137.41	34.1344	1.397		
860	400.3	5890.3	4250.9	7.056	121.88	34.4671	1.397		
900	440.3	6169.8	4452.8	8.280	108.69	34.7848	1.397		
940	480.3	6449.4	4654.5	9.650	97.410	35.0888	1.397		
980	520.3	6729.1	4856.3	11.175	87.693	35.3802	1.397		
1020	560.3	7009.0	5058.0	12.867	79.276	35.6601	1.396		
1060	600.3	7288.9	5259.8	14.734	71.940	35.9293	1.396		
1100	640.3	7569.0	5461.6	16.790	65.514	36.1887	1.396		
1140	680.3	7849.2	5663.5	19.045	59.857	36.4389	1.395		
1180	720.3	8129.7	5865.6	21.512	54.854	36.6807	1.395		
1220	760.3	8410.5	6067.8	24.202	50.410	36.9147	1.394		
1260	800.3	8691.5	6270.3	27.128	46.447	37.1414	1.394		
1300	840.3	8972.9	6473.1	30.303	42.899	37.3612	1.393		
1340	880.3	9254.6	6676.1	33.742	39.713	37.5747	1.392		
1380	920.3	9536.7	6879.6	37.457	36.842	37.7821	1.391		
1420	960.3	9819.3	7083.4	41.465	34.246	37.9839	1.391		
1460	1000.3	10102.3	7287.7	45.779	31.892	38.1805	1.390		
1500	1040.3	10385.8	7492.4	50.417	29.752	38.3721	1.389		
1540	1080.3	10669.9	7697.6	55.392	27.802	38.5590	1.388		
1580	1120.3	10954.6	7903.4	60.724	26.019	38.7415	1.387		
1620	1160.3	11239.8	8109.8	66.427	24.388	38.9198	1.385		
1660	1200.3	11525.7	8316.7	72.521	22.890	39.0941	1.384		
1700	1240.3	11812.3	8524.3	79.026	21.512	39.2647	1.383		
1740	1280.3	12099.5	8732.6	85.961	20.242	39.4317	1.382		
1780	1320.3	12387.4	8941.5	93.341	19.070	39.5953	1.380		
1820	1360.3	12676.1	9151.2	101.193	17.985	39.7557	1.379		
1860	1400.3	12965.5	9361.5	109.533	16.981	39.9129	1.378		
1900	1440.3	13255.7	9572.7	118.388	16.049	40.0673	1.376		
1940	1480.3	13546.7	9784.6	127.776	15.183	40.2189	1.375		
1980	1520.3	13838.5	9997.4	137.723	14.377	40.3677	1.373		
2020	1560.3	14131.1	10210.8	148.254	13.625	40.5141	1.372		
2060	1600.3	14424.6	10425.3	159.396	12.924	40.6580	1.370		
2100	1640.3	14718.8	10640.4	171.165	12.269	40.7994	1.369		
2140	1680.3	15014.1	10856.5	183.598	11.656	40.9387	1.367		
2180	1720.3	15310.2	11073.4	196.724	11.082	41.0758	1.366		
2220	1760.3	15607.1	11291.2	210.553	10.544	41.2107	1.364		
2260	1800.3	15905.1	11510.0	225.140	10.038	41.3437	1.363		
2300	1840.3	16203.8	11729.5	240.496	9.564	41.4747	1.361		
2340	1880.3	16503.5	11950.1	256.667	9.117	41.6040	1.360		

2380	1920.3	16804.0	12171.5	273.665	8.697	41.7313	1.358
2420	1960.3	17105.6	12393.8	291.537	8.301	41.8569	1.357
2460	2000.3	17408.0	12617.1	310.317	7.927	41.9809	1.355
2500	2040.3	17711.4	12841.2	330.038	7.575	42.1033	1.354
2540	2080.3	18015.7	13066.4	350.727	7.242	42.2240	1.352
2580	2120.3	18321.1	13292.4	372.431	6.927	42.3433	1.351
2620	2160.3	18627.3	13519.5	395.188	6.630	42.4610	1.350
2660	2200.3	18934.6	13747.4	419.029	6.348	42.5774	1.348
2700	2240.3	19242.4	13976.2	444.012	6.081	42.6924	1.347
2740	2280.3	19551.5	14206.0	470.143	5.828	42.8059	1.345
2780	2320.3	19861.4	14436.7	497.506	5.588	42.9183	1.344
2820	2360.3	20172.2	14668.2	526.107	5.360	43.0293	1.343
2860	2400.3	20483.9	14900.6	555.982	5.144	43.1389	1.341
2900	2440.3	20796.5	15133.9	587.240	4.938	43.2476	1.340
2940	2480.3	21110.2	15368.3	619.862	4.743	43.3549	1.339
2980	2520.3	21424.6	15603.4	653.922	4.557	43.4611	1.337
3020	2560.3	21739.9	15839.4	689.489	4.380	43.5663	1.336
3060	2600.3	22056.0	16076.3	726.583	4.211	43.6704	1.335
3100	2640.3	22373.2	16314.2	765.241	4.051	43.7733	1.334
3140	2680.3	22690.9	16552.8	805.452	3.898	43.8750	1.332
3180	2720.3	23009.8	16792.3	847.464	3.752	43.9760	1.331
3220	2760.3	23329.4	17032.4	891.139	3.613	44.0758	1.330
3260	2800.3	23650.2	17273.7	936.736	3.480	44.1749	1.329
3300	2840.3	23971.1	17515.6	983.986	3.354	44.2726	1.328
3340	2880.3	24293.4	17758.7	1033.37	3.232	44.3698	1.327
3380	2920.3	24616.2	18002.0	1084.55	3.116	44.4658	1.326
3420	2960.3	24939.8	18246.3	1137.85	3.006	44.5611	1.325
3460	3000.3	25264.2	18491.2	1193.24	2.900	44.6555	1.324
3500	3040.3	25589.6	18737.5	1250.77	2.798	44.7490	1.323
3540	3080.3	25916.0	18984.8	1310.49	2.701	44.8416	1.322
3580	3120.3	26242.3	19231.6	1372.46	2.608	44.9334	1.321
3620	3160.3	26570.1	19479.9	1436.67	2.520	45.0242	1.320
3660	3200.3	26898.3	19729.1	1503.57	2.434	45.1146	1.319
3700	3240.3	27227.4	19978.7	1572.68	2.353	45.2038	1.318
3740	3280.3	27557.4	20229.3	1644.49	2.274	45.2925	1.317
3780	3320.3	27887.0	20479.4	1718.79	2.199	45.3802	1.316
3820	3360.3	28218.9	20731.8	1795.98	2.127	45.4675	1.315
3860	3400.3	28550.0	20983.5	1875.66	2.058	45.5537	1.314
3900	3440.3	28882.4	21237.2	1958.71	1.991	45.6397	1.314
3940	3480.3	29215.3	21490.6	2044.45	1.927	45.7248	1.313
3980	3520.3	29549.5	21745.3	2132.74	1.866	45.8087	1.312
4020	3560.3	29883.8	22000.2	2224.60	1.807	45.8925	1.311
4060	3600.3	30219.1	22256.8	2319.38	1.750	45.9753	1.310
4100	3640.3	30555.0	22513.2	2417.69	1.696	46.0578	1.310
4140	3680.3	30891.1	22769.1	2519.14	1.643	46.1394	1.309
4180	3720.3	31227.8	23027.1	2623.96	1.593	46.2204	1.308
4220	3760.3	31566.3	23286.1	2731.96	1.545	46.3005	1.307
4260	3800.3	31904.5	23544.9	2844.50	1.498	46.3806	1.307
4300	3840.3	32243.1	23804.0	2959.95	1.453	46.4596	1.306
4340	3880.3	32582.4	24064.6	3079.53	1.409	46.5383	1.305
4380	3920.3	32922.2	24325.6	3203.30	1.367	46.6165	1.304

4420	3960.3	33263.4	24586.7	3330.60	1.327	46.6939	1.304
4460	4000.3	33604.6	24849.2	3461.81	1.288	46.7706	1.303
4500	4040.3	33947.7	25112.1	3597.46	1.251	46.8470	1.302
4540	4080.3	34288.8	25374.5	3737.92	1.215	46.9230	1.302
4580	4120.3	34632.8	25638.3	3882.32	1.180	46.9983	1.301
4620	4160.3	34976.3	25901.6	4030.11	1.146	47.0725	1.300
4660	4200.3	35318.8	26166.8	4183.69	1.114	47.1468	1.300
4700	4240.3	35664.8	26432.6	4342.71	1.082	47.2208	1.299
4740	4280.3	36010.7	26698.3	4504.54	1.052	47.2935	1.298
4780	4320.3	36354.3	26963.2	4672.92	1.023	47.3664	1.298
4820	4360.3	36702.3	27231.0	4846.26	0.995	47.4387	1.297
4860	4400.3	37049.9	27499.9	5023.59	0.967	47.5101	1.297
4900	4440.3	37397.7	27767.5	5207.93	0.941	47.5816	1.296
4940	4480.3	37745.1	28036.2	5396.59	0.915	47.6523	1.295
4980	4520.3	38094.5	28305.4	5591.04	0.891	47.7226	1.295
5020	4560.3	38442.8	28575.0	5790.58	0.867	47.7922	1.294
5060	4600.3	38793.1	28846.5	5998.17	0.844	47.8622	1.294
5100	4640.3	39141.9	29116.6	6207.91	0.822	47.9304	1.293
5140	4680.3	39495.4	29388.5	6425.75	0.800	47.9989	1.293
5180	4720.3	39846.4	29660.7	6649.98	0.779	48.0670	1.292
5220	4760.3	40196.6	29932.2	6879.93	0.759	48.1345	1.291
5260	4800.3	40549.5	30203.6	7117.84	0.739	48.2021	1.291
5300	4840.3	40902.4	30477.7	7361.83	0.720	48.2690	1.290
5340	4880.3	41256.2	30752.8	7610.55	0.702	48.3350	1.290
5380	4920.3	41610.1	31027.9	7868.25	0.684	48.4011	1.289
5420	4960.3	41960.6	31299.7	8132.56	0.666	48.4667	1.289
5460	5000.3	42316.4	31576.7	8406.08	0.650	48.5324	1.288
5500	5040.3	42674.0	31852.7	8681.65	0.634	48.5965	1.288
5540	5080.3	43026.8	32129.6	8971.08	0.618	48.6616	1.287
5580	5120.3	43385.2	32403.6	9264.15	0.602	48.7254	1.287
5620	5160.3	43743.0	32685.5	9566.16	0.587	48.7891	1.286
5660	5200.3	44099.9	32960.9	9875.62	0.573	48.8523	1.286
5700	5240.3	44455.9	33238.0	10197.0	0.559	48.9160	1.285
5740	5280.3	44814.2	33517.6	10519.0	0.546	48.9777	1.285
5780	5320.3	45171.6	33796.3	10854.5	0.532	49.0400	1.284

# **Appendix C: Thermodynamic Properties for Water**

## **C.1 Saturation Temperature vs. Pressure (SI Units)**

Press (kPa)	Temp (K)	Specific Volume (m <sup>3</sup> /kg)			Internal Energy (kJ/kg)			Enthalpy (kJ/kg)			Entropy (kJ/kg/K)		
		v <sub>f</sub>	v <sub>g</sub>	u <sub>f</sub>	u <sub>fg</sub>	u <sub>g</sub>	h <sub>f</sub>	h <sub>fg</sub>	h <sub>g</sub>	s <sub>f</sub>	s <sub>fg</sub>	s <sub>g</sub>	
0.61	273.2	0.001000	205.9975	0.00	2374.9	2374.9	0.00	2500.9	2500.9	0.00000	9.15549	9.15549	
0.80	276.9	0.001000	159.6461	15.81	2364.3	2380.1	15.81	2492.0	2507.8	0.05748	8.99925	9.05672	
1.00	280.1	0.001000	129.1833	29.30	2355.2	2384.5	29.30	2484.4	2513.7	0.10591	8.86902	8.97493	
1.20	282.8	0.001000	108.6740	40.57	2347.6	2388.2	40.57	2478.0	2518.6	0.14595	8.76236	8.90831	
1.40	285.1	0.001001	93.9033	50.28	2341.1	2391.4	50.28	2472.5	2522.8	0.18016	8.67199	8.85214	
1.60	287.2	0.001001	82.7463	58.83	2335.3	2394.2	58.84	2467.7	2526.6	0.21005	8.59355	8.80360	
1.80	289.0	0.001001	74.0143	66.49	2330.2	2396.7	66.49	2463.4	2529.9	0.23663	8.52424	8.76087	
2.00	290.6	0.001001	66.9896	73.43	2325.5	2398.9	73.43	2459.5	2532.9	0.26058	8.46214	8.72272	
2.50	294.2	0.001002	54.2421	88.43	2315.4	2403.8	88.43	2451.0	2539.4	0.313030	8.64215		
3.00	297.2	0.001003	45.6550	100.99	2306.9	2407.9	100.99	2443.9	2544.9	0.35433	8.22223	8.57656	
3.50	299.8	0.001003	39.4678	111.83	2299.6	2411.4	111.84	2437.7	2549.6	0.39066	8.13060	8.52126	
4.00	302.1	0.001004	34.7925	121.40	2293.1	2414.5	121.40	2432.3	2553.7	0.42245	8.05104	8.47349	
5.00	306.0	0.001005	28.1863	137.76	2282.1	2419.8	137.76	2423.0	2560.8	0.47625	7.91766	8.39391	
6.00	309.3	0.001006	23.7342	151.49	2272.8	2424.3	151.49	2415.2	2566.7	0.52087	7.80827	8.32915	
7.00	312.2	0.001007	20.5252	163.36	2264.7	2428.1	163.37	2408.4	2571.8	0.55908	7.71549	8.27456	
8.00	314.7	0.001008	18.0994	173.84	2257.6	2431.4	173.85	2402.4	2576.2	0.59253	7.63488	8.22741	
9.00	316.9	0.001009	16.1997	183.20	2251.2	2434.5	183.26	2397.0	2580.3	0.62233	7.56359	8.18592	
10.00	319.0	0.001010	14.6706	191.80	2245.4	2437.2	191.81	2392.1	2583.9	0.64922	7.49968	8.14889	
15.00	327.1	0.001014	10.0204	225.92	2222.1	2448.0	225.94	2372.4	2598.3	0.75484	7.25228	8.00712	
20.00	333.2	0.001017	7.6482	251.38	2204.6	2456.0	251.40	2357.5	2608.9	0.83195	7.07528	7.90724	
25.00	338.1	0.001020	6.2034	271.90	2190.5	2462.4	271.93	2345.5	2617.4	0.89309	6.93708	7.83016	
30.00	342.2	0.001022	5.2286	289.20	2178.5	2467.7	289.23	2335.3	2624.6	0.94394	6.82351	7.76745	
40.00	349.0	0.001026	3.9931	317.53	2158.8	2476.3	317.57	2318.5	2636.1	1.02590	6.64307	7.66897	
50.00	354.5	0.001030	3.2401	340.42	2142.8	2483.2	340.48	2304.7	2645.2	1.09101	6.50196	7.59296	
60.00	359.1	0.001033	2.7318	359.77	2129.2	2488.9	359.84	2293.0	2652.9	1.14524	6.38586	7.53110	
70.00	363.1	0.001036	2.3649	376.61	2117.3	2493.9	376.68	2282.7	2659.4	1.19186	6.28709	7.47895	
80.00	366.6	0.001038	2.0872	391.56	2106.6	2498.2	391.64	2273.5	2665.2	1.23283	6.20106	7.43389	
90.00	369.8	0.001041	1.8695	405.03	2097.0	2502.1	405.13	2265.2	2670.3	1.26944	6.12479	7.39423	
101.33	373.1	0.001043	1.6733	418.88	2087.1	2506.0	418.99	2256.5	2675.5	1.30672	6.04766	7.35439	
120.00	377.9	0.001047	1.4284	439.17	2072.5	2511.6	439.30	2243.8	2683.1	1.36075	5.93688	7.29763	
140.00	382.4	0.001051	1.2366	458.22	2058.6	2516.9	458.37	2231.6	2690.0	1.41085	5.83517	7.24602	
160.00	386.4	0.001054	1.0914	475.17	2046.2	2521.4	475.34	2220.7	2696.0	1.45494	5.74643	7.20137	
180.00	390.1	0.001058	0.9775	490.48	2035.0	2525.5	490.67	2210.7	2701.4	1.49437	5.66765	7.16203	
200.00	393.4	0.001061	0.8857	504.47	2024.6	2529.1	504.68	2201.6	2706.2	1.53010	5.59676	7.12686	

## Appendix C: Thermodynamic Properties for Water

Press (kPa)	Temp (K)	Specific Volume (m <sup>-3</sup> /kg)		Internal Energy (kJ/kg)			Enthalpy (kJ/kg)			Entropy (kJ/kg/K)		
		vf	vg	uf	ufg	ug	hf	hfg	hg	sf	sfg	sg
300.00	406.7	0.001073	0.6058	561.13	1982.0	2543.2	561.46	2163.4	2724.9	1.67176	5.31980	6.89517
400.00	416.8	0.001084	0.4624	604.29	1948.8	2553.1	604.72	2133.3	2738.1	1.77660	5.11882	6.89542
500.00	425.0	0.001093	0.3748	639.64	1921.1	2560.7	640.19	2107.9	2748.1	1.86060	4.95998	6.82058
600.00	432.0	0.001101	0.3156	669.84	1897.0	2566.8	670.50	2085.6	2756.1	1.93110	4.82807	6.75917
700.00	438.1	0.001108	0.2728	696.37	1875.4	2571.8	697.14	2065.6	2762.7	1.99208	4.71490	6.70698
800.00	443.6	0.001115	0.2403	720.13	1855.9	2576.0	721.02	2047.3	2768.3	2.04599	4.61555	6.66154
900.00	448.5	0.001121	0.2149	741.72	1837.9	2579.7	742.72	2030.3	2773.0	2.09440	4.52683	6.62124
1000.00	453.0	0.001127	0.1943	761.56	1821.2	2582.8	762.68	2014.4	2777.1	2.13843	4.44655	6.58498
1200.00	461.1	0.001139	0.1632	797.13	1790.7	2587.9	798.50	1985.3	2783.8	2.21630	4.30539	6.52169
1400.00	468.2	0.001149	0.1408	828.52	1763.3	2591.8	830.13	1958.8	2788.9	2.28388	4.18364	6.46752
1600.00	474.5	0.001159	0.1237	856.76	1738.2	2594.9	858.61	1934.3	2792.9	2.34381	4.07621	6.42002
1800.00	480.3	0.001168	0.1104	882.51	1714.8	2597.3	884.61	1911.4	2796.0	2.39779	3.97980	6.37760
2000.00	485.5	0.001177	0.0996	906.27	1693.0	2599.2	908.62	1889.8	2798.4	2.44702	3.89214	6.33916
2500.00	497.1	0.001197	0.0799	958.99	1643.2	2602.2	961.98	1840.1	2802.0	2.55443	3.70155	6.25597
3000.00	507.0	0.001217	0.0667	1004.72	1598.6	2603.3	1008.37	1794.9	2803.3	2.64562	3.54017	6.18579
4000.00	523.5	0.001253	0.0498	1082.42	1519.4	2601.8	1087.43	1713.5	2800.9	2.79665	3.27306	6.06971
5000.00	537.1	0.001286	0.0394	1148.07	1448.9	2597.0	1154.50	1639.7	2794.2	2.92075	3.05296	5.97370
6000.00	548.7	0.001319	0.0324	1205.82	1384.1	2589.9	1213.73	1570.8	2784.6	3.02744	2.86263	5.89007
7000.00	559.0	0.001352	0.0274	1257.97	1322.9	2580.9	1267.44	1505.1	2772.6	3.12199	2.69264	5.81463
8000.00	568.2	0.001385	0.0238	1306.00	1264.4	2570.4	1317.08	1441.5	2758.6	3.20765	2.53720	5.74485
9000.00	576.5	0.001418	0.0205	1350.89	1207.6	2558.4	1363.65	1379.2	2742.9	3.28657	2.39244	5.67901
10000.00	584.1	0.001453	0.0180	1393.34	1151.8	2545.1	1407.87	1317.6	2725.5	3.36029	2.25560	5.61589
11000.00	591.2	0.001489	0.0160	1433.90	1096.6	2530.5	1450.28	1256.1	2706.4	3.42995	2.12458	5.55453
12000.00	597.8	0.001526	0.0143	1473.01	1041.3	2514.4	1491.33	1194.3	2685.6	3.49646	1.99766	5.49412
13000.00	604.0	0.001566	0.0128	1511.04	985.6	2496.7	1531.40	1131.5	2662.9	3.56058	1.87331	5.43388
14000.00	609.8	0.001610	0.0115	1548.34	928.9	2477.3	1570.88	1067.2	2638.1	3.62300	1.75005	5.37305
15000.00	615.3	0.001657	0.0103	1585.30	870.5	2455.8	1610.15	1000.7	2610.9	3.68445	1.62636	5.31080
16000.00	620.5	0.001710	0.0093	1622.32	809.6	2431.9	1649.67	931.1	2580.8	3.74568	1.50059	5.24627
17000.00	625.4	0.001769	0.0084	1659.98	745.2	2405.1	1690.05	857.4	2547.4	3.80770	1.37081	5.17850
18000.00	630.1	0.001840	0.0075	1698.93	675.6	2374.6	1732.04	777.5	2509.5	3.87170	1.23384	5.10554
19000.00	634.6	0.001925	0.0036	1740.32	279.6	2019.9	1776.91	310.7	2087.6	3.93967	0.48827	4.42795
20000.00	638.9	0.002039	0.0034	1786.35	235.7	2022.1	1827.12	263.1	2090.2	4.01541	0.41112	4.42653
21000.00	643.0	0.002212	0.0033	1842.97	180.8	2023.8	1889.43	203.0	2092.4	4.10930	0.31555	4.42485
22064.00	647.1	0.003209	0.0032	2034.47	0.0	2034.5	2105.27	0.0	2105.3	4.43941	0.00000	4.43941

Temp (K)	Press (kPa)	Specific Volume (m <sup>-3</sup> /kg)		Internal Energy (kJ/kg)			Enthalpy (kJ/kg)			Entropy (kJ/kg/K)		
		vf	vg	uf	ufg	ug	hf	hfg	hg	sf	sfg	sg
273.1	0.61	0.001000	206.1397	0.00	2374.9	2374.9	0.00	2500.9	2500.9	0.00000	9.15591	9.15591
275.0	0.70	0.001000	181.6044	7.76	2369.7	2377.4	7.76	2496.5	2504.3	0.02831	9.07831	9.10662
280.0	0.99	0.001000	130.1941	28.79	2355.5	2384.3	28.80	2484.7	2513.5	0.10412	8.78382	8.97794
285.0	1.39	0.001001	94.6073	49.78	2341.4	2391.2	49.78	2472.8	2522.6	0.17840	8.67661	8.85501
290.0	1.92	0.001001	69.6305	70.73	2327.3	2398.1	70.73	2461.0	2531.7	0.25128	8.48623	8.73751
295.0	2.62	0.001002	51.8694	91.66	2313.2	2404.9	91.66	2449.2	2540.8	0.32283	8.30229	8.62511
300.0	3.54	0.001003	39.0821	112.57	2299.1	2411.7	112.57	2437.3	2549.9	0.39312	8.12441	8.51754
305.0	4.72	0.001005	29.7669	133.47	2285.0	2418.4	133.48	2425.4	2558.9	0.46222	7.95228	8.41451
310.0	6.23	0.001007	22.9051	154.37	2270.8	2425.2	154.38	2413.5	2567.9	0.53018	7.78559	8.31577
315.0	8.14	0.001009	17.7969	175.26	2256.6	2431.9	175.26	2401.7	2516.8	0.59704	7.62405	8.22110
320.0	10.55	0.001011	13.9557	196.16	2242.4	2438.6	196.17	2389.6	2585.7	0.66285	7.46741	8.13026
325.0	13.53	0.001013	11.0396	217.06	2228.1	2445.2	217.07	2377.5	2594.6	0.72765	7.31540	8.04305
330.0	17.21	0.001015	8.8056	237.96	2213.8	2451.8	237.98	2365.4	2603.3	0.79148	7.16779	7.95928
335.0	21.72	0.001018	7.0792	258.87	2199.4	2458.3	258.89	2353.2	2612.1	0.85438	7.02436	7.87875
340.0	27.19	0.001021	5.7341	279.80	2185.0	2464.8	279.82	2340.9	2620.7	0.91638	6.88491	7.80128
345.0	33.78	0.001024	4.6778	300.73	2170.5	2471.2	300.77	2238.2	2629.3	0.97751	6.74921	7.72673
350.0	41.68	0.001027	3.8420	321.69	2155.9	2477.6	321.73	2316.0	2637.7	1.03781	6.61710	7.65492
355.0	51.08	0.001030	3.1760	342.66	2141.2	2483.9	342.71	2303.4	2646.1	1.09731	6.48839	7.58570
360.0	62.19	0.001034	2.6415	363.66	2126.4	2490.1	363.72	2290.7	2654.4	1.15604	6.36289	7.51894
365.0	75.26	0.001037	2.2099	384.68	2111.5	2496.2	384.75	2277.8	2662.5	1.21403	6.24046	7.45449
370.0	90.54	0.001041	1.8591	405.72	2096.5	2502.3	405.81	2264.8	2670.6	1.27129	6.12094	7.39223
375.0	108.30	0.001045	1.5723	426.79	2081.4	2508.2	426.91	2251.8	2678.5	1.32787	6.00417	7.33204
380.0	128.85	0.001049	1.3365	447.90	2066.1	2514.0	448.03	2238.2	2686.3	1.38378	5.89001	7.27379
385.0	152.52	0.001053	1.1415	469.04	2050.7	2519.8	469.20	2224.7	2693.9	1.43904	5.77834	7.21738
390.0	179.64	0.001058	0.9794	490.21	2035.2	2525.4	490.40	2210.5	2701.3	1.49369	5.66901	7.16270
395.0	210.59	0.001062	0.8440	511.43	2019.5	2530.9	511.65	2197.0	2708.6	1.54775	5.56190	7.10964
400.0	245.75	0.001067	0.7303	532.68	2003.5	2536.2	532.95	2182.8	2715.7	1.60122	5.45690	7.05812
405.0	285.55	0.001072	0.6345	553.99	1987.5	2541.4	554.29	2168.3	2722.6	1.65415	5.35389	7.00804
410.0	330.42	0.001077	0.5533	575.33	1971.2	2546.5	575.69	2153.5	2729.3	1.70654	5.25277	6.95931
415.0	380.82	0.001082	0.4842	596.73	1954.7	2551.4	597.15	2138.7	2735.8	1.75843	5.15343	6.91866
420.0	437.24	0.001087	0.4253	618.19	1938.0	2556.1	618.66	2123.4	2742.1	1.80982	5.05578	6.86560
425.0	500.18	0.001093	0.3747	639.70	1921.0	2560.7	640.24	2107.9	2748.1	1.86074	4.95972	6.82046
430.0	570.18	0.001098	0.3311	661.27	1903.8	2565.1	661.90	2092.0	2753.9	1.91121	4.86516	6.77637
435.0	647.77	0.001104	0.2935	682.91	1886.4	2569.3	683.62	2075.8	2759.4	1.96124	4.77202	6.73327
440.0	733.55	0.001110	0.2609	704.61	1868.7	2573.3	705.43	2059.3	2764.7	2.01086	4.68022	6.69108
445.0	828.10	0.001117	0.2326	726.39	1850.7	2577.1	727.32	2042.4	2769.7	2.06009	4.58966	6.64975

## C.2 Saturation Pressure vs. Temperature (SI Units)

Temp (K)	Press (kPa)	Specific Volume (m <sup>3</sup> /kg)	Internal Energy			Enthalpy			Entropy		
			vf	vg	uf	ufg	ug	hf	hfg	hg	sf
455.0	1046.02	0.001130	0.1862	770.18	1813.9	2584.1	771.37	2074.4	2778.8	2.15744	4.41199
460.0	1170.68	0.001137	0.1672	792.21	1795.0	2587.2	793.54	1989.4	2782.9	2.20560	4.32472
465.0	1306.72	0.001144	0.1504	814.33	1775.8	2590.1	815.82	1970.8	2786.7	2.25345	4.23839
470.0	1454.84	0.001152	0.1356	836.55	1756.2	2592.7	838.22	1951.5	2790.1	2.30099	4.15292
475.0	1615.75	0.001159	0.1226	858.87	1736.3	2595.1	860.74	1932.4	2793.2	2.34826	4.06826
480.0	1790.19	0.001167	0.1110	881.30	1715.9	2597.2	883.39	1912.5	2795.9	2.39527	3.98431
485.0	1978.94	0.001176	0.1006	903.85	1695.2	2599.0	906.18	1892.0	2798.2	2.44204	3.90101
490.0	2182.77	0.001185	0.0914	926.53	1674.0	2600.6	929.11	1871.0	2800.1	2.48859	3.81829
495.0	2402.48	0.001194	0.0832	949.34	1652.4	2601.8	952.20	1849.3	2801.5	2.53495	3.73606
500.0	2638.90	0.001203	0.0758	972.29	1630.3	2602.6	975.46	1827.1	2802.6	2.58113	3.65426
505.0	2892.85	0.001213	0.0691	995.40	1607.8	2603.2	998.90	1804.3	2803.2	2.62717	3.57281
510.0	3165.22	0.001223	0.0632	1018.66	1584.7	2603.3	1022.53	1780.7	2803.3	2.67307	3.49163
515.0	3456.86	0.001233	0.0578	1042.10	1561.0	2603.1	1046.37	1756.5	2802.8	2.71888	3.41064
520.0	3768.70	0.001245	0.0529	1065.73	1536.8	2602.5	1070.42	1731.5	2801.9	2.76461	3.32977
525.0	4101.65	0.001256	0.0485	1089.55	1511.9	2601.4	1094.70	1705.7	2800.4	2.81029	3.24892
530.0	4456.65	0.001268	0.0445	1113.58	1486.4	2599.9	1119.23	1679.1	2798.3	2.85595	3.16802
535.0	4834.69	0.001281	0.0409	1137.84	1460.1	2598.0	1144.04	1651.5	2795.6	2.90162	3.08696
540.0	5236.75	0.001294	0.0376	1162.35	1433.1	2595.5	1169.13	1623.1	2792.2	2.94734	3.00564
545.0	5663.85	0.001308	0.0345	1187.12	1405.4	2592.5	1194.53	1593.6	2788.1	2.99314	2.92397
550.0	6117.05	0.001323	0.0318	1212.18	1376.7	2588.9	1220.27	1563.0	2783.3	3.03906	2.84182
555.0	6597.43	0.001339	0.0292	1237.54	1347.2	2584.7	1246.37	1531.3	2777.6	3.08515	2.75905
560.0	7106.12	0.001355	0.0269	1263.25	1316.6	2579.9	1272.88	1498.3	2771.2	3.13146	2.67553
565.0	7644.26	0.001373	0.0248	1289.32	1285.0	2574.3	1299.82	1464.0	2763.8	3.17805	2.59110
570.0	8213.06	0.001392	0.0228	1315.80	1252.2	2568.0	1327.23	1428.2	2755.4	3.22497	2.50557
575.0	8813.76	0.001412	0.0210	1342.73	1218.0	2560.8	1355.17	1390.8	2745.9	3.27231	2.41873
580.0	9447.69	0.001433	0.0193	1370.16	1182.5	2552.7	1383.70	1351.6	2735.3	3.32014	2.33033
585.0	10116.21	0.001457	0.0178	1398.14	1145.4	2543.5	1412.88	1310.5	2723.3	3.36858	2.24011
590.0	10820.77	0.001482	0.0163	1426.75	1106.4	2533.2	1442.79	1267.1	2709.9	3.41772	2.14771
595.0	11562.92	0.001510	0.0150	1456.07	1065.5	2521.6	1473.53	1221.4	2694.9	3.46773	2.05273
600.0	12344.30	0.001540	0.0137	1486.21	1022.2	2508.5	1505.22	1172.8	2678.0	3.51877	1.95463
605.0	13166.69	0.001573	0.0126	1517.30	976.3	2493.6	1538.01	1120.9	2658.9	3.57108	1.85272
610.0	14032.02	0.001611	0.0114	1549.53	927.1	2476.6	1572.14	1065.1	2637.3	3.62498	1.74610
615.0	14942.40	0.001654	0.0104	1583.17	873.9	2457.1	1607.89	1004.6	2612.5	3.68092	1.63352
620.0	15900.20	0.001704	0.0094	1618.61	815.8	2434.4	1645.70	938.2	2583.9	3.73955	1.51329
630.0	17969.08	0.001837	0.0075	1697.70	677.9	2375.6	1730.71	780.1	2510.8	3.86968	1.23822
640.0	20265.91	0.002076	0.0034	1799.92	222.7	2022.7	1842.00	248.9	2909.9	4.03783	0.38844
647.1	22063.97	0.003209	0.0032	2034.52	0.0	2034.5	2105.33	0.0	2105.3	4.43950	0.00000

### C.3 Superheated Steam Table (SI Units)

Press = 0.010 MPa	Tsat= 319.0 K
T(K) = 325.	350. 400. 450. 500. 550. 600. 650. 700. 800. 900. 1000.
v-m3/kg	14.9541 16.1208 18.4417 20.7557 23.0696 25.3768 27.6860 29.9947 32.3032 36.9196 41.5356 46.1514
u-kj/kg	2446.0 2482.1 2554.3 2627.2 2701.3 2776.8 2833.8 2932.4 3012.6 3177.9 3350.3 3529.6
h-kj/kg	2595.6 2643.3 2738.7 2834.7 2932.0 3030.6 3130.7 3232.3 3335.6 3547.1 3765.6 3991.2
s-kj/kg/K	8.18513 8.32676 8.58137 8.80763 9.01251 9.20046 9.37463 9.53734 9.69038 9.9727710.2300210.46758
Press = 0.015 MPa	Tsat= 327.1 K
T(K) = 350.	400. 450. 500. 550. 600. 650. 700. 800. 900. 1000. 1100.
v-m3/kg	10.7362 12.2880 13.8328 15.3748 16.9155 18.4555 19.9950 21.5343 24.6123 27.6899 30.7672 33.8444
u-kj/kg	2481.4 2553.9 2627.0 2701.2 2776.7 2832.3 2932.3 3012.5 3177.9 3350.2 3529.6 3716.1
h-kj/kg	2642.5 2738.2 2834.5 2931.8 3030.4 3130.6 3232.2 3335.5 3547.1 3765.6 3991.1 4223.8
s-kj/kg/K	8.13764 8.39336 8.62004 8.82509 9.01314 9.18737 9.35011 9.50318 9.7855910.0428610.2804310.50212
Press = 0.025 MPa	Tsat= 338.1 K
T(K) = 350.	400. 450. 500. 550. 600. 650. 700. 800. 900. 1000. 1100.
v-m3/kg	6.4284 7.3650 8.2944 9.2211 10.1464 11.0710 11.9952 12.9191 14.7664 16.6132 18.4599 20.3063
u-kj/kg	2480.0 2553.2 2626.6 2700.9 2776.5 2835.6 2932.2 3012.4 3177.8 3350.2 3529.6 3716.1
h-kj/kg	2640.7 2737.3 2833.9 2931.4 3030.2 3130.4 3232.1 3335.4 3547.0 3765.5 3991.1 4223.7
s-kj/kg/K	7.89785 8.15585 8.38335 8.58878 8.77701 8.95134 9.11416 9.26727 9.54974 9.8070410.0446310.26633
Press = 0.040 MPa	Tsat= 349.0 K
T(K) = 350.	400. 450. 500. 550. 600. 650. 700. 800. 900. 1000. 1100.
v-m3/kg	4.0050 4.5957 5.1791 5.7596 6.3388 6.9173 7.4953 8.0731 9.2281 10.3826 11.5370 12.6912
u-kj/kg	2477.8 2552.1 2625.9 2700.5 2776.2 2835.3 2932.0 3012.3 3177.7 3350.1 3529.5 3716.0
h-kj/kg	2638.0 2736.0 2833.1 2930.8 3029.8 3130.0 3231.8 3335.2 3546.9 3765.4 3991.0 4223.7
s-kj/kg/K	7.67465 7.93627 8.16504 8.37102 8.55954 8.73403 8.89695 9.05013 9.33269 9.59003 9.8276410.04936
Press = 0.060 MPa	Tsat= 359.1 K
T(K) = 400.	450. 500. 550. 600. 650. 700. 800. 900. 1000. 1100. 1200.
v-m3/kg	3.05719 3.44835 3.83661 4.22350 4.60967 4.99541 5.38086 6.15124 6.92120 7.69092 8.46050 9.22998
u-kj/kg	2550.7 2625.1 2699.9 2775.8 2853.0 2931.8 3012.0 3177.6 3350.0 3529.4 3716.0 3909.4
h-kj/kg	2734.1 2832.0 2930.1 3029.2 3129.6 3231.5 3334.9 3546.7 3765.3 3990.9 4223.6 4463.2
s-kj/kg/K	7.74553 7.97603 8.18276 8.37166 8.54637 8.70943 8.86270 9.14537 9.40277 9.64043 9.8621710.07059
Press = 0.101 MPa	Tsat= 373.1 K
T(K) = 400.	450. 500. 550. 600. 650. 700. 800. 900. 1000. 1100. 1200.
v-m3/kg	1.80206 2.03654 2.26798 2.49803 2.72735 2.95623 3.18482 3.64148 4.09772 4.55372 5.00959 5.46535
u-kj/kg	2547.7 2623.3 2698.7 2774.9 2852.4 2931.2 3011.6 3177.3 3349.8 3529.3 3715.8 3909.3
h-kj/kg	2730.3 2829.7 2928.5 3028.1 3128.7 3230.8 3334.3 3546.3 3765.0 3990.7 4223.4 4463.0
s-kj/kg/K	7.49608 7.73027 7.93859 8.12828 8.30345 8.46679 8.62025 8.90315 9.16068 9.39842 9.62020 9.82866
Press = 0.200 MPa	Tsat= 393.4 K
T(K) = 400.	450. 500. 550. 600. 650. 700. 800. 900. 1000. 1100. 1200.
v-m3/kg	0.90251 1.02507 1.14427 1.26200 1.37897 1.49549 1.61172 1.84366 2.07517 2.30645 2.53758 2.76862
u-kj/kg	2540.0 2619.0 2695.9 2772.9 2850.8 2930.0 3010.6 3176.6 3349.2 3528.8 3715.5 3909.0
h-kj/kg	2720.5 2824.0 2924.8 3025.3 3126.6 3229.1 3329.2 3545.3 3764.3 3990.1 4223.0 4462.7
s-kj/kg/K	7.16292 7.40676 7.61907 7.81074 7.98701 8.15104 8.30496 8.58842 8.84625 9.08417 9.30606 9.51459
Press = 0.300 MPa	Tsat= 406.7 K
T(K) = 450.	500. 550. 600. 650. 700. 800. 900. 1000. 1100. 1200. 1300.
v-m3/kg	0.67872 0.75960 0.83891 0.91743 0.99550 1.07327 1.22829 1.38288 1.53724 1.69145 1.84557 1.99962
u-kj/kg	2614.4 2693.0 2770.8 2849.2 2928.7 3009.6 3175.8 3348.7 3528.4 3715.1 3908.7 4108.8
h-kj/kg	2818.1 2920.8 3022.5 3124.5 3227.4 3331.5 3544.3 3763.5 3989.6 4222.6 4462.4 4708.7
s-kj/kg/K	7.20939 7.42604 7.61979 7.79722 7.96195 8.11634 8.40036 8.65851 8.89661 9.11862 9.32722 9.52438
Press = 0.400 MPa	Tsat= 416.8 K
T(K) = 450.	500. 550. 600. 650. 700. 800. 900. 1000. 1100. 1200. 1300.
v-m3/kg	0.50545 0.56722 0.62735 0.68666 0.74550 0.80405 0.92061 1.03674 1.15263 1.26838 1.38404 1.49963
u-kj/kg	2609.7 2690.0 2768.7 2847.6 2927.4 3008.4 3175.1 3348.1 3528.0 3714.8 3908.4 4108.6
h-kj/kg	2811.9 2916.9 3019.6 3123.3 3225.6 3330.1 3543.3 3762.8 3989.0 4222.2 4462.4 4708.5
s-kj/kg/K	7.06594 7.28723 7.48316 7.66177 7.82722 7.98208 8.26667 8.52513 8.76341 8.98553 9.19421 9.39142
Press = 0.500 MPa	Tsat= 425.0 K
T(K) = 450.	500. 550. 600. 650. 700. 800. 900. 1000. 1100. 1200. 1300.
v-m3/kg	0.40140 0.45177 0.50040 0.54819 0.59550 0.64251 0.73599 0.82905 0.92187 1.01455 1.10712 1.19964
u-kj/kg	2604.8 2686.9 2766.6 2846.0 2926.2 3007.5 3174.3 3347.6 3527.6 3714.5 3908.1 4108.4
h-kj/kg	2805.5 2912.8 3016.8 3120.1 3223.9 3328.7 3542.3 3762.1 3988.5 4221.7 4461.7 4708.2
s-kj/kg/K	6.95182 7.17807 7.37626 7.55608 7.72226 7.87760 8.16276 8.42153 8.66000 8.88223 9.09098 9.28825
Press = 0.600 MPa	Tsat= 432.0 K
T(K) = 450.	500. 550. 600. 650. 700. 800. 900. 1000. 1100. 1200. 1300.
v-m3/kg	0.33195 0.37477 0.41576 0.45587 0.49549 0.53482 0.61292 0.69059 0.76803 0.84532 0.92251 0.99965
u-kj/kg	2599.7 2683.8 2764.4 2844.4 2924.9 3006.4 3173.6 3347.0 3527.1 3714.1 3907.8 4108.1
h-kj/kg	2798.8 2908.7 3013.9 3117.9 3222.2 3327.3 3541.4 3761.4 3988.0 4221.3 4461.3 4707.9
s-kj/kg/K	6.85603 7.08760 7.28815 7.46921 7.63613 7.79195 8.07769 8.33677 8.57542 8.79777 9.00659 9.20392
Press = 0.700 MPa	Tsat= 438.1 K
T(K) = 450.	500. 550. 600. 650. 700. 800. 900. 1000. 1100. 1200. 1300.
v-m3/kg	0.28228 0.31976 0.35529 0.38992 0.42406 0.45789 0.52501 0.59170 0.65814 0.72444 0.79065 0.85679
u-kj/kg	2594.3 2680.6 2762.2 2842.7 2923.6 3005.4 3172.9 3346.5 3526.7 3713.8 3907.5 4107.9
h-kj/kg	2791.9 2904.4 3010.9 3115.7 3220.4 3325.9 3540.4 3760.7 3987.4 4220.9 4461.0 4707.6
s-kj/kg/K	6.77268 7.00998 7.21299 7.39533 7.56300 7.71931 8.00562 8.26502 8.50385 8.72631 8.93521 9.13258

Press = 0.800 MPa Tsat= 443.6 K
T(K) = 450. 500. 550. 600. 650. 700. 800. 900. 1000. 1100. 1200. 1300.
v-m3/kg 0.24496 0.27847 0.30993 0.34046 0.37049 0.40020 0.45908 0.51752 0.57572 0.63379 0.69175 0.74965
u-kj/kg 2588.7 2677.4 2760.0 2841.1 2922.3 3004.3 3172.1 3345.9 3526.3 3713.4 3907.3 4107.6
h-kj/kg 2784.7 2900.1 3007.9 3113.5 3218.7 3324.5 3539.4 3759.9 3986.9 4220.4 4460.7 4707.4
s-kj/kg/K 6.69816 6.94173 7.14729 7.33094 7.49938 7.65617 7.94306 8.20278 8.44180 8.66437 8.87334 9.07077
Press = 0.900 MPa Tsat= 448.5 K
T(K) = 450. 500. 550. 600. 650. 700. 800. 900. 1000. 1100. 1200. 1300.
v-m3/kg 0.21586 0.24634 0.27465 0.30199 0.32881 0.35533 0.40779 0.45983 0.51162 0.56327 0.61483 0.66632
u-kj/kg 2582.7 2674.0 2757.8 2839.4 2921.0 3003.3 3171.4 3345.4 3525.9 3713.1 3907.4 4107.4
h-kj/kg 2777.0 2894.9 3004.3 3111.2 3216.9 3323.1 3538.4 3759.2 3986.3 4220.0 4460.3 4707.1
s-kj/kg/K 6.63002 6.88060 7.08881 7.27380 7.44301 7.60031 7.88778 8.14781 8.38701 8.60970 8.81874 9.01622
Press = 1.000 MPa Tsat= 453.0 K
T(K) = 500. 550. 600. 650. 700. 800. 900. 1000. 1100. 1200. 1300. 1400.
v-m3/kg 0.22063 0.24641 0.27121 0.29547 0.31943 0.36677 0.41368 0.46034 0.50687 0.55329 0.59966 0.64598
u-kj/kg 2670.6 2755.5 2837.8 2919.7 3002.2 3170.6 3344.8 3525.4 3712.7 3906.7 4107.1 4313.9
h-kj/kg 2891.3 3001.9 3109.0 3215.2 3321.6 3537.4 3758.5 3985.8 4219.6 4460.0 4706.8 4959.9
s-kj/kg/K 6.82505 7.03601 7.22237 7.39237 7.55017 7.83828 8.09857 8.33796 8.56076 8.76988 8.96741 9.15493
Press = 1.200 MPa Tsat= 461.1 K
T(K) = 500. 550. 600. 650. 700. 800. 900. 1000. 1100. 1200. 1300. 1400.
v-m3/kg 0.18201 0.20405 0.22503 0.24546 0.26557 0.30523 0.34445 0.38342 0.42225 0.46099 0.49966 0.53829
u-kj/kg 2663.7 2750.9 2834.4 2917.1 3000.1 3169.2 3343.7 3524.6 3712.0 3906.1 4106.7 4313.5
h-kj/kg 2882.1 2995.7 3104.4 3211.6 3318.8 3535.4 3757.1 3984.7 4218.7 4459.3 4706.2 4959.4
s-kj/kg/K 6.72656 6.94336 7.13256 7.30417 7.46298 7.75221 8.01319 8.25296 8.47598 8.68525 8.88289 9.07048
Press = 1.400 MPa Tsat= 468.2 K
T(K) = 500. 550. 600. 650. 700. 800. 900. 1000. 1100. 1200. 1300. 1400.
v-m3/kg 0.15437 0.17376 0.19203 0.20974 0.22711 0.26127 0.29500 0.32848 0.36181 0.39506 0.42823 0.46137
u-kj/kg 2656.4 2746.2 2831.0 2914.4 2998.0 3167.3 3342.6 3523.7 3711.3 3905.5 4106.2 4313.1
h-kj/kg 2872.5 2989.4 3099.8 3208.1 3315.9 3533.4 3755.6 3983.6 4217.9 4458.6 4705.7 4959.0
s-kj/kg/K 6.64047 6.86348 7.05567 7.22894 7.38878 7.67920 7.94082 8.18096 8.40421 8.61362 8.81137 8.99904
Press = 1.600 MPa Tsat= 474.5 K
T(K) = 500. 550. 600. 650. 700. 800. 900. 1000. 1100. 1200. 1300. 1400.
v-m3/kg 0.13360 0.15103 0.16728 0.18294 0.19825 0.22830 0.25791 0.28727 0.31649 0.34561 0.37466 0.40368
u-kj/kg 2648.8 2741.3 2827.5 2911.8 2995.8 3166.2 3341.5 3522.9 3710.7 3905.0 4105.7 4312.6
h-kj/kg 2862.6 2983.0 3095.2 3204.5 3313.0 3531.5 3754.2 3982.5 4217.0 4457.9 4705.1 4958.5
s-kj/kg/K 6.56317 6.79289 6.98820 7.16319 7.32408 7.61571 7.87796 8.11847 8.34195 8.55151 8.74936 8.93711
Press = 1.800 MPa Tsat= 480.3 K
T(K) = 500. 550. 600. 650. 700. 800. 900. 1000. 1100. 1200. 1300. 1400.
v-m3/kg 0.11740 0.13334 0.14802 0.16209 0.17581 0.20266 0.22906 0.25522 0.28123 0.30715 0.33300 0.35881
u-kj/kg 2640.9 2736.4 2824.0 2909.1 2993.7 3164.7 3340.4 3522.0 3710.0 3904.4 4105.2 4312.2
h-kj/kg 2852.2 2976.4 3090.5 3200.9 3310.1 3529.5 3752.7 3981.4 4216.2 4457.2 4704.6 4958.1
s-kj/kg/K 6.49238 6.72934 6.92792 7.10466 7.26663 7.55947 7.82237 8.06326 8.28696 8.49667 8.69463 8.88246
Press = 2.000 MPa Tsat= 485.5 K
T(K) = 500. 550. 600. 650. 700. 800. 900. 1000. 1100. 1200. 1300. 1400.
v-m3/kg 0.10439 0.11917 0.13261 0.14541 0.15786 0.18215 0.20599 0.22958 0.25303 0.28123 0.30715 0.33300 0.35881
u-kj/kg 2632.6 2731.3 2820.5 2906.4 2991.5 3163.2 3339.3 3521.2 3709.3 3903.8 4104.7 4311.8
h-kj/kg 2841.4 2969.7 3085.7 3197.2 3307.2 3527.5 3751.3 3980.3 4215.3 4456.6 4704.0 4957.6
s-kj/kg/K 6.42645 6.67128 6.87328 7.05184 7.21490 7.50897 7.77251 8.01377 8.23771 8.44757 8.64563 8.83353
Press = 2.500 MPa Tsat= 497.1 K
T(K) = 500. 550. 600. 650. 700. 800. 900. 1000. 1100. 1200. 1300. 1400.
v-m3/kg 0.08080 0.09361 0.10484 0.11538 0.12553 0.14552 0.16445 0.18342 0.20226 0.22099 0.23967 0.25830
u-kj/kg 2609.7 2718.1 2811.4 2899.5 2986.1 3159.4 3326.5 3519.0 3707.5 3902.4 4103.5 4310.8
h-kj/kg 2811.7 2952.2 3073.5 3188.0 3299.9 3522.5 3747.6 3977.6 4213.2 4454.8 4702.7 4956.5
s-kj/kg/K 6.27535 6.54361 6.75484 6.93818 7.10407 7.40126 7.66643 7.90864 8.13314 8.34338 8.54170 8.72980
Press = 3.000 MPa Tsat= 507.0 K
T(K) = 550. 600. 650. 700. 800. 900. 1000. 1100. 1200. 1300. 1400. 1500.
v-m3/kg 0.07650 0.08631 0.09534 0.10397 0.12060 0.13675 0.15265 0.16841 0.18407 0.19967 0.21522 0.23074
u-kj/kg 2704.1 2801.9 2892.5 2980.5 3155.6 3333.7 3516.8 3705.8 3900.9 4102.3 4309.7 4523.0
h-kj/kg 2933.7 3060.9 3178.9 3292.5 3517.4 3744.0 3974.8 4210.1 4451.4 4701.3 4955.4 5215.2
s-kj/kg/K 6.43310 6.65462 6.84310 7.01196 7.31236 7.57918 7.82233 8.04742 8.25802 8.45662 8.64491 8.82414
Press = 3.500 MPa Tsat= 517.5 K
T(K) = 550. 600. 650. 700. 800. 900. 1000. 1100. 1200. 1300. 1400. 1500.
v-m3/kg 0.06422 0.07304 0.08102 0.08857 0.10301 0.11697 0.13068 0.14424 0.15770 0.17110 0.18445 0.19777
u-kj/kg 2689.3 2792.2 2885.4 2974.9 3151.8 3330.9 3514.7 3704.1 3899.5 4101.0 4308.7 4522.1
h-kj/kg 2914.0 3047.8 3168.9 3284.9 3512.4 3740.3 3972.1 4208.9 4451.4 4699.9 4954.3 5214.3
s-kj/kg/K 6.33371 6.56677 6.76077 6.93274 7.23644 7.50492 7.74903 7.97469 8.18567 8.38453 8.57302 8.75240
Press = 4.000 MPa Tsat= 523.5 K
T(K) = 550. 600. 650. 700. 800. 900. 1000. 1100. 1200. 1300. 1400. 1500.
v-m3/kg 0.05494 0.06306 0.07027 0.07701 0.08982 0.10213 0.11419 0.12610 0.13792 0.14967 0.16138 0.17305
u-kj/kg 2673.4 2782.0 2878.1 2969.3 3148.0 3328.1 3512.5 3702.3 3898.0 4099.8 4307.6 4521.2
h-kj/kg 2893.1 3034.3 3159.1 3277.3 3507.3 3736.7 3969.3 4206.7 4449.7 4698.5 4953.1 5213.4
s-kj/kg/K 6.24171 6.48774 6.68767 6.86291 7.17000 7.44017 7.68524 7.91147 8.12284 8.32196 8.51064 8.69017

Press = 4.500 MPa Tsat= 530.6 K  
T(K) = 550. 600. 650. 700. 800. 900. 1000. 1100. 1200. 1300. 1400. 1500.  
v-m3/kg 0.04765 0.05528 0.06189 0.06802 0.07955 0.09059 0.10137 0.11200 0.12254 0.13300 0.14343 0.15382  
u-kj/kg 2656.3 2771.5 2870.6 2963.5 3144.1 3235.3 3510.4 3700.6 3896.6 4098.6 4306.6 4520.3  
h-kj/kg 2870.7 3020.3 3149.1 3269.6 3502.1 3733.0 3966.5 4204.6 4448.0 4697.1 4952.0 5212.5  
s-kj/kg/K 6.15444 6.41525 6.62155 6.80022 7.11079 7.38267 7.62871 7.85553 8.06727 8.26666 8.45554 8.63521

Press = 5.000 MPa Tsat= 537.1 K  
T(K) = 550. 600. 650. 700. 800. 900. 1000. 1100. 1200. 1300. 1400. 1500.  
v-m3/kg 0.04175 0.04904 0.05519 0.06082 0.07134 0.08136 0.09112 0.10072 0.11023 0.11967 0.12907 0.13843  
u-kj/kg 2637.7 2760.6 2862.9 2957.7 3140.3 3232.5 3508.2 3698.8 3895.1 4097.4 4305.5 4519.4  
h-kj/kg 2846.5 3005.8 3138.9 3261.8 3497.0 3729.3 3963.8 4202.4 4446.2 4695.7 4950.9 5211.6  
s-kj/kg/K 6.06984 6.34772 6.56087 6.74313 7.05728 7.33089 7.57790 7.80531 8.01743 8.21709 8.40617 8.58598

Press = 6.000 MPa Tsat= 548.7 K  
T(K) = 550. 600. 650. 700. 800. 900. 1000. 1100. 1200. 1300. 1400. 1500.  
v-m3/kg 0.03267 0.03961 0.04510 0.05001 0.05902 0.06751 0.07573 0.08380 0.09177 0.09967 0.10753 0.11536  
u-kj/kg 2594.6 2737.5 2847.1 2945.8 3132.5 3316.8 3503.8 3695.3 3892.2 4094.9 4303.5 4517.6  
h-kj/kg 2790.6 2975.2 3117.7 3245.9 3486.6 3721.9 3958.2 4198.1 4442.8 4693.0 4948.7 5209.7  
s-kj/kg/K 5.90115 6.22319 6.45166 6.64164 7.24041 7.48939 7.71798 7.93087 8.13107 8.32035 8.50064

Press = 7.000 MPa Tsat= 559.0 K  
T(K) = 600. 650. 700. 800. 900. 1000. 1100. 1200. 1300. 1400. 1500. 1600.  
v-m3/kg 0.03280 0.03787 0.04227 0.05022 0.05762 0.06474 0.07171 0.07858 0.08539 0.09215 0.09967 0.10558  
u-kj/kg 2712.3 2830.5 2933.5 3124.5 3311.1 3499.4 3691.8 3889.3 4092.5 4301.4 4515.8 4735.4  
h-kj/kg 2941.9 3095.6 3229.5 3476.1 3714.4 3952.6 4193.8 4439.4 4690.2 4946.4 5207.9 5474.5  
s-kj/kg/K 6.10772 6.35409 6.55258 6.88213 7.16288 7.41385 7.64363 7.85730 8.05804 8.24789 8.48289 8.60030

Press = 8.000 MPa Tsat= 568.2 K  
T(K) = 600. 650. 700. 800. 900. 1000. 1100. 1200. 1300. 1400. 1500. 1600.  
v-m3/kg 0.02761 0.03241 0.03646 0.04361 0.05020 0.05650 0.06264 0.06869 0.07468 0.08061 0.08652 0.09239  
u-kj/kg 2684.6 2813.1 2920.9 3116.5 3305.3 3495.0 3689.3 3886.4 4090.0 4299.3 4514.0 4733.8  
h-kj/kg 2905.5 3072.4 3212.6 3465.4 3706.9 3947.0 4189.4 4435.9 4687.4 4944.2 5206.1 5473.0  
s-kj/kg/K 5.99692 6.26455 6.47242 6.81035 7.09482 7.34781 7.57880 7.79324 7.99453 8.18477 8.36547 8.53770

Press = 9.000 MPa Tsat= 576.5 K  
T(K) = 600. 650. 700. 800. 900. 1000. 1100. 1200. 1300. 1400. 1500. 1600.  
v-m3/kg 0.02349 0.02815 0.03193 0.03847 0.04442 0.05009 0.05559 0.06100 0.06634 0.07164 0.07690 0.08214  
u-kj/kg 2653.8 2794.8 2907.9 3108.4 3299.5 3490.6 3684.7 3883.4 4087.5 4297.2 4512.2 4732.3  
h-kj/kg 2865.2 3048.1 3195.2 3454.6 3699.3 3941.4 4185.1 4432.5 4684.6 4941.9 5204.3 5471.5  
s-kj/kg/K 5.88729 6.18066 6.39887 6.74568 7.03398 7.28902 7.52122 7.73645 7.93828 8.12892 8.30991 8.48236

Press = 10.000 MPa Tsat= 584.1 K  
T(K) = 600. 650. 700. 800. 900. 1000. 1100. 1200. 1300. 1400. 1500. 1600.  
v-m3/kg 0.02009 0.02471 0.02829 0.03436 0.03980 0.04496 0.04995 0.05485 0.05968 0.06446 0.06921 0.07393  
u-kj/kg 2618.9 2775.4 2894.4 3100.1 3293.7 3486.2 3681.2 3880.5 4085.1 4295.1 4510.4 4730.7  
h-kj/kg 2819.8 3022.5 3177.3 3443.7 3691.7 3935.8 4180.7 4429.0 4681.9 4939.7 5202.5 5470.0  
s-kj/kg/K 5.77538 6.10069 6.33038 6.68660 6.97883 7.23595 7.46938 7.68539 7.88777 8.07881 8.26009 8.43276

Press = 12.000 MPa Tsat= 597.8 K  
T(K) = 600. 650. 700. 750. 800. 850. 900. 950. 1000. 1050.  
v-m3/kg 0.01459 0.01947 0.02280 0.02562 0.02818 0.03058 0.03287 0.03510 0.03727 0.03940  
u-kj/kg 2528.8 2733.1 2866.2 2979.0 3083.3 3183.5 3281.9 3379.6 3477.2 3575.3  
h-kj/kg 2703.9 2966.8 3139.8 3286.5 3421.4 3550.4 3676.4 3800.7 3924.4 4048.1  
s-kj/kg/K 5.52472 5.94753 6.20430 6.40683 6.58105 6.73752 6.88148 7.01595 7.14285 7.26349

Press = 14.000 MPa Tsat= 609.8 K  
T(K) = 650. 700. 750. 800. 850. 900. 950. 1000. 1050.  
v-m3/kg 0.01563 0.01885 0.02145 0.02376 0.02589 0.02792 0.02987 0.03177 0.03363  
u-kj/kg 2684.9 2835.9 2957.0 3066.0 3169.3 3269.9 3369.2 3468.2 3567.3  
h-kj/kg 2903.7 3099.8 3257.3 3398.6 3531.8 3660.8 3787.5 3913.0 4038.1  
s-kj/kg/K 5.79671 6.08799 6.30540 6.48786 6.64947 6.79693 6.93391 7.06267 7.18475

Press = 16.000 MPa Tsat= 620.5 K  
T(K) = 650. 700. 750. 800. 850. 900. 950. 1000. 1050.  
v-m3/kg 0.01263 0.01586 0.01831 0.02044 0.02238 0.02421 0.02596 0.02765 0.02930  
u-kj/kg 2628.3 2803.4 2933.9 3048.2 3154.8 3257.8 3358.8 3459.1 3559.3  
h-kj/kg 2830.4 3057.1 3226.9 3375.1 3512.9 3645.1 3774.1 3901.5 4028.1  
s-kj/kg/K 5.64059 5.97752 6.21205 6.40350 6.57059 6.72171 6.86128 6.99195 7.11548

Press = 18.000 MPa Tsat= 630.1 K  
T(K) = 650. 700. 750. 800. 850. 900. 950. 1000. 1050.  
v-m3/kg 0.01014 0.01350 0.01586 0.01785 0.01964 0.02132 0.02291 0.02445 0.02594  
u-kj/kg 2559.0 2768.3 2909.9 3029.8 3140.1 3245.4 3348.3 3449.9 3551.2  
h-kj/kg 2741.5 3011.2 3195.3 3351.1 3493.7 3629.2 3760.7 3890.0 4018.1  
s-kj/kg/K 5.46893 5.87012 6.12446 6.32572 6.49863 6.65356 6.79580 6.92843 7.05344

Press = 20.000 MPa Tsat= 638.9 K  
T(K) = 650. 700. 750. 800. 850. 900. 950. 1000. 1050.  
v-m3/kg 0.00790 0.01158 0.01388 0.01577 0.01745 0.01901 0.02047 0.02188 0.02325  
u-kj/kg 2466.8 2730.1 2884.7 3011.0 3125.0 3232.9 3337.6 3440.7 3543.0  
h-kj/kg 2624.9 2961.6 3162.4 3326.5 3474.1 3613.1 3747.1 3878.4 4008.0  
s-kj/kg/K 5.26183 5.76355 6.04101 6.25298 6.43206 6.59096 6.73595 6.87059 6.99709

```

Press = 22.000 MPa  Tsat= 646.9 K
T(K) =      650.    700.    750.    800.    850.    900.    950.    1000.    1050.
v-m3/kg     0.00147  0.00997  0.01226  0.01407  0.01566  0.01711  0.01848  0.01979  0.02105
u-kj/kg     1596.4   2688.3   2858.4   2991.6   3109.7   3220.3   3326.9   3431.4   3534.9
h-kj/kg     1698.6   2907.8   3128.1   3301.2   3454.2   3596.8   3733.5   3866.7   3997.9
s-kj/kg/K   3.69088  5.65591  5.96051  6.18419  6.36978  6.53282  6.68065  6.81732  6.94536

Press = 24.000 MPa
T(K) =      650.    700.    750.    800.    850.    900.    950.    1000.    1050.
v-m3/kg     0.00146  0.00861  0.01090  0.01265  0.01416  0.01554  0.01682  0.01804  0.01921
u-kj/kg     1590.2   2642.3   2830.8   2971.7   3094.1   3207.5   3316.1   3422.0   3526.6
h-kj/kg     1695.8   2848.9   3092.4   3275.4   3434.0   3580.4   3719.7   3855.0   3987.8
s-kj/kg/K   3.68017  5.54534  5.88208  6.11853  6.31101  6.47834  6.62908  6.76784  6.89743

Press = 26.000 MPa
T(K) =      650.    700.    750.    800.    850.    900.    950.    1000.    1050.
v-m3/kg     0.00145  0.00742  0.00974  0.01145  0.01290  0.01420  0.01542  0.01656  0.01766
u-kj/kg     1584.4   2591.2   2801.9   2951.2   3078.2   3194.5   3305.1   3412.6   3518.4
h-kj/kg     1693.3   2784.1   3055.2   3248.9   3413.6   3563.8   3705.9   3843.2   3977.7
s-kj/kg/K   3.67008  5.42987  5.80500  6.05541  6.25513  6.42692  6.58065  6.72153  6.85270

Press = 28.000 MPa
T(K) =      650.    700.    750.    800.    850.    900.    950.    1000.    1050.
v-m3/kg     0.00144  0.00637  0.00874  0.01042  0.01182  0.01306  0.01421  0.01530  0.01634
u-kj/kg     1578.9   2533.7   2771.6   2930.2   3062.0   3181.4   3294.1   3403.1   3510.1
h-kj/kg     1691.1   2712.0   3016.4   3221.9   3392.8   3547.1   3692.0   3831.5   3967.5
s-kj/kg/K   3.66050  5.30724  5.72875  5.99434  6.20169  6.37808  6.53487  6.67792  6.81068

Press = 30.000 MPa
T(K) =      650.    700.    750.    800.    850.    900.    950.    1000.    1050.
v-m3/kg     0.00143  0.00543  0.00787  0.00952  0.01088  0.01207  0.01317  0.01420  0.01519
u-kj/kg     1573.7   2468.6   2739.9   2908.7   3045.6   3168.1   3283.0   3393.6   3501.8
h-kj/kg     1689.1   2631.5   2976.2   3194.4   3371.8   3530.2   3678.1   3819.7   3957.4
s-kj/kg/K   3.65138  5.17540  5.65290  5.93499  6.15032  6.33146  6.49139  6.63664  6.77102

Press = 35.000 MPa
T(K) =      650.    700.    750.    800.    850.    900.    950.    1000.    1050.
v-m3/kg     0.00141  0.00141  0.00613  0.00773  0.00900  0.01010  0.01109  0.01201  0.01289
u-kj/kg     1561.7   1701.7   2654.4   2852.5   3003.4   3134.3   3254.9   3369.6   3480.9
h-kj/kg     1685.0   1899.7   2868.9   3123.2   3318.4   3487.6   3643.0   3790.1   3932.0
s-kj/kg/K   3.63027  3.83785  5.46347  5.79237  6.02927  6.22286  6.39089  6.54179  6.68027

```

## C.4 H<sub>2</sub>O Compressed Liquid Table (SI units)

```

Press = 40.000 MPa
T(K) =      650.    700.    750.    800.    850.    900.    950.    1000.    1050.
v-m3/kg     0.00139  0.00139  0.00483  0.00640  0.00760  0.00862  0.00953  0.01038  0.01117
u-kj/kg     1550.8   1691.1   2560.8   2793.3   2959.9   3099.8   3226.4   3345.4   3459.9
h-kj/kg     1681.8   1897.7   2754.1   3049.3   3263.9   3444.6   3607.7   3760.4   3906.6
s-kj/kg/K   3.61114  3.81901  5.27412  5.65605  5.91650  6.12322  6.29967  6.45636  6.59905

```

Temperature=	0.001 MPa									
	273.1 K	Psat=								
Press(MPa)=	1	2	5	8	10	15	20	25	30	50
v-m3/kg	0.001	0.001	0.001	0.001	0.001	0.00099	0.00099	0.00099	0.00099	0.00098
u-kj/kg	0	0	0	0.1	0.1	0.2	0.2	0.3	0.3	0.3
h-kj/kg	1	2	5	8.1	10.1	15.1	20	25	29.9	49.1
s-kj/kg/K	0	0	0.00014	0.00027	0.00034	0.00045	0.00047	0.00041	0.00028	0
Temperature=	280.0 K	Psat=	0.001 MPa							
Press(MPa)=	1	2	5	8	10	15	20	25	30	50
v-m3/kg	0.001	0.001	0.001	0.001	0.001	0.00099	0.00099	0.00099	0.00099	0.00098
u-kj/kg	28.8	28.8	28.7	28.7	28.7	28.6	28.5	28.4	28.3	27.9
h-kj/kg	29.8	30.8	33.7	36.7	38.6	43.5	48.3	53.1	57.9	76.7
s-kj/kg/K	0.10407	0.10402	0.10386	0.10368	0.10354	0.10315	0.1027	0.10219	0.10162	0.09879
Temperature=	300.0 K	Psat=	0.004 MPa							
Press(MPa)=	1	2	5	8	10	15	20	25	30	50
v-m3/kg	0.001	0.001	0.001	0.001	0.001	0.001	0.00099	0.00099	0.00099	0.00098
u-kj/kg	112.5	112.4	112.2	111.9	111.8	111.4	111	110.6	110.2	108.6
h-kj/kg	113.5	114.4	117.2	119.9	121.7	126.3	130.8	135.4	139.9	157.8
s-kj/kg/K	0.39285	0.39257	0.39174	0.39089	0.39033	0.3889	0.38744	0.38597	0.38448	0.37831
Temperature=	320.0 K	Psat=	0.011 MPa							
Press(MPa)=	1	2	5	8	10	15	20	25	30	50
v-m3/kg	0.00101	0.00101	0.00101	0.00101	0.00101	0.001	0.001	0.001	0.001	0.00099
u-kj/kg	196	195.9	195.5	195	194.8	194.1	193.4	192.8	192.1	189.7
h-kj/kg	197	197.9	200.5	203.1	204.8	209.2	213.5	217.8	222.1	239.2
s-kj/kg/K	0.66242	0.66198	0.66066	0.65934	0.65847	0.65628	0.65409	0.65191	0.64973	0.64104
Temperature=	340.0 K	Psat=	0.027 MPa							
Press(MPa)=	1	2	5	8	10	15	20	25	30	50
v-m3/kg	0.00102	0.00102	0.00102	0.00102	0.00102	0.00101	0.00101	0.00101	0.00101	0.001
u-kj/kg	279.6	279.4	278.8	278.3	277.9	276.9	276	275.1	274.2	270.9
h-kj/kg	280.6	281.5	283.9	286.4	288	292.2	296.3	300.4	304.5	320.9
s-kj/kg/K	0.91582	0.91524	0.91352	0.91181	0.91067	0.90785	0.90504	0.90226	0.89949	0.88862
Temperature=	360.0 K	Psat=	0.062 MPa							
Press(MPa)=	1	2	5	8	10	15	20	25	30	50
v-m3/kg	0.00103	0.00103	0.00103	0.00103	0.00103	0.00103	0.00102	0.00102	0.00102	0.00101
u-kj/kg	363.4	363.2	362.4	361.7	361.2	360	358.8	357.7	356.5	352.2
h-kj/kg	364.5	365.2	367.6	369.9	371.5	375.4	379.3	383.2	387.1	402.8
s-kj/kg/K	1.15538	1.15468	1.15259	1.15052	1.14914	1.14573	1.14236	1.13902	1.13572	1.12283
Temperature=	380.0 K	Psat=	0.129 MPa							
Press(MPa)=	1	2	5	8	10	15	20	25	30	50
v-m3/kg	0.00105	0.00105	0.00105	0.00104	0.00104	0.00104	0.00104	0.00104	0.00103	0.00102
u-kj/kg	447.6	447.3	446.4	445.5	444.9	443.4	441.9	440.5	439.1	433.8
h-kj/kg	448.7	449.4	451.6	453.8	455.3	459	462.7	466.4	470.1	485.1
s-kj/kg/K	1.38306	1.38224	1.37978	1.37735	1.37574	1.37175	1.36782	1.36394	1.36011	1.34526
Temperature=	400.0 K	Psat=	0.246 MPa							
Press(MPa)=	1	2	5	8	10	15	20	25	30	50
v-m3/kg	0.00107	0.00107	0.00106	0.00106	0.00106	0.00106	0.00106	0.00105	0.00105	0.00104
u-kj/kg	532.4	532	530.9	529.8	529	527.3	525.5	523.8	522.1	515.8
h-kj/kg	533.5	534.1	536.2	538.3	539.7	543.1	546.6	550.1	553.6	567.8
s-kj/kg/K	1.60051	1.59955	1.59672	1.59392	1.59207	1.58749	1.58298	1.57854	1.57417	1.5573



Press(MPa)=	1	2	5	8	10	15	20	25	30	50
v-m3/kg				0.00143	0.00141	0.00139	0.00137	0.00135	0.00131	
u-kj/kg				1368.5	1355.1	1343.3	1332.8	1323.2	1313.5	1291.5
h-kj/kg				1382.9	1376.2	1371.1	1367	1363.8	1356.7	
s-kj/kg/K				3.31731	3.29363	3.27272	3.25386	3.23661	3.17855	

Temperature=	600.0 K	Psat=	12.34 MPa							
Press(MPa)=	1	2	5	8	10	15	20	25	30	50
v-m3/kg					0.00152	0.00148	0.00145	0.00143	0.00136	
u-kj/kg					1474.8	1456.6	1441.5	1428.3	1387.5	
h-kj/kg					1497.5	1486.3	1477.8	1471.2	1455.6	
s-kj/kg/K					3.49917	3.46794	3.44163	3.41862	3.34608	

Temperature=	620.0 K	Psat=	15.9 Mpa							
Press(MPa)=	1	2	5	8	10	15	20	25	30	50
v-m3/kg					0.00163	0.00157	0.00153	0.00143		
u-kj/kg					1588.6	1562.9	1542.9	1487.6		
h-kj/kg					1621.2	1602.3	1588.9	1559.1		
s-kj/kg/K					3.68902	3.64556	3.6115	3.5159		

Temperature=	640.0 K	Psat=	20.27 Mpa							
Press(MPa)=	1	2	5	8	10	15	20	25	30	50
v-m3/kg						0.01322	0.01322	0.01322		
u-kj/kg						2616.4	2616.4	2616.4		
h-kj/kg						2815.1	2815.1	2815.1		
s-kj/kg/K						5.63646	5.63646	5.63646		

## C.5 Saturation Temperature vs. Pressure (English Units)

Press (psi)	Temp (R)	Specific Volume (ft <sup>3</sup> *3/lbm)	Internal Energy			Enthalpy			Entropy		
			vf	vg	uf	ufg	ug	hf	hfg	hg	sf
0.1	494.7	0.0161	2951.1577		3.01	1021.2	1024.2	3.02	1075.8	1078.8	0.00611
0.2	512.8	0.0161	1529.1317		21.25	1008.9	1030.2	21.25	1065.5	1086.8	0.04231
0.3	524.1	0.0161	1041.6294		32.60	1001.3	1033.9	32.60	1059.1	1091.7	0.06421
0.4	532.5	0.0161	793.5160		41.00	995.6	1036.6	41.00	1054.4	1095.4	0.08010
0.6	544.8	0.0161	541.0339		53.35	987.3	1040.6	53.36	1047.4	1100.7	0.10305
0.8	554.0	0.0161	412.4360		62.52	981.1	1043.6	62.52	1042.1	1104.7	0.11973
1.0	561.4	0.0162	334.2068		69.88	976.1	1046.0	69.88	1037.9	1107.8	0.13292
1.5	575.3	0.0162	228.1557		83.83	966.6	1050.4	83.83	1029.9	1113.8	0.15746
2.5	594.1	0.0163	141.1594		102.58	953.8	1056.4	102.59	1019.1	1121.7	0.18954
3.0	601.1	0.0163	118.9527		109.62	949.0	1058.6	109.63	1015.1	1124.6	0.20132
3.5	607.2	0.0164	102.9342		115.73	944.7	1060.5	115.74	1011.4	1127.1	0.21143
4.0	612.6	0.0164	90.8181		121.13	941.0	1062.1	121.15	1008.2	1129.4	0.22030
5.0	621.9	0.0164	73.6775		130.43	934.6	1065.0	130.44	1002.7	1133.2	0.23536
6.0	629.7	0.0165	62.1094		138.27	929.1	1067.4	138.29	998.0	1136.3	0.24789
7.0	636.5	0.0165	53.7612		145.08	924.3	1069.4	145.11	994.1	1139.1	0.25865
8.0	642.5	0.0166	47.4442		151.13	920.1	1071.2	151.15	990.3	1141.5	0.26811
10.0	652.8	0.0166	38.5033		161.54	912.7	1074.3	161.57	984.0	1145.5	0.28418
12.5	663.6	0.0167	31.2495		172.36	905.0	1077.4	172.40	977.3	1149.7	0.30062
14.7	671.6	0.0167	26.8597		180.48	899.2	1079.7	180.52	972.1	1152.8	0.31278
20.0	687.6	0.0169	20.1340		196.61	887.6	1084.2	196.67	962.1	1158.7	0.33651
25.0	699.7	0.0170	16.3406		208.88	878.6	1087.5	208.96	954.1	1163.1	0.35421
30.0	710.0	0.0170	13.7771		219.30	870.9	1090.2	219.40	947.3	1166.6	0.36900
35.0	718.9	0.0171	11.9251		228.41	864.1	1092.5	228.52	941.2	1169.7	0.38175
40.0	726.9	0.0172	10.5224		236.53	857.9	1094.5	236.66	935.7	1172.4	0.39298
45.0	734.1	0.0172	9.4220		243.88	852.3	1096.2	244.02	930.7	1174.7	0.40304
50.0	740.7	0.0173	8.5350		250.61	847.2	1097.8	250.77	926.0	1176.8	0.41217
55.0	746.7	0.0174	7.8041		256.82	842.4	1099.2	257.00	921.6	1178.6	0.42052
60.0	752.4	0.0174	7.1912		262.61	837.9	1100.5	262.80	917.5	1180.3	0.42824
65.0	757.6	0.0175	6.6696		268.02	833.7	1101.7	268.24	913.7	1181.9	0.43542
70.0	762.6	0.0175	6.2201		273.13	829.6	1102.8	273.35	910.0	1183.3	0.44213
75.0	767.3	0.0176	5.8286		277.95	825.8	1103.8	278.19	906.5	1184.7	0.44844
80.0	771.7	0.0176	5.4844		282.53	822.2	1104.7	282.79	903.1	1185.9	0.45439
85.0	775.9	0.0176	5.1794		286.89	818.7	1105.6	287.17	899.9	1187.0	0.46003
90.0	779.9	0.0177	4.9071		291.06	815.3	1106.4	291.36	896.8	1188.1	0.46539
95.0	783.8	0.0177	4.6626		295.05	812.1	1107.1	295.37	893.7	1189.1	0.47049

Press (psi)	Temp (R)	Specific Volume (ft**3/lbm)	Internal Energy (Btu/lbm)	Enthalpy (Btu/lbm)	Entropy (Btu/lbm/R)			
		vf    vg	uf    ufg    ug	hf    hfg    hg	sf    sfg    sg			
100.0	787.5	0.0178	4.4417	298.89	809.0 1107.9	299.22	890.8 1190.1	0.47538 1.13124 1.60661
				Internal Energy (Btu/lbm)	Enthalpy (Btu/lbm)	Entropy (Btu/lbm/R)		
110.0	794.5	0.0178	4.0581	306.14	803.0 1109.2	306.50	885.3 1191.8	0.48454 1.11432 1.59886
120.0	800.9	0.0179	3.7365	312.90	797.4 1110.3	313.29	880.0 1193.3	0.49302 1.09874 1.59176
130.0	807.0	0.0180	3.4626	319.24	792.1 1111.4	319.67	875.0 1194.7	0.50091 1.08429 1.58520
140.0	812.7	0.0181	3.2267	325.22	787.1 1112.3	325.69	870.2 1195.9	0.50830 1.07080 1.57910
150.0	818.1	0.0181	3.0211	330.89	782.3 1113.2	331.40	865.7 1197.1	0.51525 1.05814 1.57340
160.0	823.2	0.0182	2.8404	336.28	777.7 1114.0	336.82	861.3 1198.1	0.52183 1.04622 1.56805
170.0	828.1	0.0183	2.6802	341.43	773.3 1114.7	342.00	857.0 1199.0	0.52806 1.03494 1.56300
180.0	832.8	0.0183	2.5373	346.35	769.0 1115.4	346.96	852.9 1199.9	0.53399 1.02423 1.55822
190.0	837.2	0.0184	2.4088	351.07	764.9 1116.0	351.72	849.0 1200.7	0.53965 1.01403 1.55367
200.0	841.5	0.0184	2.2928	355.62	760.9 1116.5	356.30	845.1 1201.4	0.54506 1.00429 1.54935
250.0	860.7	0.0187	1.8478	376.11	742.6 1118.7	376.97	827.2 1204.2	0.56915 0.96114 1.53029
300.0	877.0	0.0189	1.5467	393.80	726.3 1120.1	394.85	811.1 1206.0	0.58953 0.92485 1.51438
350.0	891.4	0.0192	1.3290	409.48	711.5 1121.0	410.72	796.3 1207.1	0.60728 0.89335 1.50063
400.0	904.3	0.0194	1.1640	423.66	697.8 1121.5	425.09	782.6 1207.6	0.62308 0.86537 1.48845
450.0	916.0	0.0196	1.0345	436.64	685.0 1121.6	438.27	769.5 1207.8	0.63737 0.84010 1.47747
500.0	926.7	0.0198	0.9301	448.67	672.9 1121.6	450.50	757.1 1207.8	0.65045 0.81698 1.46743
600.0	945.9	0.0202	0.7718	470.48	650.3 1120.8	472.72	733.7 1206.5	0.67378 0.77569 1.44947
700.0	962.8	0.0206	0.6572	490.01	629.3 1119.4	492.63	711.8 1204.5	0.69430 0.73931 1.43361
800.0	977.9	0.0209	0.5704	507.83	609.6 1117.4	510.93	691.0 1201.9	0.71271 0.70654 1.41925
900.0	991.7	0.0213	0.5021	524.31	590.8 1115.1	527.86	670.9 1198.7	0.72950 0.67650 1.40600
1000.0	1004.3	0.0216	0.4470	539.73	572.7 1112.4	543.73	651.4 1195.1	0.74501 0.64861 1.39362
1100.0	1016.0	0.0220	0.4015	554.27	555.1 1109.4	558.75	632.4 1191.1	0.75948 0.62242 1.38190
1200.0	1026.9	0.0224	0.3632	568.10	538.0 1106.1	573.07	613.7 1186.8	0.77310 0.59760 1.37069
1300.0	1037.2	0.0227	0.3306	581.34	521.2 1102.5	586.81	595.2 1182.0	0.78600 0.57389 1.35990
1400.0	1046.8	0.0231	0.3023	594.07	504.6 1098.6	600.06	576.9 1177.0	0.79831 0.55110 1.34941
1500.0	1055.9	0.0235	0.2776	606.38	488.1 1094.5	612.91	556.8 1171.5	0.81012 0.52904 1.33916
1600.0	1064.6	0.0239	0.2558	618.34	471.7 1090.0	625.42	540.4 1165.8	0.82151 0.50757 1.32907
1800.0	1080.7	0.0248	0.2189	641.42	438.9 1080.3	649.67	503.5 1153.2	0.84327 0.46589 1.30916
2000.0	1095.5	0.0257	0.1886	663.74	405.4 1069.2	673.25	465.7 1139.0	0.86408 0.42510 1.28918
2250.0	1112.4	0.0270	0.1573	691.19	361.7 1052.9	702.44	416.0 1118.4	0.88942 0.37393 1.26335
2500.0	1127.8	0.0287	0.1309	719.11	314.2 1033.3	732.37	361.5 1093.9	0.91498 0.32054 1.23552
2750.0	1142.0	0.0308	0.0573	749.09	212.1 870.3	764.78	134.6 899.4	0.94233 0.11756 1.05990
3000.0	1155.1	0.0345	0.0531	785.51	86.3 871.8	804.64	96.7 901.3	0.97571 0.08362 1.05933
3200.0	1164.8	0.0517	0.0517	877.11	0.0 877.1	907.70	0.0 907.7	1.06317 0.00000 1.06317

## C.6 Saturation Pressure vs. Temperature (English Units)

Temp (R)	Press (psi)	Specific Volume (ft**3/lbm)	Internal Energy (Btu/lbm)	Enthalpy (Btu/lbm)	Entropy (Btu/lbm/R)
		vf    vg	uf    ufg    ug	hf    hfg    hg	sf    sfg    sg
491.7	0.09	0.0161 3308.9548	0.00 1023.2 1023.2	0.00 1077.5 1077.5	0.00000 2.19152 2.19152
500.0	0.12	0.0161 2418.8743	8.38 1017.6 1026.0	8.38 1072.8 1081.2	0.01690 2.14557 2.12647
510.0	0.18	0.0161 1686.7268	18.44 1010.8 1029.3	18.44 1067.1 1085.6	0.03681 2.09238 2.12920
520.0	0.26	0.0161 1195.2240	28.47 1004.1 1032.5	28.47 1061.5 1089.9	0.05630 2.04126 2.09755
530.0	0.37	0.0161 859.8069	38.49 997.3 1035.8	38.49 1055.8 1094.3	0.07538 1.99205 2.06744
540.0	0.51	0.0161 627.3451	48.50 990.6 1039.1	48.50 1050.1 1098.6	0.09410 1.94466 2.03876
550.0	0.71	0.0161 463.8765	58.51 983.8 1042.3	58.51 1044.4 1102.9	0.11246 1.89896 2.01142
560.0	0.96	0.0162 347.3375	68.51 977.0 1045.5	68.51 1038.7 1107.2	0.13048 1.85486 1.98535
570.0	1.29	0.0162 263.1730	78.51 970.2 1048.7	78.52 1033.0 1111.5	0.14819 1.81227 1.96045
580.0	1.71	0.0162 201.6415	88.52 963.4 1051.9	88.52 1027.2 1115.8	0.16558 1.77109 1.93668
590.0	2.25	0.0163 156.1334	98.52 956.6 1055.1	98.53 1021.4 1120.0	0.18269 1.73126 1.91395
600.0	2.92	0.0163 122.1055	108.53 949.7 1058.2	108.54 1015.6 1124.2	0.19951 1.69269 1.89220
610.0	3.75	0.0164 96.3962	118.55 942.8 1061.3	118.56 1009.7 1128.3	0.21606 1.65531 1.87137
620.0	4.78	0.0164 76.7798	128.57 935.9 1064.4	128.58 1003.8 1132.4	0.23236 1.61906 1.85142
630.0	6.05	0.0165 61.6720	138.60 928.9 1067.5	138.62 997.8 1136.5	0.24841 1.58387 1.83228
640.0	7.57	0.0165 49.9327	148.64 921.8 1070.5	148.66 991.8 1140.5	0.26422 1.54969 1.81391
650.0	9.42	0.0166 40.7337	158.69 914.8 1073.4	158.72 985.7 1144.4	0.27981 1.51645 1.79626
660.0	11.62	0.0167 33.4671	168.76 907.6 1076.4	168.79 979.5 1148.3	0.29518 1.48411 1.77928
670.0	14.23	0.0167 27.6832	178.84 900.4 1079.2	178.88 973.3 1152.1	0.31034 1.45261 1.76294
680.0	17.31	0.0168 23.0457	188.93 893.1 1082.1	188.99 966.9 1155.9	0.32529 1.42190 1.74720
690.0	20.92	0.0169 19.3017	199.05 885.8 1084.8	199.11 960.5 1159.6	0.34006 1.39195 1.73201
700.0	25.13	0.0170 16.2589	209.18 878.4 1087.5	209.26 953.9 1163.2	0.35464 1.36270 1.71734
710.0	30.02	0.0170 13.7705	219.33 870.8 1090.2	219.43 947.2 1166.7	0.36904 1.33412 1.70316
720.0	35.64	0.0171 11.7232	229.51 863.2 1092.7	229.62 940.4 1170.1	0.38327 1.30616 1.68943
730.0	42.10	0.0172 10.0291	239.71 855.5 1095.2	239.84 933.5 1173.4	0.39734 1.27880 1.67613
740.0	49.48	0.0173 8.6197	249.93 847.7 1097.6	250.09 926.5 1176.6	0.41125 1.25198 1.66323
750.0	57.86	0.0174 7.4409	260.18 839.8 1100.0	260.37 919.3 1179.6	0.42501 1.22569 1.65070
760.0	67.35	0.0175 6.4501	270.46 831.7 1102.2	270.68 911.9 1182.6	0.43863 1.19989 1.63852
770.0	78.05	0.0176 5.6133	280.77 823.6 1104.3	281.03 904.4 1185.4	0.45211 1.17454 1.62665
780.0	90.07	0.0177 4.9034	291.12 815.3 1106.4	291.41 896.7 1188.1	0.46546 1.14963 1.61509
790.0	103.52	0.0178 4.2985	301.50 806.8 1108.3	301.84 888.8 1190.7	0.47869 1.12511 1.60380
800.0	118.52	0.0179 3.7809	311.92 798.2 1110.2	312.31 880.8 1193.1	0.49180 1.10098 1.59277
810.0	135.18	0.0180 3.3362	322.38 789.5 1111.9	322.83 872.5 1195.4	0.50480 1.07719 1.58198
820.0	153.64	0.0181 2.9527	328.89 780.6 1113.5	333.40 864.1 1197.5	0.51769 1.05372 1.57141
830.0	174.03	0.0183 2.6207	343.44 771.5 1115.0	344.03 855.4 1199.4	0.53048 1.03055 1.56104

Temp (R)	Press (psi)	Specific Volume (ft <sup>3</sup> /lbm)	Internal Energy (Btu/lbm)	Enthalpy (Btu/lbm)	Entropy (Btu/lbm/R)
840.0	196.49	0.0184	2.3323	354.04	762.3 1116.3
850.0	221.14	0.0185	2.0809	364.69	752.9 1117.6
860.0	248.15	0.0187	1.8611	375.41	743.2 1118.6
870.0	277.66	0.0188	1.6683	386.18	733.4 1119.6
880.0	309.82	0.0190	1.4986	397.02	723.3 1120.3
890.0	344.79	0.0191	1.3488	407.93	713.0 1120.9
900.0	382.74	0.0193	1.2163	418.91	702.4 1121.3
910.0	423.83	0.0195	1.0986	429.98	691.6 1121.6
920.0	468.23	0.0197	0.9940	441.13	680.5 1121.6
930.0	516.12	0.0199	0.9006	452.37	669.1 1121.5
940.0	567.68	0.0201	0.8171	463.72	657.4 1121.1
950.0	623.10	0.0203	0.7422	475.17	645.3 1120.5
960.0	682.56	0.0205	0.6749	486.74	632.9 1119.6
970.0	746.26	0.0207	0.6143	498.44	620.1 1118.5
980.0	814.41	0.0210	0.5595	510.28	606.9 1117.1
990.0	887.21	0.0212	0.5100	522.27	593.2 1115.4
1000.0	964.87	0.0215	0.4651	534.42	579.0 1113.4
1010.0	1047.63	0.0218	0.4243	546.75	564.3 1111.0
1020.0	1135.71	0.0221	0.3871	559.29	549.0 1108.3
1030.0	1229.35	0.0225	0.3531	572.04	533.0 1105.1
1040.0	1328.81	0.0229	0.3220	585.05	516.4 1101.4
1050.0	1434.35	0.0233	0.2935	598.34	498.9 1097.2
1060.0	1546.25	0.0237	0.2672	611.95	480.5 1092.5
1070.0	1664.83	0.0242	0.2429	625.93	461.1 1087.0
1080.0	1790.40	0.0247	0.2205	640.33	440.4 1080.8
1090.0	1923.31	0.0253	0.1995	655.24	418.3 1073.6
1100.0	2063.95	0.0260	0.1800	670.78	394.5 1065.3
1110.0	2212.74	0.0268	0.1616	687.10	368.4 1055.5
1120.0	2370.19	0.0278	0.1441	704.47	339.5 1044.0
1130.0	2536.83	0.0289	0.1274	723.34	306.7 1030.0
1140.0	2713.33	0.0305	0.0580	744.45	125.6 870.1
1150.0	2900.52	0.0327	0.0547	769.61	101.6 871.2
1160.0	3099.69	0.0371	0.0517	805.97	65.9 871.9
1164.8	3200.12	0.0515	0.0515	876.57	0.0 876.6

### C.7 Superheated Steam Table (English Units)

```

Press =   1.0 psi, Tsat = 561.4 R
T(R) =    .600.   .650.   .700.   .750.   .800.   .850.   .900.   1.000.   1.100.   1.200.   1.300.   1.400.
v-ft3/lbm = 357.745 387.798 417.779 447.720 477.638 507.541 537.435 597.207 656.965 716.715 776.461 836.203
u-Btu/lbm = 1059.3   1076.5   1093.7   1111.0   1128.5   1146.1   1163.9   1200.1   1237.0   1274.9   1313.6   1353.1
h-Btu/lbm = 1125.5   1148.2   1170.9   1193.8   1216.8   1240.0   1263.3   1310.5   1358.6   1407.4   1452.7   1507.8
s-Btu/lbm/R = 0.01229 0.024862 0.02838 2.11392 2.14360 2.17168 2.19835 2.24811 2.29388 2.33640 2.37620 2.41372

```

```

Press =   2.5 psi, Tsat = 594.1 R
T(R) =    600.   650.   700.   750.   800.   850.   900.   1000.   1100.   1200.   1300.   1400.
v-ft3/lbm 142.701 154.841 166.904 178.926 190.924 202.909 214.883 238.816 262.735 286.646 310.553 334.456
u-Btu/lbm 1058.5 1076.0 1093.3 1110.7 1128.3 1145.9 1163.8 1200.0 1237.0 1274.8 1313.5 1353.1
h-Btu/lbm 1124.5 1147.5 1170.5 1193.5 1216.5 1239.8 1263.1 1310.4 1358.5 1407.4 1457.1 1507.7
s-Btu/lbm/R 1.90967 1.94663 1.98065 2.01236 2.04214 2.07028 2.09699 2.14680 2.19260 2.23513 2.27495 2.31247

```

```

Press =      5.0 psi, Tsat = 621.9 R
T(R) =      .650.    .700.    .750.    .800.    .850.    .900.    .1000.   .1100.   .1200.   .1300.   .1400.   .1500.
v-fft3/lbm = 77.183. 83.277. 89.337. 95.353. 101.364. 107.366. 119.353. 131.325. 143.290. 155.250. 167.206. 179.161
u-Btu/lbm = 1076.1. 1092.7. 1110.3. 1127.9. 1145.7. 1163.6. 1199.8. 1236.9. 1274.7. 1313.4. 1353.0. 1393.6
h-Btu/lbm = 1146.4. 1169.7. 1192.9. 1216.1. 1239.4. 1262.8. 1310.2. 1358.3. 1407.2. 1457.0. 1517.7. 1559.2
s-Btu/(lbm R) = 68670. 69032. 69531. 69651. 69940. 2.00208. 2.07008. 2.11592. 2.16848. 2.19932. 2.23586. 2.23422

```

```

Press =    7.5 psi, Tsat = 639.6 R
T(°R) =   650.    700.    750.    800.    850.    900.    1000.   1100.   1200.   1300.   1400.   1500.
v-ft3/lbm 51.297  55.400  59.460  63.495  67.516  71.527  79.531  87.521  95.504 103.482 111.457 119.429
u-Btu/lbm 1074.2 1092.1 1109.9 1127.6 1145.4 1163.4 1199.7 1236.8 1274.6 1313.4 1353.0 1393.5
h-Btu/lbm 1145.3 1169.0 1192.4 1215.7 1239.1 1262.6 1310.0 1358.2 1407.1 1456.9 1507.6 1559.2

```

```

Press = 10.0 psi, Tsat = 652.8 R
T     =    700.   750.   800.   850.   900.   1000.   1100.   1200.   1300.   1400.   1500.   1600.
v-ft3/lbm 41.4602 44.5258 47.5662 50.5914 53.6069 59.6202 65.6198 71.6115 77.5984 83.5819 89.5631 95.5426
u-Btu/lbm 1091.5 1109.8 1127.3 1145.2 1163.1 1199.5 1236.7 1274.6 1313.3 1352.9 1393.5 1434.9
h-Btu/lbm 1168.2 1191.8 1215.3 1238.7 1262.3 1309.8 1358.0 1407.0 1456.8 1507.5 1559.1 1611.6

```

```

Press = 12.5 psi, Tsat = 663.6 R
T(R) = 700. 750. 800. 850. 900. 1000. 1100. 1200. 1300. 1400. 1500. 1600.
v-ft3/lbm 33.0955 35.5648 38.0085 40.4367 42.8550 47.6737 52.4787 57.2759 62.0681 66.8570 71.6435 76.4284
u-Btu/lbm 1090.9 1109.0 1126.9 1142.9 1162.0 1199.4 1236.5 1274.5 1313.2 1352.9 1393.4 1434.9
h-Btu/lbm 1167.4 1191.2 1214.8 1238.4 1262.0 1309.6 1357.9 1406.9 1456.7 1507.4 1559.0 1611.6

```

T(R) = 700. 750. 800. 850. 900. 1000. 1100. 1200. 1300. 1400. 1500. 1600.  
v-ft3/lbm 28.0952 30.2085 32.2956 34.3669 36.4283 40.5332 44.6241 48.7072 52.7854 56.8603 60.9328 65.0036  
u-Btu/lbm 1090.3 1108.6 1126.7 1144.7 1162.7 1199.3 1236.4 1274.4 1313.2 1352.8 1393.4 1434.8  
h-Btu/lbm 1166.7 1190.7 1214.4 1238.1 1261.8 1309.4 1357.7 1406.8 1456.6 1507.4 1559.0 1611.5  
s-Btu/lbm/R 1.78065 1.81380 1.84444 1.87311 1.90018 1.95040 1.99643 2.03910 2.07901 2.11659 2.15220 2.18611

Press = 20.0 psi, Tsat = 687.6 R  
T(R) = 700. 750. 800. 850. 900. 1000. 1100. 1200. 1300. 1400. 1500. 1600.  
v-ft3/lbm 20.5449 22.1217 23.6710 25.2040 26.7268 29.7540 32.7671 35.7724 38.7726 41.7696 44.7642 47.7572  
u-Btu/lbm 1088.9 1107.6 1125.9 1144.1 1162.3 1198.9 1236.2 1274.2 1313.0 1352.7 1393.3 1434.8  
h-Btu/lbm 1164.9 1189.4 1213.5 1237.3 1261.2 1309.0 1357.4 1406.5 1456.4 1507.2 1558.8 1611.4  
s-Btu/lbm/R 1.74461 1.77846 1.80949 1.83841 1.86564 1.91605 1.96217 2.00490 2.04485 2.08246 2.11809 2.15201

Press = 40.0 psi, Tsat = 726.9 R  
T(R) = 750. 800. 850. 900. 1000. 1100. 1200. 1300. 1400. 1500. 1600. 1700.  
v-ft3/lbm 10.9125 11.7197 12.5083 13.2855 14.8242 16.3406 17.8527 19.3597 20.8634 22.3648 23.8644 25.3628  
u-Btu/lbm 1103.8 1123.1 1142.0 1160.6 1197.8 1235.3 1273.5 1312.4 1352.2 1392.9 1434.4 1476.9  
h-Btu/lbm 1184.5 1209.8 1234.5 1258.9 1307.4 1356.2 1405.6 1455.7 1506.6 1558.3 1611.0 1664.5  
s-Btu/lbm/R 1.69668 1.72936 1.75928 1.78714 1.83827 1.88478 1.92774 1.96784 2.00555 2.04126 2.07523 2.10768

Press = 60.0 psi, Tsat = 752.4 R  
T(R) = 800. 850. 900. 1000. 1100. 1200. 1300. 1400. 1500. 1600. 1700. 1800.  
v-ft3/lbm 7.7325 8.2745 8.8041 9.8422 10.8650 11.8794 12.8887 13.8947 14.8983 15.9002 16.9008 17.9005  
u-Btu/lbm 1120.1 1139.4 1158.0 1196.5 1234.4 1272.8 1311.9 1351.8 1392.5 1434.1 1476.6 1520.0  
h-Btu/lbm 1205.9 1231.5 1256.5 1305.8 1355.0 1404.6 1454.9 1505.9 1557.8 1610.5 1664.1 1718.6  
s-Btu/lbm/R 1.68079 1.71180 1.74036 1.79226 1.83917 1.88236 1.92261 1.96043 1.99620 2.03022 2.06272 2.09388

Press = 80.0 psi, Tsat = 771.7 R  
T(R) = 800. 850. 900. 1000. 1100. 1200. 1300. 1400. 1500. 1600. 1700. 1800.  
v-ft3/lbm 5.7361 6.1561 6.5625 7.3528 8.1271 8.8927 9.6532 10.4103 11.1650 11.9180 12.6698 13.4206  
u-Btu/lbm 1117.0 1137.4 1157.0 1195.3 1233.5 1272.1 1311.3 1351.3 1392.1 1433.7 1476.3 1519.8  
h-Btu/lbm 1201.8 1228.4 1254.1 1304.1 1353.7 1403.7 1454.1 1505.3 1557.3 1610.1 1663.8 1718.3  
s-Btu/lbm/R 1.64497 1.67722 1.70652 1.75924 1.80656 1.84999 1.89039 1.92831 1.96416 1.99823 2.03077 2.06196

Press = 100.0 psi, Tsat = 787.5 R  
T(R) = 800. 850. 900. 1000. 1100. 1200. 1300. 1400. 1500. 1600. 1700. 1800.  
v-ft3/lbm 4.5358 4.8839 5.2169 5.8589 6.4842 7.1007 7.7119 8.3196 8.9250 9.5287 10.1312 10.7327  
u-Btu/lbm 1113.6 1134.9 1155.1 1194.1 1232.6 1271.4 1310.7 1350.8 1391.7 1433.4 1476.0 1519.5  
h-Btu/lbm 1197.5 1225.2 1251.6 1302.4 1352.5 1402.7 1453.4 1504.7 1556.7 1609.6 1663.4 1718.0  
s-Btu/lbm/R 1.61596 1.64965 1.67975 1.73333 1.78107 1.82474 1.86529 1.90332 1.93924 1.97337 2.00595 2.03717

Press = 120.0 psi, Tsat = 800.9 R

T(R) = 850. 900. 1000. 1100. 1200. 1300. 1400. 1500. 1600. 1700. 1800. 1900.  
v-ft3/lbm 4.0347 4.3192 4.8628 5.3889 5.9059 6.4176 6.9259 7.4317 7.9359 8.4388 8.9407 9.4420  
u-Btu/lbm 1132.4 1153.2 1192.8 1231.7 1270.7 1310.2 1350.3 1391.3 1433.1 1475.7 1519.7 1563.7  
h-Btu/lbm 1221.9 1249.0 1300.7 1351.3 1401.7 1452.6 1504.0 1556.2 1609.2 1663.0 1717.7 1773.2  
s-Btu/lbm/R 1.62645 1.65742 1.71191 1.76009 1.80401 1.84471 1.88284 1.91884 1.95302 2.01689 2.04692

Press = 140.0 psi, Tsat = 812.7 R  
T(R) = 850. 900. 1000. 1100. 1200. 1300. 1400. 1500. 1600. 1700. 1800. 1900.  
v-ft3/lbm 3.4272 3.6775 4.1511 4.6064 5.0525 5.4931 5.9303 6.3651 6.7981 7.2299 7.6608 8.0909  
u-Btu/lbm 1129.7 1151.2 1191.5 1230.7 1269.9 1309.6 1349.9 1390.9 1432.7 1475.4 1519.0 1563.5  
h-Btu/lbm 1218.5 1246.4 1299.0 1350.0 1400.8 1451.8 1503.4 1555.7 1608.8 1662.6 1717.4 1772.9  
s-Btu/lbm/R 1.60622 1.63813 1.693358 1.74221 1.78638 1.82724 1.86547 1.90154 1.93578 1.96844 1.99972 2.02977

Press = 160.0 psi, Tsat = 823.2 R  
T(R) = 850. 900. 1000. 1100. 1200. 1300. 1400. 1500. 1600. 1700. 1800. 1900.  
v-ft3/lbm 2.9707 3.1958 3.6172 4.0195 4.4124 4.7998 5.1836 5.5651 5.9448 6.3233 6.7008 7.0776  
u-Btu/lbm 1127.0 1149.1 1190.2 1229.8 1269.2 1309.0 1349.4 1390.5 1432.4 1475.1 1518.7 1563.2  
h-Btu/lbm 1214.9 1243.7 1297.2 1348.7 1398.9 1450.1 1502.8 1555.2 1608.3 1662.2 1717.0 1772.7  
s-Btu/lbm/R 1.58812 1.62105 1.67750 1.72659 1.77102 1.81204 1.85038 1.88653 1.92082 1.95351 1.98482 2.01490

Press = 180.0 psi, Tsat = 832.8 R  
T(R) = 850. 900. 1000. 1100. 1200. 1300. 1400. 1500. 1600. 1700. 1800. 1900.  
v-ft3/lbm 2.6148 2.8207 3.2017 3.5630 3.9145 4.2605 4.6029 4.9428 5.2811 5.6181 5.9541 6.2895  
u-Btu/lbm 1124.1 1147.0 1188.9 1228.8 1268.5 1308.4 1348.9 1390.1 1432.1 1474.8 1518.5 1563.0  
h-Btu/lbm 1211.1 1240.9 1295.4 1347.5 1398.8 1450.3 1502.1 1554.6 1607.9 1661.9 1716.7 1772.4  
s-Btu/lbm/R 1.57158 1.60564 1.66314 1.71272 1.75740 1.79858 1.83703 1.87325 1.90759 1.94033 1.97167 2.00177

Press = 200.0 psi, Tsat = 841.5 R  
T(R) = 850. 900. 1000. 1100. 1200. 1300. 1400. 1500. 1600. 1700. 1800. 1900.  
v-ft3/lbm 2.3291 2.5202 2.8693 3.1977 3.5162 3.8290 4.1382 4.4451 4.7501 5.0540 5.3568 5.6590  
u-Btu/lbm 1121.0 1144.8 1187.5 1227.9 1267.8 1307.8 1348.4 1389.7 1431.7 1474.6 1518.2 1562.8  
h-Btu/lbm 1207.2 1238.1 1293.6 1346.2 1397.8 1449.5 1501.5 1554.1 1607.4 1661.5 1716.4 1772.1  
s-Btu/lbm/R 1.55619 1.59152 1.65013 1.70020 1.74515 1.78649 1.82505 1.86134 1.89574 1.92852 1.95989 1.99002

Press = 250.0 psi, Tsat = 860.7 R  
T(R) = 900. 1000. 1100. 1200. 1300. 1400. 1500. 1600. 1700. 1800. 1900. 2000.  
v-ft3/lbm 1.9779 2.2703 2.5400 2.7991 3.0523 3.3019 3.5490 3.7944 4.0385 4.2816 4.5241 4.7660  
u-Btu/lbm 1139.1 1184.1 1225.5 1265.9 1306.4 1347.2 1388.7 1430.9 1473.8 1517.6 1562.2 1607.7  
h-Btu/lbm 1230.6 1289.0 1342.9 1395.4 1447.5 1499.9 1552.8 1606.3 1660.5 1715.6 1771.4 1828.1  
s-Btu/lbm/R 1.56033 1.62195 1.67333 1.71896 1.76072 1.79954 1.83603 1.87056 1.90344 1.93489 1.96507 1.99414

Press = 300.0 psi, Tsat = 877.0 R

T(R) = 900. 1000. 1100. 1200. 1300. 1400. 1500. 1600. 1700. 1800. 1900. 2000.  
 v-ft3/lbm 1.6144 1.8704 2.1013 2.3209 2.5345 2.7443 2.9517 3.1572 3.3615 3.5649 3.7675 3.9696  
 u-Btu/lbm 1133.0 1180.5 1223.0 1264.1 1304.9 1346.0 1387.7 1430.0 1473.1 1517.0 1561.7 1607.2  
 h-Btu/lbm 1222.6 1284.2 1339.6 1392.9 1445.5 1498.3 1551.5 1605.2 1659.6 1714.8 1770.7 1827.5  
 s-Btu/lbm/R 1.53305 1.59813 1.65091 1.69726 1.73944 1.77854 1.81522 1.84989 1.88287 1.91439 1.94463 1.97375

Press = 350.0 psi, Tsat = 891.4 R  
 T(R) = 900. 1000. 1100. 1200. 1300. 1400. 1500. 1600. 1700. 1800. 1900. 2000.  
 v-ft3/lbm 1.3527 1.5842 1.7877 1.9793 2.1646 2.3460 2.5250 2.7021 2.8780 3.0529 3.2270 3.4007  
 u-Btu/lbm 1126.2 1176.7 1220.5 1262.2 1303.4 1344.8 1386.7 1429.2 1472.4 1516.3 1561.1 1606.7  
 h-Btu/lbm 1213.8 1279.3 1336.2 1390.3 1443.6 1496.7 1550.1 1604.1 1658.7 1713.9 1770.7 1826.8  
 s-Btu/lbm/R 1.50812 1.57726 1.63155 1.67865 1.72127 1.76065 1.79752 1.83233 1.86541 1.89701 1.92731 1.95647

Press = 400.0 psi, Tsat = 904.3 R  
 T(R) = 1000. 1100. 1200. 1300. 1400. 1500. 1600. 1700. 1800. 1900. 2000. 2100.  
 v-ft3/lbm 1.3691 1.5523 1.7230 1.8871 2.0473 2.2049 2.3608 2.5153 2.6689 2.8217 2.9741 3.1259  
 u-Btu/lbm 1172.8 1217.9 1260.3 1302.0 1343.6 1385.7 1428.3 1471.6 1515.7 1560.5 1606.2 1652.7  
 h-Btu/lbm 1274.1 1332.7 1397.8 1441.6 1495.1 1548.8 1603.0 1657.7 1713.1 1769.3 1826.2 1884.0  
 s-Btu/lbm/R 1.55851 1.61441 1.66230 1.70536 1.74503 1.78209 1.81704 1.85022 1.88190 1.91226 1.94146 1.96963

Press = 450.0 psi, Tsat = 916.0 R  
 T(R) = 1000. 1100. 1200. 1300. 1400. 1500. 1600. 1700. 1800. 1900. 2000. 2100.  
 v-ft3/lbm 1.2012 1.3691 1.5236 1.6712 1.8149 1.9560 2.0953 2.2332 2.3702 2.5065 2.6422 2.7775  
 u-Btu/lbm 1169.8 1215.3 1258.4 1300.5 1342.4 1384.7 1427.5 1470.9 1515.0 1560.0 1605.7 1652.3  
 h-Btu/lbm 1268.8 1329.2 1385.2 1439.5 1493.5 1547.5 1601.8 1656.8 1712.3 1768.6 1825.6 1883.4  
 s-Btu/lbm/R 1.54131 1.59895 1.64767 1.69119 1.73115 1.76840 1.80349 1.83678 1.86653 1.89895 1.92820 1.95640

Press = 500.0 psi, Tsat = 926.7 R  
 T(R) = 1000. 1100. 1200. 1300. 1400. 1500. 1600. 1700. 1800. 1900. 2000. 2100.  
 v-ft3/lbm 1.0665 1.2223 1.3640 1.4985 1.6290 1.7568 1.8828 2.0075 2.1313 2.2543 2.3767 2.4987  
 u-Btu/lbm 1164.6 1212.6 1256.4 1298.9 1341.2 1383.7 1426.6 1470.2 1514.4 1559.4 1605.2 1651.8  
 h-Btu/lbm 1263.2 1325.6 1382.6 1437.5 1491.8 1546.1 1600.7 1655.8 1711.5 1767.9 1825.0 1882.9  
 s-Btu/lbm/R 1.52530 1.58481 1.63438 1.67838 1.71863 1.75608 1.79132 1.82471 1.85654 1.88702 1.91631 1.94454

Press = 550.0 psi, Tsat = 936.7 R  
 T(R) = 1000. 1100. 1200. 1300. 1400. 1500. 1600. 1700. 1800. 1900. 2000. 2100.  
 v-ft3/lbm 0.9559 1.1021 1.2333 1.3572 1.4769 1.5939 1.7091 1.8229 1.9358 2.0479 2.1595 2.2707  
 u-Btu/lbm 1160.2 1209.8 1254.5 1297.4 1340.0 1382.6 1425.7 1469.4 1513.8 1558.8 1604.7 1651.3  
 h-Btu/lbm 1257.5 1321.9 1379.9 1435.5 1490.2 1544.8 1599.6 1654.8 1710.7 1767.2 1824.4 1882.3  
 s-Btu/lbm/R 1.51020 1.57171 1.62218 1.66666 1.70722 1.74487 1.78025 1.81374 1.84565 1.87619 1.90552 1.93380

Press = 600.0 psi, Tsat = 945.9 R

### C.8 H<sub>2</sub>O Compressed Liquid Tables (English Units)

T(R) =	1000.	1100.	1200.	1300.	1400.	1500.	1600.	1700.	1800.	1900.	2000.	2100.
v-ft3/lbm	0.8632	1.0017	1.1243	1.2394	1.3501	1.4581	1.5642	1.6690	1.7729	1.8760	1.9785	2.0806
s-Btu/lbm	1155.7	1207.0	1252.5	1295.9	1338.7	1381.6	1424.9	1468.7	1513.1	1558.3	1604.2	1650.9
h-Btu/lbm	1251.5	1318.2	1377.2	1433.4	1488.5	1543.4	1598.5	1653.9	1709.8	1766.4	1823.7	1881.8
s-Btu/lbm/R	1.49578	1.55946	1.61087	1.65586	1.69672	1.73458	1.77010	1.80369	1.83568	1.86628	1.89566	1.92397

```

Press = 700.0 psi, Tsat = 962.8 R
T(R) =      1000.    1100.    1200.    1300.    1400.    1500.    1600.    1700.    1800.    1900.    2000.    2100.
v-ft3/lbm   0.7162   0.8437   0.9530   1.0541   1.1508   1.2447   1.3366   1.4272   1.5169   1.6057   1.6941   1.7820
u-Btu/lbm   1145.9   1201.2   1248.4   1292.8   1336.2   1379.6   1423.2   1467.2   1511.8   1557.1   1603.2   1650.0
h-Btu/lbm   1238.6   1310.4   1371.8   1429.3   1485.2   1540.7   1596.2   1652.0   1708.2   1765.0   1822.5   1880.7
s-Btu/lbm/R 1.46837  1.53696  1.59037  1.63641  1.67790  1.71617  1.75198  1.78579  1.81793  1.84865  1.87812  1.90650

```

```

Press = 800.0 psi, Tsat = 977.9 R
T(R) = 1000. 1100. 1200. 1300. 1400. 1500. 1600. 1700. 1800. 1900. 2000. 2100.
v-ft3/lbm 0.6041 0.7246 0.8243 0.9151 1.0013 1.0846 1.1659 1.2459 1.3249 1.4031 1.4807 1.5580
u-Btu/lbm 1134.9 1195.1 1244.2 1289.6 1333.7 1377.5 1421.4 1465.7 1510.5 1556.0 1602.1 1649.0
h-Btu/lbm 1224.3 1302.3 1366.2 1425.0 1481.9 1538.0 1593.9 1650.0 1706.6 1763.6 1821.2 1879.6
s-Btu/lbm/R 1.44194 1.51644 1.57205 1.61919 1.66134 1.70004 1.73614 1.77016 1.80246 1.83330 1.86286 1.89131

```

```

Press = 900.0 psi, Tsat = 991.7 R
T(R) =      1000.    1100.    1200.    1300.    1400.    1500.    1600.    1700.    1800.    1900.    2000.    2100.
v-ft3/lbm   0.5148   0.6315   0.7239   0.8069   0.8850   0.9600   1.0331   1.1048   1.1755   1.2454   1.3148   1.3838
u-Btu/lbm   1122.5   1188.7   1239.9   1286.4   1331.2   1375.4   1419.7   1464.2   1509.2   1554.9   1601.1   1648.1
h-Btu/lbm   1208.2   1293.8   1360.4   1420.7   1478.5   1535.2   1591.6   1648.1   1704.9   1762.2   1820.0   1878.5
s-Btu/lbm/R 1.41552  1.49735  1.55536  1.60367  1.64649  1.68563  1.72203  1.75627  1.78873  1.81969  1.84934  1.87787

```

```

Press = 1000.0 psi, Tsat = 1004.3 R
T(R) =    1100.   1200.   1300.   1400.   1500.   1600.   1700.   1800.   1900.   2000.   2100.   2200.
v-ft3/lbm   0.5565  0.6435  0.7203  0.7919  0.8604  0.9269  0.9920  1.0560  1.1193  1.1821  1.2444  1.3063
u-Btu/lbm   1181.9  1235.5  1283.2  1328.6  1373.3  1417.9  1462.7  1507.9  1553.7  1600.1  1647.2  1695.1
h-Btu/lbm   1284.9  1335.4  1416.4  1475.1  1535.2  1589.3  1646.2  1703.2  1760.7  1818.7  1877.4  1936.7
s-Btu/lbm/R 1.47927 1.53992 1.58948 1.63300 1.67258 1.70929 1.74374 1.77636 1.80744 1.83719 1.86579 1.89338

```

```

Press = 1100.0 psi, Tsat = 1016.0 R
T(R) =      1100.    1200.    1300.    1400.    1500.    1600.    1700.    1800.    1900.    2000.    2100.    2200.
v-ft3/lbm   0.4947   0.5776   0.6493   0.7157   0.7788   0.8399   0.8996   0.9583   1.0162   1.0735   1.1304   1.1869
u-Btu/lbm   1174.8   1230.9   1279.8   1326.1   1371.2   1416.1   1461.2   1506.6   1552.6   1599.1   1646.3   1694.2
h-Btu/lbm   1275.5   1348.4   1411.9   1471.6   1529.7   1587.0   1644.2   1701.6   1759.3   1817.5   1876.2   1935.7
s-Btu/lbm/R 1.46191  1.52547  1.57634  1.62060  1.66064  1.69765  1.73233  1.76511  1.79631  1.82615  1.85482  1.88247

```

Press = 1200.0 psi, Tsat = 1026.9 R

T(R) =	1100.	1200.	1300.	1400.	1500.	1600.	1700.	1800.	1900.	2000.	2100.	2200.
v-ft3/lbm	0.4428	0.5224	0.5901	0.6521	0.7109	0.7675	0.8227	0.8768	0.9302	0.9830	1.0353	1.0873
u-Btu/lbm	1167.3	1226.2	1276.5	1323.4	1369.1	1414.4	1459.7	1505.3	1551.4	1598.1	1645.4	1693.4
h-Btu/lbm	1265.6	1342.2	1407.4	1468.2	1526.9	1584.7	1642.3	1699.9	1757.9	1816.2	1875.1	1934.7
s-Btu/lbm/R	1.44502	1.51180	1.56408	1.60909	1.64959	1.68692	1.72182	1.75477	1.78609	1.81602	1.84477	1.87248

```

Press = 1300.0 psi, Tsat = 1037.2 R
T(R) =    1100.   1200.   1300.   1400.   1500.   1600.   1700.   1800.   1900.   2000.   2100.   2200.
v-ft3/lbm   0.3983   0.4756   0.5400   0.5983   0.6533   0.7062   0.7576   0.8079   0.8575   0.9064   0.9549   1.0031
u-Btu/lbm   1159.3   1221.4   1273.0   1320.8   1367.0   1412.6   1458.2   1504.0   1550.3   1597.0   1644.4   1692.6
h-Btu/lbm   1255.0   1335.8   1402.9   1464.6   1524.0   1582.4   1640.3   1698.2   1756.4   1815.0   1874.0   1933.7
s-Btu/lbm/R 1.42838  1.49877  1.55252  1.59832  1.63931  1.67696  1.71208  1.74519  1.77664  1.80667  1.83549  1.86326

```

```

Press = 1400.0 psi, Tsat = 1046.8 R
T(R) =    1100.   1200.   1300.   1400.   1500.   1600.   1700.   1800.   1900.   2000.   2100.   2200.
v-ft3/lbm   0.3596   0.4354   0.4969   0.5522   0.6040   0.6536   0.7017   0.7488   0.7951   0.8408   0.8860   0.9309
u-Btu/lbm   1150.7   1216.4   1269.5   1318.1   1364.8   1410.8   1456.6   1502.7   1549.1   1596.0   1643.5   1691.7
h-Btu/lbm   1243.8   1329.2   1398.2   1461.1   1521.2   1580.0   1638.3   1696.6   1755.0   1813.7   1872.9   1932.8
s-Btu/lbm/R 1.41181  1.48626  1.54158  1.58819  1.62967  1.66764  1.70300  1.73627  1.76785  1.79796  1.82686  1.85470

```

```

Press = 1500.0 psi, Tsat = 1055.9 R
T(R) =      1100.    1200.    1300.    1400.    1500.    1600.    1700.    1800.    1900.
v-ft3/lbm   0.3255   0.4003   0.4596   0.5122   0.5613   0.6081   0.6534   0.6976   0.7411
u-Btu/lbm   1141.5   1211.3   1266.0   1315.4   1362.6   1409.0   1455.1   1501.4   1547.9
h-Btu/lbm   1231.7   1323.4   1393.5   1457.5   1518.3   1577.7   1636.4   1694.9   1753.5
s-Btu/lbm/R 1.39510  1.47415  1.53114  1.57860  1.62058  1.65889  1.69447  1.72792  1.75962

```

```

Press = 1600.0 psi, Tsat = 1064.6 R
T(R) =      1100.    1200.    1300.    1400.    1500.    1600.    1700.    1800.    1900.
v-ft3/lbm   0.2950   0.3695   0.4268   0.4772   0.5238   0.5682   0.6110   0.6528   0.6938
u-Btu/lbm   1131.4   1206.0   1262.4   1312.7   1360.4   1407.2   1453.6   1500.0   1546.8
h-Btu/lbm   1218.7   1315.3   1388.7   1453.9   1515.5   1575.3   1634.4   1692.3   1752.1
s-Btu/lbm/R 1.37804  1.46238  1.52113  1.56948  1.61198  1.65062  1.68643  1.72005  1.75187

```

```

Press = 1700.0 psi, Tsat = 1072.9 R
T(R) =    1100.   1200.   1300.   1400.   1500.   1600.   1700.   1800.   1900.
v-ft3/lbm = 0.2673  0.3422  0.3979  0.4462  0.4908  0.5330  0.5737  0.6133  0.6521
u-Btu/lbm = 1120.4  1200.5  1258.7  1309.9  1358.2  1405.4  1452.0  1498.7  1545.6
h-Btu/lbm = 1204.5  1308.1  1383.8  1450.2  1512.6  1572.9  1632.4  1691.5  1750.6
s-Btu/lbm/R = 1.36037  1.45087  1.51150  1.56076  1.60379  1.64277  1.67883  1.71261  1.75000

```

Press = 1800.0 psi, Tsat = 1080.7 R

T(R) =	1100.	1200.	1300.	1400.	1500.	1600.	1700.	1800.	1900.
v-ft3/lbm	0.2418	0.3178	0.3721	0.4187	0.4614	0.5017	0.5405	0.5781	0.6150
u-Btu/lbm	1108.2	1194.8	1254.9	1307.1	1356.0	1403.5	1450.5	1497.4	1544.4
h-Btu/lbm	1188.7	1300.6	1378.8	1446.5	1509.6	1570.6	1630.4	1689.8	1749.2
s-Btu/lbm/R	1.34174	1.43955	1.50219	1.55240	1.59598	1.63531	1.67160	1.70555	1.73764

Press = 1900.0 psi, Tsat = 1088.3 R									
T(R) =	1100.	1200.	1300.	1400.	1500.	1600.	1700.	1800.	1900.
v-ft3/lbm	0.2179	0.2958	0.3490	0.3941	0.4351	0.4738	0.5108	0.5467	0.5818
u-Btu/lbm	1094.2	1189.0	1251.1	1304.3	1353.8	1401.7	1448.9	1496.0	1543.3
h-Btu/lbm	1170.8	1292.9	1373.7	1442.7	1506.7	1568.2	1628.4	1688.1	1747.7
s-Btu/lbm/R	1.32165	1.42838	1.49317	1.54436	1.58849	1.62817	1.66471	1.69884	1.73105

Press = 2000.0 psi, Tsat = 1095.5 R									
T(R) =	1100.	1200.	1300.	1400.	1500.	1600.	1700.	1800.	1900.
v-ft3/lbm	0.1949	0.2758	0.3281	0.3719	0.4115	0.4486	0.4840	0.5184	0.5519
u-Btu/lbm	1077.8	1182.8	1247.2	1301.4	1351.5	1399.8	1447.4	1494.7	1542.1
h-Btu/lbm	1149.9	1284.9	1368.5	1439.0	1503.7	1565.8	1626.4	1686.4	1746.2
s-Btu/lbm/R	1.29918	1.41730	1.48438	1.53660	1.58130	1.62134	1.65812	1.69242	1.72476

Press = 2500.0 psi, Tsat = 1127.8 R								
T(R) =	1200.	1300.	1400.	1500.	1600.	1700.	1800.	1900.
v-ft3/lbm	0.1980	0.2483	0.2873	0.3214	0.3528	0.3824	0.4109	0.4385
u-Btu/lbm	1148.2	1226.4	1286.5	1340.0	1390.4	1439.5	1487.9	1536.2
h-Btu/lbm	1239.7	1341.3	1419.4	1488.6	1553.6	1616.3	1677.9	1738.9
s-Btu/lbm/R	1.36160	1.44310	1.50107	1.54884	1.59077	1.62881	1.66401	1.69701

Press = 3000.0 psi, Tsat = 1155.1 R								
T(R) =	1200.	1300.	1400.	1500.	1600.	1700.	1800.	1900.
v-ft3/lbm	0.1421	0.1943	0.2307	0.2613	0.2889	0.3147	0.3392	0.3629
u-Btu/lbm	1103.1	1203.5	1270.8	1328.0	1380.8	1431.5	1481.1	1530.2
h-Btu/lbm	1181.9	1311.3	1398.8	1473.0	1541.1	1606.1	1669.3	1731.6
s-Btu/lbm/R	1.30046	1.40439	1.46935	1.52058	1.56455	1.60393	1.64007	1.67375

Press = 3500.0 psi								
T(R) =	1200.	1300.	1400.	1500.	1600.	1700.	1800.	1900.
v-ft3/lbm	0.0244	0.1550	0.1900	0.2183	0.2433	0.2663	0.2881	0.3089
u-Btu/lbm	720.0	1177.7	1254.1	1315.6	1370.9	1423.3	1474.1	1524.2
h-Btu/lbm	768.0	1278.1	1377.1	1456.9	1528.4	1595.7	1660.6	1724.2
s-Btu/lbm/R	0.91193	1.36649	1.44004	1.49513	1.54131	1.58210	1.61920	1.65358

Press = 4000.0 psi

T(R) =	1200.	1300.	1400.	1500.	1600.	1700.	1800.	1900.
v-ft3/lbm	0.0240	0.1249	0.1594	0.1860	0.2091	0.2301	0.2497	0.2685
u-Btu/lbm	714.7	1148.8	1236.4	1302.7	1360.8	1415.0	1467.1	1518.2
h-Btu/lbm	765.3	1241.1	1354.3	1440.3	1515.5	1585.2	1651.9	1716.8
s-Btu/lbm/R	0.90685	1.32818	1.41226	1.47167	1.52020	1.56247	1.60058	1.63567

Press = 4500.0 psi								
T(R) =	1200.	1300.	1400.	1500.	1600.	1700.	1800.	1900.
v-ft3/lbm	0.0237	0.1009	0.1355	0.1609	0.1825	0.2019	0.2200	0.2370
u-Btu/lbm	709.9	1116.0	1217.7	1289.4	1350.5	1406.6	1460.0	1512.1
h-Btu/lbm	763.2	1200.0	1330.4	1423.4	1502.4	1574.6	1643.1	1709.3
s-Btu/lbm/R	0.90232	1.28852	1.38550	1.44969	1.50072	1.54453	1.58367	1.61949

Press = 5000.0 psi								
T(R) =	1200.	1300.	1400.	1500.	1600.	1700.	1800.	1900.
v-ft3/lbm	0.0234	0.0815	0.1163	0.1409	0.1613	0.1794	0.1962	0.2119
u-Btu/lbm	705.6	1079.1	1198.0	1275.8	1340.0	1398.1	1452.9	1505.9
h-Btu/lbm	761.3	1154.4	1305.5	1406.0	1489.1	1564.0	1634.3	1701.9
s-Btu/lbm/R	0.89820	1.24703	1.35941	1.42885	1.48252	1.52792	1.56811	1.60468

Temperature=	500.0 R	Psat=	0.1 psi							
Press(psi)=	250	500	1000	1500	2000	2500	3000	3500	4000	5000
v-ft3/lbm	0.016	0.016	0.016	0.016	0.016	0.0159	0.0159	0.0159	0.0159	0.0158
u-Btu/lbm	8.4	8.4	8.4	8.4	8.3	8.3	8.3	8.3	8.3	8.3
h-Btu/lbm	9.1	9.9	11.3	12.8	14.3	15.7	17.1	18.6	20	22.9
s-Btu/lbm/R	0.0169	0.01689	0.01687	0.01684	0.0168	0.01675	0.0167	0.01664	0.01657	0.01641
Temperature=	550.0 R	Psat=	0.7 psi							
Press(psi)=	250	500	1000	1500	2000	2500	3000	3500	4000	5000
v-ft3/lbm	0.0161	0.0161	0.0161	0.0161	0.016	0.016	0.016	0.016	0.016	0.0159
u-Btu/lbm	58.4	58.4	58.2	58.1	57.9	57.8	57.6	57.5	57.4	57.1
h-Btu/lbm	59.2	59.9	61.2	62.5	63.9	65.2	66.5	67.8	69.2	71.8
s-Btu/lbm/R	0.11232	0.11219	0.11192	0.11165	0.11137	0.1111	0.11082	0.11054	0.11026	0.1097
Temperature=	600.0 R	Psat=	2.9 psi							
Press(psi)=	250	500	1000	1500	2000	2500	3000	3500	4000	5000
v-ft3/lbm	0.0163	0.0163	0.0163	0.0163	0.0162	0.0162	0.0162	0.0162	0.0161	0.0161
u-Btu/lbm	108.4	108.3	108	107.8	107.5	107.3	107	106.8	106.5	106.1
h-Btu/lbm	109.2	109.8	111	112.3	113.5	114.8	116	117.2	118.5	120.9
s-Btu/lbm/R	0.19929	0.19907	0.19864	0.1982	0.19777	0.19734	0.19691	0.19648	0.19606	0.19521
Temperature=	650.0 R	Psat=	9.4 psi							
Press(psi)=	250	500	1000	1500	2000	2500	3000	3500	4000	5000
v-ft3/lbm	0.0166	0.0166	0.0166	0.0165	0.0165	0.0165	0.0165	0.0164	0.0164	0.0164
u-Btu/lbm	158.5	158.3	158	157.6	157.2	156.9	156.5	156.2	155.8	155.2
h-Btu/lbm	159.3	159.9	161	162.2	163.3	164.5	165.6	166.8	168	170.3
s-Btu/lbm/R	0.27953	0.27924	0.27866	0.27809	0.27752	0.27695	0.27639	0.27584	0.27529	0.27419
Temperature=	700.0 R	Psat=	25.1 psi							
Press(psi)=	250	500	1000	1500	2000	2500	3000	3500	4000	5000
v-ft3/lbm	0.017	0.0169	0.0169	0.0169	0.0169	0.0168	0.0168	0.0168	0.0167	0.0167
u-Btu/lbm	209	208.7	208.2	207.7	207.2	206.8	206.3	205.8	205.4	204.5
h-Btu/lbm	209.7	210.3	211.3	212.4	213.5	214.5	215.6	216.7	217.8	219.9
s-Btu/lbm/R	0.35431	0.35395	0.35323	0.35252	0.35182	0.35113	0.35044	0.34976	0.34908	0.34775
Temperature=	750.0 R	Psat=	57.9 psi							
Press(psi)=	250	500	1000	1500	2000	2500	3000	3500	4000	5000
v-ft3/lbm	0.0174	0.0174	0.0173	0.0173	0.0173	0.0172	0.0172	0.0172	0.0171	0.0171
u-Btu/lbm	259.9	259.6	259	258.3	257.7	257.1	256.5	255.9	255.3	254.2
h-Btu/lbm	260.7	261.2	262.2	263.1	264.1	265.1	266	267	268	270
s-Btu/lbm/R	0.42467	0.42423	0.42337	0.42251	0.42167	0.42083	0.42001	0.41919	0.41839	0.41681
Temperature=	800.0 R	Psat=	118.5 psi							
Press(psi)=	250	500	1000	1500	2000	2500	3000	3500	4000	5000
v-ft3/lbm	0.0179	0.0179	0.0178	0.0178	0.0178	0.0177	0.0177	0.0176	0.0176	0.0175
u-Btu/lbm	311.7	311.3	310.4	309.6	308.8	308.1	307.3	306.5	305.8	304.4
h-Btu/lbm	312.5	312.9	313.7	314.6	315.4	316.2	317.1	318	318.8	320.6
s-Btu/lbm/R	0.49152	0.49099	0.48994	0.48891	0.4879	0.4869	0.48592	0.48495	0.484	0.48212
Temperature=	850.0 R	Psat=	221.1 psi							
Press(psi)=	250	500	1000	1500	2000	2500	3000	3500	4000	5000
v-ft3/lbm	0.0185	0.0185	0.0185	0.0184	0.0184	0.0183	0.0183	0.0182	0.0182	0.0181
u-Btu/lbm	364.6	364.1	363	362	360.9	359.9	358.9	358	357.1	355.2
h-Btu/lbm	365.5	365.8	366.4	367.1	367.7	368.4	369.1	369.8	370.5	372
s-Btu/lbm/R	0.55573	0.55508	0.5538	0.55255	0.55132	0.55012	0.54894	0.54778	0.54664	0.54442

Temperature=	900.0 R	Psat=	382.7 psi							
Press(psi)=	250	500	1000	1500	2000	2500	3000	3500	4000	5000
v-ft3/lbm		0.0193	0.0192	0.0192	0.0191	0.019	0.019	0.0189	0.0188	0.0187
u-Btu/lbm		418.6	417.1	415.8	414.4	413.1	411.8	410.6	409.4	407.1
h-Btu/lbm		420.4	420.7	421.1	421.5	421.9	422.4	422.9	423.4	424.4
s-Btu/lbm/R		0.61744	0.61584	0.61428	0.61277	0.61129	0.60985	0.60844	0.60706	0.6044
Temperature=	950.0 R	Psat=	623.1 psi							
Press(psi)=	250	500	1000	1500	2000	2500	3000	3500	4000	5000
v-ft3/lbm			0.0202	0.0201	0.02	0.0199	0.0198	0.0197	0.0197	0.0195
u-Btu/lbm			473.7	471.8	470	468.2	466.6	464.9	463.4	460.4
h-Btu/lbm			477.4	477.4	477.4	477.4	477.6	477.7	477.9	478.4
s-Btu/lbm/R			0.67717	0.67515	0.67321	0.67133	0.66951	0.66775	0.66604	0.66277
Temperature=	1000.0 R	Psat=	964.9 psi							
Press(psi)=	250	500	1000	1500	2000	2500	3000	3500	4000	5000
v-ft3/lbm			0.0215	0.0214	0.0212	0.0211	0.0209	0.0208	0.0207	0.0205
u-Btu/lbm			534.2	531.4	528.8	526.3	524	521.8	519.6	515.7
h-Btu/lbm			538.2	537.4	536.7	536.1	535.6	535.2	534.9	534.6
s-Btu/lbm/R			0.73949	0.73666	0.73399	0.73146	0.72905	0.72675	0.72454	0.72038
Temperature=	1050.0 R	Psat=	1434.3 psi							
Press(psi)=	250	500	1000	1500	2000	2500	3000	3500	4000	5000
v-ft3/lbm				0.0232	0.0229	0.0227	0.0224	0.0222	0.0221	0.0217
u-Btu/lbm				597.7	593.4	589.5	585.9	582.6	579.5	573.9
h-Btu/lbm				604.2	601.9	599.9	598.3	597	595.8	594
s-Btu/lbm/R				0.80183	0.7976	0.79376	0.79024	0.78696	0.7839	0.7783
Temperature=	1100.0 R	Psat=	2063.9 psi							
Press(psi)=	250	500	1000	1500	2000	2500	3000	3500	4000	5000
v-ft3/lbm						0.0254	0.0249	0.0244	0.024	0.0234
u-Btu/lbm						663.3	656.4	650.6	645.4	636.7
h-Btu/lbm						675.1	670.2	666.4	663.2	658.4
s-Btu/lbm/R						0.86361	0.85706	0.85149	0.8466	0.83821



# Appendix D: Thermodynamic Property Tables for Carbon Dioxide

## D.1 CO<sub>2</sub> Saturation Temperature Table (SI Units)

T(K)	P(MPa)	Volume (m <sup>3</sup> /kg)			Energy (kJ/kg)			Enthalpy (kJ/kg)			Entropy (kJ/kg/K)		
		vf	vfg	vg	uf	ufg	ug	hf	hfg	hg	sf	sfg	sg
216.5	0.5173	0.000847	0.071931	0.072778	0.00	314.66	314.23	0.00	351.87	351.87	0.00000	1.62497	1.62497
220.0	0.6000	0.000857	0.062281	0.063137	6.49	308.75	315.24	7.01	346.12	353.12	0.03175	1.57326	1.60501
225.0	0.7365	0.000871	0.050940	0.051811	16.89	299.69	316.57	17.52	337.21	354.73	0.07948	1.49872	1.57720
230.0	0.8949	0.000885	0.041984	0.042869	27.28	290.46	317.73	28.07	328.03	356.09	0.12425	1.42620	1.55046
235.0	1.0769	0.000901	0.034828	0.035729	37.55	281.17	318.72	38.52	318.68	357.19	0.16850	1.35607	1.52457
240.0	1.2849	0.000918	0.029049	0.029967	47.72	271.77	319.49	48.90	309.10	358.00	0.21142	1.28791	1.49934
245.0	1.5211	0.000936	0.024333	0.025269	57.89	262.15	320.04	59.32	299.16	358.48	0.25348	1.22106	1.47454
250.0	1.7875	0.000956	0.020449	0.021405	68.15	252.18	320.33	69.85	288.74	358.59	0.29503	1.15495	1.44998
255.0	2.0866	0.000977	0.017223	0.018199	78.52	241.80	320.32	80.56	277.73	358.30	0.33630	1.08914	1.42545
260.0	2.4208	0.001001	0.014516	0.015516	89.06	230.91	319.97	91.49	266.05	357.53	0.37744	1.02326	1.40070
265.0	2.7924	0.001027	0.012227	0.013254	99.79	215.43	319.22	102.66	253.57	356.23	0.41856	0.95688	1.37544
270.0	3.2043	0.001056	0.010272	0.011328	110.77	207.22	317.99	114.16	240.13	354.29	0.45995	0.88937	1.34933
275.0	3.6592	0.001090	0.008586	0.009676	122.13	194.04	316.17	126.12	225.46	351.57	0.50204	0.81985	1.32188
280.0	4.1602	0.001129	0.007113	0.008242	134.02	179.57	313.59	138.72	209.16	347.88	0.54545	0.74701	1.29246
285.0	4.7106	0.001177	0.005805	0.006982	146.67	163.35	310.01	152.21	190.69	342.90	0.59086	0.66910	1.26006
290.0	5.3143	0.001239	0.004616	0.005954	160.36	144.62	304.98	166.94	169.15	336.09	0.63666	0.58327	1.22294
295.0	5.9765	0.001324	0.003484	0.004808	175.75	121.81	297.55	183.66	142.62	326.29	0.69391	0.48347	1.17739
300.0	6.7058	0.001471	0.002278	0.003749	195.40	39.57	234.56	205.06	104.89	309.95	0.76240	0.34960	1.11200
304.2	7.3834	0.002155	0.000000	0.002155	241.37	0.0	241.37	257.31	0.00	257.31	0.93116	0.00000	0.93116

## D.2 CO<sub>2</sub> Saturation Pressure Table (SI Units)

P(MPa)	T(K)	Volume (m <sup>3</sup> /kg)			Energy (kJ/kg)			Enthalpy (kJ/kg)			Entropy (kJ/kg/K)		
		vf	vfg	vg	uf	ufg	ug	hf	hfg	hg	sf	sfg	sg
0.5173	216.5	0.000847	0.071926	0.072774	0.00	314.66	314.23	0.00	351.87	351.87	0.00001	1.62495	1.62496
0.6000	220.0	0.000857	0.062281	0.063137	6.49	308.75	315.24	7.01	346.12	353.12	0.03175	1.57326	1.60501
0.7001	223.7	0.000867	0.053559	0.054425	14.23	302.01	316.24	14.84	339.50	354.34	0.06669	1.51745	1.58413
0.8000	227.1	0.000877	0.046942	0.047819	21.24	295.84	317.08	21.94	333.39	355.33	0.09780	1.46810	1.56590
0.9000	230.2	0.000886	0.041744	0.042630	27.59	290.18	317.77	28.38	327.75	356.13	0.12561	1.42406	1.54967
1.0000	233.0	0.000895	0.037547	0.038442	33.39	284.95	318.34	34.29	322.50	356.49	0.15071	1.38428	1.53499
1.5000	244.6	0.000935	0.024695	0.025630	57.04	262.97	320.00	58.44	300.01	358.45	0.24998	1.22664	1.47662
2.0000	255.6	0.000971	0.018062	0.019033	75.62	244.73	320.36	77.56	280.86	358.42	0.32484	1.10744	1.43229
2.5000	261.1	0.001006	0.013974	0.014981	91.43	228.41	319.84	93.94	263.35	357.29	0.38657	1.00857	1.39514
3.0000	267.6	0.001041	0.011180	0.012221	105.43	213.22	318.65	108.55	246.76	355.32	0.43989	0.92220	1.36208
3.5000	273.3	0.001078	0.009131	0.010209	118.23	198.63	316.86	122.00	230.59	352.59	0.48766	0.84371	1.33137
4.0000	278.5	0.001116	0.007549	0.008665	130.27	184.22	314.48	134.73	214.41	349.15	0.53182	0.77001	1.30183
4.5000	283.1	0.001158	0.006275	0.007433	141.86	169.62	311.48	147.07	197.86	344.93	0.57374	0.69880	1.27254
5.0000	289.5	0.001205	0.005210	0.006415	153.23	154.53	307.77	159.26	180.58	339.84	0.61437	0.62821	1.24258
5.5000	291.5	0.001260	0.004289	0.005545	164.60	138.54	303.14	171.53	162.11	333.64	0.65465	0.55620	1.21085
6.0000	295.2	0.001328	0.003445	0.004773	176.32	120.92	297.23	184.28	141.59	325.87	0.69592	0.47968	1.17560
6.5000	298.6	0.001420	0.002199	0.003619	189.34	77.22	266.56	198.56	90.42	288.95	0.74169	0.30631	1.04800
7.0000	301.9	0.001571	0.000955	0.002526	205.65	14.70	220.35	216.64	39.24	255.88	0.79940	0.13294	0.93234
7.3834	304.2	0.002155	0.000000	0.002155	241.37	0.0	241.37	257.31	0.00	257.31	0.93116	0.00000	0.93116

### D.3 Superheated CO<sub>2</sub> Table - (SI Units)

P= 0.5173 MPa T(K) 216.5	220.	250.	300.	350.	400.	500.	600.	700.	800.	900.	1000.	
v,m**3/kg 0.07277	0.07429	0.08691	0.10672	0.12586	0.14469	0.18190	0.21881	0.25559	0.29229	0.32895	0.36557	
u,kJ/kg 314.23	316.52	336.19	369.47	404.41	441.28	520.67	606.76	698.42	794.67	894.67	997.77	
h,kJ/kg 351.87	354.95	381.15	424.68	469.52	516.13	614.77	719.95	830.64	945.88	1064.84	1186.88	
s,kJ/kg/K 1.62496	1.63907	1.75074	1.90943	2.04760	2.17203	2.39184	2.58344	2.75397	2.90778	3.04786	3.17642	
P= 0.6000 MPa T(K) 220.0	220.	250.	300.	350.	400.	500.	600.	700.	800.	900.	1000.	
v,m**3/kg 0.06314	0.00000	0.07429	0.09163	0.10824	0.12454	0.15673	0.18861	0.22036	0.25202	0.28365	0.31524	
u,kJ/kg 315.24	0.00	335.31	368.92	404.01	440.97	520.47	606.60	698.30	794.57	894.58	997.69	
h,kJ/kg 353.12	378.34	423.89	468.96	515.71	614.50	719.77	830.51	945.78	1064.77	1186.83		
s,kJ/kg/K 1.60501	0.00000	1.71914	1.87954	2.01844	2.14324	2.36341	2.55516	2.72578	2.87964	3.01975	3.14832	
P= 0.7000 MPa T(K) 223.7	250.	300.	350.	400.	500.	600.	700.	800.	900.	1000.	1200.	
v,m**3/kg 0.05443	0.06301	0.07811	0.09250	0.10566	0.13244	0.16162	0.18887	0.21604	0.24316	0.27202	0.34249	
u,kJ/kg 316.24	334.23	368.24	403.52	440.60	520.21	606.41	698.15	794.44	894.48	997.60	1211.21	
h,kJ/kg 354.34	378.34	422.91	468.27	515.19	614.18	719.55	830.36	945.67	1064.69	1186.78	1438.28	
s,kJ/kg/K 1.58413	1.68559	1.84813	1.98793	2.11318	2.33376	2.52573	2.69644	2.85036	2.99051	3.11911	3.34826	
P= 0.8000 MPa T(K) 227.1	250.	300.	350.	400.	500.	600.	700.	800.	900.	1000.	1200.	
v,m**3/kg 0.04782	0.05454	0.06798	0.08069	0.09307	0.11737	0.14138	0.16526	0.18905	0.21280	0.23652	0.28390	
u,kJ/kg 317.08	333.12	367.55	403.04	440.22	519.96	606.23	698.00	794.32	894.37	997.50	1211.13	
h,kJ/kg 355.33	376.75	421.94	467.59	514.68	613.86	719.33	830.21	945.56	1064.61	1186.72	1438.26	
s,kJ/kg/K 1.56590	1.62060	1.96130	2.04702	2.30805	2.50019	2.67100	2.82498	2.96516	3.03973		3.32297	
P= 0.9000 MPa T(K) 230.2	250.	300.	350.	400.	500.	600.	700.	800.	900.	1000.	1200.	
v,m**3/kg 0.04263	0.04794	0.06010	0.07150	0.08258	0.10425	0.12564	0.14689	0.16806	0.18919	0.21028	0.25242	
u,kJ/kg 317.77	331.99	366.86	402.55	439.85	519.71	604.04	697.85	794.20	894.27	997.43	1211.06	
h,kJ/kg 356.13	375.13	420.95	466.90	514.17	613.54	719.11	830.03	945.45	1064.54	1186.67	1438.23	
s,kJ/kg/K 1.54967	1.62888	1.79601	1.93764	2.06383	2.28530	2.47762	2.64854	2.80257	2.94280	3.07145	3.30066	
P= 1.0000 MPa T(K) 233.0	250.	300.	350.	400.	500.	600.	700.	800.	900.	1000.	1200.	
v,m**3/kg 0.03844	0.04265	0.05379	0.06416	0.07748	0.09376	0.11305	0.13220	0.15127	0.17030	0.18929	0.22723	
u,kJ/kg 318.34	330.83	366.16	403.05	439.47	519.46	605.85	697.70	794.07	894.16	997.32	1210.99	
h,kJ/kg 356.78	373.47	419.95	466.21	513.65	613.22	718.90	829.90	945.34	1064.46	1186.61	1438.21	
s,kJ/kg/K 1.53499	1.60415	1.77374	1.91632	2.04798	2.26489	2.45741	2.62842	2.78251	2.92277	3.05145	3.28069	
P= 1.5000 MPa T(K) 244.6	250.	300.	350.	400.	500.	600.	700.	800.	900.	1000.	1200.	
v,m**3/kg 0.02563	0.02665	0.030485	0.04211	0.046899	0.06228	0.07572	0.08812	0.10090	0.11362	0.12632	0.15166	
u,kJ/kg 320.00	324.48	362.54	399.55	437.58	518.19	604.91	696.95	793.45	893.63	996.86	1210.62	
h,kJ/kg	358.45	364.46	414.82	462.71	511.06	611.61	717.81	829.13	944.80	1064.07	1186.34	1438.11
s,kJ/kg/K 1.47662	1.50091	1.68488	1.83254	1.96164	2.18577	2.37925	2.55078	2.70515	2.84559	2.97439	3.20379	
P= 2.0000 MPa T(K) 253.6	300.	350.	400.	500.	600.	700.	800.	900.	1000.	1200.	1400.	
v,m**3/kg 0.01903	0.02535	0.03107	0.03640	0.04654	0.05638	0.06608	0.07571	0.08529	0.09484	0.11398	0.13287	
u,kJ/kg 320.36	358.72	396.99	435.65	516.92	603.97	696.21	792.83	893.10	996.40	1210.25	1431.83	
h,kJ/kg 358.42	409.41	459.13	508.51	610.01	716.73	828.37	944.25	1063.68	1186.07	1438.01	1697.57	
s,kJ/kg/K 1.43229	1.61745	1.77081	1.90250	2.12891	2.32335	2.49535	2.65003	2.79066	2.91959	3.14914	3.34913	
P= 2.5000 MPa T(K) 261.1	300.	350.	400.	500.	600.	700.	800.	900.	1000.	1200.	1400.	
v,m**3/kg 0.01498	0.01962	0.02445	0.02884	0.03170	0.04505	0.05286	0.06060	0.06829	0.07595	0.09121	0.10642	
u,kJ/kg 319.84	354.65	394.35	433.71	515.65	603.03	695.46	792.22	892.58	995.94	1209.89	1431.53	
h,kJ/kg 357.29	403.69	455.48	505.81	608.40	715.66	827.62	943.71	1063.30	1185.81	1437.91	1697.58	
s,kJ/kg/K 1.39514	1.56125	1.72105	1.85548	2.08423	2.27964	2.45215	2.60711	2.74793	2.87698	3.10668	3.30675	
P= 3.0000 MPa T(K) 267.6	300.	350.	400.	500.	600.	700.	800.	900.	1000.	1200.	1400.	
v,m**3/kg 0.01222	0.01577	0.02020	0.02381	0.03081	0.03750	0.04405	0.05050	0.05695	0.06335	0.07069	0.08879	
u,kJ/kg 318.65	350.28	391.64	431.73	514.38	602.09	694.72	791.60	892.06	995.49	1209.53	1431.22	
h,kJ/kg 355.32	397.58	451.73	503.15	606.80	714.59	826.87	943.18	1062.92	1185.55	1437.81	1697.60	
s,kJ/kg/K 1.36208	1.51160	1.67877	1.81611	2.04724	2.43645	2.61782	2.72191	2.84208	3.07193		3.27210	
P= 3.5000 MPa T(K) 273.3	300.	350.	400.	500.	600.	700.	800.	900.	1000.	1200.	1400.	
v,m**3/kg 0.01021	0.01299	0.01687	0.02021	0.02632	0.03211	0.03776	0.04333	0.04886	0.05436	0.06530	0.07620	
u,kJ/kg 316.86	345.55	388.85	429.73	513.10	601.65	693.98	790.90	891.53	995.03	1209.17	1430.92	
h,kJ/kg 352.59	391.01	447.90	500.47	605.21	713.52	826.13	942.65	1062.55	1185.29	1437.72	1697.61	
s,kJ/kg/K 1.43654	1.61457	1.78201	2.01563	2.21299	2.38650	2.54204	2.68321	2.81251	3.04251		3.24276	
P= 4.0000 MPa T(K) 278.5	300.	350.	400.	500.	600.	700.	800.	900.	1000.	1200.	1400.	
v,m**3/kg 0.00867	0.01087	0.01450	0.01751	0.02295	0.02806	0.03304	0.03794	0.04279	0.04761	0.05720	0.06675	
u,kJ/kg 314.48	340.37	385.98	427.71	511.82	600.21	693.24	790.38	891.02	994.58	1208.81	1430.62	
h,kJ/kg 349.15	383.86	443.96	497.76	603.61	712.47	825.39	942.13	1062.18	1185.03	1437.62	1697.63	
s,kJ/kg/K 1.30183	1.42218	1.60799	1.75173	1.98788	2.18624	2.36023	2.51606	2.65742	2.78684	3.01699	3.21732	
P= 4.5000 MPa T(K) 283.1	300.	350.	400.	500.	600.	700.	800.	900.	1000.	1200.	1400.	
v,m**3/kg 0.00743	0.00919	0.01265	0.01541	0.02033	0.02492	0.02937	0.03374	0.03807	0.04237	0.05091	0.05940	
u,kJ/kg 307.77	328.03	379.95	423.57	509.24	598.34	691.77	789.17	889.98	993.68	1208.09	1430.03	
h,kJ/kg 339.84	366.98	435.76	492.26	600.43	710.37	823.93	941.10	1061.45	1184.53	1437.45	1697.67	
s,kJ/kg/K 1.27254	1.37913	1.57711	1.72436	1.96311	2.16246	2.33695	2.49307	2.63460	2.76414	2.99444	3.19486	
P= 5.0000 MPa T(K) 287.5	300.	350.	400.	500.	600.	700.	800.	900.	1000.	1200.	1400.	
v,m**3/kg 0.00641	0.00779	0.01116	0.01374	0.01824	0.02241	0.02643	0.03039	0.03429	0.03817	0.04587	0.05353	
u,kJ/kg 307.77	328.03	379.95	423.57	509.24	598.34	691.77	789.17	889.98	993.68	1208.09	1430.03	
h,kJ/kg 339.84	366.98	435.76	492.26	600.43	710.37	823.93	941.10	1061.45	1184.53	1437.45	1697.67	
s,kJ/kg/K 1.24258	1.33514	1.54862	1.69927	1.94068	2.14103	2.31602	2.47242	2.61414	2.74380	2.97424	3.17474	

## Appendix D: Thermodynamic Property Tables for Carbon Dioxide

389

P= 5.5000 MPa T(K) 291.5	300.	350.	400.	500.	600.	700.	800.	900.	1000.	1200.	1400.
v,m**3/kg	0.00554	0.00659	0.00995	0.01236	0.01653	0.02023	0.02403	0.02764	0.03120	0.03474	0.04175
u,kJ/kg	303.14	320.24	376.78	421.47	507.95	597.40	691.03	788.56	889.47	993.23	1207.73
h,kJ/kg	333.64	356.46	431.48	489.47	598.84	709.33	823.21	940.59	1061.09	1184.29	1437.36
s,kJ/kg/K	1.21085	1.28013	1.52098	1.67602	1.92015	2.12151	2.29699	2.45368	2.59557	2.72535	2.95594
P= 6.0000 MPa T(K) 295.2	300.	350.	400.	500.	600.	700.	800.	900.	1000.	1200.	1400.
v,m**3/kg	0.00477	0.00548	0.00893	0.01122	0.01510	0.01864	0.02203	0.02535	0.02863	0.03188	0.03832
u,kJ/kg	297.23	310.38	373.50	419.33	506.66	596.47	690.30	787.96	888.95	992.78	1207.38
h,kJ/kg	325.87	343.29	427.06	486.66	597.26	708.29	822.50	940.08	1060.73	1184.04	1437.28
s,kJ/kg/K	1.17560	1.23416	1.49490	1.65426	1.90119	2.10356	2.27954	2.43650	2.57858	2.70848	2.93921
P= 6.5000 MPa T(K) 298.6	300.	350.	400.	500.	600.	700.	800.	900.	1000.	1200.	1400.
v,m**3/kg	0.00142	0.00435	0.00806	0.01025	0.01389	0.01719	0.02034	0.02342	0.02645	0.02946	0.03541
u,kJ/kg	189.33	295.63	370.09	417.16	505.36	595.54	689.57	787.36	888.44	992.34	1207.02
h,kJ/kg	198.55	323.90	422.50	483.81	595.68	707.26	821.79	939.58	1060.38	1183.80	1437.19
s,kJ/kg/K	0.74165	1.16131	1.46975	1.63375	1.88354	2.08694	2.26341	2.42065	2.56290	2.69929	2.92380
P= 7.0000 MPa T(K) 301.9	350.	400.	500.	600.	700.	800.	900.	1000.	1200.	1400.	1600.
v,m**3/kg	0.00157	0.00732	0.00943	0.01286	0.01595	0.01889	0.02176	0.02459	0.02738	0.03292	0.03842
u,kJ/kg	205.74	366.55	414.96	504.06	594.61	688.84	786.76	887.93	991.90	1206.67	1428.85
h,kJ/kg	216.75	417.79	480.95	594.10	706.24	821.08	939.09	1060.03	1183.57	1437.11	1697.76
s,kJ/kg/K	0.79975	1.44529	1.61425	1.86703	2.07144	2.28480	2.40593	2.54833	2.67849	2.90951	3.11034
P= 7.3834 MPa T(K) 304.2	350.	400.	500.	600.	700.	800.	900.	1000.	1200.	1400.	1600.
v,m**3/kg	0.00221	0.00692	0.00987	0.01217	0.01511	0.01791	0.02064	0.02333	0.02598	0.03124	0.03645
u,kJ/kg	243.72	363.73	413.26	503.07	593.89	688.29	786.30	887.55	991.56	1206.40	1428.62
h,kJ/kg	260.02	414.06	478.73	592.89	705.46	820.55	938.71	1059.77	1183.39	1437.05	1697.78
s,kJ/kg/K	0.94013	1.42690	1.59999	1.85053	2.06026	2.23756	2.39530	2.53786	2.66808	2.89922	3.10011
P= 7.5000 MPa T(K) 304.2	350.	400.	500.	600.	700.	800.	900.	1000.	1200.	1400.	1600.
v,m**3/kg	0.00166	0.00667	0.00871	0.01197	0.01487	0.01764	0.02032	0.02297	0.02558	0.03076	0.03590
u,kJ/kg	214.30	362.86	412.74	502.76	593.68	688.12	786.16	887.43	991.46	1206.32	1428.56
h,kJ/kg	226.75	412.90	478.05	592.53	705.23	820.38	938.59	1059.69	1183.33	1437.03	1697.78
s,kJ/kg/K	0.83007	1.42135	1.59573	1.85148	2.05691	2.23437	2.39217	2.53477	2.66502	2.89619	3.09710
P= 8.0000 MPa T(K) 304.2	350.	400.	500.	600.	700.	800.	900.	1000.	1200.	1400.	1600.
v,m**3/kg	0.00148	0.00610	0.00808	0.01119	0.01393	0.01654	0.01907	0.02153	0.02401	0.02887	0.03369
u,kJ/kg	200.44	359.01	410.48	501.46	592.75	687.39	785.57	886.92	991.02	1205.97	1428.27
h,kJ/kg	212.29	407.83	475.13	590.96	704.22	819.69	938.11	1059.35	1183.10	1436.96	1697.81
s,kJ/kg/K	0.78001	1.39775	1.57794	1.83678	2.04324	2.22118	2.37926	2.52203	2.65240	2.88371	3.08470
P= 9.0000 MPa T(K) 304.2	350.	400.	500.	600.	700.	800.	900.	1000.	1200.	1400.	1600.
v,m**3/kg	0.00137	0.00515	0.00704	0.00989	0.01237	0.01471	0.01697	0.01920	0.02139	0.02573	0.03002
u,kJ/kg	189.73	350.78	405.88	498.85	590.90	685.95	784.39	885.92	990.14	1205.27	1427.69
h,kJ/kg	202.07	397.10	469.21	587.83	702.21	818.32	937.15	1058.68	1182.65	1436.81	1697.87
s,kJ/kg/K	0.74177	1.35107	1.54429	1.80950	2.01803	2.19696	2.35559	2.49870	2.62930	2.86089	3.06204
P= 10.0000 MPa T(K) 304.2	350.	400.	500.	600.	700.	800.	900.	1000.	1200.	1400.	1600.
v,m**3/kg	0.00132	0.00437	0.00602	0.00885	0.01112	0.01325	0.01530	0.01731	0.01929	0.02321	0.02708
u,kJ/kg	183.35	341.76	401.15	496.24	589.05	684.52	783.21	884.92	989.27	1204.58	1427.11
h,kJ/kg	196.51	385.51	463.19	584.73	700.24	816.97	936.20	1058.02	1182.21	1436.67	1697.94
s,kJ/kg/K	0.71907	1.30438	1.51273	1.78460	1.99520	2.17516	2.33428	2.47773	2.60855	2.84042	3.04175
P= 12.5000 MPa T(K) 304.2	350.	400.	500.	600.	700.	800.	900.	1000.	1200.	1400.	1600.
v,m**3/kg	0.00124	0.00300	0.00472	0.00659	0.00888	0.01062	0.01229	0.01392	0.01552	0.01868	0.02180
u,kJ/kg	173.03	315.85	388.84	489.68	584.47	680.97	780.30	882.45	987.12	1202.87	1425.69
h,kJ/kg	188.49	353.29	447.78	577.07	695.41	813.69	933.93	1056.45	1181.16	1436.36	1698.12
s,kJ/kg/K	0.68224	1.18642	1.44045	1.73002	1.94585	2.12816	2.28687	2.43295	2.56433	2.79688	2.99857
P= 15.0000 MPa T(K) 304.2	350.	400.	500.	600.	700.	800.	900.	1000.	1200.	1400.	1600.
v,m**3/kg	0.00119	0.00222	0.00374	0.00576	0.00739	0.00887	0.01029	0.01166	0.01301	0.01566	0.01827
u,kJ/kg	165.95	289.68	376.00	483.13	579.93	677.47	777.44	880.02	985.01	1201.19	1424.28
h,kJ/kg	183.79	322.92	432.17	569.58	690.74	810.55	931.75	1054.96	1180.18	1436.10	1698.34
s,kJ/kg/K	0.65685	1.08136	1.37520	1.68334	1.90438	2.08905	2.25087	2.39596	2.52788	2.76108	2.96315
P= 20.0000 MPa T(K) 304.2	350.	400.	500.	600.	700.	800.	900.	1000.	1200.	1400.	1600.
v,m**3/kg	0.00113	0.00163	0.00262	0.00442	0.00554	0.00670	0.00779	0.00885	0.00988	0.01189	0.01387
u,kJ/kg	155.78	255.86	350.57	470.16	571.04	670.64	771.86	875.29	980.90	1197.91	1421.54
h,kJ/kg	178.36	288.43	403.03	555.30	681.94	804.67	927.73	1052.23	1178.42	1435.70	1698.87
s,kJ/kg/K	0.61997	0.95621	1.26338	1.60545	1.83658	2.02578	2.19009	2.33671	2.46965	2.70411	2.90680



# Appendix E: Thermodynamic Property Tables for Sodium

## E.1 Sodium Temperature Saturation Table: SI units

T (K)	P (MPa)	Volume (m**3/kg)			Energy (kJ/kg)			Enthalpy (kJ.kg)			Entropy (kJ/kg)		
		v <sub>f</sub>	v <sub>fg</sub>	v <sub>g</sub>	u <sub>f</sub>	u <sub>fg</sub>	u <sub>g</sub>	h <sub>f</sub>	h <sub>fg</sub>	h <sub>g</sub>	s <sub>f</sub>	s <sub>fg</sub>	s <sub>g</sub>
800.0	0.001	0.001211	298.0341	298.0353	0.0	4034.4	4034.3	0.0	4315.6	4315.5	0.0000	5.3945	5.3944
850.0	0.002	0.001229	127.4088	127.4100	66.4	3970.8	4037.2	66.4	4267.0	4333.4	0.0804	5.0200	5.1004
900.0	0.005	0.001247	60.0689	60.0702	132.7	3904.9	4037.6	132.7	4215.5	4348.2	0.1563	4.6839	4.8401
950.0	0.011	0.001266	30.7359	30.7372	200.2	3836.0	4036.2	200.2	4160.4	4360.6	0.2292	4.3793	4.6085
1000.0	0.020	0.001286	16.8576	16.8587	268.5	3765.2	4033.7	268.5	4102.8	4371.3	0.2991	4.1028	4.4019
1050.0	0.036	0.001306	9.8134	9.8148	336.6	3694.3	4030.9	336.7	4044.6	4381.2	0.3653	3.8520	4.2172
1100.0	0.060	0.001327	6.0137	6.0150	405.1	3623.4	4028.5	405.2	3986.0	4391.2	0.4285	3.6236	4.0521
1154.6	0.101	0.001351	3.7069	3.7083	479.9	3547.6	4027.5	480.0	3923.2	4403.2	0.4939	3.3979	3.8917
1200.0	0.150	0.001372	2.5685	2.5699	542.4	3486.0	4028.4	542.6	3872.2	4414.9	0.5457	3.2269	3.7725
1250.0	0.224	0.001395	1.7722	1.7736	611.0	3421.1	4032.2	611.3	3818.9	4430.1	0.5996	3.0550	3.6547
1300.0	0.325	0.001419	1.2599	1.2613	682.9	3356.1	4039.0	683.3	3765.0	4448.4	0.6526	2.8962	3.5490
1400.0	0.625	0.001469	0.6880	0.6899	831.8	3232.2	4064.0	832.7	3662.8	4495.5	0.7528	2.6163	3.3691
1500.0	1.101	0.001523	0.4091	0.4106	998.1	3107.4	4105.5	999.7	3557.9	4557.7	0.8494	2.3719	3.2213
1600.0	1.802	0.001581	0.2590	0.2606	1194.0	2970.8	4164.8	1196.8	3437.4	4634.2	0.9463	2.1484	3.0947
1700.0	2.776	0.001642	0.1713	0.1729	1440.8	2804.2	4245.0	1445.4	3279.7	4725.1	1.0487	1.9292	2.9780

## E.2 Sodium Pressure Saturation Table: SI units

P (MPa)	T (K)	Volume (m**3/kg)			Energy (kJ/kg)			Enthalpy (kJ.kg)			Entropy (kJ/kg)		
		v <sub>f</sub>	v <sub>fg</sub>	v <sub>g</sub>	u <sub>f</sub>	u <sub>fg</sub>	u <sub>g</sub>	h <sub>f</sub>	h <sub>fg</sub>	h <sub>g</sub>	s <sub>f</sub>	s <sub>fg</sub>	s <sub>g</sub>
0.009	941.1	0.001263	34.4471	34.4483	188.2	3848.4	4036.6	188.2	4170.3	4358.5	0.2165	4.4313	4.6479
0.020	999.9	0.001286	16.8773	16.8798	268.2	3765.0	4033.7	268.2	4103.1	4371.3	0.2988	4.1035	4.4023
0.040	1060.5	0.001311	8.8223	8.8236	351.0	3679.4	4030.3	351.0	4032.3	4383.3	0.3788	3.8024	4.1811
0.060	1099.5	0.001327	6.0411	6.0425	404.3	3624.2	4028.6	404.4	3986.7	4391.1	0.4278	3.6258	4.0536
0.080	1129.1	0.001340	4.6196	4.6209	444.9	3582.8	4027.7	445.0	3952.4	4397.4	0.4637	3.5006	3.9643
0.100	1153.1	0.001351	3.7528	3.7541	477.9	3549.6	4027.5	478.0	3924.9	4402.9	0.4921	3.4036	3.8958
0.100	1154.6	0.001351	3.7070	3.7084	480.0	3547.5	4027.5	480.1	3923.1	4403.2	0.4939	3.3978	3.8917
0.200	1235.2	0.001388	1.9714	1.9728	591.3	3439.4	4030.7	591.5	3833.7	4425.3	0.5844	3.1038	3.6882
0.300	1289.0	0.001413	1.3548	1.3562	667.1	3370.0	4037.2	667.6	3776.5	4444.0	0.6414	2.9298	3.5712
0.400	1330.2	0.001434	1.0398	1.0404	726.6	3318.3	4044.9	727.2	3733.9	4461.1	0.6836	2.8070	3.4905
0.500	1364.1	0.001451	0.8459	0.8474	777.0	3276.3	4053.2	777.7	3699.2	4476.9	0.7175	2.7118	3.4293
0.750	1430.6	0.001485	0.5826	0.5841	880.3	3194.6	4074.9	881.4	3631.6	4513.0	0.7825	2.5385	3.3210
1.000	1481.9	0.001513	0.4471	0.4486	966.2	3130.5	4096.8	967.7	3577.6	4545.3	0.8320	2.4142	3.2461
2.000	1623.0	0.001594	0.2348	0.2364	1245.1	2936.1	4181.1	1248.3	3405.6	4653.8	0.9691	2.0983	3.0675
3.000	1719.4	0.001655	0.1586	0.1603	1497.8	2766.0	4263.7	1502.7	3241.9	4744.6	1.0698	1.8855	2.9553

### E.3 Superheated Sodium Table: SI Units

$P = 0.0093 \text{ MPa } T(K) 941.1$	950.	1000.	1050.	1100.	1150.	1200.	1250.	1300.	1350.	1400.	1450.
$v, m^*3/kg$	34.44834	34.94240	37.4751	39.7787	41.9451	44.0527	46.0856	48.0955	50.0854	52.0603	54.0195
$u, kJ/kg$	4036.59	4053.95	4131.43	4187.49	4231.91	4269.71	4303.53	4334.91	4364.73	4393.52	4421.62
$h, kJ/kg$	4358.54	4380.48	4481.67	4559.26	4623.98	4681.33	4734.23	4784.41	4832.83	4880.08	4926.55
$s, kJ/kg/K$	4.64786	4.6711	4.7751	4.8509	4.9111	4.9622	5.0072	5.0481	5.0861	5.1218	5.1555
$P = 0.0500 \text{ MPa } T(K) 1081.6$	1100.	1150.	1200.	1250.	1300.	1350.	1400.	1450.	1500.	1600.	1700.
$v, m^*3/kg$	7.16339	7.3656	7.8738	8.3370	8.7728	9.1880	9.5989	9.9813	10.3661	10.7461	11.1220
$u, kJ/kg$	4029.30	4067.54	4152.25	4217.57	4315.56	4355.73	4394.29	4424.85	4456.64	4487.15	4516.73
$h, kJ/kg$	4387.47	4435.77	4545.94	4634.47	4709.21	4774.96	4834.71	4890.39	4943.17	4993.95	5043.27
$s, kJ/kg/K$	4.11076	4.1553	4.2536	4.3291	4.3902	4.4418	4.4870	4.5275	4.5645	4.5990	4.6619
$P = 0.1000 \text{ MPa } T(K) 1153.1$	1200.	1250.	1300.	1350.	1400.	1450.	1500.	1550.	1600.	1700.	1800.
$v, m^*3/kg$	3.75411	4.0095	4.4909	4.7099	4.9198	5.1238	5.3224	5.5175	5.7113	6.0886	6.4619
$u, kJ/kg$	4027.47	4118.13	4194.78	4257.01	4309.31	4354.73	4395.35	4432.52	4467.19	4500.04	4561.93
$h, kJ/kg$	4402.87	4519.07	4620.66	4706.08	4780.30	4846.74	4907.72	4964.76	5018.94	5071.02	5170.79
$s, kJ/kg/K$	3.89575	3.9956	4.0790	4.1462	4.2023	4.2507	4.2936	4.3322	4.3678	4.4009	4.4614
$P = 0.1013 \text{ MPa } T(K) 1154.6$	1200.	1250.	1300.	1350.	1400.	1450.	1500.	1550.	1600.	1700.	1800.
$v, m^*3/kg$	3.70836	3.9531	4.2086	4.4293	4.6460	4.8546	5.0551	5.2515	5.4449	5.6342	6.0083
$u, kJ/kg$	4027.46	4115.61	4193.14	4255.49	4308.11	4353.79	4394.57	4431.88	4466.67	4509.59	4561.62
$h, kJ/kg$	4403.21	4516.16	4618.74	4704.29	4778.88	4845.62	4906.79	4963.99	5018.31	5070.48	5170.40
$s, kJ/kg/K$	3.89173	3.9887	4.0736	4.1403	4.1967	4.2453	4.2883	4.3271	4.3627	4.3998	4.4564
$P = 0.2000 \text{ MPa } T(K) 1235.2$	1250.	1300.	1350.	1400.	1450.	1500.	1550.	1600.	1700.	1800.	1900.
$v, m^*3/kg$	2.0149	2.1492	2.2746	2.3923	2.5043	2.6118	2.7161	2.8176	3.0193	3.2077	3.3977
$u, kJ/kg$	4030.70	4060.32	4148.92	4222.58	4284.70	4338.27	4385.53	4428.13	4467.23	4538.19	4602.85
$h, kJ/kg$	4425.26	4463.26	4578.76	4677.48	4763.15	4839.12	4907.90	4971.33	5030.76	5141.23	5244.38
$s, kJ/kg/K$	3.68618	3.7197	3.8120	3.8874	3.9501	4.0036	4.0503	4.0920	4.1297	4.1968	4.2557
$P = 0.3000 \text{ MPa } T(K) 1289.0$	1300.	1350.	1400.	1450.	1500.	1550.	1600.	1700.	1800.	1900.	2000.
$v, m^*3/kg$	1.35620	1.3768	1.41673	1.5524	1.6330	1.7094	1.7830	1.8541	1.9910	2.1230	2.2530
$u, kJ/kg$	4037.18	4057.97	4145.04	4219.93	4284.39	4340.57	4390.39	4435.34	4514.89	4585.34	4660.37
$h, kJ/kg$	4444.04	4471.01	4585.23	4685.67	4774.27	4853.41	4925.30	4991.58	5112.20	5222.25	5342.25
$s, kJ/kg/K$	3.57121	3.5931	3.6823	3.7568	3.8197	3.8736	3.9210	3.9632	4.0364	4.0994	4.2094
$P = 0.4000 \text{ MPa } T(K) 1330.2$	1350.	1400.	1450.	1500.	1550.	1600.	1700.	1800.	1900.	2000.	2100.
$v, m^*3/kg$	1.04040	1.0678	1.1349	1.1987	1.2593	1.3172	1.3729	1.4792	1.5807	1.6820	1.7837
$u, kJ/kg$	4044.92	4079.76	4161.92	4234.45	4298.05	4354.22	4404.49	4492.10	4568.10	4646.10	4726.10
$h, kJ/kg$	4461.08	4506.88	4615.92	4713.95	4801.77	4881.10	4953.64	5038.78	5200.44	5280.44	5358.44
$s, kJ/kg/K$	3.49055	3.5271	3.6100	3.6806	3.7410	3.7935	3.8398	3.9190	3.9858	4.0598	4.1398

### E.4 Sodium Temperature Saturation Table: English Units

(T(R))	(P(psi))	Volume (ft <sup>*3</sup> /lbm)	Energy (Btu/lbm)	Enthalpy (Btu/lbm)	Entropy (Btu/lbm)
		vf    vfg    vg	uf    ufg    ug	hf    hfg    hg	hg    sf    sfg    sg
1440.0	0.1	0.01944 4784.0732 4784.0928	-0.1 8412.9 8412.8	-0.1 8999.3 8999.2	2.77752 3.47195 6.24947
1500.0	0.3	0.01963 2683.4263.4597	91.3 8326.1 8417.4	91.3 8933.5 9024.8	2.70908 3.30871 6.01779
1600.0	0.6	0.01996 1131.0094 1131.0293	245.7 8174.2 8419.9	245.7 8815.3 9061.0	2.61041 3.06085 5.67126
1700.0	1.4	0.02029 527.3803 527.4006	436.5 779.5 8160.6	436.6 8652.6 9089.1	2.53727 2.82764 5.36491
1800.0	2.9	0.02065 270.5976 270.6182	559.9 7851.7 8411.6	559.9 8555.6 9115.5	2.45985 2.64062 5.09957
1900.0	5.5	0.02101 146.8262 148.8472	717.8 7687.2 8405.0	717.9 8420.5 9138.1	2.40120 2.46215 4.86335
2000.0	9.8	0.02139 87.1279 87.1493	876.3 7523.6 8400.0	876.5 8285.3 9161.1	2.35325 2.30148 4.65473
2100.0	16.4	0.02178 53.8157 53.8375	1035.4 7363.3 8398.6	1035.7 8152.4 9188.1	2.31376 2.15673 4.47049
2200.0	26.2	0.02218 34.8169 34.8391	1195.4 7207.7 8403.2	1195.9 8028.3 9219.7	2.28164 2.02621 4.30784
2300.0	40.1	0.02260 23.4509 23.4735	1357.7 7057.5 8415.3	1358.6 7898.9 9258.4	2.25603 1.90818 4.16421
2400.0	59.2	0.02304 16.3607 16.3838	1523.8 6912.6 8436.4	1525.0 7807.7 9305.7	2.23610 1.80108 4.03717
2500.0	84.7	0.02349 11.7652 11.7887	1698.8 6768.5 8467.3	1700.6 7661.5 9362.1	2.22161 1.70256 3.92417
2600.0	117.8	0.02396 8.6896 8.7136	1882.8 6626.0 8508.8	1885.3 7543.0 9428.3	2.21143 1.61176 3.82319
2800.0	211.7	0.02495 5.0603 5.0853	2298.4 6326.7 8625.1	2303.1 7286.1 9589.2	2.20253 1.44566 3.64818
3000.0	350.7	0.02602 3.1440 3.1700	2819.0 5971.7 8790.7	2827.1 6959.5 9786.6	2.20581 1.28880 3.49461

### E.5 Sodium Pressure Saturation Table: English Units

(P(psi))	(T(R))	Volume (ft <sup>*3</sup> /lbm)	Energy (Btu/lbm)	Enthalpy (Btu/lbm)	Entropy (Btu/lbm)
		vf    vfg    vg	uf    ufg    ug	hf    hfg    hg	hg    sf    sfg    sg
1.4	1694.0	0.02027 552.9115 552.9318	392.7 8024.8 8417.5	392.7 8696.2 9088.9	0.25091 5.13362 5.38454
2.5	1778.1	0.02057 311.3963 311.4169	525.6 7887.4 8412.9	525.6 8584.7 9110.3	0.32730 4.82810 5.15540
5.0	1884.3	0.02095 162.7399 162.7609	693.0 7713.0 8406.0	693.0 8441.9 9134.9	0.41842 4.48007 4.89849
7.5	1952.7	0.02121 111.4133 111.4345	801.4 7600.7 8402.0	801.4 8349.2 9150.6	0.47446 4.27565 4.75011
10.0	2004.5	0.02140 85.1990 883.8	876.1 7516.0 8399.8	883.8 8279.1 9162.9	0.51564 4.13034 4.64598
12.5	2046.6	0.02157 69.1843 69.2059	950.6 7448.2 8398.7	950.6 8223.0 9173.6	0.54812 4.01794 4.56606
14.7	2078.3	0.02169 59.5053 59.5270	1001.2 7397.3 8398.5	1001.2 8180.9 9182.1	0.57219 3.93639 4.50858
15.0	2082.4	0.02171 58.3823 58.4040	1007.5 7391.0 8398.5	1007.5 8175.6 9183.2	0.57520 3.92615 4.50135
17.5	2113.6	0.02183 50.5836 50.6055	1057.4 7341.4 8398.9	1057.4 8134.7 9192.1	0.59845 3.84866 4.44711
20.0	2141.5	0.02194 44.6815 44.7031	1101.8 7297.9 8399.7	1101.8 8098.7 9200.5	0.61875 3.78177 4.40052
25.0	2189.8	0.02214 36.3213 36.3435	1179.6 7222.8 8402.4	1179.6 8036.6 9216.2	0.65350 3.66995 4.32345
30.0	2231.0	0.02231 36.7461 36.7694	1246.1 7176.0 8406.0	1246.1 7984.8 9230.9	0.68238 3.57897 4.26135
45.0	2328.6	0.02272 21.0823 21.1050	1405.9 7014.4 8420.3	1405.9 7865.1 9271.0	0.74668 3.37755 4.12623
60.0	2403.4	0.02305 16.1681 16.1911	1531.9 6905.3 8437.2	1531.9 7775.5 9307.4	0.79783 3.23519 4.03302
75.0	2464.9	0.02333 13.1648 13.1881	1638.8 6816.4 8455.2	1638.8 7687.0 9341.2	0.83749 3.12481 3.96230
100.0	2549.2	0.02372 10.1038 10.1275	1790.1 6696.3 8486.4	1790.1 7603.4 9393.5	0.89046 2.98265 3.87311
200.0	2779.2	0.02485 5.3337 5.3586	2256.0 6534.9 8610.9	2256.0 7314.8 9570.8	1.03310 2.63194 3.66503
300.0	2935.0	0.02567 3.6502 3.6758	2640.2 6090.6 8730.7	2640.2 7078.3 9718.5	1.13168 2.41166 3.54334

## E.6 Superheated Sodium Table: English Units

P=	1.4 psi	T(R)1694.0	1700.	1800.	1900.	2000.	2100.	2200.	2300.	2400.	2500.	2600.	2700.
v,ft**3/lbm	552.9318	555.9260	561.5211	642.4615	680.8981	717.9449	754.1944	789.7718	825.1837	860.1784	895.1399	929.9736	
u,Btu/lbm	8417.5	8431.5	8615.3	8743.4	8843.3	8927.9	9003.8	9074.5	9142.0	9207.5	9271.7	9334.9	
h,Btu/lbm	9088.9	9106.5	9345.6	9525.3	9670.0	9799.6	9919.4	10033.4	10143.8	10250.2	10358.5	10464.1	
s,Btu/lbm/R	5.3845	5.3949	5.5319	5.6282	5.7034	5.7667	5.8224	5.8731	5.9201	5.9642	6.0060	6.0459	
P=	2.5 psi	T(R)1778.1	1800.	1900.	2000.	2100.	2200.	2300.	2400.	2500.	2600.	2700.	2800.
v,ft**3/lbm	311.4169	317.4174	342.4559	365.0533	386.2126	406.6337	426.4664	446.1012	465.3131	484.4529	503.5057	522.4739	
u,Btu/lbm	8412.9	8464.1	8647.7	8780.0	8884.3	8972.8	9051.9	9125.1	9196.9	9261.5	9326.9	9391.0	
h,Btu/lbm	9110.3	9174.9	9414.5	9597.4	9749.3	9883.4	10069.4	10123.8	10236.5	10346.3	10454.3	10561.0	
s,Btu/lbm/R	5.1554	5.1916	5.3214	5.4153	5.4895	5.5519	5.6068	5.6566	5.7026	5.7457	5.7864	5.8252	
P=	5.0 psi	T(R)1884.3	1900.	2000.	2100.	2200.	2300.	2400.	2500.	2600.	2700.	2800.	2900.
v,ft**3/lbm	162.7609	164.9819	178.0859	189.8740	200.8626	211.3520	221.7053	231.4523	241.2410	250.9281	260.5435	270.0991	
u,Btu/lbm	8406.0	8451.3	8644.1	8795.0	8905.9	9002.9	9088.3	9166.3	9239.4	9309.2	9376.8	9442.7	
h,Btu/lbm	9134.9	9183.3	9441.7	9640.8	9805.5	9949.4	10080.3	10208.2	10319.8	10433.0	10543.6	10652.3	
s,Btu/lbm/R	4.8985	4.9242	5.0571	5.1545	5.2312	5.2952	5.3509	5.4009	5.4468	5.4895	5.5298	5.5679	
P=	7.5 psi	T(R)1952.7	2000.	2100.	2200.	2300.	2400.	2500.	2600.	2700.	2800.	2900.	3000.
v,ft**3/lbm	111.4345	115.8719	124.4683	132.3047	139.6526	146.6837	153.5009	160.1333	166.7368	173.2347	179.6686	186.0625	
u,Btu/lbm	8402.0	8513.1	8698.8	8840.1	8954.4	9051.8	9138.2	9217.4	9291.7	9362.6	9431.1	9497.8	
h,Btu/lbm	9150.6	9291.4	9534.9	9728.9	9862.6	10037.2	10169.4	10293.4	10411.8	10526.3	10638.1	10747.8	
s,Btu/lbm/R	4.7501	4.8217	4.9410	5.0314	5.1043	5.1658	5.2198	5.2684	5.3132	5.3548	5.3940	5.4312	
P=	10.0 psi	T(R)2004.5	2100.	2200.	2300.	2400.	2500.	2600.	2700.	2800.	2900.	3000.	3100.
v,ft**3/lbm	85.1990	91.8108	98.0478	103.8181	109.2796	114.5324	119.1342	124.6441	129.5703	134.5207	139.2899	144.2899	
u,Btu/lbm	8399.8	8609.7	8775.6	8906.7	9015.7	9110.4	9195.6	9274.3	9348.5	9419.5	9488.2	9557.8	
h,Btu/lbm	9162.9	9432.0	9653.8	9836.6	9994.5	10136.3	10267.2	10390.7	10509.1	10623.8	10735.8	10847.8	
s,Btu/lbm/R	4.6460	4.7781	4.8816	4.9630	5.0303	5.0882	5.1396	5.1862	5.2293	5.2697	5.3075	5.3432	
P=	12.5 psi	T(R)2046.6	2100.	2200.	2300.	2400.	2500.	2600.	2700.	2800.	2900.	3000.	3100.
v,ft**3/lbm	69.2059	72.2589	77.5131	82.3293	86.8434	91.1549	95.3236	99.3923	103.3869	107.3276	111.2298		
u,Btu/lbm	8398.7	8523.8	8712.5	8859.6	8980.9	9082.8	9173.9	9257.0	9334.5	9408.0	9478.6	9557.8	
h,Btu/lbm	9173.6	9332.9	9580.3	9781.4	9952.3	10103.4	10241.2	10369.8	10492.0	10609.6	10723.9	10847.8	
s,Btu/lbm/R	4.5661	4.6436	4.7594	4.8491	4.9220	4.9837	5.0378	5.0863	5.1308	5.1721	5.2108	5.2507	
P=	14.7 psi	T(R)2078.3	2100.	2200.	2300.	2400.	2500.	2600.	2700.	2800.	2900.	3000.	3100.
v,ft**3/lbm	59.5270	60.6702	65.2546	69.4941	73.4376	77.1835	80.7923	84.2977	87.7346	91.1159	94.4552	97.4080	
u,Btu/lbm	8398.5	8451.6	8658.4	8819.0	8949.0	9058.8	9155.0	9241.8	9322.2	9397.9	9470.2	9557.8	
h,Btu/lbm	9182.1	9249.3	9517.4	9737.3	9915.7	10074.8	10218.4	10351.5	10477.0	10597.2	10713.5	10847.8	
s,Btu/lbm/R	4.5086	4.5412	4.6670	4.7637	4.8413	4.9063	4.9627	5.0129	5.0586	5.1008	5.1402	5.1802	
P=	0.5000 MPa	T(K)1364.1	1400.	1450.	1500.	1550.	1600.	1650.	1700.	1750.	1800.	1850.	1900.
v,m**3/kg	0.84736	0.8867	0.9396	0.9901	1.0382	1.0845	1.1302	1.1723	1.2157	1.2557	1.2957	1.3357	
u,kJ/kg	4053.23	4121.29	4189.33	4258.40	4319.85	4374.83	4436.84	4496.86	4551.15	4611.50	4671.85	4731.20	
h,kJ/kg	4476.92	4555.62	4659.12	4753.43	4838.98	4917.08	4997.27	5078.97	5157.89	5237.24	5317.59	5397.89	
s,kJ/kg/K	3.49232	3.4912	3.5674	3.6332	3.6903	3.7404	3.8252	3.8957	3.9657	4.0357	4.1057	4.1757	
P=	0.6000 MPa	T(K)1393.2	1400.	1450.	1500.	1550.	1600.	1650.	1700.	1750.	1800.	1850.	1900.
v,m**3/kg	0.71675	0.7229	0.7679	0.8113	0.8529	0.8926	0.9323	0.9720	1.0117	1.0514	1.0911	1.1309	
u,kJ/kg	4061.83	4072.44	4149.78	4222.09	4287.59	4346.48	4414.24	4482.86	4551.55	4620.24	4688.93	4757.62	
h,kJ/kg	4491.87	4560.21	4610.55	4708.07	4799.27	4882.03	5028.97	5157.89	5287.74	5417.53	5547.32	5677.11	
s,kJ/kg/K	3.39018	3.3918	3.4718	3.5419	3.6030	3.6564	3.7264	3.7964	3.8664	3.9364	4.0064	4.0764	
P=	0.7000 MPa	T(K)1418.8	1450.	1500.	1550.	1600.	1650.	1700.	1750.	1800.	1850.	1900.	1950.
v,m**3/kg	0.62230	0.6464	0.6843	0.7208	0.7558	0.8220	0.8842	0.9462	1.0082	1.0702	1.1322	1.1942	
u,kJ/kg	4070.56	4116.64	4189.55	4257.59	4319.61	4427.27	4518.19	4607.07	4696.95	4785.83	4874.71	4963.59	
h,kJ/kg	4506.11	4569.10	4638.64	4702.13	4762.13	4848.67	5002.68	5137.18	5272.68	5407.18	5541.68	5676.18	
s,kJ/kg/K	3.33927	3.3893	3.4624	3.5268	3.5833	3.6564	3.7368	3.8064	3.8764	3.9464	4.0164	4.0864	
P=	0.8000 MPa	T(K)1441.8	1450.	1500.	1550.	1600.	1650.	1700.	1750.	1800.	1850.	1900.	1950.
v,m**3/kg	0.55049	0.5561	0.5895	0.6221	0.6535	0.6850	0.7172	0.7489	0.7816	0.8133	0.8450	0.8768	
u,kJ/kg	4079.29	4090.60	4161.22	4230.19	4294.39	4407.05	4502.25	4607.52	4702.72	4807.92	4913.12	5023.32	
h,kJ/kg	4519.68	4535.45	4602.32	4676.97	4787.66	4952.69	5097.06	5237.74	5407.44	5577.14	5746.84	5916.54	
s,kJ/kg/K	3.31049	3.3172	3.3922	3.4592	3.5184	3.6178	3.7172	3.8164	3.9154	4.0146	4.1136	4.2126	
P=	0.9000 MPa	T(K)1462.7	1500.	1550.	1600.	1650.	1700.	1750.	1800.	1850.	1900.	1950.	2000.
v,m**3/kg	0.44859	0.4583	0.4849	0.5147	0.5458	0.5754	0.6051	0.6350	0.6649	0.6948	0.7247	0.7546	
u,kJ/kg	4096.75	4181.89	4184.13	4249.42	4368.93	4471.50	4581.07	4690.64	4800.21	4909.78	5019.35	5128.92	
h,kJ/kg	4545.34	4577.20	4669.06	4760.28	4829.03	5077.67	5275.34	5473.01	5670.68	5868.35	6066.02	6263.70	
s,kJ/kg/K	3.24613	3.2730	3.3433	3.4066	3.5136	3.6102	3.7062	3.8032	3.8992	4.0062	4.1032	4.2002	
P=	1.0000 MPa	T(K)1481.9	1500.	1550.	1600.	1650.	1700.	1750.	1800.	1850.	1900.	1950.	2000.
v,m**3/kg	0.44859	0.4583	0.4849	0.5147	0.5458	0.5754	0.6051	0.6350	0.6649	0.6948	0.7247	0.7546	
u,kJ/kg	4096.75	4181.89	4184.13	4249.42	4368.93	4471.50	4581.07	4690.64	4800.21	4909.78	5019.35	5128.92	
h,kJ/kg	4545.34	4577.20	4669.06	4760.28	4829.03	5077.67	5275.34	5473.01	5670.68	5868.35	6066.02	6263.70	
s,kJ/kg/K	3.24613	3.2730	3.3433	3.4066	3.5136	3.6102	3.7062	3.8032	3.8992	4.0062	4.1032	4.2002	
P=	2.0000 MPa	T(K)1623.0	1700.	1800.	1900.	2000.	2100.	2200.	2300.	2400.	2500.	2600.	2700.
v,m**3/kg	0.23636	0.2574	0.2834	0.3144	0.3454	0.3764	0.4074	0.4384	0.4694	0.5004	0.5314	0.5624	
u,kJ/kg	4181.14	4241.43	4347.27	4453.51	4560.75	4668.01	4775.25	4882.51	4989.77	5097.03	5204.29	5311.55	
h,kJ/kg	4653.85	4756.31	4914.13	5072.95	5231.77	5400.59	5569.41	5738.23	5907.05	6075.87	6244.69	6413.51	
s,kJ/kg/K	3.06745	3.1640	3.2716	3.3845	3.5003	3.6160	3.7216	3.8284	3.9352	4.0419	4.1486	4.2553	

P= 15.0 psi T(R)2082.4 2100. 2200. 2300. 2400. 2500. 2600. 2700. 2800. 2900. 3000.  
 v,ft\*\*3/lbm 58.4040 59.2735 63.8431 68.0124 71.8927 75.5716 79.1147 82.5565 85.9165 89.2437 92.5195  
 u,Btu/lbm 8398.6 8441.9 8651.0 8813.4 8948.4 9055.5 9152.4 9239.7 9320.5 9396.5 9469.0  
 h,Btu/lbm 9183.2 9238.1 9508.8 9727.2 9910.7 10070.9 10215.3 10348.9 10474.9 10595.5 10712.1  
 s,Btu/lbm/R 4.5013 4.5280 4.6551 4.7526 4.8309 4.8964 4.9531 5.0036 5.0494 5.0917 5.1312

P= 20.0 psi T(R)2141.5 2200. 2300. 2400. 2500. 2600. 2700. 2800. 2900. 3000.  
 v,ft\*\*3/lbm 44.7034 46.8068 50.1409 53.2172 56.1055 58.8591 61.5165 64.1042 66.6435 69.1359  
 u,Btu/lbm 8399.7 8534.1 8723.8 8875.8 9001.7 9109.8 9205.6 9292.7 9373.6 9450.0  
 h,Btu/lbm 9200.5 9372.6 9621.1 9894.1 10066.7 10164.2 10307.6 10441.0 10567.4 10688.5  
 s,Btu/lbm/R 4.4005 4.4811 4.5931 4.6817 4.7544 4.8162 4.8704 4.9190 4.9633 5.0044

P= 25.0 psi T(R)2189.8 2200. 2300. 2400. 2500. 2600. 2700. 2800. 2900. 3000.  
 v,ft\*\*3/lbm 36.3435 36.6472 39.4482 42.0280 44.4280 46.7122 48.8966 51.0140 53.0731 55.1066  
 u,Btu/lbm 8402.4 8426.7 8538.6 8809.8 8949.0 9067.9 9171.9 9265.2 9350.9 9431.1  
 h,Btu/lbm 9216.2 9247.2 9521.9 9750.0 9944.0 10113.9 10266.8 10407.5 10539.5 10665.0  
 s,Btu/lbm/R 4.3235 4.3379 4.4623 4.5603 4.6399 4.7067 4.7643 4.8157 4.8620 4.9046

P= 30.0 psi T(R)2231.0 2200. 2300. 2400. 2500. 2600. 2700. 2800. 2900. 3000.  
 v,ft\*\*3/lbm 30.6964 32.3466 34.5823 36.6599 38.6280 40.4872 42.2885 44.0402 45.7548  
 u,Btu/lbm 8406.0 8558.4 8744.6 8897.8 9026.9 9138.6 9238.0 9328.4 9412.3  
 h,Btu/lbm 9230.9 9427.6 9673.9 9849.2 10064.6 10226.5 10374.3 10511.8 10641.7  
 s,Btu/lbm/R 4.2614 4.3505 4.4569 4.5429 4.6146 4.6750 4.7294 4.7779 4.8220

P= 45.0 psi T(R)2236.8 2400. 2500. 2600. 2700. 2800. 2900. 3000.  
 v,ft\*\*3/lbm 21.1050 22.2378 23.7421 25.1384 26.4846 27.5569 28.9821 30.1735  
 u,Btu/lbm 8420.3 8570.1 8753.6 8909.8 9042.1 9158.4 9262.3 9356.8  
 h,Btu/lbm 9271.0 9466.5 9710.6 9922.5 10109.5 10277.2 10430.4 10572.9  
 s,Btu/lbm/R 4.1262 4.2126 4.3147 4.3988 4.4703 4.5313 4.5852 4.6336

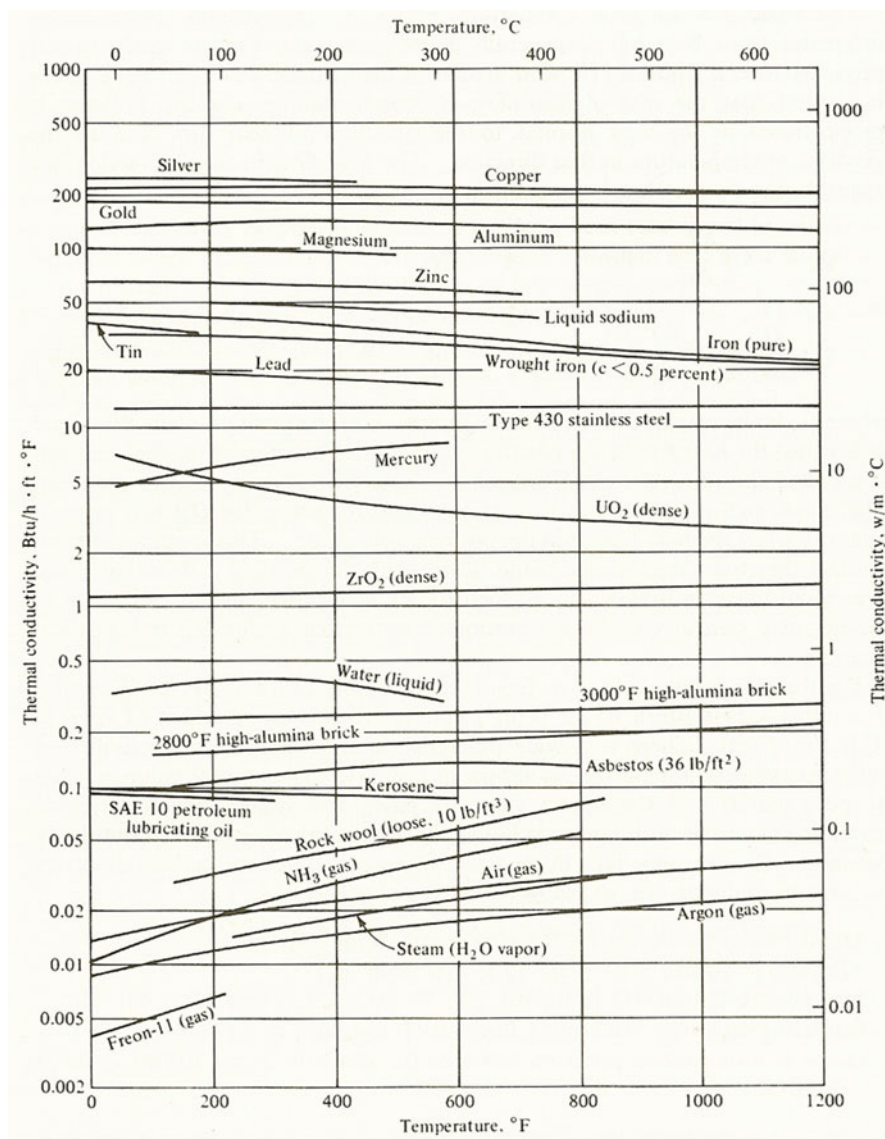
P= 60.0 psi T(R)2403.4 2500. 2600. 2700. 2800. 2900. 3000.  
 v,ft\*\*3/lbm 16.1911 17.3290 19.4446 19.4999 20.5009 21.4601 22.3860  
 u,Btu/lbm 8432.7 8620.0 8800.6 8951.1 9082.2 9198.3 9302.7  
 h,Btu/lbm 9307.4 9558.3 9791.9 9999.0 10184.0 10351.6 10505.8  
 s,Btu/lbm/R 4.0330 4.1415 4.2360 4.3155 4.3834 4.4426 4.4951

P= 75.0 psi T(R)2464.9 2500. 2600. 2700. 2800. 2900. 3000.  
 v,ft\*\*3/lbm 13.1891 13.4599 14.4440 15.3240 16.1567 16.9534 17.7190  
 u,Btu/lbm 8455.2 8582.0 8703.9 8865.7 9009.9 9136.7 9250.3  
 h,Btu/lbm 9342.1 9428.0 9674.2 9896.0 10095.6 10275.6 10440.6  
 s,Btu/lbm/R 3.9623 3.9992 4.1034 4.1899 4.2633 4.3277 4.3840

P= 100.0 psi T(R)2549.2 2600. 2700. 2800. 2900. 3000.  
 v,ft\*\*3/lbm 10.1275 11.1702 11.1120 11.8280 12.4567 13.0588  
 u,Btu/lbm 8486.4 8573.8 8743.2 8899.6 9040.4 9166.8  
 h,Btu/lbm 9393.5 9512.9 9743.8 9959.1 10156.1 10336.5  
 s,Btu/lbm/R 3.8731 3.9260 4.0204 4.1022 4.1732 4.2353

P= 200.0 psi T(R)2779.2 2800. 2900. 3000.  
 v,ft\*\*3/lbm 5.3586 5.4301 5.7768 6.1134  
 u,Btu/lbm 8610.9 8633.3 8760.4 8899.8  
 h,Btu/lbm 9570.8 9606.2 9795.2 9994.0  
 s,Btu/lbm/R 3.6650 3.6835 3.7690 3.8462

P= 300.0 psi T(R)2953.0 2900. 3000.  
 v,ft\*\*3/lbm 3.7586 3.8233 3.9923  
 u,Btu/lbm 8730.7 8776.3  
 h,Btu/lbm 9718.5 9806.6  
 s,Btu/lbm/R 3.5433 3.5974





# Nuclear System Acronyms

## Glossary of Nuclear Terms (US Nuclear Regulatory Commission)

<b>AECB</b>	Atomic Energy Control Board
<b>AECL</b>	Atomic Energy of Canada Ltd.
<b>AESOP</b>	Atomic Energy Simulation of Optimization (computer code)
<b>AFCI</b>	Advanced Fuel Cycle Initiative
<b>AHTR</b>	Advanced High-Temperature Reactor
<b>ASDV</b>	Atmospheric Steam Discharge Valve
<b>ASME</b>	American Society of Mechanical Engineers
<b>ASSERT</b>	Advanced Solution of Subchannel Equations in Reactor Thermal Hydraulics (computer code)
<b>ASTM</b>	American Society for Testing Materials
<b>AVR</b>	Arbeitsgemeinschaft Versuchsreaktor
<b>BLC</b>	Boiler Level Control
<b>BLW</b>	Boiling Light Water
<b>BPC</b>	Boiler Pressure Controller
<b>CBA</b>	Core Barrel Assembly
<b>CCGT</b>	Combined-Cycle Gas Turbine
<b>CCP</b>	Critical Channel Power
<b>CHE</b>	Capillary Heat Exchanger
<b>CHF</b>	Critical Heat Flux
<b>CHP</b>	Combined Heat and Power
<b>CPR</b>	Critical Power Ratio
<b>CRL</b>	Chalk River Laboratories
<b>CRT</b>	Cathode Ray Tube
<b>CS</b>	Core Structures
<b>CSA</b>	Canadian Standards Association
<b>CSC</b>	Core Structure Ceramics

<b>CSDV</b>	Condenser Steam Discharge Valve
<b>CSNI</b>	Canadian Standards for the Nuclear Industry
<b>CV</b>	Cross Vessel
<b>DBE</b>	Design Basis Earthquake
<b>DBE</b>	Design Basis Event
<b>DCC</b>	Digital Control Computer
<b>DDN</b>	Design Data Need
<b>DF-ET</b>	Drift Flux-Equal Temperature
<b>DF-UT</b>	Drift Flux-Unequal Temperature
<b>DHI</b>	Doosan Heavy Industries and Construction
<b>DHX</b>	Dump Heat Exchanger
<b>DID</b>	Defense-in-Depth Principle
<b>DNB</b>	Departure from Nucleate Boiling
<b>DOE</b>	Department of Energy
<b>DRACS</b>	Direct Reactor Auxiliary Cooling System
<b>EBR-II</b>	Experimental Breeder Reactor
<b>ECC</b>	Emergency Core Cooling
<b>ECI</b>	Emergency Core Injection
<b>EFPH</b>	Effective Full Power Hours
<b>EVET</b>	Equal Velocity-Equal Temperature
<b>EVUT</b>	Equal Velocity-Unequal Temperature
<b>EWS</b>	Emergency Water Supply
<b>FBR</b>	Feed, Bleed, and Relief
<b>FHSS</b>	Fuel Handling and Storage System
<b>FP</b>	Full Power
<b>FP</b>	Fission Product
<b>FSV</b>	Fort Saint Vrain
<b>GA</b>	General Atomics
<b>GFR</b>	Gas-Cooled Fast Reactor
<b>GTHTR</b>	Gas-Turbine High-Temperature Reactor
<b>GT-MHR</b>	Gas-Turbine Modular Helium Reactor
<b>HEM</b>	Homogeneous Equilibrium Model
<b>HPS</b>	Hydrogen Production System
<b>HRSG</b>	Heat Recovery Steam Generator
<b>HT</b>	Heat Transfer
<b>HTGR</b>	High-Temperature Gas-Cooled Reactor
<b>HTR</b>	High-Temperature Reactor
<b>HTS</b>	Heat Transport System
<b>HTTR</b>	High-Temperature Engineering Test Reactor
<b>HWP</b>	Heavy Water Plant
<b>HX</b>	Heat Exchanger
<b>HYDNA</b>	Hydraulic Network Analysis (extinct computer code)
<b>I&amp;C</b>	Instrumentation and Control
<b>IBIF</b>	Intermittent Buoyancy-Induced Flow

<b>ICRP</b>	International Commission on Radiological Protection
<b>IGCC</b>	Integrated Gasification Combined Cycle
<b>IHX</b>	Intermediate Heat Exchanger
<b>INL</b>	Idaho National Laboratory
<b>ISI</b>	In-Service Inspection
<b>JAERI</b>	Japan Atomic Energy Research Institute
<b>KAERI</b>	Korean Atomic Energy Research Institute
<b>KVK</b>	Komponenten Versuchskreislauf (Component Test Facility)
<b>LEU-TRISO:</b>	Low Enriched Uranium Triple-Coated Isotropic
<b>LFR</b>	Lead-Alloy-Cooled Fast Reactor
<b>LMTD</b>	Logarithmic Mean Temperature Difference
<b>LOC</b>	Loss of Coolant
<b>LOC/LOECC</b>	Loss of Coolant with Coincident Loss of Emergency Core Cooling
<b>LOCA</b>	Loss of Coolant Accident
<b>LOP</b>	Loss of Pumping
<b>LOR</b>	Loss of Regulation
<b>LOSP</b>	Loss of Secondary Pressure
<b>LWR</b>	Light Water Reactor
<b>MCCR</b>	Ministry of Corporate and Consumer Relations
<b>MCS</b>	Maintenance Cooling System
<b>MHD</b>	Magneto Hydrodynamics
<b>MHR</b>	Modular Helium Reactor
<b>milli-k</b>	Unit of reactivity for reactor physics
<b>NERI</b>	Nuclear Energy Research Initiative
<b>NGNP</b>	Next Generation Nuclear Plant
<b>NHDD</b>	Nuclear Hydrogen Development and Demonstration
<b>NHS</b>	Nuclear Heat Source
<b>NHSS</b>	Nuclear Heat Steam System
<b>NPD</b>	Nuclear Power Demonstration
<b>NPSH</b>	Net Positive Suction Head
<b>NRC</b>	Nuclear Regulatory Commission
<b>NTU</b>	Number of Transfer Units
<b>NUCIRC</b>	Nuclear Circuits (computer code)
<b>OECD</b>	Organization for Economic Co-operation and Development
<b>OH</b>	Ontario Hydro
<b>ORNL</b>	Oak Ridge National Laboratory
<b>PBMR</b>	Pebble-Bed Modular Reactor
<b>PCDSR</b>	Preconceptual Design Studies Report
<b>PCHE</b>	Printed Circuit Heat Exchanger
<b>PCS</b>	Power Conversion System
<b>PCU</b>	Power Conversion Unit
<b>PFHE</b>	Plate-Fin Heat Exchanger
<b>PGSA</b>	Pickering Generating Station A

<b>PHTS</b>	Primary Heat Transport System
<b>PHW</b>	Pressurized Heavy Water
<b>PHWR</b>	Pressurized Heavy Water Reactor
<b>PMHE</b>	Plate Machined Heat Exchanger
<b>PMR</b>	Prismatic Modular Reactor
<b>PNP</b>	Process Nuclear Heat Plant
<b>PRESCON2</b>	Pressure Containment (computer code)
<b>PSHE</b>	Plate Stamped Heat Exchanger
<b>PWR</b>	Pressurized Water Reactor
<b>QA</b>	Quality Assurance
<b>R&amp;D</b>	Research and Development
<b>R&amp;M</b>	Reliability and Maintainability
<b>RAMA</b>	Reactor Analysis Implicit Algorithm
<b>RB</b>	Reactor Building
<b>RCS</b>	Reactivity Control System
<b>RIH</b>	Reactor Inlet Header
<b>ROH</b>	Reactor Outlet Header
<b>RPV</b>	Reactor Pressure Vessel
<b>RSS</b>	Reserve Shutdown System
<b>RTD</b>	Resistance Temperature Detector
<b>RU</b>	Reactor Unit
<b>SDM</b>	Safety Design Matrix
<b>SG</b>	Steam Generator
<b>SHTS</b>	Secondary Heat Transport System
<b>SOPHT</b>	Simulation of Primary Heat Transport (computer code)
<b>SOX</b>	Sarbanes-Oxley
<b>SRV</b>	Safety Relief Valve
<b>SSC</b>	Structures, Systems, and Components
<b>TH</b>	Thermal Hydraulic
<b>THTR</b>	Thorium High-Temperature Reactor
<b>TMI</b>	Three Mile Island
<b>TOFFEA</b>	Two Fluid Flow Equation Analysis (computer code)
<b>TRIS</b>	Triple-Coated Isotropic
<b>TRISO</b>	Tristructural Isotropic
<b>TRISO</b>	Tri-Isotopic
<b>URS-WD</b>	URS – Washington Division
<b>UVUT</b>	Unequal Velocity Unequal Temperature
<b>VB</b>	Vacuum Building
<b>VC</b>	Vacuum Chamber
<b>VHTR</b>	Very-High-Temperature Reactor
<b>WRE</b>	White-Shell Research Establishment

# Index

## A

Adiabatic compressed air energy storage (AA-CAES), 28  
Adiabatic compressed air energy storage for electricity (ADELE), 26, 28  
Adiabatic flame temperature, 57  
Advanced high temperature reactor (AHTR), 116  
Alkaline water electrolysis, 75  
Anode, 65  
Area density, 142

## B

Base load, 66  
Brayton combined cycle (BCC), 248  
Brayton cycle, 169, 175

## C

California Energy Commission (CEC), 34  
California Public Utilities Commission (CPUC), 34  
Carnot efficiency, 177  
Cathode, 65  
Chemical fuels, 46  
Clean-in-place (CIP), 256  
Closed circuit, 149  
Closed cycle, 175  
Cogeneration, 83  
Coiled tube air heat exchanger (CTAH), 31  
Combined cycle efficiency, 150  
Combined cycle gas turbine (CCGT), 150, 151  
Combined heat and power (CHP), 83  
Combustion, 46

Compact heat exchangers (CHEs), 142, 254  
Compact heat exchangers with precision formed surfaces, 254  
Compressed air energy storage (CAES), 32  
Compressed air energy systems (CAES), 26  
Compressibility factor, 181  
Computational fluid dynamics (CFD), 277  
Cooling towers, 222  
Cost of electricity (COE), 161  
Counter flow, 236  
Cross flow, 236

## D

Darcy friction factor, 305  
Department of Energy (DOE), 92  
Dynamic pressure, 305

## E

Effectiveness method, 135, 280  
Electric hydrolysis, 65  
Energy and Industrial Technology Development Organization (NEDO), 61  
Energy Technology List, 254  
Enhanced capital allowance (ECA), 254  
Enthalpy, 53, 54, 56, 57  
Environmental program requirements (EPR), 157  
Extensive security measures, 95

## F

Fanning friction factor, 306  
Final Safety Analysis Report (FSAR), 95

Finite elements method (FEM), 105  
 Firebrick resistance-heated energy storage (FIRES), 30  
 Fluoride-salt-cooled high-temperature reactor (FHR), 30  
 Fuel Cells, and Infrastructure Technologies (HFCIT), 92, 93  
 Fuel cell vehicle (FCV), 61, 81, 85  
 Fukushima, 94

**G**

Gas cooled fast reactor (GFR), 202  
 Gas turbine high temperature tractor (GTHTTR), 202  
 Generation IV, 10–14, 124, 151, 153, 156

**H**

Head loss, 307  
 Heat exchanger (HX), 106, 129, 131, 215, 221, 247  
     counter flow, 133  
     cross flow, 133  
     parallel flow, 133  
 Heat of combustion, 56  
 Heat recovery steam generator (HRSG), 31, 149, 151, 159, 161  
 Higher heating value (HHV), 42, 57  
 High pressure compressor (HPC), 170, 184  
 High temperature electrolysis (HTE), 165, 201  
 High temperature gas cooled reactor (HTGR), 31, 103  
 High temperature test reactor (HTTR), 106  
 Hydraulic diameter, 268  
 Hydrogen fuel cell vehicle (HFCV), 81, 89  
 Hydrogen Network (HyNet), 101

**I**

Ideal thermodynamic efficiency, 10  
 Independent power producers (IPPs), 160  
 In-service inspection (ISI), 116  
 Intermediate heat exchanger (IHX), 97, 98, 106, 111, 114, 168, 188, 190, 249  
 Intermediate heat transport loop (IHTL), 190

**J**

Joule–Thompson expansion cycle, 76

**L**

Light water reactor (LWR), 30  
 Linde cycle, 76  
 Liquefied natural gas (LNG), 85  
 Liquid salt (LS), 103  
 Logarithmic (Log) mean temperature difference (LMTD), 106, 116, 135, 227, 280  
 Lower heating value (LHV), 42  
 Low pressure compressor (LPC), 170, 184

**M**

Million metric (MM), 39, 41  
 Minimum fluid capacity rate, 235  
 Mixed or unmixed flow, 133  
 Molten salt energy storage (MSES), 26  
 Molten salt reactor (MSR), 31

**N**

National Institute of Standards and Technology (NIST), 184  
 National Renewable Energy Laboratory (NREL), 89, 92  
 Next Generation Nuclear Plant (NGNP), 80, 86, 87, 106, 124, 125, 153, 188, 211, 247, 263, 266, 308  
 North American Electric Reliability Corporation (NERC), 89  
 Nuclear air-Brayton Combined Cycle (NACC), 248  
 Nuclear hydrogen development and demonstration (NHDD), 166  
 Nuclear power plants, 95, 225  
 Nuclear Steam Supply Systems, 9  
 Number of transfer units (NTU), 135

**O**

Office of Nuclear Energy, 153  
 Open circuit, 149  
 Open cycle, 175  
 Organization for Economic Co-operation and Development (OECD), 69

**P**

Parallel flow, 213, 235  
 Peak load, 66  
 Photovoltaic (PV), 23  
 Plate-finned heat exchangers, 254

- Plate heat exchangers, 254  
Power conversion cycle (PCU), 168  
Power conversion system (PCS), 124, 129, 157  
Power conversion unit (PCU), 169, 173, 188, 196, 201  
Pressure swing adsorption (PSA), 63  
Preventive maintenance (PM), 106  
Printed circuit heat exchanger (PCHE), 116, 185, 190, 195, 258  
Process heat exchanger (PHX), 103, 188  
Proof stress (PS), 308
- R**  
Ratio of stream capacity rates, 285  
Reactor outlet temperature (ROT), 116  
Reduced pressure, 182  
Reduced temperature, 182  
Research and development (R&D), 61  
Return on investment (ROI), 38, 248  
Reynolds number, 233, 244  
Risk of radioactive release, 95
- S**  
Secondary heat exchanger (SHX), 170, 188  
Small modular reactors (SMR), 143  
Solar PV (SPV), 24  
Solid polymer electrolyte membrane water electrolysis (SPE), 75
- Standard cubic feet per day (SCFD), 39, 41  
Standards development organizations (SDO), 93  
State emergency response, 95  
Steam cycle (SC), 196  
Steam reforming technology, 38, 65  
Stoichiometric air, 48  
Sulfur iodine (SI), 165, 199, 201
- T**  
T boundary condition, 299  
Theoretical air, 48  
Thermosyphon, 263  
Total cost of ownership (TCO), 38, 248  
Total direct cost (TDC), 196  
Tri-isotopic (TRISO), 112
- U**  
Ultimate tensile stress (UTS), 308  
U.S. Department of Energy's Office of Science, 153  
U.S. Nuclear Regulatory Commission, 152
- V**  
Very high temperature reactor (VHTR), 80, 114, 166, 193, 201, 202